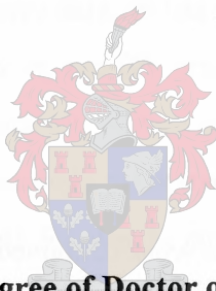


**LONGSHORE SEDIMENT TRANSPORT: APPLIED
WAVE POWER APPROACH, FIELD DATA
ANALYSIS AND EVALUATION OF FORMULAE**

by

Jacobus Stefanus Schoonees



**Dissertation approved for the degree of Doctor of Philosophy (Engineering (Civil))
at the University of Stellenbosch**

Supervisor: Prof A Rooseboom

December 2001

Declaration:

I, the undersigned, hereby declare that the work contained in this dissertation is my own original work and has not previously in its entirety or in part been submitted at any university for a degree.

Signature:

Date: 2001-12-11

ABSTRACT

The process of sand being moved parallel to the coast by wave and current action is called longshore (sediment) transport. Knowledge of longshore transport is essential for the design of breakwaters at harbour entrances, for navigation channels and for calculating the amount of dredging they require, for beach improvement schemes and for the determination of the stability of inlets and estuaries.

Different aspects of longshore transport have been investigated, namely, (1) analysis of field data, (2) evaluation of longshore transport formulae and (3) the development of the wave power approach as an alternative method to calculate longshore transport.

In the development of a better understanding of longshore sediment transport, the following has been done for the first time: (1) a comprehensive data set has been compiled covering almost a full range of conditions occurring on natural beaches; and (2) virtually all longshore transport formulae have been evaluated against this extensive data set. A new improved method, the applied wave power approach, has been developed and extensively calibrated against the same data set. Based on this evaluation, guidelines are now available for design engineers as to which are the best bulk and detailed predictors of longshore sediment transport. These are respectively, the recalibrated Kamphuis formula and the applied wave power approach.

Another useful first, is the derivation of confidence intervals for a longshore transport formula, showing what accuracy can be obtained and that accurate predictions are now possible. In addition, it has now been determined what the minimum required measurement period should be and what the most cost-effective way is for obtaining the true long-term mean net longshore transport rate at a particular site.

SAMEVATTING (Abstract in Afrikaans)
LANGSSTRANDSE SEDIMENTVERVOER: AANGEWENDE
GOLFDRYWINGSBENADERING, VELDDATA-ONTLEDING EN
BEOORDELING VAN FORMULES

Die proses waarvolgens sand ewewydig aan die kus deur golf- en stroomwerking vervoer word, word langsstrandse (sediment-) vervoer of langsvervoer genoem. Kennis van langsvervoer is noodsaaklik vir die ontwerp van golfbrekers by hawe-ingange, navigasiekanale en vir die berekening van die hoeveelheid baggerwerk daarvoor benodig, strandverbeteringskemas en vir die bepaling van die stabiliteit van inlate en getyriwiere.

Verskillende aspekte van langsvervoer is ondersoek, naamlik, (1) die ontleding van velddata, (2) die beoordeling van langsvervoerformules en (3) die ontwikkeling van die golfdrywingsbenadering as 'n alternatiewe metode om langsvervoer mee te bereken..

Tydens die ontwikkeling van 'n beter begrip van langsstrandse sedimentvervoer is die volgende vir die eerste keer gedoen: (1) 'n omvattende datastel is versamel wat bykans alle toestande wat aan natuurlike strande voorkom, dek; en (2) feitlik alle langsvervoerformules is teen hierdie uitgebreide datastel beoordeel. 'n Nuwe verbeterde metode, die aangewende golfdrywingsbenadering, is ontwikkel en omvattend teen dieselfde datastel geëyk. Gebaseer op hierdie beoordeling, is riglyne nou vir ontwerp-ingenieurs beskikbaar rakende watter totaal- en detail-langsvervoervoorspellers die beste is. Dit is onderskeidelik die hergeëykte Kamphuisformule en die aangewende golfdrywingsbenadering.

Nog 'n nuttige eerste is die afleiding van betroubaarheidsgrense vir 'n langsvervoerformule, wat wys watter akkuraatheid nou haalbaar is en dat noukeurige voorspellings nou moontlik is. Verder is dit nou vasgestel wat die vereiste meettydperk behoort te wees en wat die mees koste-effektiewe manier is waarop die ware langtermyn-gemiddelde netto langsvervoertempo by 'n spesifieke terrein verkry kan word.

ACKNOWLEDGEMENTS

I would like to express special thanks to the following persons:

- The Lord Jesus Christ for peace and joy, granting me the privilege to carry out the study and giving me the courage to continue when I was at the end of my tether. He deserves all praise.
- Andre Theron for compiling the longshore transport data, assisting me with the analysis thereof and for many valuable discussions.
- Juanita van Heerden for excellently typing, retyping, changing the text ... and still managing a smile. I appreciate your efforts.
- Dr Harry Swart for introducing me to the subject, training me as an engineer and for his critical review of the thesis manuscript.
- Johan Serdyn, Rob Coppoolse and Chris Els for helping me with the programming of the many formulae and the plotting of their results.
- Prof Rooseboom for explanations and discussions about the stream power concept.
- CSIR (as an organisation) for the opportunity to carry out the work.

I would like to dedicate this thesis to my wife Anelene and our children Anel, Pieter, Talia and Carlie as a token of my appreciation of their love and support throughout the years.

The one insight that came out of this study is that it is not advisable to do a PhD part-time. Dit het voorwaar vasbyt gekos!



(Photograph : D Phelp)



(Photograph : D Phelp)

LONGSHORE SEDIMENT TRANSPORT PROBLEMS AT A HARBOUR

CONTENTS

	Page
ABSTRACT	i
SAMEVATTING (Abstract in Afrikaans)	ii
ACKNOWLEDGEMENTS	iii
LIST OF TABLES	viii
LIST OF FIGURES	ix
LIST OF SYMBOLS	xi
 1. INTRODUCTION	 1.1
1.1 General	1.1
1.2 Objectives	1.5
1.3 Layout of the Thesis	1.6
 2. FIELD DATA ANALYSIS	 2.1
2.1 General	2.1
2.2 Review of Longshore Transport Database	2.1
2.2.1 Field data database	2.1
2.2.2 Data evaluation	2.2
2.3 Annual Variation in the Net Longshore Transport	2.3
2.3.1 Sites and available data	2.3
2.3.2 Analysis method	2.4
2.3.3 Results	2.4
2.3.4 Conclusions and recommendations	2.5
2.4 Main Findings	2.5
 3. EXISTING LONGSHORE TRANSPORT FORMULAE	 3.1
3.1 General	3.1
3.2 Brief History	3.1
3.3 Classification	3.2
3.4 Description of the Types of Formulae	3.2
3.4.1 General	3.2
3.4.2 Energetics (energy flux) approach	3.3
3.4.3 Shear stress (modified steady flow) approach	3.3
3.4.4 Approach using the product of the shear stress and current velocity	3.4
3.4.5 Approach using dimensional analysis	3.4
3.4.6 Approach using the suspended sediment concentration and the longshore current velocity	3.4
3.4.7 Empirical formulae	3.5
3.4.8 Conclusion	3.5
3.5 Summary	3.5
 4. EVALUATION OF THE LONGSHORE TRANSPORT FORMULAE	 4.1
4.1 General	4.1
4.2 Previous Studies	4.1
4.3 Typical Grain Size Relationships	4.2

4.4	Method of Testing	4.2
4.5	Field Data	4.4
4.6	Evaluating Existing Formulae	4.4
4.6.1	General	4.4
4.6.2	Results	4.4
4.6.3	Discussion of the results	4.6
4.6.4	Testing the package deal approach	4.10
4.6.5	Recalibration of the Kamphuis formula	4.12
4.7	Conclusions	4.17
5.	APPLIED WAVE POWER CONCEPT	5.1
5.1	General	5.1
5.2	Stream Power Concept	5.3
5.3	General Approach for the Applied Wave Power Concept	5.6
5.3.1	Background	5.6
5.3.2	Previous studies	5.7
5.3.3	Philosophy	5.8
5.3.4	Basic formulations	5.9
5.3.5	Underlying aspects	5.10
5.4	Choice and Consistency of the Concentration Data	5.14
5.5	Local Longshore Transport Rate Outside the Surf Zone	5.16
5.5.1	General	5.16
5.5.2	Theory	5.16
5.5.3	Calibration of the mean concentration	5.17
5.5.4	Calibration of the local longshore transport rate	5.18
5.6	Local Longshore Transport Rate Inside the Surf Zone	5.21
5.6.1	General	5.21
5.6.2	Derivation of the Wave Power Equations	5.21
5.6.3	Results of the initial calibration	5.26
5.6.4	Distribution of the coefficient a_4	5.27
5.6.5	Effect of beach profile variations caused by cross-shore transport	5.31
5.6.6	Calibration	5.33
5.6.7	Final results	5.38
5.7	Flow Chart and Equations Recommended for the Applied Wave Power Approach ..	5.40
5.8	Recommendations for Further Work	5.43
5.9	Conclusion	5.44
6.	SUMMARY, CONCLUSIONS AND RECOMMENDATIONS	6.1
6.1	General	6.1
6.2	Field Data Analysis	6.1
6.3	Existing Longshore Transport Formulae	6.2
6.4	Evaluation of the Existing Longshore Transport Formulae	6.2
6.5	Applied Wave Power Concept	6.4
6.6	Miscellaneous Findings	6.7
6.7	Final Conclusion	6.7

REFERENCES	R.1
------------------	-----

TABLES

FIGURES

Appendix A:	Review of the field-data base for longshore sediment transport
B:	Annual variation in the net longshore sediment transport rate
C:	Longshore transport formulae

- D: Typical grain size distributions
- E: Accuracy and applicability of the SPM longshore transport formula
- F: Improvement of the most accurate longshore transport formula
- G: Vertical distribution of the time-averaged longshore current velocity
- H: Sediment concentrations: Extrapolation method, consistency of the data and detailed calibrations
- I: Accuracy of the White (1987) data set on local longshore transport rates outside the surf zone
- J: Accuracy of one data point of the Kraus *et al.* (1982) data set on local longshore transport inside the surf zone

LIST OF TABLES

Table	2.1: Longshore transport data evaluation
	2.2: Confidence bands of the factor, floating mean net longshore transport/true long-term mean net transport
	3.1: Summary of the longshore transport formulae
	4.1: Standard error of estimate (σ) for each formula
	4.2: Percentage occurrence of the discrepancy ratios (r_d) for each formula

LIST OF FIGURES

Figure	2.1: Longshore transport data evaluation
	2.2: Variation of the running mean net longshore transport rates over time
	2.3: Richards Bay: floating mean net longshore transport (S) / long-term mean net S
	4.1: Comparing predictions with measured data
	4.2a: Predicted versus measured longshore transport rates for the Kamphuis formula
	4.2b: Residuals versus the predicted longshore transport rates for the Kamphuis formula
	4.2c: Histogram of the discrepancy ratio for the Kamphuis formula
	4.3a: Predicted versus measured longshore transport rates for the Van Hijum, Pilarczyk and Chadwick formula
	4.3b: Residuals versus the predicted longshore transport rates for the Van Hijum, Pilarczyk and Chadwick formula
	4.3c: Histogram of the discrepancy ratio for the Van Hijum, Pilarczyk and Chadwick formula
	4.4a: Predicted versus measured longshore transport rates for the Van der Meer formula
	4.4b: Residuals versus the predicted longshore transport rates for the Van der Meer formula
	4.4c: Histogram of the discrepancy ratio for the Van der Meer formula
	4.5a: Predicted versus measure longshore transport rates for the Larras, Bonnefille and Pernecker, 2 formula
	4.5b: Residuals versus the predicted longshore transport rates for the Larras, Bonnefille and Pernecker, 2 formula
	4.5c: Histogram of the discrepancy ratio for the Larras, Bonnefille and Pernecker, 2 formula
	4.6a: Predicted versus measured longshore transport rates for the SPM, Kamphuis and Readshaw formula
	4.6b: Residuals versus the predicted longshore transport rates for the SPM, Kamphuis and Readshaw formula
	4.6c: Histogram of the discrepancy ratio for the SPM, Kamphuis and Readshaw formula
	4.7a: Predicted versus measured longshore transport rates for the Sauvage de Saint Marc, Vincent and Larras, 1 formula
	4.7b: Residuals versus the predicted longshore transport for the Sauvage de Saint Marc, Vincent and Larras, 1 formula
	4.7c: Histogram of the discrepancy ratio for the Sauvage de Saint Marc, Vincent and Larras, 1 formula
	4.8a: Predicted versus measured longshore transport rates for the Hou, Lee and Lin, 2 formula
	4.8b: Residuals versus the predicted longshore transport rates for the Hou, Lee and Lin, 2 formula
	4.8c: Histogram of the discrepancy ratio for the Hou, Lee and Lin, 2 formula
	4.9a: Predicted versus measured longshore transport rates for the Engelund, Hansen and Swart formula
	4.9b: Residuals versus the predicted longshore transport rates for the Engelund, Hansen and Swart formula
	4.9c: Histogram of the discrepancy ratio for the Engelund, Hansen and Swart formula
	4.10a: Predicted versus measured longshore transport rates for the Fleming formula
	4.10b: Residuals versus the predicted longshore transport rates for the Fleming formula
	4.10c: Histogram of the discrepancy ratio for the Fleming formula
	4.11a: Predicted versus measured longshore transport rates for the Watanabe formula
	4.11b: Residuals versus the predicted longshore transport rates for the Watanabe formula
	4.11c: Histogram of the discrepancy ratio for the Watanabe formula
	4.12a: Predicted versus measured longshore transport rates for the Ackers, White, Swart and Lenhoff formula
	4.12b: Residuals versus the predicted longshore transport rates for the Ackers, White, Swart and Lenhoff formula
	4.12c: Histogram of the discrepancy ratio for the Ackers, White, Swart and Lenhoff formula
	4.13: Predicted versus measured longshore transport rates for the median of the predictions of the 5 best formulae

- Figure 4.14: Predicted versus measured longshore transport rates for the mean of the 3 middle predictions of the 5 best formulae
- 4.15: Predicted versus measured longshore transport rates for the weighted mean of the predictions of the 5 best formulae
- 4.16: Consistency in the predictions of the 5 best formulae
- 4.17: Confidence intervals for the original Kamphuis formula
- 4.18: Confidence intervals for the recalibrated Kamphuis formula: $S = 38\,900 z_{\text{Kamphuis}}$
- 4.19: Confidence intervals for the recalibrated Kamphuis formula: $S = 30\,700 z_{\text{Kamphuis}}$
- 4.20: Confidence intervals in terms of the transport factor for the recalibrated Kamphuis formula: $S = 38\,900 z_{\text{Kamphuis}}$
- 4.21: Confidence intervals for three sub-ranges of the data for the recalibrated Kamphuis formula: $S = 38\,900 z_{\text{Kamphuis}}$
- 5.1a: Velocity and shear stress variation across a small fluid element
- 5.1b: Variation over depth of the stream power applied per unit volume and the amount of power made available by the element
- 5.1c: Calibration of the exponent e_1 for fluvial sediment transport in terms of the applied stream power
- 5.2: Cross-shore variation of the longshore $(\overline{c'v'})$ and cross-shore $(\overline{c'u'})$ flux couplings
- 5.3: Scatterplot of the observed net flux for thirty-one 64 s segments: (A) $\overline{C.U}$ versus \overline{CU} and (B) $\overline{C.V}$ versus \overline{CV}
- 5.4: Computed vertical mixing gradient / wave celerity ratio as a function of estimated breaker index
- 5.5: Computed reference mixing / velocity ratio as a function of estimated breaker index
- 5.6: Comparison between measured and computed reference concentrations
- 5.7: Comparison between measured and computed reference concentrations on linear scales
- 5.8: Coefficient a_2 versus H_{is}/d
- 5.9: Predicted versus measured mean concentrations (outside the surf zone)
- 5.10: Local longshore transport rate against $C_{\text{gem}} \cdot v \cdot d$ for all the realistic data points
- 5.11: Local longshore transport rate against $C_{\text{gem}} \cdot v \cdot d$ for the most accurate data points
- 5.12: Calibration of coefficient a_3 versus H_{is}/d
- 5.13: Predicted versus measured local longshore transport rates for the most accurate data points (outside the surf zone)
- 5.14: Predicted versus measured local longshore transport rates for all the realistic data points (outside the surf zone)
- 5.15a & b: Breaker types
- 5.16: Curves of a_4 fitted through data on local longshore transport rates
- 5.17: Different types of theoretical a_4 distributions
- 5.18: Constant, stepwise and Mountain peak distributions of a_4
- 5.19: Curves allowing for the effect of beach profile variations
- 5.20: Optimization of a constant a_4 while allowing for beach profile variations
- 5.21: Factor allowing for beach profile variations
- 5.22: Histogram of the occurrence of the local surf similarity parameter in Data Set 1
- 5.23: Optimization of a_4 in Zone (i) of the stepwise distribution
- 5.24: Types A, B and C curves in relation to the stepwise a_4 distribution
- 5.25a: Varying points Z, Y and X to optimize the Mountain peak a_4 distribution
- 5.25b: Varying points U, V and W to optimize the Mountain peak a_4 distribution
- 5.26: Varying Point U to optimize a_4
- 5.27: Predicted versus measured longshore transport rates for the applied wave power approach
- 5.28: Percentage occurrence of the discrepancy ratio for the applied wave power approach
- 5.29: Predicted versus measured longshore transport rates for coarse sediment for the applied wave power approach

LIST OF SYMBOLS

A	=	cross-sectional area
a	=	distance above the bed (where the reference concentration C_a is known)
a_o	=	orbital amplitude on the bottom
a_1, a_2, a_3, a_4	=	calibration coefficients
$a_{3,BJ}$ and $a_{4,BJ}$	=	a_3 and a_4 respectively using the Battjes and Janssen (1978) approach
C	=	suspended sediment concentration
C_a	=	(reference) sediment concentration at a distance a above the bed
C_c	=	wave celerity
(Cd_B)	=	coefficient defined in Eq. (5.43)
C_{gem}	=	time- and depth-averaged sediment concentration
C_1	=	coefficient
D	=	energy dissipation per unit time per unit area of the sea bottom
d	=	water depth
D_b	=	energy dissipation per unit time and per unit area due to wave breaking
d_b	=	depth at the breaker line
$D_{b,BJ}$	=	D_b according to the Battjes and Janssen (1978) method
D_f	=	energy dissipation per unit time per unit area due to bottom friction
D_i	=	grain size that exceeds $i\%$ of the sample by mass with i typically equal to 10, 16, 25, 35, 50, 60, 65, 75, 84 and 90%
e_i	=	residual of the i th data (= difference between the measured and predicted transport rates)
e_1	=	exponent (= $0,833 \sqrt{2\pi} w/u_*$ or $a_1 w/u_*$)
F	=	energy flux
f	=	frequency of occurrence of the wave condition
f_c	=	maximum concentration/minimum concentration at a particular elevation
f_f	=	floating average net longshore transport rate divided by the long-term mean net longshore transport rate
f_r	=	running mean net longshore transport rate divided by the long-term mean net longshore transport rate
f_s	=	higher local transport rate/lower local transport rate for the measurements of White (1987)
f_w	=	Jonsson wave friction factor
f_1	=	factor to allow for the effect of beach profile variations
g	=	gravitational acceleration
H	=	local wave height
h	=	local water depth including wave set-up or set-down
H_b	=	breaker wave height
H_{bs}	=	significant breaker height
H_{is}	=	H_s = local significant wave height
H_m	=	maximum wave possible in the specific water depth considered

H_{rms}	=	local root-mean-square wave height
i_r	=	slope of the river or stream
K	=	calibration coefficient used by Dally <i>et al.</i> (1985)
K_D	=	coefficient
K_1	=	coefficient in the general longshore transport formula based on the energy flux approach
L	=	wavelength
L_o	=	deep-water wavelength
m_1, m_2	=	exponents
n	=	number of data points
n_w	=	factor which is a function of the water depth and wavelength
	=	$0,5 \{1 + (4\pi d/L) / (\sinh 4\pi d/L)\}$
p	=	porosity
P_c	=	mean available power supply to a column of water per unit bed area
P_{ls}	=	wave energy flux factor using the significant wave height
P_0	=	energy dissipation per volume and time raised to the power e_1
P_1	=	energy dissipation per volume and time raised to the power e_1 , allowing for beach profile variations
Q	=	ratio of broken waves to the total number of waves at the particular position
Q_r	=	discharge of the river or stream
R^2	=	coefficient of determination
r	=	bed roughness
r_d	=	$r_{d,i}$ = discrepancy ratio of the i th data point
S	=	total longshore transport rate
S_{down}	=	total downcoast longshore transport rate
S_{gross}	=	gross longshore transport rate
S_i	=	longshore transport rate predicted by formula i ($i = 1 \dots 5$)
s_i	=	local longshore transport rate at point i
S_m	=	$S_{m,i}$ = measured longshore transport rate of the i th data point
S_{net}	=	net longshore transport rate
S_p	=	$S_{p,i}$ = predicted longshore transport rate of the i th data point
S_{up}	=	total upcoast longshore transport rate
t	=	time
T_p	=	peak wave period
T_z	=	zero-crossing wave period
u	=	cross-shore current velocity
u_*	=	shear velocity
u_{gem}	=	time-averaged cross-shore current velocity

u_o	=	orbital velocity on the bottom
v	=	longshore current velocity
v_{gem}	=	time- and depth-averaged longshore current velocity
v_{kom2}	=	longshore current velocity calculated with the Komar (1975) approach
v_r	=	mean current velocity of the river or stream
v_x	=	longshore current velocity computed with the Swart and Fleming (1980) method
w	=	fall velocity of the sediment
x	=	the horizontal distance measured from the stillwater line seawards
x_D	=	horizontal distance measured landwards from the breaker line as defined by Dally <i>et al.</i> (1985)
$x_{Kamphuis}$	=	parameter containing the variables used by Kamphuis (see Eq. 4.5)
x_r	=	length dimension measured along the channel/river
z	=	vertical dimension measured from the bed upwards
$z_{Kamphuis}$	=	parameter containing the variables used by Kamphuis (see Eq. 4.5)
α	=	beach slope
α_{BJ}	=	calibration constant in the Battjes and Janssen method
α_D	=	coefficient defined in Eq. (5.34)
β_D	=	coefficient defined in Eq. (5.38)
Γ	=	calibration coefficient
γ	=	breaker index
θ_b	=	wave incidence angle at the breakerline
ξ_b	=	surf similarity parameter evaluated at the breakerline
ξ_i	=	local surf similarity parameter
π	=	pi (= 3,1519 ...)
ρ	=	density of water
ρ_s	=	density of the sediment grains
σ	=	standard error of estimate
σ_i	=	standard error of estimate for formula i
τ	=	shear stress
τ_b	=	shear stress at the bed of the river
τ_c	=	critical bed shear stress
τ_o	=	shear stress at the seabed

1. INTRODUCTION

1.1 General

The process whereby sediment is moved parallel to the coastline by wave and current action, is called longshore sediment transport, or longshore transport. The bottom material or sediment, is stirred up (suspended) by wave action. In the nearshore zone, breaking waves suspend most of the transported sediment. Considerably less sediment is suspended outside the surf zone. Waves approaching the coastline obliquely generate longshore currents. In addition, other mechanisms such as tidal variation, wind and a longshore variation in (wave) breaker height can also generate longshore currents. These currents transport the sediment which has been stirred up by the waves, alongshore. The longshore transport rate, or littoral drift, is the rate at which sediment is moved parallel to the coast in the littoral zone. It is expressed as a volume per time; that is, in m^3/s or m^3/year .

Knowledge of longshore sediment transport is essential for the design of breakwaters at harbour and marina entrances, for navigation channels and their dredging requirements, for beach improvement schemes incorporating groynes, for detached breakwaters and beach fill, as well as for the determination of the stability of inlets and estuaries. Sometimes the economic viability of these projects depends primarily on the siltation and therefore the longshore transport rate. It is therefore of paramount importance that this quantity can be determined accurately.

How are longshore transport rates usually determined? Normally a wave refraction study is conducted to calculate a nearshore wave climate at a number of locations in the particular study area. This climate is then used to compute the longshore transport for each wave condition at a specific location in the study area. Waves and currents can cause longshore transport in either of two directions at a location: up- or downcoast. Therefore a convention for the longshore transport direction is (arbitrarily) chosen. Positive and negative transport represent, for example, up- and downcoast transports respectively. By adding up all the transport rates caused by the different wave conditions in the upcoast direction, the total upcoast longshore transport rate (S_{up}) is obtained. The total downcoast transport rate (S_{down}) is determined in a similar way. The gross and net longshore transport rates at a specific location (S_{gross} and S_{net}) are then determined as follows:

$$S_{\text{gross}} = |S_{\text{up}}| + |S_{\text{down}}|$$

and

$$S_{\text{net}} = S_{\text{up}} + S_{\text{down}}$$

The sign of S_{net} then indicates the net longshore transport direction. This process is then repeated for the other locations in the study area.

Longshore transport formulae can be classified as either bulk or detailed formulae (Swart and Fleming, 1980). For the bulk formulae, a single longshore transport rate is obtained for each wave condition. This means that all the sand (total load) that is moved per time parallel to the coastline at different depths past a line perpendicular to the beach (the location), is estimated. Although it is known that more sand is transported in

the surf zone than outside it, no information about the distribution of the transport is given by bulk formulae. On the other hand, detailed formulae (or predictors) provide information on the transport rate at different depths at each location. The local longshore transport rate is the transport rate at the particular depth. Each of these local transport rates is multiplied by the cross-shore (horizontal) distance that it represents to obtain the local transport product. These local transport products are then added up to acquire the total (integrated) transport rate at the specific location (or line perpendicular to the beach). By dividing the local transport product at each depth by the total transport rate, the so-called cross-shore distribution of the longshore transport is obtained. Normally a depth increment is chosen and calculations are done at depths which are multiples of this depth increment. These calculations usually involve the determination of the dimensions of bed forms (if any), the local bed roughness, the local shear stress on the bed, the local longshore current velocity and the local longshore transport rate (s_i where i is the number of the point on the line perpendicular to the beach). The longshore (or total) transport rate is then acquired by integration normal to the shore as described above. This rate can then be compared to the answers obtained with bulk formulae.

If at all possible, the transport rates computed in the study area should be compared with transport rates measured nearby; for example, accretion at an adjacent harbour as proposed by US Army, Corps of Engineers (1984). It is even better to calibrate the prediction method(s) with data at the same site as was done by Laubscher *et al.* (1991) and Coppoolse and Schoonees (1991). Sometimes, however, no measurements are available. In such instances it is customary to calculate the longshore transport regime at a number of locations in the study area and to compare the transport pattern with trends obtained from beach surveys and aerial photographs. For example, if the net longshore transport increases from one location to the next and the direction remains the same, it means that erosion has to take place between the two locations in order to achieve a larger longshore transport rate. This erosion is usually either revealed as a retreating coastline or a denuded rocky beach. Schoonees and Barwell (1991) resorted to such an approach in analysing beach erosion at Waenhuiskrans in South Africa.

Even if the formula which is used to compute the longshore transport is perfect, the results may not mean much unless the wave conditions are representative for the particular study area. Rossouw (1989) has concluded that for South African conditions, recordings over at least five years are required to obtain a representative annual wave climate. Laubscher *et al.* (1991) and Coppoolse and Schoonees (1991) have clearly illustrated the effect of a varying annual wave climate on the yearly predicted net longshore transport rate at Richards Bay. They found large variations in the annual net longshore transport rate, including a few reversals in the direction of the net rate.

Although numerous formulae that have been developed over the last sixty years are available to compute longshore transport rates, experience has shown that predictions from different formulae can easily vary by orders of magnitude. This causes a problem for the design engineer who usually requires an accurate assessment of the average annual longshore transport rate at a site. He is faced with the following questions:

- Which answer(s) is (are) the most accurate? / Which formula(e) is (are) the best?
- Do the formulae have a sound theoretical basis? / What theoretical approaches have been used in deriving the formulae?
- Have the formulae been calibrated against a wide range of data or for conditions similar to those at

the particular site?

- How accurate are these calibration data?
- What is the most cost-effective way of obtaining the true *long-term* net longshore transport rate at the site?

Schoonees (1997) evaluated the theoretical bases and the ranges of the data for a number of longshore transport formulae. It is valuable to know the ranges of applicability of the formulae. However, no testing against data was performed other than that by the original authors.

The well-known longshore transport formula from the Shore Protection Manual (SPM formula; US Army, Corps of Engineers, 1984) has, for example, been validated against only 41 field data points. Surely, more data must be available in the literature. It is therefore also important to compile and objectively evaluate available field data on longshore transport and to test the accuracy of existing longshore transport formulae against a common and comprehensive field data set. The best formula might then also be improved by calibrating it against the comprehensive data set. Guidance on the above questions can then be given which would be very valuable to all engineers practising in the coastal engineering field.

Formulae for the prediction of longshore transport rates can only be as good as the data on which they are based. Although this is especially true for empirical methods, even the most sophisticated formula requires verification. In this study only field data of longshore transport rates are used. Laboratory data usually contain scale effects. Furthermore, the ultimate aim is to use formulae to predict longshore transport rates in the field, not in the laboratory. The basic philosophy in this thesis is that if a formula has been validated successfully against field data covering a wide range of conditions, then it can be used with confidence to predict longshore transport rates at other similar sites. Emphasis is therefore placed on verification, for, without it, the results of even sophisticated formulae can be meaningless.

In order to obtain the true long-term mean net longshore transport rate at a site, it is necessary to know the annual variation in the net transport rates. This annual variation can be determined either by computing the longshore transport rates with a reliable formula from wave data spanning a number of years, or by measuring the longshore transport over a number of years. In the latter case, it must be known over how many years measurements should be done. This aspect (the required measurement period) will be determined. However, sometimes it may not be possible to take measurements for this required period (for example, time and cost limitations). An alternative question that needs to be resolved, is what is the range within which the long-term mean net transport rate can vary if measurements are done over a shorter than recommended period. This issue will also be addressed. While comparing the two ways of obtaining the true long-term mean net transport rate (predictions or measurements), another question arises: What is the most cost-effective way of obtaining the true long-term mean net longshore transport rate? An answer to this question will be given.

Although numerous investigations have been undertaken since Münch-Petersen published the first longshore transport formula in 1933 (Münch-Petersen, 1933), the above questions have remained unanswered until now. The main reasons for this are the inaccuracy in the predictions and the lack of guidance in the choice of the best formulae. In addition, most formulae have been verified against only a limited range of data.

One aspect of this thesis on longshore sediment transport is derived from the successful concept of defining and predicting fluvial sediment loads in terms of the applied stream power (Rooseboom, 1974, 1992) and by the possibility of extending this concept to nearshore coastal conditions. (Power refers to work done per unit time; that is, the energy dissipation per unit time). Furthermore the applied stream power approach has been shown to be fundamentally sound (Rooseboom, 1974, 1992).

Rooseboom (1974, 1992) derived the theory which was subsequently applied by Mülke (1981) and Rooseboom and Mülke (1982) to investigate incipient motion and ways of controlling erosion on steep slopes (e.g. railway cuttings). Another application of the theory is the prediction of the maximum scour in rivers during floods (Rooseboom and Le Grange, 1992). The question which then comes to mind is, how successfully can longshore transport be described in terms of the applied wave power approach compared with the success of determining the fluvial transport by means of the applied stream power approach? Although it is generally accepted that sediment transport in the sea is more complex than sediment transport in unidirectional flow, it is reasonable to assume that the same basic concepts should hold. An important aim of this thesis is therefore to develop the concept of predicting longshore transport in terms of the applied wave power approach and to evaluate the success (or failure) thereof. The approach followed was to formulate a robust model, realizing that improvements to various aspects could be incorporated at a later stage. However, such improvements will necessarily complicate the method.

The terms “stream power” and “wave power” which will be defined in Chapter 5, will only be used in this thesis if the power per unit volume is meant. Otherwise, the term “the product of the shear stress and the velocity” will be used.

Another important aspect in studying longshore transport at a site is the effect of rocky areas. This effect is mainly twofold, namely:

- the rocky areas limit the availability of sediment to be transported
- usually the local bottom roughness is considerably increased. This is augmented by individual rocks inducing wave breaking, thereby dissipating wave energy.

If rocky areas are present at a site, the potential longshore transport rates (that is, the rate if adequate sediment is available) are normally computed. The real transport rates are then estimated on the basis of the extent of the rocky areas. This approach has, for example, been followed in the design of a small-craft harbour at Gordons Bay, South Africa (CSIR, 1990). However, in this thesis it has been assumed that no rocky areas are present and that an average annual long-term wave climate is known. It should be noted here that a sandy bed under wave action will change in form (profile) and develop different bed forms such as ripples and dunes, thereby also limiting the capacity of sediment transport. This effect is taken into account.

Only particulate (non-cohesive) sediment has been considered. The range considered in this thesis includes sand bigger than about 0,100 mm up to pebbles and shingle. Although the emphasis is on the transport of sand, guidance is also given on the prediction of the longshore transport of coarse material in terms of the applied wave power approach. In addition, as longshore sediment transport in the vicinity of the surf zone is the subject of this thesis, typical water depths vary from 0 m to 10 m or up to about 2 to 3 times the significant

breaker height. It has been assumed that wave action and wave-generated longshore currents dominate, as will be discussed in Chapter 3. The purpose of this study is also to predict the time-averaged longshore transport rate per wave condition and not to consider short-term fluctuations in the transport.

1.2 Objectives

To summarize then, the main aims of this thesis are, with regard to each of the following aspects:

Field data

- to compile a really comprehensive database containing field data on (measured) longshore transport rates and the associated parameters; for example, wave characteristics. Most conditions encountered on natural beaches all over the world should be covered.
- to evaluate the quality of the available field data objectively by employing a method developed in this study.
- to determine the measurement period required to obtain an accurate long-term mean net longshore transport rate at a site. In addition, guidance must be given on how to obtain in the most cost-effective way, this long-term mean net longshore transport rate.

Evaluation of the longshore transport formulae

- to compile a large number of longshore transport formulae (including the commonly used ones) from the literature and classify them into different types of formulae based upon their different approaches.
- to describe briefly the characteristics and theoretical bases of these existing longshore transport formulae.
- to evaluate the existing longshore transport formulae against the comprehensive database.
- to identify the most accurate existing longshore transport formulae by using objective measures to compare the predicted with the measured transport rates. Both bulk and detailed predictors must be considered.
- to improve the best existing longshore transport formula by recalibrating it against the comprehensive database.

Applied wave power approach

- to develop the applied wave power approach to predict longshore transport rates. The aim is to develop a detailed predictor using a process-based, fundamentally sound, yet robust approach.
- to validate the predictions of the applied wave power approach against the (same) comprehensive database. In addition, the accuracy of the applied wave power approach will be compared with the accuracy of the existing longshore transport formulae.

- to determine whether the applied wave power approach is a promising method to predict the longshore transport of coarse material.

Apart from deriving and testing a new method to predict longshore transport, the study will resolve the dilemma of the design engineer because the most accurate existing longshore transport formulae will be identified. Guidance will be given on the required measurement period and the most cost-effective way of obtaining the true long-term mean net longshore transport rate at a site.

1.3 Layout of the Thesis

The layout of this thesis is as follows: the next chapter (Chapter 2) deals with the field data analysis. This is followed by a discussion of the existing longshore transport formulae in Chapter 3. Using the results of Chapters 2 and 3, the existing longshore transport formulae are evaluated against the data in Chapter 4. The development of the applied wave power approach to predict longshore transport rates is treated in Chapter 5. The thesis ends with a summary, conclusions and recommendations (Chapter 6).

2. FIELD DATA ANALYSIS

2.1 General

This chapter consists of two parts: firstly, an in-depth review of the available field data database for longshore transport; and secondly, an analysis of annual net longshore transport rates to obtain the long-term average longshore transport rate at a particular site.

The **review of the available field data** was performed to determine the accuracy of the data. These data consist of simultaneous measurements of the longshore transport rate and wave and sediment characteristics at a variety of sites. The accuracy of longshore transport predictions by means of existing longshore transport formulae (described in Chapter 4) and the wave power related formula derived in Chapter 5 are tested against these data. In turn, these verified formulae and a representative wave climate must be available to predict longshore transport rates (including the long-term net rate) accurately at a particular site. The full data review was published in Coastal Engineering (Schoonees and Theron, 1993) and is attached as Appendix A. One of the aims of this chapter is to extract the most important findings of this review with regard to the compilation and nature of the data (the field data database) and the evaluation of the quality of the data. These two aspects are treated in Section 2.2.

In Section 2.3 the **annual variation in the net longshore transport rate** is investigated with the aim of determining for what length of time measurements should be taken at a particular site in order to obtain a reliable mean net longshore transport rate. This time period will be determined by analysing available time series of net longshore transport rates at three sites. Guidance will also be given on the possible variation in the estimated long-term net rate if measurements are conducted over a shorter than recommended period. A discussion will be presented on what is the most cost-effective way to obtain the long-term mean net longshore transport at a site. Both measurements and predictions will be considered. The complete analysis, contained in Schoonees (2000), was published in Coastal Engineering and was attached as Appendix B. This paper is summarized in Section 2.3.

The main findings of the field data analysis are presented in Section 2.4.

2.2 Review of Longshore Transport Database

2.2.1 Field data database

A literature search was undertaken to collect field data on longshore transport. Only field data are evaluated because laboratory investigations contain possible scale effects and/or use regular waves. Furthermore, the ultimate aim of this study is to be able to predict longshore transport accurately in the field (Komar, 1988). This search yielded a large number of data sets for both bulk and local transport rates, far in excess of the 41 data points used by US Army, Corps of Engineers (1984). Altogether 273 data sets were collected for bulk transport rates. The data originated from a large variety of sites around the world.

2.2

The transport rates were determined by measuring accretion and erosion rates adjacent to coastal structures and at sand spits, by using sand tracers and by different kinds of samplers and traps. Wave conditions were determined by a variety of methods ranging in sophistication from visual estimates, to wave hindcasting to the use of recorders such as pressure transducers.

Most of the data were obtained during mild wave conditions for fine to medium sand. Data are especially lacking for:

longshore transport rate (S)	>	$0,2 \times 10^6 \text{ m}^3 / \text{year}$ ($0,0634 \text{ m}^3 / \text{s}$)
significant breaker height (H_{bs})	>	1,8 m
median grain size (D_{50})	>	0,6 mm
beach slope ($\tan\alpha$)	>	0,06 (= 1 / 14)

A serious consequence of this lack of data is that longshore transport formulae are calibrated almost exclusively against data for mild conditions whereas, in the case of an average annual longshore transport budget, a few storms usually make the major contribution to the total sediment transport. In other words, the most important predictions for which the formulae are used, are for conditions outside the calibration range of the formulae. It is therefore strongly recommended that data be collected in these ranges.

2.2.2 Data evaluation

Method

A point rating system was devised to compare different data sets with regard to the most important parameters for longshore transport. Points were allocated to a data set according to the quality of the data of the six physical parameters deemed most appropriate (important) in determining longshore transport rates. These parameters and the relative importance ("weighting") allocated to the parameters were:

●	longshore transport rate	40
●	wave height	20
●	wave period	10
●	wave direction (angle of incidence)	20
●	beach profile (bottom) slope	5
●	grain size	<u>5</u>
		100

The data sets were further evaluated with respect to each parameter in terms of three sub-divisions namely:

- method by which the data were determined for a specific parameter
- accuracy with which the data were determined or measured
- representativeness of the data

The data sets were each given a score out of a total of 10 points in terms of each of these sub-divisions with respect to each specific parameter. The details of the allocation of points can be found in Appendix A (in both the paper and in a table in Section A2).

The scores for the sub-divisions were added and after the relative weighting of the parameters had been applied, the total points were converted to give a total score out of 100.

Results

The results of evaluating the overall quality of the longshore transport data are presented in Table 2.1 (tables with numbers can be found after the text; tables without numbers are generally referred to only locally) and Figure 2.1. (Some references are listed more than once because the specific data sets contained in that reference differ in quality.) The data were sorted according to the final point rating.

Discussion

Based on the evaluation, the data sets were divided into three categories, namely, lower, middle and higher categories. Most of the data sets fell in the middle category which exhibited a very gradual increase in the overall accuracy of the data (Figure 2.1). Distinguishing between short- and long-term bulk transport data yielded similar trends in the accuracy of the data.

It was found that the evaluation was done reasonably objectively and consistently within the limitations of evaluating the accuracy of measurements (Schoonees and Theron, 1993 - Appendix A). A limited sensitivity study indicated that the data evaluation was not overly sensitive to the weighting allocated to the different parameters.

It is recommended that longshore transport formulae be tested against these data, covering as many different conditions and different sites as possible.

It is already known that it is difficult to measure longshore transport rates, and the parameters that influence them, accurately. This is supported by the fact that the highest score achieved in the evaluation was only 71%. It is recommended that multiple measurements of the transport rate be made simultaneously using different techniques in order to be able to estimate the random error involved in the data and to demonstrate the consistency of the measurements.

2.3 Annual Variation in the Net Longshore Transport

2.3.1 Sites and available data

The three sites where time series data of the net longshore transport rates are available, are located on the east (Indian Ocean) coast of South Africa. These are: Durban Bight, the sand trap of the Port of Durban, and the beaches around the Port of Richards Bay. For comparative purposes, the data for Nouakchott, Mauritania from Shi-Leng and Teh-Fu (1987) are also given.

2.3.2 Analysis method

Both a *running* and a *floating* mean net longshore transport rate were used in the analysis of the time series of the net longshore transport rates as will be discussed below.

The running mean net transport rate is calculated as follows: the first point is the mean rate over 1 year; the second point is the mean rate of the first 2 years; the third point is average of the first 3 years; and so on. A factor (f_r), being the running mean rate divided by the long-term mean net longshore transport rate, was plotted against time for each of the three sites. The advantage of plotting this factor, instead of just the running mean rate, against time, is that it is known that the factor will tend towards unity. It is then easy to see over how many years the running average needs to be taken to ensure that a certain variation is not exceeded.

Due to cost limitations, it is usually not possible also to measure the longshore transport over the required number of years. Guidance is therefore needed on how much a shorter-term average can deviate from the long-term average rate. A *floating* average was used for this purpose. The floating average is computed over a specified number of years. For example, the floating average over 3 years is calculated as follows: the first mean value is the average of the first, second and third net rates, the second mean value is the average of the second, third and fourth net rates, the third mean value is the average of the third, fourth and fifth net rates, etcetera. As for the running mean, the floating mean is divided by the long-term mean rate to obtain a factor (f_f) which will tend towards unity over time. Confidence bands based on the data can then be drawn in on a plot of this factor versus the period over which the floating mean was computed. Therefore, for a certain confidence level, the factors can be obtained within which the estimate of the long-term rate will fall if measurements are taken during a period shorter than the recommended period.

2.3.3 Results

The factor (f_r) or ratio of the running mean net longshore transport divided by the long-term mean net longshore transport, is plotted versus time in Figure 2.2.

Figure 2.3 shows the variation in the factor (f_f) of the floating mean longshore transport divided by the long-term mean transport rate versus the period over which the averaging was done. The Richards Bay data set, which is the longest data set and shows the most variation, has been used.

Four confidence bands (95%, 80%, 20% and 5%) were determined based on the occurrence of the above-mentioned factor f_r . The 95% limit indicates that 95% of the values of f_r will exceed the given value for the particular period over which the averaging was done. The data points showing the position of these four confidence limits (which were determined by means of linear interpolation) are also plotted in Figure 2.3. Smooth curves were drawn through these points. Table 2.2, in which the values of f_r are tabulated, summarizes the confidence limits.

2.3.4 Conclusions and recommendations

Based on data from three sites on the South African east coast, it was found that measurements of the longshore transport rates should be conducted continuously for 5 years to 8 years in order to obtain an accurate value (within 10%) of the long-term mean net longshore transport rate. It was also found that the order (sequence) in which the net longshore transport rates occur is not critical as long as the required measurement period is adhered to. In other words, it does not matter whether the measurements start at a time when the net longshore transport rates are low or high.

Four confidence bands (95%, 80%, 20% and 5%) were determined for the factor f_r , the floating mean net longshore transport/long-term mean net transport, for different measurement periods (Table 2.2). This table can be used to estimate the long-term net transport rate if measurements were done over a shorter period than the 5 years to 8 years recommended above. That is, if measurements cover only, for example, a 2 year period, the values of f_r in Table 2.2 can be applied to determine the range in which the true long-term mean net transport rate will fall for a given confidence band.

For example, if measurements which were taken continuously over two years, yielded a mean net longshore transport rate of 300 000 m³/year, it would mean that the long-term mean net rate can vary as follows by using Table 2.2:

With a confidence of 90% (between 5% and 95%): from $-0,05 \times 300\ 000 = -15\ 000$ m³/year to $2,20 \times 300\ 000 = 660\ 000$ m³/year.

Although the above conclusions are derived from data originating from specific sites, it is reasonable to expect that the conclusions are more widely applicable, especially for exposed sites (such as the three South African sites considered here). For protected sites, the above results are most probably conservative. It is recommended that the above analysis be repeated for protected and partly protected coasts when data become available.

It is also recommended that an accurate assessment of the long-term mean net longshore transport rate at a site can best be made cost-effectively by doing limited site-specific measurements, calibrating the best longshore transport formula (Schoonees and Theron, 1996) for the particular site, and predicting the transport rates using a representative wave climate. Measurements can be made using a variety of methods as described in Schoonees and Theron (1993). If possible these predictions should be augmented by comparing the net rate with the net rates from nearby sites.

2.4 Main Findings

For the first time in coastal engineering, a really comprehensive database has been compiled containing field data on longshore transport rates. Virtually all conditions encountered on natural beaches are covered and the data were collected on beaches from many different sites from around the world. Specific conditions were identified for which data still need to be collected. A point rating system was devised and applied to evaluate the quality of the available data objectively. It is recommended that multiple measurements of the transport rate

2.6

be made simultaneously using different techniques in order to be able to estimate the random error involved in the data and to evaluate the consistency of the measurements.

It was found for exposed sites that measurements of the longshore transport rates should be conducted continuously for 5 years to 8 years in order to obtain an accurate value (within 10 %) of the true long-term mean net longshore transport rate. A table was compiled to estimate the range in which the true long-term mean net transport rate will fall for a given confidence band if measurements were done over a shorter period than the recommended 5 years to 8 years. An accurate assessment of the long-term mean net longshore transport rate at a site can best be made cost-effectively by doing limited site-specific measurements, calibrating the best longshore transport formula (Schoonees and Theron, 1996) for the particular site, and predicting the transport rates using a *representative* wave climate.

3. EXISTING LONGSHORE TRANSPORT FORMULAE

3.1 General

The coastal engineer is faced with a multitude options regarding the choice of the best longshore transport formula. The theoretical bases of these methods vary considerably, as do the complexity of the formulations and the extent of calibrations. How can the formulations which are the best in general or for a particular application be determined? Surely the proof of the pudding is in the eating; that is, the predictions must be accurate over a wide range of conditions. However, the best formula(e) must have a sound theoretical basis. For this purpose, the different theoretical bases of the formulae are discussed in this chapter.

The chapter starts (Section 3.2) with a brief description of the history of the development of longshore transport formulae. In Section 3.3 a new classification is presented for longshore transport formulae. This classification relies on the theoretical bases of the formulae. Section 3.4 is a description of each of the types of formulae. Details of the formulae (including improvements to the formulae and the way in which they were applied) can be found in Appendix C. The chapter ends with a brief review (Section 3.6).

3.2 Brief History

Münch-Petersen (1933, 1936, 1938) was apparently the first researcher to propose a longshore transport formula - see also Knapps (1938) and Slomianko (1960). He related the longshore transport rate exclusively to the characteristics of the wind which generated the waves because of a lack of wave data and measuring equipment - see also Johnson (1953) and Sayao and Kamphuis (1983).

Subsequent investigations included mobile bed model studies by Krumbein (1944), Saville (1950), Shay and Johnson (1951) and Savage (1959, 1962) (in the United States of America). Some prototype measurements were reported by Caldwell (1950, 1956), Watts (1953) and Johnson (1953, 1957). In 1947 the Scripps Institute of Oceanography proposed a longshore transport formula (Scripps Institute of Oceanography, 1947 and Sayao and Kamphuis, 1983). Early theoretical work was carried out by Bagnold (1963) and Inman and Bagnold (1963).

Similar developments were taking place in Japan. Iwagaki and Sawaragi (1962) quoted studies by Sawaragi and Murakami (1957) in which a longshore transport formula based on energy considerations was derived and calibrated with prototype data collected at Miyazu Beach, Akaishi Strait. Mashima (1958, 1960) discussed littoral drift in general. Adachi *et al.* (1959) and Shiraishi (1959) also conducted field studies. Horikawa (1978) gave details of early formulae proposed by Ijima *et al.* (1960), Ichikawa *et al.* (1961) and Ijima *et al.* (1964). Shinohara *et al.* (1958) conducted a model study of littoral drift.

In France, Sauvage de Saint Marc and Vincent (1954) measured longshore transport in a model basin. Other early French publications are Larras (1957, 1961). Field studies have been carried out since 1947 (Delorme, 1981 and Sireyjol, 1964). In Britain, Russell (1960) and in the Netherlands, Svasek and Engel (1960) developed tracer techniques to determine the longshore transport rates. Spring (1920) reported on the sediment problems at Madras harbour (India) while Manohar (1957) investigated sand transport at south Indian ports.

In Germany, Wyrski (1953) was one of the first investigators to study longshore transport.

Since these early studies, interest in the prediction of longshore transport has grown considerably, possibly also stimulated by an increase in coastal, shipping and port development.

In the next section, a classification of existing longshore transport formulae will be presented whereafter the main characteristics of each type of formula will be briefly discussed.

3.3 Classification

A number of different classifications of longshore transport formulae have been proposed. On the one hand, there are the classifications of Sayao and Kamphuis (1983) who distinguished between the wave energy flux approach and the steady flow modification approach. On the other hand, Bailard (1984) noted two types, namely, energetics-based and traction-based models. In this study and in Schoonees (1997) the formulae were classified according to the following approaches:

- (a) An energetics or energy flux approach. (Following Longuet-Higgins (1972), some researchers refer to this category as radiation stress predictors, for example, Vitale, 1981);
- (b) The shear stress or modified steady flow approach;
- (c) An approach using the product of the shear stress and the longshore current velocity (including using the Shields parameter). (As mentioned in the Introduction, the terminology of wave power per unit area will not be used.)
- (d) Applying dimensional analysis;
- (e) Combining the predictions of the suspended concentration and the longshore current velocity;
- (f) Empirical methods.

As with virtually all classifications, ambiguity persists if a formula contains elements of more than one approach. In such cases, the formula was classified according to the approach which was considered to be dominant.

In the subsequent section, each formula, whether a detailed or bulk predictor, is listed in chronological order under its relevant approach. The main characteristics of each type of formula are then described.

3.4 Description of the Types of Formulae

3.4.1 General

Previous reviews of longshore transport formulae include Sayao and Kamphuis (1983) and Bodge (1986). The latter concentrated mainly on detailed predictors. Schoonees (1997) evaluated some longshore transport formulae in detail by examining the theory and the data on which they were based.

The available longshore transport formulae (and how they were applied) are presented in Appendix C and Schoonees (1997). The two longshore transport formulae by Hallermeier (1982) were improved significantly,

while the range for the Bonnefille and Pernecker (1967) methods was extended by extrapolation (Schoonees, 1997). Table 3.1 lists all the formulae per category. It also contains the abbreviations of the formulae as used subsequently on the figures showing their prediction capabilities.

3.4.2 Energetics (energy flux) approach

Most of the 21 formulae in this category (Table 3.1) are adaptations of the Shore Protection Manual (=SPM) formula (US Army, Corps of Engineers, 1984):

$$S = K_1 P_{ls} f \quad (3.1)$$

where S = longshore transport rate (m^3/year)
 P_{ls} = wave energy flux factor using the significant wave height in the calculation (Longuet-Higgins, 1972 proposed using rather the product of the radiation stress component and the wave celerity ($=P_{ls}$), because these are meaningful quantities)
 K_1 = coefficient
 f = frequency of occurrence of the wave condition

Generally speaking, the formulae in this category can be represented by:

$$S = K P_{ls}^{m_1} f \quad (3.2)$$

with m_1 = exponent

Mostly, K in these formulae is not a constant as in the SPM formula, but a function of amongst others, the median grain size (or fall velocity), the surf similarity parameter (Battjes, 1974), the wave incidence angle, the friction factor, the wave period, the beach slope and the sediment density. Although the value of m_1 is usually assumed to be unity, its value ranges from 0,79 to 1,07 (Schoonees, 1997).

Eighteen of the methods in this category are bulk predictors and only three provide detailed transport rates (Table 3.1).

When examining Equation (3.2), it can be deduced that what is essentially assumed in this category is that a certain energy flux is available at the breakerline to transport sediment. Following Bailard (1985), K can be regarded as an efficiency factor of the “wave-current machine” transporting the sediment. In most cases, no attention is given to the processes in the surf zone and how energy is dissipated.

3.4.3 Shear stress (modified steady flow) approach

The methods in this category (Table 3.1) vary considerably, namely, from simple to complicated formulations. For this reason, it is not possible to give one general equation summarizing the different formulae. These

formulae are usually dependent on the formulae for sediment transport in rivers which have been adapted for use in the sea.

The early river formulae which were adapted are the Kalinske and Brown (Rouse, 1950) and the Frijlink (1952) methods. Following an evaluation to determine the best formulae for sediment transport in rivers, the attention focussed on the Ackers and White, and Engelund and Hansen methods (Swart and Fleming, 1980). Essentially, the adaptation usually involves introducing the average bed shear stress due to combined wave current action instead of the bed shear stress due to current action alone. Bijker's (1967) adaptation along these lines constituted a breakthrough because it became possible for the first time to calculate the local longshore transport rate and thus the distribution of the longshore transport across the surf zone and beyond.

In this category the emphasis is clearly on detailed predictors because eight of the nine formulae can be classified as such (Table 3.1).

3.4.4 Approach using the product of the shear stress and current velocity

Typically the formulation can be represented here by:

$$S = C_1 v^{m_2} (\tau - \tau_c)^{m_2} \quad (3.3)$$

with	v	=	longshore current velocity
	τ	=	bed shear stress
	τ_c	=	critical bed shear stress
	m_2	=	exponent being either 1,0 or 1,1
	C_1	=	coefficient depending on, for example, the sediment density, median grain size (or fall velocity) and the density of sea water

Most of the four formulae in this group (Table 3.1) contain an incipient motion criterion (being τ_c). Three of the four methods provide detailed longshore transport predictions.

3.4.5 Approach using dimensional analysis

Here the longshore sediment transport rate is related to groups of variables determined by dimensional analysis. A single general equation cannot be formulated because of the different groupings of the variables. The formulations listed in Table 3.1, although containing quite a number of variables, are simple and easy to use. All three formulae in this group are bulk predictors.

3.4.6 Approach using the suspended sediment concentration and the longshore current velocity

Five methods correspond to this classification (Table 3.1). They vary considerably and as such, cannot be represented by a single general formula. Of these methods, three are bulk predictors which have reasonably

simple formulations. Extensive integration (that is, over the depth and across the surf zone) is required for these detailed predictors.

3.4.7 Empirical formulae

These formulae have been derived from data. The earlier French formulae (derived from 1954 to 1967), are based mainly on laboratory data while the more recent formulae have been calibrated against field data. Despite the variability in these formulae, they are all simple expressions which are easy to use. Of the nine methods classified as having an empirical basis (Table 3.1), seven are bulk predictors.

3.4.8 Conclusion

By far the majority of researchers favour the energetics or energy flux approach; the shear stress (or modified steady flow / Shield number) and empirical approaches are the second most popular approaches. The most recent studies, however, use the product of the shear stress and current velocity, dimensional analysis and empirical approaches.

3.5 Summary

The historical development of longshore transport formulae (since 1933) has been briefly described. In total, 51 longshore transport formulae have been compiled from the literature. A new process-based classification system for longshore transport formulae has been devised and applied by analysing the theoretical bases of almost all existing longshore transport formulae. The characteristics of the different types of formulae are described in this chapter while the individual formulae are summarised in Appendix C. These 51 formulae can now be tested against the field data.

4. EVALUATION OF THE LONGSHORE TRANSPORT FORMULAE

4.1 General

Section 4.2 provides background by describing briefly and evaluating previous longshore transport formulae. The testing of the existing formulae in this section implies that the predicted longshore transport rates can be compared with the measured rates as will be discussed further on (Section 4.4). The input data are, however, lacking certain parameters of the grain size distribution. Therefore it is necessary, firstly, to derive typical grain size relationships (Section 4.3). Thereafter, the method of comparing the predicted and measured rates is discussed (Section 4.4), followed by ranges of the field data (Section 4.5).

Then follows the evaluation of the existing longshore transport formulae against the field data (Section 4.6). Conclusions on the accuracy of the formulae are drawn and recommendations are given. The so-called “package deal approach” advocated by Swart and Fleming (1980), as well as variations of it, are also tested in this section. Briefly, the aim of the investigation is to determine whether the mean or median of the predictions by the best formulae can be used to obtain an improved prediction. Finally, the best formula is recalibrated to improve it and guidelines are given on its usage.

4.2 Previous Studies

Van de Graaff and Van Overeem (1979) compared the Bijker, Engelund, Hansen and Swart and two versions of the Ackers and White formulae against the SPM formula. They assumed that the SPM formula gives a fairly reliable prediction because it is based on a number of prototype measurements. Willis (1980), however, is of the opinion that the SPM formula is not a reasonable standard by which to judge other methods and pointed out that the SPM formula has been extrapolated far beyond the range of the data on which it is based. In addition, both Van de Graaff and Van Overeem (1979) and Willis (1980) warn that the grain size, beach slope and bed roughness should not be varied independently of one other. Because of these objections and because it has been shown in Schoonees and Theron (1994) that the SPM formula is indeed not a reliable yardstick, the conclusions by Van de Graaff and Van Overeem (1979) on the accuracy of these formulae are questionable.

As part of the Canadian Coastal Sediment Study, Fleming *et al.* (1984, 1986a and b) evaluated nine longshore transport formulae. These were three adaptations of the Ackers and White formula, the SPM, the Engelund, Hansen and Swart, Fleming, Nielsen and two forerunners of the eventual Kamphuis, Davies, Nairn and Sayao formula (Fleming *et al.*, 1986b and Kamphuis *et al.*, 1986). The two forerunners outperformed the SPM formula (all three are bulk predictors) when compared to data of two storms at Pointe Sapin (Kooistra and Kamphuis, 1984). (This is in accordance to the results of Schoonees (1997)). By using the same data, the Nielsen formula proved to be the best detailed predictor evaluated, although some anomalies were found in the trend of the bed roughness with varying grain size and wave height.

Kamphuis *et al.* (1986) tested the SPM, Bijker, Ackers, White and Willis formulae and their own method against 38 prototype data points. Their own formula outperformed the others and also showed good agreement with an additional event, namely, at Pointe Sapin (Kooistra and Kamphuis, 1984).

In conclusion then, it is apparent that only a small number of longshore transport formulae have been tested against a limited database. A need therefore exists for an assessment of virtually all the longshore transport formulae against a comprehensive database. This has been done as discussed further in this chapter.

4.3 Typical Grain Size Relationships

In order to be able to test the calculated longshore transport rates against the measured rates, different grain size characteristics are required such as D_{35} and D_{90} . (D_i is the grain size that exceeds i % of the sample by mass). Very few of the references on longshore transport data, however, report grain sizes other than the median grain size. To overcome this, typical grain size relationships were derived, based on grain size data for sand collected along the South African coastline.

The results of the grain size analysis are given in Appendix D. The relationships found between D_{10} and D_{50} , D_{16} and D_{50} , etc. exhibit remarkably low scatter (Appendix D) with a mean coefficient of determination (R^2) of 0,969. These relationships are not necessarily representative of the grain size distributions of the bottom material at the field sites around the world where prototype data have been collected (Chapter 2). However, it is felt that it is reasonable to use these relationships, especially in the light of the good fit. Where the grain size distributions have been reported, they have been used (Appendix D).

4.4 Method of Testing

The only correct standard by which to judge the accuracy of the predicted longshore transport rates (and therefore the respective transport formulae) is by comparing the predictions with measured rates. As has been shown above, another formula (in this case the SPM formula) is not a suitable yardstick. Neither can it, for example, be assumed that the median value of a number of predicted transport rates is the correct transport rate. Figure 4.1 illustrates this principle: in Figure 4.1a it can be seen that the measured transport rate is indeed close to the median of the six predicted rates. In this particular case, the median would be a reasonable estimate of the true transport rate. However, in Figure 4.1b, it can clearly be seen that the median of the predicted values is not a good estimate of the measured transport rate. In this last figure only one of the predictions is really close to the true, measured transport rate. It is therefore clear that the median of the predictions cannot be used as a measure for the accuracy of the transport formulae. Neither can the range of the data be extended by performing some simulations and then make conclusions about the accuracy of the longshore transport formulae. This is because the true longshore transport rates are unknown for the simulated cases.

The accuracy of the predictions and formulae have in the analysis that follows, been tested against measured data and not against any estimates of what the true transport rates could be.

The results of the testing of the formulae will be presented in a number of ways in order to facilitate interpretation. These are:

- A plot of the predicted longshore transport rates (S_p) versus the measured rates (S_m).
- The standard error of estimate (σ) was calculated (Kamphuis, *et al.*, 1986):

4.3

$$\sigma = \left[\sum_{i=1}^n \frac{(\log S_{p,i} - \log S_{m,i})^2}{n-1} \right]^{0,5}$$

(n = number of data points)

(4.1)

- The discrepancy ratio (r_d) (Van Rijn, 1984) and its distribution were determined.

$$r_{d,i} = S_{p,i} / S_{m,i} \quad (4.2)$$

A histogram of the percentage occurrence versus r_d gives this distribution.

- The residuals (e_i) were computed and plotted against S_p to check whether there is a systematic trend in the residuals, or not.

$$e_i = S_{m,i} - S_{p,i} \quad (4.3)$$

On the plot of the predicted transport rates versus the measured rate, the line of perfect agreement was drawn in. The closer the points lie to this line, the better the predictions. Clearly, a good formula must predict transport rates well over the full range of the data. Because the standard error of estimate both evaluates and totals a function of the discrepancy between the predicted and measured longshore transport rates (Equation 4.1), it is logical that the smaller σ is, the better the predictions.

Following Van Rijn (1984), it was determined what percentage of the predictions had discrepancy ratios between 0,5 and 2,0 and within the range 0,25 to 4,0. Naturally, the assumption is that the higher the percentage of the predictions having smaller discrepancy ratios (in the above-mentioned ranges), the better the formula. The choice of these ranges (for example, 0,5 to 2,0) is based to some extent on the large variations found in measurements and predictions of sediment transport rates. Local longshore transport rates for low to medium waves in the surf zone are accurate within a factor 2 (Kraus *et al.*, 1989). Outside the surf zone, the ratio (f_s) between the higher transport rate/lower rate, was on average 8,3 (Appendix I).

The residual $e_i = S_{m,i} - S_{p,i}$ will be negative if a formula overpredicts (and positive for a transport rate that is too low). Thus, if the scatter lies predominantly below $e_i = 0$, then the formula tends to overpredict. Keeping in mind that $e_i = 0$ represents perfect agreement, it is clear that the smaller the scatter of the residuals, the better the predictions. It should also be noted that the plot of the residuals should show no trend if the particular formula (theory) represents the processes properly. If a trend is present, it means that a certain process(es) is(are) simulated inadequately or not at all.

Missing data, apart from the grain size parameters, presented a problem. Wherever possible, the gaps were filled by calculating the values. For example, if the energy flux factor (P_b) is given as well as the significant breaker wave height (H_{bs}) and the peak wave period (T_p) it is possible to compute the wave incidence angle at the breakerline.

4.5 Field Data

From the field data compiled and reviewed by Schoonees and Theron (1993) (Chapter 2 above) a data set, called Data Set 1, was extracted. The sources of Data Set 1 are listed in Schoonees and Theron (1994) (see Appendix E). Data Set 1 contains 123 data points, consisting of data possessing all the required parameters. In order to test the existing formulae, Data Set 1 was also used to enable a comparison to be made of the accuracy of the applied wave power method with the existing formulae.

It is important to note that the data ranges of the particular Data Set 1 are:

0,058	<	H_{bs} (m)	<	3,400
2,32	<	T_p (s)	<	16,60
0,30	<	θ_b (°)	<	35,00
0,0070 (=1/142,9)	<	beach slope	<	0,1380 (=1/7,2)
0,154	<	D_{50} (mm)	<	15,000
600	<	S (m ³ /year)	<	14 793 000

(θ_b = wave incidence angle at the breakerline)

From the above values it is clear that the data ranges of this data set are quite wide. Most conditions encountered on natural beaches are covered and the data were collected on beaches from a variety of sites from around the world. The wide ranges of the data lend credibility to the conclusions drawn in the comparison of the predictions of the existing formulae with the measured transport rates.

4.6 Evaluating Existing Formulae

4.6.1 General

The full evaluation of the existing formulae is presented in Schoonees (1997). Presented here is an extract of the most important findings from this evaluation. Fifty-one existing formulae which are listed in Table 3.1, were tested against Data Set 1. Plots of the predicted longshore transport rates versus the measured rates were prepared for each formula. Furthermore, the standard error of estimate, the distribution of the discrepancy ratios and the residuals were determined for each formula.

4.6.2 Results

Tables 4.1 and 4.2 summarize the findings of the testing with the presentation of the standard error of estimate and the percentage occurrence of the discrepancy ratio per formula. An extract from Table 4.1 was made to list the fifteen best formulae for the particular data set used, based on the standard error of estimate. The following table was obtained:

4.5

Order of accuracy	Number of the formula	Name	Relative standard error of estimate (σ)	Number of data points	Category	Type*
1	37	Kamphuis	0,413	123	Dimensional analysis	Bulk
2	20	Van Hijum, Pilarczyk and Chadwick	0,417	123	Energetics (energy flux)	Bulk
3	51	Van der Meer	0,447	123	Empirical	Bulk
4	46	Larras, Bonnefille and Pernecker, 2	0,504	66	Empirical	Bulk
5	3	SPM, Kamphuis and Readshaw	0,515	123	Energetics (energy flux)	Bulk
6	43	Sauvage de Saint Marc, Vincent and Larras, 1	0,530	89	Empirical	Bulk
7	15	Hou, Lee and Lin, 2	0,561	123	Energetics (energy flux)	Bulk
8	16	Hallermeier, 1	0,563	123	Energetics (energy flux)	Bulk
9	14	Hou, Lee and Lin, 1	0,569	123	Energetics (energy flux)	Bulk
10	7	Caldwell	0,579	123	Energetics (energy flux)	Bulk
11	35	Kamphuis, Davies, Nairn and Sayao	0,599	119	Dimensional analysis	Bulk
12	45	Larras, Bonnefille and Pernecker, 1	0,601	109	Empirical	Bulk
13	25	Engelund, Hansen and Swart	0,611	123	Shear stress (modified steady flow)	Detail
14	40	Tsuchiya	0,619	123	Suspended sediment concentration and longshore current velocity	Bulk
15	47	Kraus, Isobe, Igarashi, Sasaki and Horikawa	0,625	123	Empirical	Bulk

* Type of formula is either a bulk or a detailed predictor.

Figures 4.2a, 4.2b, 4.2c to 4.8c contain the results of the comparison of the seven best formulae (according to σ) with the measured data. (These seven formulae will be encountered later on.) The figures with postscripts "a" show the predicted longshore transport rates (S_p) versus the measured rates (S_m). Postscript "b" indicates the graphs showing the residuals (e_i) versus the predicted transport rates. Similarly, postscript "c" distinguishes the histograms of the discrepancy ratios. Table 3.1 contains the names and abbreviations of the formulae

which were applied to the figures. Note that in these figures:

m^3/yr means m^3/yr ;

$1E+00$ is $10^0=1$;

$1E+02$ is 10^2 ; and

$1E4$ designates 10^4 , etc.

If the five best formulae are chosen from Table 4.2 according to the highest percentage of the discrepancy ratio (r_d) between 0,5 and 2, the following order is obtained:

Order of accuracy	Number of the formula	Name of the formula	% of the predictions for which r_d is between 0,5 and 2
1	3	SPM, Kamphuis and Readshaw	65,0
2	20	Van Hijum, Pilarczyk and Chadwick	64,2
3	51	Van der Meer	60,2
4	43	Sauvage de Saint Marc, Vincent and Larras, 1	57,3
5	8 16	Manohar Hallermeier, 1 (as improved in Appendix C)	56,9 56,9

4.6.3 Discussion of the results

Best measure of the accuracy of the formulae

Since the ranking of formulae in terms of accuracy is dependent on the measure (for example, σ) used, it is relevant to examine which measure is the most appropriate. The graphs of the predicted versus the measured transport rates are most suitable for seeing the scatter of the predictions and in a way, for seeing whether the trends in the predictions are correct (for example, do the predictions follow the line of perfect agreement or do they have a different slope). The same applies to the plots of residuals where the emphasis is especially on trends. However, these types of graphs do not allow for a quantitative comparison as is illustrated by the difficulty of seeing from Figures 4.2a and 4.3a that the Kamphuis formula is superior to the Van Hijum, Pilarczyk and Chadwick formula.

Both the relative standard error of estimate (σ) and the percentage occurrence of the discrepancy ratio (r_d) in a certain range provide a quantitative measure. However, it was found that using the percentage of the predictions where r_d is between 0,25 and 4, is misleading. The reason for this is that the range of 0,25 to 4 is too wide. Formulae, especially those that underpredicted consistently, obtained percentages of 100% yet the

4.7

graphs for the predicted versus measured transport rates revealed the inadequacy of the formulae. It was found that both σ and the percentage of predictions with r_d values in the range 0,5 to 2 could be used. However, σ is a better yardstick to use if the purpose for determining the longshore transport budget at a site is taken into account. The reason for this is that a single badly predicted transport rate can greatly distort the acquired budget. This will be best reflected in σ because its value will be greatly affected while at the same time, the percentage of r_d can still be very high. Thus, σ is preferred as the measure.

The most accurate predictor: the Kamphuis formula

From the first of the above two tables which list the existing longshore formulae according to their accuracies based on σ , it was found that the Kamphuis formula produced the best results for this particular data set. However, it could be argued that, with minor recalibration, any other formula exhibiting less scatter, could achieve better results than the Kamphuis formula. This scatter need not necessarily be around the line of perfect agreement between predicted and measured longshore transport rates. Inspection of all these graphs revealed (Schoonees, 1997) that this is not the case. One can possibly argue further that the Kamphuis formula has been calibrated against most of the data in this particular data set and that is why it performs well. In fact, the Kamphuis formula used none of the 123 data points in this data set. Interestingly, the Kamphuis formula was completely calibrated on data collected in a physical sediment model and verified with field data. This indicates that, provided that a physical model is properly designed and the simulation is carefully done, scale effects can be controlled to acceptably low levels.

It is reasonable to assume that the Kamphuis formula will also perform well, and most probably better than all the other formulae, when applied to other data sets. In this regard, it is important to note that the data ranges of the particular data set (Data Set 1) used above are quite wide (Section 4.5). Most conditions encountered on natural beaches are covered, which gives credibility to the conclusions drawn in this comparison with data.

It is hypothesised that the Kamphuis formula achieved the best results because it contains all the most important parameters, yet is very simple to use. By including fewer parameters, a lower degree of inaccuracy ("noise") is introduced into the prediction by, for example, measurement errors.

Although the Kamphuis formula does not have an incipient motion criterion, it fared well over the full range of the data (which include low transport rates of amongst others, coarse sediment).

Other reliable formulae

By using σ as the measure, the best three formulae are the:

- Kamphuis formula
- Van Hijum, Pilarczyk and Chadwick formula
- Van der Meer formula

The latter two formulae are like the Kamphuis formula, simple and easy to use. Again, a lower degree of inaccuracy is or can be introduced by using only the most important input parameters.

When comparing the sequence of the formulae in the table based on the percentage predictions with r_d between 0,5 and 2, with the sequence of the formulae according to the standard error of estimate in the previous ranking, three of the same five formulae are present (except the Kamphuis and Larras, Bonnefille and Pernecker, 2 methods). The sixth formula on the previous table (Sauvage de Saint Marc, Vincent and Larras, 1) is now ranked number four. The order is, however, somewhat different. It is interesting to note that these two French formulae were published in the 1950s and 1960s; however, they could not be applied to all the data points because the input conditions were outside their ranges of applicability. Note that the SPM, Kamphuis and Readshaw formula, although having the top ranking according to r_d , tends to underpredict high transport rates (Figure 4.6a). This confirms that σ is a better measure than r_d to determine the accuracy of the formulae. At present, the accuracy achievable for the best formula is such that only about 65% of the predictions have r_d values between 0,5 and 2. Ample room for improvement therefore exists.

Most of the 15 best formulae (according to σ) fall in the “Energetics (energy flux)” and “Empirical” categories. This is partly due to the fact that the former category (“Energetics”) is the most popular approach. The categories “Shear stress x longshore current velocity”, “Shear stress (modified steady flow)” and “Suspended sediment concentration and longshore current velocity” did not fare very well. However, it must be kept in mind that the classification of certain formulae was sometimes ambiguous.

Most accurate detailed predictors

In the tables above which rank the most accurate formulae, there is only one detailed predictor, namely, the Engelund, Hansen and Swart method. It can be argued that detailed predictors should not be compared directly with bulk formulae. The detailed predictors are usually more prone to inaccuracies of various input parameters. Moreover, the fact that the bulk predictors are more accurate could merely indicate the inadequacy of the models for calculating the longshore current velocity (D H Swart, pers. comm., 1995). In order to compare the detailed predictors among themselves, the following table was compiled:

Order according to σ	Number of the formula	Name of the formula	Number of data points	σ
1	25	Engelund, Hansen and Swart	123	0,611
2	38	Fleming	123	0,684
3	31	Watanabe	123	0,707
4	27	Ackers, White, Swart and Lenhoff	123	0,750
5	18	Bailard	123	0,753

Figures 4.9a to 4.12c show the performances of the four best existing detailed formulae.

From the above table, it can be seen that the Engelund, Hansen and Swart formula performed the best ($\sigma = 0,611$), followed by Fleming ($\sigma = 0,684$), according to the standard error of estimate. Taking the percentage occurrence of the discrepancy ratio between 0,5 and 2 as the guideline, the Fleming formula with 56,1% leads, while the Engelund, Hansen and Swart method (50,4%) comes second. Roughly speaking, about 50% of the predictions by the five best detailed predictors have discrepancy ratios between 0,5 and 2. There is, therefore, vast room for improvement.

Of the five best detailed formulae, two (Engelund, Hansen and Swart and Watanabe predictors) can be classified as relatively simple. As for the bulk formulae, their accuracy is improved by including fewer variables. However, logically, all the significant variables must be included in the formulation if it is to be accurate. The Ackers, White, Swart and Lenhoff formula requires by far the most computations.

It is hypothesized that the results which show that bulk predictors are at present more accurate indicate that profile variations impact on detailed predictors far more seriously. These profile variations are caused by changes in cross-shore transport due to variations in the wave conditions. The correct choice of a representative beach profile which determines the energy dissipation, is therefore very important for detailed predictors. However, comparing detailed predictors among themselves is realistic because the choice of beach profile is consistent. However, beach profile changes caused by cross-shore sediment transport, impact on the wave energy dissipation and hence, on the longshore transport. It is therefore preferable that beach profile changes due to cross-shore transport be calculated interactively with the longshore transport. That is, beach profile changes are first computed for a certain time step followed by longshore transport calculations. This series of computations of profile changes and longshore transport is then repeated for the duration of the particular wave condition.

Detailed predictors can be validated by comparing the predicted local longshore transport rates with measured rates for both inside and outside the surf zone. Measuring the longshore current velocity eliminates the possible

inaccuracy which is introduced by computing the velocity, and which in turn will affect the accuracy of the particular formula. As discussed in Sections 5.5.4 and 5.6.4, only limited data are available. It is recommended that such measurements be undertaken.

Another factor which could influence the accuracy of detailed predictors, is the depth interval chosen. That is, the local longshore transport is computed at depths 0,1 x depth increment, 2 x depth increment and so on before integrating the transport across the surf zone and beyond. Fleming *et al.* (1986a and b) recommended 0,250 m or smaller steps; in this study 0,125 m was used. Thus the integration can contribute to the inaccuracy of detailed predictors.

4.6.4 Testing the package deal approach

It is common practice to compare the predictions from different longshore transport formulae when computing the annual longshore transport regime at a site. Swart and Fleming (1980) advocated the use of a so-called package deal approach because it was then unknown which formulae were the best. In this approach, the highest and lowest transport rates predicted by six formulae were ignored and the median of the remaining values was determined. An advantage of the package deal approach is that it limits or eliminates the influence of rapidly varying formulae, especially when extrapolating formulae beyond their calibration ranges. Clearly the ideal situation is to know which formula is the best over the full ranges of possible conditions experienced on natural beaches.

The question then remains whether better results can be achieved with this package deal approach or in a related way. Three approaches were tried, namely: first, by considering the median of the predictions by the five best formulae; second, the mean of the three middle values after discarding the highest and lowest predictions and third, a weighted mean transport of the five predictions. The weighting was done according to $1/\sigma$ as follows:

$$S_{\text{weighted mean}} = \frac{S_1/\sigma_1 + S_2/\sigma_2 + S_3/\sigma_3 + S_4/\sigma_4 + S_5/\sigma_5}{(1/\sigma_1 + 1/\sigma_2 + 1/\sigma_3 + 1/\sigma_4 + 1/\sigma_5)} \quad (4.4)$$

where S_i = transport rate according to formula i ($i = 1, 2, 3, 4, 5$)
 σ_i = standard error of estimate of formula i

The five best formulae which are also based on all (123 in this instance) data points were chosen. These formulae are:

Kamphuis

Van Hijum, Pilarczyk and Chadwick

Van der Meer

SPM, Kamphuis and Readshaw

Hou, Lee and Lin, 2

The following table contains the results:

Method	Standard error of estimate (σ)
Median of 5 predictions	0,421
Mean of middle 3 predictions	0,418
Weighted mean of 5 predictions	0,426

Figures 4.13 to 4.15 show the predicted versus the measured longshore transport rates for these three approaches. From these figures it is obvious that there is very little difference between these three package deal approaches since their σ values range only from 0,418 to 0,426. Taking the "mean of the middle three predictions" is marginally better than the other two approaches. The best formula (the Kamphuis method) on its own is better ($\sigma = 0,413$) than the best of the package deal approaches ($\sigma = 0,418$). Even the second best formula, the Van Hijum, Pilarczyk and Chadwick method, on its own ($\sigma = 0,417$) fares slightly better than the best of the package deal approaches ($\sigma = 0,418$).

Figure 4.16 shows the variation in the transport rates predicted by the five best formulae. It can be seen that these predictions are reasonably consistent; that is, the individual formulae do not yield excessive outliers.

It can therefore be concluded that none of the package deal approaches yields better answers than the best formula (the Kamphuis method) and as such, is not worth pursuing if the above-mentioned five best formulae are used within the wide data ranges of Data Set 1. This result is not totally unexpected: adding results of lesser accuracy to the Kamphuis formula is likely to decrease the overall accuracy. Another reason for this lies most probably in the consistency of the five best formulae. It can be argued that the package deal approaches could be preferable if less reliable formulae are applied which tend to deviate. This is, however, not recommended. It is proposed to use the Kamphuis formula alone (in its recalibrated form as given in the next section), for data falling within the data range given above. For data outside this wide range, it is proposed to examine the transport rates predicted by the five best formulae and use engineering judgement. Most probably it would be best also to apply the recalibrated Kamphuis formula alone to data outside the range; however, depending on the consistency of the predictions, it may be advantageous to use the package deal approach (the mean of the middle three predictions) if deviations are prevalent among the transport rates. The reason for this recommendation is that the Kamphuis formula, which was calibrated against physical model data, has shown that it extrapolates well as indicated by it being the best formula tested against field data. It is therefore reasonable to expect that it will also extrapolate well to beyond the data ranges of Data Set 1.

4.6.5 Recalibration of the Kamphuis formula

The recalibration of the Kamphuis formula is described in detail in Schoonees and Theron (1996) which is reproduced as Appendix F. Only the most important aspects are covered here.

The Kamphuis formula can be rewritten:

$$\begin{aligned}
 S &= (31557600.1, 3.10^{-3})(\rho_s / (\rho_s - \rho)) \cdot x_{\text{Kamphuis}} \\
 &= 41025 (\rho_s / (\rho_s - \rho)) \cdot x_{\text{Kamphuis}} \\
 &= 41025 z_{\text{Kamphuis}} \quad (4.5) \\
 &\quad (\text{m}^3/\text{year})
 \end{aligned}$$

$$\text{with } z_{\text{Kamphuis}} = \frac{1}{(1-p)(\rho_s - \rho)} (\rho / T_p) L_0^{1,25} H_{bs}^2 (\tan \alpha)^{0,75} \cdot (1/D_{50})^{0,25} (\sin 2\theta_b)^{0,6}$$

(See Appendix F for definitions of these variables.)

Equation (4.5), the original Kamphuis formula, is plotted on linear scales in Figures 4.17a and b. Note that Figure 4.17b shows the detail of Figure 4.17a for z_{Kamphuis} values up to 100 (instead of 350).

The 80%, 90% and 95% confidence intervals using the t distribution (according to Walpole and Myers, 1978) for the predicted responses of the original Kamphuis formula are also shown in Figures 4.17a and b. The curves (confidence intervals) shown in Figures 4.17a and b, which may appear straight at a first glance, are, in fact, not straight. These curves have been plotted over the range of Data Set 1 and therefore have not been extrapolated. Also note the distorted scales of Figures 4.17a and b. Despite the fact that the Kamphuis formula is the best of the 51 formulae tested, it is immediately apparent that the confidence intervals are very wide. For example, at an 80% confidence level, the predicted transport rate for $z_{\text{Kamphuis}} = 14,2$ varies between $-690\,000 \text{ m}^3/\text{year}$ and $+1\,885\,000 \text{ m}^3/\text{year}$ (predicted response = $+580\,000 \text{ m}^3/\text{year}$) - Figure 4.17b. It should be noted that the confidence intervals shown in Figures 4.17a and b are based on all the data over the full range of z_{Kamphuis} . However, inspection of these figures clearly shows that the scatter of the data increases at higher z_{Kamphuis} values. The preferred approach would therefore be to determine separately the confidence intervals for various z_{Kamphuis} intervals; for example, for $z_{\text{Kamphuis}} \leq 12$ and for $z_{\text{Kamphuis}} > 12$ (Figures 4.17a and b). From Figure 4.17b, it is clear that the scatter is limited for $z_{\text{Kamphuis}} \leq 12$, and as such, the confidence intervals will be much narrower. Note that the coefficient of determination (R^2) is 0,688, meaning that about 69% of the variance is explained by the original Kamphuis formula.

Two approaches were employed to improve the calibration of the Kamphuis formula, namely:

- Linear regression and taking cognizance of outliers and ensuring a good fit over the full range of the data.
- Minimizing the standard error of estimate by choosing the right coefficient (instead of 41 025 in Equation (4.5)).

The following two relationships were obtained, namely:

$$S = 38\,900 \, z_{\text{Kamphuis}} \quad (4.6)$$

(m³/year)

(which gives the same answers as

$$S = 63\,433 \, x_{\text{Kamphuis}}$$

in Appendix F, provided $\rho_s = 2\,650 \text{ kg/m}^3$ and $\rho = 1\,025 \text{ kg/m}^3$).

and

$$S = 30\,700 \, z_{\text{Kamphuis}} \quad (4.7)$$

(m³/year)

(which gives the same answers as

$$S = 50\,000 \, x_{\text{Kamphuis}}$$

in Appendix F, provided $\rho_s = 2\,650 \text{ kg/m}^3$ and $\rho = 1\,025 \text{ kg/m}^3$).

Figures 4.18a to 4.19b present respectively the confidence intervals for the future predicted responses of Equations (4.6) and (4.7) using the t distribution according to Walpole and Myers (1978). As for the original Kamphuis formula, the confidence intervals in Figures 4.18a to 4.19b have been determined for all the data. Although the confidence intervals are still wide, they are similar and wider respectively compared with the intervals for the original Kamphuis formula. For comparative purposes, at an 80% confidence level and for $z_{\text{Kamphuis}} = 14,2$ the values are:

Equation (4.6): $-780\,000 \text{ m}^3/\text{year}$ to $+1\,880\,000 \text{ m}^3/\text{year}$

(Predicted response = $550\,000 \text{ m}^3/\text{year}$)

Equation (4.7): $-1\,090\,000 \text{ m}^3/\text{year}$ to $+1\,960\,000 \text{ m}^3/\text{year}$

(Predicted response = $440\,000 \text{ m}^3/\text{year}$)

These confidence intervals can be presented in terms of a transport factor such that it is easier to generalize the results. The transport factor is defined as a ratio, namely, the transport rate at the limit of the confidence interval divided by the predicted transport rate (response). For example, for Equation (4.6) with $x_{\text{Kamphuis}} = 8,7$, the transport factors at an 80% confidence level for the upper and lower limits are $(+1\,880\,000 / 550\,000) = 3,4$ and $(-780\,000 / 550\,000) = -1,4$ respectively. Rooseboom (1992) found that for river catchments the

transport factor calculated for sediment yield decreased with increasing size (area) of the river catchment. A similar pattern can be expected for the longshore transport predicted by the recalibrated Kamphuis formula, except that the sediment yield from a river catchment cannot be negative while the longshore transport rate can be negative.

Figure 4.20, which has a hyperbolic form, shows that the transport factor does indeed decrease with increasing z_{Kamphuis} over the range of the data (the transport factor has not been extrapolated beyond the range of the data). Furthermore, the upper and lower limit curves are symmetrical around a transport factor of 1 (which corresponds with the predicted response). Roughly, for $z_{\text{Kamphuis}} \geq 85$, the upper and lower transport factors (for an 80% confidence interval) are between 1,4 and 0,6. The ratio of the transport factor of the upper limit divided by the transport factor of the lower limit for $z_{\text{Kamphuis}} = 85$ (80% confidence interval) = $1,4/0,6 = 2,3$. This ratio, which is not very high, reduces with increasing z_{Kamphuis} values. (Note that this ratio is equal to the transport rate at the upper limit of the confidence interval divided by the rate at the lower limit of the confidence interval.) The following table summarizes these ratios (of the transport factors for the upper limit divided by the transport factor for the lower limit) for typical z_{Kamphuis} values as shown in Figure 4.20.

z_{Kamphuis}	Ratio of upper and lower limit transport factors	
	80% confidence interval	95% confidence interval
85	2,4	4,3
127	1,8	2,5
170	1,6	2,0
212	1,4	1,8
255	1,4	1,6
283	1,3	1,6 ⁽¹⁾

(1) This value is shown on Figure 4.20.

The ratios at $z_{\text{Kamphuis}} = 283$ for the 80% and 95% confidence intervals are 1,3 and 1,6 respectively. Comparing these values with a variation of a factor 2, it is clear that the transport factors for predictions with the recalibrated Kamphuis formula are very good for high z_{Kamphuis} values. For lower values of z_{Kamphuis} the ratios are 1,8 and 2,5 for 80% and 95% confidence limits respectively. The transport factors for predictions in this range are good.

It may be asked how serious the higher transport factors that are found for low z_{Kamphuis} values (Figure 4.20) are. They are not too serious because a very small value times a larger transport factor is still small. As most of the longshore transport at a site is caused by a few high wave conditions, the longshore sediment transport budget at the site will not be affected too much. In fact, Seymour and Castel (1985) investigated the episodicity of the longshore transport at seven sites along the United States west coast. They found that almost half of the

gross transport occurs during only 10% of the time. A higher transport factor in the predicted response for low wave conditions is therefore not too important. Rather, the high rates should be predicted well.

The situation at Richards Bay was chosen to illustrate the accuracy achieved with the recalibrated Kamphuis formula. A brief site description is given in Appendix B while Figure 6 (Appendix B) shows the measured versus predicted longshore transport rates at Richards Bay. The four data points (Figure 6 in Appendix B) can, however, not be plotted directly on Figure 4.20. This is because the four data points are the cumulative total transport during the particular year whilst Figure 4.20 is valid for individual wave conditions only. Despite this, z_{Kamphuis} values were computed for typical Richards Bay wave conditions. The typical values chosen (CSIR, 1994 and Laubscher *et al.*, 1991), were: peak wave period = 12 s, wave incidence angle at the breakerline = 3° , and median grain size = 0,30 mm. A range of significant breaker heights from 1,5 m (the median height) to 4,0 m (the 1 in 1 year significant height is about 4,2 m; CSIR, 1994) was used. The corresponding z_{Kamphuis} values were then calculated:

H_{bs} (m)	z_{Kamphuis}
1,5	44,2
2,0	78,5
3,0	176,5
4,0	313,8

Comparing these z_{Kamphuis} values with the x axis of Figure 4.20, it is clear that these values fall on the part of the graph where the transport factor is the lowest. In fact, the ratio of the upper and lower limit transport factors is between:

about 1,3 and 2,4 (80% confidence interval)

and from

about 1,6 to 4,4 (95% confidence interval)

by using Figure 4.20 and the table with the transport factors on page 4.14. It can therefore be concluded that, for Richards Bay, the predictions of the longshore transport rate per wave condition, are within a factor 2 (on average about 1,8) for an 80% confidence limit.

The variables contributing to the longshore transport rate have been ordered in such a manner in Data Set 1 that the transport rate is always positive. It can therefore be argued that physically the range of transport rates at say the 80% or 95% confidence intervals cannot drop below zero. The fact that it happens is partly attributable to using data in the entire range to calculate the confidence intervals.

Inspection of Figures 4.18a and b reveals that because of the increased scatter for z_{Kamphuis} values higher than 12, it is preferable that the confidence intervals be derived for $z_{\text{Kamphuis}} \leq 12$ and $z_{\text{Kamphuis}} > 12$. Considering also

the number of data points in each sub-range of z_{Kamphuis} , it was decided to determine the confidence intervals for three sub-ranges:

- (1) $z_{\text{Kamphuis}} \leq 6$
- (2) $6 < z_{\text{Kamphuis}} \leq 12$
- (3) $z_{\text{Kamphuis}} > 12$

Figures 4.21a and b (Figure 4.21b shows the detail of Figure 4.21a) illustrate the confidence intervals for the three sub-ranges for the recalibrated Kamphuis formula ($S = 38\,900\, z_{\text{Kamphuis}}$). As expected, these figures depict considerably narrower confidence intervals for the first two sub-ranges ($z_{\text{Kamphuis}} \leq 12$) because of the reduced scatter in the data (Figure 4.21a and b) compared with the third sub-range. These narrower confidence intervals appear to be contradictory to the higher transport factors found for low z_{Kamphuis} values. However, Figures 4.18a and b illustrate the slowly varying width of the confidence intervals around the predicted response, whilst the predicted response rapidly increases with increasing z_{Kamphuis} values. The result is therefore that the transport factor decreases with increasing z_{Kamphuis} values because the width of the confidence interval is divided by an ever increasing predicted response as depicted in the table below.

The following table presents typical values from the three confidence intervals of each of the z_{Kamphuis} sub-ranges given in Figures 4.21a and b:

z_{Kamphuis} value approximately in the middle of the sub- range	Predicted longshore transport rate (m ³ /year)	95% confidence interval		Width of the confidence interval (=upper limit - lower limit) (m ³ /year)	Ratio of upper and lower limit factors (= upper limit/ lower limit)	Ratio of the width of the confidence interval and the predicted transport rate
		Lower limit (m ³ /year)	Upper limit (m ³ /year)			
3,5	140 000	9 000	260 000	251 000	28,9	1,79
9,4	370 000	6 000	730 000	724 000	121,7	1,96
147,8	5 750 000	1 860 000	9 630 000	7 770 000	5,2	1,35

This table shows that although the scatter for the third sub-range is the largest (7 770 000 m³/year), its ratio of the upper limit/lower limit is the lowest (5,2) of the three sub-ranges as illustrated in Figures 4.21a. On the other hand, the ratio of the width of the confidence interval (95% in this example) and the predicted transport rate is of similar magnitude: 1,35 to 1,96, say 1,5 to 2,0. This can be regarded as a handy rule of thumb.

The standard errors of estimate for Equations (4.6) and (4.7) show a small improvement compared with the original Kamphuis formula:

Name of the formula	Formula	Standard error of estimate (σ)	% improvement according to σ
Original Kamphuis	$S = 41\,025 z_{\text{Kamphuis}}$	0,413	-
Equation (4.6)	$S = 38\,900 z_{\text{Kamphuis}}$	0,405	2
Equation (4.7)	$S = 30\,700 z_{\text{Kamphuis}}$	0,387	6

Equations (4.6) and (4.7) are therefore slight improvements of the original Kamphuis formula. Whether to use Equation (4.6) or Equation (4.7) needs to be resolved. Equation (4.6) is the best relationship based on linear regression, while Equation (4.7) has the smallest standard error of estimate. It is recommended (Appendix F) that Equation (4.6) be applied at sites where the significant wave heights normally exceed about 0,3 m and where the sediment grain size is usually less than 1 mm, that is, at partly protected and exposed sites. Only at sites where very calm conditions prevail and/or where the sediment size is coarse, is Equation (4.7) expected to yield better answers.

4.7 Conclusions

In all previous studies only a small number of longshore transport formulae have been tested against very limited data. For the first time, virtually all (51) longshore transport formulae have been tested against a really comprehensive database. Two of the four different measures used were found to be the best with which to judge the accuracy of a formula. These are (i), the plot of the predicted transport rates versus the measured rates combined with (ii), the standard error of estimate.

The Kamphuis formula, a bulk predictor, was found to perform the best of the 51 formulae tested. This formula, which performed well over the full range of the data, was recalibrated and slightly improved. For specific conditions, two different versions of the recalibrated Kamphuis formula were determined (Equations (4.6) and (4.7)). Accurate predictions are now possible. Another first, is the derivation of confidence intervals have been derived for a longshore transport formula (Figures 4.18a to 4.19b and 4.21a and b). Figure 4.20 presents, for the recalibrated Kamphuis formula, these confidence intervals in terms of a transport factor. For medium to high wave conditions (the most important conditions when determining the longshore transport budget at a site), the transport factor is smaller than 1,6 (at an 80% confidence interval).

It was found that the Engelund, Hansen and Swart method is the most accurate of the existing detailed predictors.

None of the package deal approaches (using five of the best longshore transport formulae) yields better answers within the wide ranges of Data Set 1 than the best formula (the Kamphuis method). Because of the consistency in the predictions of the recalibrated Kamphuis formula, there is no need for a package deal approach within the present data range. For data outside this wide range, it is proposed to examine the transport rates predicted by the five best formulae and use engineering judgement. Most probably it would be the best also to apply the recalibrated Kamphuis formula alone because it had been shown to extrapolate well.

5. APPLIED WAVE POWER CONCEPT

5.1 General

Definitions

The terms “stream” and “wave power” are used in different contexts in the literature. It is therefore appropriate to define clearly what is meant by these terms, especially as the wave power concept is further developed in this thesis. Bagnold (1966) derived the available stream power as follows: The rate of energy supply per unit length of a stream is the rate at which potential energy is transformed into kinetic energy as the water descends under gravity down a slope of i_r . Therefore:

available stream power per unit length of a stream = $\rho g Q_r i_r$

where ρ = density of water
 g = gravitational acceleration
 and Q_r = discharge of the stream

The mean available power supply to the column of water per unit bed area (P_c) is

$$P_c = \frac{\text{available stream power}}{\text{flow width}} = \frac{\rho g Q_r i_r}{\text{flow width}}$$

but $Q_r = A v_r$
 with A = cross-sectional area
 = (flow width) d
 $\therefore Q_r = (\text{flow width}) d v_r$
 v_r = mean current velocity
 and $\tau_b = \rho g d i_r$
 where d = water depth
 and τ_b = shear stress at the bed

Thus, by substitution

$$P_c = \tau_b v_r$$

Note that the units of P_c which is per unit area, are kg/s^3 . On the other hand, Rooseboom (1974, 1992) used the stream power per unit volume as presented in Section 5.2. Therefore in this case the units are $\text{kg}/(\text{m.s}^3)$.

Aim

A detailed longshore transport formula based on the applied wave power approach will be derived in this chapter. The derivation will be done by treating the transport inside the surf zone separately from the transport outside the surf zone. The results will thus provide expressions for the local longshore transport rate (dependent on, amongst others, the water depth) in each of these zones. Essentially, the mean (time and depth-averaged) suspended sediment concentration will be derived in terms of the applied wave power approach. The

sediment concentration (including the bedload concentration) is in turn combined with the mean (time and depth-averaged) longshore current velocity to give the local longshore transport rate.

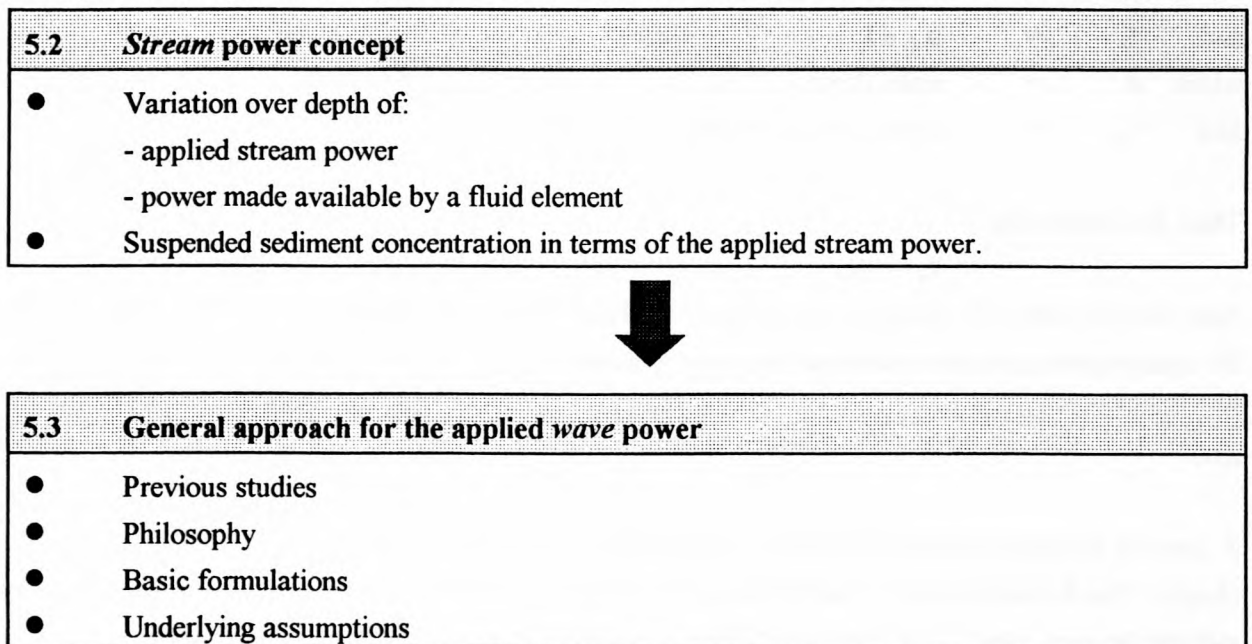
It will be recalled from Chapter 4 that the best existing detail predictor, the Engelund, Hansen and Swart method, obtained a standard error of estimate (σ) of 0,611 (Table 4.1) when tested against the comprehensive Data Set 1. In order to be successful, the applied wave power approach should attain a lower or similar value of σ when tested against the same data set. It will be shown that this has been achieved.

Methodology

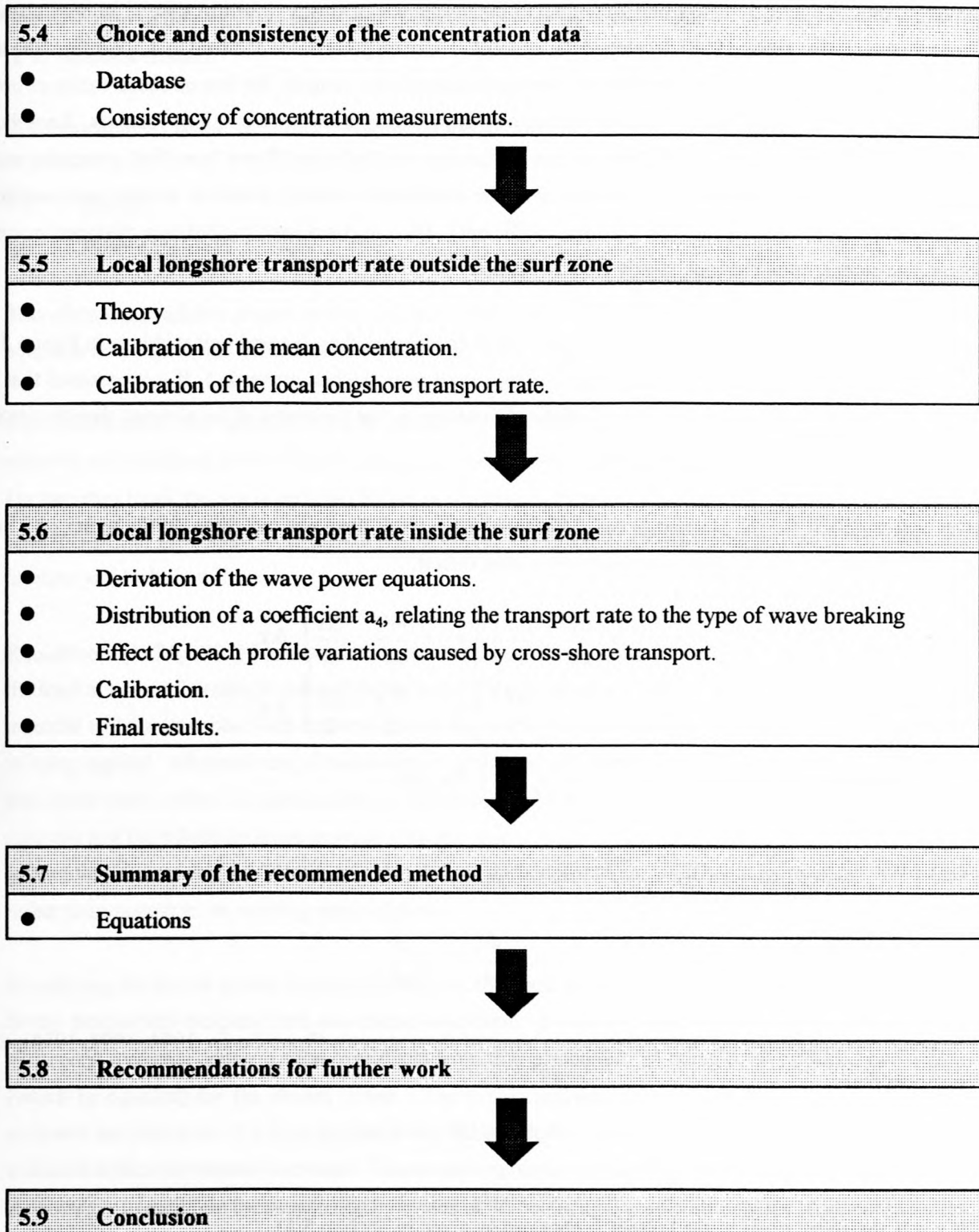
In order to adapt the applied stream power approach in fluvial hydraulics for use in the sea, it is necessary to understand the essence of the applied stream power approach. An explanation of this approach will therefore be presented in Section 5.2. Thereafter the adaptation of the applied stream power approach to the situation in the sea will be treated. The general approach in relating the longshore transport (in the sea) to the applied wave power concept is explained in Section 5.3. Results from previous studies are presented in support of the philosophy adopted. The basic formulations of the local longshore transport rate in the two regions (inside and outside the surf zone) will be given. However, certain assumptions underlie these formulations. The implications and validity of these assumptions will be discussed.

Because sediment concentration data are used in the calibration, it is relevant to analyse their consistency and accuracy (Section 5.4). In Sections 5.5 and 5.6 the theory is derived which enables the local longshore transport rate outside and inside the surf zone to be computed. This theory is then calibrated against both concentration data and measured local transport rates. The theory is then calibrated further (validated) against the comprehensive field data set of *bulk (total)* transport rates.

The following flow diagram explains the development of the longshore transport formula in terms of the applied wave power concept and the layout of Chapter 5 (the numbers given are the relevant section numbers):



5.3

**5.2 Stream Power Concept**

This section is a summary of the work by Rooseboom (1974, 1992, 1998) on the stream power approach. At the end of the section, the concept of applied wave power derived from the concept of stream power is explained. The derived concept will be used further to determine a method for computing the longshore transport. The development of the applied wave power concept and the rest of Chapter 5 are work by the author.

In an attempt to obtain a clearer understanding of the mechanics of steady, uniform flow in an open channel, Rooseboom (1974, 1992, 1998) developed the concept of stream power. He deduced that apart from the laws of conservation of mass, energy and momentum, an additional law, namely, the law of conservation of power is applicable (Rooseboom, 1992). This law provides insight into sediment transporting processes. Rooseboom (1974, 1992) derived the velocity distributions for laminar and turbulent flows from first principles and in doing so, determined theoretically the values of the coefficients usually found in present semi-empirical relationships (for example, the Von Karman coefficient). He also considered the balance of stream power in one-dimensional, open channel, steady flow as follows:

Consider the movement of a small fluid element with dimensions $\Delta x_r, \Delta z$ and unit width as in Figure 5.1a. (The x_r axis is along the channel bed while z is measured from the bed upwards.) If it is assumed that this element moves with a mean velocity of v_r and the shear stress is τ at the centre of the element, then the velocity and shear stress vary as shown in Figure 5.1a.

The power deficit for the element is the difference in the work done per unit time on the upper and lower surfaces of the element. Therefore the stream power deficit

$$\begin{aligned}
 &= \left(\tau + \frac{d\tau}{dz} \cdot \frac{\Delta z}{2} \right) \left(v_r + \frac{dv_r}{dz} \cdot \frac{\Delta z}{2} \right) \Delta x_r \\
 &- \left(\tau - \frac{d\tau}{dz} \cdot \frac{\Delta z}{2} \right) \left(v_r - \frac{dv_r}{dz} \cdot \frac{\Delta z}{2} \right) \Delta x_r \\
 &= \left(\tau \frac{dv_r}{dz} + v_r \frac{d\tau}{dz} \right) \Delta x_r \Delta z
 \end{aligned}$$

\therefore stream power deficit per unit volume

$$= \tau \frac{dv_r}{dz} + v_r \frac{d\tau}{dz}$$

However, by considering the flow resistance in terms of shear stresses (Rooseboom, 1974, 1992, 1998), it can be shown that

$$\tau = \rho g (d - z) i_r$$

(If $z = 0$, the shear stress at the bottom is obtained as given in Section 5.1)

$$\therefore \frac{d\tau}{dz} = -\rho g i_r$$

Substituting then the stream power deficit per unit volume

$$= \tau \frac{dv_r}{dz} - \rho g i_r v_r$$

The first term in this equation represents the stream power applied per unit volume to deform a fluid element or to maintain motion.

From Section 5.1 it will be recalled that the available stream power per unit length of a stream

$$= \rho g Q_r i_r$$

$$= \rho g \Delta x_r \Delta z i_r v_r \text{ by using } Q_r = A v_r$$

Therefore the available stream power per unit volume is $\rho g i_r v_r$. The second term in the above-mentioned equation thus represents the amount of power (per unit volume) made available by the element.

Figure 5.1b shows the variation of the functions $\tau \frac{dv_r}{dz}$ and $\rho g i_r v_r$. From this figure it is evident that for the majority of elevations above the bed there is a considerable difference between the value of these functions. On the other hand, the areas enclosed by the two graphs in Figure 5.1b should be equal in order to satisfy the principle of the conservation of power (Rooseboom, 1974, 1992, 1998). This proves to be valid for both laminar and turbulent flows.

Rooseboom (1974, 1992) postulated that whenever alternative modes of flow exist, that mode which requires the least amount of stream power will be followed. Therefore it can be stated that fluid flowing over movable material will not transport such material unless this results in a decrease in the amount of stream power which is being applied. Alternatively, if two modes of structural yielding exist, yielding will take place according to that mode which offers the least resistance (Rooseboom, 1974, 1992). Where flow takes place over movable material and the relatively large amount of stream power required to maintain motion along the bed becomes greater than that which would be required to deform the bed, the stream will begin to transport the bed material rather than persist in its existing mode of flow.

In applying the stream power concept to sediment transport in unidirectional flow, Rooseboom (1974, 1992) firstly determined incipient bed movement conditions. He then proceeded to derive the variation of the suspended sediment concentration over depth from first principles. In doing so he obtained two expressions (which he equated) for the stream power. The first expression is that the power necessary to change the sediment concentration of a fluid element at any stage is equal to the rate of change of the kinetic energy of the sediment within the element over time. The second expression is based on the average amount of power which is necessary to maintain the suspension by means of the centrifugal acceleration of the sediment particles. The result is the following differential equation:

$$\frac{dC}{C} = \left(\frac{10}{12} \sqrt{2\pi} \cdot w/u_* \right) \left(\frac{d \cdot dz}{z(d-z)} \right) \quad (5.1)$$

where	C	=	sediment concentration
	w	=	sediment fall velocity
	d	=	water depth
	u_*	=	shear velocity

This equation by Rooseboom is identical to the one derived by Rouse (1937) using diffusion theory except for the factor $= 10/12 = 0,833$. The solution of Equation (5.1) is similar to the Rouse equation if the exponent $0,833e_1$ is used instead of e_1 ($e_1 = \sqrt{2\pi} w/u_*$). The solution of Equation (5.1) is:

$$\frac{C}{C_a} = \left\{ \frac{(d-z)}{z} \frac{a}{(d-a)} \right\}^{e_1} \quad (5.2)$$

where C_a = (reference) sediment concentration at $z = a$ (a = distance above the bed)

The ratio w/u_* can be shown to represent the ratio of the power required to suspend particles to the power being applied by the moving fluid.

Equation (5.2) is equivalent to (Rooseboom, 1974, 1992):

$$\frac{C}{C_a} = \frac{\left(\tau \frac{dv_r}{dz} \right)^{e_1}}{\left(\tau \frac{dv_r}{dz} \right)^{e_1} \text{ at } z = a} \quad (5.3)$$

Based on data of measured values given in Chien (1954), Rooseboom (1974, 1992) showed that $0,833e_1$ fits the data better than e_1 (Figure 5.1c). The solution of Equation (5.1) can be given in words as: the concentration at any elevation is proportional to the applied stream power raised to the power $0,833e_1$, where $e_1 = \sqrt{2\pi} w/u_*$. Rooseboom (1975, 1992) proceeded to use this relationship in determining the total sediment load in river flow. (*This concludes the summary of the work by Rooseboom.*)

In the case of wave-driven sediment transport, the same concept will be used; that is, the concentration (here the mean concentration will be used) is proportional to the applied wave power raised to the power e_1 ($= a_1 w/u_*$ where a_1 is a coefficient). Clearly, the shear velocity will now have to be evaluated in terms of the wave friction factor which is dependent on the wave and sediment characteristics.

5.3 General Approach for the Applied Wave Power Concept

5.3.1 Background

In this section *previous studies* employing the stream and wave power concept are reviewed and the *philosophy* of representing longshore transport in terms of the applied wave power is given. This is followed by the *basic formulations* that will be developed further in Sections 5.5 and 5.6 for the local longshore transport both outside and inside the surf zone. However, certain *assumptions* underlie these formulations. The validity of these assumptions will be discussed in the rest of this section.

5.3.2 Previous studies

In the past, a number of studies have been conducted on the relationship between *sediment transport and the product of the shear stress and the current velocity*. Bagnold (1963, 1966) developed the concept of comparing a river or stream to a machine having specific efficiencies in transporting bedload and suspended load. In doing so, Bagnold found that the bedload sediment transport rate (in terms of the immersed weight) is proportional to the time-averaged rate of energy dissipation per area of the stream. Inman and Bagnold (1963) applied the same concept in the sea and averaged, using a control volume, to estimate the total longshore sediment transport rate past a given section of beach. Bailard (1981, 1982, 1984) re-examined the Bagnold (1966) concept and derived a sediment transport model for a plane, sloping beach based on the following assumption: the instantaneous sediment transport rate is directly proportional and reacts immediately to the instantaneous energy dissipation rate per unit bed area. Komar (1977) also related the local longshore transport rate to the product of the shear stress and the current velocity. Later, Watanabe (1985) used a somewhat different formulation successfully, namely, relating the local sediment transport rate to the product of the excess shear stress (above the critical shear stress) and the current velocity.

A different approach has been followed in which the *sediment transport was related to the power per unit volume*. As shown in Section 5.2, Rooseboom (1974) found for river flow that the suspended sediment concentration is proportional to the applied stream power raised to a power of 0,833 e_1 . Dean (1977) analysed numerous beach profiles and found that the depth along a profile is usually a function of the distance from the shoreline raised to a power 0,67. Dean then theoretically showed that the form of the beach profile is consistent with uniform wave energy dissipation per unit volume. Moore (1982) developed a numerical model for simulating beach profile changes using a transport equation for the cross-shore sand movement in which the transport rate was proportional to the wave energy dissipation rate per unit volume. Similarly, Kriebel and Dean (1984) assumed that the cross-shore sand transport rate was proportional to the excess energy dissipation rate per unit volume, that is, the difference between the actual and the equilibrium values of the energy dissipation rate per unit volume (Schoonees and Theron, 1995). Kriebel and Dean obtained good results when modelling beach profile changes caused by storms (Schoonees and Theron, 1995). Larson and Kraus (1989) found that the net cross-shore transport rate showed good correlation with the energy dissipation rate per unit volume, better than the correlation with the energy dissipation rate per unit area.

Considering the above literature, it is clear that sediment transport has successfully been related to either the power per unit volume or the product of the shear stress and the current velocity. Furthermore, as noted above, Larson and Kraus (1989) found good correlation between the net cross-shore transport rate and the energy dissipation rate per unit volume. It is also a fact that the cross-shore transport rate is a function of the suspended sediment concentration coupled with the cross-shore flow. This then means that the suspended sediment concentration is related to the energy dissipation rate per unit volume. It is therefore logical to relate the suspended sediment concentration to the energy dissipation rate per unit volume. This deduction of relating the concentration to the energy dissipation rate per unit volume is also intuitively appealing. Surely, if sufficient energy is expended during a given period, sediment will be suspended.

When considering longshore transport rather than cross-shore transport, the concept to be considered is that the suspended sediment (related to the energy dissipation rate per unit volume) will be transported alongshore by the longshore current. The local longshore transport rate is then the product of the local suspended sediment concentration (including the bedload concentration) and the local longshore current velocity. This concept is in essence partly similar to the basic approach that has been widely used by, for example, Bijker (1967) and Swart (1976b): wave action mobilizes sediment which is transported alongshore by the longshore current.

5.3.3 Philosophy

As explained in Section 5.3.2, in the approach being followed here, the key process of sediment suspension is fundamentally modelled in terms of the energy dissipation rate per unit volume (the applied wave power). This approach is motivated by the analogy of stream power successfully applied in fluvial hydraulics as explained in Section 5.2. The local longshore transport rate is then the product of the local suspended sediment concentration and the local longshore current velocity. In even further support of this method, Mülke (1981) has shown that the final product of the stream power approach (river flow) can be adapted and applied to determine the initiation of severe erosion along a steep slope by unidirectional flow. Furthermore, Bailard (1981, 1982) used the product of the shear stress and the current velocity by Bagnold (1966) in an analogous way, in the sea. Bailard obtained reasonable success.

The method of employing the applied wave power concept in this way is to start with the proven fundamental concept of the suspended sediment concentration being a function of the energy dissipation rate per unit volume. This concept is built up from the most basic approach whereafter it progressively increases in complexity whilst still fundamentally modelling the appropriate coastal processes correctly. If the method shows promise, more elaborate refinements can be added at any stage (though some of the promising elaborations will not form part of this thesis).

A possible alternative method of using the applied wave power concept is the purely “mathematical” method. This implies the mathematical derivation of the applied wave power. A starting point can be to use the continuity principle and Newton’s second law to derive the velocity and shear stress variations over the water depth (for cross-shore and longshore flow) both inside and outside the surf zone. However, because water motion in the sea is a combination of oscillatory and unidirectional flow, the method for the sea is considerably more complex than for rivers. Despite being reasonably simple in essence, the mathematics involved in the treatment of stream power are already cumbersome. Therefore, in order to keep the mathematics manageable, a number of simplifying assumptions will have to be made in deriving the wave power from first principles. For example, in the sea the bottom shear stress is a function of, among others, the wave friction factor (Section 5.5.1) which is in turn dependent on the bottom roughness, wave characteristics and water depth. The factors influencing the bottom roughness include the sediment grain size. In contrast, the equation for the shear stress distribution in river flow is relatively simple (Section 5.2). Making these simplifying assumptions is likely to result in an oversimplification of the processes, thus causing in the coastal processes to be represented in a way not true to reality. The attractiveness of a method to compute the longshore transport is neither the length of the equations nor the complexity of the mathematics involved, but lies in having a sound theoretical basis and in the quality of its predictions. Likewise, the evaluation of the longshore transport formulae

(Chapter 4) has conclusively shown that the simpler formulae which have a sound theoretical basis generally provide the best predictions. For these reasons the fundamental method as explained above has been chosen.

In order to derive the longshore sediment transport rate in terms of the applied wave power, different formulations are required inside and outside the surf zone respectively, as the processes differ. Inside the surf zone, wave breaking is the dominant mechanism in suspending sediment. Outside the surf zone, energy is primarily dissipated by bottom friction. The derivation of formulae for these two zones is treated separately in the following sections. In each of these two zones, the local longshore transport rates at different depths can be computed with the newly derived formulae. These rates have to be integrated across the surf zone and beyond. In this way, the bulk (total rate across the shore) transport rate for the particular wave condition is determined.

Emphasis is placed on the calibration of the formulae. The reason for this is simply to obtain formulae which can be used with confidence under a wide variety of conditions. Associated with this emphasis on calibration, is the importance of the accuracy and reliability of the data, as it is highly unlikely, if not impossible, to obtain calibrated formulae which are more accurate than the data on which they are based.

5.3.4 Basic formulations

By analogy with the stream power concept and based on the findings from previous studies mentioned above, it was assumed that the mean sediment concentration (C_{gem}) over the water depth (d) and over time at the particular position (inside or outside the surf zone) is proportional to the wave power (or the energy dissipation per time and per unit volume) raised to the power e_1 . That is:

$$C_{gem} \propto (D/d)^{e_1} \quad (5.4)$$

where D = energy dissipation per unit area of the sea bottom
 e_1 = exponent
 = function of the sediment fall velocity (w) and the bottom shear velocity (u_*)
 = $a_1 w/u_*$ (a_1 = dimensionless coefficient which was found to be

$$0,833\sqrt{2\pi} = 2,089 \text{ by Rooseboom (1974, 1992) for river flow.})$$

The bottom shear velocity u_* is a function of the bottom shear stress and therefore, among other things, also of the bed roughness and orbital motion as will be presented later on.

$$C_{gem} = a_2 (D/d)^{e_1} \quad (5.5)$$

with a_2 = calibration coefficient (units: $(m.s^3/kg)^{e_1}$ if C_{gem} is in m^3/m^3)

and subscript "gem" denotes a mean value over depth and over time.

In the simplest form then, the local time-averaged longshore transport rate (s_i) is:

$$s_i = a_3 C_{gem} v_{gem} d \quad (5.6)$$

where v_{gem} = local longshore current velocity averaged over the depth

and a_3 = dimensionless calibration coefficient (if C_{gem} is in m^3/m^3)

A double calibration is possible by determining a_2 in Equation (5.5) using totally independent concentration data and then using the result to obtain a_3 in Equation (5.6). Obtaining a_3 in this manner is done by using local longshore transport data. The potential advantage of this approach is twofold, namely:

- Because of the rather limited local longshore transport data, the formulae are tested against the relatively wider concentration database that is currently available. A more representative result based on more degrees of freedom is thus achieved.
- The adequacy of both the assumptions inherent in Equations (5.5) and (5.6) and their validity are tested separately.

In addition, a direct calibration was carried out. By eliminating C_{gem} from Equation (5.5) and (5.6), the following relationship is obtained:

$$s_i = a_4 (D/d)^{e_1} v_{gem} d \quad (5.7)$$

with a_4 = calibration coefficient (units: $(m.s^3/kg)^{e_1}$)

Therefore a_4 can be determined directly with local longshore transport data.

The final and most important calibration is, however, against the extensive database for bulk longshore transport rates that is presented in Chapter 2 and used in Chapter 4.

The same basic formulations (Equations (5.5) to (5.7)) were used both outside and inside the surf zone; however, the energy dissipation per time and volume and the shear velocity were evaluated differently with respect to each zone.

5.3.5 Underlying aspects

The following underlying aspects are treated briefly:

- Wave-current interaction.
- Representing the local longshore transport rate by the product of the time-averaged concentration and the time-averaged longshore current velocity.
- Distributions of the concentration and longshore current velocity over the depth.

- Implications of not using non-linear wave theory.
- Expressing the longshore transport solely as suspended load compared with both bedload and suspended load.
- Effect of beach profile variations caused by cross-shore sediment transport.

Wave-current interaction

The presence of strong currents in addition to waves affects not only the longshore current velocity, but also influences the orbital motion and thus the bottom roughness and the shear velocity. Furthermore, the energy dissipation due to bottom friction is changed. Wave-current interaction therefore plays a role in determining D , u_* and v_{gem} .

In the derivation that follows, it has been assumed that wave-driven currents predominate. If tidal or wind-driven currents are important, energy dissipation due to breaking and bottom friction (while also taking wave-current interaction into account) can be computed by methods such as those of O'Connor and Yoo (1987, 1988). Because the ripple dimensions and thus the bottom roughness and friction factor are also affected, the value of the exponent e_1 will also change. It is therefore possible to explicitly include wave-current interaction in the method. This inclusion is, however, outside the scope of the thesis. One can, however, argue that wave-current interaction is to some extent implicitly allowed for in the model. This is because the calibration data include the effects of wave-current interaction, especially in the surf zone where strong currents are sometimes found. It therefore depends whether the data have been obtained at sites where tidal or wind-driven currents are important. Both local and bulk longshore transport data have been used in the calibration of the method. For the *local* longshore transport data only, the ranges of the measured longshore current velocity, are as follows:

Inside the surf zone: 0,01 m/s to 0,53 m/s

Outside the surf zone: 0,02 m/s to 0,08 m/s

For the bulk longshore transport data, the ranges of longshore current velocities were considerably higher (although these velocities were predicted and not measured). From these ranges of the longshore current velocities, it can be seen that moderate to reasonably strong currents are included in the data for inside the surf zone; however, generally speaking, the currents are low outside the surf zone. Limited wave-current interaction is therefore included for transport inside the surf zone.

Despite this implicit inclusion of (limited) wave-current interaction, the method must be considered applicable only at sites where wave-driven currents predominate.

Longshore transport in terms of the mean concentration and mean velocity over time

It may be asked whether the basic approach is correct of assuming that the time-averaged local longshore transport rate can be represented by $C_{gem} \cdot v_{gem}$. It is well-known that both the concentration (C) and the

longshore current velocity (v) vary considerably over time. Therefore if peaks of these variables coincide (showing so-called coupling), it means that

$$\frac{1}{t} \int_0^t C v dt = (C \cdot v)_{gem} \neq C_{gem} \cdot v_{gem} \quad (5.8)$$

where t = time

Since $s_i = \int C v dt$, it is clear that if C and v are correlated, then the local longshore transport (s_i) cannot be represented by $C_{gem} \cdot v_{gem}$. If this is the case, both the time variations of C and v have to be known together with their phase difference in order to perform the integration of Equation (5.8).

A number of studies have been conducted to investigate the relationships between $(C \cdot v)_{gem}$ and $C_{gem} \cdot v_{gem}$ and between $(C \cdot u)_{gem}$ and $C_{gem} \cdot u_{gem}$ (u is the cross-shore current velocity) as a function of time (Sternberg *et al.*, 1984; Jaffe *et al.*, 1984; Hanes and Vincent, 1987; Beach and Sternberg, 1992; and Jaffe and Sallenger, 1992). Using detailed measurements at four sites during, amongst other conditions, storms, the researchers found conclusively that C and v are uncorrelated but that there is a coupling between C and u . (Steetzel (1993), however, presented an argument for presenting the cross-shore transport rate by $C_{gem} \cdot u_{gem}$.) Figures 5.2 and 5.3 illustrate the results of the measurements. Note that in Figure 5.2 a low (approximately zero) suspended-sediment flux coupling indicates no correlation between C and v . Figure 5.3 (plot B) shows that $C_{gem} \cdot v_{gem} = (C \cdot v)_{gem}$.

It can therefore be concluded that the local longshore transport rate can be represented by $C_{gem} \cdot v_{gem}$ as a good first approximation.

Distributions of the concentration and longshore current velocity over the depth

Apart from the representation of the concentration and longshore current velocity by their respective time-averaged values, the variations of the concentration and the longshore current velocity over depth should be considered. It is therefore relevant to briefly review the distributions of C and v over the depth. In numerous studies it has been found that the time-averaged concentration is distributed exponentially over the depth (for example, Nielsen, 1979, 1984; Sternberg *et al.*, 1984 and Schoonees, 1990).

In Appendix G it is shown from measurements and from theory that the time-averaged longshore current velocity is almost constant throughout the water depth. Therefore, assuming $v = v_{gem}$ is well justified. Using C_{gem} does not allow adequately for the variation of C over the depth. However, applying C_{gem} remains the simplest approach as explained previously and is expected nevertheless to give reasonable results.

It can therefore be concluded that v_{gem} provides an adequate representation of v over the depth. The calibration and verification of the method will show whether it is sufficiently accurate to use C_{gem} .

Non-linear wave theory

Since all the waves under consideration are in shallow water, the question can be asked whether non-linear wave theory should not rather be used. Such a theory would change (and possibly improve) the predictions of the orbital motion, the bottom roughness, the shear velocity and the energy dissipation per time and volume. If the longshore current velocity is computed, the prediction thereof will also be affected. However, the calibration and verification of the above-mentioned parameters were accomplished with the aid of linear wave theory. If non-linear wave theory is applied, then the calibration of these parameters should be repeated. Therefore, in order to be consistent and because it is simpler to use, linear wave theory was applied throughout. If the validity of the method of applied wave power is proved, then it will be possible to investigate the use of non-linear wave theory later.

Total load versus bedload and suspended load

The differentiation between bedload and suspended load is considered somewhat artificial, with the former being a special case of the latter. Following Nielsen (1979) and Rooseboom (1992), it has therefore been assumed that all sediment is carried in suspension. The so-called bedload layer is therefore considered as a zone in which a high concentration of suspended sediment occurs.

If the exponent e_1 (in Equations (5.2), (5.3) and (5.5) for example) is small, the sediment concentration varies very little with depth and an almost homogenous suspension is present (Rooseboom, 1992). For high e_1 values virtually all sediment will be found close to the bed and only so-called bedload transport occurs (Rooseboom, 1992). The suspension theory therefore accounts for both extremes, namely, a homogenous suspension and only bedload. At the same time, intermediate cases are also covered. It is therefore reasonable to relate the total load to the mechanism of suspension. Furthermore, Rooseboom and Mülke (1982) have shown for stream flow that incipient motion criteria could be established by means of suspension theory even though the transport is almost purely bedload just after the start of motion.

Effect of beach profile variations caused by cross-shore sediment transport

It is well-known that offshore sediment transport is usually a swift process whereby a beach is usually eroded near the water-line during a storm. The sand is transported seawards and deposited to form an underwater bar in deeper water on which the storm waves break. When the sea calms down again, sand is slowly transported back to the beach, thus re-establishing approximately the original beach profile if no net loss of sand has occurred. If a wave condition persists long enough, an equilibrium beach profile is formed. On such a profile, there are no significant net changes in the form of the profile. Various studies have proved the equilibrium beach profile concept; for example, Nayak (1970), Swart (1974), Dean (1977) and Larson and Kraus (1989).

Related to the equilibrium beach profile concept, Larson and Kraus (1989) found a rapid decay over time in the net cross-shore transport rate. This finding is based on measurements during 33 experiments in large waves tanks. This decay corresponds to the fact that the cross-shore transport rate is related to the extent of difference

5.14

between the existing profile and the equilibrium profile (Swart, 1974). An initial large difference between these profiles will cause the profile to adapt reasonably quickly. When the difference becomes small, the change towards the equilibrium profile will take place much more slowly.

Based on the beach profile variations that are caused by cross-shore transport, it is hypothesized that the local longshore transport rates will change over time because of these beach profile variations. In order to substantiate this hypothesis, limited modelling with a cross-shore sediment transport and morphological model, Sbeach by Larson and Kraus (1989), was used to simulate typical beach profile changes. This model has a sound theoretical basis and is well verified against field data (Schoonees and Theron, 1995). The following output from the Sbeach model was used: the variation over time of the water depth and the local wave height. This output was then employed to calculate separately the parameter called the energy dissipation per unit volume and time raised to the power e_1 ($= (D_{b,BJ}/d)^{e_1}$). According to Equation (5.7), this parameter is directly related to the local longshore transport rate. Three different areas were identified in the modelling along the beach profile, namely, (1) an area where significant erosion occurred, (2) an area along the beach profile characterised by low deposition, and (3) an area where high deposition (crest of a sand bar) occurred. It was found in all these areas that the parameter $(D_{b,BJ}/d)^{e_1}$, representing the local longshore transport rate, varied over time. After initial larger variations, an equilibrium value of the parameter was established. In the second area it was found that only minor changes occurred. Clearly, this is to be expected in Area (2) because both the water depth and the local wave height changed only very slightly over time.

It is customary in computing longshore transport to assume that the beach profile does not change during the period that a particular wave condition occurs. The above analysis, however, clearly shows that the local longshore transport rate will vary over time because of beach profile changes. It is therefore important to take into account this variation over time in the longshore transport rate. This aspect will be addressed later.

5.4 Choice and Consistency of the Concentration Data

Because independent concentration data are employed in the calibration, it is important to consider briefly the accuracy and reliability of these data. This is done in this section and thereafter the theory for both outside and inside the surf zone is developed.

Van Rijn (1991) compiled a comprehensive database on sand concentration profiles through the water depth. From this database all data collected in the field as well as in prototype-sized flumes were chosen for calibration. The advantage of this approach is that possible scale effects are virtually eliminated. On the other hand, it is more difficult to measure accurately in the field (see for example, Derks and Stive, 1984; Schoonees, 1990 and Coppoolse *et al.*, 1992). In addition, the input variables cannot be controlled. However, it was felt, concerning the longshore transport data (Schoonees and Theron, 1993 - Appendix A) that the most important consideration was to be able to predict sediment concentrations accurately in the field. Data obtained in wave tunnels were excluded because the effects of vertical accelerations and wave breaking are not produced.

5.15

A wide variety of conditions are covered by the data in the database. Apart from non-breaking waves (outside the surf zone), spilling, spilling/plunging and plunging breaking waves (inside the surf zone) are included. For the laboratory data from large flume tests, mostly irregular wave spectra of the Pierson-Moskowitz type were used. However, irregular waves with a Jonswap spectrum and regular waves were also generated in these tests. Detailed information regarding the wave heights (the significant wave height was used unless otherwise stated), wave periods, water depths, grain sizes, different bed forms, et cetera is given where the calibrations are described.

Data from the following authors were used as given by Van Rijn (1991):

Nielsen (1984)

Vellinga (1984)

Vessem for Project Geomor, Rijkswaterstaat, The Netherlands (Van Rijn, 1991)

Roelvink (1987)

Steetzel (1987)

Van Rijn (1989)

Dette and Uliczka (1986, 1986a)

Details regarding these investigations are given in Van Rijn (1991) together with the original references and will not be repeated here. In Appendix H, one of the methods used by Van Rijn to extrapolate concentration measurements to the bed in order to determine a mean concentration, is described. The results of this method were used in the present study.

It is important to note that no data points of the selected recordings (as explained above) were left out simply because they did not fit the model(s) that were calibrated.

Nielsen (1984) repeatedly measured sediment concentrations in the field, while Dette and Uliczka (1986) did so in a big wave flume in Hannover. Both these sets of data are analysed in Appendix H. It was found that the factor (f_c), being the maximum concentration/minimum concentration at a particular elevation, varied between 1,4 and 19,9 with an average value of 3,2. This means that even if a particular theoretical model is perfect, its accuracy in calibration against these data can be accurate only within an average factor (f_c) of 3,2.

In Appendix H various reasons are given for these large variations in measured concentrations. One of the most important reasons is the sampling interval which is believed to be too short. Typically, the sampling interval is from 3,5 minutes to 15 minutes. Arguments are presented in Appendix H which indicate that the interval should be not less than 30 minutes and preferably an hour or longer.

The consistency of the concentration measurements (on average within a factor of 3,2) must be kept in mind when the calibration of the applied wave power approach is carried out. Outliers deviating from the calibration curve can be expected because an outlier is found even in the limited number of repetitive measurements (Table H1 in Appendix H). This finding is confirmed in Figures 5.4 and 5.5 which show a spread in the data

in the calibration of the method by Steetzel (1993) at Delft University of Technology. Steetzel (1993) developed a method to compute cross-shore sediment transport in terms of the concentrations. Outliers are evident in his subsequent comparison of the measured and calculated bottom reference concentrations (Figures 5.6 and 5.7). Despite the spread in the concentration data, Steetzel showed that his cross-shore transport model predicts the beach response reasonably accurately.

5.5 Local Longshore Transport Rate Outside the Surf Zone

5.5.1 General

Equations (5.5), (5.6) and (5.7) will be used to calibrate coefficients a_1 to a_4 for transport outside the surf zone. The energy dissipation caused by bottom friction will be applied. The theory for predicting the energy dissipation and the calibrations of the mean concentration and local transport rate is developed.

5.5.2 Theory

After defining the wave power, the equations for the shear and fall velocities are presented.

By using the wave energy equation for steady state conditions, the energy dissipation per unit time and unit volume for a turbulent boundary layer (Horikawa, 1988; O'Connor and Yoo, 1988) is given by:

$$\begin{aligned} D_f/d &= \frac{1}{d} \frac{\partial F}{\partial x} \\ &= \frac{2}{3\pi} \rho f_w u_o^3 / d \end{aligned} \quad (5.9)$$

where D_f = energy dissipation per unit time and area due to bottom friction

The mean sediment concentration over depth (and time) is then

$$\begin{aligned} C_{gem} &= a_2 (D_f / d)^{e_1} \\ \text{with } e_1 &= a_1 w / u_* \\ \text{and } a_1, a_2 &= \text{calibration coefficients} \end{aligned} \quad (5.10)$$

In the same way, Equation (5.7) can be applied with $D = D_f$ being the appropriate energy dissipation per unit time and area.

To obtain u_* in the exponent e_1 in Equations (5.4) and (5.5) the following approach was used:

$$u_* = (\tau_o / \rho)^{0.5} \quad (5.11)$$

5.17

where τ_o = bottom shear stress

$$= 0,5f_w\rho u_o^2 \quad (5.12)$$

and f_w = Jonsson wave friction factor

$$= \exp \{-5,98 + 5,21(a_o/r)^{-0,19}\} \quad \text{for } a_o/r > 1,57 \quad (5.13)$$

$$0,30 \quad \text{for } a_o/r \leq 1,57$$

(Swart, 1974)

Here r = bed roughness which was determined with the Van Rijn (1989) method

a_o = orbital amplitude on the bottom

$$= \frac{H}{2\sinh(2\pi d/L)} \quad (5.14)$$

Also u_o = orbital velocity on the bed

$$= \frac{\pi H}{T_p \sinh(2\pi d/L)} \quad (5.15)$$

The fall velocity (w) was evaluated using the method by Fromme (1977).

5.5.3 Calibration of the mean concentration

The values of the coefficients a_1 and a_2 in Equation (5.5) are determined here in the calibration of the mean concentration. Firstly, the ranges of the data are given, then the curve fitting is shown and the relationship for the mean concentration is given.

The ranges of the data outside the surf zone were as follows:

0,20	\leq	H_s (m)	\leq	1,55
4,6	\leq	T_p (s)	\leq	16,6
1,10	\leq	d (m)	\leq	3,00
0,110	\leq	D_{50} (mm)	\leq	0,500
0,0111	\leq	C_{gem} ($\times 10^{-3} \text{ m}^3/\text{m}^3$)	\leq	0,3400
0,095	\leq	H_s/d	\leq	0,589

The data therefore cover a reasonably wide range.

Appendix H presents the detailed calibration. A summary of the calibration follows. By using Marquart's maximum neighbourhood method (Daniel and Wood, 1980), the optimal value of 1,16 was found for a_1 . To improve the fit, the variation of a_2 as a function of the local surf similarity parameter, the factor H_s/L , and H_s/d , was investigated ($H_s = H_{is}$ = local significant wave height). The best result was obtained by the latter factor (H_s/d). Although the scatter is still large (Figure 5.8), a line was fitted through the data giving:

$$a_2 = 0,15 \cdot 10^{-3} (H_s/d) \quad (5.16)$$

Figure 5.9 illustrates the measured versus the predicted mean concentrations in which

$$C_{gem} = 0,15 \cdot 10^{-3} (H_s/d) (D_f/d)^{1,16w/u} \quad (5.17)$$

This figure (note the linear scales) shows that despite some scatter, this equation can predict the mean concentrations reasonably well over quite a wide range of conditions. The dotted lines indicate 0,5 and 2 times the measured mean concentration. Most of the points fall within this range. However, recalling from Section 5.4 that on average the accuracy of the data is within a factor of 3,2, and comparing the variations in Figures 5.9 and 5.7, the predictions are actually quite good.

5.5.4 Calibration of the local longshore transport rate

The calibration involves the determination of relationships for coefficients a_3 and a_4 in Equations (5.6) and (5.7) to obtain the local longshore transport rate outside the surf zone. Firstly, the selection of the data employed is discussed. This is followed by a list of the ranges of the data. Finally, the relationship for a_3 is presented.

In selecting data for calibration purposes, it was surprising to find that few data are available which met the following criteria:

- Both the suspended and bedload were locally measured outside the surf zone.
- The local longshore current velocity was measured outside the surf zone near the measurement position (this is to limit inaccuracies due to current prediction).

The latter criterion ruled out the data by Mangor *et al.* (1984) and Kraus *et al.* (1989). The data by Rosati *et al.* (1991) and White (1987) are the best according to Schoonees and Theron (1993). However, Rosati *et al.* concentrated their efforts inside the surf zone with the result that only very few data points outside the surf zone were available and only at their Ludington site. Because considerable effort would be needed to extract the data of Rosati *et al.* which would yield only a few points, it was decided to use only the data by White (1987). It should be noted that White's (1987) data received a score of 50% from Schoonees and Theron (1993) which

is within their “middle” data quality category. Because of the scarcity of data outside the surf zone, it is recommended that more measurements be conducted there.

White (1987) used red and green tracer sand to simultaneously measure the longshore transport rates. The accuracy of the White (1987) data set analysed in Appendix I must be kept in mind when considering the calibration. It was found that the mean factor between the higher and lower transport rates (from the red and green tracer) was 8,3 (Appendix I).

By using Equation (5.17) the factor C_{gem} v.d. was calculated and plotted as depicted in Figure 5.10. Outliers can be seen; the main one being data point 11 Aug '80 # 1 (with the high transport rate) which was shown to be inaccurate (Appendix I). This point was therefore disregarded in the calibration. Calibration was carried out and when the predicted longshore transport rates were plotted versus the measured rates, it was found that the low rates were well predicted. However, the higher rates which cause most of the transport, were badly predicted. It was thus concluded that the data of lower accuracy (generally speaking those representing low rates) contributed significantly to the calibration. Consequently, it was decided to select only the data points of which the percentage difference between the green and red tracers is less or equal to 100%. Altogether 12 points remained. It would of course be better to impose a stricter criterion such as 50% or even 25%. However, too few points would then be retained (Table I1 in Appendix I); for example, only 6 points remain if 50% is chosen.

The data ranges of these 12 points are as follows:

0,42	≤	H_s (m)	≤	1,13
7,70	≤	T_p (s)	≤	22,70
2,30	≤	d (m)	≤	5,00
0,177	≤	D_{50} (mm)	≤	0,250
0,02	≤	s_i ($\times 10^{-9} m^2/s$)	≤	35,34
0,162	≤	H_s/d	≤	0,396

Figure 5.11 illustrates the relationship between C_{gem} v.d. and s_i where Equation (5.17) was used to compute C_{gem} . Again some scatter is apparent.

It can be argued that a_3 could be a function of either the wave steepness (H_s/L , which is an important parameter in cross-shore sediment transport), the local wave agitation as represented by H_s/d or the local surf similarity parameter (as defined in Equation (5.45) in Section 5.6.4). Clearly, the higher the local wave height is, the higher the wave agitation H_s/d will be and the higher the local transport should be. On the other hand, the local surf similarity parameter contains both the beach slope and the local wave steepness.

5.20

When tested against the data, it was found that the wave agitation parameter H_s/d gave the most accurate representation of a_3 (Figure 5.12). The reason for this is that H_s/d directly determines the wave agitation and thus the local transport rate as explained above. From Figure 5.12 it can be seen that the data lie between $H_s/d = 0,16$ and $0,40$, with a single point between about $H_s/d = 0,27$ and $0,40$. Clearly the trend of a_3 increasing with higher values of H_s/d , is correct as explained above. This trend is supported by the data point at $H_s/d = 0,40$. In addition, further calibration is carried out later (Section 5.6) against the comprehensive bulk data set which does contain data in this H_s/d range. It can therefore be concluded that the single data point at $H_s/d = 0,40$ in the local transport data does not impede the calibration.

The best-fit curve was adjusted slightly to prevent a_3 from being negative in the region around $H_s/d = 0,22$ (Figure 5.12). Attention should also be paid to the wider range of H_s/d values, that is, less than $0,16$ and from about $0,40$ to the breakerline (say $0,70$ or $0,80$). As data in these areas are lacking, it is proposed to keep a_3 constant for low H_s/d values because it is highly unlikely that a_3 will increase in this region. Extrapolating the curve to the breakerline produced reasonable results. The value of a_3 will increase by a factor of $6,8$ when extrapolating from $H/d = 0,4$ to the breakerline. This increase is reasonable because Nielsen (1979, 1984) found an approximately ten- to twentyfold increase in the sediment concentrations under non-breaking and breaking waves which had the same wave height. The following relationships are therefore adopted:

$$\begin{aligned} a_3 &= 2 \times 10^{-3} \quad \text{for } H_s/d \leq 0,16 \\ &= [678,9(H_s/d)^2 - 289,9(H_s/d) + 31,0] \times 10^{-3} \\ &\quad \text{for } 0,16 < H_s/d \leq 0,7 \text{ or } 0,8 \text{ (the breakerline)} \end{aligned} \quad (5.18)$$

The local longshore transport beyond the surf zone is then given by:

$$s_l = a_3 C_{gem} v_{gem} d \quad (5.19)$$

Figure 5.13 shows the predicted versus measured transport rates. The broken lines represent the predicted rate = $0,5$ (or 2) times the measured rate. It can be seen that the higher rates are reasonably well predicted. However, some overprediction at low rates is evident. As explained before, the accuracy of especially the data points having low transport rates, is suspect. If the accuracy of the data is taken into account, the fit is reasonably good.

In Figure 5.14 the correlation between the predicted and measured transport rates of White's original 21 data points can be seen. (The broken lines have the same meaning as in Figure 5.13.) Apart from the one outlier (that is, the data point of 11 Aug '80 # 1 which has been shown to be unrealistic), the agreement is reasonable.

Calibration against the independent large data set containing the bulk longshore transport rates (Chapter 4) is carried out in the next section (Section 5.6) in conjunction with the longshore transport inside the surf zone.

5.6 Local Longshore Transport Rate Inside the Surf Zone

5.6.1 General

In Section 5.6 an expression is derived and comprehensively calibrated for the local longshore transport rate inside the surf zone. The section starts with the derivation of different equations to compute the energy dissipation caused by wave breaking. After taking into account the results of an initial calibration, the distribution of the coefficient a_4 (in Equation (5.7) for inside the surf zone) is treated in detail. Different possible distributions are postulated and subsequently tested against data. Allowance for the effect of beach profile variations caused by cross-shore transport is discussed next. Full calibration and optimization is carried out for the different distributions of the coefficient a_4 . Thereafter the final results are presented, showing the accuracy of the predictions.

5.6.2 Derivation of the Wave Power Equations

Background

Four different methods were used to compute the energy dissipation per unit area due to wave breaking (D_b). Three of these were used as given by the original authors, namely, Dean (1977), Battjes and Janssen (1978) - abbreviated to BJ, usually as a subscript - and Morfett (1990). The fourth method was derived here based on the equation given by Dally for the variation in wave height across the surf zone (Dally *et al.*, 1984) as will be shown below. The four methods are discussed below.

The Dean method

Dean (1977) explained the concave shape of beach profiles by considering the energy dissipation per unit time and volume in the surf zone under equilibrium wave conditions. Later on, Kriebel and Dean (1984) and Kriebel (1990) developed a cross-shore sediment transport model in which Dean's derivation was also applied (see also Schoonees and Theron, 1995). Kriebel calibrated his model successfully and obtained quite accurate predictions of beach profile behaviour. Dean's derivation is as follows:

$$D_b/d = \frac{1}{d} \frac{\partial F}{\partial x} \quad (5.20)$$

where x = horizontal distance measured from the still water line seawards

$$F = \text{energy flux} = E n_w C_c \quad (5.21)$$

$$\text{with } E = 0,125 \rho g H^2 \quad (5.22)$$

$$n_w = 0,5 \{1 + (4\pi d/L)/(\sinh 4\pi d/L)\}$$

$$H = \text{wave height}$$

5.22

L = local wavelength
and C_c = wave celerity

Assuming shallow water and linear wave theory, then

$$n_w = 1 \quad (5.23)$$

$$\text{and } C_c = (gd)^{0.5} \quad (5.24)$$

Equations (5.22), (5.23) and (5.24) in (5.21) yield:

$$F = 0,125 \rho g^{1.5} d^{0.5} H^2 \quad (5.25)$$

Assuming spilling breaking:

$$H = \gamma d \quad (5.26)$$

with γ = breaker index
= 0,78 (Dean, 1977).

Substituting Equation (5.26) in Equation (5.55) and then differentiating Equation (5.20), the result is:

$$D_b / d = \frac{5}{16} \rho g^{1.5} \gamma^2 d^{0.5} \frac{dd}{dx} \quad (5.27)$$

If a uniform beach slope is assumed such that $dd/dx = \tan \alpha$ then

$$D_b / d = \frac{5}{16} \rho g^{1.5} \gamma^2 d^{0.5} \tan \alpha \quad (5.28)$$

This equation was then used in conjunction with Equations (5.5) and (5.7).

The Battjes and Janssen model

Battjes and Janssen (1978) used the analogy of energy loss in a hydraulic jump to determine the energy dissipation of a broken wave. Later Battjes and Stive (1985) extensively calibrated the Battjes and Janssen model which predicts the wave height distribution through the surf zone. Battjes and Stive obtained accurate results.

Battjes and Janssen derived the following expression:

$$D_b = 0,25 \alpha_{BJ} Q \rho g H_m^2 / T_p \quad (5.29)$$

where α_{BJ} = calibration constant
= 1 (Battjes and Stive, 1985)

5.23

Q = ratio of broken waves to the total number of waves at the particular position
 and H_m = maximum wave height possible in the specific water depth considered

$$= 0,88 \frac{L}{2\pi} \tanh\left(\frac{2\pi h}{L} \cdot \frac{\gamma}{0,88}\right) \quad (5.30)$$

with h = local water depth including wave set-up or set-down

Battjes and Stive (1985) gave an expression for γ based on the deep-water wave steepness; however, in the data available in this study (e.g. Van Rijn, 1991), the deep-water wave height which is used to compute the wave steepness is unknown. Therefore an average breaker index γ of 0,7 was used (Battjes, 1974).

To obtain Q , Battjes and Janssen (1978) assumed a Rayleigh distribution for the wave heights and acquired the following expression:

$$\frac{1-Q}{-\ln Q} = \left(\frac{H_{rms}}{H_m} \right)^2 \quad (5.31)$$

where H_{rms} = root-mean-square wave height

This leads to

$$1 - Q + (H_{rms}/H_m)^2 \ln Q = 0 \quad (5.32)$$

which has to be solved iteratively taking into account that $H_{rms} = H_s / \sqrt{2}$ (US Army, Corps of Engineers, 1984).

Equation (5.29) is then applied (with $D = D_b$) in conjunction with Equations (5.5) and (5.7).

Derivation based on the approach by Dally et al. (1985)

Like Battjes and Janssen (1978), Dally et al. (1985) also used the analogy of energy loss in a hydraulic jump to determine the energy dissipation of a broken wave, although in a different form. Dally et al. derived the following equations (Equations (5.33) to (5.38)) for wave height variation across a surf zone which has a uniform beach slope:

For $K/\tan\alpha \neq 2,5$:

$$\begin{aligned}
 H &= \text{local wave height} \\
 &= H_b \left[(d/d_b)^{K/\tan\alpha - 0,5} \cdot (1 + \alpha_D) - \alpha_D (d/d_b)^2 \right]^{0,5} \quad (5.33)
 \end{aligned}$$

$$\text{with } \alpha_D = \frac{K\Gamma^2}{\tan\alpha(2,5 - K/\tan\alpha)} \left(\frac{d_b}{H_b} \right)^2 \quad (5.34)$$

$$K = \text{calibration coefficient} \quad (5.35)$$

$$= 0,15 \text{ (Dally et al., 1985)}$$

$$\text{and } \Gamma = \text{calibration coefficient} \quad (5.36)$$

$$= 0,40 \text{ (Dally et al., 1985)}$$

$$d_b = \text{depth at the breakerline}$$

$$H_b = \text{breaker height}$$

$$H = H_b(d/d_b)[1 - \beta_D \ln(d/d_b)]^{0,5} \quad (5.37)$$

For $K/\tan\alpha = 2,5$:

$$\text{where } \beta_D = 2,5\Gamma^2(d_b/H_b)^2 \quad (5.38)$$

The above equations by Dally *et al.* (1985), however, present the wave height through the surf zone. In the derivation which follows, it is shown how D_b can be obtained by using these Dally *et al.* (1985) equations. Firstly, either Equation (5.33) or (5.37) is substituted (whichever is applicable) in Equation (5.25) to acquire F . This equation is then differentiated to obtain $\partial F / \partial x_D$ which is substituted in Equation (5.20) to obtain D_b .

Differentiating Equation (5.25) yields

$$\frac{\partial F}{\partial x_D} = 0,125\rho g^{1,5} \left[2d^{0,5} H \frac{\partial H}{\partial x_D} + 0,5d^{-0,5} H^2 \frac{\partial d}{\partial x_D} \right] \quad (5.39)$$

Expressions for $\partial H / \partial x_D$ and $\partial d / \partial x_D$ are required to be able to compute $\partial F / \partial x_D$ from Equation (5.39). Furthermore, the relationship between $\partial F / \partial x$ and $\partial F / \partial x_D$ needs to be established.

Assuming a uniform beach slope and remembering that x_D is measured landwards from the breakerline in the Dally *et al.* (1985) notation:

$$d = d_b - x_D \tan\alpha$$

$$\therefore \frac{\partial d}{\partial x_D} = -\tan\alpha$$

5.25

To obtain $\frac{\partial H}{\partial x_D}$, Equations (5.33) and (5.37) are differentiated:

For $K/\tan\alpha \neq 2,5$:

$$\frac{\partial H}{\partial x_D} = 0,5H_b \left[(d/d_b)^{K/\tan\alpha - 0,5} \cdot (1 + \alpha_D) - \alpha_D (d/d_b)^2 \right]^{0,5} \cdot \left\{ (1 + \alpha_D)(d/d_b)^{K/\tan\alpha - 1,5} \cdot (K/\tan\alpha - 0,5) \cdot (1/d_b) \frac{\partial d}{\partial x} - 2\alpha_D (d/d_b)(1/d_b) \frac{\partial d}{\partial x} \right\} \quad (5.40)$$

For $K/\tan\alpha = 2,5$:

$$\begin{aligned} \frac{\partial H}{\partial x_D} &= (H_b/d_b) [1 - \beta_D \ln(d/d_b)]^{0,5} \cdot \frac{\partial d}{\partial x} \\ &- (H_b \beta_D / 2d_b) [1 - \beta_D \ln(d/d_b)]^{-0,5} \cdot \frac{\partial d}{\partial x} \end{aligned} \quad (5.41)$$

But to be consistent with the definition of x which is measured from the still-water line seawards, it is noted that

$$\begin{aligned} x_D &= x_b - x \\ \therefore \partial x_D &= -\partial x \\ \therefore \frac{\partial F}{\partial x} &= -\frac{\partial F}{\partial x_D} \end{aligned}$$

which must be used in conjunction with Equation (5.39).

The energy dissipation per unit time and area is then found from Equations (5.39) and (5.20) and used together with Equations (5.5) and (5.7). Note that the breaker height (H_b) is required in this formulation. However, in the concentration data bank (Van Rijn, 1991) only the local wave height is given. To circumvent this problem, H_b was computed from either Equation (5.33) or (5.37), whichever is applicable.

The Morfett method

In deriving his own longshore transport model, Morfett (1990) adapted the expression given by O'Connor and Yoo (1987) for the energy dissipation by wave breaking. The result was:

$$D_b = 0,125 \rho g (Cd_b) H_r^3 \quad (5.42)$$

where

$$(Cd_B) = K_D \frac{(\tan \alpha)^{0.33}}{g} \left(\frac{2\pi}{T_z} \right)^3 \left(\frac{\pi H_s}{L} \right)^2 \cdot \frac{1}{\{\tan h(2\pi d / L)\}^5} \quad (5.43)$$

with $K_D = 1,3$

and $T_z =$ zero-crossing wave period.

Equation (5.42) is then used together with Equations (5.5) and (5.7).

5.6.3 Results of the initial calibration

An initial calibration was carried out to determine the value of the coefficient a_1 (in Equation 5.5), to determine which method gives the best results when the energy dissipation per unit time and volume is calculated and also whether the use of coefficient a_4 is preferable to using coefficient a_3 (in Equations (5.6) and (5.7)). Details of the initial calibration are described in Appendix H. The results of the initial calibration are presented below.

Of the four methods tested against concentration data, the Battjes and Janssen approach was found to be best for predicting the energy dissipation due to wave breaking. Marquart's maximum neighbourhood method (Daniel and Wood, 1980) was then used to optimize the values of a_1 while using the Battjes and Janssen approach and the Van Rijn (1991) database for sediment concentrations. Thus the value of coefficient a_1 was found to be 1,94.

According to Schoonees and Theron (1993) (Chapter 2), the best measurements of the local longshore transport rate (s_i) were made by Kraus *et al.* (1982). These data which scored 63%, fell in the "higher" data quality category of Schoonees and Theron (1993). Features which enhanced the data of Kraus *et al.* (1982) were that measurements were carried out at four widely varying beaches (for example, Hirono beach), and that the local longshore current velocity was measured. Although this data set contains only 15 data points, it was chosen for the initial calibration because of its better quality. The local significant wave height was calculated from the measured breaker height with the Dally *et al.* (1985) method.

It was found that using coefficient a_4 produced better results than coefficient a_3 . The advantage of a_3 is that it contains the intermediate calibration of a_1 and a_2 in C_{gem} (Equations (5.5) and (5.6)). This is unfortunately also its drawback since it inherits the scatter/noise in the concentration data. This result of a_4 giving better results than a_3 was confirmed during the initial calibration against the large bulk longshore sediment transport data set. It was also concluded that it is better to use the Swart and Fleming (1980) method than the Komar (1975) method for calculating the longshore current velocities ($= v_x$) when the present method is tested against the bulk longshore transport data.

Since it is known that breaker type (that is, spilling, plunging, collapsing and surging) heavily influences the concentration of suspended sediment (Kana, 1976, 1977, 1978, 1979), it is logical to assume that a_4 is a function of the breaker type. The relationship between a_4 and the breaker type is determined in the next section.

5.6.4 Distribution of the coefficient a_4

General

Before the distribution of coefficient a_4 in terms of the breaker type can be determined and verified (as proposed by Kamphuis, personal communication, 1998), it is necessary to describe the different types of wave breaking and the energy dissipation associated with each type. In addition, the local longshore transport data by Kraus *et al.* (1982) will also be analysed. These three aspects, namely, types of wave breaking, analysis of the local longshore transport data, and the distribution of a_4 in terms of the wave breaking, are dealt with in the rest of this section.

Types of wave breaking

Galvin (1968) and Battjes (1974) are among the researchers who have studied wave breaking. The main wave breaker types are: spilling, plunging, collapsing and surging breakers (Figure 5.15a and b).

Battjes (1974) describes spilling and plunging breakers as follows:

In plunging breakers the crest becomes strongly asymmetric; it curls over, enclosing an air pocket, after which it impinges on the trough water ahead. It imparts some forward momentum to this trough water, entraining air and generating turbulence in the process. The water motion in the impact area is not at all wave-like in appearance. However, some distance shoreward from this area a travelling bore is formed, carrying the relatively small wave momentum and energy which is left after the plunge. With increasing wave steepness and for decreasing slope angle the crest of a plunging breaker becomes less asymmetric, and the forward-projected jet of water from the crest becomes less and less pronounced. Its point of impact moves closer to the point of detachment, that is, it moves from the trough to the sloping face of the breaker; the violence of the impact thereby decreases. The enclosed air pocket diminishes in size, and for sufficiently steep waves and gentle slopes the air pocket and the jet of water emanating from the crest are no longer identifiable. One then speaks of spilling breakers. The wave form as a whole in these breakers is fairly stable, since the zone of instability is confined to the crest region. The wave-energy dissipation takes place much more gradually than in plunging breakers.

In collapsing breakers, the breaking occurs over the lower half of the wave. Although bubbles and foam are present, there is usually no splash-up (Galvin, 1968 and U S Army, Corps of Engineers, 1984). In contrast, a wave which slides up and down the slope with minor air entrainment at the base only (little or no bubble production), is a surging breaker (Galvin, 1968 and U S Army, Corps of Engineers, 1984).

The importance of large-scale vortices (containing large numbers of air bubbles) in wave breaking in suspending sediment has been studied by various investigators, namely, Nadaoka and Kondoh (1982), Nielsen (1984) and

5.28

Nadaoka *et al.* (1988). Air rising through the water column creates an upward flow of water, thereby assisting the entrainment of sediment from the bottom. Nielsen (1984) presented a photograph showing a sediment-laden water jet rising above the general water level because of plunging breaking. Other evidence was also presented by these investigators to substantiate their conclusion of the important role played by air bubbles associated with wave breaking on suspending sediment.

The main breaker types of spilling, plunging, collapsing and surging occur in this order as the beach slope ($\tan \alpha$) increases and/or the wave steepness decreases. Although there is a gradual transition from one breaker type to another, Battjes (1974) has shown that the surf similarity parameter or Iribarren number at breaking (ξ_b) can be used to classify the breaker type. The equation is:

$$\xi_b = \frac{\tan \alpha}{(H_{bs}/L_o)^{0,5}} \quad (5.44)$$

L_o = deep-water wavelength

Battjes (1974) gives the following classification:

Spilling breakers:	$\xi_b < 0,4$
Plunging breakers:	$0,4 < \xi_b < 2,0$
Collapsing and surging breakers:	$\xi_b > 2,0$

A maximum value of 8,5 for the surf similarity parameter at breaking was found in the data used by Battjes (1974).

It was considered that it would be more advantageous to link coefficient a_4 to the *local* wave breaking rather than to assume that the surf similarity parameter at the *breakerline* characterises the breaking throughout the surf zone. The local surf similarity parameter, is defined as follows:

$$\xi_i = \frac{\tan \alpha}{(H_i/L_o)^{0,5}} \quad (5.45)$$

where $H_s = H_{is}$ = local significant wave height

By assuming that $H_{is} = \gamma \cdot H_{bs}$ (γ = breaker index) which is a reasonable assumption, it is possible to relate the local surf similarity parameter to the surf similarity parameter at breaking. From Equations (5.44) and (5.45) it is found that

$$\xi_i = \xi_b / \gamma^{0,5} \quad (5.46)$$

5.29

By using Equation (5.46) and assuming typical values of the breaker index between 0,7 and 1,0 (Battjes, 1974), the corresponding classification of the wave breaker type in terms of the local surf similarity parameter is as follows:

Spilling breakers:	$\xi_i < 0,5$
Plunging breakers:	$0,5 < \xi_i < 2,3$
Collapsing and surging breakers:	$\xi_i > 2,3$

A probable maximum value of the local surf similarity parameter is about 10.

Values of a_4 as portrayed by the local transport data

Figure 5.16 shows the distribution of the data points when plotting a_4 against the Kraus *et al.* (1982) local longshore transport data. These points illustrate the form of the curve: a gradual increase in a_4 as the local surf similarity parameter increases to about 0,5 followed by a drastic increase to $\xi_i = 1,0$. Thereafter, the reverse is true : a sudden decrease of up to $\xi_i = 1,4$ followed by a slow decrease.

The two data points around $\xi_i = 1,5$ represent the points from Hirono Beach where surging breakers occurred according to Kraus *et al.* (1982) . The two values of a_4 should indeed be very low considering the very low degree of turbulence associated with surging breaking. However, the local surf similarity parameter should have values for these two data points that exceed about 2,3 to be in the range of collapsing and surging breaking. These two data points should therefore, according to breaker type theory, lie further towards the right of the figure.

Two other points, potentially outliers, immediately catch the eye in Figure 5.16. The first value, at $\xi_i = 0,37$, is conclusively shown in Appendix J to be an outlier (and therefore incorrect). It is also clear from Figure 5.16 that the highest point (at about $\xi_i = 0,94$) represents the complete range of values from about $\xi_i = 0,65$ to 1,4. The curve fitted through this data point (the one with highest peak in Figure 5.16) is therefore completely defined by one single point in this range. Clearly, if this point is incorrect, the predictions in this range will also be incorrect. For this reason three other curves were also fitted as shown in Figure 5.16. All these curves were determined based on the measured values. However, when these curves were used and the accuracy of the method evaluated against the large bulk data set (Data Set 1), poor results were obtained. The standard error of estimate (σ) exceeded 1,3 for all these curves. Furthermore, it was found that for ξ_i between 0,4 and 1,2, the transport rates were overpredicted while underpredictions occurred in the range of ξ_i between 1,5 and 1,9. These over- and underpredictions substantiate the view that the peak of the a_4 curve is expected to be between $\xi_i = 1,5$ and 2,3 for strongly plunging breakers, and not at 0,94 as indicated by the single data point.

It was also found that, in order to predict bulk longshore transport rates accurately for a wide variety of conditions, the applied wave power approach needed to be evaluated against the large bulk data set and not only against the limited local longshore transport rates. (*The local longshore transport data and the curves shown in Figure 5.16 are therefore not used further in the calibration.*) These poor results (of $\sigma > 1,3$ for the curves

in Figure 5.16) clearly point to the fact that a more fundamental approach is required in determining the distribution of a_4 . This approach is outlined below.

Distributions of coefficient a_4

Plausible arguments based on physical processes are presented to determine possible distributions of coefficient a_4 in terms of the local surf similarity parameter. As breaking changes from spilling to plunging, the turbulence associated with the breaking also increases. If the breaking changes from plunging to collapsing and surging, the turbulence will decrease rapidly to lower levels than would be the case for spilling breaking. Associated with the turbulence is the air entrainment during breaking. Bubble entrainment is initially at a medium level during spilling breaking and changes to high and very high during plunging breaking as has been found by Nadaoka and Kondoh (1982), Nielsen (1984) and Nadaoka *et al.* (1988). However, low to very low air entrainment is found in collapsing and surging breakers (Galvin, 1968 and U S Army, Corps of Engineers, 1984).

Comprehensive measurements by Kana (1978) and Fairchild (1977) indicate a drastic increase in the suspended sediment concentrations under plunging breaking compared with spilling breaking. In fact, Kana (1978) found that the sediment concentration increased between 3,5 to 6,8 times when the wave breaking changed from spilling to plunging breaking. Based on these results he concludes that plunging breaking suspends an order of magnitude more sand than spilling breaking. Analysis of the data given by Fairchild (1977) shows about a fivefold increase in the sediment concentration with the change from spilling to plunging breaking. Using these values as a rough guide, it is therefore reasonable to assume that the value of a_4 must increase by about the same ratio as the suspended sediment concentration when the breaking changes from spilling to plunging.

Synthesizing the information presented in the above studies on types of wave breaking, air entrainment and measurements of suspended sediment concentrations, the following can be concluded about the distribution of a_4 :

Coefficient a_4 will rapidly increase as the type of breaking changes from spilling to plunging. This increase can be by a factor of about 4 or 5, but up to about 10. This increase of a_4 is also substantiated by the local longshore transport data of Kraus *et al.* (1982). The coefficient a_4 will very rapidly decrease when wave breaking changes from plunging to collapsing and surging. The value of a_4 will be less for collapsing and surging breaking compared with spilling breaking.

Based on these conclusions, a possible distribution of a_4 (called the Type A curve) is a symmetric curve with smooth yet rapid changes in the value of coefficient a_4 in the transitional areas between the different breaker types (that is, where $\xi_i = 0,5$ and 2,3). Another curve of a_4 (Type B) can be deduced which is similar to the previous one (the Type A curve), except that it has a flat top between $\xi_i = 0,5$ and 2,3, indicating a saturation point for the entrainment of air during plunging breaking. In addition, the flat top indicates that only a limited volume of water can be enclosed during plunging breaking. The third possible curve (Type C) is asymmetric:

5.31

because of a rapid increase in the turbulence from spilling to plunging breaking, there is a rapid increase in the value of coefficient a_4 between $\xi_i = 0,5$ and $2,3$. However, the value of a_4 decreases extremely rapidly when the wave breaking changes from plunging to collapsing and surging breaking (at about $\xi_i = 2,3$). For spilling breaking, the values of a_4 are very similar for the Type C curve compared with the Type A curve.

These three distributions are depicted in Figure 5.17. In order to distinguish the three distributions visually, they have been given descriptive names, namely:

- Type A: Hillock
 B: Table Mountain
 C: Mountain peak

With only the limited number of values for a_4 (as portrayed by the limited local longshore transport data), it was found to be difficult to obtain the correct numerical values for the three types of curves presented above. In order to facilitate the calibration of these three curves to the bulk data set (Data Set 1), two additional (empirical) distributions of a_4 were determined. These are a constant a_4 and a stepwise function (Figure 5.18).

The stepwise function was determined from the data in order that the three types of curves (A, B and C) could be fitted through the stepwise function to ensure that the curves would approximately predict the correct numerical values. Clearly, if a_4 is constant, it means that the coefficient a_4 is not dependent on the type of breaking. If it is therefore found in the calibration that the most accurate predictions are obtained with a constant value of a_4 , it means that this theory is incorrect. On the other hand, if it is found from the calibration that either a Type A, B or C curve fits the data well, it will substantiate the physical arguments for the distribution of a_4 presented above. Another use of the constant a_4 function is to prove that, when allowing for the effect of beach profile variations caused by cross-shore transport, the predictions will be more accurate as will be explained below.

The calibration of the a_4 distributions is described in Section 5.6.6.

5.6.5 Effect of beach profile variations caused by cross-shore transport

In Section 5.3 it has been shown that the local longshore transport rate will vary over time because of beach profile changes. If the existing beach profile is far from the equilibrium profile, the incoming waves will initially cause a high energy dissipation per unit volume and time at certain locations along the profile. This in turn will cause high suspended sediment concentrations locally with the result that the beach profile will initially adapt relatively quickly. Essentially, the energy dissipation per unit volume and time will be limited because of these beach profile variations.

The fact that the energy dissipation per unit volume and time is limited, will be simulated in order to account

for the beach profile changes caused by cross-shore sediment transport. Clearly, the accuracy of the predictions must confirm the success, or otherwise, of allowing for beach profile variation by limiting the energy dissipation per unit volume and time.

Based on physical processes, it has now been proven that the energy dissipation per unit volume and time should be limited. The question now is the extent (or the numerical values) of this limitation. The suspended sediment concentration data provided some guidelines; however, to ensure that the results will be widely applicable, a wide range of numerical values were tested by using various relationships (curves).

The method that was employed to allow for the effect of beach profile variations is as follows:

- A number of different curves were tested for limiting the energy dissipation per unit volume and time.
- For each of these curves, a constant a_4 distribution was used. The optimal (constant) value of a_4 for each of the curves was then determined by using the bulk data set (Data Set 1).
- The process was repeated without allowing for the beach profile changes by not limiting the energy dissipation per unit volume and time and also by using a constant a_4 distribution. The optimal value of a_4 for this case was also obtained.

The effect of allowing for the beach profile changes does not include the influence of the distribution of coefficient a_4 because constant a_4 values were used in each case. In this way, the effect of the beach profile changes could be singled out and a consistent comparison could be carried out.

Figure 5.19 shows the different curves that were used to limit the parameter P_0 representing the energy dissipation per unit volume and time raised to the power e_1 .

$$P_0 = (D_{b,BJ} / d)^{e_1} \quad (5.47)$$

This parameter P_0 is directly proportional to the local longshore transport rate (Equation 5.7). These curves were chosen to cover a feasible, yet wide range of values.

The optimization process which was followed to determine the best constant a_4 value for each curve was: a value was chosen for a_4 which was used to predict the longshore transport rates for Data Set 1. Based on the predicted rates, the standard error of estimate (σ) was computed. Different constant values of a_4 were also chosen and the corresponding standard errors of estimate were calculated. The different values of the standard error were then plotted, which enabled the optimal constant value a_4 to be found. Curve (i) (Figure 5.19) produced the best results, namely the lowest standard error, which is 0,713 for Curve (i) (Figure 5.20).

5.33

Mathematically, the limitation of the parameter P_0 (and thereby allowing for beach profile changes) was treated as follows (Figure 5.19):

$$P_1 = (C_{gem,1} / C_{gem,0}) \cdot P_0 \quad (5.48)$$

where P_0 = original $(D_{b,B}/d)^{e_1}$ (that is, without taking into account the beach profile variations)

$P_1 = (D_{b,B}/d)^{e_1}$ including the effect of beach profile variations

$C_{gem,0}$ = original C_{gem} (straight line in Figure 5.19)

$C_{gem,1} = C_{gem}$ as limited by Curve (i), thereby accounting for the effect of beach profile variations

Alternatively

$$P_1 = f_1 \cdot P_0 \quad (5.49)$$

where f_1 = factor to allow for the effect of beach profile variations

$$= (0,20 \ln P_0 + 0,28) / (0,06 \cdot P_0) \quad \text{if } P_0 > 13,29$$

$$= 1 \quad \text{if } P_0 \leq 13,29 \quad (5.50)$$

The factor f_1 is plotted in Figure 5.21.

If no allowance is made for the beach profile changes and a constant a_4 is used, the optimal standard error of estimate (σ) found is 1,079. Comparing this standard error (1,079) with the corresponding standard error of estimate after allowing for beach profile changes (0,713), it is clear that considerably better (about 34% better) predictions are obtained. This drastic improvement in the accuracy of the predictions confirms the importance of allowing for the effects of beach profile variations.

5.6.6 Calibration

General

This section which deals with the calibration of the applied wave power approach, consists of a description of the method used in the calibration, determining the stepwise distribution of a_4 , fitting the three distributions (Types A, B and C, that is, the Hillock, Table Mountain and Mountain peak curves) and the optimization of the distribution (Type A, B or C) that produced the best predictions.

Method used in the calibration of the stepwise distribution of a_4

The calibration method can be described as follows:

- The range of values of the local surf similarity parameter (0 to 10) were divided up into different zones (Zones (i), (ii)...). In each of these zones the optimal value of the coefficient a_4 (being constant over the zone) was determined.

- Iteration 1
 - Step 1: Typical initial values of a_4 were assumed for each of the zones mentioned above. While keeping the values of all but the first zone constant, it was possible to vary the value of a_4 in Zone (i). Each time the value of a_4 was changed, the bulk longshore transport rates were predicted for all the data points in Data Set 1 and the standard error of estimate could be calculated. The value of a_4 which produced the lowest standard error of estimate, was taken to be the best constant a_4 value for Zone (i).

 - Step 2: Iteration 1, Step 2: The best constant value of a_4 for Zone (i) (found in Step 1 above) was used together with the initially chosen values for Zones (iii), (iv)... to optimize the value of a_4 in Zone (ii). As for Zone (i), the best constant a_4 for Zone (ii) is the a_4 which produces the lowest standard error of estimate.

 - Step 3 and further: The best constant value of a_4 for Zone (iii) was determined in a similar manner as for Zones (i) and (ii). The process was repeated for the other zones.

- Iteration 2
 - Step 1: All the best values obtained during Iteration 1 for Zones (ii), (iii)... were assumed as input values while the new best value for Zone (i) was again determined.

 - Step 2 and further: The best values of a_4 for Zones (ii), (iii)... were obtained in a similar manner as was done during Iteration 1.

- Iteration 3: The process was repeated until the new best values of a_4 for each of the zones did not differ significantly from the old best values of a_4 .

The method used later to optimize the best of the three distributions (either Type A, B or C), was very similar to the above method as will be described further below.

Stepwise a_4 distribution

Two different aspects were mainly considered when the range of values of the local surf similarity parameter was divided into different zones. These two aspects are: (1) the different zones should roughly correspond to the different breaker types; and (2) the distribution of the values of the local surf similarity parameter in the whole of Data Set 1.

Figure 5.22 shows the distribution of the local surf similarity parameter for all the data points at all different cross-shore positions in Data Set 1 (12 230 points). It can be seen from this graph that the majority of the values fall between 0 and 1, although there are still a significant number of values between 1 and 2. This is to be expected because these values correspond to spilling and plunging breaking (Section 5.6.4) which are by far the most commonly occurring breaker types found on natural beaches.

The division of the range of the local surf similarity parameter is:

- Zone (i): $0 \leq \xi_i \leq 0,5$
 (ii): $0,5 < \xi_i \leq 1,5$
 (iii): $1,5 < \xi_i \leq 2,3$
 (iv): $\xi_i > 2,3$

Figure 5.23 illustrates the optimization process in finding the best value for a_4 in Zone (i). This figure shows that there is a drastic improvement in the accuracy achieved between the predictions using the a_4 values of Iteration 1 compared with Iteration 2. However, the accuracy of the predictions is the same when using the a_4 values of Iteration 2 and the values of Iteration 3. Two iterations were therefore sufficient to obtain optimized results.

The optimized stepwise distribution of a_4 (Figure 5.18) is as follows:

Zone	ξ_i	a_4 ($\times 10^{-6}$)
(i)	0 to 0,5	22
(ii)	0,5 to 1,5	310
(iii)	1,5 to 2,3	2100
(iv)	2,3 to 10	20

The standard error of estimate (σ) for the optimized stepwise distribution of a_4 is 0,453 (Figure 5.23). Recalling from Chapter 4 that the previous best detailed longshore transport predictor has a σ of 0,611, it is clear that a significant improvement (about 26%) has been obtained. In addition, the standard error of estimate for the optimized stepwise distribution ($=0,453$) is considerably better than the corresponding value for a constant a_4 ($=0,713$); this therefore confirms the theory that a_4 is in fact dependent on the breaker type.

Having successfully calibrated the stepwise distribution of a_4 , it was conceived to divide up the range of the local surf similarity parameter into a large number of different zones. If enough zones are investigated and the value of a_4 can be optimized for each of these zones, then it may be possible to determine the optimized distribution of a_4 directly from all the data points of the comprehensive Data Set 1. This concept of having many different zones was applied. It was found that the method worked only if a maximum of three to five different zones was chosen. If more zones are chosen, then the curves of the standard error of estimate versus the chosen value of a_4 (curves like those in Figure 5.23) become very flat without distinct inflexion points. The reasons for the flat curves include the numerical characteristics of the method and the distribution of the values of the local surf similarity parameter as illustrated in Figure 5.22.

Types A, B and C distributions of a_4

An advantage of having the optimized stepwise a_4 distribution is that near optimal values of the three theoretical distributions of a_4 , namely, Types A, B and C (the Hillock, Table Mountain and Mountain peak distributions) could easily be obtained. Figure 5.24 shows not only the stepwise a_4 distribution but also the three theoretical distributions that were fitted around the stepwise distribution. The fitting process was conducted so that the step values of the stepwise distribution would be approximately average values (in each zone) for each of the three theoretical curves (Figure 5.24). From this figure it can be seen that the largest difference in the value of a_4 given by the three theoretical distributions, occurs in the region where the local surf similarity parameter is between 1,5 and 3. In contrast, it has been shown that for the available data, most of the local values of the local surf similarity parameter lie between the 0 and 1 (Figure 5.22).

The question can be asked why the value of a_4 in the stepwise distribution changes rapidly from 2 100 to 20 ($\times 10^{-6}$) at a value of 2,3 of the local surf similarity parameter (Figure 5.24). The answer lies in the sudden change in the turbulence intensity produced by plunging breaking compared with virtually no turbulence found during collapsing and surging breaking. In addition, air entrainment plays an important role by causing extreme vertical flows (air lift) during plunging breaking while almost no air is entrained during collapsing and surging breaking (Section 5.6.4). Furthermore, measurements of the suspended sediment concentrations show a drastic increase in the concentration for plunging breaking compared with spilling breaking (which produces considerably more turbulence than collapsing breaking).

Considering then the sudden change in the value of a_4 from plunging to collapsing breaking, it is clear that the applied wave power approach is sensitive to small uncertainties in the value of the local surf similarity parameter around 2,3 (Figure 5.24). Fortunately this concern is not too serious because collapsing breaking is not commonly found on natural sandy beaches. This fact is supported by the extensive data (12 230 points) in Data Set 1 which show that few data points lie in the interval $\xi_i > 2,3$ (Figure 5.22).

5.37

The standard error of estimate is as follows for the different types of curves shown in Figure 5.24:

Type	σ
A: Hillock	0,760
B: Table Mountain	0,756
C: Mountain peak	0,508

By comparing the values of the standard error of estimate in the table above, it is clear that the Type C curve (Mountain peak) is by far the most accurate of the three types of curves. However, the accuracy of the Types A and B curves (Hillock and Table Mountain) is comparable. However, because Type C (Mountain peak) curve predicts so much more accurately than Types A and B curves, it was decided to optimize only the Type C (Mountain peak) curve. The accuracy of the Type C curve ($\sigma = 0,508$) is somewhat worse than the optimized stepwise distribution of a_4 ($\sigma = 0,453$); however, it should be possible to achieve comparable accuracy with the Mountain peak curve once it has been optimized.

Optimization of the Type C (Mountain peak) curve

The method used for the optimization of the Mountain peak curve was similar to the method used to determine the stepwise distribution of a_4 . However, instead of choosing constant a_4 values in different zones, the vertical positions of Points Z, Y and X (Figure 5.25a) were varied in turn, equations fitted through these points and the positions optimized. In a similar way, the positions of Points U, V and W were also optimized. Points U, V and W are located at different values of the local surf similarity parameter to Points Z, Y and X (Figures 5.25a and b).

Figure 5.26 illustrates the optimization of Point U during the optimization of the Mountain peak curve with Points U, V and W. In Figure 5.18 the optimized Mountain peak curve using Points U, V and W is shown.

The following values for the standard error of estimate were found for the two versions of the Mountain peak curve:

Optimization using Points	Standard error of estimate (σ)
Z, Y and X	0,467
U, V and W	0,457

From the values of the standard error of estimate for the two versions of the Mountain peak curve given in the table above, it is clear that the version of the curve using Points U, V and W is more accurate than the version using Points Z, Y and X. In addition, the accuracy of the Mountain peak curve using Points U, V and W is almost the same as the value for the stepwise distribution of a_4 ($\sigma = 0,453$). In fact, the difference in accuracy

is less than 1%. Since the Mountain peak curve using Points U, V and W has virtually the same accuracy as the stepwise distribution of a_4 , and because the Mountain peak curve is based on sound physical arguments, it is recommended that this distribution of a_4 be used.

The equations of the Mountain peak distribution using Points U, V and W are as follows:

$$\begin{aligned}
 a_{4,BJ} &= 110 \times 10^{-6} \xi_i && \text{if } 0 \leq \xi_i \leq 0,4 \\
 &= (660 \xi_i - 220) \times 10^{-6} && \text{if } 0,4 < \xi_i \leq 1,0 \\
 &= (1151,11 \xi_i - 1071,11) \times 10^{-6} && \text{if } 1,0 < \xi_i \leq 2,3 \\
 &= (-15896,3 \xi_i + 38965,8) \times 10^{-6} && \text{if } 2,3 < \xi_i \leq 2,45 \\
 &= 20 \times 10^{-6} && \text{if } \xi_i > 2,45
 \end{aligned} \tag{5.51}$$

The local longshore transport rate is then

$$s_i = a_{4,BJ} \cdot P_1 \cdot v_{gem} \cdot d \tag{5.52}$$

where $v_{gem} = v_x$ (applying the Swart and Fleming (1980) method)

5.6.7 Final results

Accuracy of the applied wave power approach against all the data of Data Set 1

The predicted longshore transport rates versus the measured longshore transport rates for the applied wave power approach (optimized Mountain peak curve using U, V and W) are shown in Figure 5.27. It can be seen on this figure that, although there is still scatter, the transport rates are well predicted over the full range of the conditions covered in Data Set 1. When comparing the scatter present in Figure 5.27 with similar figures for the best bulk predictors in existence (Figures 4.2a, 4.3a and 4.4a), it is clear that the scatter is of the same order. With the standard error of estimate being 0,457 for the applied wave power approach, it can be seen from Table 4.1 that the applied wave power approach is the fourth best longshore transport predictor of the 52 formulae tested in total (Chapter 4).

Comparing the applied wave power approach with the other detailed longshore transport predictors, it can be seen that the applied wave power approach is by far the most accurate of the detailed transport predictors evaluated. In fact, the applied wave power approach is 25% more accurate than the second best detailed longshore transport predictor (the Engelund, Hansen and Swart method) which has a standard error of estimate of 0,611.

5.39

The distribution of the discrepancy ratios (= predicted transport rate / measured transport rate) for the applied wave power approach is shown in Figure 5.28. This figure illustrates that most of the discrepancy ratios are less than or equal to one. About 44% of the predictions with the applied wave power approach have discrepancy ratios of between 0,5 and 2.

Reasons for the success of the applied wave power approach

The success of the applied wave power approach in predicting longshore transport can be ascribed to the following:

- the approach has a sound theoretical basis
- all the significant physical processes are adequately represented
- the approach does not contain inappropriate assumptions
- inaccuracies (“noise”) are not introduced by the incorporation of physical processes of minor importance
- well verified methods have been applied to provide the required input on, for example, the wave height decay through the surf zone, bed roughness and the longshore current velocity.

Longshore transport of coarse material

Interestingly, the applied wave power approach predicts the transport of coarse material (median grain size from 1 mm up to 15 mm) reasonably well (Figure 5.29), despite the fact that the recorded rates in these instances varied between 1 490 m³/year and 1 310 000 m³/year with a median value of about 8100 m³/year. (Note that the broken lines on Figure 5.29 indicate 0,5 and 2 times the measured transport rate, while the solid line is the line of perfect agreement between the predicted and measured rates).

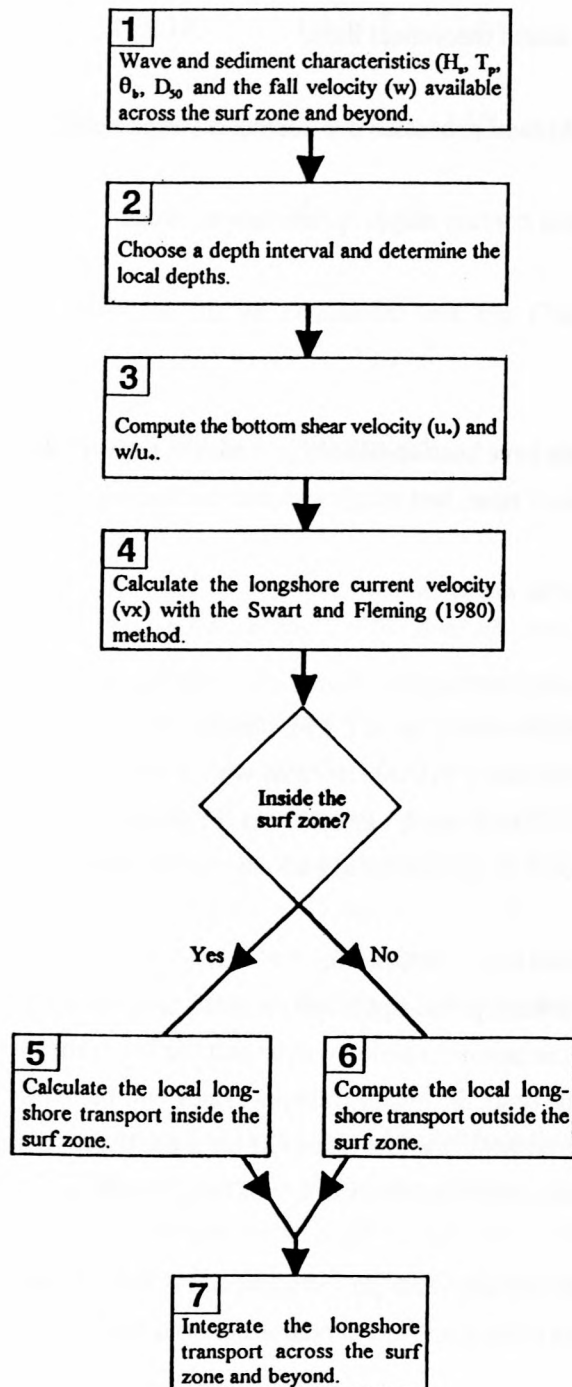
The average discrepancy ratio is 2,5, which indicates a tendency for overprediction. This is, however, to be expected because the applied wave power approach presently does not include an incipient motion criterion. The effect of including an incipient motion criterion will be that the low transport rates will be predicted much more accurately while, at the same time, the higher transport rates will be hardly influenced. The fact that the high transport rate is well predicted while the low transport rates are overpredicted (Figure 5.29), confirms that an incipient motion criterion will improve the accuracy of the predictions.

It can be concluded that the applied wave power approach is at least sufficiently accurate to be able to give order of magnitude estimates of the transport of coarse material (with D_{50} between 1 mm and 15 mm). However,

caution is necessary because of the few (8) data points and because of the tendency for overprediction. It is recommended that the accuracy of the method be tested against more data from coarse material having a wider range, after incorporating an incipient motion criterion. Only then can the method be used with confidence for design purposes in the specialized cases where coarse material is transported.

5.7 Flow Chart and Equations Recommended for the Applied Wave Power Approach

The following flow chart summarizes schematically the method recommended for determining longshore transport with the applied wave power approach:



5.41

The detail of some of the above items is given below (the numbers correspond to the numbers in the flow chart):

3. Compute the bottom shear velocity (u_*) and w/u_* .
<ul style="list-style-type: none"> ● Determine the orbital velocity (u_o) and amplitude (a_o) on the bottom according to linear wave theory (Eq. (5.15) and 5.14)).
<ul style="list-style-type: none"> ● Calculate the bed forms (if any) and the bed roughness with the Van Rijn (1989) method.
<ul style="list-style-type: none"> ● $f_w = \exp \{-5,98 + 5,21 (a_o / r)^{-0,19}\}$ for $a_o / r > 1,57$ $= 0,30$ for $a_o / r \leq 1,57$ (Swart, 1974) (Eq. 5.13)
<ul style="list-style-type: none"> ● $\tau_o = 0,5 f_w \rho u_o^2$ (Eq. 5.12)
<ul style="list-style-type: none"> ● $u_* = (\tau_o / \rho)^{0,5}$ (Eq. 5.11)

5. Calculate the local longshore transport inside the surf zone

- Determine $c_1 = 1,94 w/u_*$.
- Compute the energy dissipation per unit time and area (D_b) following Battjes and Janssen (1978).

$$H_m = 0,88 \frac{L}{2\pi} \tanh \left(\frac{2\pi h}{L} \cdot \frac{\gamma}{0,88} \right) \quad (\text{Eq. 5.30})$$

Q from

$$1 - Q + (H_{rms} / H_m)^2 \ln Q = 0 \quad (\text{Eq. 5.32})$$

$$D_{b,BJ} = 0,25 \alpha_{BJ} Q \rho g H_m^2 / T_p \quad (\text{Eq. 5.29})$$

- Allow for the effect of beach profile variations:

$$P_o = (D_{b,BJ} / d)^{c_1} \quad (\text{Eq. 5.47})$$

$$P_1 = f_1 P_o \quad (\text{Eq. 5.49})$$

$$\begin{aligned} \text{with } f_1 &= 1 \text{ if } P_o \leq 13,29 \\ &= (0,20 \ln P_o + 0,28) / (0,06 P_o) \text{ if } P_o > 13,29 \end{aligned} \quad (\text{Eq. 5.50})$$

- Calculate $a_{4,BJ}$

$$\xi_i = \frac{\tan \alpha}{(H_i / L_o)^{0,5}} \quad (\text{Eq. 5.45})$$

$$\begin{aligned} a_{4,BJ} &= 110 \times 10^{-6} \xi_i && \text{if } 0 \leq \xi_i \leq 0,4 \\ &= (660 \xi_i - 220) \times 10^{-6} && \text{if } 0,4 < \xi_i \leq 1 \\ &= (1151,11 \xi_i - 1071,11) \times 10^{-6} && \text{if } 1 < \xi_i \leq 2,3 \\ &= (-15896,3 \xi_i + 38965,8) \times 10^{-6} && \text{if } 2,3 < \xi_i \leq 2,45 \\ &= 20 \times 10^{-6} && \text{if } \xi_i > 2,45 \end{aligned} \quad (\text{Eq. 5.51})$$

- Compute the local longshore transport rate (s_i)

$$s_i = a_4 P_1 v_{gem} d \quad (\text{Eq. 5.52})$$

$$\text{where } a_4 = a_{4,BJ}$$

$$\text{with } v_{gem} = v_x. \text{ (Longshore current velocity using the Swart and Fleming (1980) method)}$$

6. Compute the local longshore transport rate <u>outside</u> the surf zone	
● Determine $e_1 = 1,16 \text{ w/u}$.	
● Calculate the energy dissipation per unit time and volume (D_f/d)	
$D_f/d = \frac{2}{3\pi} \rho f_w u_o^3 / d$	(Eq. 5.9)
● Compute a_3	$= 2,0 \times 10^{-3} \quad \text{for } H_s/d \leq 0,16$ $= [678,9 (H_s/d)^2 - 289,9 (H_s/d) + 31] \times 10^{-3} \quad \text{for } 0,16 < H_s/d \leq 0,7 \text{ or } 0,8$
	(Eq. 5.18)
● Obtain the depth- and time-averaged concentration (C_{gem})	
$C_{gem} = 0,15 \cdot 10^{-3} (H_s/d)(D_f/d)^{1,16w/u}$	(Eq. 5.17)
● Determine the local longshore transport rate (s_i)	
$s_i = a_3 C_{gem} \cdot v_{gem} \cdot d$	(Eq. 5.19)
with v_{gem}	$= vx$

From the above, it is clear that the applied wave power approach properly takes into account all the significant processes and that application of the approach is convenient.

5.8 Recommendations for Further Work

By relating the sediment concentration to $\left(\tau \frac{dv}{dy}\right)^{e_1}$ (see for example, Equation 5.3) at different elevations above the bottom, the vertical distribution of the concentration can be determined. In combination with the distribution of the longshore current velocity (Appendix G) it is possible to derive the vertical distribution for the local longshore transport rate. It is recommended that this be done for further refinement of the approach. If the variation in applied wave power per volume over time is known, it is also possible theoretically to determine the fluctuation of the local longshore transport rate over time which is useful in some instances.

It is recommended that a bulk longshore transport formula be derived based on the applied wave power approach. This can be done by integration, yielding a formula which is even more convenient to apply. It would also be advantageous to investigate the prediction of sediment transport in situations where strong tidal and wind-driven currents occur because the applied wave power approach should also perform well in this instance.

Cross-shore sediment transport and its associated beach profile variations (including tidal fluctuations) should be modelled interactively with longshore transport to obtain more accurate longshore transport rates. Although computationally intensive, it is recommended that interactive modelling be investigated and developed further.

To achieve an even better calibration it is important to obtain more data on local longshore transport rates for plunging to surging breakers, that is, (referring to Figure 5.16) for values of the local surf similarity parameter between 0,6 and 1,4. Data are sorely needed for high concentrations and high $(D_{b/BJ} / d)^c$ values, as well as for the region outside the surf zone (Section 5.5). It is important that the longshore current velocity be measured when obtaining these data so as to minimize the potential inaccuracy in the local transport rate due to the prediction of the longshore current velocity.

It is recommended that the accuracy of the applied wave power approach be validated against more data for coarse material having a wider range, after incorporating an incipient motion criterion. Such validation would allow an even wider application (from very fine sand to rock) of the approach.

5.9 Conclusion

The theory for the prediction of the longshore transport in terms of the applied wave power approach has been developed based on the principles of wave phenomena such as breaking. This approach resulted in a detailed predictor which accounts for the different processes inside and outside the surf zone. The applied wave power approach has been successfully calibrated against a comprehensive database containing bulk longshore transport rates. Of the 52 longshore transport formulae tested, the applied wave power approach was found to be the fourth best. The wave power approach is by far the best detailed longshore transport predictor (25% more accurate than the second best predictor). Based on the theory, calibration and performance, it can be concluded that the applied wave power approach is successful in predicting longshore transport rates. The main reasons for the success of the applied wave power approach are: (1) it has a sound theoretical basis; (2) it does not have inappropriate assumptions; and (3) it takes into account all the significant physical processes.

6. SUMMARY, CONCLUSIONS AND RECOMMENDATIONS

6.1 General

A study was undertaken on different aspects of longshore sediment transport. These aspects are the analysis of field data, evaluation of existing longshore transport formulae and the development and validation of the applied wave power approach in order to predict longshore transport rates.

The aims of the field data analysis were to compile a comprehensive database, to evaluate the quality of the available field data objectively and to determine the measurement period required to obtain an accurate long-term mean net longshore transport rate at a site. Guidance is required on how to obtain in the most cost-effective way, this long-term mean net longshore transport rate. The objectives of the evaluation of the longshore transport formulae were to compile a large number of formulae and to evaluate these formulae against the comprehensive database. From this evaluation it was possible to identify and to improve the most accurate longshore transport formula. The aims of the applied wave power approach were to develop a detailed predictor using a fundamentally sound, yet robust approach and to validate the predictions against the comprehensive database. In addition, the accuracy of the applied wave power approach had to be compared with the accuracy of the existing longshore transport formulae.

6.2 Field Data Analysis

General

The field data analysis consisted of two parts: firstly, a review of the available field data for longshore transport; and secondly, an analysis of the annual variation in the net longshore transport rate.

Review of the available field data

For the first time in coastal engineering, a really comprehensive database has been compiled containing field data on longshore transport rates. A data set, called Data Set 1, was extracted from the database. Virtually all conditions encountered on natural beaches are covered in this data set. The data were collected on beaches from many different sites from around the world. This wide range of conditions give credibility to the conclusions drawn in the evaluation of the formulae presented in Section 6.4.

Most of the longshore transport data from around the world were obtained during mild wave conditions for fine to medium sand. Data are especially lacking for transport rates exceeding $200\,000\text{ m}^3/\text{year}$, significant wave heights higher than 1,8 m, sediment grain sizes coarser than 0,6 mm, and beach slopes steeper than 0,06 ($=1/14$). This means that longshore transport formulae are calibrated almost exclusively against data for mild conditions. As a result, the most important predictions for which the formulae are used, are for conditions outside their calibration range. It is therefore strongly recommended that data be collected in the above-mentioned ranges.

A point rating system was devised whereby the quality of all the available data could be assessed objectively. The data sets were divided into three categories, namely, the lower, middle and higher categories. The highest score achieved in the evaluation was only 71%, thus reflecting the difficulty of measuring the longshore transport accurately. It is recommended that multiple measurements of the transport rate be made simultaneously, in order to be able to estimate the random error contained in the data and to demonstrate the consistency of the measurements.

Annual variation in the net longshore transport rate

Based on data from three sites on the South African east coast, it is recommended that measurements of the longshore transport rates should be conducted for 5 years to 8 years in order to obtain an accurate value (within 10%) of the long-term mean net longshore transport rate (Figure 2.2). It was also found that the order in which the net longshore transport rate occurs (for example, a few years of high net rates), is not critical as long as the required measurement period is adhered to.

Four confidence bands (95%, 80%, 20% and 5%) were determined for the factor (floating mean net longshore transport/long-term mean net transport), for different measurement periods (Figure 2.3 and Table 2.2). This table can be used to estimate the range of possible long-term net transport rates if measurements were done over a shorter period than the 5 years to 8 years recommended above.

Although the above conclusions are derived from data originating from specific sites, it is reasonable to expect that the conclusions are more widely applicable, especially for exposed sites. For protected sites, the above results are most probably conservative.

It is recommended that an accurate assessment of the long-term mean net transport rate at a site can best be made cost-effectively by combining calculations and measurements. It is proposed that limited site-specific measurements be made, that the best longshore transport formula (the improved Kamphuis formula- see below) be calibrated for the particular site and then be used to predict the longshore transport rates by using a representative wave climate. If possible, these predictions should be augmented by comparing the net rate with the known net rates from nearby sites.

6.3 Existing Longshore Transport Formulae

The historical development of longshore transport formulae (since 1933) has been briefly described. In total, 51 longshore transport formulae have been compiled from the literature. A new process-based classification system for longshore transport formulae has been devised and applied by analysing the theoretical bases of almost all existing longshore transport formulae. The characteristics of the different types of formulae have been presented in Chapter 3 while the individual formulae have been summarised in Appendix C.

6.4 Evaluation of the Existing Longshore Transport Formulae

In all previous studies only a small number of longshore transport formulae have been tested against very limited data. For the first time, virtually all (51) longshore transport formulae have been tested against a really

comprehensive database. Two of the four different measures used, were found to be the best measures with which to judge the accuracy of a formula. These are (1), the plot of the predicted transport rates versus the measured rates combined with (2), the standard error of estimate.

The Kamphuis formula, a bulk predictor, was found to perform the best of the 52 formulae (51 existing formulae plus the applied wave power approach) when tested against Data Set 1. Because of the wide ranges of this data set, it is reasonable to assume that the Kamphuis formula will perform best for most other sites too. It is hypothesised that the Kamphuis formula performed the best because it contains all the most important parameters. By including fewer parameters, a lower degree of inaccuracy is introduced into the prediction. The Van Hijum, Pilarczyk and Chadwick and the Van der Meer formulae are rated second and third respectively. Figures 5.8a, 5.9a and 5.10a illustrate the fit of the predicted transport rates against the measured rates for the three best formulae.

The best longshore transport formula was recalibrated to improve its predictions. Two approaches were used to recalibrate the *Kamphuis formula* (Equations (4.6) and (4.7)), yielding the following two relationships:

$$S = 38\,900 \, z_{\text{Kamphuis}} \, (\text{m}^3/\text{year}) \quad (4.6)$$

and

$$S = 30\,700 \, z_{\text{Kamphuis}} \, (\text{m}^3/\text{year}) \quad (4.7)$$

For obtaining bulk longshore transport rates, it is recommended that Equation (4.6) be applied at sites where the significant wave heights normally exceed about 0,3 m and where the sediment grain size is usually less than 1 mm; that is, at partly protected and exposed sites. Only at sites where very calm conditions prevail and/or where the sediment size is coarse, is Equation (4.7) expected to yield better results. A slight improvement of 2% in the standard error of estimate in the predicted transport rates was obtained by the recalibration.

Another first, is the derivation of confidence intervals for a longshore transport formula (Figure 4.18a - 4.19b and 4.21a and b). Accurate predictions are now possible. Figure 4.20 presents, for the recalibrated Kamphuis formula, these confidence intervals in terms of a transport factor. For medium to high wave conditions (the most important conditions when determining the longshore transport budget at a site), the transport factor is smaller than 1,6 at an 80% confidence interval.

The best *existing* detailed predictor is the Engelund, Hansen and Swart formula which is only number 13 of the 15 best formulae when considering the existing bulk and detailed formulae together. It can be argued that detailed predictors should not be compared directly with bulk formulae. The detailed predictors are usually more susceptible to inaccuracies resulting from the larger number of input parameters normally required. When comparing the detailed predictors among themselves, it was found that the applied wave power approach, the Engelund, Hansen and Swart formula and the Fleming formula are the first, second and third most accurate formulae respectively. It is believed that the results which show that bulk predictors are at present more accurate, indicate that beach profile variations impact on detailed predictors far more seriously than on bulk

predictors. These profile variations are caused by changes in cross-shore transport due to variations in the wave conditions. It is therefore preferable that beach profile changes due to cross-shore transport be calculated interactively with the longshore transport.

The so-called *package deal approach* (analysing the variation in the predictions of the longshore transport by different formulae) was tested by using the five of the best formulae. The best single formula (the Kamphuis method) on its own is better than the best of the package deal approaches. It can therefore be concluded that none of the package deal approaches yields better answers than the best formula on its own (the Kamphuis method) within the wide data ranges of Data Set 1. For data outside this wide range, it is proposed to examine the transport rates predicted by the five best formulae and use engineering judgement. Most probably it would be best also to apply the recalibrated Kamphuis formula alone to data outside the range; however, depending on the consistency of the predictions, it may be advantageous to use the package deal approach (the mean of the middle three predictions) if deviations are prevalent among the transport rates. The reason for this recommendation is that the Kamphuis formula, which was calibrated against physical model data, has shown that it extrapolates well as indicated by it being the best formula tested against field data. It is therefore reasonable to expect that it will also extrapolate well to beyond the data ranges of Data Set 1.

6.5 Applied Wave Power Concept

General

The stream power concept developed and applied successfully by Rooseboom (1974, 1992), for river flow has been adapted for use in the sea. The applied wave power principle was used both inside and outside the surf zone in order to obtain expressions for the local longshore transport rate at any particular location in these two regions. These rates were integrated across the surf zone and beyond to obtain the bulk rate. Although the method which was derived here, is valid only for strong wave action and weak currents, it can be adapted for strong currents.

In developing the applied wave power approach, it was assumed that the time- and depth-averaged sediment concentration at a particular position is proportional to the energy dissipation per unit time and volume raised to a power e_1 . Exponent e_1 is a function of a coefficient a_1 , the fall velocity of the sediment and the bottom shear of velocity.

Initial calibration was carried out by using suspended sediment concentration data in the regions inside and outside the surf zone. Therefore the quality of the concentration data was assessed. It was found that the ratio between the maximum and minimum concentration can be expected to be about 3,2 on average for repetitive measurements.

Outside the surf zone

Outside the surf zone, it was found that the mean concentration can be given by:

$$C_{gem} = 0,15 \cdot 10^{-3} (H_s / d) (D_f / d)^{1,16w/u} \quad (5.17)$$

Figure 5.9 shows that a reasonable fit is obtained.

The data by White (1987) based on simultaneously measured red and green tracer movement were used. Analysis of the data revealed that the mean factor f (= higher transport rate/lower transport rate) was 8,3. Eventually 12 (of the initial 21) data points of this data set were used. For each of the 12 data points, the percentage difference between the transport rates which were measured separately with the red and the green tracers, was below 100%. The data ranges are given in Section 5.5.4 and the method is summarized in Section 5.7. The local longshore transport rate is then:

$$s_i = a_3 C_{gem} \cdot v_{gem} \cdot d \quad (5.19)$$

with coefficient a_3 defined by Equation (5.18).

The predicted versus the measured local transport rates are plotted in Figure 5.13 for the eventual 12 points and in Figure 5.14 for the original 21 points. The fit in Figures 5.13 and 5.14 is quite good, considering the accuracy of the data.

Inside the surf zone

The derivation of different equations to compute the energy dissipation caused by wave breaking, led to the testing of four of these methods against data. These data have reasonably wide ranges. The approach using the Battjes and Janssen (1978) method yielded the best results. An initial calibration showed, among other things, that the best value for coefficient a_1 was 1,94 and that, for inside the surf zone, coefficient a_4 gave better results than coefficient a_3 . Therefore the local transport rate is:

$$s_i = a_4 (D/d)^e_1 v_{gem} \cdot d \quad (5.7)$$

It was shown that the local longshore transport rate will vary over time because of beach profile changes resulting from cross-shore sediment transport. If the existing beach profile is far from the equilibrium profile, the incoming waves will initially cause high energy dissipation per volume and time at certain locations along the profile. This in turn, will locally result in high suspended sediment concentrations with the result that the beach profile will initially adapt rather quickly. Essentially the energy dissipation per volume and time will be limited because of these beach profile variations. Figure 5.21 shows the factor that was derived to allow for these beach profile changes. Mathematically it means

$$P_1 = f_1 \cdot P_0 \quad (5.49)$$

$$\text{where } P_0 = (D_{b,B}/d)^e_1 \quad (5.47)$$

Employing this factor improved the accuracy of the predictions significantly, thus confirming the importance of allowing for the effects of beach profile variations.

The mechanics of wave breaking were investigated for the different breaker types, namely, spilling, plunging, collapsing and surging breaking. The local wave breaking was categorised by the local surf similarity parameter. It was postulated that different distributions of a_4 (as a function of the local surf similarity

parameter) can be either of three types of distributions (called Types A, B and C). Physically plausible arguments were presented for each of these types. In addition, a step-wise function for a_4 was determined from Data Set 1 (the comprehensive data set of bulk longshore transport rates) in order that the three types of curves could be fitted through the step-wise function to ensure that curves will predict the correct numerical values. A numerical method requiring several iterations, was employed for this purpose.

It was found that the Type C (called the Mountain peak curve) was the most accurate. This type of curve was therefore optimized in two different ways. Figure 5.26 shows the best of the optimized curves while the relationship for a_4 is given by Equation (5.51). The local longshore transport rate inside the surf zone is then

$$s_i = a_4 \cdot P_1 \cdot v_{gem} \cdot d \quad (5.52)$$

Final results

The applied wave power approach to compute the longshore sediment transport rate is summarised in Section 5.7.

The predicted longshore transport rates versus the measured longshore transport rates for the applied wave power approach are shown in Figure 5.27. With the standard of error of estimate being 0,457 for the applied wave power approach, it means that this approach is the fourth best longshore transport predictor of the 52 formulae tested.

The applied wave power approach is by far the most accurate of the detailed transport predictors evaluated. In fact, this approach is 25% more accurate than the second best detailed longshore transport predictor (the Engelund, Hansen and Swart method) which has a standard error of estimate of 0,611. It is therefore recommended that the applied wave power approach be used if the local longshore transport rates are required (for obtaining the cross-shore distribution of the longshore transport). The total transport rate integrated across the surf zone and acquired using the applied wave power approach could be adjusted (scaled) according to the prediction with the recalibrated Kamphuis formula.

It was found that the applied wave power approach is at least sufficiently accurate to be able to give order of magnitude estimates of the transport of coarse material (with D_{50} between 1 mm and 15 mm). However, caution is necessary because of the few (8) data points and because of the tendency for overprediction. It is recommended that the accuracy of this method be tested against more data from coarse material having a wider range, after incorporating an incipient motion criterion. Only then can the method be used with confidence for design purposes where coarse material is transported.

It is recommended that a bulk longshore transport formula be derived based on the applied wave power approach, in addition to the detailed predictor presented above. This approach could be adapted to determine the vertical distribution of the local longshore transport rate; this should be investigated.

6.6 Miscellaneous Findings

Only limited data are available for high concentrations inside (plunging to surging breakers) and outside the surf zone where the longshore current velocity has also been measured. It is therefore recommended that such detailed concentration and transport measurements be undertaken in order to validate detailed predictors.

Based on measurements and theory, it was found that the longshore current velocity is almost constant over depth (Appendix G). This fact was used in the derivation of the applied wave power approach.

The variations in repeated sediment concentration measurements can be drastically reduced by increasing the sampling period to at least 30 minutes (preferably an hour or longer). Thus, it is recommended that sampling/measuring of the local longshore transport should also be done over at least half an hour and preferably an hour or longer in order to improve the accuracy of short-term measurements.

Typical sediment grain size relationships were derived expressing D_{10} , D_{16} , D_{25} , D_{35} , D_{60} , D_{65} , D_{75} , D_{84} , and D_{90} in terms of the median grain size (D_{50}) - see Appendix D. Very good correlations (mean $R^2 = 0,97$) were obtained. These relationships are very useful if the grain size parameters other than the median grain size are not available.

6.7 Final Conclusion

In the development of a better understanding of longshore sediment transport, the following has been done for the first time: (1) a comprehensive data set have been compiled covering almost a full range of conditions occurring on natural beaches; and (2) virtually all longshore transport formulae have been evaluated against such an extensive data set. A new improved method, the applied wave power approach, has been developed and extensively calibrated against the same data set. Based on this evaluation, guidelines are now available for design engineers as to which are the best bulk and detailed predictors of longshore sediment transport. These are respectively, the recalibrated Kamphuis formula and the applied wave power approach.

Another useful first, is the derivation of confidence intervals for a longshore transport formula, showing that accurate predictions can now be obtained. In addition, it has been determined what the required measurement period should be and what the most cost-effective way are for obtaining the true long-term mean net longshore transport rate at a particular site.

REFERENCES

- Ackers, P. and White, W.R. (1973). Sediment transport: new approach and analysis. *J. Hydr. Div., Proc. ASCE*, Vol. 99(HY11): 2041-2060.
- Adachi, S., Sawaragi, T. And Ogo, A. (1959). The effects of coastal structures on the littoral sand drifts. *Coastal Engineering in Japan*, Vol. 2: 85-98.
- Anderson, O.H. and Fredsøe, J. (1983). *Transport of suspended sediment along the coast*. Progress Report 59, ISVA, Technical University of Denmark, Lyngby, pp. 33-46.
- Bagnold, R.A. (1963). Mechanics of marine sedimentation. In: *The sea*. Vol. 3, *The earth beneath the sea*. Hill, M.N. (ed.). Interscience Publ., New York, pp. 507-528.
- Bagnold, R.A. (1966). *An approach to the sediment transport problem from general physics*. Prof. Paper 422-I, US Dept. of Interior, Geological Survey, 37pp.
- Bailard, J.A. (1981). An energetics total load sediment transport model for a plane sloping beach. *J. of Geophysical Res.*, Vol. 86, (C11): 10938-10954.
- Bailard, J.A. (1982). An energetics total load sediment transport model for a plane, sloping beach. *Ocean Science and Engineering*, Vol. 7(2): 229-277.
- Bailard, J.A. (1984). A simplified model for longshore sediment transport. *19 Intern. Conf. on Coastal Eng.*, ASCE, Houston. Vol 2: 1454-1470.
- Bailard, J.A. (1985). *Simple models for surf zone sediment transport*. Technical Note N 1740, Naval Civil Engineering Laboratory, Port Hueneme, California.
- Bajorunas, L. (1960). Littoral transport in the Great Lakes. *7 Intern. Conf. on Coastal Eng., ASCE, The Hague, Netherlands*. Vol. 1: 326-341.
- Bajorunas, L. (1970). Littoral transport and energy relationships. *12 Intern. Conf. on Coastal Eng., ASCE, Washington DC*. Vol. 2: 787-798.
- Bakker, W.T. (1969). *Berekening van het langstransport door golven met die methode van evenwijdige dieptelijnen*. Studierapport WWK 69-70, Rijkswaterstaat, The Netherlands, 57 pp. (in Dutch).
- Bakker, W.T. (1971). *Computation of the wave induced littoral drift according to the Svasek-method adapted to parallel depth contours*. Study report WWK 71-2, Rijkswaterstaat, The Netherlands.
- Bakker, W.T., Ten Hoopen, H.G.H. and Grieve, G.R.H. (1971). *Berekening van het zandtransport volgens de methode Svasek bij een strand en een vooroever die een hoek met elkaar maken*. Study report WWK 71-18, Rijkswaterstaat, The Netherlands, 28 pp. (In Dutch).
- Battjes (1974). Computation of set-up, longshore currents, run-up and overtopping due to wind-generated waves. Ph.D. thesis, Technical University of Delft, Delft.
- Battjes and Janssen, J.P.F.M. (1978). Energy loss and set-up due to breaking of random waves. *16 Intern. Conf. on Coastal Eng., ASCE, Hamburg, Germany*. Vol. 1: 569-587.
- Battjes, J.A. and Stive, M.J.F. (1985). Calibration and verification of a dissipation model for random breaking waves. *J. of Geophysical Res.*, Vol. 90(C5): 9159-9167.
- Beach, R.A. and Sternberg, R.W. (1992). Suspended sediment transport in the surf zone: response to incident wave and longshore current interaction. *Marine Geology*, Vol. 108: 275-294.
- Bijker, E.W. (1967). *Some considerations about scales for coastal models with movable bed*. Publ. 50, Delft Hydraulics Laboratory. 142pp.
- Bijker, E.W. (1968). Littoral drift as a function of waves and current. *11 Intern. Conf. on Coastal Eng., ASCE, London*. Vol 1: 415-435.

- Bijker, E.W. (1971a). *Littoral drift computations and mutual wave and current influence*. Report No. 71-2, Dept. Of Civil Eng., Delft University of Technology. 20pp.
- Bijker, E.W. (1971b). Longshore transport computations. *Proc. ASCE, J. of Waterways, Harbors and Coastal Engineering Division*, Vol. 97 (WW4): 687-701.
- Bodge, K.R. (1986). Short-term impoundment of longshore sediment transport. Ph.D. thesis, University of Florida, Gainesville. 346 pp.
- Bonnefille R. And Pernecker, L. (1967). Étude théorique et expérimentale du transport littoral. Bulletin de la Direction des Étude théorique et expérimentale du transport littoral. *Bulletin de la Direction des Études et Recherches, Série A (3)*: 97-102. (In French).
- Bosman, J.J. (1982). *Concentration measurements under oscillatory water motion*. Report M 1695 Part II, Delft Hydraulics Laboratory, Delft.
- Bosman, J.J. and Steetzel, H.J. (1986). Time and bed averaged concentrations under waves. *20 Intern. Conf. on Coastal Eng., ASCE, Taipei, Taiwan*. Vol. 2: 986-1000.
- Brampton, A. and Motyka, J.M. (1984). Modelling the plan shape of shingle beaches. *Estuarine Studies*, Vol. 12. Springer Verlag, Berlin.
- Bruno, R.O., Dean R.G., Gable, C.G. and Walton, T.L. (1981). *Longshore sand transport study at Channel Islands Harbor, California*. Technical paper no. 81-2, CERC, US Army Corps of Engineers, Fort Belvoir. 48pp.
- Caldwell, J.M. (1950). Sedimentation in harbors. In: Trask, P.D. (Ed.) *Applied sedimentation*. John Wiley and Sons, New York, pp. 291-299.
- Caldwell, J.M. (1956). *Wave action and sand movement near Anaheim Bay, California*. Tech. Memorandum 68, US Army, Beach Erosion Board. 21pp.
- Carter, D.J.T. (1982). Prediction of wave height and period for a constant wind velocity using the JONSWAP results. *Ocean Eng.* Vol. 9(1): 17-33.
- Castanho, J. (1966). *Wave breaking and littoral drift (Rebentacão das ondas e transporte litoral)*. Paper No. 275, Laboratorio Nacional de Engenharia Civil, Lisbon. 278pp. (in Portuguese).
- Caviglia, F.J., Pousa, J.L. and Lanfredi, N.W. (1991). A determination of the energy flux constant from dredge records. *J. of Coastal Research*, Vol. 7(2): 543-549.
- Chadwick, A.J. (1989). Field measurements and numerical model verification of coastal shingle transport. In: Palmer, M.H. (ed.) *Advances in Water Modelling and Measurement*. . BHRA, Cranfield, Bedford.
- Chang, T.T. and Wang, Y.H. (1978). Field verification of sediment transport model. *26 Speci-ality Conf. of Hydraulics Div., ASCE, University of Maryland, Maryland*. pp. 737-744.
- Chien, H. (1954). The present status of research on sediment transport. *Proc. ASCE*, Vol. 80.
- Coppoolse, R.C. and Schoonees, J.S. (1991). Maintenance dredging at Richards Bay: sensitivity analysis of predictive models and the location of an offshore dump site. In: *CEDA-PIANC Conference, Amsterdam*.
- Coppoolse, R.C., Schoonees, J.S., Smith, G.G. and Mocke, G.P. (1992). Hydrodynamics and sediment concentrations at Walker Bay. *23 Intern. Conf. on Coastal Eng., ASCE, Venice, Italy*. Vol. 3: 3026-3039.
- CSIR (1976). *Evaluation of beaches along the Natal South Coast*. CSIR Report C/SEA 7604, National Research Institute for Oceanology, Stellenbosch.

- CSIR (1987). *Ondersoek na die omgewingsfaktore en daarmee gepaardgaande baaigeskiktheid van die strande aan die Noordoos-Valsbaaise kus*. CSIR Report C/SEA 8718/1,2 and 3, National Research Institute for Oceanology, Stellenbosch. (in Afrikaans).
- CSIR (1989). *A calibrated longshore sediment transport model for Richards Bay*. CSIR Report EMA-C 89121, Ematek, Stellenbosch.
- CSIR (1990). *Environmental factors affecting the marine recreational potential of the coastal zone between the Strand and Gordon's Bay*. CSIR Report EMA-C 90153/1-3, Ematek, Stellenbosch.
- CSIR (1994). *Erosion and sedimentation problems at Richards Bay*. CSIR Report EMAS-C 94035, Stellenbosch.
- CSIR (1996). *Durban beach monitoring*. Progress Report: July 1994 to June 1995. Volume 1: Main Report. CSIR Report 96014/1, Stellenbosch.
- Dally, W.R., Dean, R.G. and Dalrymple, R.A. (1984). A model for breaker decay on beaches. *19 Intern. Conf. on Coastal Eng., ASCE, Houston, Texas*. Vol 1: 82-98.
- Dally, W.R., Dean, R.G. and Dalrymple, R.A. (1985). Wave height variation across beaches of arbitrary profile. *J. of Geophysical Res.*, Vol. 90(C6): 11917-11927.
- Daniel, C. and Wood, F.S. (1980). *Fitting equations to data*. John Wiley and Sons, New York.
- Das, M.M. (1971). Longshore sediment transport rates: a compilation of data. Miscellaneous Paper No. 1-71, US Army, Coastal Eng. Res. Center, Washington DC. 75pp.
- Das, M.M. (1972). Suspended sediment and longshore sediment transport data review. *13 Intern. Conf. on Coastal Eng., ASCE, Vancouver*. Vol 2: 1027-1048.
- Dean, R.G. (1973). Heuristic models of sand transport in the surf zone. *Conf. on Eng. Dynamics in the Surf Zone, Sydney*. pp. 208-214.
- Dean, R.G. (1977). *Equilibrium beach profiles: US Atlantic and Gulf Coasts*. Report No. 12, Ocean Engineering. Univ. of Delaware, Newark.
- Dean, R.G. (1978). Review of sediment transport relationships and the data base. *Workshop on Coastal Sediment Transport with Emphasis on the National Sediment Transport Study, DEL-SG-15-78*. Sea Grant College Program, Univ. Of Delaware, Newark, pp. 25-39.
- Dean, R.G. (1987). Equilibrium beach profiles: characteristics and applications. *J. Coastal Res.* 7(1): 53-84.
- Dean, R.G., Berek, E.P., Bodge, K.R. and Gable, C.B. (1987). NSTS measurements of total longshore transport. *Coastal Sediments '87, New Orleans, Louisiana*, Vol. 1: 652-667.
- Dean, R.G., Berek, E.P., Gable, C.G. and Seymour, R.J. (1982). Longshore transport determined by an efficient trap. *18 Intern. Conf. on Coastal Engineering, ASCE, Cape Town*. Vol. 2: 954-968.
- Deigaard, R., Fredsøe, J. and Hedegaard, I.B. (1986). Mathematical model for littoral drift. *J. Waterway, Port, Coastal and Ocean Eng.*, Vol. 112(3): 351-369.
- Delorme, J.-L. (1981). Erosion des côtes due à des travaux portuaires et mesures visant à y remédier. *Permanent International Association of Navigation Congresses, Edinburgh*. Vol. 5: 771-797. (in French).
- Derks, H. and Stive, M.J.G. (1984). Field investigations in the TOW programme for coastal sediment transport in the Netherlands. *19 Intern. Conf. on Coastal Eng., ASCE, Houston, Texas*. Vol. 2: 1830-1845.
- Detle, H-H and Uliczka, K. (1986). Velocity and sediment concentration fields across surf zones. *20 Intern. Conf. on Coastal Eng., ASCE, Taipei, Taiwan*. Vol. 2: 1062-1076.

- Dette, H-H and Uliczka, K., (1986a). *Sediment Concentration at Prototype Equilibrium Profile*. Technical Report No. 4 - SFB 205/TP A6, University of Hannover, Hannover.
- Dong, P. and Anastasiou, K. (1991). A numerical model of the vertical distribution of longshore currents on a plane beach. *Coastal Eng.* Vol. 15: 279-298.
- Downing, J.P. (1984). Suspended sand transport on a dissipative beach. *19 Intern. Conf. on Coastal Eng., ASCE, Houston, Texas*. Vol. 2: 1765-1781.
- Duane, D.B. and James, W.R. (1980). Littoral transport in the surf zone elucidated by a Eulerian sediment tracer experiment. *J. Sedimentary Petrology*. Vol. 50(3): 929-942.
- Edelman, T. (1963). Littoral transport in the breaker zone, caused by oblique waves. *10 Congress IAHR, London*. Vol 1: 61-67.
- Engelund, F. and Hansen, E. (1967). *A monograph on sediment transport in alluvial streams*. Teknisk Forlag, Copenhagen. 63pp.
- Fairchild, J.C. (1972). Longshore transport of suspended sediment. *13 Intern. Conf. on Coastal Eng., ASCE, Vancouver*. Vol. 2: 1069-1088.
- Fairchild, J.C. (1977). *Suspended sediment in the littoral zone at Ventnor, New Jersey, and Nags Head, North Carolina*. Report TP 77-5, US Army, Coastal Eng. Research Center, Fort Belvoir. 97pp.
- Fleming, C.A. (1977). The development and application of a mathematical sediment transport model. Ph.D. thesis, University of Reading.
- Fleming, C.A. and Hunt, J.N. (1976). A mathematical sediment transport model for unidirectional flow. *Proc. Inst. Civil Eng., Great Britain*. Part 2, Vol. 61: 297-310.
- Fleming, C.A., Pinchin, B.M. and Nairn, R.B. (1986a). *Evaluation of coastal sediment transport estimation techniques. Phase 2: Comparison with measured data*. Canadian Coastal sediment study (C²S²); Report C²S² - 19. Keith Philpott Consulting Ltd, Thornhill, Ontario.
- Fleming, C.A. Pinchin, B.M. and Nairn, R.B. (1986b). Evaluation of models of nearshore processes. *20 Intern. Conf. on Coastal Eng., ASCE, Taipei, Taiwan.*, Vol. 2: 1116-1131.
- Fromme, G.A.W. (1977). *Establishment of a standard relationship between settling velocity and grain size of coastal sand*. CSIR Research Report 356, National Research Institute for Oceanology, Stellenbosch.
- Frijlink, H.C. (1952). Discussion des formules de débit solide de Kalinske, d'Einstein, et de Meyer-Peter et Muller (Zurich) compte tenu des mesures récentes de transport dans les rivières néerlandaises. *2 Journ. Hydraulique, Soc. Hydr. de France, Grenoble*. pp. 98-103 (in French).
- Gable, C.B. (1981). *Report on data from the nearshore sediment transport study experiment at Leadbetter Beach, Santa Barbara, California, Jan-Feb 1980*. IMR Report No. 80-5. Institute of Marine Resources, University of California.
- Galvin, C.J. (1968). Breaker type classification on three laboratory beaches. *J. Geophysical Res.*, Vol. 72(12): 3651-3659.
- Greer, M.N. and Madsen, O.S. (1978). Longshore sediment transport data: a review. *16 Intern. Conf. on Coastal Eng., ASCE, Hamburg*. Vol. 2: 1563-1576.
- Hallermeier, R.J. (1982). Bedload and wave thrust computations of alongshore sand transport. *J. Geophysical Res.*, Vol. 87(C8): 5741-5751.
- Hanes, D.M. and Vincent, C.E. (1987). Detailed dynamics of nearshore suspended sediment. *Coastal Sediments '87, ASCE, New Orleans, Louisiana*, Vol. 1: 285-299.

- Horikawa, K. (1978). *Coastal engineering: an introduction to ocean engineering*. University of Tokyo Press, Tokyo. 402pp.
- Horikawa, K. (ed.) (1988). *Nearshore dynamics and coastal processes: theory, measurement and predictive models*. University of Tokyo. Tokyo.
- Hou, H. (1988). Study of shelf waves vs. sand drift in NW coast of Taiwan. *21 Intern. Conf. on Coastal Eng., ASCE, Malaga*. Vol. 2: 1152-1165.
- Hou, H., Lee, C. and Lin, L. (1980). Relationship between alongshore wave energy and littoral drift in the midwest coast at Taiwan. *17 Intern. Conf. on Coastal Eng., ASCE, Sydney*. Vol. 2: 1255-1274.
- Ichikawa, T., Ochiai, O., Tomita, K. and Murobuse, K. (1961). Waves and coastal sediment characteristics at Tagono-ura coast, Suruga Bay. *8 Conf. on Coastal Eng. in Japan*, pp. 161-167 (in Japanese).
- Ijima, T., Sato, S., Aona, H. and Ishii, K. (1960). Wave and coastal sediment characteristics at Fukue coast, Atsumi Bay. *7 Conf. on Coastal Eng. in Japan*. pp 69-79 (in Japanese).
- Inman, D.L. and Bagnold, R.A. (1963). Littoral processes. In: *The sea*. Vol. 3, *The earth beneath the sea*. Hill, M.N. (ed). Interscience Publ., New York, pp. 529-553.
- Inman, D.L., Zampol, J.A., White, T.E., Hanes, D.M., Waldorf, B.W. and Kastens, K.A. (1980). Field measurements of sand motion in the surf zone. *17 Intern. Conf. on Coastal Eng., ASCE, Sydney*. Vol. 2: 1215-1234.
- Ishihara, T., Iwagaki, Y. and Murakami, M. (1958). On the investigation of beach erosion along the north coast of Akashi Strait. *Coastal Eng. in Japan*, Vol. 1: 97-109.
- Isobe, M. (1983). *Field observation of vertical distribution of mean velocity in the nearshore zone*. NERC Report, No 17, TR-82-1: 66-73. (in Japanese).
- Iwagaki, Y. and Sawagari, T. (1962). A new method of estimation of the rate of littoral sand drift. *Coastal Eng. in Japan*, Vol. 5: 69-79.
- Jaffe, B.E. and Sallenger, A.H. (1992). The contribution of suspension events to sediment transport in the surf zone. *23 Intern. Conf. on Coastal Eng., ASCE, Venice, Italy*. Vol. 3: 2680-2693.
- Jaffe, B.E., Sternberg, R.W. and Sallenger, A.H. (1984). The role of suspended sediment in shore-normal beach profile changes. *19 Intern. Conf. on Coastal Eng., ASCE, Houston, Texas*. Vol. 2: 1983-1996.
- Johnson, J.W. (1953). Sand transport by littoral currents. *5 Hydraulics Conf., Iowa Inst. of Hydr. Research Studies in Eng., Iowa*. pp. 89-109.
- Johnson, J.W. (1957). The littoral drift problem at shoreline harbors. *J. Waterways and Harbors Div., Proc. ASCE*, Vol. 83 (WW1) Paper 1211. 37pp.
- Johnson, I.G. (1966). Wave boundary layers and friction factors. *10 Intern. Conf. on Coastal Eng., ASCE, Tokyo*. Vol. 1: 127-148.
- Kamphuis, J.W. (1990). Alongshore sediment transport rate. *22 Intern. Conf. on Coastal Eng., ASCE, Delft*. Vol. 3: 2402-2415.
- Kamphuis, J.W. (1991). Alongshore sediment transport rate. *J. Waterway, Port, Coastal and Ocean Eng., ASCE*, Vol. 117(6): 624-640.
- Kamphuis, J.W. (1995). Comparison of two-dimensional and three dimensional beach profiles. *J. Waterway, Port, Coastal and Ocean Eng., ASCE*, Vol. 121 (3): 155-161.
- Kamphuis, J.W., Davies, M.H., Nairn, R.B. and Sayao, O.J. (1986). Calculations of littoral sand transport rate. *Coastal Engineering*, Vol. 10:1-21
- Kamphuis, J.W. and Readshaw, J.S. (1978). A model study of alongshore sediment transport rate. *16 Intern. Conf. on Coastal Eng., ASCE, Hamburg*. Vol. 2: 1656-1674.

- Kana, T.W. (1976). Sediment transport rates and littoral processes near Price Inlet, S.C.: terrigenous clastic depositional environments. In: Hayes, M.O. and Kana, T.W. (eds.). *AAPG Tech. Report No. 11-DRD*. Univ. South Carolina, Columbia. pp. 158-171.
- Kana, T.W. (1977). Suspended sediment transport at Price Inlet, S.C. *Coastal Sediments '77, Charleston*. pp. 366-382.
- Kana, T.W. (1978). Surf zone measurements of suspended sediment. *16 Intern. Conf. on Coastal Eng., ASCE, Hamburg*. Vol. 2: 1725-1743.
- Kana, T.W. (1979). *Suspended sediment in breaking waves*. Tech. Report No. 18-CRD. Dept. of Geology, Univ. of South Carolina, Columbia. 153 pp.
- Kana, T.W. and Ward, L.G. (1980). Nearshore suspended sediment load during storm and post-storm conditions. *17 Intern. Conf. on Coastal Eng., ASCE, Sydney*. Vol. 2: 1158-1173.
- Katoh, K., Tanaka, N., Kondoh, T., Akaishi, M. and Terasaki, K. (1985). *Field observations of local sand movements in the surf zone using fluorescent sand tracer (second report)*. Report of the Port and Harbour Research Institute, Ministry of Transport, Japan, Vol. 24, No. 4.
- Katori, S., Sakakiyama, T. and Watanabe, A. (1984). Measurement of sand transport in a cross unidirectional-oscillatory flow tank. *Coastal Eng. in Japan*. Vol. 27: 193-203.
- Kim, K.H., Sawaragi, T. and Deguchi, I. (1986). Lateral mixing and wave direction in the wave-current interaction region. *20 Intern. Conf. on Coastal Eng., ASCE, Taipei, Taiwan*, Vol. 1:366-380.
- Knaps, R.J. (1938). Prüfung der formel von Prof Münch-Petersen über material wanderung an der lettischen küste. *VI Hydrologische Konferenz der Baltischen Staaten*. (In German).
- Knoth, J.S. and Nummedal, D. (1977). Longshore sediment transport using fluorescent tracer. *Coastal Sediments '77, Charleston*. pp. 383-398.
- Komar, P.D. (1969). The longshore transport of sand on beaches. Ph.D. thesis, Scripps Institute of Oceanography, University of California, San Diego.
- Komar, P.D. (1975). Nearshore currents: generation by obliquely incident waves and longshore variations in breaker height. In: Hails, J.R. and Carr, A. (eds.). *Symposium on Nearshore Sediment Dynamics*. Wiley, London. pp. 17-45.
- Komar, P.D. (1977). Beach sand transport: distribution and total drift. *J. Waterway, Port, Coastal and Ocean Div. ASCE*, Vol. 103 (WW2): 225-239.
- Komar, P.D. (1983). Beach Processes and erosion: an introduction. In: Komar, P.D. (ed.). *CRC Handbook of coastal processes and erosion*. CRC Press, Boca Raton, Florida. pp. 1-20.
- Komar, P.D. (1988). Environmental controls on littoral sand transport. *21 Intern. Conf. on Coastal Eng., ASCE, Malaga*. Vol. 2: 1238-1252.
- Komar, P.F. and Inman, D.L. (1970). Longshore sand transport on beaches. *J. Geophysical Res.*, Vol. 76 (30): 5914-5927.
- Kooistra, J. and Kamphuis, J.W. (1984). *Scale effects in alongshore sediment transport rates*. Report No. C2S2-13. Canadian Coastal Sediment Study. Kingston, Ontario
- Kraus, N.C. (1985). Field experiments on vertical mixing of sand in the surf zone. *J. Sedimentary Petrology*, Vol. 55(1): 3-14.
- Kraus, N.C., Farinato, R.S. and Horikawa, K. (1981). Field experiments on longshore sand transport in the surf zone. *Coastal Eng. in Japan*, Vol. 24: 171-194.
- Kraus, N.C., Gingerich, K.J. and Rosati, J.D. (1988). Towards an improved empirical formula for longshore sand transport. *21 Intern. Conf. On Coastal Eng., ASCE, Malaga*. Vol. 2: 1182-1196.

- Kraus, N.C., Gingerich, K.J. and Rosati, J.D. (1989). *Duck 85 surf zone sand transport experiment*. Tech. Report CERC-89-5, US Army, Corps of Engineers, Waterways Experiment Station.
- Kraus, N.C., Isobe, M., Igarashi, H., Sasaki, T.O. and Horikawa, K. (1982). Field experiments on longshore sand transport in the surf zone. *18 Intern. Conf. on Coastal Eng., ASCE, Cape Town*. Vol. 2: 969-988.
- Kriebel, D.L., (1990). Advances in numerical modelling of dune erosion. *21 Intern. Conf. on Coastal Engineering, ASCE, Delft*. Vol. 3: 2304-2317.
- Kriebel, D.L. and Dean, R.G. (1984). Beach and dune response to severe storms. *19 Intern. Conf. on Coastal Eng., ASCE, Houston, Texas*. Vol. 2: 1584-1599.
- Krumbein, W.C. (1944). *Shore currents and sand movement on a model beach*. Tech. Memo no. 7, US Army, Beach Erosion Board, Washington, D.C..
- Larras, J. (1957). *Plages et côtes de sable: collection du laboratoire national d'hydraulique*, Eyrolles, Paris, 117 pp. (in French).
- Larras, J. (1961). *Cours d'hydraulique maritime et de travaux maritimes*. Dunod, Paris, 459 pp. (in French).
- Larras, J. (1966). Cubes de sable charriés par la houle parallèlement à la côte. *Annales des Ponts et Chaussées*, No. 2: 71-76. (in French).
- Larras, J. and Bonnefille, R. (1965). Quantités de sable charriées par la houle parallèlement à la côte. *Congress IAHR, Leningrad*. Vol. 5: 233-236. (in French).
- Larson, M. and Kraus, N.C. (1989). *SBEACH: numerical model for simulating storm-induced beach change*. Report 1: Empirical foundation and model development. Tech. Report CERC-89-9, CERC, WES, US Army Corps of Eng., Vicksburg, M.S.
- Laubscher, W.I., Coppoolse, R.C., Schoonees, J.S. and Swart, D.H. (1991). A calibrated longshore transport model for Richards Bay. *Proc. of Coastal Sediments '91. ASCE, Seattle*. Vol. 1: 197-211.
- Laubscher, W.I., Schoonees, J.S., and Swart, D.H. (1989). *A calibrated longshore sediment transport model for Richards Bay*. CSIR Report EMA-C 89121, Ematek, Stellenbosch.
- Laubscher, W.I., Swart, D.H., Schoonees, J.S., Pfaff, W.M. and Davis A.B. (1990). The Durban beach restoration scheme after 30 years. *22 Intern. Conf. on Coastal Eng., ASCE, Delft*, Vol. 3: 3227-3238.
- Lee K.K. (1975). Longshore currents and sediment transport in west shore of Lake Michigan. *Water Resources Research*, Vol. 2 (6): 1029-1032.
- Longuet-Higgins, M.S. (1970). Longshore currents generated by obliquely incident sea waves, 1 and 2. *J. of Geophysical Res.*, Vol. 75(33): 6778-6801.
- Madsen, O.S. (1978). An analytical model of longshore sediment transport. *Workshop on Coastal Sediment Transport with Emphasis on the National Sediment Transport Study*. DEL-SG-15-78, Sea Grant College Program, Univ. of Delaware, Newark, Delaware.
- Madsen, O.S. (1987). Use of tracers in sediment transport studies. *Coastal Sediments '87, New Orleans*, Vol. 1: 424-435.
- Mangor, K., Sørensen, T. and Navntoft, E. (1984). Shore approach at the Danish North Sea Coast, monitoring of sedimentation in a dredged trench. *19 Intern. Conf. on Coastal Eng., ASCE, Houston*. Vol. 2: 1816-1829.
- Manohar, M. (1957). Sediment movement at south Indian ports. *6 Intern. Conf. On Coastal Eng., ASCE, Gainesville*. pp. 359-405.

- Manohar, M. (1962). Discussion of "Laboratory determination of littoral transport rate" by R.P. Savage. *J. of Waterways and Harbors Division, Proc. ASCE*, Vol. 88 (WW4): 144-147.
- Marama, K., Kajima, R., Narihiro, A. and Kondo, K., (1982). Study on sediment transport in a power station harbour basin. *18 Intern. Conf. on Coastal Eng., ASCE, Cape Town*. Vol. 2: 2357-2375.
- Mashima, Y., (1958). Study on littoral drift and longshore current. *Coastal Eng. in Japan*, Vol. 1: 85-96.
- Mashima, Y. (1960). A study on the volume of littoral drift. *Coastal Eng. in Japan*, Vol. 3: 63-88.
- McDougal, W.G. and Hudspeth, R.T. (1983). Longshore sediment transport on non-planar beaches. *Coastal Engineering*, Vol. 7(2): 119-131.
- Meadows, G.A. (1976). Time dependent fluctuations in longshore currents. *15 Intern. Conf. on Coastal Eng., ASCE, Honolulu, Hawaii*. Vol. 1: 660-680.
- Mizuguchi, M. and Horikawa, K. (1978). Experimental study on longshore current velocity distribution. *Bull. Fac. Sci. Eng., Chuo University, Tokyo*, Vol. 21: 123-150.
- Moore, B.D. (1982). Beach profile evolution in response to changes in water level and wave height. M.S. thesis, Univ. of Delaware, Newark, DE.
- Moore, G.W. and Cole, J.Y. (1960). *Coastal processes in the vicinity of Cape Thompson, Alaska: Geologic investigations in support of Project Chariot in the vicinity of Cape Thompson. Northwestern Alaska: preliminary report*. Report No. 753. Final Report US Geol. Survey Trace Elements Investigations.
- Morfett, J.C. (1990). A "virtual power" function for estimating the alongshore transport of sediment by waves. *Coastal Engineering*, Vol. 14: 439-456.
- Morfett, J.C. (1991). Numerical model of longshore transport of sand in the surf zone. *Proc. Instn. Civil Eng., Part 2*, Vol. 91: 55-70.
- Morsi, S.A. and Alexander, A.J. (1972). An investigation of particle trajectories in two-phase flow systems. *J. Fluid Mech.* Vol. 55(2): 193-208.
- Mülke, F.J. (1981). Stormwaterdreinerung van spoorbane. D. Ing. Thesis, University of Pretoria, Pretoria. (in Afrikaans).
- Münch-Petersen, (1933). Materialwanderung längs meerküsten ohne ebbe und flut. *IV Hydrologische Konferenz der Baltischen Staaten*. (in German).
- Münch-Petersen, (1936). Über Materialwanderung an Meeresküsten. *V. Hydrologische Konferenz der Baltischen Staaten, Helsinki*. (in German).
- Münch-Petersen (1938). Münch-Petersen's littoral drift formula. *The Bulletin of the Beach Erosion Board*, Vol. 4 (4): 1-31.
- Nadaoka, K. and Kondoh, T. (1982). Laboratory measurements of velocity field structure in the surf zone by LDV. *Coastal Eng. in Japan* 25: 125-145.
- Nadaoko, K., Ueno, S. and Igarashi, T. (1988). Field observations of three-dimensional large-scale eddies and sediment suspension in the surf zone. *Coastal Eng. in Japan* 31(2): 277-287.
- Nairn, R.B. (1990). Prediction of cross-shore sediment transport and beach profile evolution. Ph.D. thesis, Imperial College, University of London, London.
- Nakato, T. (1974). Wave-induced sediment entrainment from rippled beds. Ph.D. thesis, University of Iowa, Iowa City, Iowa.
- Nakato, T. (1984). Numerical integration of Einstein's integrals, I1 and I2. *J. Hydr. Eng., ASCE*, Vol. 110(12): 1863-1868.
- Nakato, T. (1990). Tests of selected sediment-transport formulas. *J. Hydr. Eng., ASCE*, Vol. 116(3): 362-379.

- Nayak, I.V. (1970). Equilibrium profiles of model beaches. 12 Intern. Conf. on Coastal Eng., ASCE, Washington, DC. Vol. 2: 1321-1340.
- Nichols, R.J. (1985). The stability of the shingle beaches in the eastern half of Christchurch Bay. Ph.D. thesis, University of Southampton, Southampton.
- Nicholls, J.N. and Wright, P. (1991). Longshore transport of pebbles: experimental estimates of K. *Coastal Sediments '91*, ASCE, Seattle. Vol. 1: 920-933.
- Nielsen, P. (1979). *Some basic concepts of wave sediment transport*. Series paper no. 20, Institute of Hydrodynamics and Hydraulic Engineering, Technical University of Denmark, Lyngby.
- Nielsen, P. (1984). Field measurements of time averaged suspended sediment concentrations under waves. *Coastal Eng.*, Vol. 8: 51-72.
- Nielsen, P. (1985). *A short manual of coastal bottom boundary layers and sediment transport*. Tech. Memo., Public Works Dept. New South Wales.
- Nielsen, P., Svendsen, I.A. and Staub, C. (1978). Onshore-offshore sediment movement on a beach. 16 *Intern. Conf. on Coastal Eng., ASCE, Hamburg*. Vol. 2: 1475-1492.
- O'Connor, B.A. and Yoo, D. (1987). Turbulence modelling of surf zone mixing processes. *Speciality Conf. on Hydrodynamics*, ASCE, Newark, Delaware. pp. 371-383.
- O'Connor, B.A. and Yoo, D. (1988). Mean bed friction of combined wave/current flow. *Coastal Eng.* 12:1-21.
- Oelerich, J. (1990). Zur berechnung des küstenparallelen sandtransportes. Dr. Ing. thesis, Technical University of Braunschweig, Braunschweig. (in German).
- Ostendorf, D.W. and Madsen, O.S. (1979). *An analysis of longshore currents and associated sediment transport in the surf zone*. Report MITSG 79-13, MIT, Cambridge, Massachusetts.
- Physkin, B.A., Maksimtchouk, V.L. and Zaitz, E.S. (1965). The investigation of littoral sand transport in seas and reservoirs. 11 *Congress IAHR, Leningrad*. Vol. 5: 151-152.
- Raw, P.N. (1993). *Determination of net longshore sediment transport rate in the sandtrap, Port of Durban, using volumetric calculations*. Internal Portnet report, Portnet, Durban.
- Readshaw, J.A. (1979). A model study of alongshore sediment transport. M. Sc. Thesis, Dept. of Civil Engineering, Queen's University, Kingston, Ontario.
- Riedel, H.J.P., Kamphuis, J.W. and Brebner, A. (1972), Measurement of bed shear stress under waves. 13 *Intern. Conf. on Coastal Eng., ASCE, Vancouver*. Vol. 1:587-603.
- Roelvink, J.A. (1987). *Large scale investigation of cross-shore sediment transport*. Report H596, Delft Hydraulics, Delft.
- Rooseboom, A. (1974). *Open channel fluid mechanics*. Technical Report TR 62, Dept. of Environment Affairs, Pretoria.
- Rooseboom, A. (1975). Sedimentafvoer in riviere en damkomme. (Sediment transport in rivers and reservoirs) D.Sc. Ing. Thesis, University of Pretoria, Pretoria (in Afrikaans).
- Rooseboom, A. (1992). *Sediment transport in rivers and reservoirs: a Southern African perspective*. Report 297/1, Water Research Commission, Pretoria.
- Rooseboom, A. (1998). The Cinderella of hydraulics - the law of the conservation of power. 3 Intern. Conf. on Hydrosience and Eng., Cottbus, Germany.
- Rooseboom, A. and Le Grange, A. (1992). Equilibrium scour in rivers with sandbeds. *Water SA*, Vol. 18: 287-292.

- Rooseboom, A. and Mülke, F.J. (1982). Erosion initiation. In: Walling, D.E. (ed.). *Recent developments in the explanation and prediction of erosion and sediment yield*. Publ. 137. IAHS, Paris.
- Rosati, J.D., Gingerich, K.J., Kraus, N.C., McKee Smith, J. and Beach, R.A. (1991). Longshore transport rate distributions measured in Lake Michigan. *Coastal Sediments '91, ASCE, Seattle*. Vol. 1: 156-169.
- Rossouw, J. (1989). Design waves for the South African coastline. Ph.D. thesis, University of Stellenbosch, Stellenbosch.
- Rouse, H. (1937). Modern conceptions of the mechanics of turbulence. *Trans. ASCE*, Vol. 102.
- Rouse, H. (1950). *Engineering Hydraulics*. John Wiley and Sons, New York. 770pp.
- Russell, R.C.H. (1960). Use of fluorescent tracers for the measurement of littoral drift. *7 Conf. on Coastal Eng., ASCE, Berkeley*. Vol. 1: 418-444.
- Sánchez-Arcilla, A., Vidas, A. and Pous, J. (1988). Improved longshore sand transport evaluation. *21 Intern. Conf. on Coastal Eng., ASCE, Malaga*. Vol. 2: 1382-1395.
- Sato, S. (1962). Sand movement at Fukue Coast in Atsumi Bay, Japan, and its observation by radioactive glass sand. *Coastal Eng. in Japan*, Vol. 5: 81-92.
- Sato, S. and Tanaka, N. (1966). Field investigation on sand drift at Port Kashima facing the Pacific Ocean. *10 Intern. Conf. on Coastal Eng., ASCE, Tokyo*. Vol. 1: 595-614.
- Sauvage de Saint Marc, M.G. and Vincent, M.G. (1954). Transport littoral formation de fleches et de tombolos. *5 Intern. Conf. on Coastal Eng., ASCE, Grenoble*. pp. 296-328. (in French).
- Savage, R.P., (1959). *Laboratory study of the effect of groins on the rate of littoral transport: equipment development and initial tests*. Tech. Memo No. 114, U.S. Army, Beach Erosion Board. 56pp.
- Savage, R.P. (1962). Laboratory determination of littoral-transport rates. *J. Waterways and Harbors Division*, Vol. 88 (WW2): 69-92.
- Saville, T. (Jr.) (1950). Mode of sand transport along an infinitely long, straight beach. *Transactions, American Geophysical Union*, Vol. 31 (4): 555-565.
- Sawaragi, T. and Deguchi, I. (1978). Distribution of sand transport rate across a surf zone. *16 Intern. Conf. On Coastal Eng., ASCE, Hamburg*. Vol. 2: 1596-1613.
- Sawaragi, T. and Murakami T. (1957). On the estimation of the rate of littoral sand drift. *4 Conf. on Coastal Eng. in Japan*.
- Sayao, O.S.F.J. and Kamphuis, J.W. (1983). *Littoral sand transport: review of the state of the art (1982)*. Civil Engineering Report no. 78, Queens University, Kingston, Ontario.
- Schoonees, J.S. (1990). Field measurements of suspended sediment concentrations in the surf zone at Walker Bay. In: Soulsby, R. and Bettess, R. (eds.) *Euromech 262: sand transport in rivers, estuaries and the sea*. Wallingford.
- Schoonees, J.S. (1997). *Evaluation of a number of longshore transport formulae*. CSIR Research Report, Stellenbosch. (in preparation).
- Schoonees, J.S. (2000). Annual variation in the net longshore sediment transport rate. *Coastal Eng.*, Vol. 40(2): 141-160.
- Schoonees, J.S. and Bartels, A. (1991). North-eastern False Bay: physical environmental factors and bathing suitability. False Bay Symposium, Cape Town. *Trans. of Royal Society of South Africa*, Vol. 47 (Parts 4 and 5): 757-770.
- Schoonees, J.S. and Barwell, L. (1991). Waenhuiskrans: sediment budget and reactivation of a sediment pathway. *Coastal Sediments '91, ASCE, Seattle, Washington*. Vol. 2: 2277-2291.

- Schoonees, J.S. and Theron, A.K. (1993). Review of the field-data base for longshore sediment transport. *Coastal Eng.*, Vol. 19: 1-25.
- Schoonees, J.S. and Theron, A.K. (1994). Accuracy and applicability of the SPM longshore transport formula. *24 Intern. Conf. on Coastal Eng., ASCE, Kobe*. Vol. 3: 2595-2609.
- Schoonees, J.S. and Theron, A.K. (1995). Evaluation of 10 cross-shore sediment transport/morphological models. *Coastal Eng.*, Vol. 25: 1-41.
- Schoonees, J.S. and Theron, A.K. (1996). Improvement of the most accurate longshore transport formula. *25 Intern. Conf. on Coastal Eng., ASCE, Orlando, Florida*. Vol. 3: 3652-3665.
- Seymour, R.J. and Castel, D. (1985). Episodicity in longshore sediment transport. *J. Waterways, Port, Coastal and Ocean Eng.*, Vol. 111 (3): 542-551.
- Scripps Institute of Oceanography (1974). *A statistical study of wave conditions at five locations along the California Coast*. Wave Report No. 68. University of California, San Diego.
- Shay, E.A. and Johnson, J.W. (1951). *Model studies on the movement of sand transported by wave action along a straight beach*. Issue 7. Series 14, Inst. Of Eng. Research, University of California, Berkeley, California.
- Shi-Leng, X. and Teh-Fu, L. (1987). Long-term variation of longshore sediment transport. *Coastal Eng.* 11:131-140.
- Shinohara, K., Tsubaki, T., Yoshitaka, M. and Agemori, C. (1958). Sand transport along a model sandy beach by wave action. *Coastal Eng. in Japan*, Vol. 1: 111-130.
- Shiraishi, N. (1959). The measurement of littoral drift at shoreline harbors. *Coastal Eng. in Japan*, Vol. 2: 59-71.
- Sireyjol, P. (1964). Communication sur la construction du port de Cotonou (Dahomey). *9 Intern. Conf. on Coastal Eng., ASCE, Lisbon*. pp. 580-595. (in French).
- Slomianko, P. (1960). Sur l'évaluation de certaines caractéristiques du transport littoral à la base des données météorologiques. *7 Intern. Conf. on Coastal Eng., ASCE, The Hague*. Vol. 1: 375-385. (in French).
- Spring, F.J.E. (1920). Coastal sand travel near Madras Harbour. *Min. Proc. Inst. of Civil Eng., London*, Vol. 210: 27-52.
- Steezel, H. (1987). *Systematic Investigation of Dune Revetments: Large-scale model tests*. Report H298-I, Delft Hydraulics, Delft.
- Steezel, H.J. (1993). Cross-shore transport during storm surges. D.Sc. Thesis, Delft University of Technology, Delft.
- Sternberg, R.W., Shi, N.C. and Downing, J.P. (1984). Field investigations of suspended sediment transport in the nearshore zone. *19 Intern. Conf. on Coastal Eng., ASCE, Houston, Texas*. Vol. 2: 1782-1798.
- Svasek, J.N. and Engel, H. (1960). Use of a radio-active tracer for the measurement of sediment transport in the Netherlands. *7 Intern. Conf. on Coastal Eng., ASCE, The Hague*. Vol. 1: 445:454.
- Svendsen, I.A. and Lorentz, R.S. (1989). Velocities in combined undertow and longshore currents. *Coastal Eng.*, Vol. 13: 55-79.
- Swart, D.H. (1974). *Offshore sediment transport and equilibrium beach profiles*. Publication no. 131, Delft Hydraulics Laboratory, 302pp.
- Swart, D.H. (1976a). Predictive equations regarding coastal transports. *15 Intern. Conf. on Coastal Eng., ASCE, Honolulu, Hawaii*. Vol. 2: 1113-1132.

- Swart, D.H. (1976b). *Coastal sediment transport: Computation of longshore transport*. Report R968, Part 1, Delft Hydraulics Laboratory. 112pp.
- Swart, D.H. (1981). Effect of Richards Bay harbour development on the adjacent coastline. 25 *PIANC, Edinburgh*, Vol. 5: 899-917.
- Swart, D.H. and Fleming, C.A. (1980). Longshore water and sediment movement. 17 *Intern. Conf. on Coastal Eng., ASCE, Sydney*. Vol. 2: 1275-1294.
- Tanaka, H. and Shuto, N. (1981). Friction coefficient for a wave-current coexistent system. *Coastal Eng. in Japan*, Vol. 24: 105-128.
- Tsuchiya, Y. (1982). The rate of longshore sediment transport and beach erosion control. 18 *Intern. Conf. on Coastal Eng., ASCE, Cape Town*. Vol. 2: 1326-1334.
- US Army, Corps of Engineers (1984). *Shore Protection Manual*, Volumes I and II, Coastal Engineering Research Center, Vicksburg.
- Van de Graaff, J. and Van Overeem, J. (1979). Evaluation of sediment transport formulae in coastal engineering practice. *Coastal Eng.* Vol. 3 (1): 1-32.
- Van der Meer, J.W. (1990). Static and dynamic stability of loose materials. In: Pilarczyk, K.W. (ed.) *Coastal protection*. Balkema, Rotterdam.
- Van der Meer, J.W. and Veldman, J.J. (1992). Singular points at berm breakwaters: scale effects, rear, round head and longshore transport. *Coastal Eng.*, Vol. 17:153-171.
- Van Hijum, E. and Pilarczyk, K.W. (1982). *Equilibrium profile and longshore transport of coarse material under regular and irregular wave attack*. Publication No. 274, Delft Hydraulics Laboratory, Delft.
- Van Rijn, L.C. (1984). Sediment transport, Part I: Bed load transport. *J. Hydr. Eng., ASCE*, Vol. 110 (10): 1431-1456.
- Van Rijn, L.C. (1989). *Handbook: sediment transport by currents and waves*. Report H461, Delft Hydraulics Laboratory, Delft.
- Van Rijn, L.C. (1991). *Data base: sand concentration profiles and sand transport for currents and/or waves*. Report H1148, Delft Hydraulics Laboratory, Delft.
- Vellinga, P. (1984). *Large-scale Dune Erosion Tests in the Deltaflume*. Report M1263-III A/B, Delft Hydraulics Laboratory, Delft. (in Dutch).
- Visser, P.J. (1991). Laboratory measurements of uniform longshore currents. *Coastal Eng.*, Vol. 15:563-593.
- Vitale, P. (1981). *Movable-bed laboratory experiments comparing radiation stress and energy flux factor as predictors of longshore transport*. Miscellaneous Report No. 81-4, U.S. Army, Coastal Eng. Res. Center. 94pp.
- Voitsekhovich, O.V. (1986). *Longshore sediment transport: generalized relations and observation data*. Ukrainian State Planning, Surveying, and Scientific-Research Institute of Water-Management Construction. Translated from: *Vodnye Resursy*, No. 5, September - October, 1986, pp. 108-115.
- Walpole, R.E. and Myers, R.H. (1978). *Probability and statistics for engineers and scientists*. MacMillan Publishing Co., New York.
- Walton, T.L. (Jr) (1978). Sediment trap at Panama City. *Workshop on Coastal Sediment Transport with Emphasis on the National Sediment Transport Study, DEL-SG-15-78*. Sea Grant College Program, University of Delaware, Newark, Delaware, pp. 93-94.

- Walton, T.L. (Jr.) and Chiu, T.Y. (1979a). *Littoral sand transport on beaches*. Report no. UFL-COEL-TR-041, Univ. Of Florida, Gainesville.
- Walton, T.L. (Jr.) and Chiu, T.Y. (1979b). A review of analytical techniques to solve the sand transport equation and some simplified solutions. *Coastal Structures '79, Alexandria*. Vol. 2: 809-837.
- Wang, Y.-H. And Chang, T.H. (1978). Littoral drift along bayshore of a barrier island. *16 Intern. Conf. on Coastal Eng., ASCE, Hamburg*. Vol. 2: 1614-1625.
- Watanabe, A. (1985), Three-dimensional predictive model of beach evolution around a structure. *Water wave research: theory, laboratory and field*. Hannover, pp. 121-141.
- Watanabe, A., Shimizu, T. and Kondo, K. (1991). Field application of a numerical model of beach topography change. *Coastal Sediments '91, ASCE, Seattle, Washington*. Vol. 2: 1814-1828.
- Watts, G.M. (1953). *A study of sand movement at South Lake Worth inlet, Florida*. Tech. memo No. 42, U.S. Army, Beach Erosion Board. 24pp.
- White, T.E. (1987). Nearshore sand transport. Ph.D. thesis, University of California, San Diego. 210pp.
- White, W.R., Milli, H. and Crabbe, A.D. (1973). *Sediment transport: an appraisal of available methods*, Volumes 1 and 2. Report INT 119, Hydr. Res. Station, Wallingford. 150pp.
- Willis, D.H. (1978). Sediment load under waves and currents. *16 Intern. Conf. on Coastal Eng., ASCE, Hamburg*. Vol. 2: 1626-1637.
- Willis, D.H. (1979). Sediment load under waves and currents. Reprint of article from *DME/NAE Quarterly Bulletin* No. 1979(3), National Research Council Canada, Ottawa.
- Willis, D.H. (1980). Evaluation of sediment transport formulae in coastal engineering practice: discussion. *Coastal Eng.* Vol. 4 (2): 177-180.
- Willis, D.H. and Price, W.A. (1975), Trends in the application of research to solve coastal engineering problems. In: Hails, J.R. and Carr, A. (eds.). *Nearshore sediments dynamics and sedimentation*. John Wiley and Sons, New York. ch. 5.
- Wyrski, K. (1953). The balance of littoral transport in the surf zone. *Deutsche Hyd. Zeit.* Vol. 6: 65-76 (in German).

TABLE 2.1: LONGSHORE TRANSPORT DATA EVALUATION

NO	REFERENCE	LOCATION AND DATA SET	TOTAL
<i>Bulk transport rates</i>			
12	Bijker (1968)	Abidjan	19
4	Adachi <i>et al.</i> (1959)	Miyazu	24
10	Fairchild (1977)	Ventnor	36
3	Ishihara <i>et al.</i> (1958)	North Akashi, Miyazu	37
10	Fairchild (1977)	Nags Head	37
2	Watts (1953)	South Lake Worth	42
1	Caldwell (1956)	Anaheim Bay	46
17	Kana (1977)	Price Inlet	48
25	Nicholls and Wright (1991)	South England	48
6	Delorme (1981)	North Africa	49
5	Moore and Cole (1960)	Cape Thompson	50
8	Sireyjol (1964)	Cotonou	51
9	Castanho (1966)	Aveiro	52
9	Castanho (1966)	Lobito	52
20	Knoth and Nummedal (1977)	Bull Island	52
30	Laubscher <i>et al.</i> (1989, 1991)	Richards Bay	54
18	Bruno <i>et al.</i> (1981)	Channel Islands Harbor, 1	55
19	Chang and Wang (1978)	Santa Rosa Island	55
27	Mangor <i>et al.</i> (1981)	Danish North Sea	55
31	Kraus <i>et al.</i> (1989)	Duck	55
14	Duane and James (1980)	Point Mugu	56
29	Bodge (1986)	Duck, 2	56
15	Hou <i>et al.</i> (1980)	Taichung Harbour	57
16	Lee (1975)	Lake Michigan	57
22	Kana and Ward (1980)	Duck	57
29	Bodge (1986)	Duck, 3	57
33	Chadwick (1989)	Shoreham, M6, M7	57
11	Sato and Tanaka (1966)	Port Kashima	58
32	Voitsekhovich (1986)	Black Sea	58
34	Hou (1988)	North-west Taiwan	58
35	Caviglia <i>et al.</i> (1991)	Mar del Plata	58
28	Kooistra and Kamphuis (1984)	Pointe Sapin NOV4	60
33	Chadwick (1989)	Shoreham, M1-M5	60
7	Sato (1962)	Fukue, Atsumi	61
29	Bodge (1986)	Duck, 4	61
13	Komar and Inman (1970)	El Moreno, Silver Strand	62
24	Dean <i>et al.</i> (1982, 1987)	Rudee Inlet	63
26	Kraus <i>et al.</i> (1982)	Japan	63
21	Inman <i>et al.</i> (1980)	Torrey Pines	64
18	Bruno <i>et al.</i> (1981)	Channel Islands Harbor, 2	67
23	Gable (1981)	Leadbetter Beach	68
28	Kooistra and Kamphuis (1984)	Pointe Sapin, OCT25	71
<i>Local transport rates</i>			
2	Downing (1984)	Twin Harbors Beach	44
1	Sawaragi and Deguchi (1978)	Isonoura	47
1	Sawaragi and Deguchi (1978)	Matsubo	49
6	White (1987)	Torrey Pines, SIO	50
7	Kraus <i>et al.</i> (1988, 1989)	Duck	55
4	Mangor <i>et al.</i> (1984)	Danish North Sea	56
5	Bodge (1986)	Duck, 2	56
5	Bodge (1986)	Duck, 3	57
5	Bodge (1986)	Duck, 4	61
3	Kraus <i>et al.</i> (1982)	Japan	63

TABLE 2.2: CONFIDENCE BANDS OF THE FACTOR, FLOATING MEAN NET LONGSHORE TRANSPORT / TRUE LONG-TERM MEAN NET TRANSPORT

Confidence limit (%)	Period (years) over which the mean was computed							
	1	2	3	4	5	6	7	8
95	-0,37	-0,05	0,17	0,32	0,41	0,48	0,55	0,62
5	2,40	2,20	2,03	1,84	1,70	1,51	1,38	1,25
80	0,28	0,44	0,52	0,58	0,63	0,68	0,70	0,74
20	1,70	1,60	1,51	1,46	1,37	1,28	1,18	1,13

TABLE 3.1: SUMMARY OF THE LONGSHORE TRANSPORT FORMULAE

CATEGORY	NUMBER*	NAME OF THE FORMULA	ABBREVIATION**	TYPE OF FORMULA
(a) Energetics (energy flux) approach	1	SPM	SPM	Bulk
	2	SPM and Swart	SPMSW	Bulk
	3	SPM, Kamphuis and Readshaw	SPMKR	Bulk
	4	SPM and Bailard (bulk transport rate)	SPMBA	Bulk
	5	SPM and Komar	SPMVER	Detailed
	6	Watts	WATTS	Bulk
	7	Caldwell	CALDW	Bulk
	8	Manohar	MANO	Bulk
	9	Pyshkin, Maksimtchouk and Zaitz	PMZ	Bulk
	10	Castanho	CAST	Bulk
	11	Dean	DEAN	Bulk
	12	Walton and Chiu, 1	WALT + C1	Bulk
	13	Walton and Chiu, 2	WALT + C2	Detailed
	14	Hou, Lee and Lin, 1	HLL1	Bulk
	15	Hou, Lee and Lin, 2	HLL2	Bulk
	16	Hallermeier, 1	HALLER1	Bulk
	17	Hallermeier, 2	HALLER2	Bulk
	18	Bailard (local transport rate)	BAILARD	Detailed
	19	Chadwick	CHADWK	Bulk
	20	Van Hījum, Pilarczyk and Chadwick	SVHPC	Bulk
	21	Brampton, Motyka and Chadwick	SBMC	Bulk
(b) Shear stress (modified steady flow) approach	22	Iwagaki and Sawaragi	IWSA	Bulk
	23	Bijker, 1	BIJKER1	Detailed
	24	Bijker, 2	BIJKER2	Detailed
	25	Engelund, Hansen and Swart	EHS	Detailed
	26	Ackers, White and Willis	WIL/1000	Detailed
	27	Ackers, White, Swart and Lenhoff	SWART	Detailed
	28	Sawaragi and Deguchi	SAD/1000	Detailed
	29	Madsen	MADSEN	Bulk
	30	Ostendorf and Madsen	OSMAD	Detailed

Table 3.1 (continued)

CATEGORY	NUMBER*	NAME OF THE FORMULA	ABBREVIATION**	TYPE OF FORMULA
(c) Product of the shear stress and longshore longshore current velocity	31	Watanabe	WATANABE	Detailed
	32	Bodge	BODGE	Detailed
	33	Kraus, Gingerich and Rosati, 3	KGR3	Detailed
	34	Morfett	MORFETT	Bulk
(d) Dimensional analysis	35	Kamphuis, Davies, Naim and Sayao	KDNS	Bulk
	36	Sánchez-Arcilla, Vidoar and Pous	SAVP	Bulk
	37	Kamphuis	KAMPH2	Bulk
(e) Suspended sediment concentration and longshore current velocity	38	Fleming	FLEMING	Detailed
	39	Nielsen	NIELSEN	Detailed
	40	Tsuchiya	TSUCHIYA	Bulk
	41	Voitsekhovich	VOITSEK	Bulk
	42	Deigaard, Fredsøe and Hedegaard	DFH	Bulk
	43	Sauvage de Saint Marc, Vincent and Larras, 1	SVL1	Bulk
(f) Empirical	44	Sauvage de Saint Marc, Vincent and Larras, 2	SVL2	Bulk
	45	Larras, Bonnefille and Pernecker, 1	LBP1	Bulk
	46	Larras, Bonnefille and Pernecker, 2	LBP2	Bulk
	47	Kraus, Isobe, Igarashi, Sasaki and Horikawa	KIISH	Bulk
	48	Kraus, Gingerich and Rosati, 1	KGR1	Bulk
	49	Kraus, Gingerich and Rosati, 2a	KGR2a	Detailed
	50	Kraus, Gingerich and Rosati, 2b	KGR2b	Detailed
	51	Van der Meer	VDMEEER	Bulk

* Number of the formula as used in the text.

** The abbreviation is displayed for identification on Figures 4.2a to 4.12c.

TABLE 4.1: STANDARD ERROR OF ESTIMATE (σ) FOR EACH FORMULA

CATEGORY	NUMBER*	NAME OF THE FORMULA	NUMBER OF DATA POINTS**	σ
(a) Energetics (energy flux) approach	1	SPM	119	0,708
	2	SPM and Swart	119	0,720
	3	SPM, Kamphuis and Readshaw	123	0,515
	4	SPM and Bailard (bulk transport rate)	119	0,741
	5	SPM and Komar	119	1,069
	6	Watts	123	0,685
	7	Caldwell	123	0,579
	8	Manohar	123	0,709
	9	Pyshkin, Maksimtchouk and Zaitz	109	1,017
	10	Castanho	123	1,118
	11	Dean	123	0,633
	12	Walton and Chiu, 1	123	0,734
	13	Walton and Chiu, 2	123	1,114
	14	Hou, Lee and Lin, 1	123	0,569
	15	Hou, Lee and Lin, 2	123	0,561
	16	Hallermeier, 1	123	0,563
	17	Hallermeier, 2	123	0,723
	18	Bailard (local transport rate)	123	0,753
	19	Chadwick	114	1,073
	20	Van Hijum, Pilarczyk and Chadwick	123	0,417
	21	Brampton, Motyka and Chadwick	123	0,793
(b) Shear stress (modified steady flow) approach	22	Iwagaki and Sawaragi	123	1,312
	23	Bijker, 1	123	0,928
	24	Bijker, 2	118	0,776
	25	Engelund, Hansen and Swart	123	0,611
	26	Ackers, White and Willis	123	1,278***
	27	Ackers, White, Swart and Lenhoff	123	0,750
	28	Sawaragi and Deguchi	123	2,895
	29	Madsen	123	0,959
	30	Ostendorf and Madsen	123	0,824

Table 4.1 (continued)

CATEGORY	NUMBER*	NAME OF THE FORMULA	NUMBER OF DATA POINTS**	σ
(c) Product of the shear stress and longshore current velocity	31	Watanabe	123	0,707
	32	Bodge	119	2,063
	33	Kraus, Gingerich and Rosati, 3	123	1,869
	34	Morfett	109	1,046
(d) Dimensional analysis	35	Kamphuis, Davies, Naim and Sayao	119	0,599
	36	Sánchez-Arcilla, Vidoar and Pous	118	0,655
	37	Kamphuis	123	0,413
(e) Suspended sediment concentration and longshore current velocity	38	Fleming	123	0,684
	39	Nielsen	123	1,130
	40	Tsuchiya	123	0,619
	41	Voitsekhovich	123	1,184
	42	Deigaard, Fredsøe and Hedegaard	109	0,640
(f) Empirical	43	Sauvage de Saint Marc, Vincent and Larras, 1	89	0,530
	44	Sauvage de Saint Marc, Vincent and Larras, 2	58	0,812
	45	Larras, Bonnefille and Pernecker, 1	109	0,601
	46	Larras, Bonnefille and Pernecker, 2	66	0,504
	47	Kraus, Isobe, Igarashi, Sasaki and Horikawa	123	0,625
	48	Kraus, Gingerich and Rosati, 1	115	1,092
	49	Kraus, Gingerich and Rosati, 2a	72	1,732
	50	Kraus, Gingerich and Rosati, 2b	37	1,945
	51	Van der Meer	123	0,449

* Number of the formula as used in the text.

** The number of data points varies because some formulae could not be applied for all the data points.

*** Predictions were divided by 1 000 before calculating σ .

TABLE 4.2: PERCENTAGE OCCURRENCE OF THE DISCREPANCY RATIOS (r_d) FOR EACH FORMULA

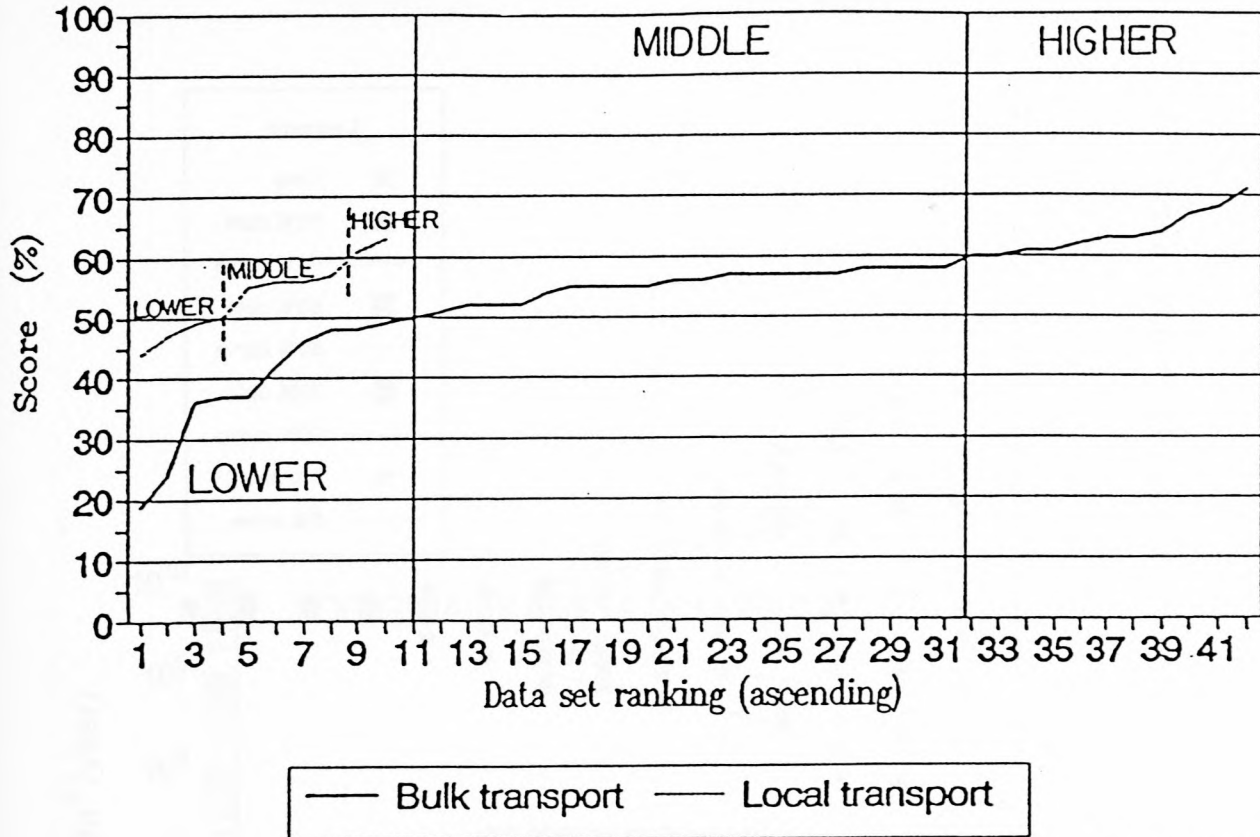
CATEGORY	NUMBER*	NAME OF THE FORMULA	PERCENTAGE OCCURRENCE OF r_d BETWEEN:	
			0,5 and 2	0,25 and 4
(a) Energetics (energy flux) approach	1	SPM	42,0	58,0
	2	SPM and Swart	42,0	58,0
	3	SPM, Kamphuis and Readshaw	65,0	95,1
	4	SPM and Bailard (bulk transport rate)	46,2	66,7
	5	SPM and Komar	10,9	33,6
	6	Watts	42,2	65,0
	7	Caldwell	56,1	75,6
	8	Manohar	56,9	78,9
	9	Pyshkin, Maksimtchouk and Zaitz	10,1	22,0
	10	Castanho	21,6	82,4
	11	Dean	36,6	62,6
	12	Walton and Chiu, 1	40,7	75,6
	13	Walton and Chiu, 2	35,8	95,9
	14	Hou, Lee and Lin, 1	53,7	73,2
	15	Hou, Lee and Lin, 2	52,8	76,4
	16	Hallermeier, 1	56,9	94,3
	17	Hallermeier, 2	53,6	92,7
	18	Bailard (local transport rate)	39,2	60,0
	19	Chadwick	28,9	100,0
	20	Van Hijum, Pilarczyk and Chadwick	64,2	90,2
	21	Brampton, Motyka and Chadwick	46,3	99,2
(b) Shear stress (modified steady flow) approach	22	Iwagaki and Sawaragi	35,8	100,0
	23	Bijker, 1	33,1	76,9
	24	Bijker, 2	50,8	99,2
	25	Engelund, Hansen and Swart	50,4	87,0
	26	Ackers, White and Willis	23,1**	54,5**
	27	Ackers, White, Swart and Lenhoff	47,4	84,5
	28	Sawaragi and Deguchi	0,8**	9,8**
	29	Madsen	23,5	42,0
	30	Ostendorf and Madsen	23,6	45,5

Table 4.2: (continued)

CATEGORY	NUMBER*	NAME OF THE FORMULA	PERCENTAGE OCCURRENCE OF r_d BETWEEN:	
			0,5 and 2,0	0,25 and 4,0
(c) Product of the shear stress and longshore current velocity	31	Watanabe	49,6	91,2
	32	Bodge	5,9	98,3
	33	Kraus, Gingerich and Rosati, 3	2,4	98,4
	34	Morfett	40,4	98,2
(d) Dimensional analysis	35	Kamphuis, Davies, Naim and Sayao	42,0	73,1
	36	Sánchez-Arcilla, Vidoor and Pous	36,4	60,2
	37	Kamphuis	52,0	83,7
(e) Suspended sediment concentration and longshore current velocity	38	Fleming	56,1	97,6
	39	Nielsen	11,4	23,6
	40	Tsuchiya	52,0	69,9
	41	Voitsekovich	19,0	86,0
	42	Deigaard, Fredsøe and Hedegaard	52,3	73,4
(f) Empirical	43	Sauvage de Saint Marc, Vincent and Larras, 1	57,3	92,1
	44	Sauvage de Saint Marc, Vincent and Larras, 2	46,6	100,0
	45	Larras, Bonnefille and Pernecker, 1	47,7	72,5
	46	Larras, Bonnefille and Pernecker, 2	55,9	88,2
	47	Kraus, Isobe, Igarashi, Sasaki and Horikawa	46,3	86,2
	48	Kraus, Gingerich and Rosati, 1	41,0	75,2
	49	Kraus, Gingerich and Rosati, 2a	12,5	100,0
	50	Kraus, Gingerich and Rosati, 2b	2,7	100,0
	51	Van der Meer	60,2	82,9

* Number of the formula as used in the text.

** Predictions were divided by 1 000 before calculating the percentages.



(From Schoonees and Theron, 1993)

Figure 2.1: Longshore transport data evaluation

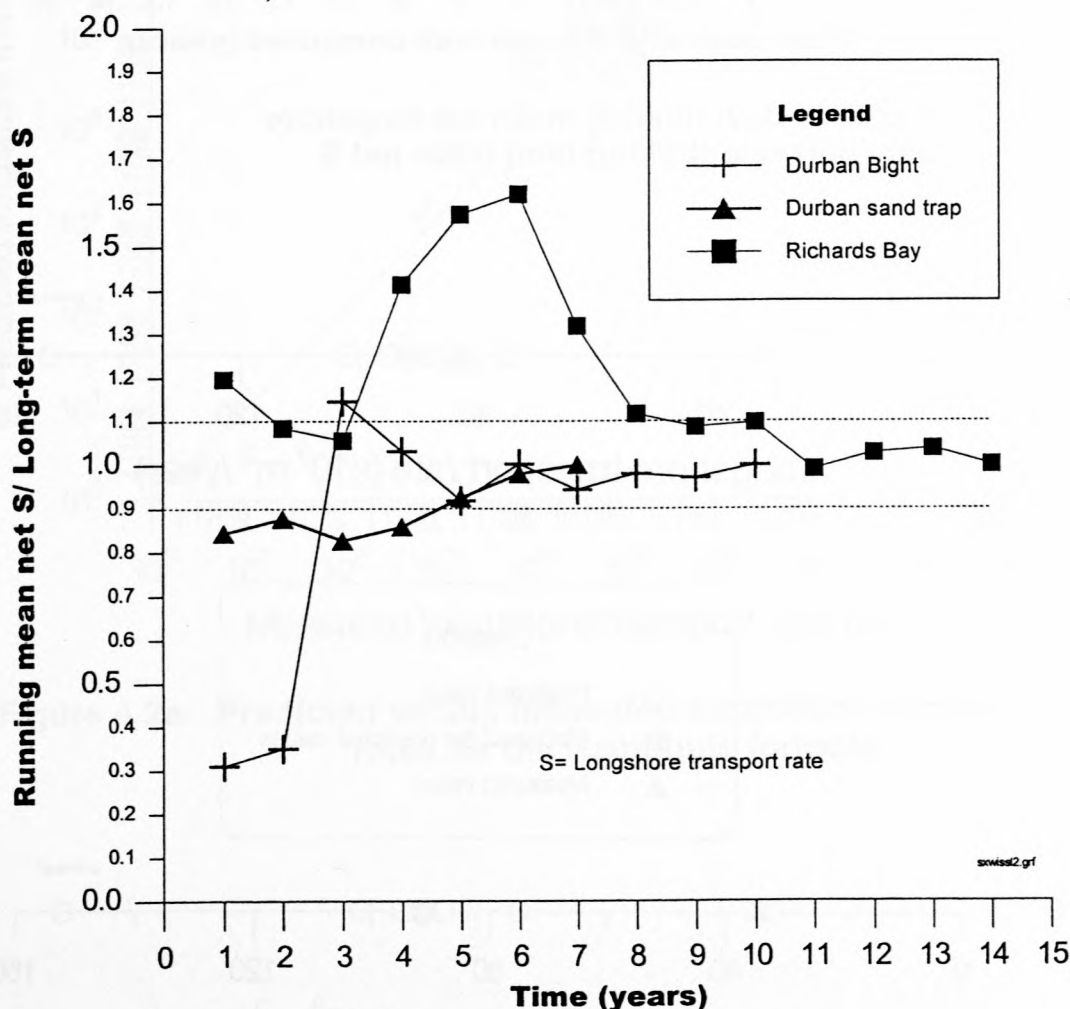


Figure 2.2: Variation of the running mean net longshore transport rates over time

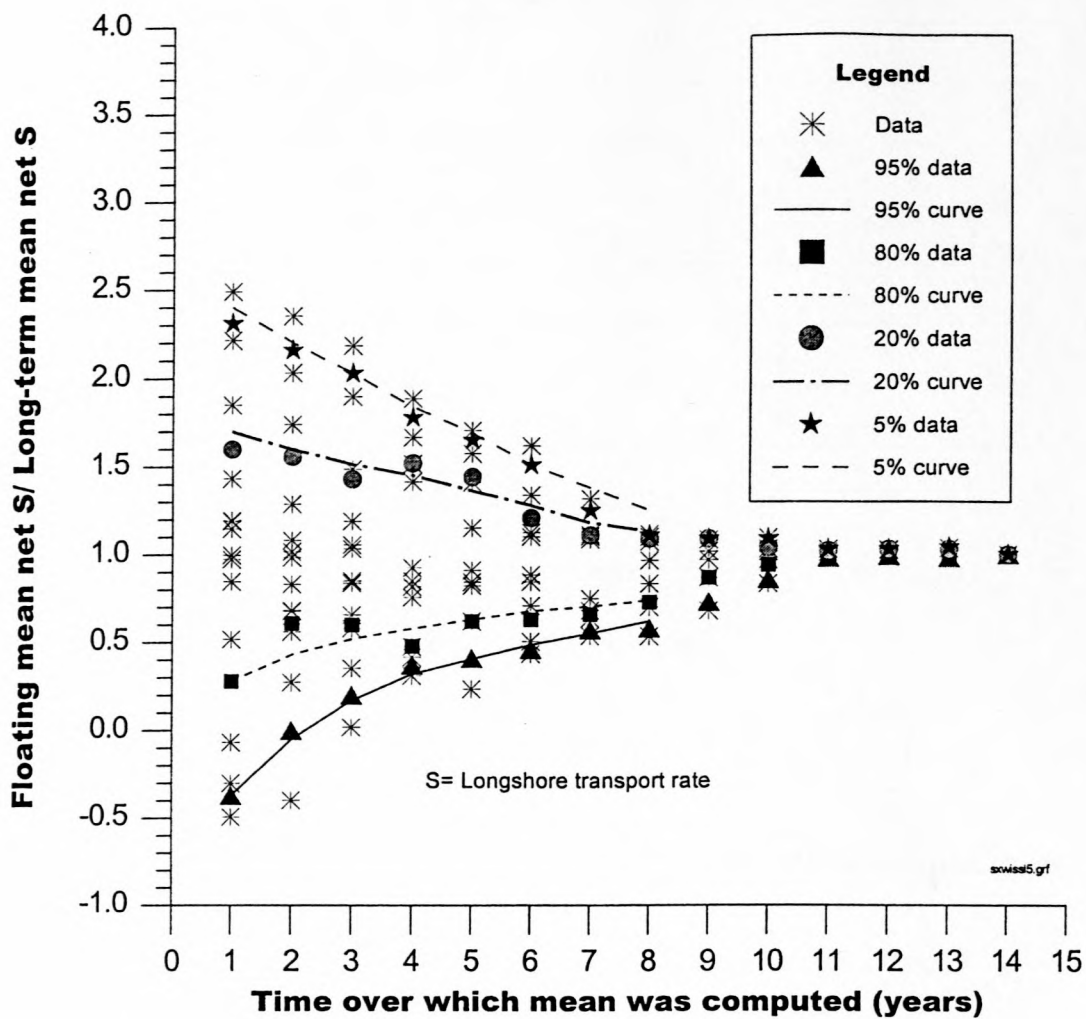


Figure 2.3: Richards Bay: floating mean net longshore transport rate (S)/long-term mean net S

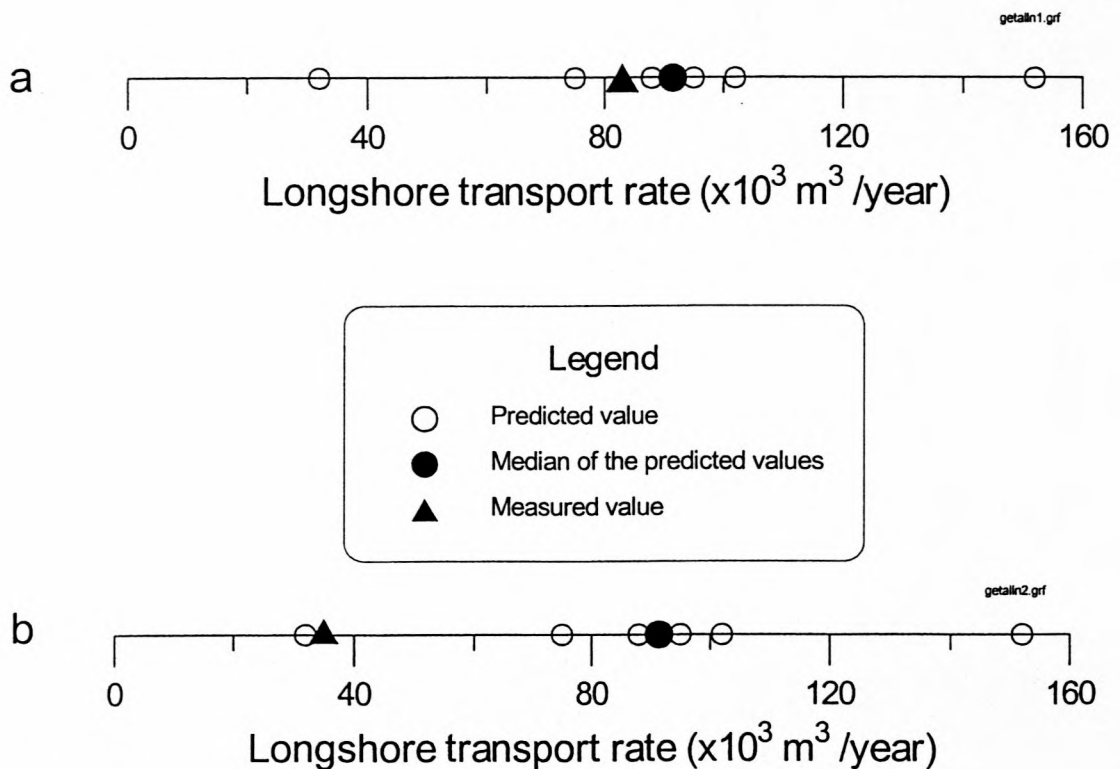


Figure 4.1: Comparing predictions with measured data

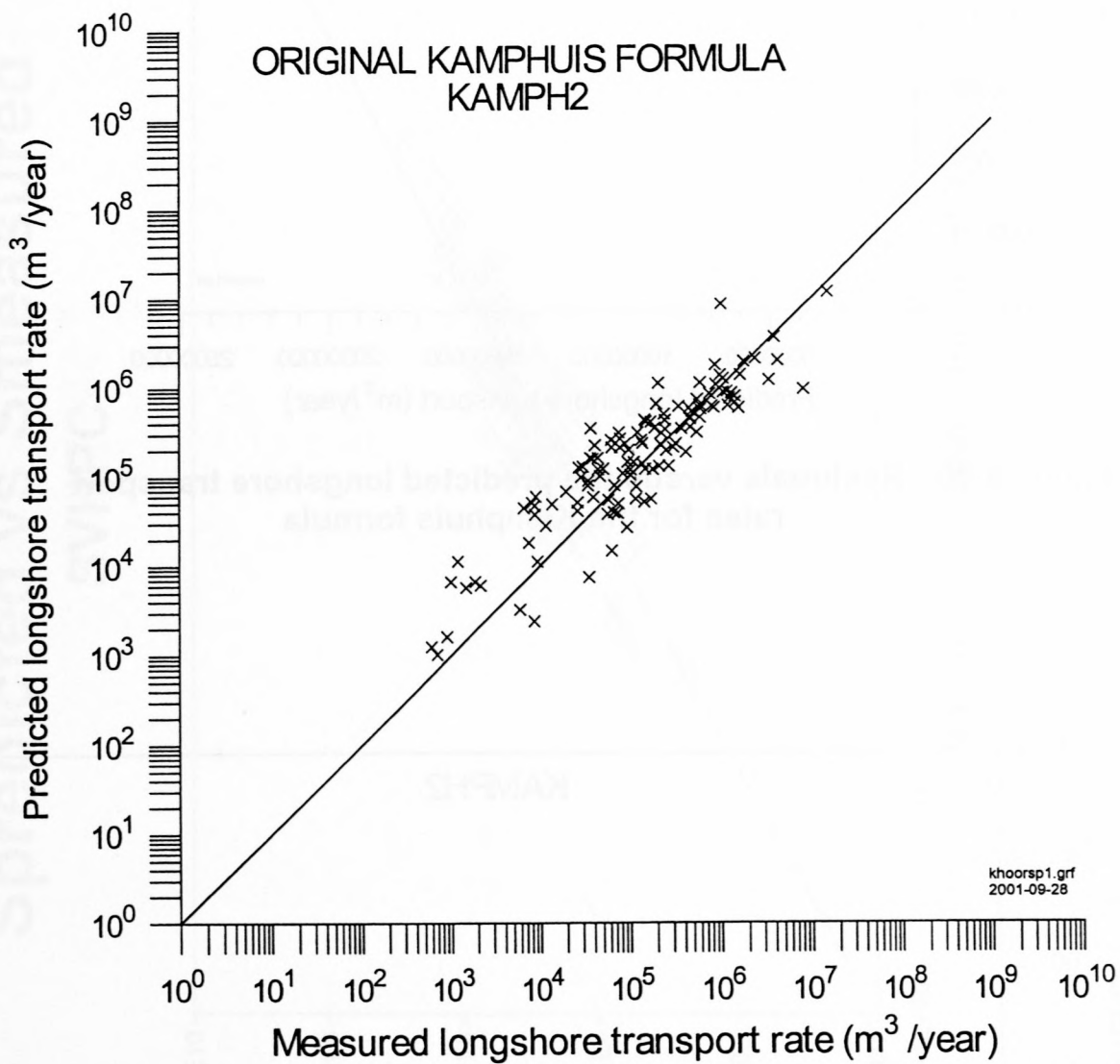


Figure 4.2a: Predicted versus measured longshore transport rates for the Kamphuis formula

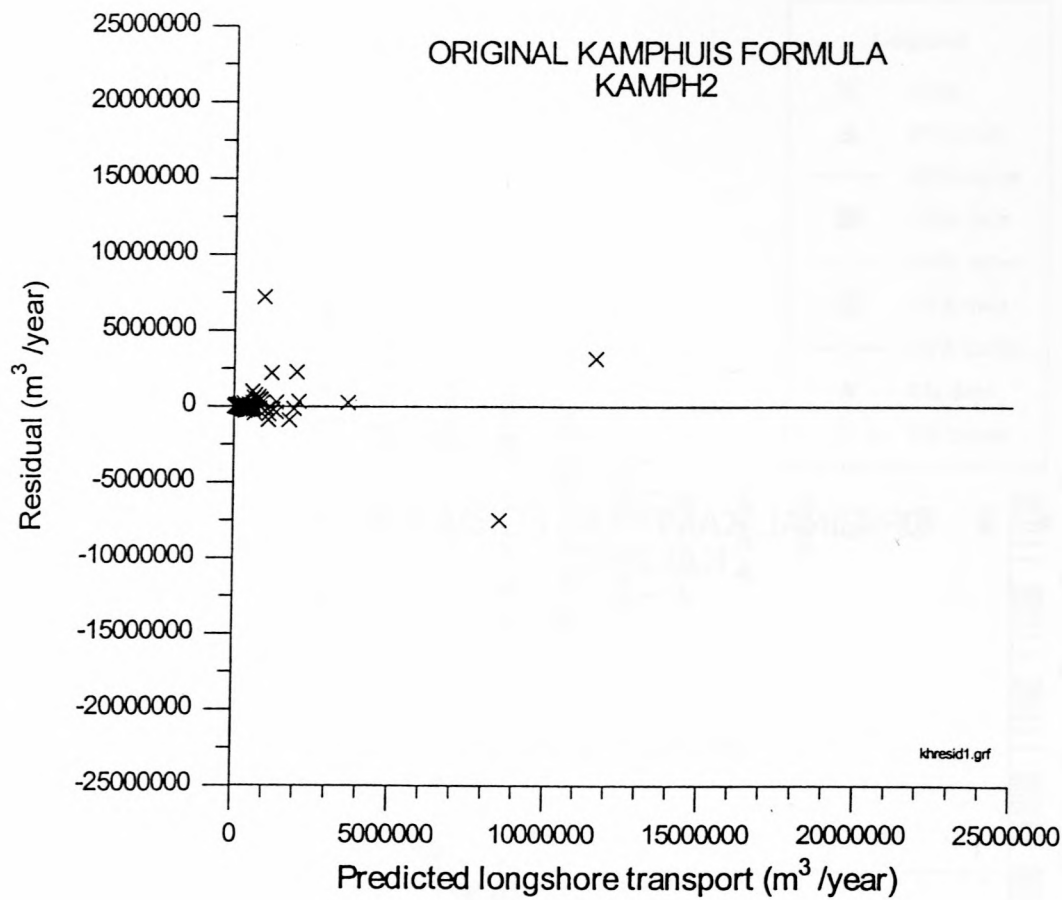


Figure 4.2b: Residuals versus the predicted longshore transport rates for the Kamphuis formula

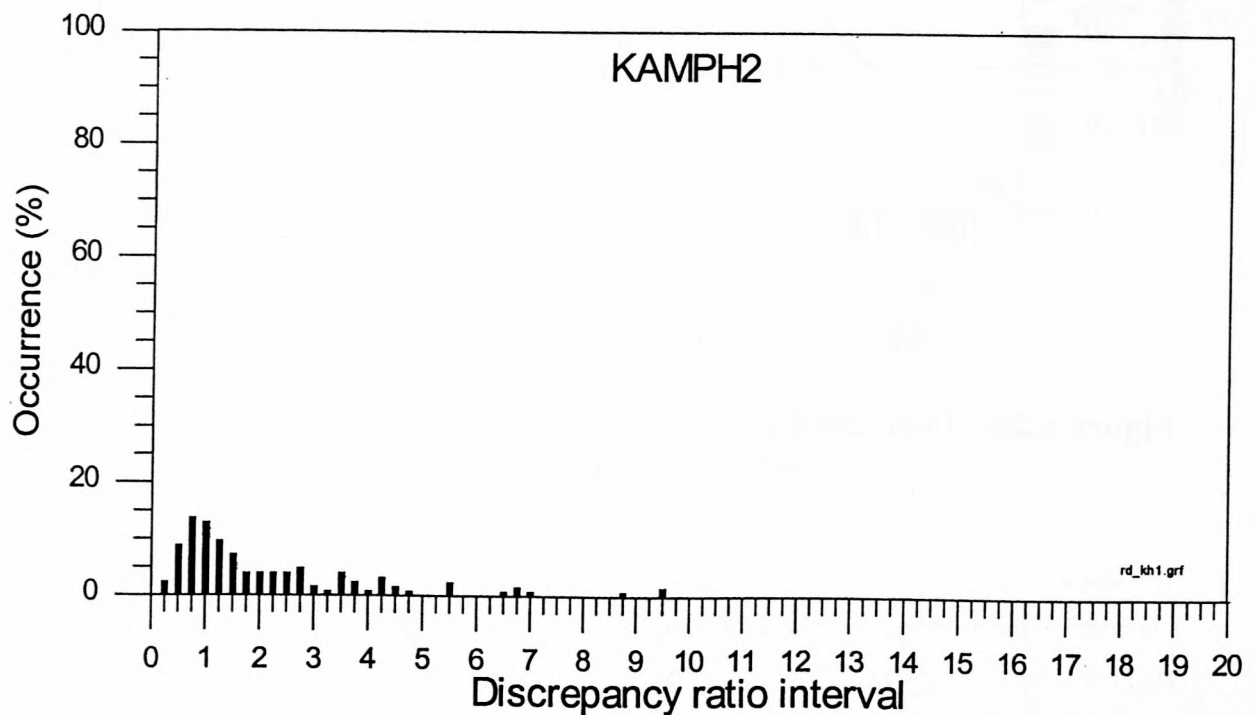


Figure 4.2c: Histogram of the discrepancy ratio for the Kamphuis formula

Spredicted vs Smeasured SVHPC

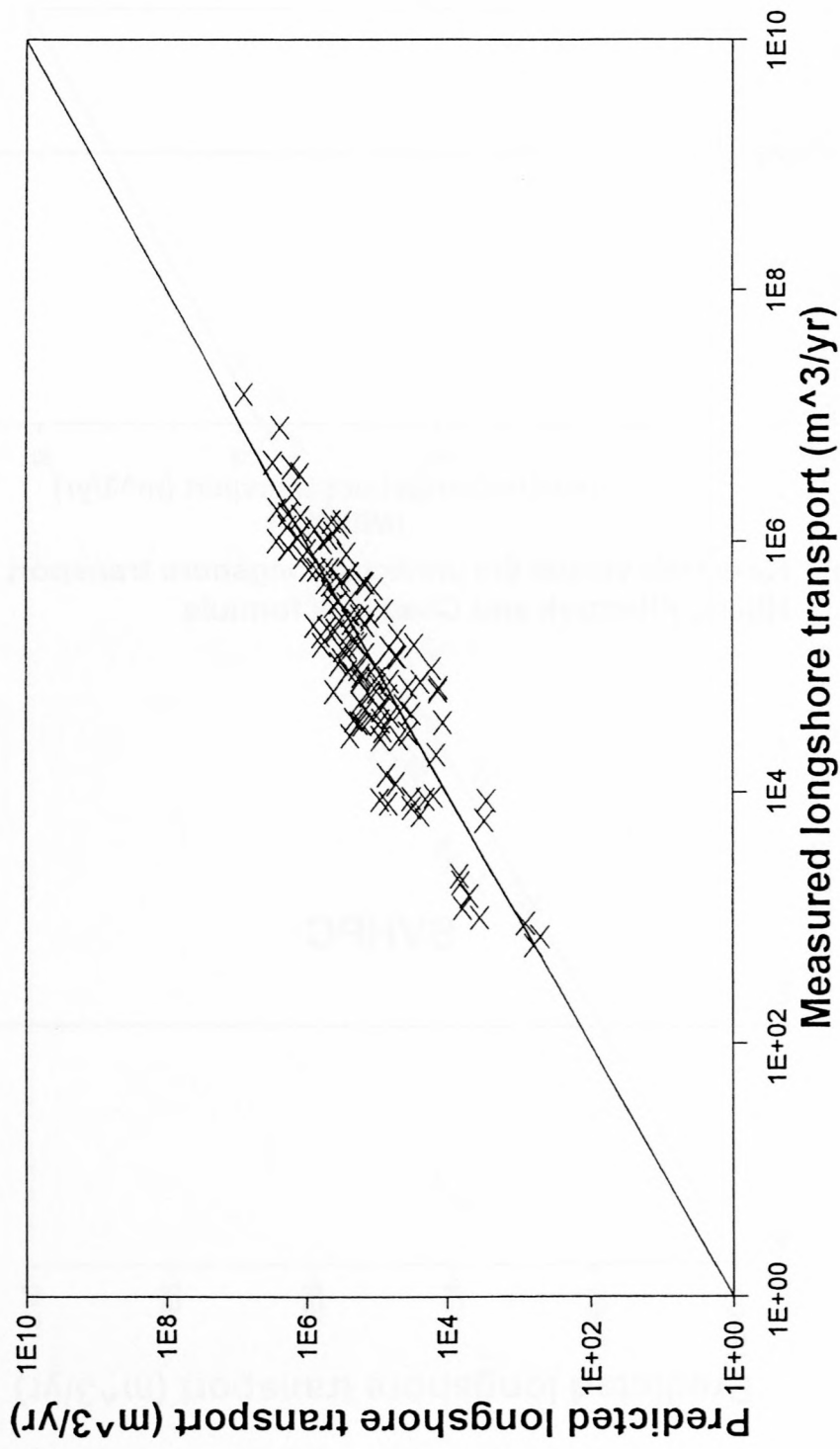


Figure 4.3a: Predicted versus measured longshore transport rates for the Van Hijum, Pilarczyk and Chadwick formula

SVHPC

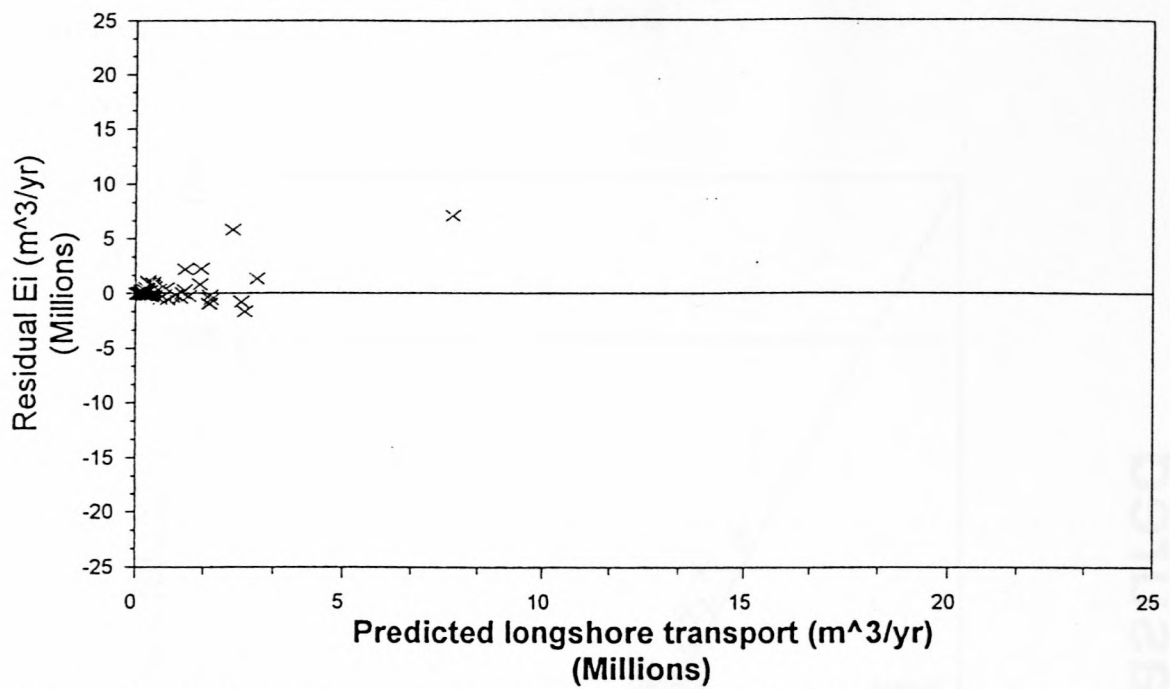


Figure 4.3b: Residuals versus the predicted longshore transport rates for the Van Hijum, Pilarczyk and Chadwick formula

SVHPC

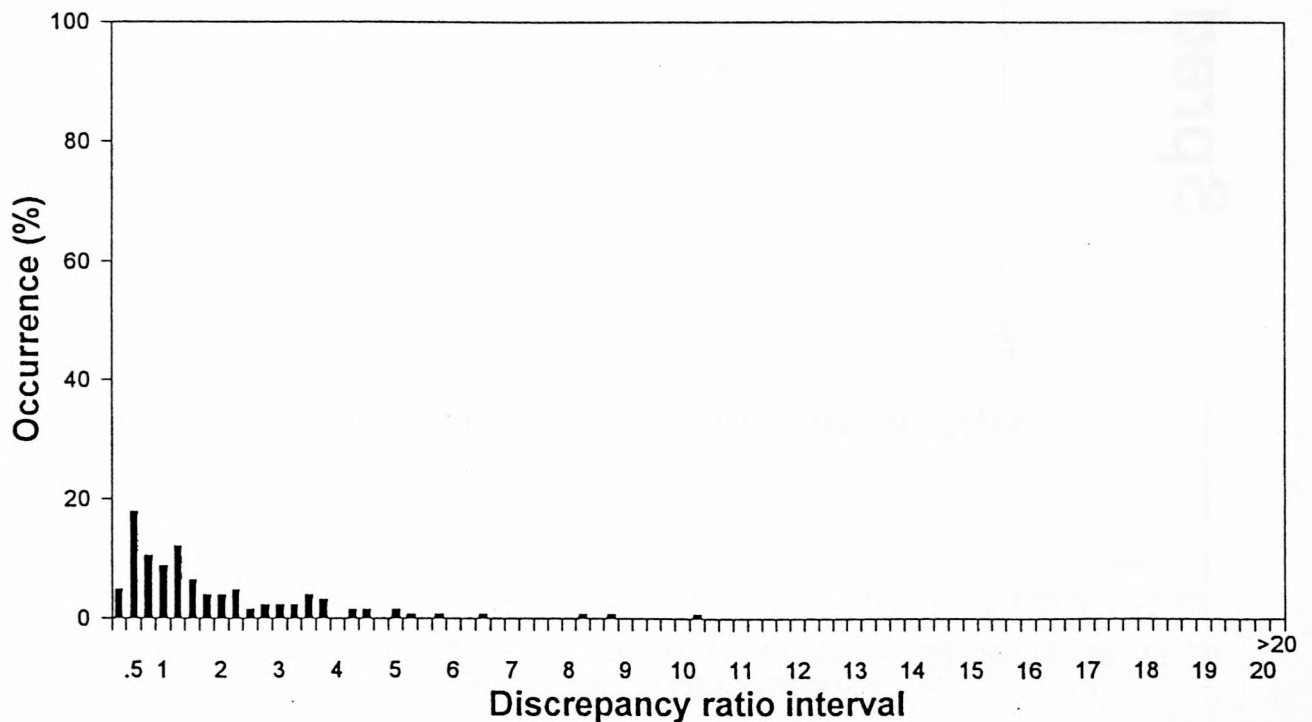


Figure 4.3c: Histogram of the discrepancy ratio for the Van Hijum, Pilarczyk and Chadwick formula

Spredicted vs Smeasured

VDMEER

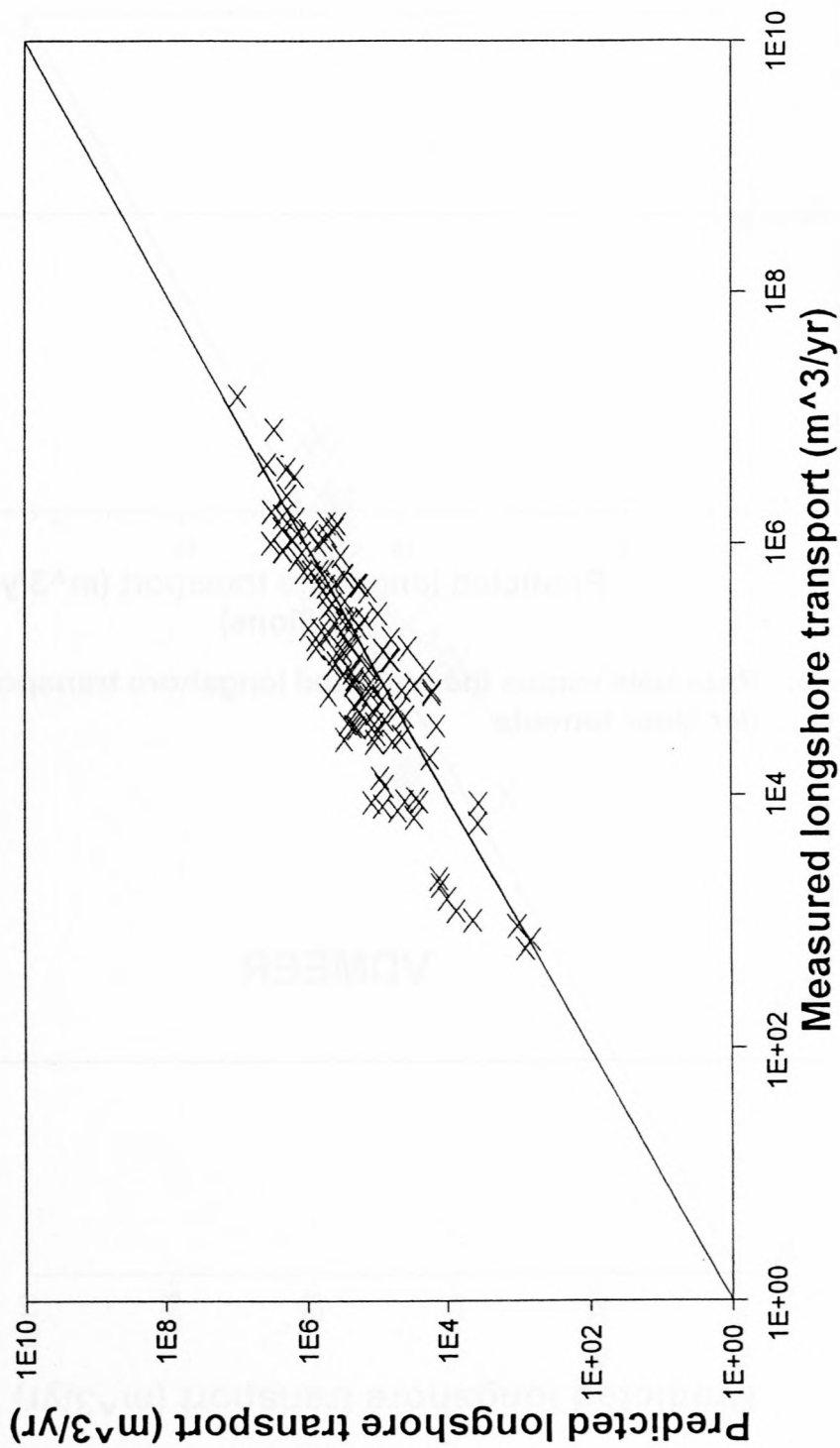


Figure 4.4a: Predicted versus measured longshore transport rates for the Van der Meer formula

VDMEER

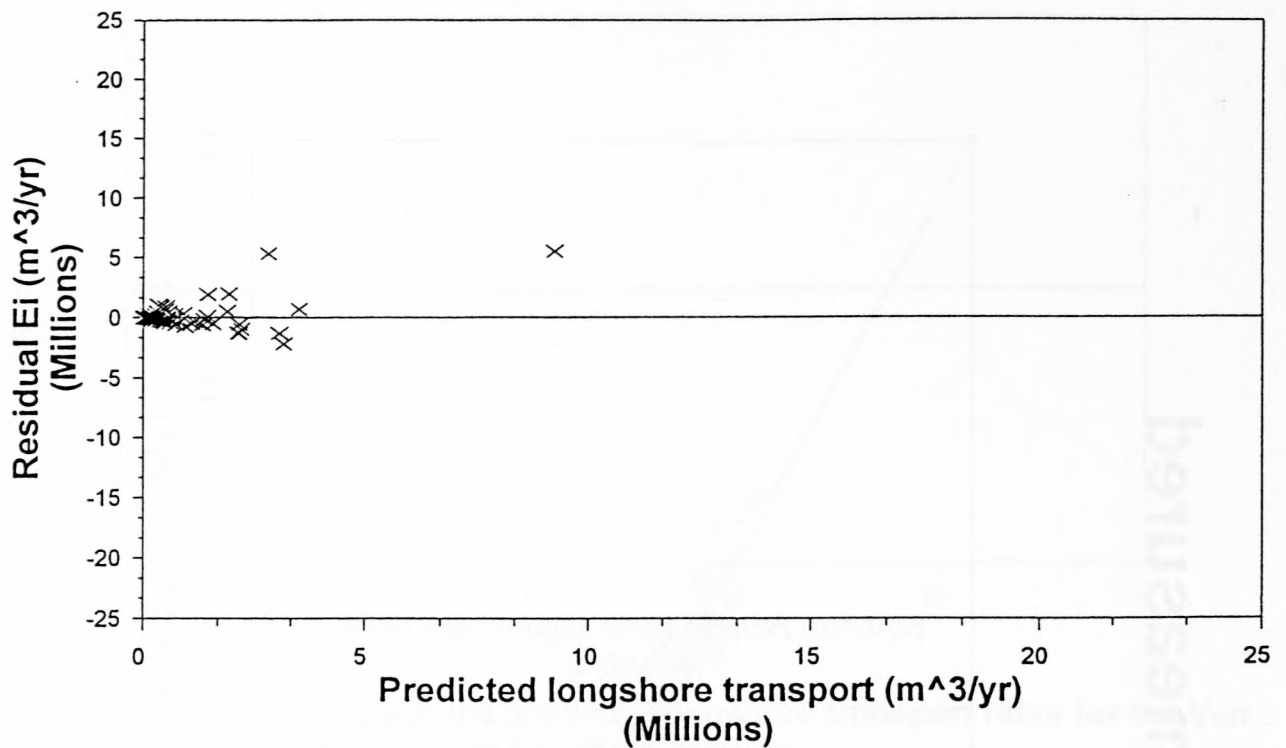


Figure 4.4b: Residuals versus the predicted longshore transport rates for the Van der Meer formula

VDMEER

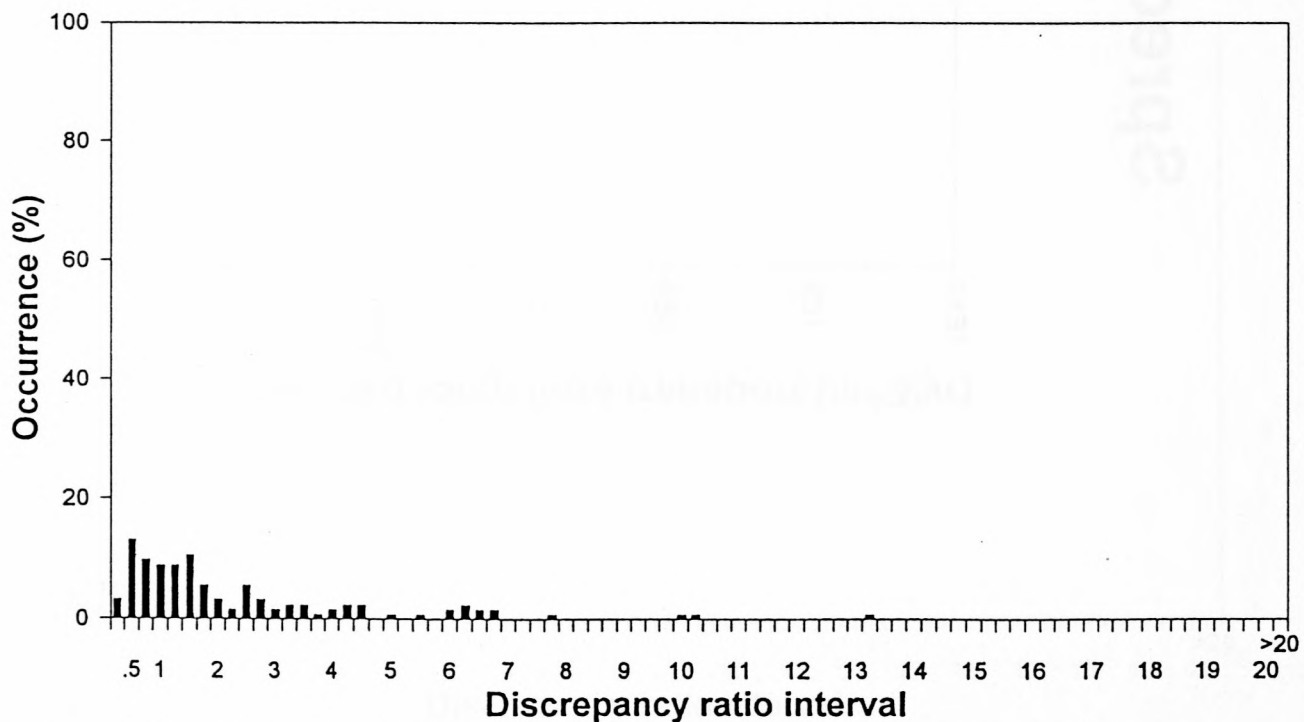


Figure 4.4c: Histogram of the discrepancy ratio for the Van der Meer formula

Spredicted vs Smeasured

LBP2

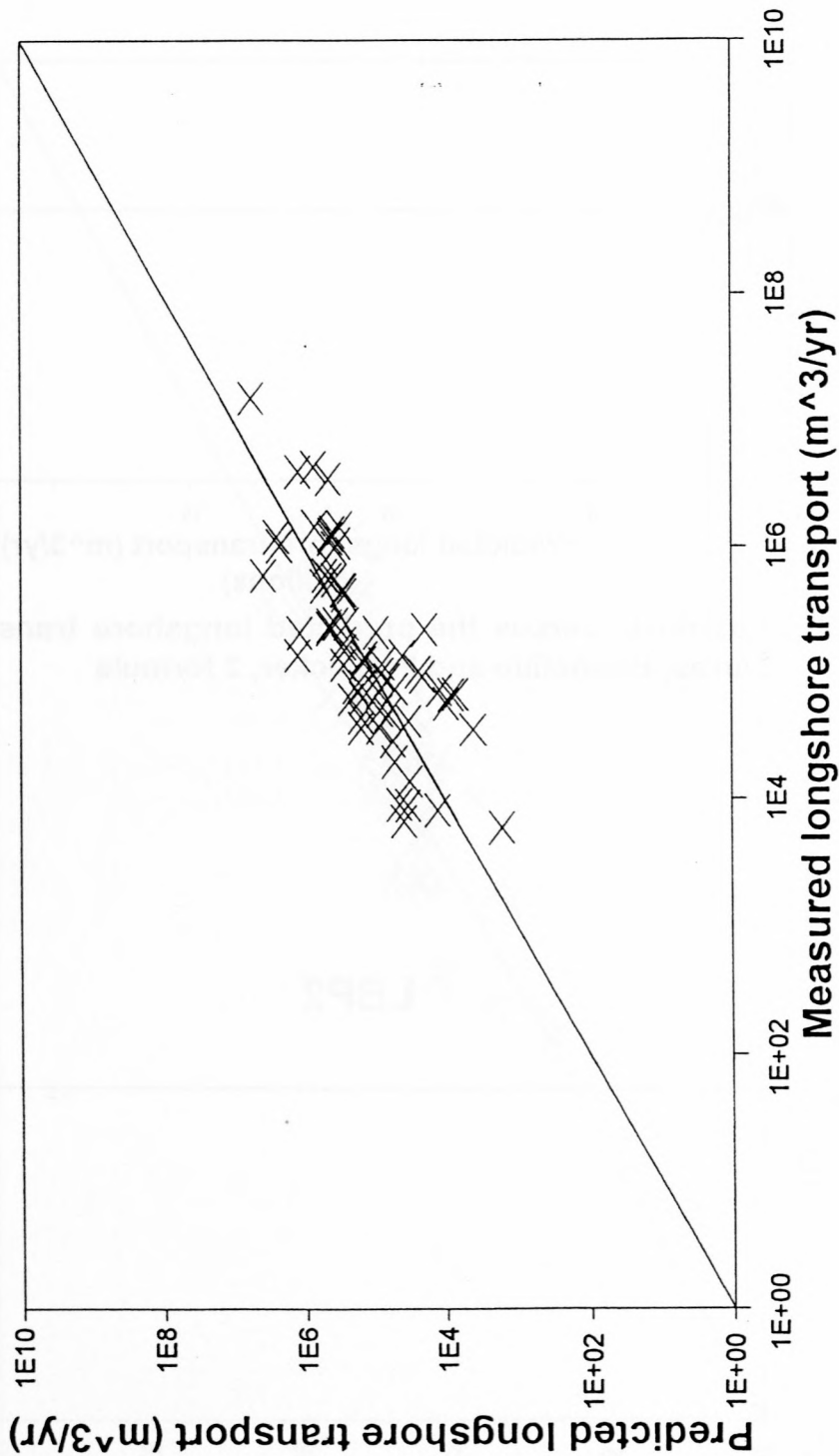


Figure 4.5a: Predicted versus measured longshore transport rates for the Larras, Bonnefille and Pernecker, 2 formula

LBP2

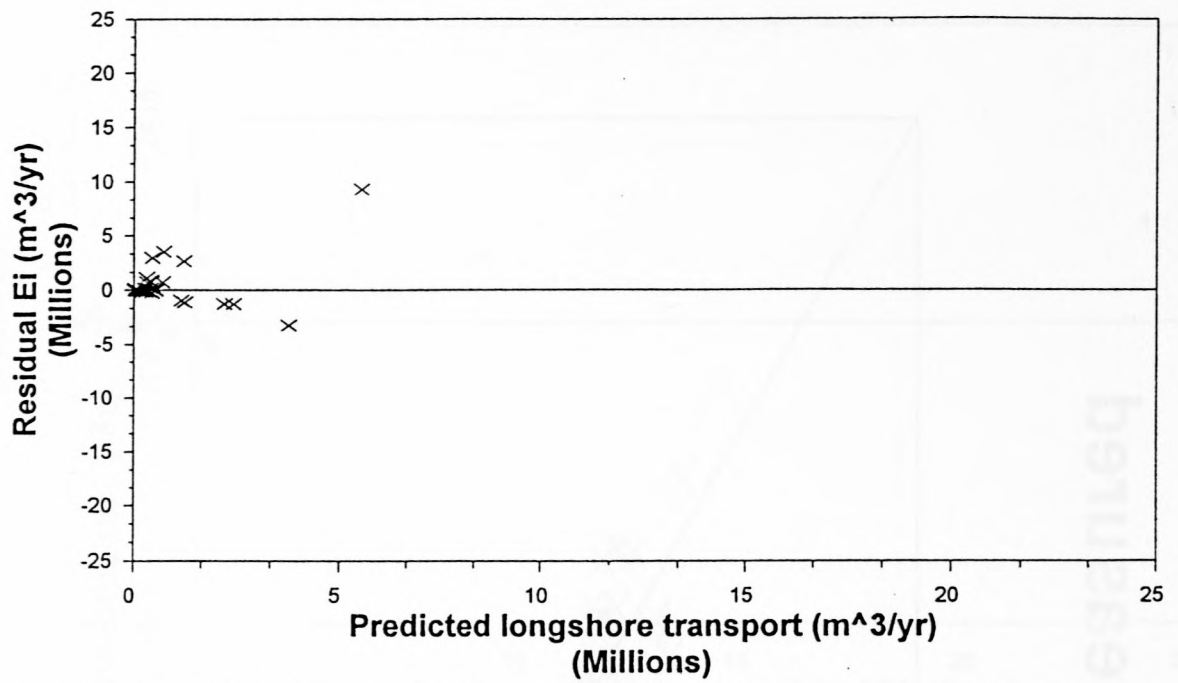


Figure 4.5b: Residuals versus the predicted longshore transport rates for the Larras, Bonnefille and Pernecker, 2 formula

LBP2

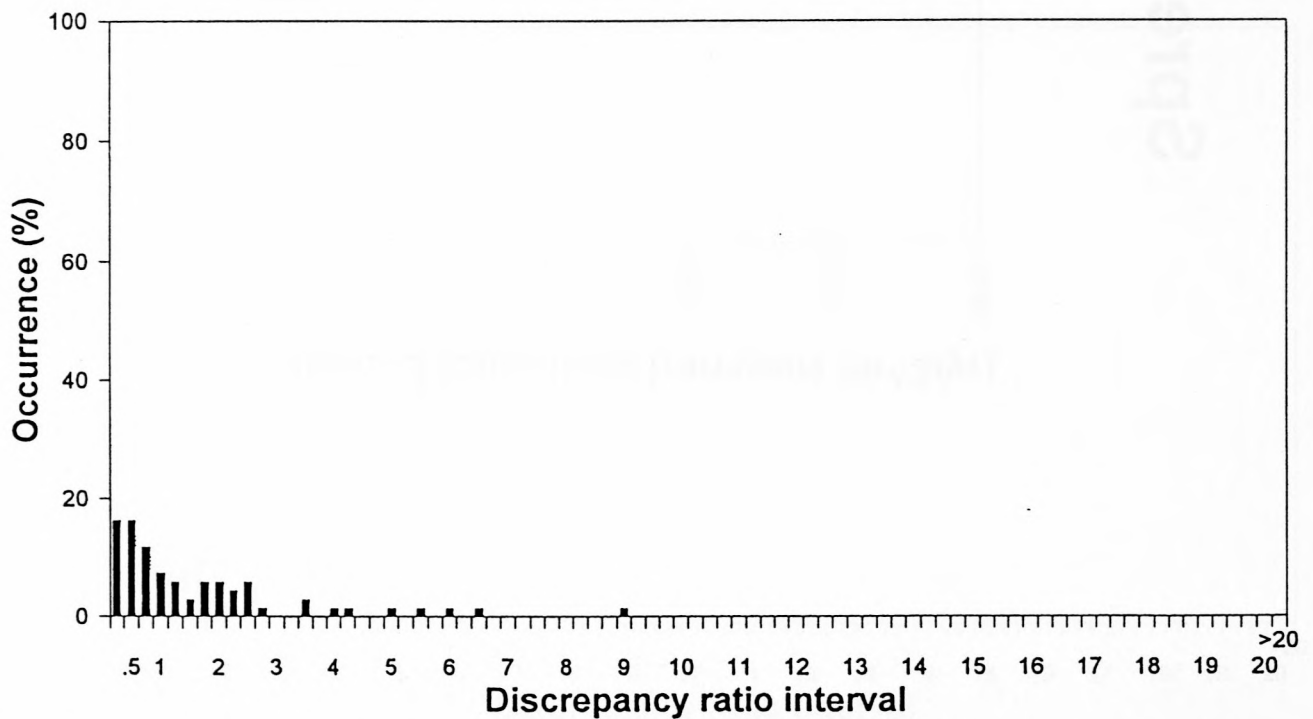


Figure 4.5c: Histogram of the discrepancy ratio for the Larras, Bonnefille and Pernecker, 2 formula

Spredicted vs Smeasured SPMKR

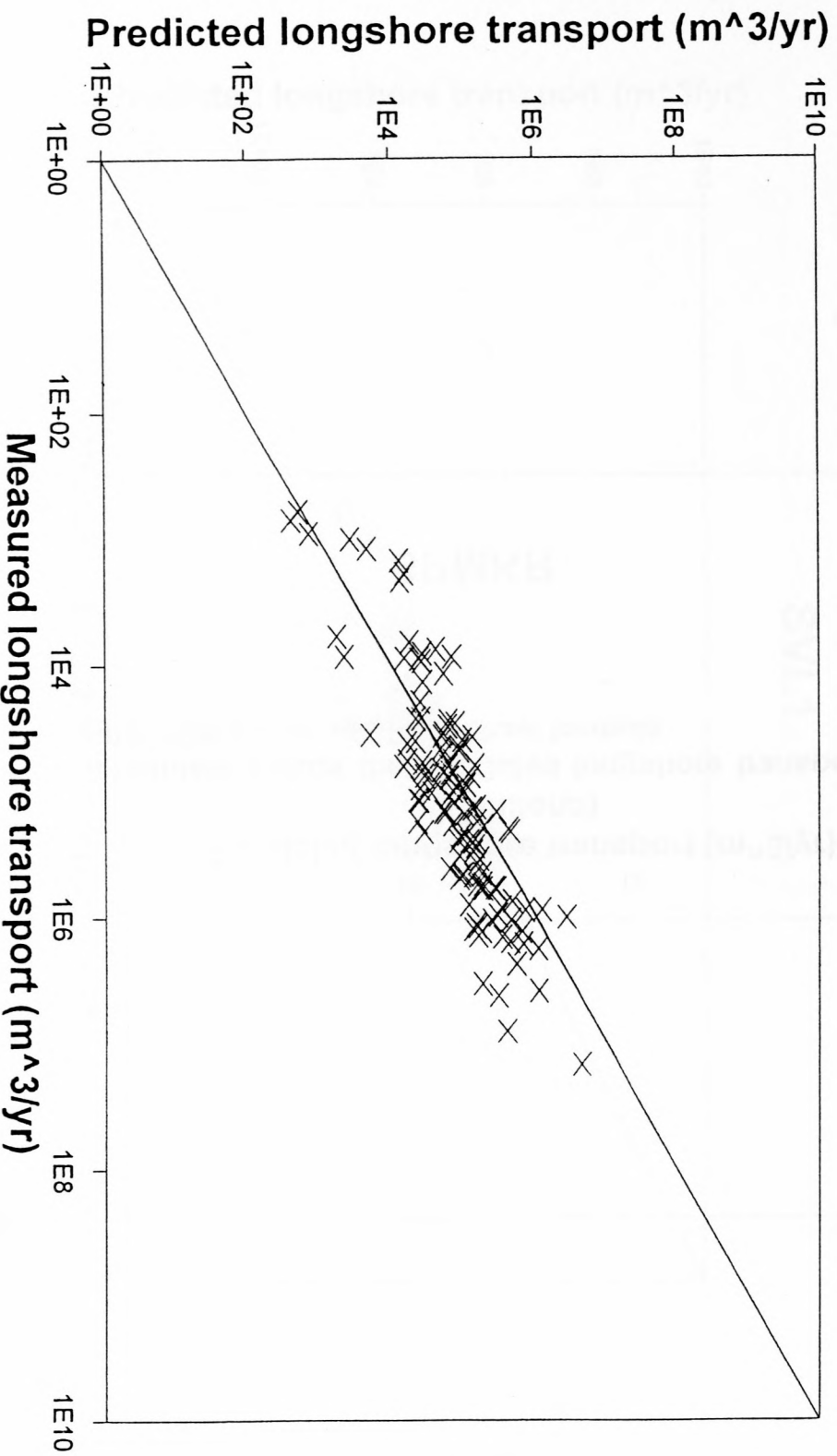


Figure 4.6a: Predicted versus measured longshore transport rates for the SPM, Kamphuis and Readshaw formula

SPMKR

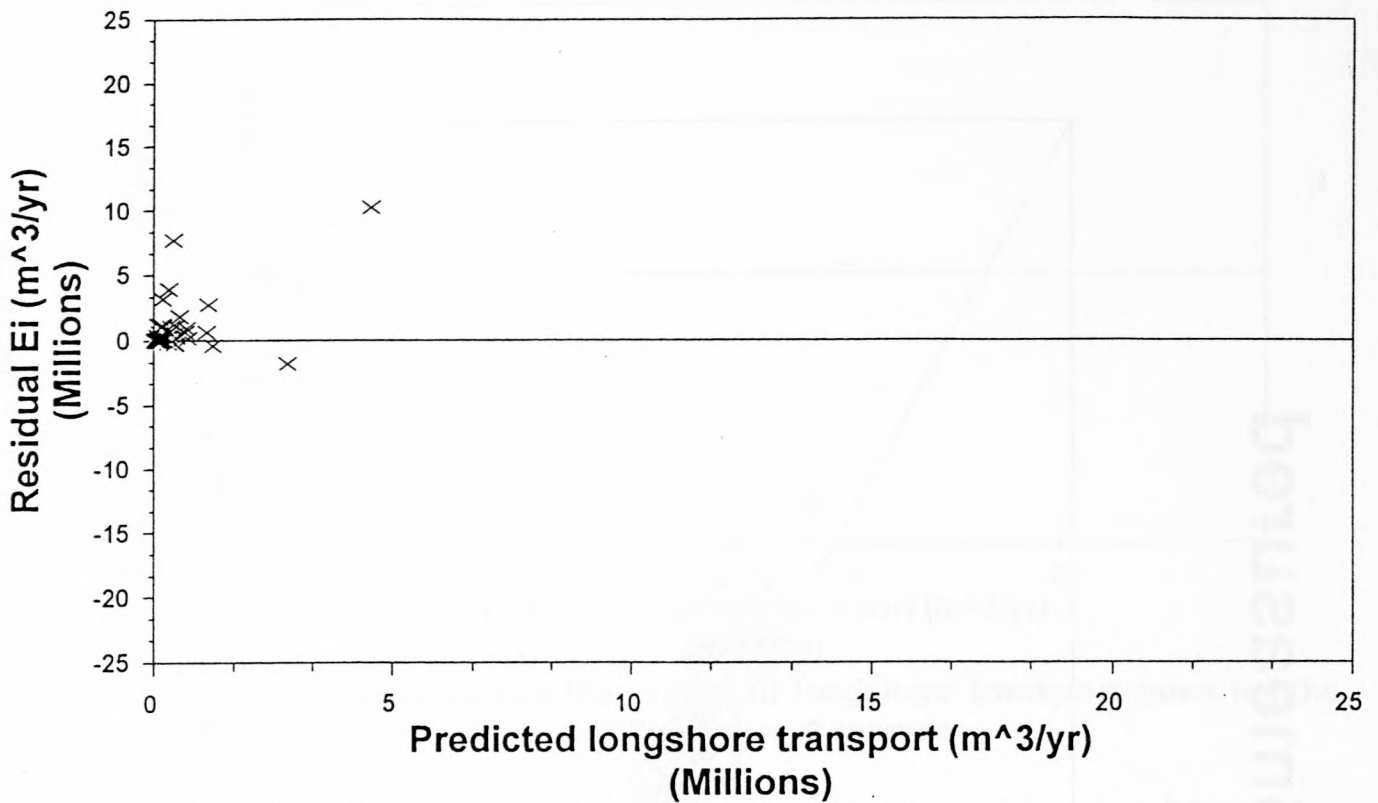


Figure 4.6b: Residuals versus the predicted longshore transport rates for the SPM, Kamphuis and Readshaw formula

SPMKR

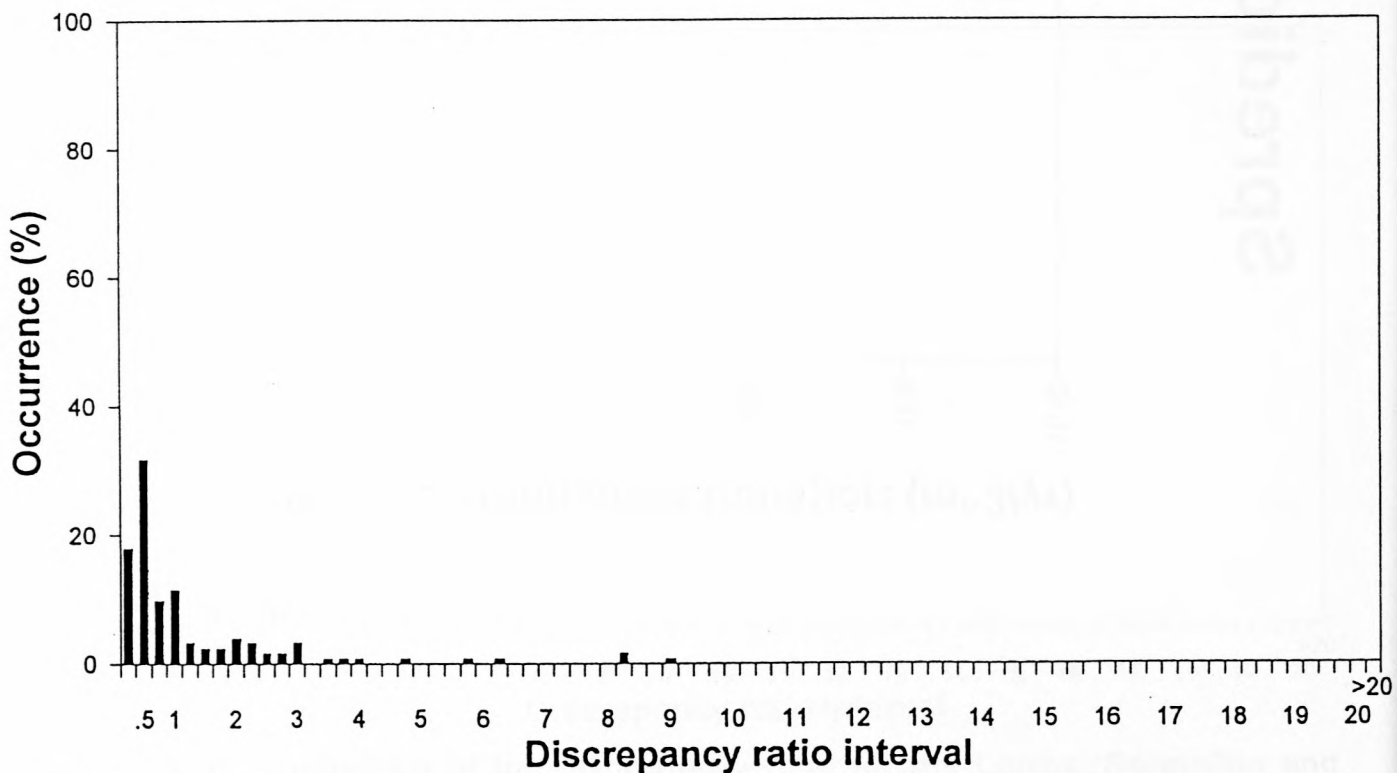


Figure 4.6c: Histogram of the discrepancy ratio for the SPM, Kamphuis and Readshaw formula

Spredicted vs Smeasured SVL1

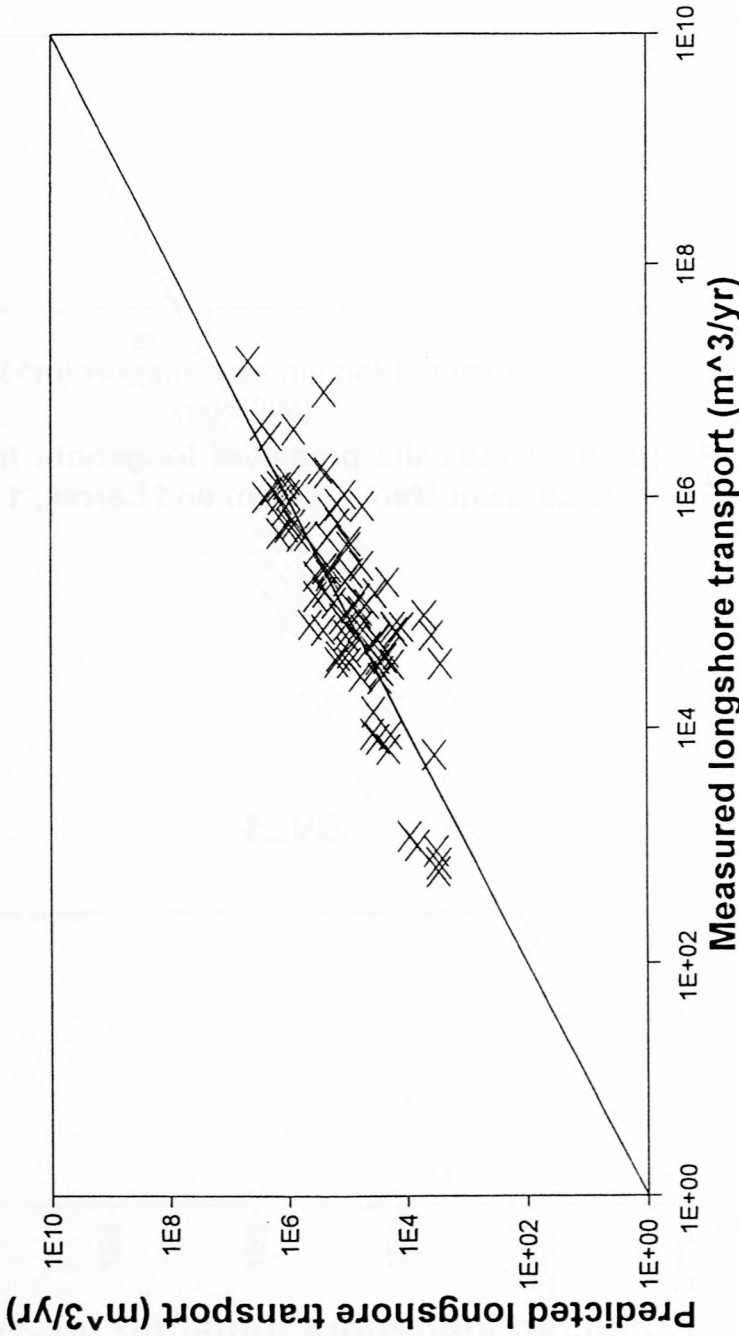


Figure 4.7a: Predicted versus measured longshore transport rates for the Sauvage de Saint Marc, Vincent and Larras, 1 formula

SVL1

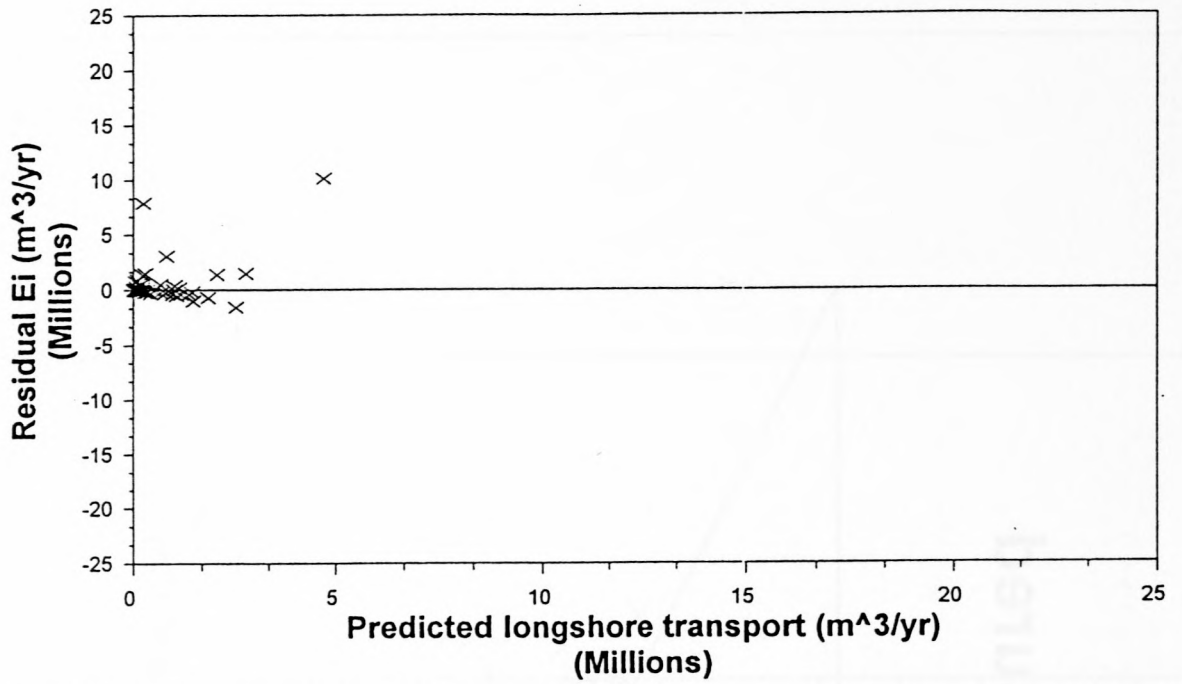


Figure 4.7b: Residuals versus the predicted longshore transport rates for the Sauvage de Saint Marc, Vincent and Larras, 1 formula

SVL1

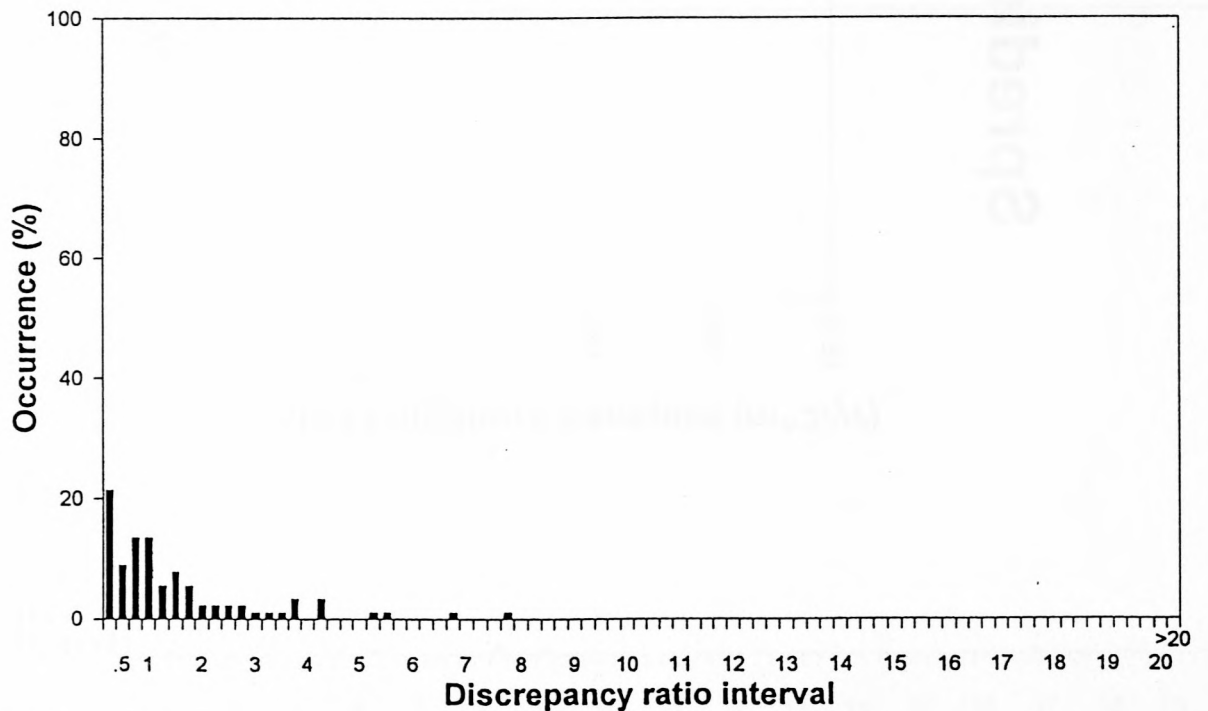


Figure 4.7c: Histogram of the discrepancy ratio for the Sauvage de Saint Marc, Vincent and Larras, 1 formula

Spredicted vs Smeasured

HLL2

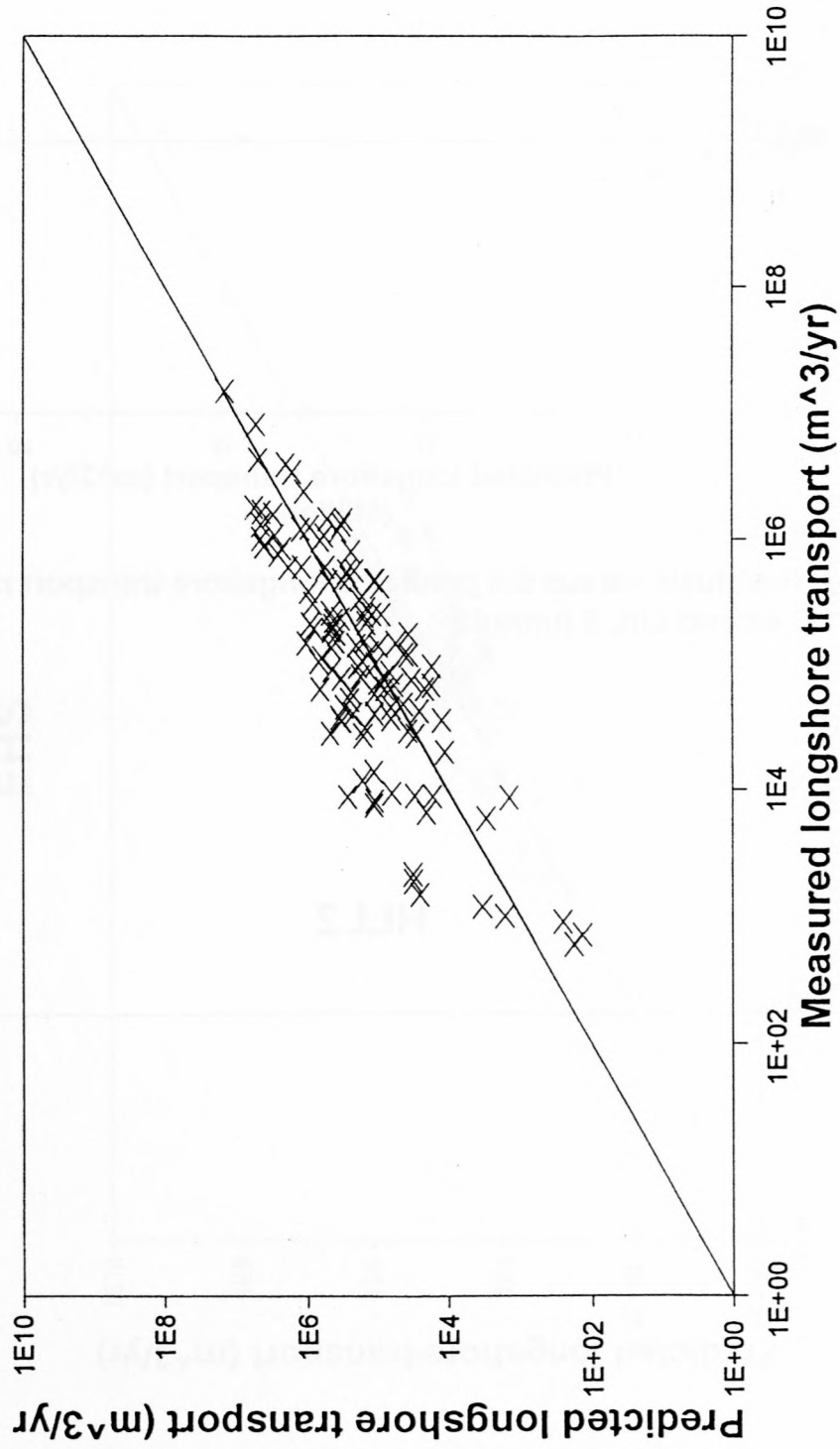


Figure 4.8a: Predicted versus measured longshore transport rates for the Hou, Lee and Lin, 2 formula

HLL2

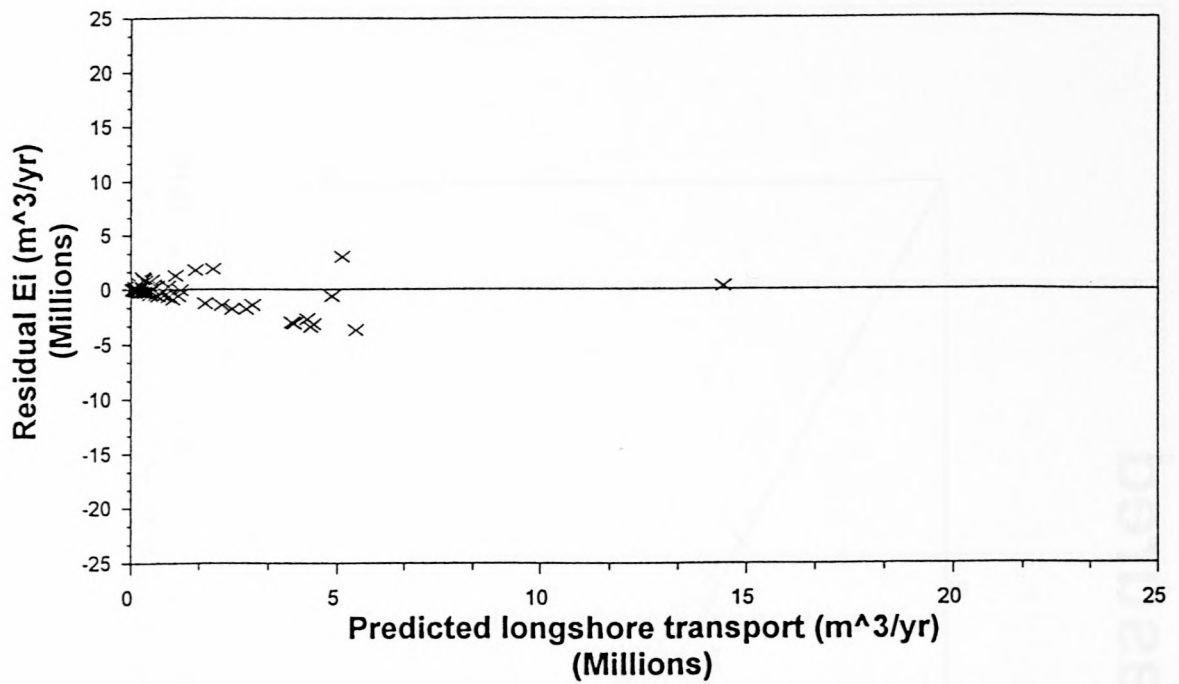


Figure 4.8b: Residuals versus the predicted longshore transport rates for the Hou, Lee and Lin, 2 formula

HLL2

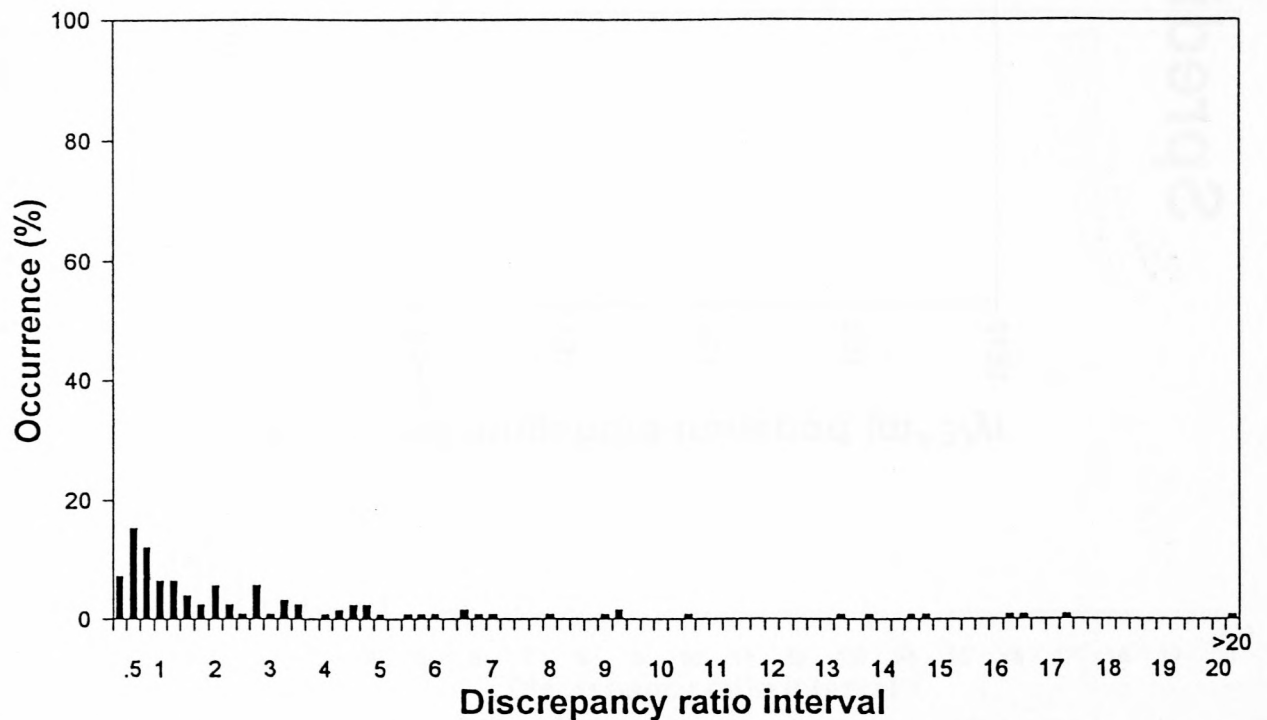


Figure 4.8c: Histogram of the discrepancy ratio for the Hou, Lee and Lin, 2 formula

Spredicted vs Smeasured **EHS**

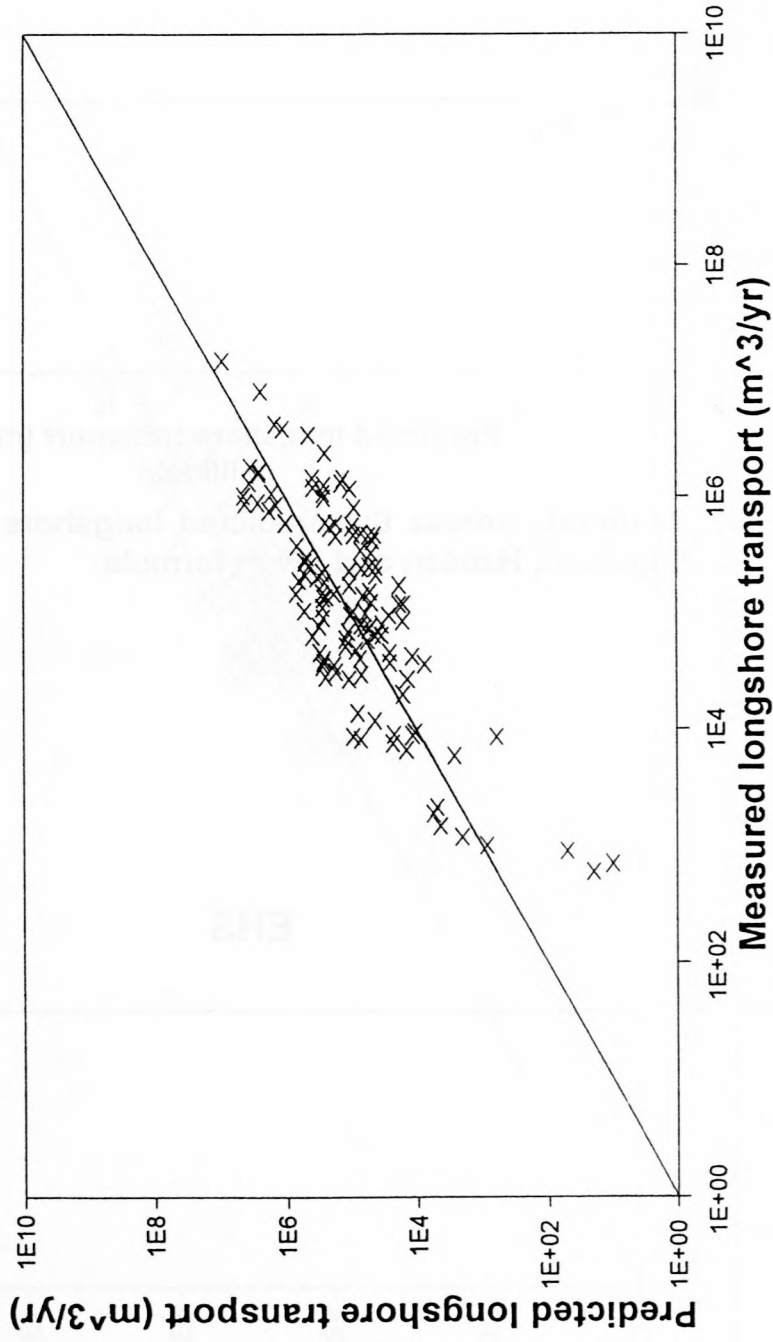


Figure 4.9a: Predicted versus measured longshore transport rates for the Engelund, Hansen and Swart formula

EHS

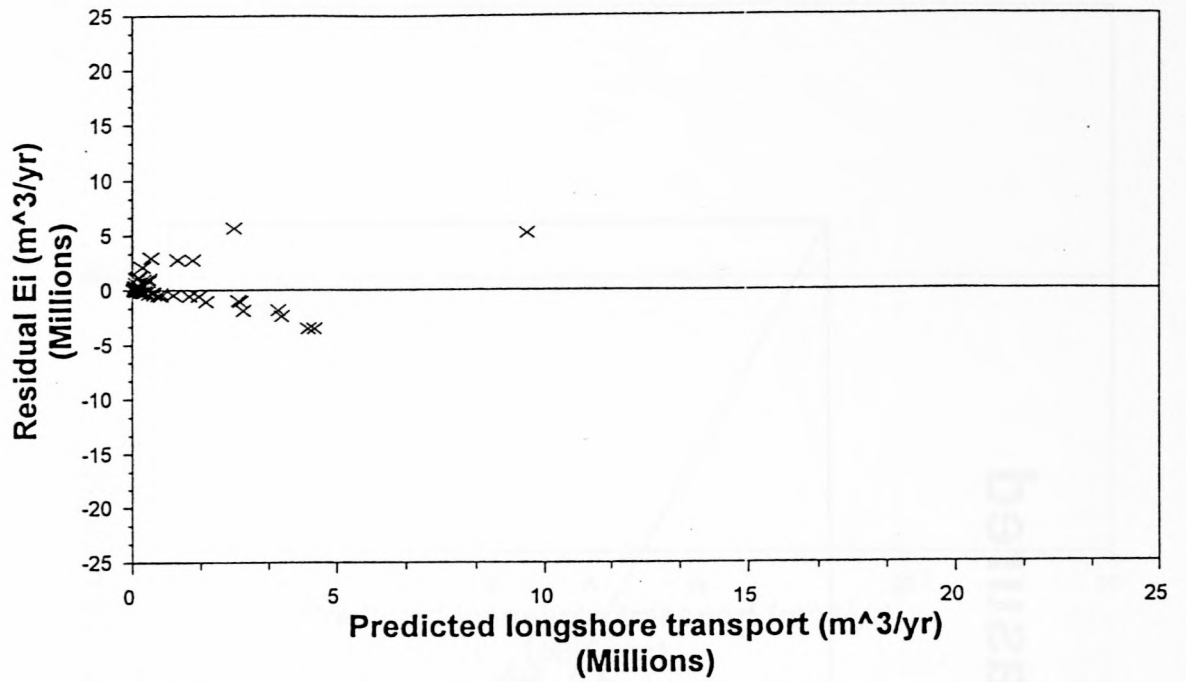


Figure 4.9b: Residuals versus the predicted longshore transport rates for the Engelund, Hansen and Swart formula

EHS

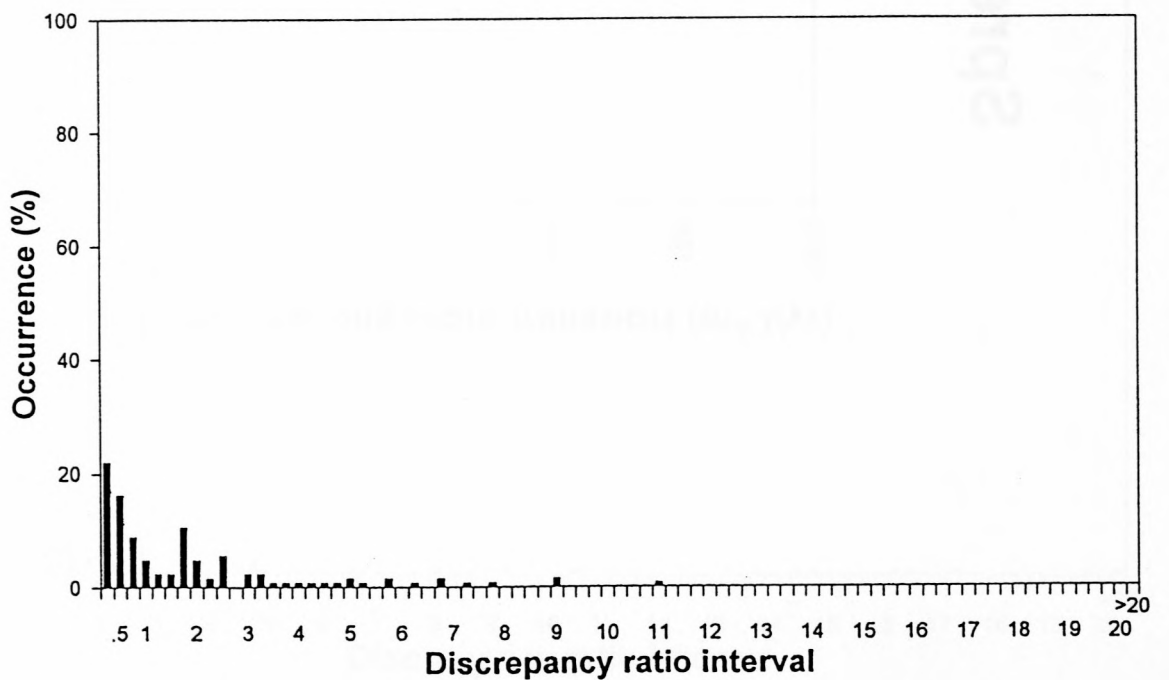


Figure 4.9c: Histogram of the discrepancy ratio for the Engelund, Hansen and Swart formula

Spredicted vs Smeasured

FLEMING

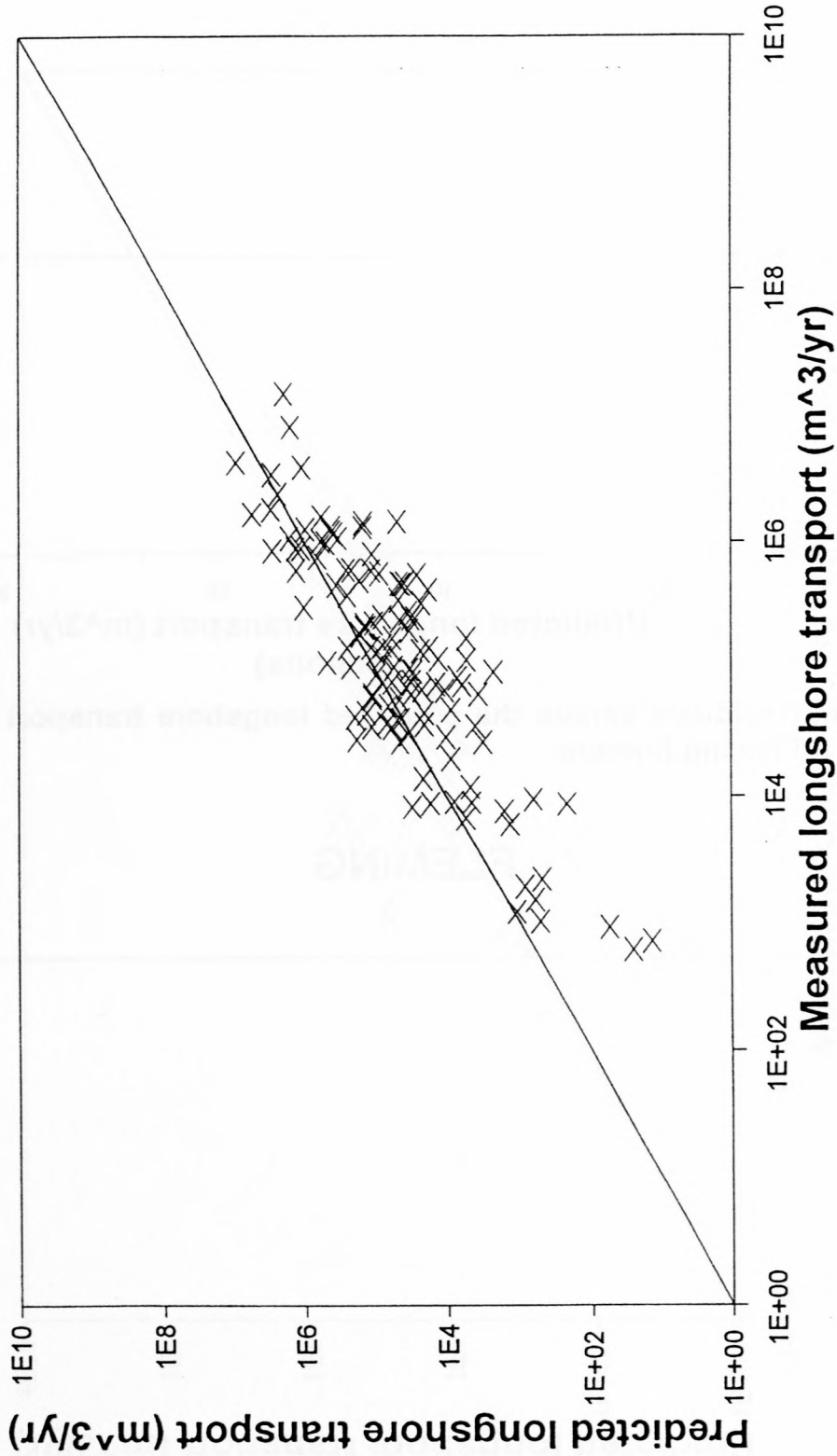


Figure 4.10a: Predicted versus measured longshore transport rates for the Fleming formula

FLEMING

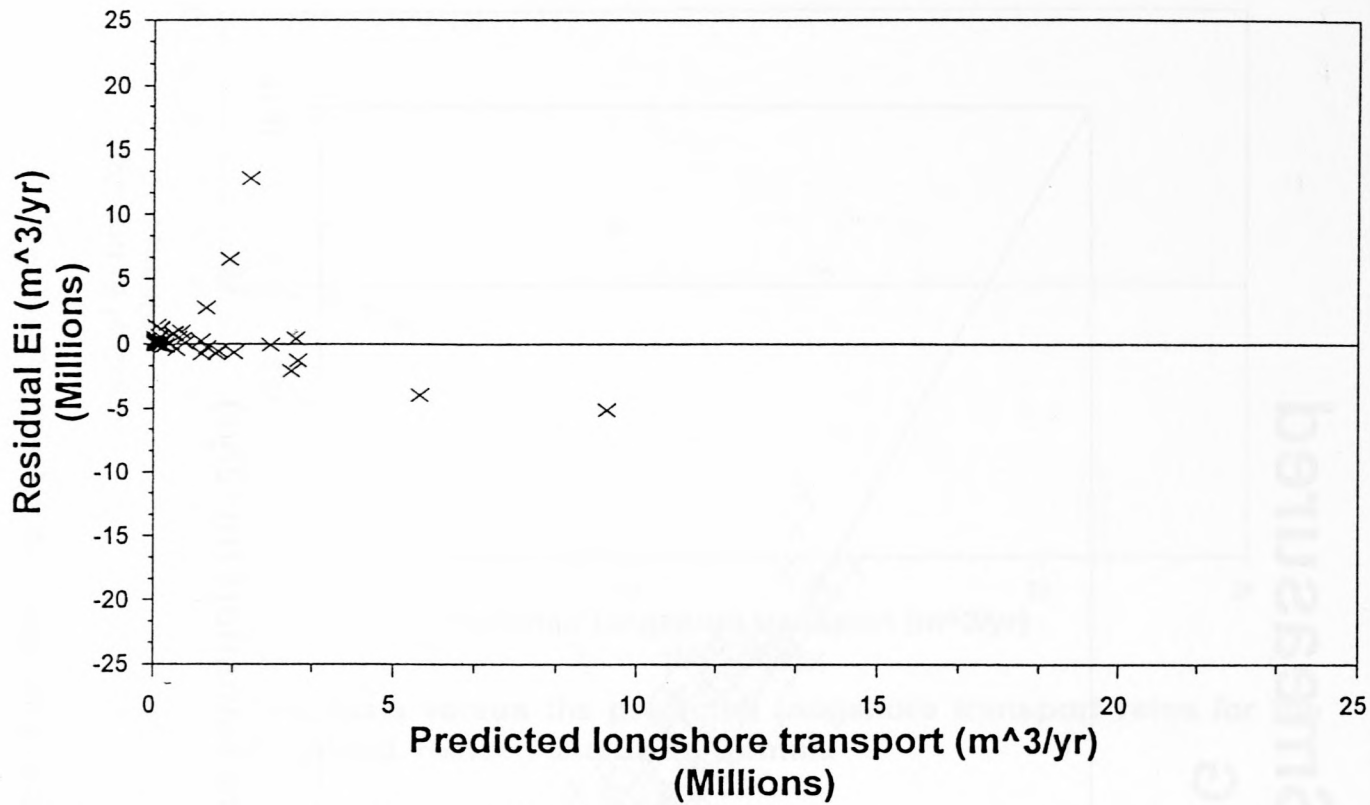


Figure 4.10b: Residuals versus the predicted longshore transport rates for the Fleming formula

FLEMING

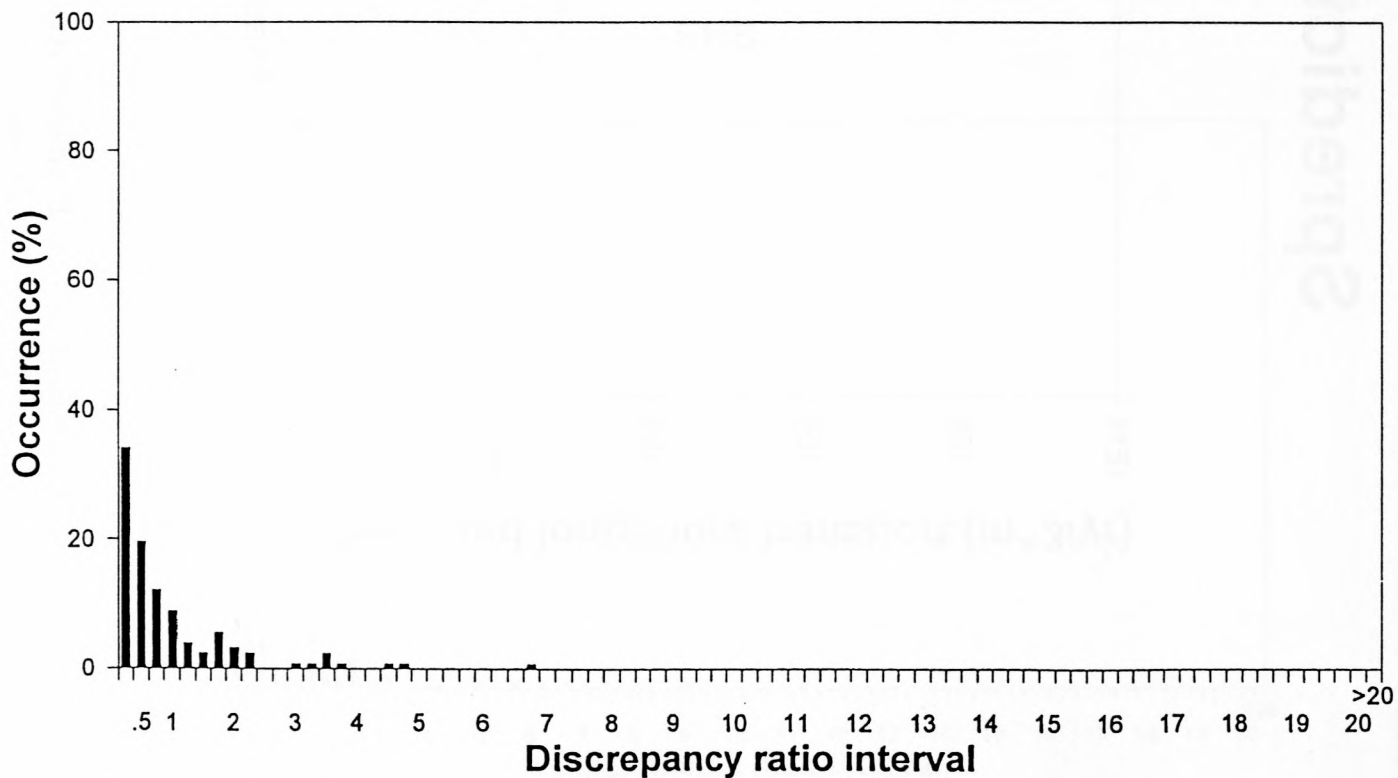


Figure 4.10c: Histogram of the discrepancy ratio for the Fleming formula

Spredicted vs Smeasured

WATANABE

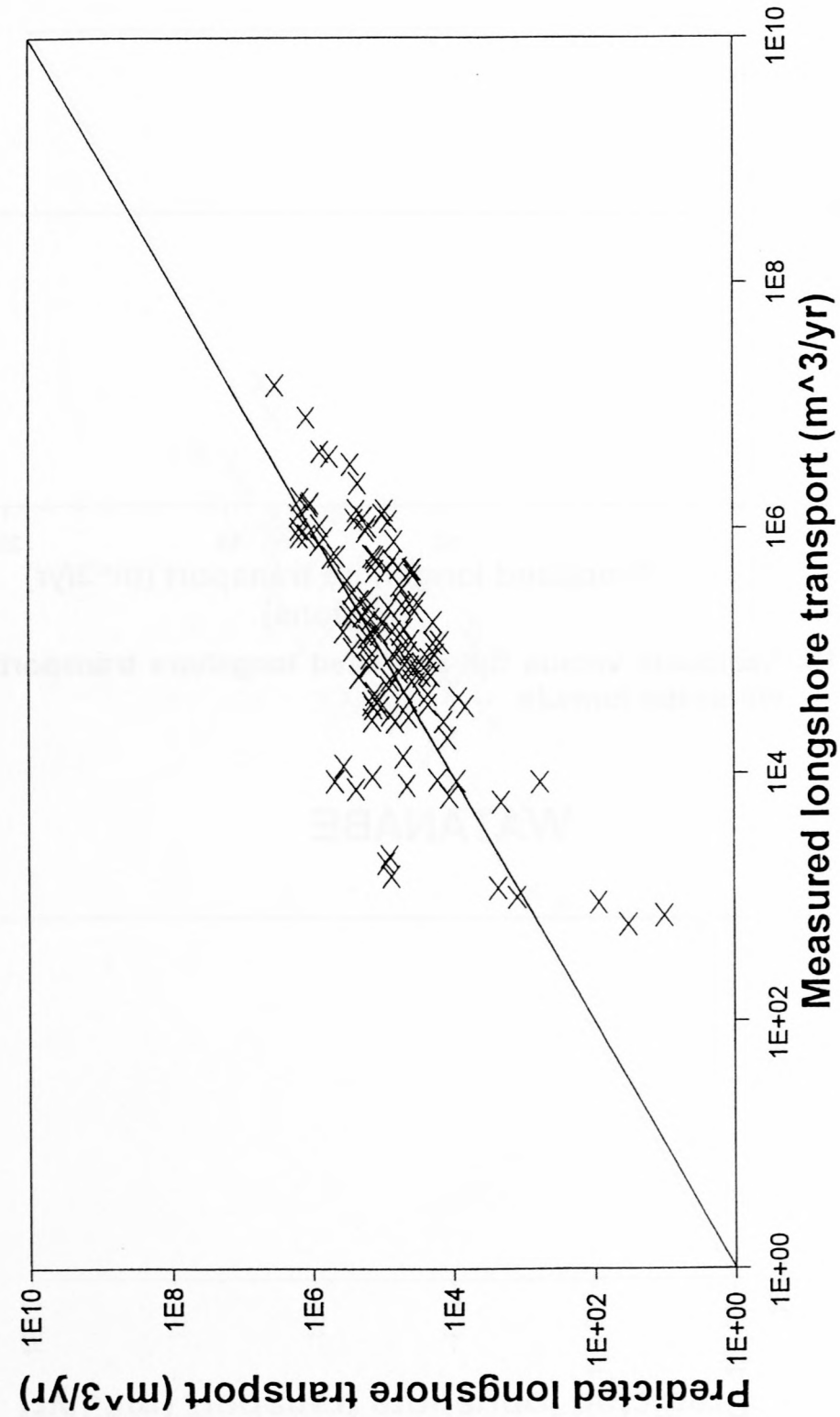


Figure 4.11a: Predicted versus measured longshore transport rates for the Watanabe formula

WATANABE

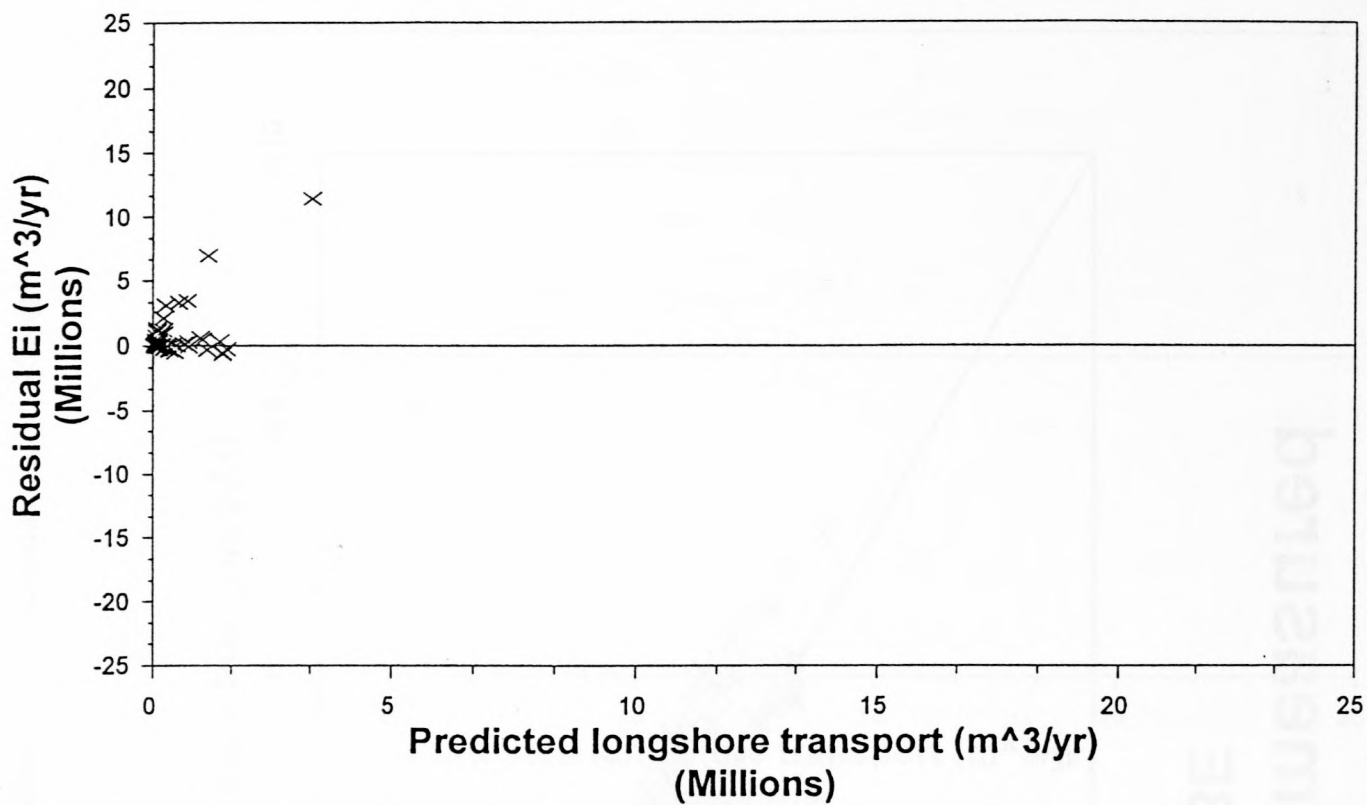


Figure 4.11b: Residuals versus the predicted longshore transport rates for the Watanabe formula

WATANABE

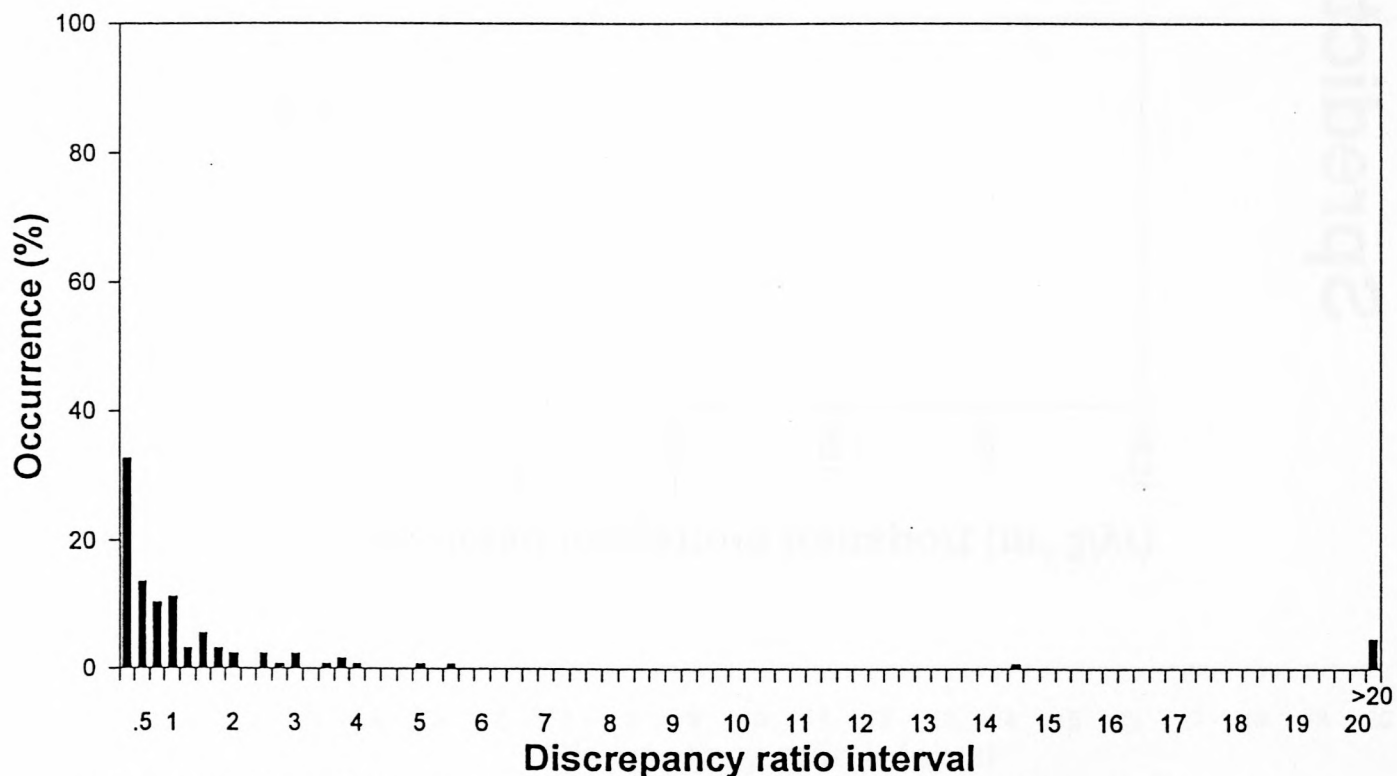


Figure 4.11c: Histogram of the discrepancy ratio for the Watanabe formula

Spredicted vs Smeasured

SWART

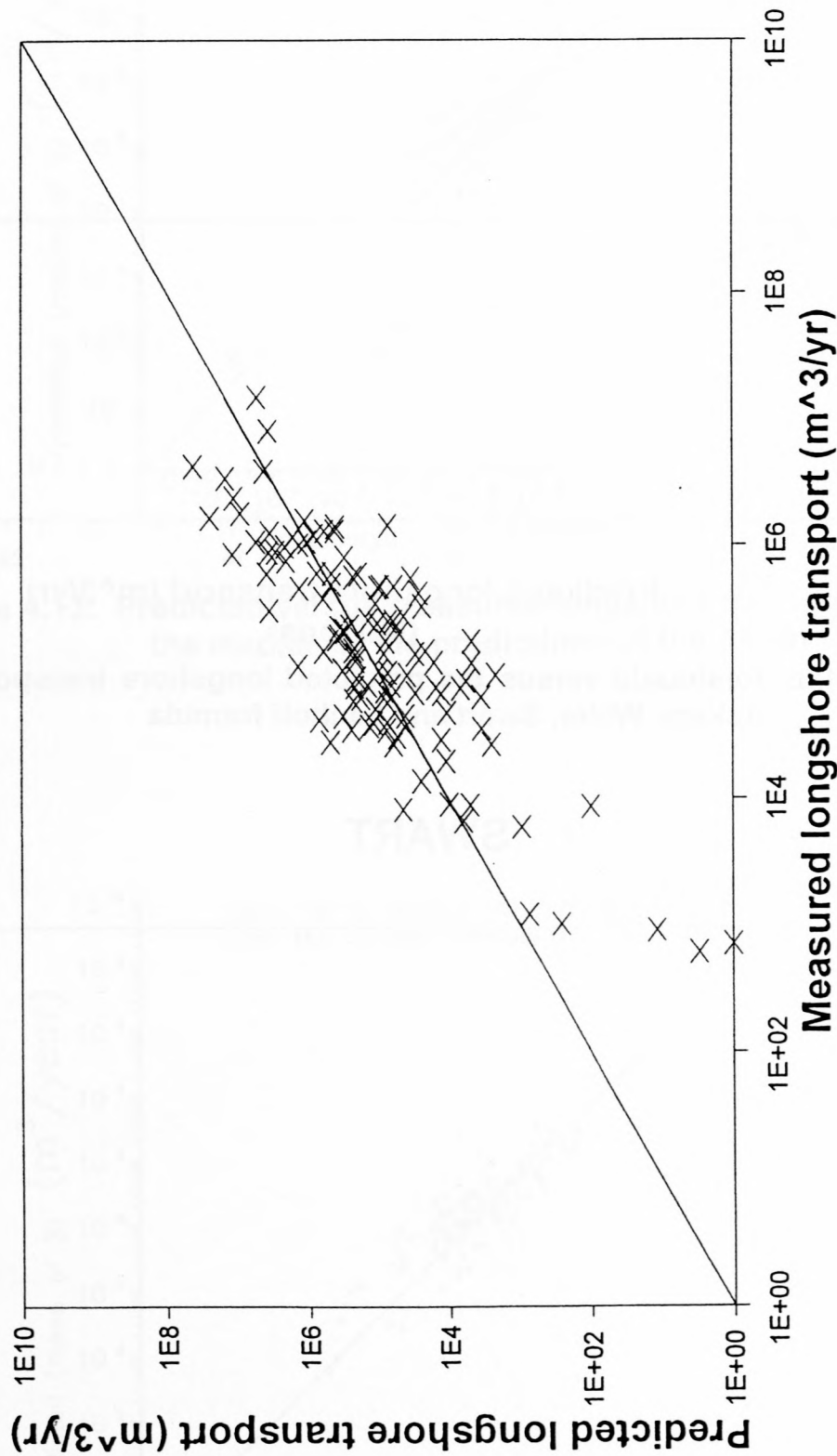


Figure 4.12a: Predicted versus measured longshore transport rates for the Ackers, White, Swart and Lenhoff formula

SWART

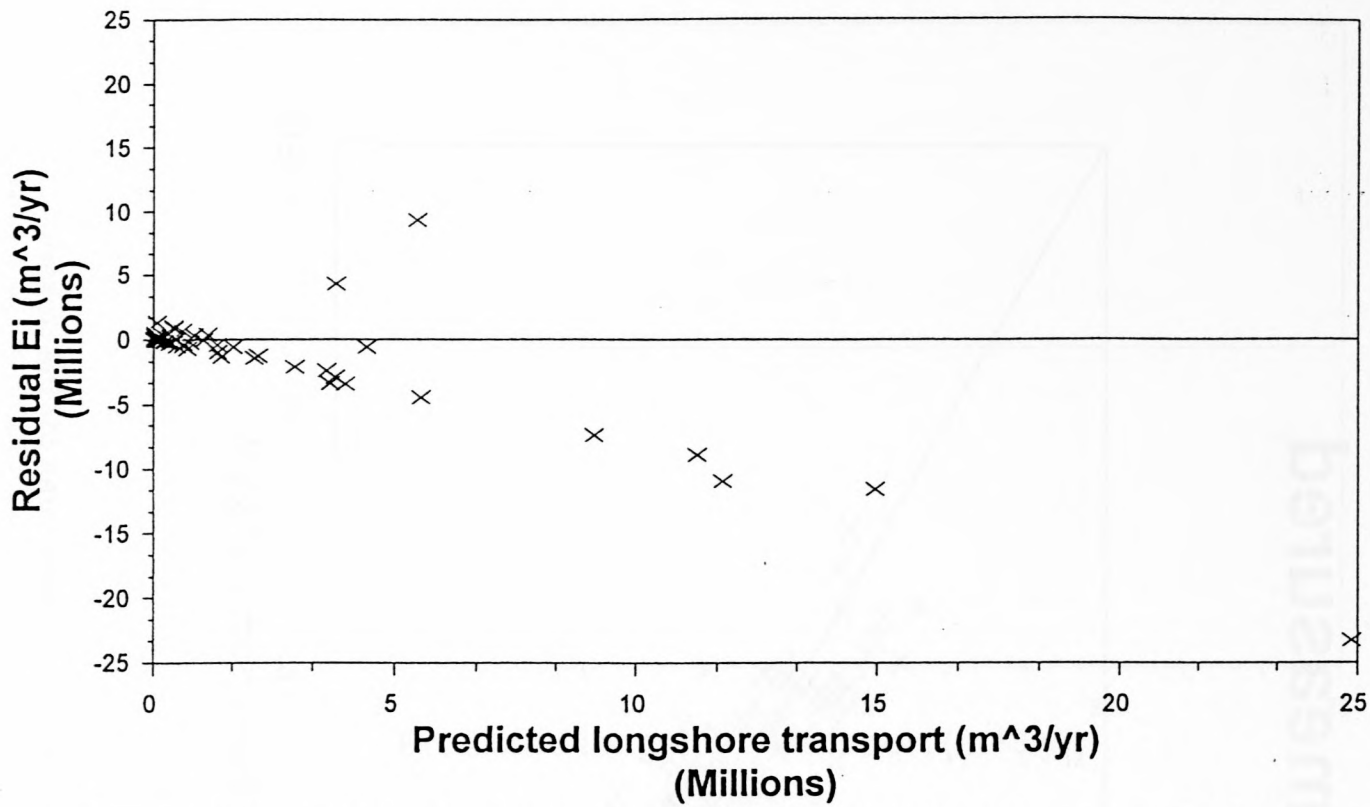


Figure 4.12b: Residuals versus the predicted longshore transport rates for the Ackers, White, Swart and Lenhoff formula

SWART

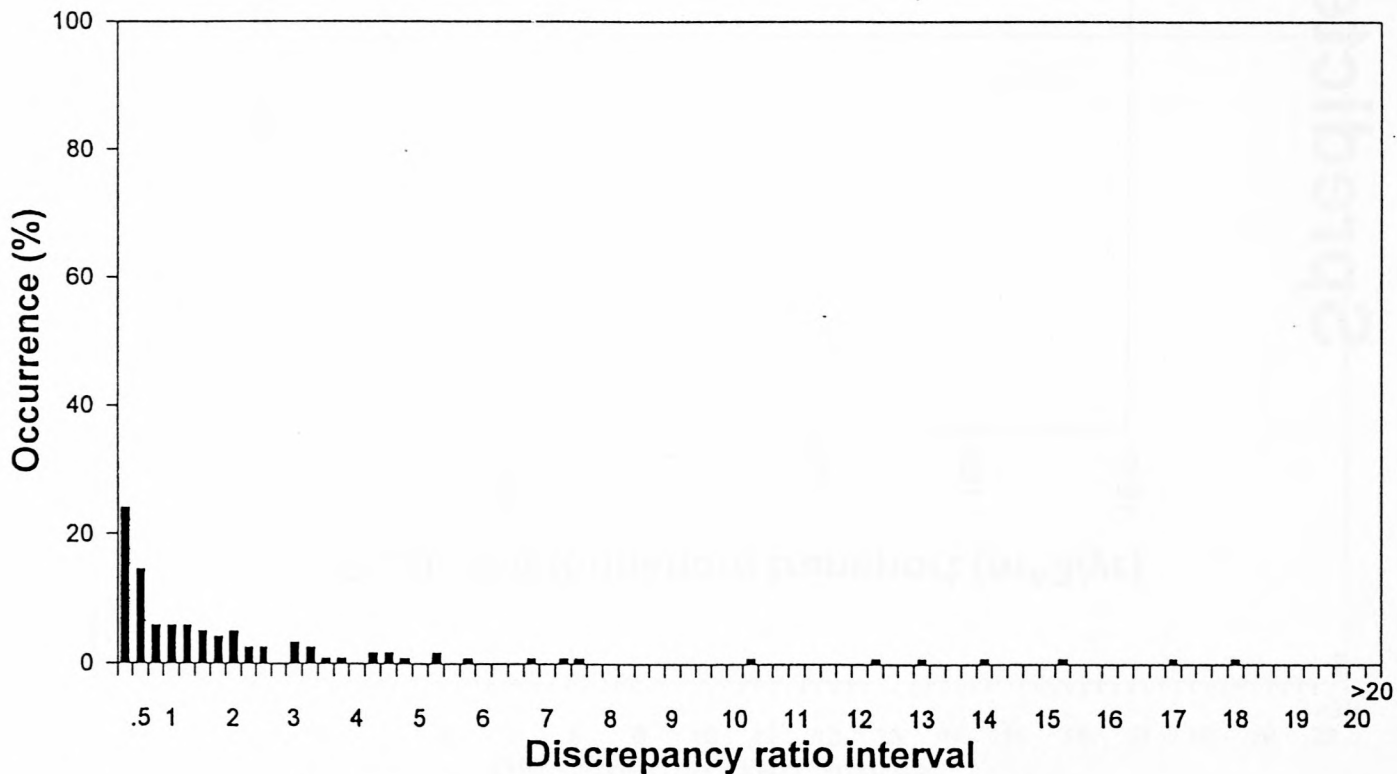


Figure 4.12c: Histogram of the discrepancy ratio for the Ackers, White, Swart and Lenhoff formula

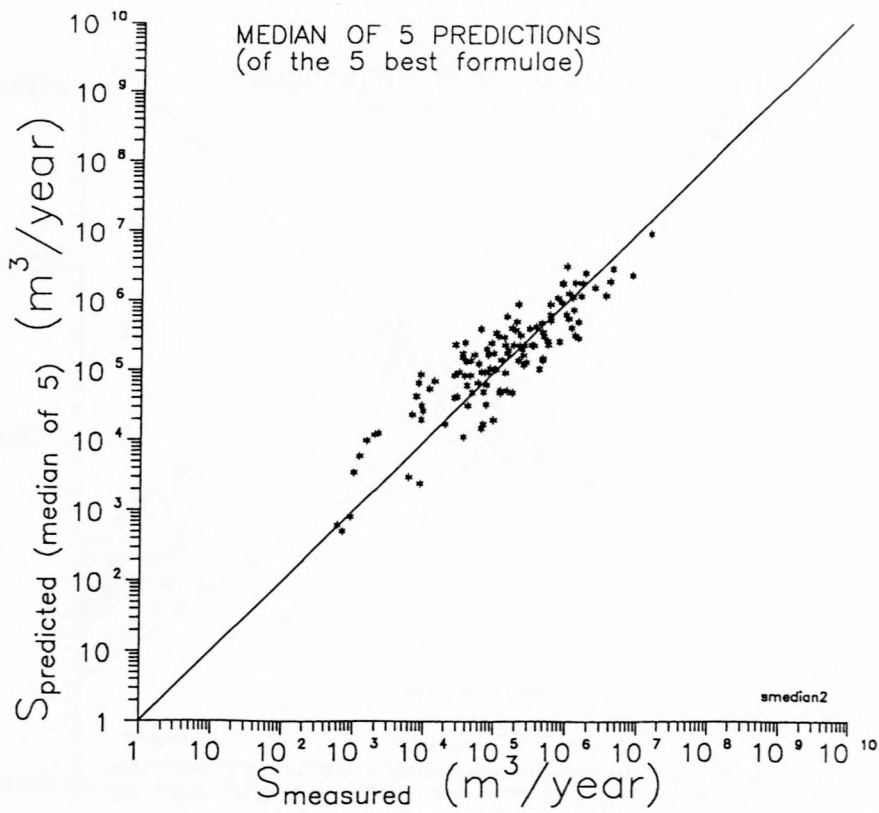


Figure 4.13: Predicted versus measured longshore transport rates for the median of the predictions of the 5 best formulae

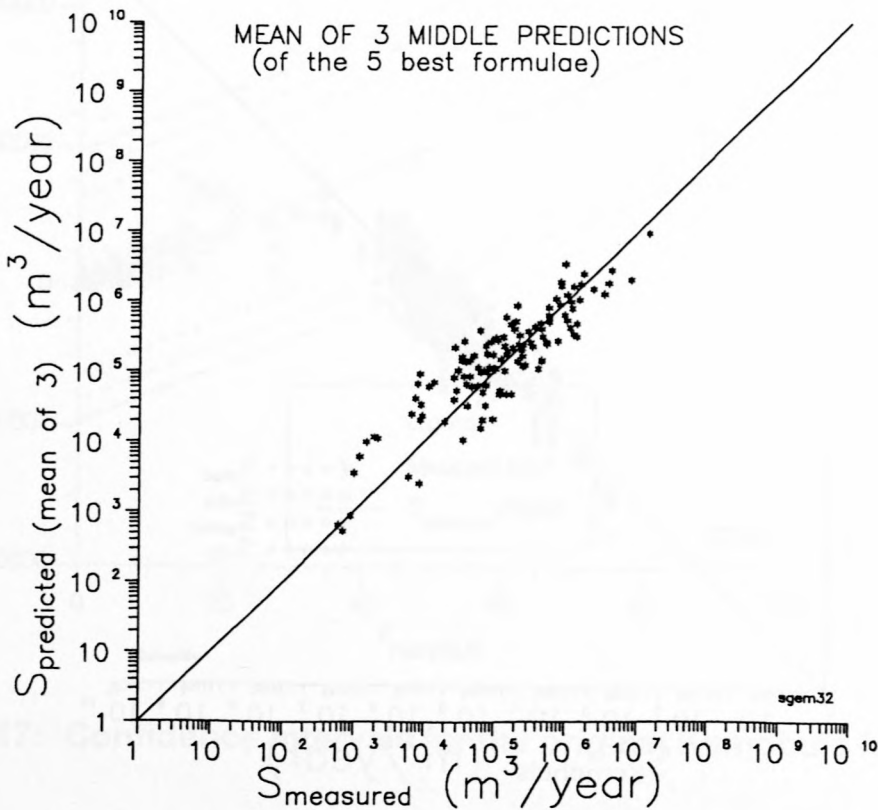


Figure 4.14: Predicted versus measured longshore transport rates for the mean of the 3 middle predictions of the 5 best formulae

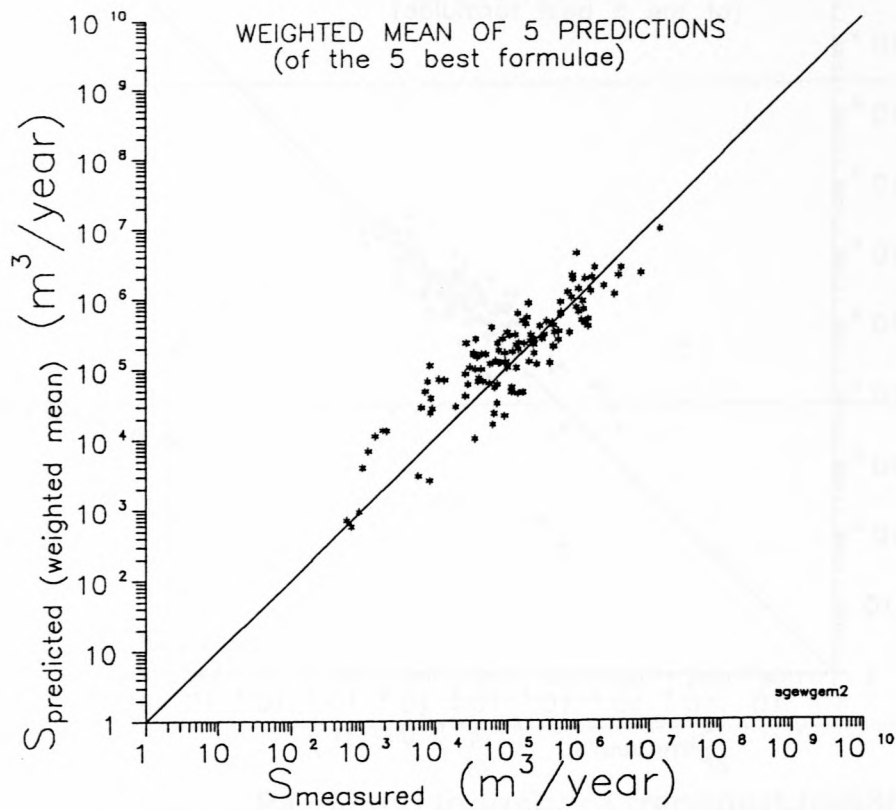


Figure 4.15: Predicted versus measured longshore transport rates for the weighted mean of the predictions of the 5 best formulae

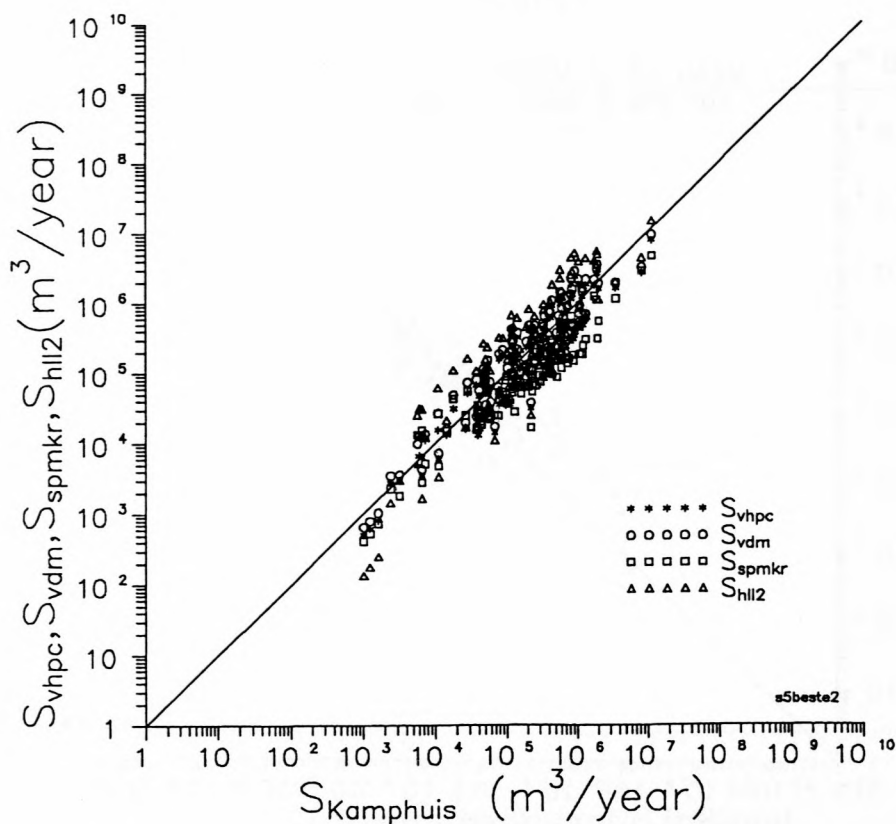


Figure 4.16: Consistency in the predictions of the 5 best formulae

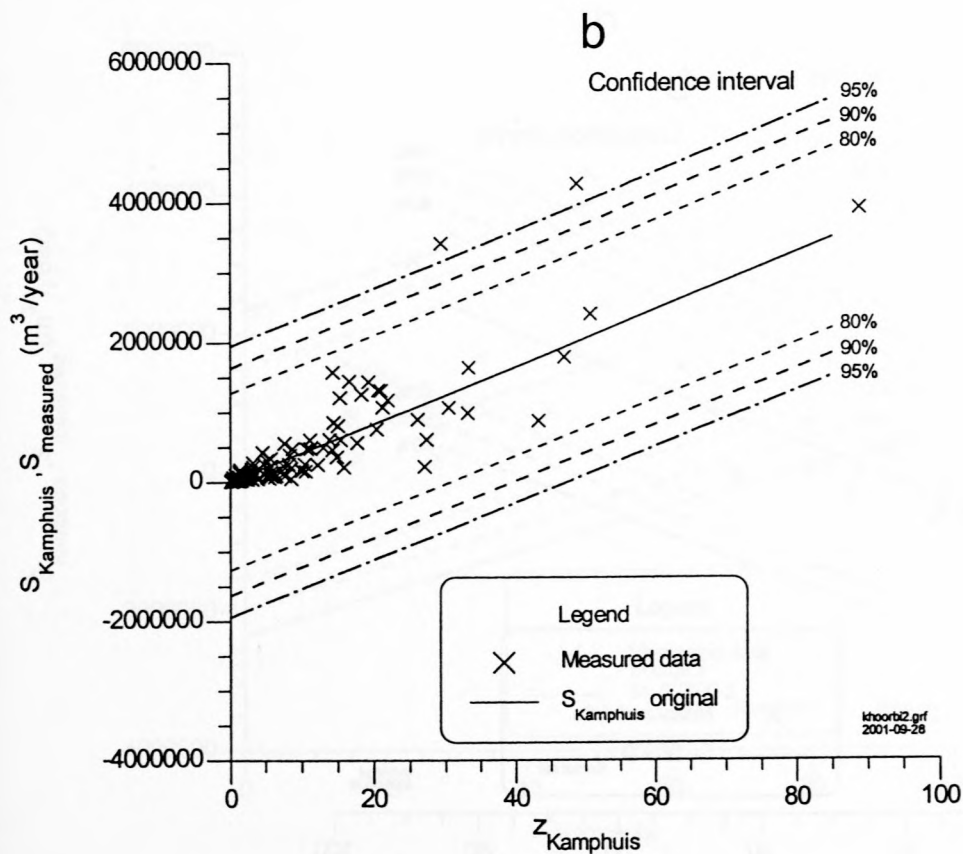
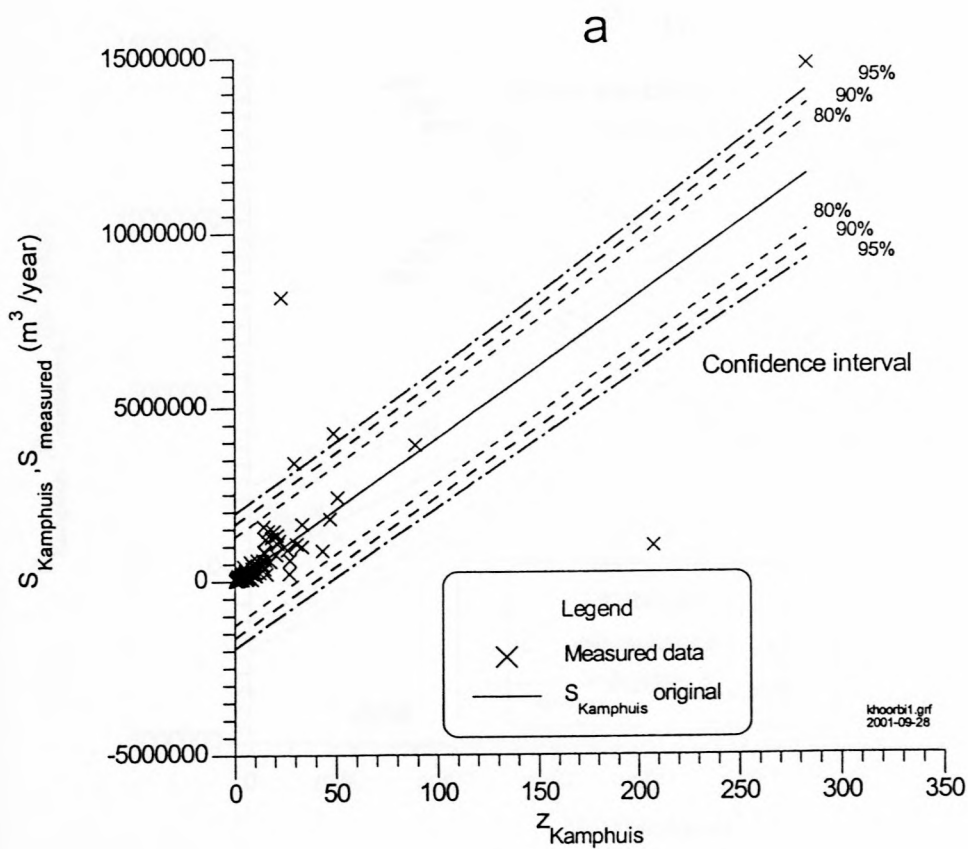


Figure 4.17: Confidence intervals for the original Kamphuis formula

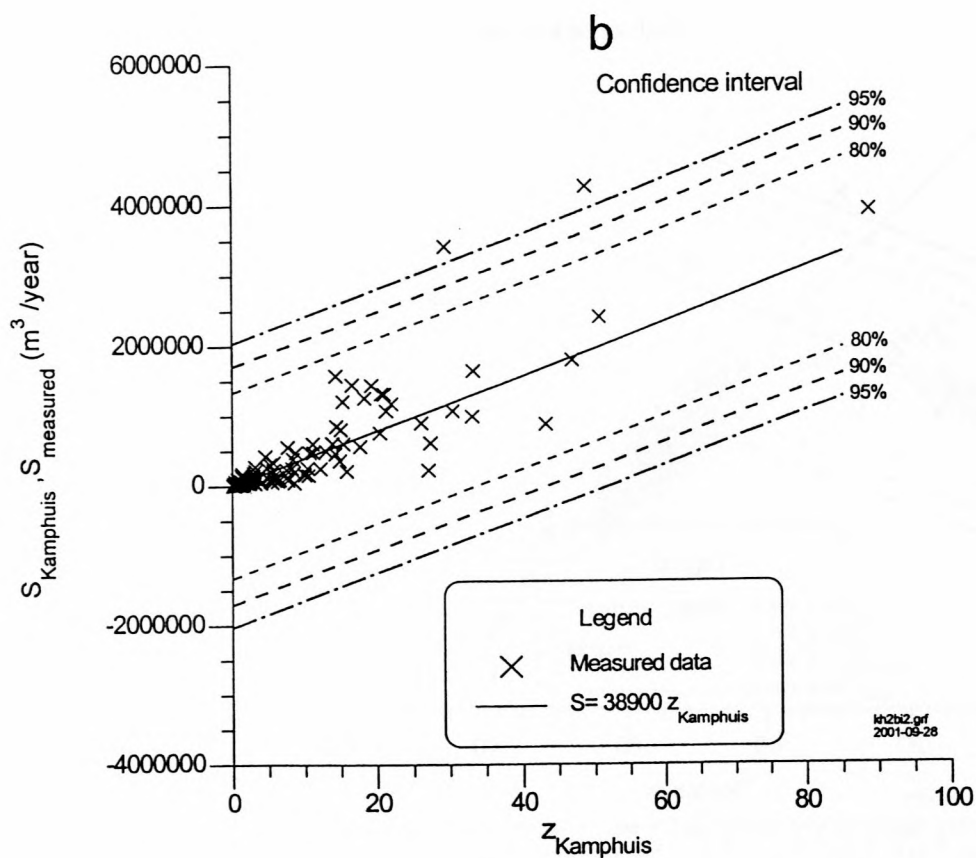
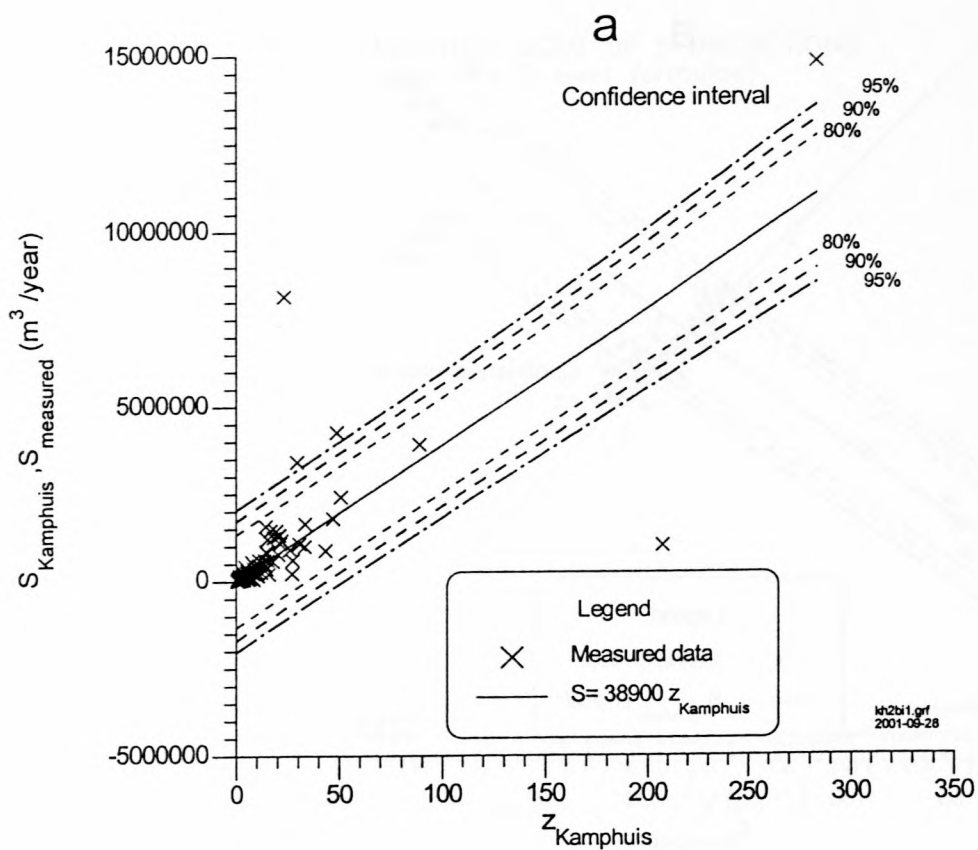


Figure 4.18: Confidence intervals for the recalibrated Kamphuis formula: $S = 38\,900 z_{\text{Kamphuis}}$

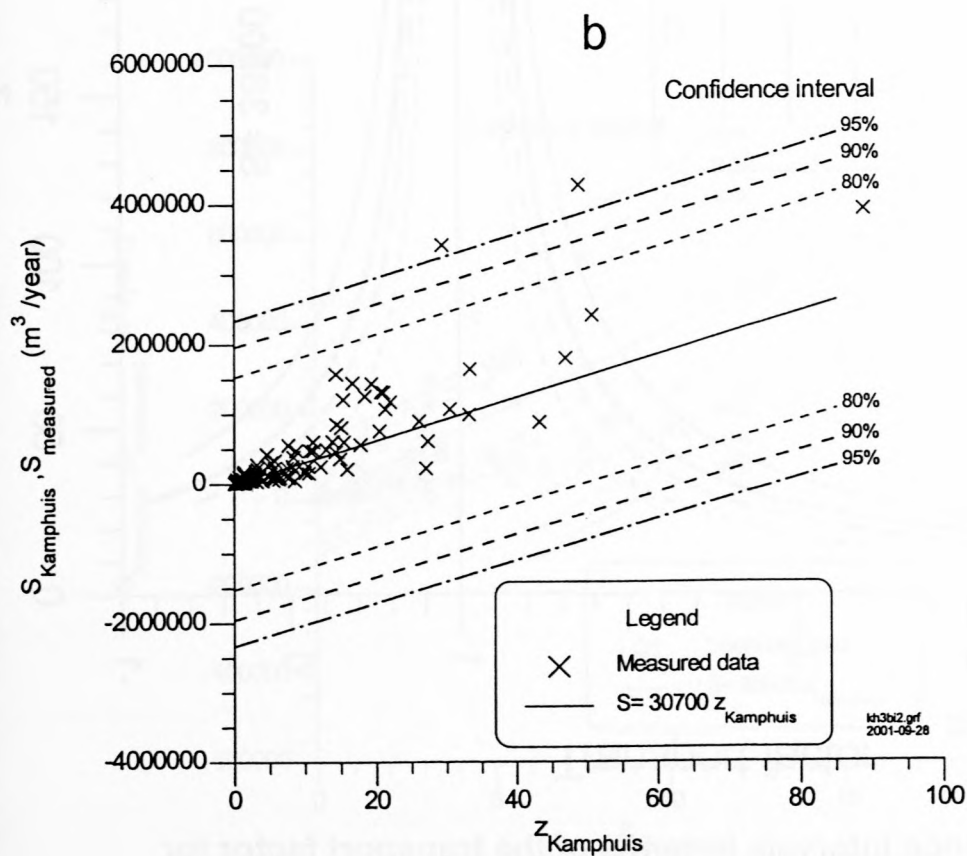
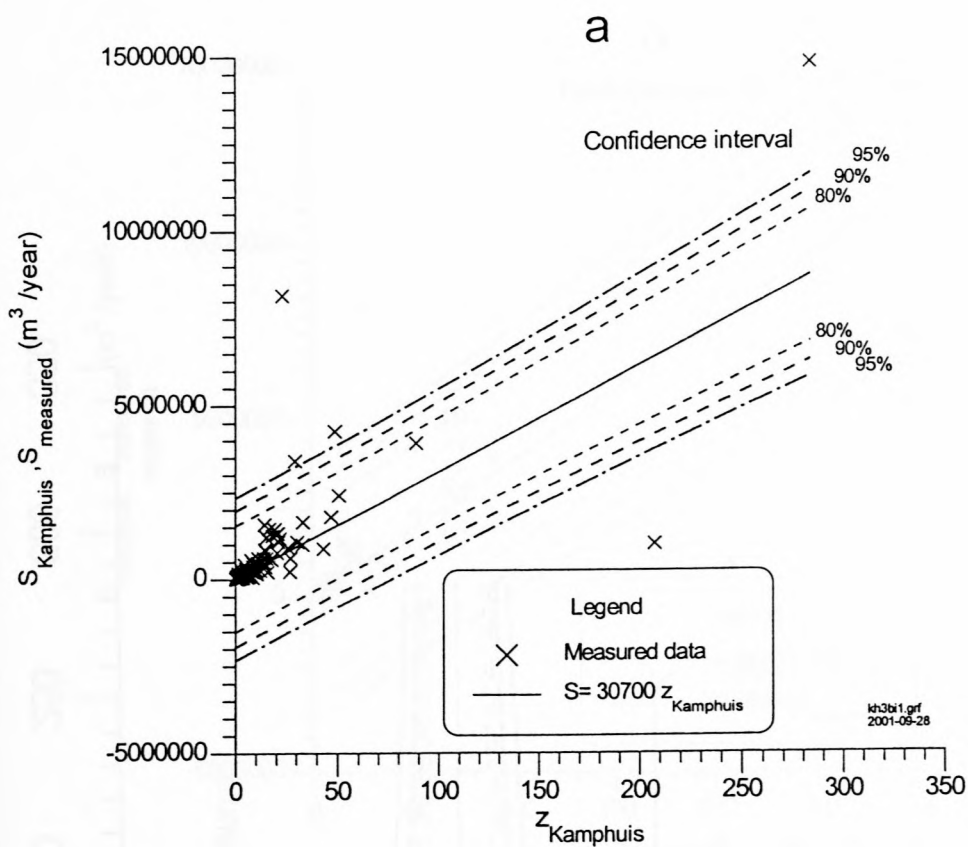


Figure 4.19: Confidence intervals for the recalibrated Kamphuis formula: $S = 30\,700 z_{\text{Kamphuis}}$

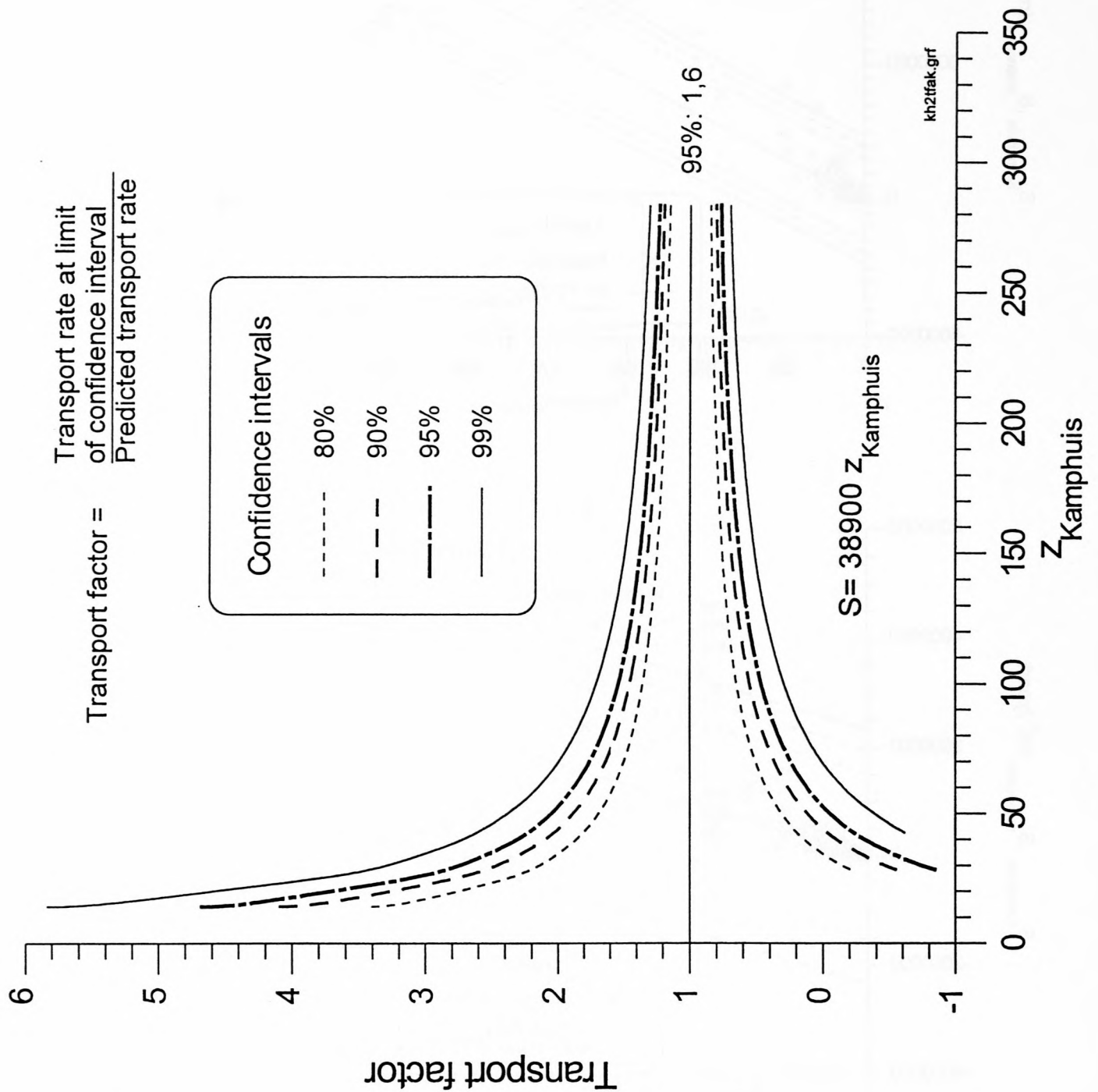


Figure 4.20: Confidence intervals in terms of the transport factor for the recalibrated Kamphuis formula: $S = 38\,900 z_{\text{Kamphuis}}$

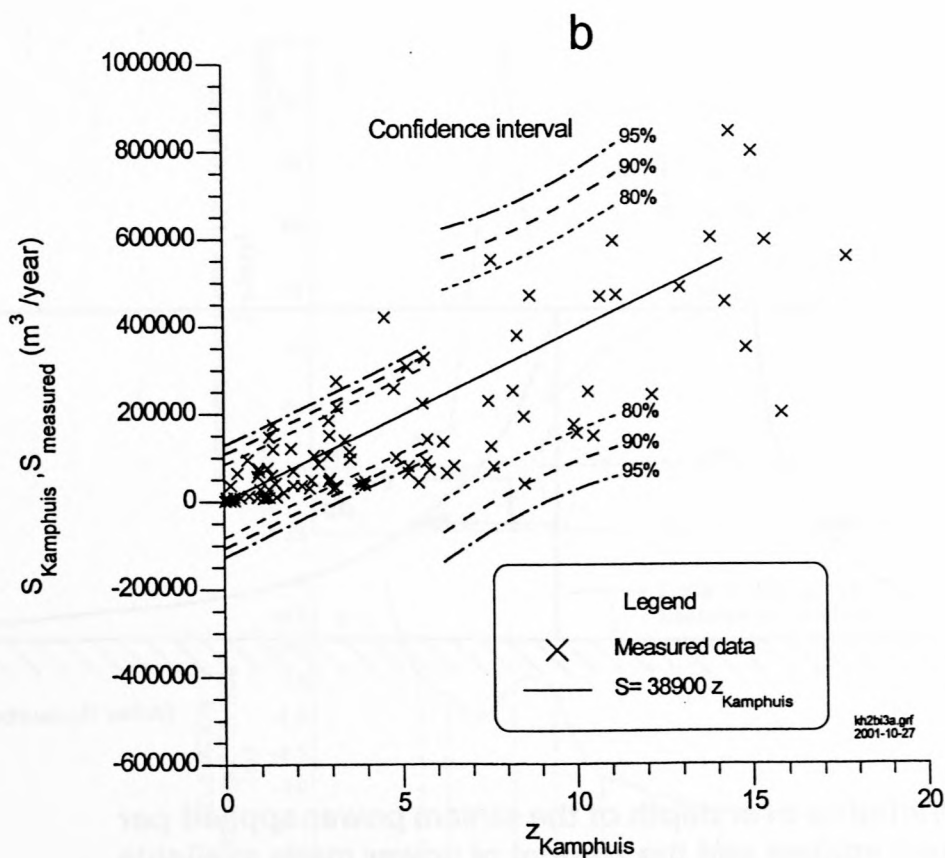
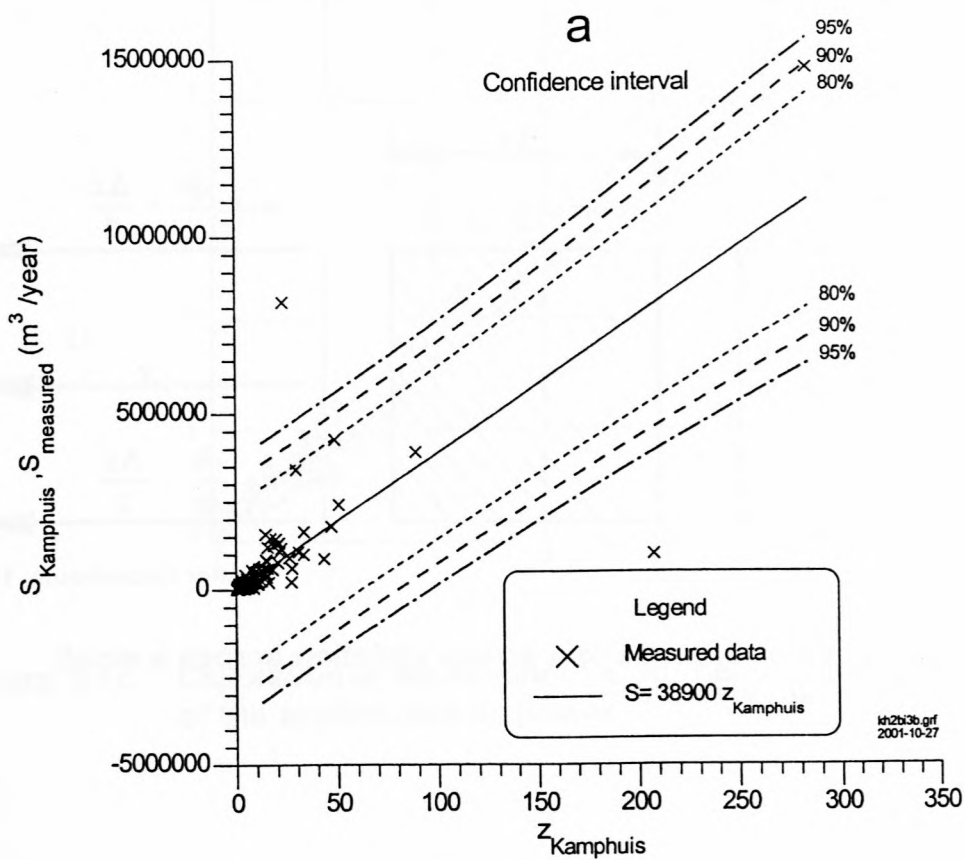


Figure 4.21: Confidence intervals for three sub-ranges of the data for the recalibrated Kamphuis formula: $S = 38\,900 z_{Kamphuis}$

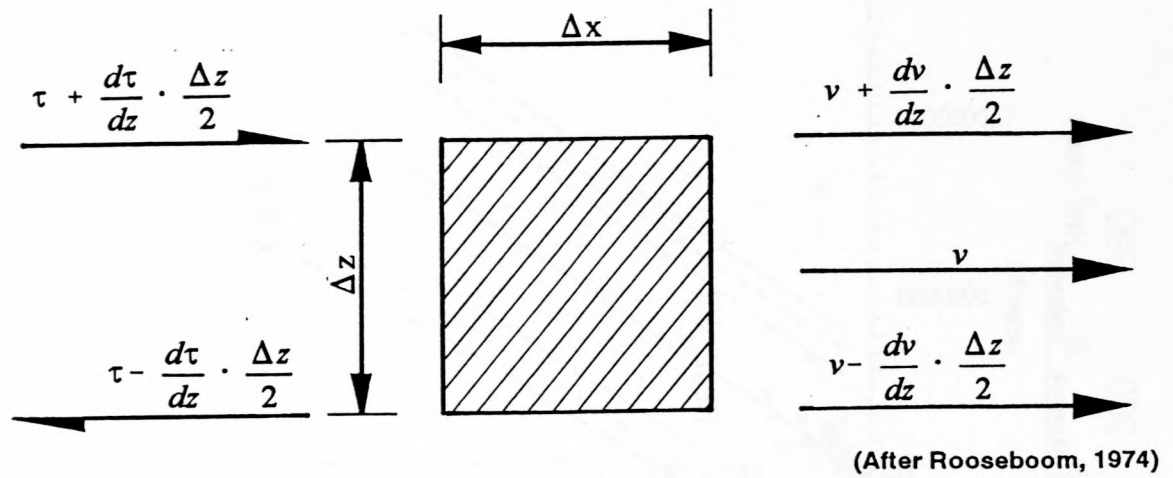


Figure 5.1a: Velocity and shear stress variation across a small fluid element

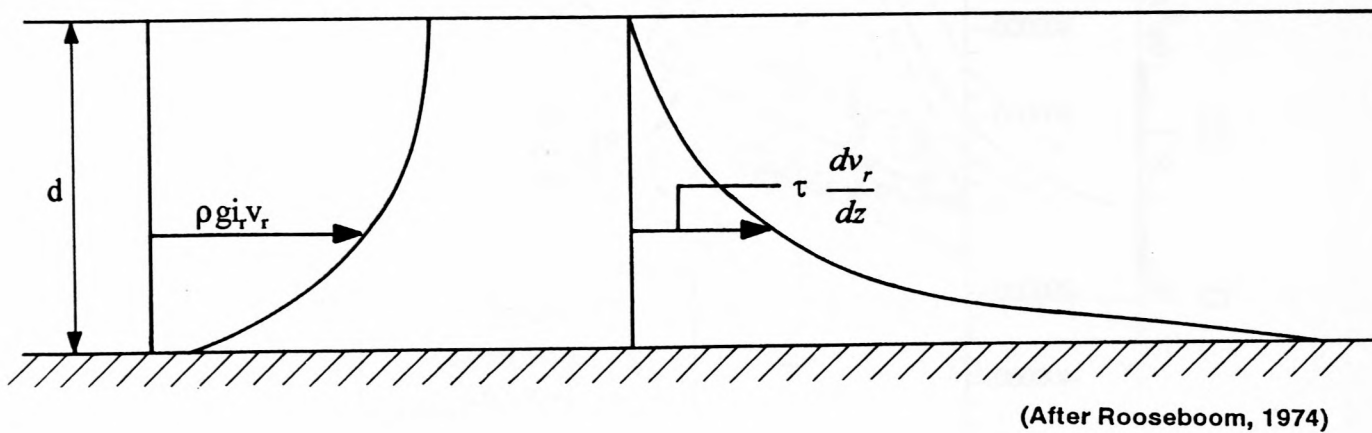


Figure 5.1b: Variation over depth of the stream power applied per unit volume and the amount of power made available by the element.

Z1

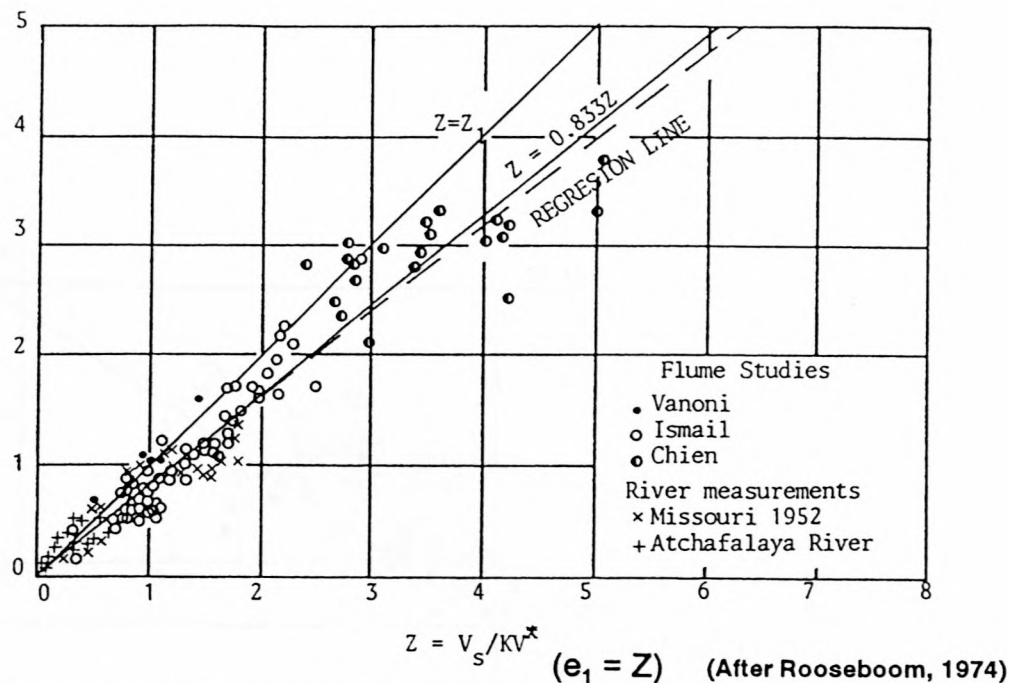
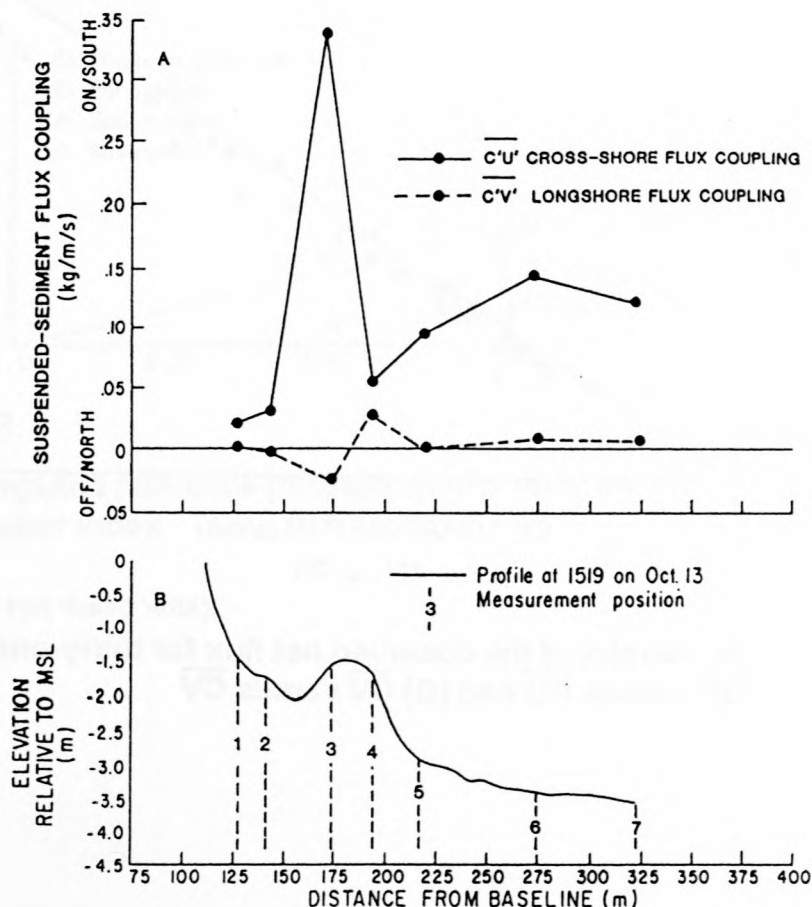
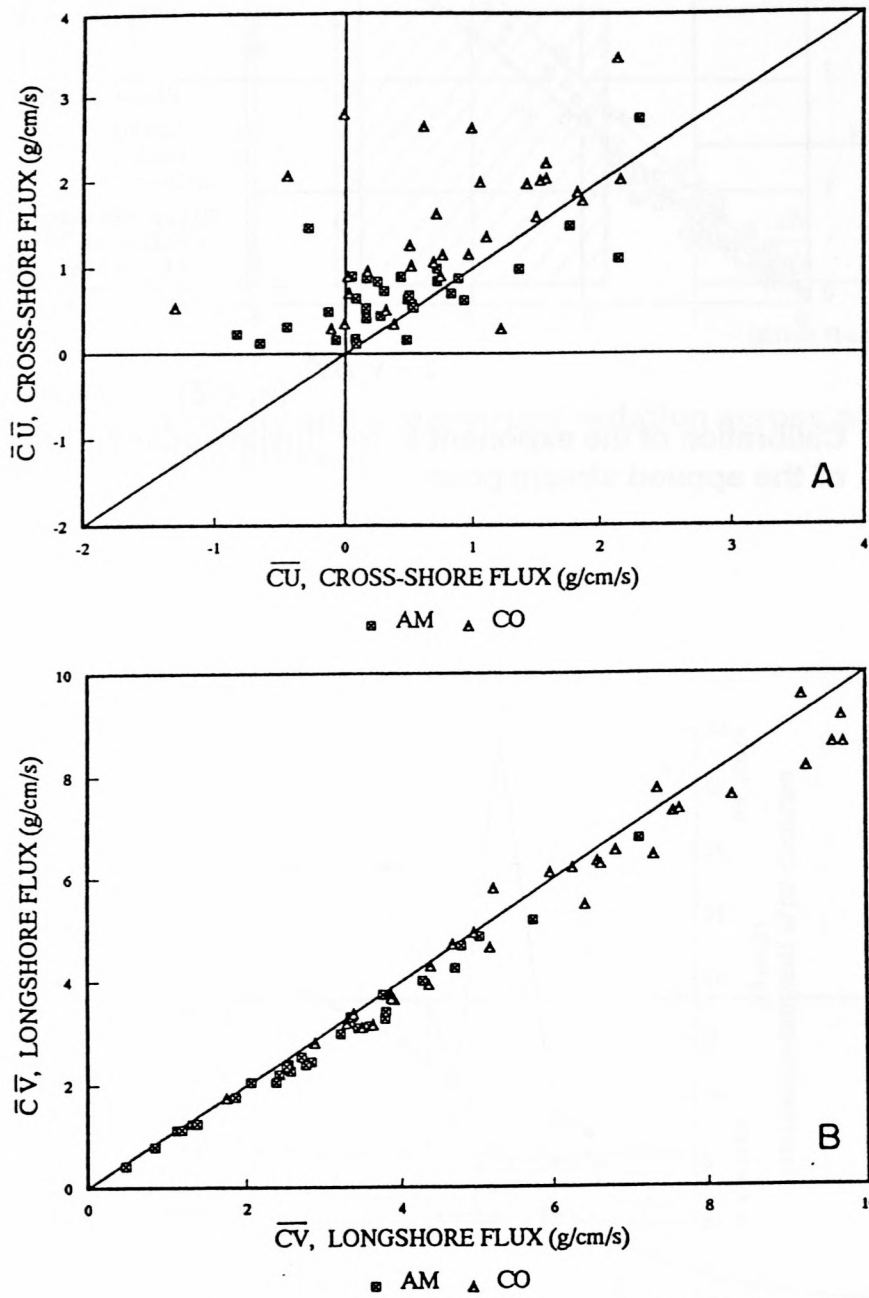


Figure 5.1c: Calibration of the exponent e_1 for fluvial sediment transport in terms of the applied stream power



(After Jaffe et al., 1984)

Figure 5.2: Cross-shore variation of the longshore ($\overline{c'v'}$) and cross-shore ($\overline{c'u'}$) flux couplings



(After Beach and Sternberg, 1992)

Figure 5.3: Scatterplot of the observed net flux for thirty-one 64 s segments: (A) \bar{C}_U versus \bar{C}_U and (B) \bar{C}_V versus \bar{C}_V

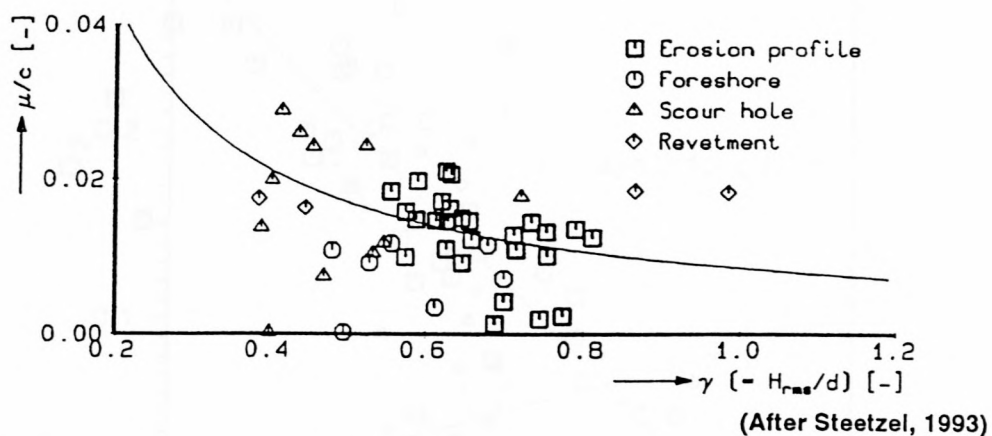


Figure 5.4: Computed vertical mixing gradient/wave celerity ratio as a function of estimated breaker index

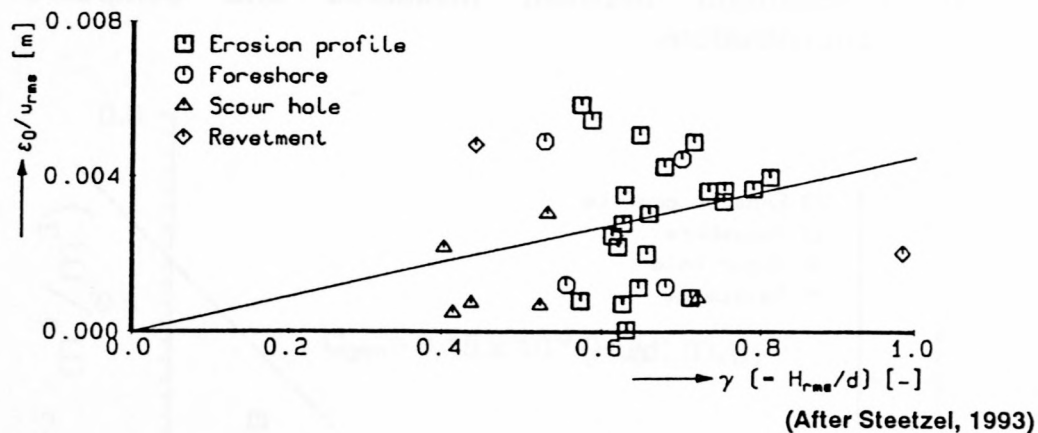


Figure 5.5: Computed reference mixing/velocity ratio as a function of estimated breaker index

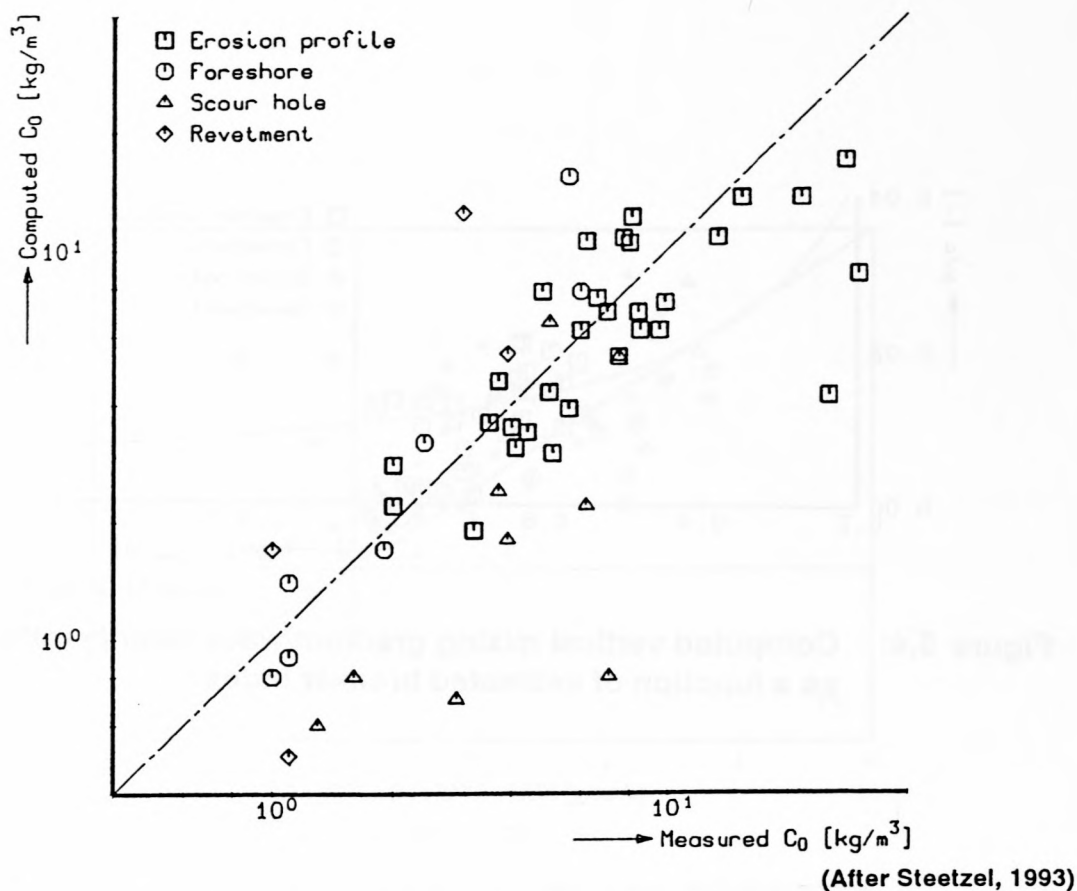


Figure 5.6: Comparison between measured and computed reference concentrations

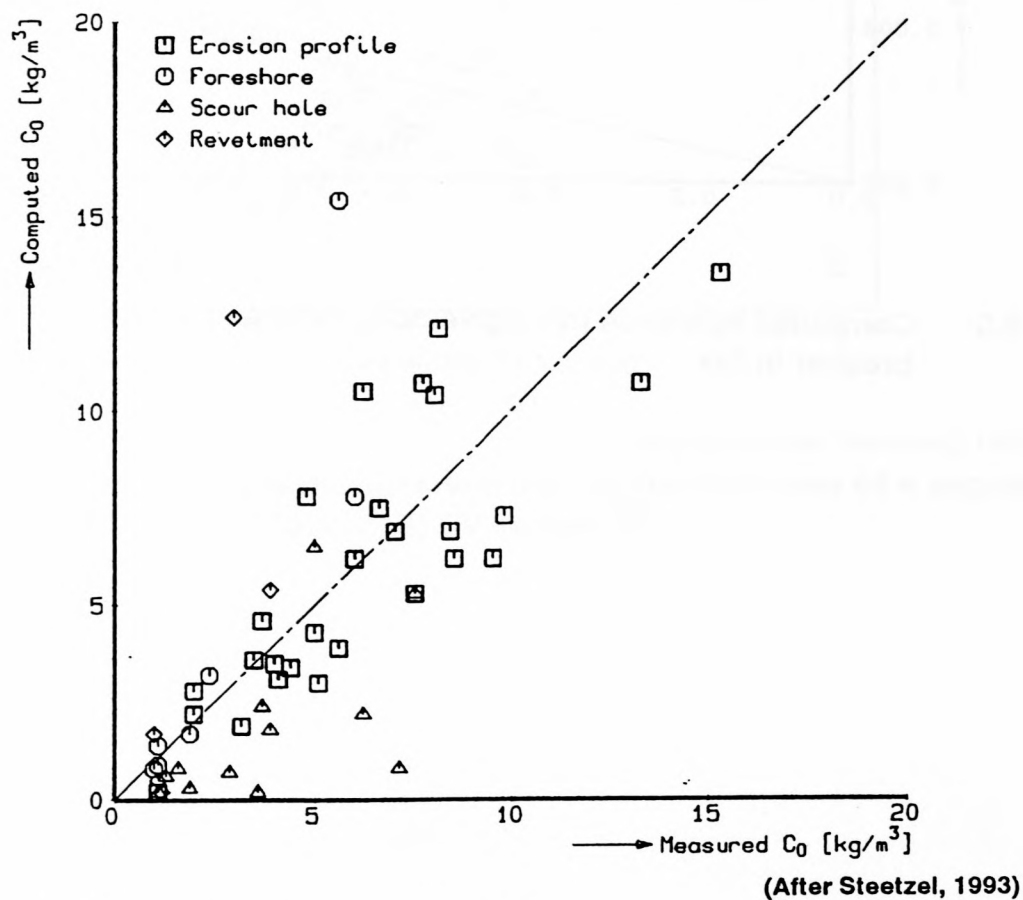


Figure 5.7: Comparison between measured and computed reference concentrations on linear scales

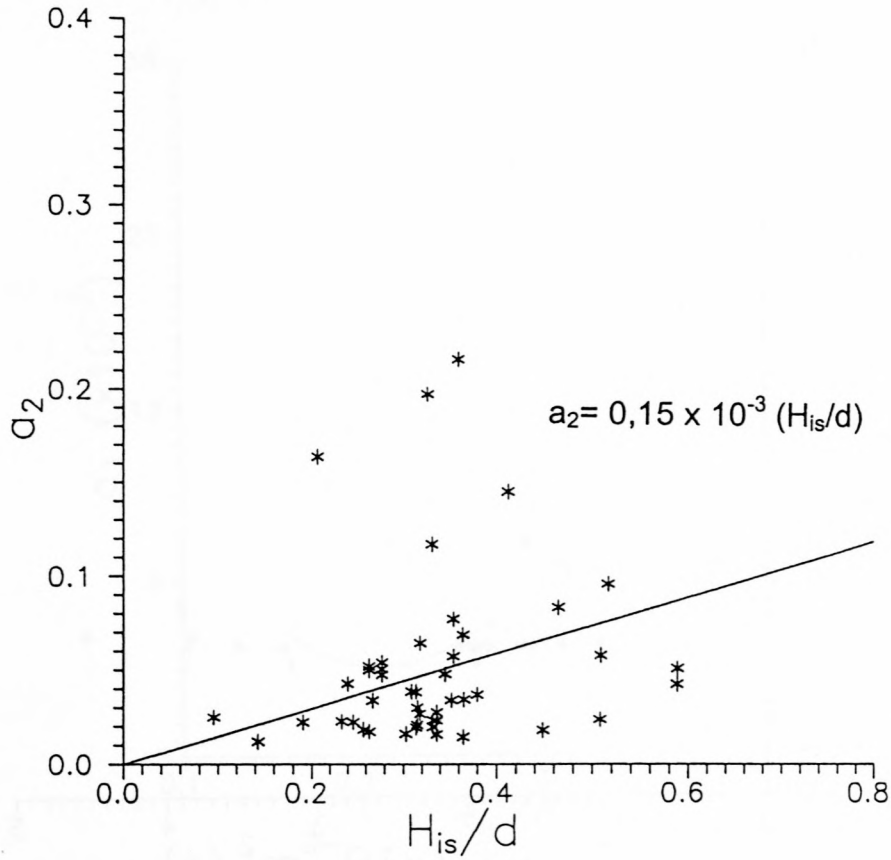


Figure 5.8: Coefficient a_2 versus H_{is}/d

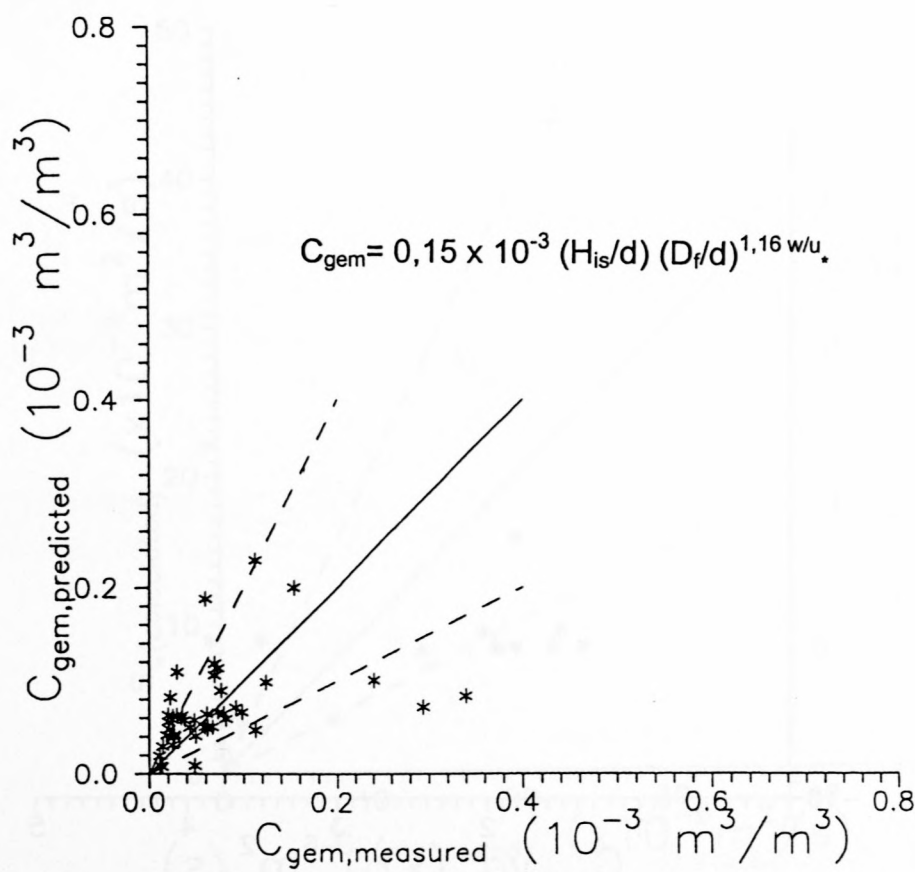


Figure 5.9: Predicted versus measured mean concentrations (outside the surf zone)

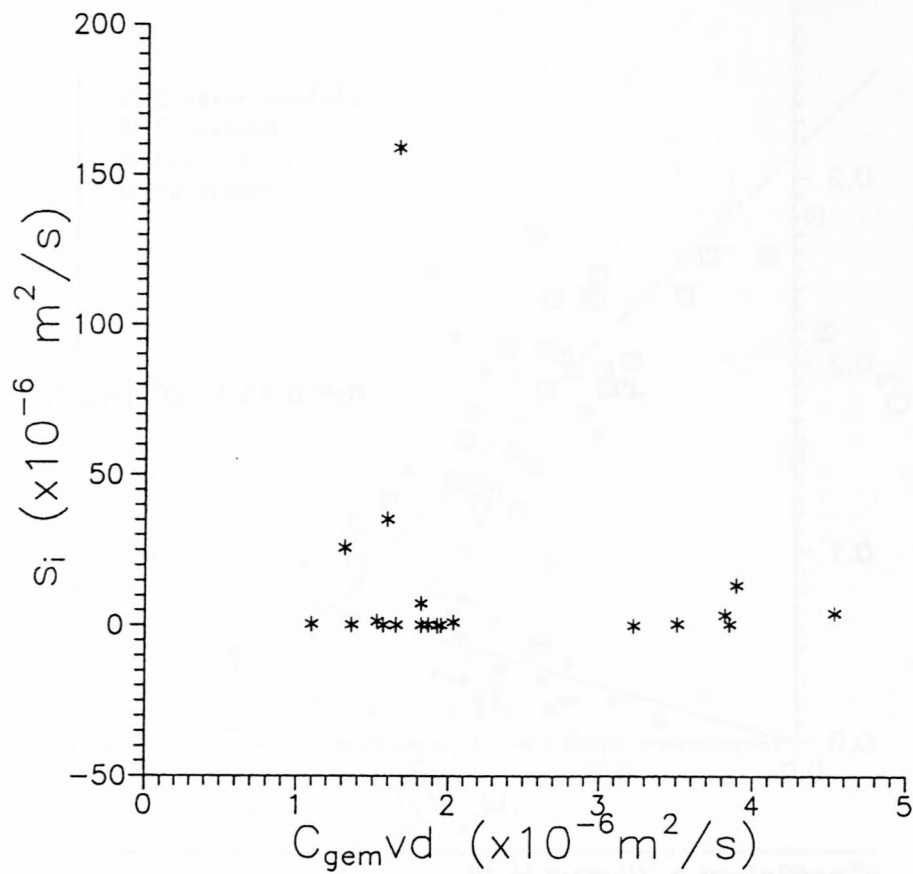


Figure 5.10: Local longshore transport rate against $C_{\text{gem}} \cdot v \cdot d$ for all the realistic data points

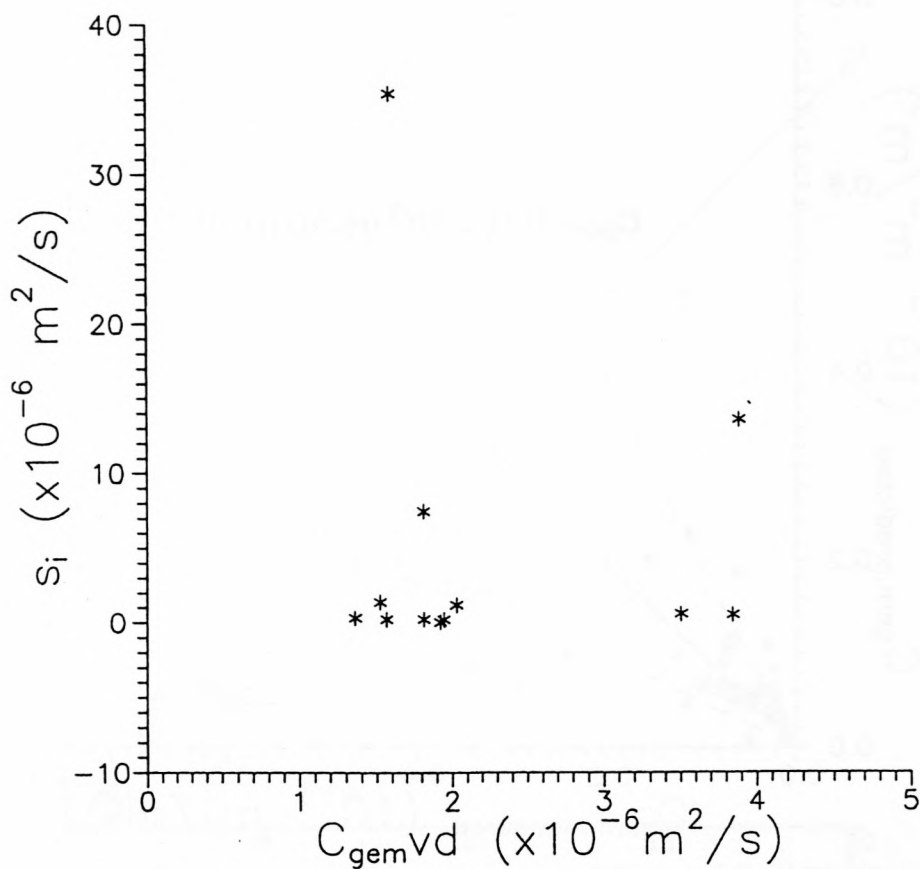


Figure 5.11: Local longshore transport rate against $C_{\text{gem}} \cdot v \cdot d$ for the most accurate data points

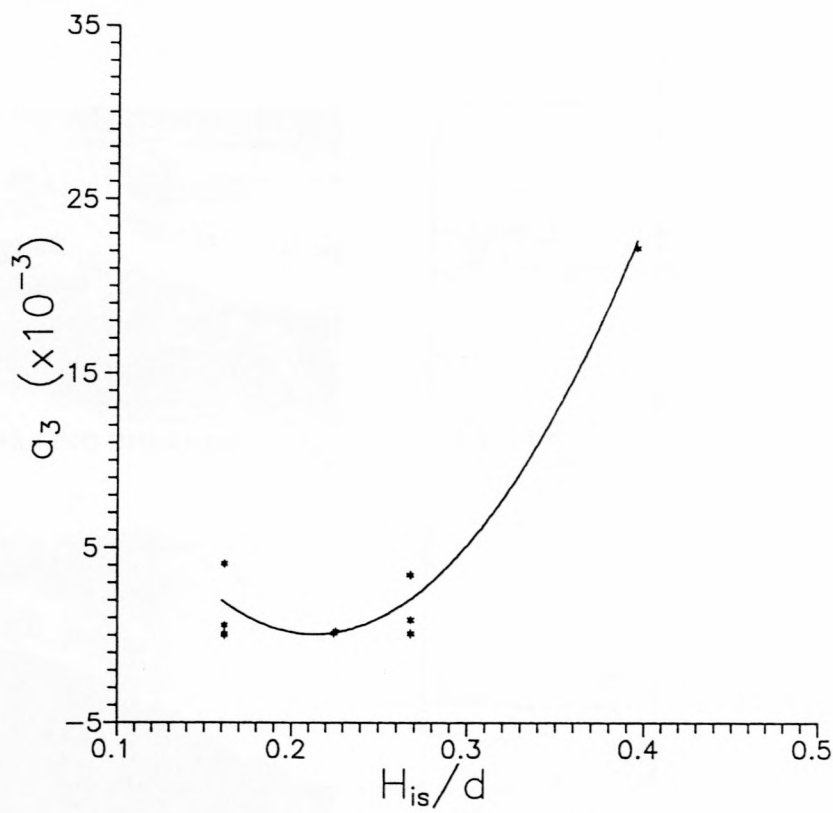


Figure 5.12: Calibration of coefficient a_3 versus H_{is}/d

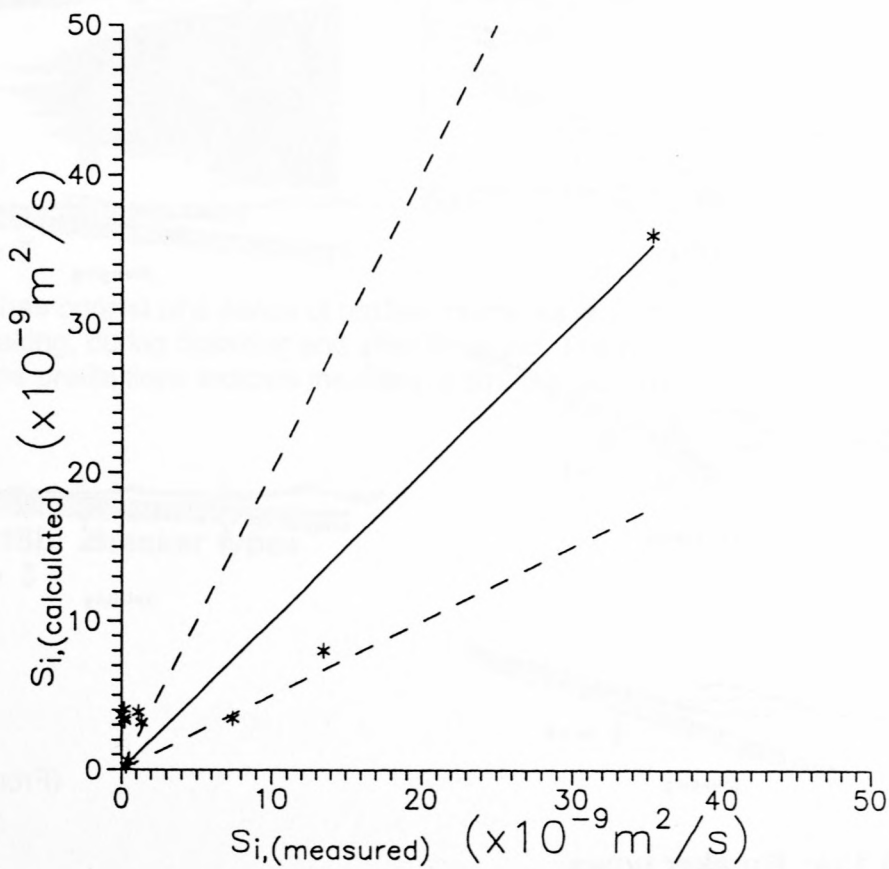


Figure 5.13: Predicted versus measured local longshore transport rates for the most accurate data points (outside the surf zone)

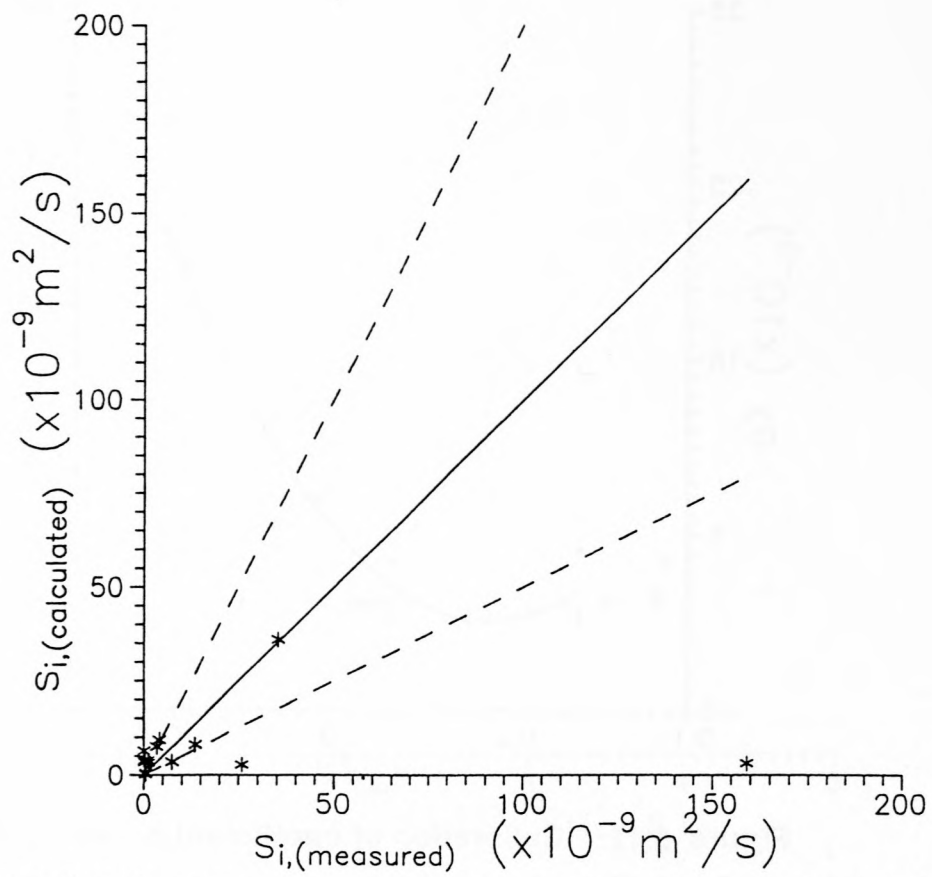
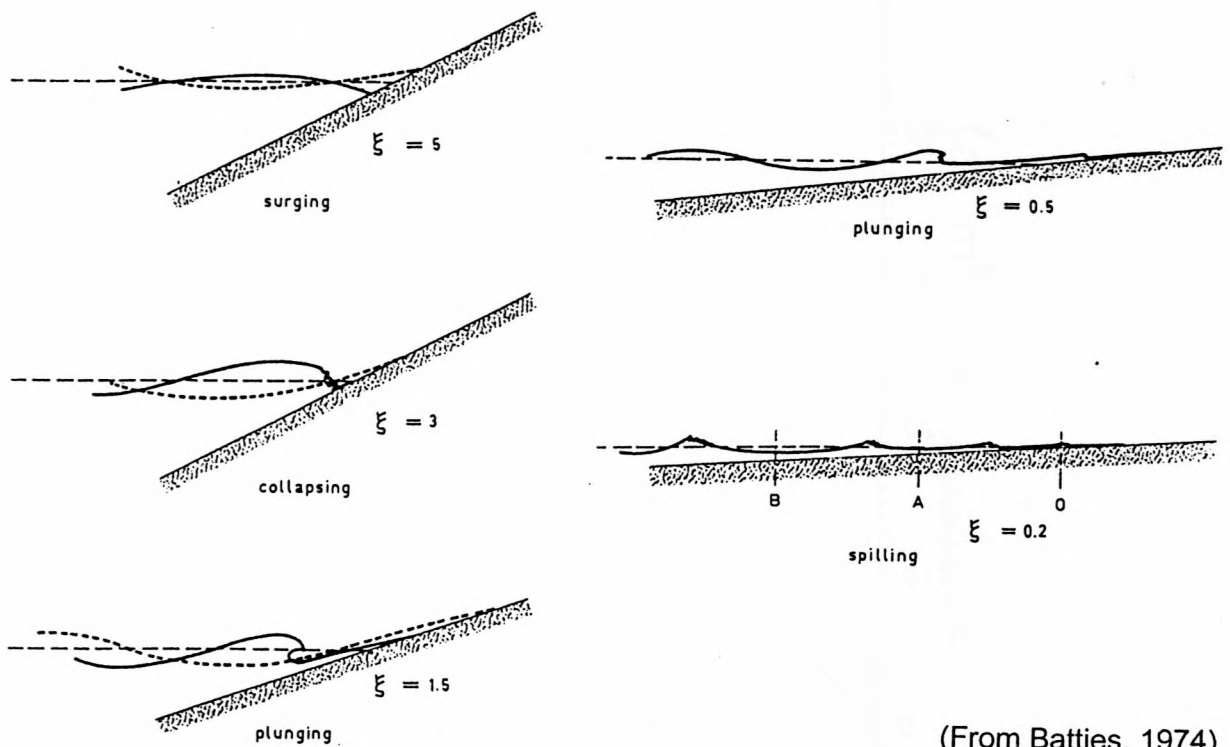


Figure 5.14: Predicted versus measured local longshore transport rates for all the realistic data points (outside the surf zone)

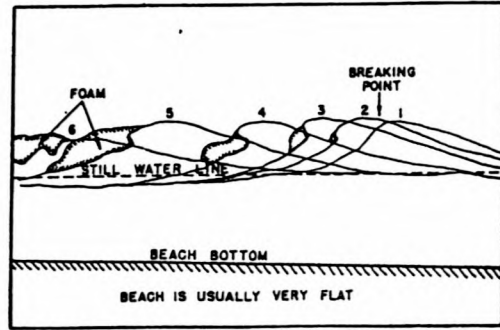


(From Battjes, 1974)

Figure 5.15a: Breaker types



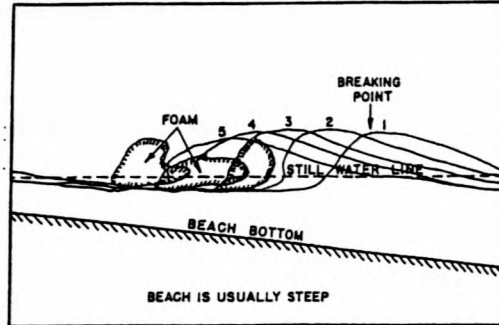
SPILLING BREAKER



SKETCH SHOWING THE GENERAL CHARACTER OF SPILLING BREAKER



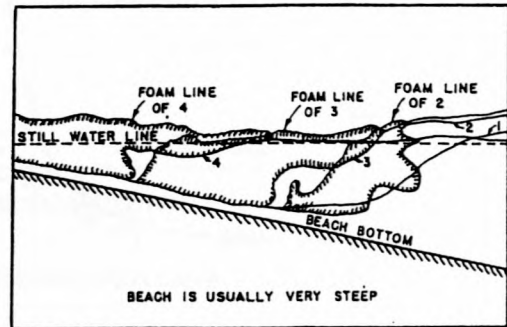
PLUNGING BREAKER



SKETCH SHOWING THE GENERAL CHARACTER OF PLUNGING BREAKER



COLLAPSING BREAKER



SKETCH SHOWING THE GENERAL CHARACTER OF COLLAPSING BREAKERS

The sketches consist of a series of profiles of the wave from as it appears before breaking, during breaking and after breaking. The numbers opposite the profile lines indicate the relative times of occurrences

(adapted from US Army, Corps of Engineers, 1984)

Figure 5.15b: Breaker types

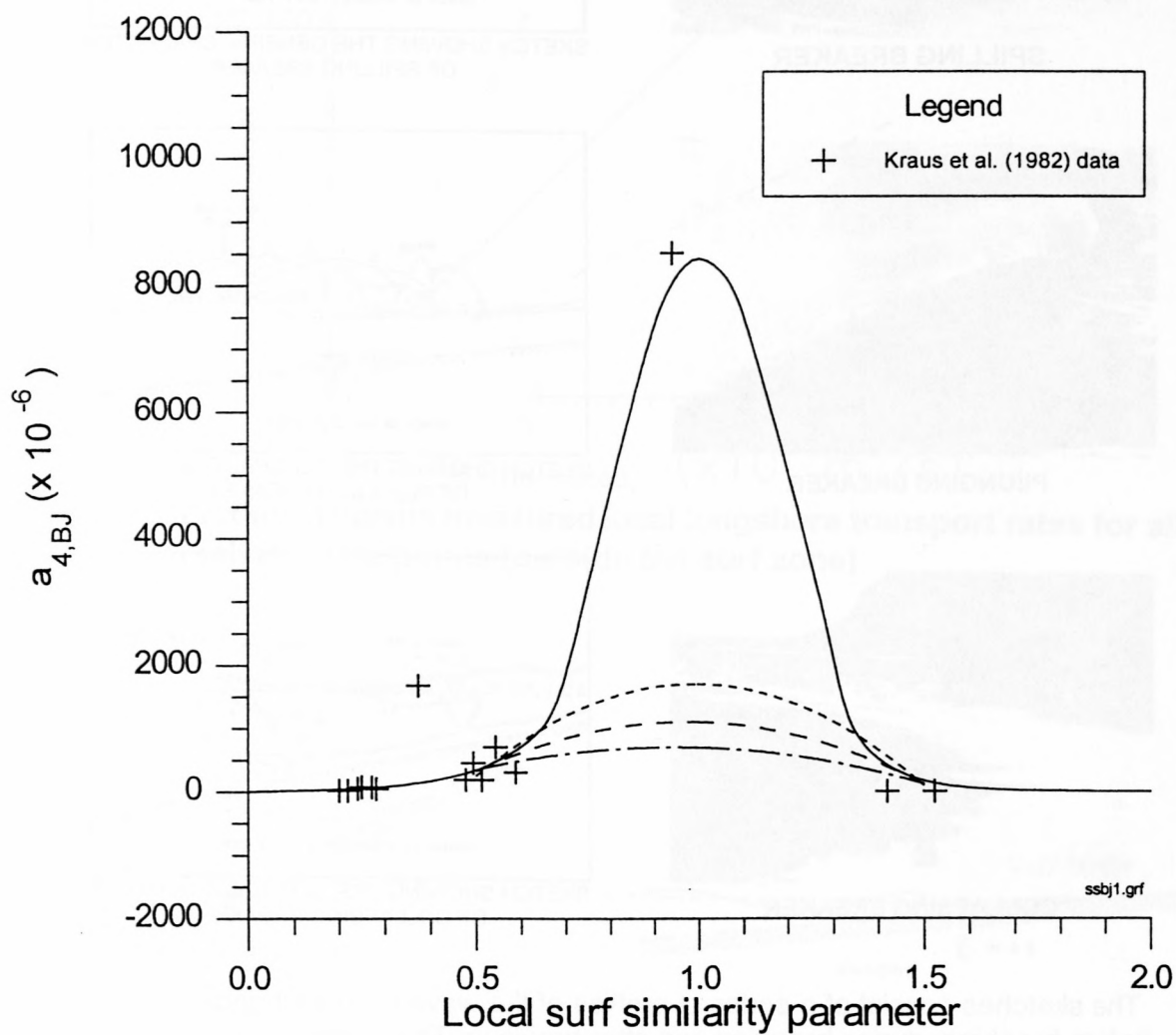


Figure 5.16: Curves of a_4 fitted through data on local longshore transport rates

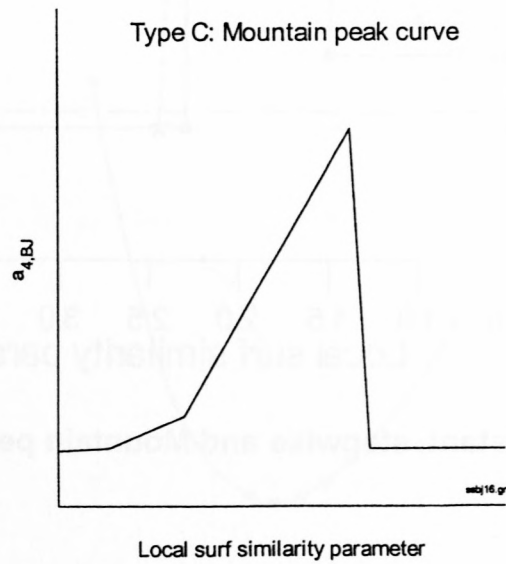
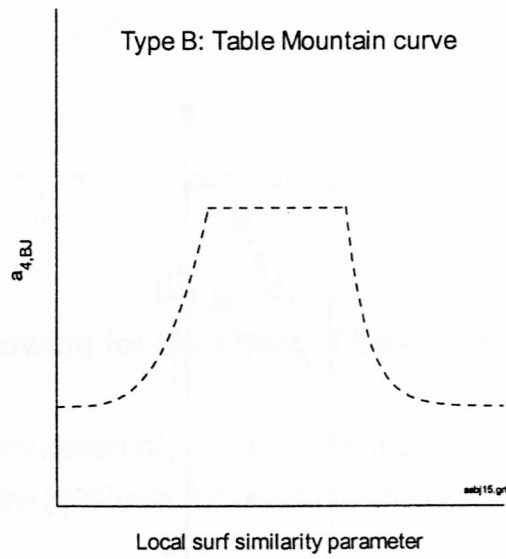
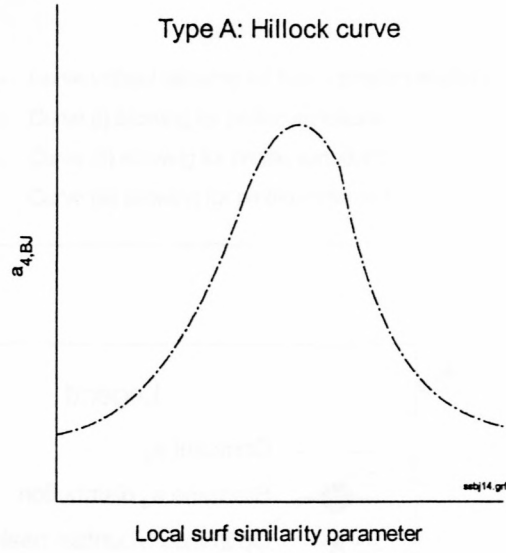


Figure 5.17: Different types of theoretical a_4 distributions

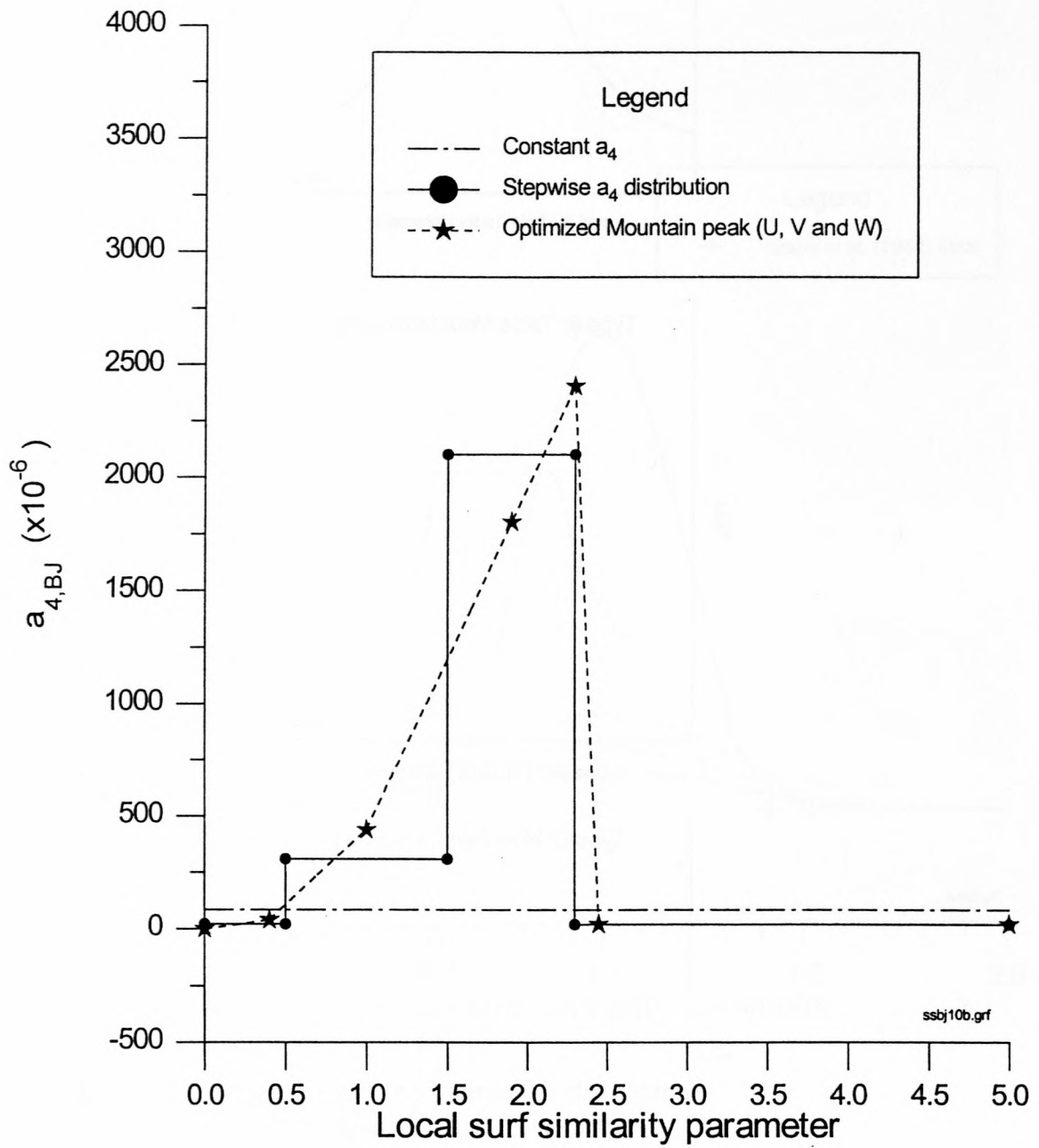


Figure 5.18: Constant, stepwise and Mountain peak distributions of a_4

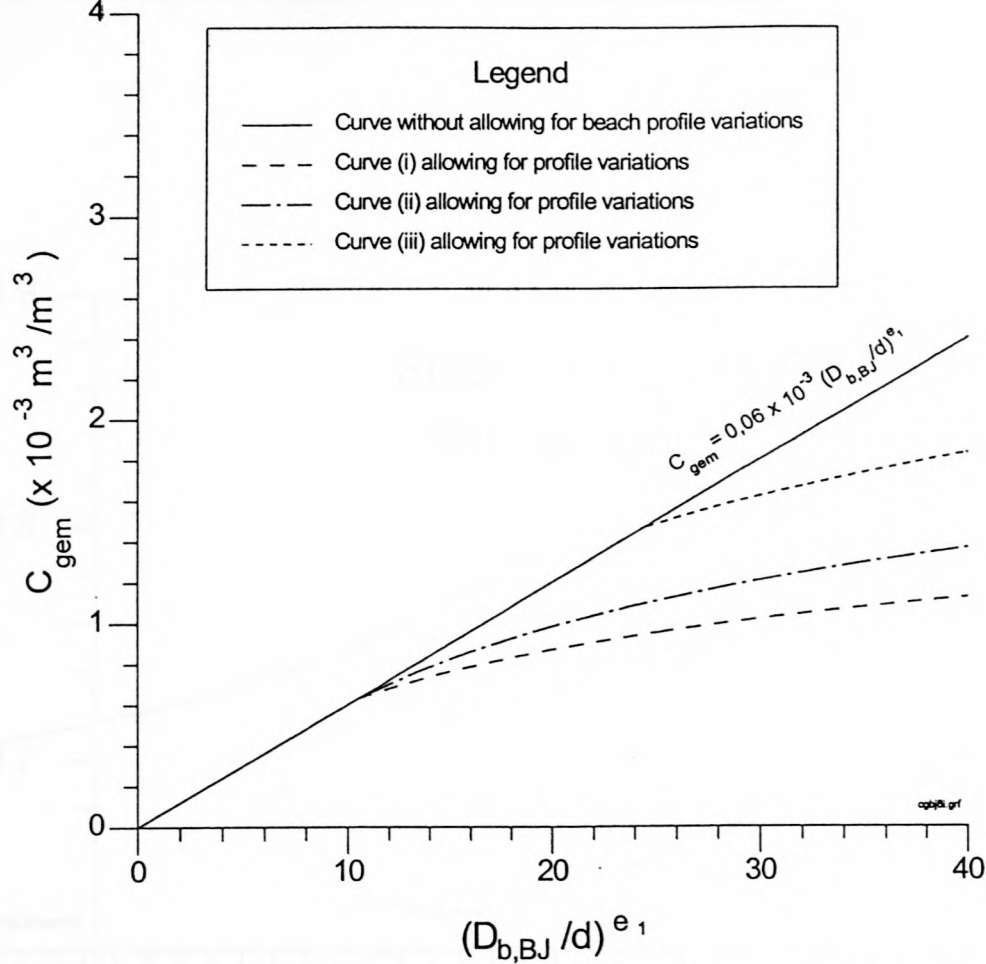


Figure 5.19: Curves allowing for the effect of beach profile variations

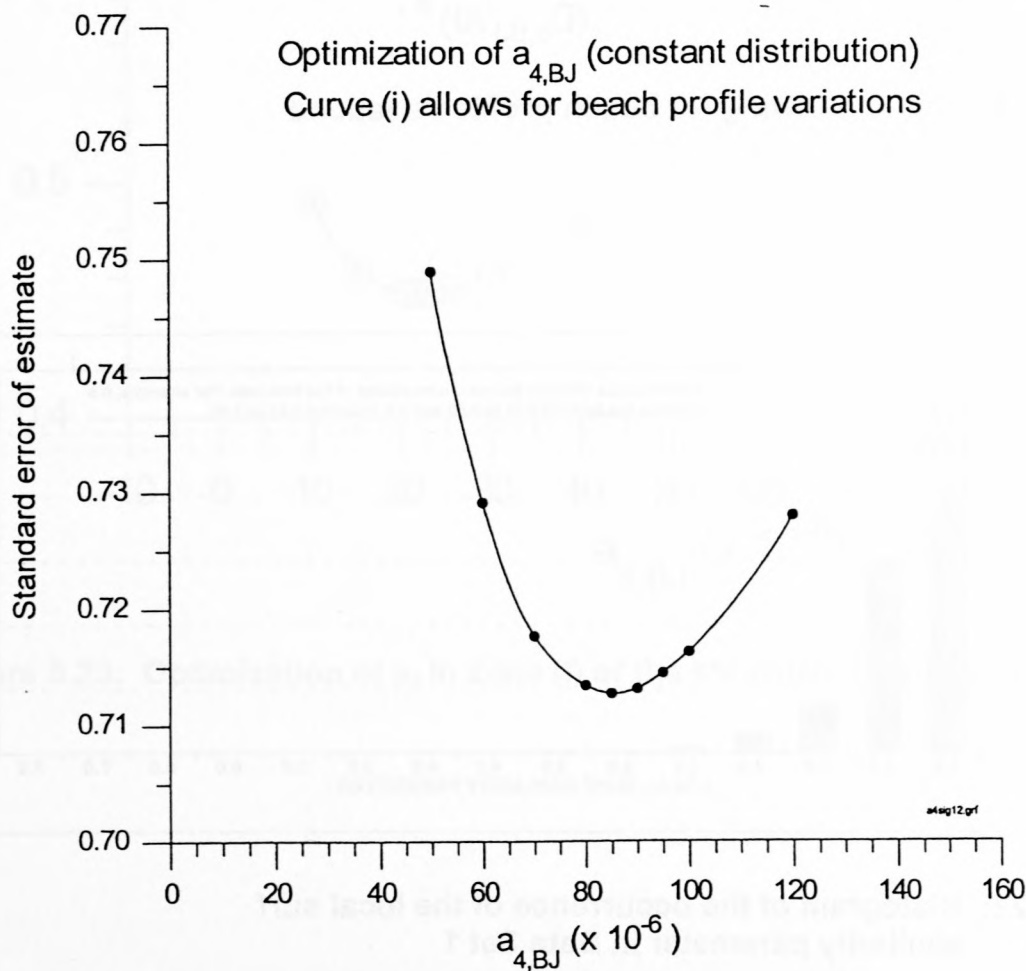


Figure 5.20: Optimization of a constant a_4 while allowing for beach profile variations

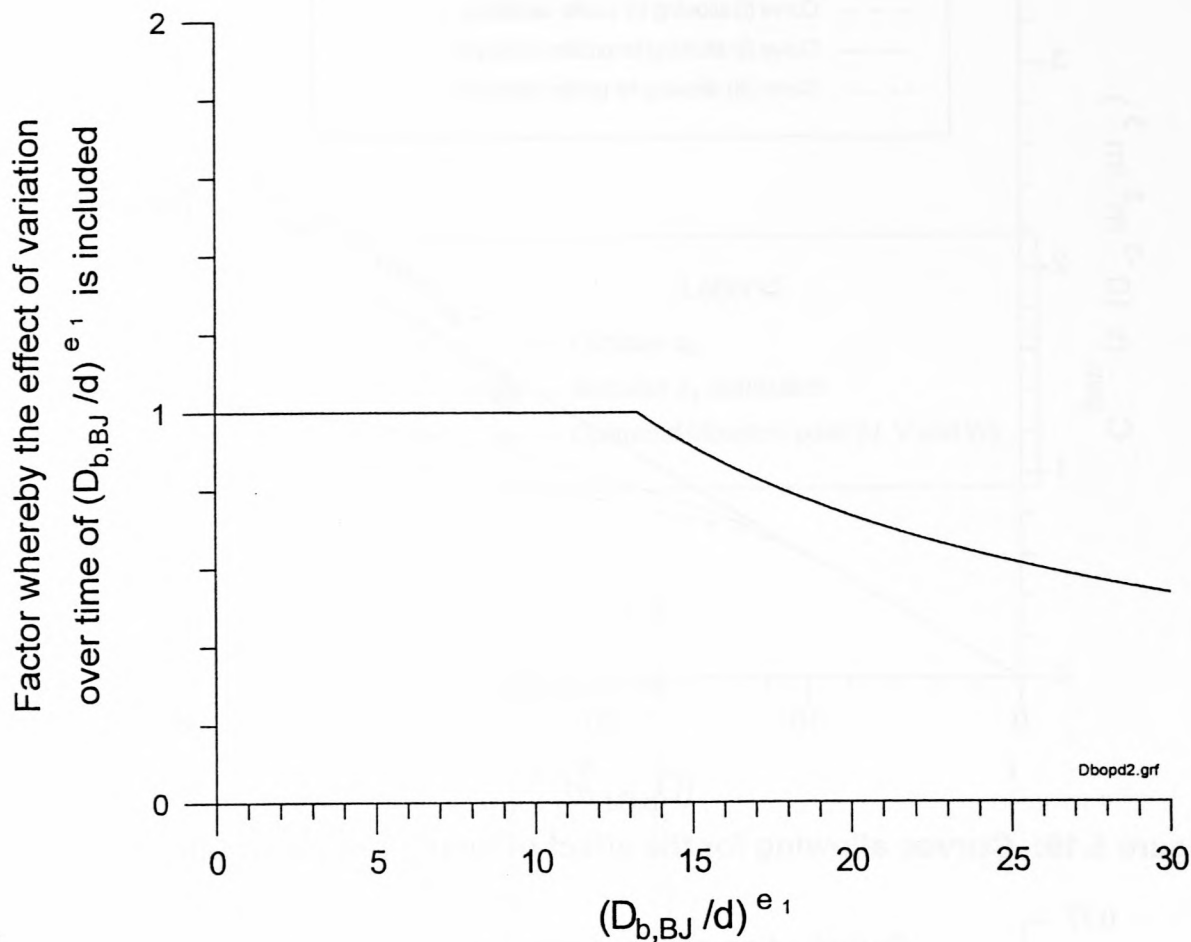


Figure 5.21: Factor allowing for beach profile variations

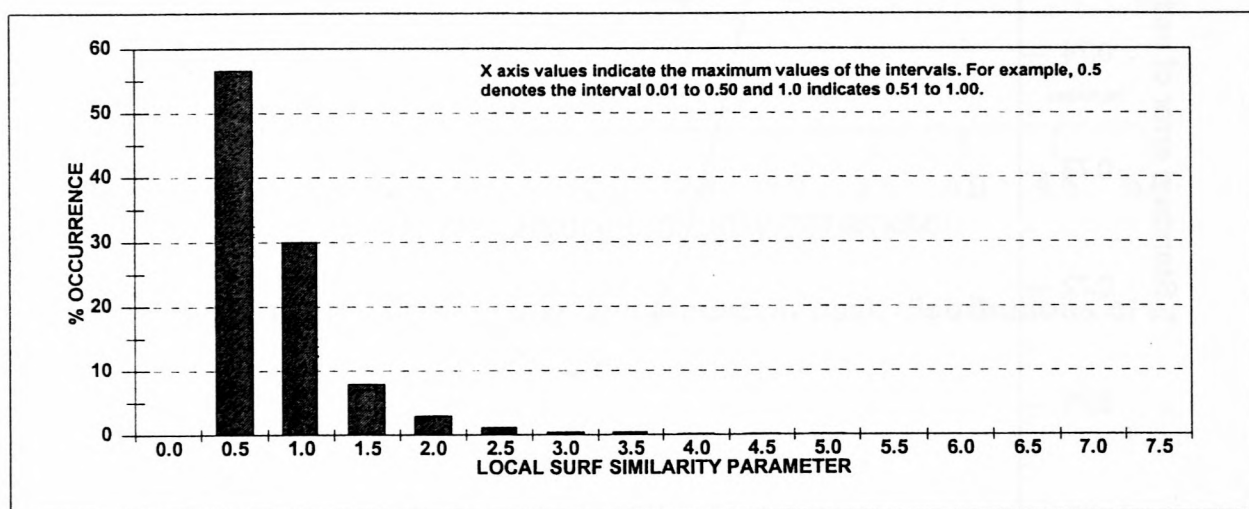


Figure 5.22: Histogram of the occurrence of the local surf similarity parameter in Data Set 1

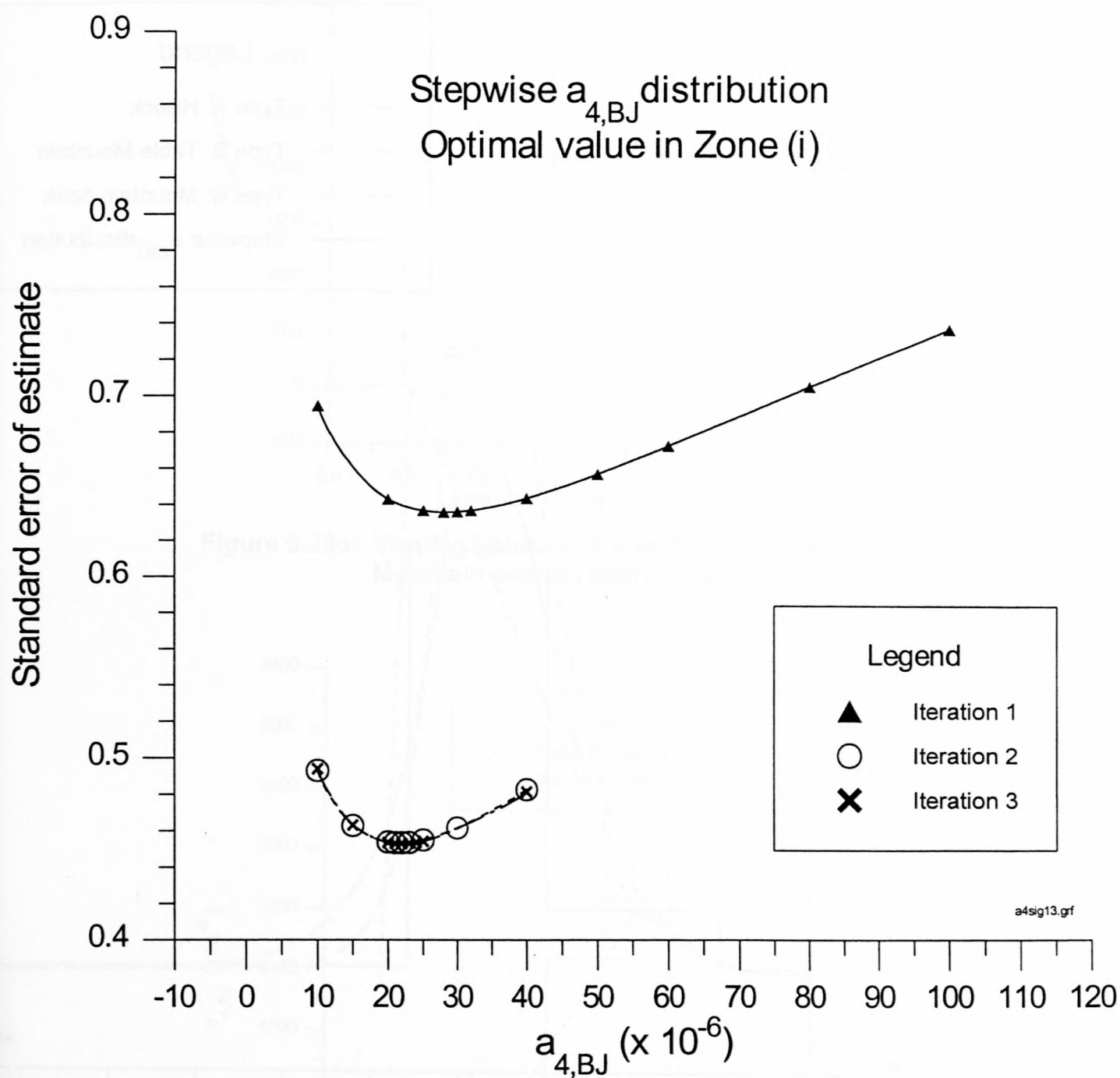


Figure 5.23: Optimization of a_4 in Zone (i) of the stepwise distribution

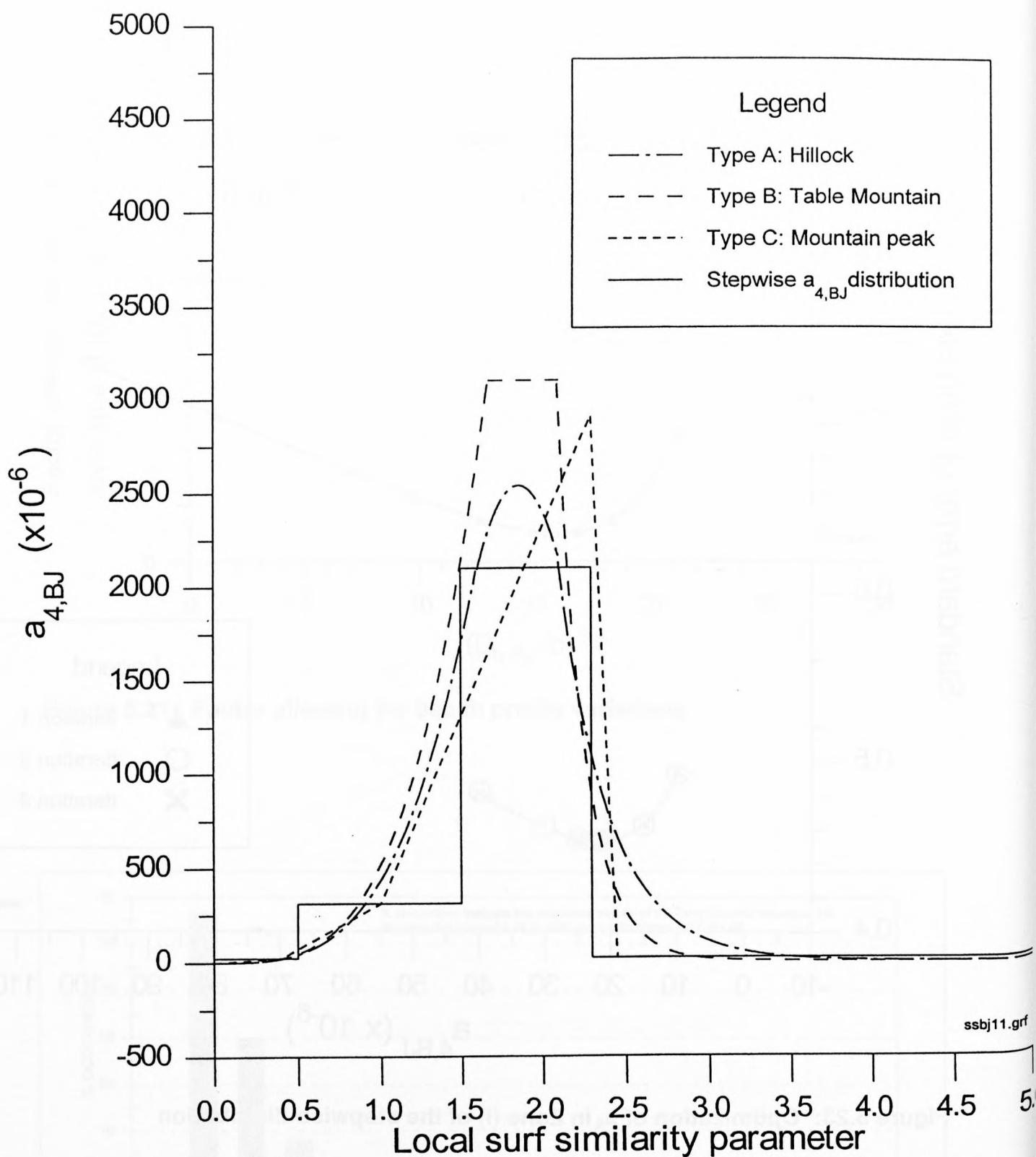


Figure 5.24: Types A, B and C curves in relation to the stepwise a_4 distribution

Figure 5.22: Histogram of the occurrence of the local surf similarity parameter in Data Set 1

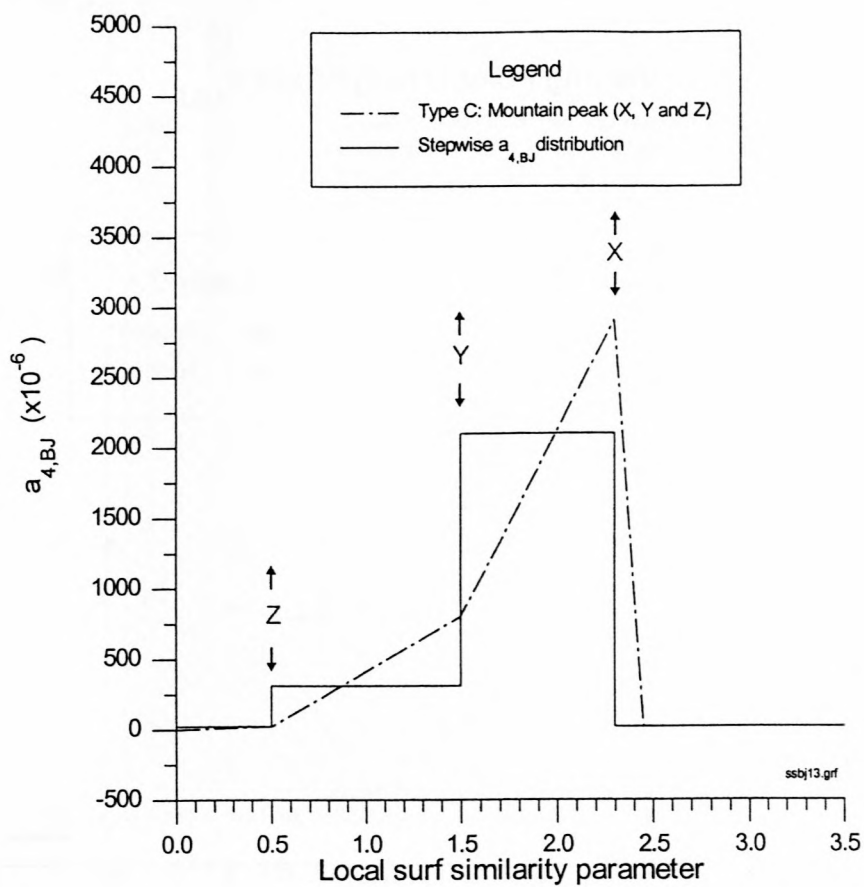


Figure 5.25a: Varying points Z, Y and X to optimize the Mountain peak a_4 distribution

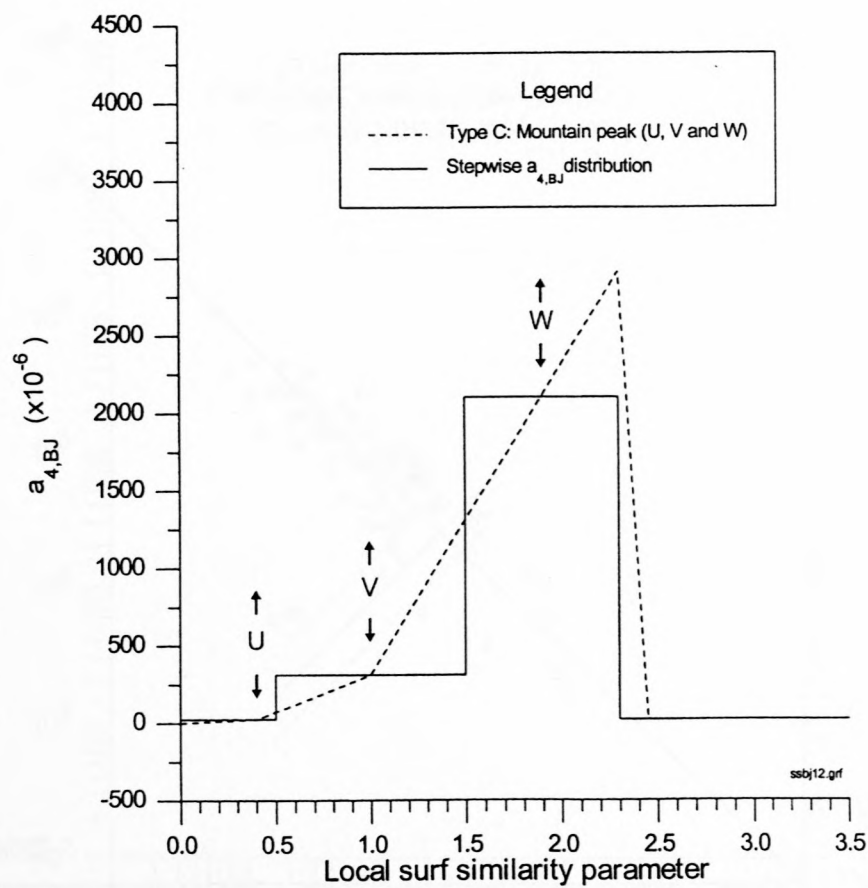


Figure 5.25b: Varying points U, V and W to optimize the Mountain peak a_4 distribution

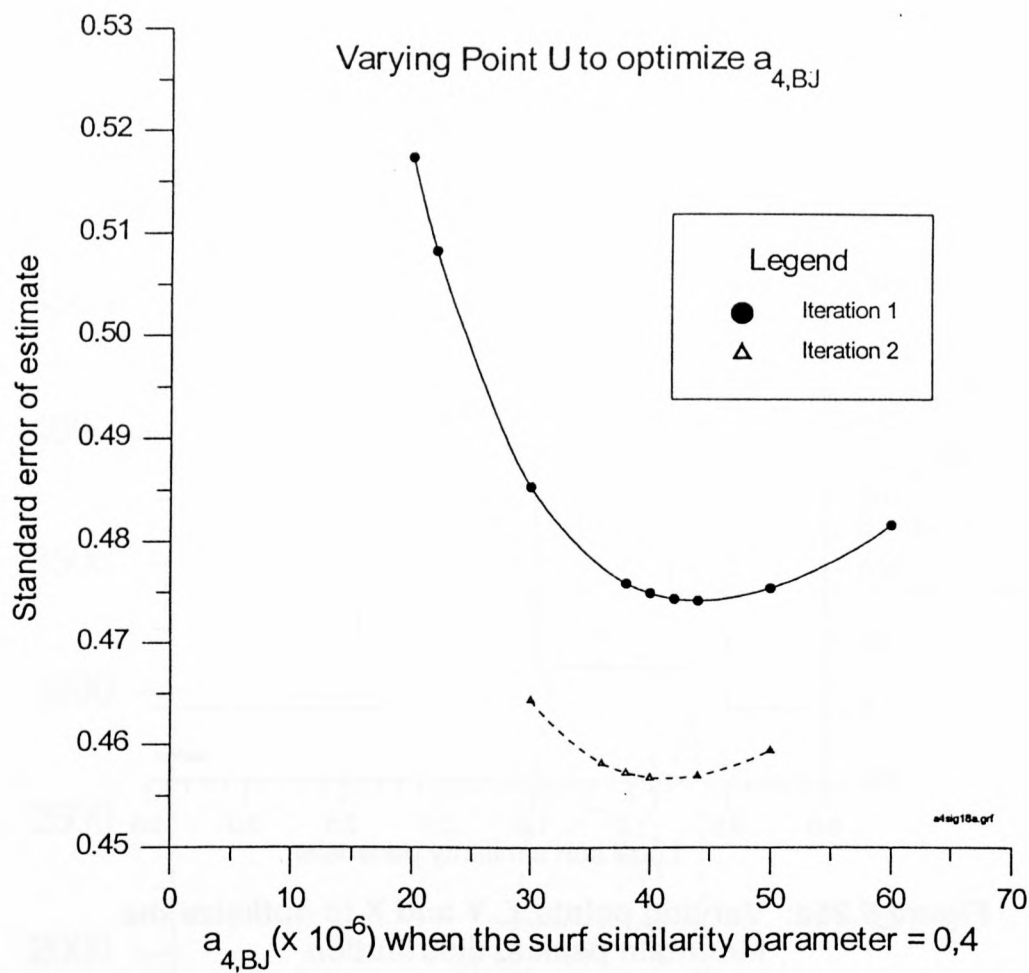


Figure 5.26: Varying Point U to optimize a_4

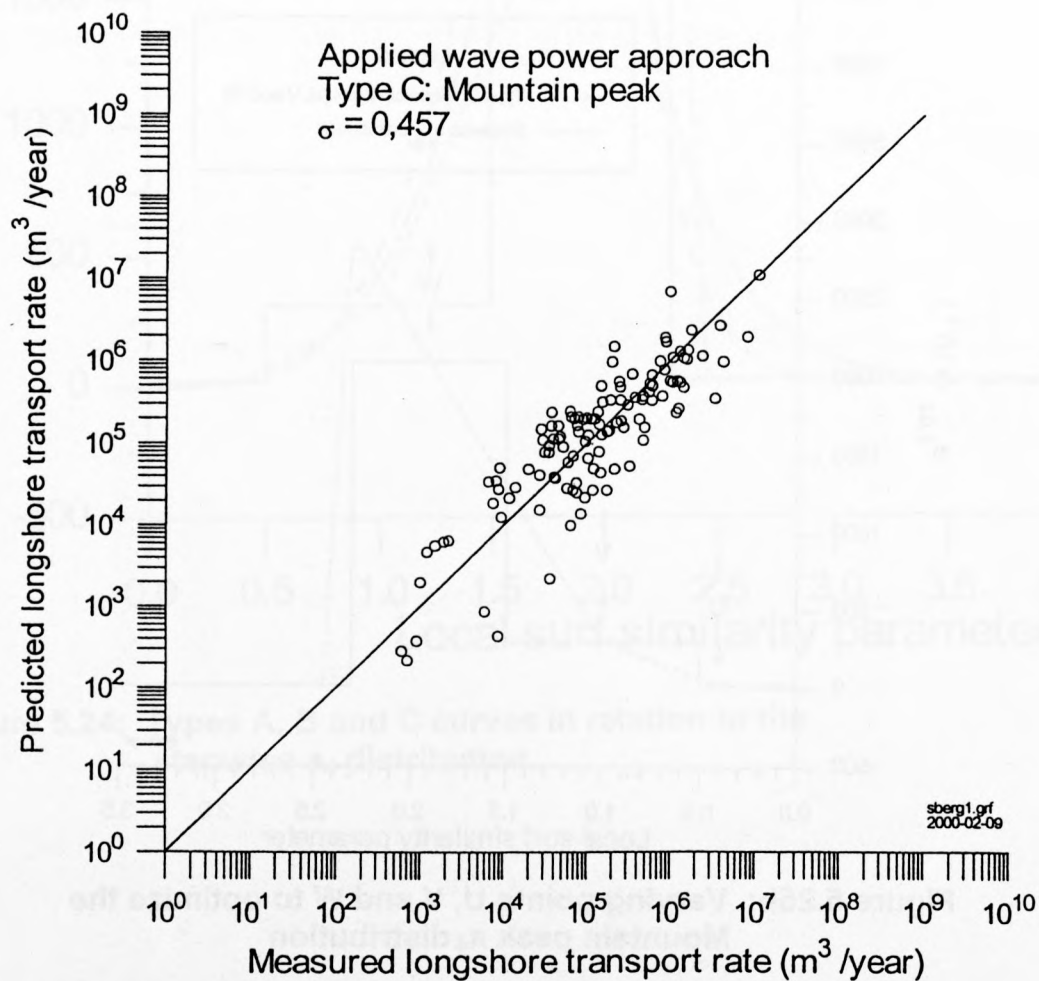


Figure 5.27: Predicted versus measured longshore transport rates for the applied wave power approach

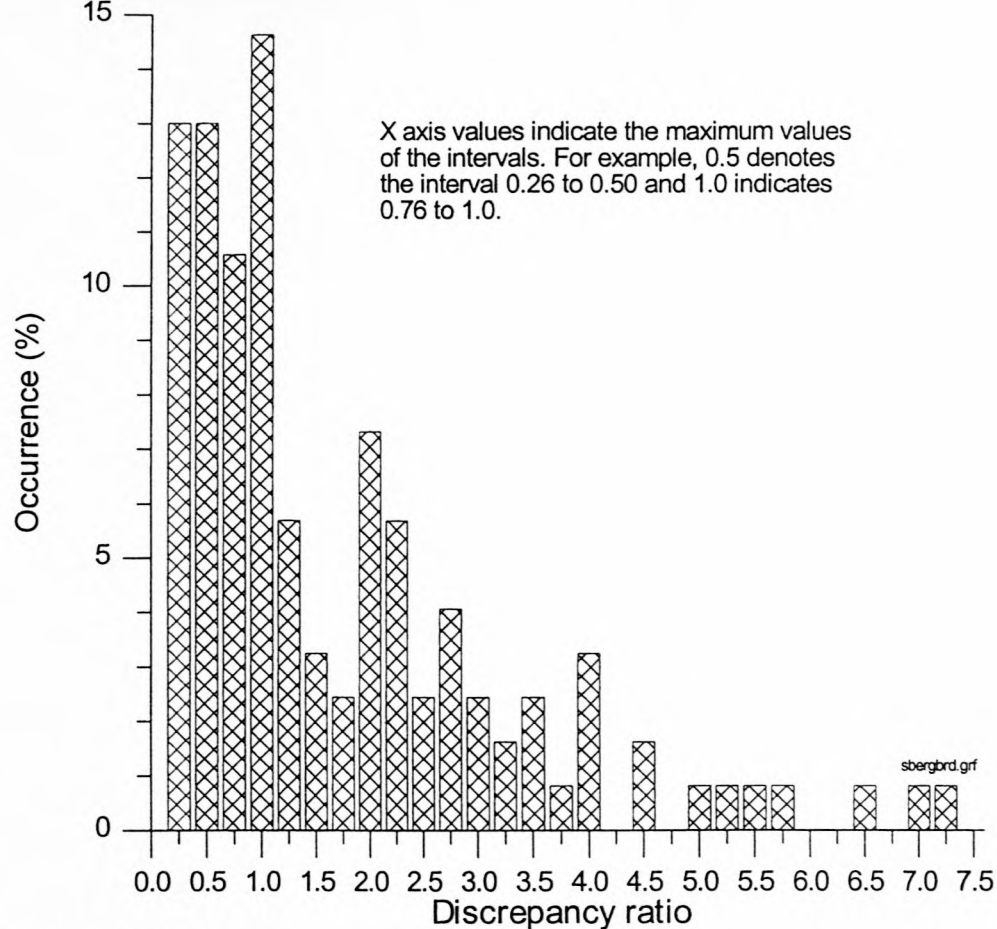


Figure 5.28: Percentage occurrence of the discrepancy ratio for the applied wave power approach

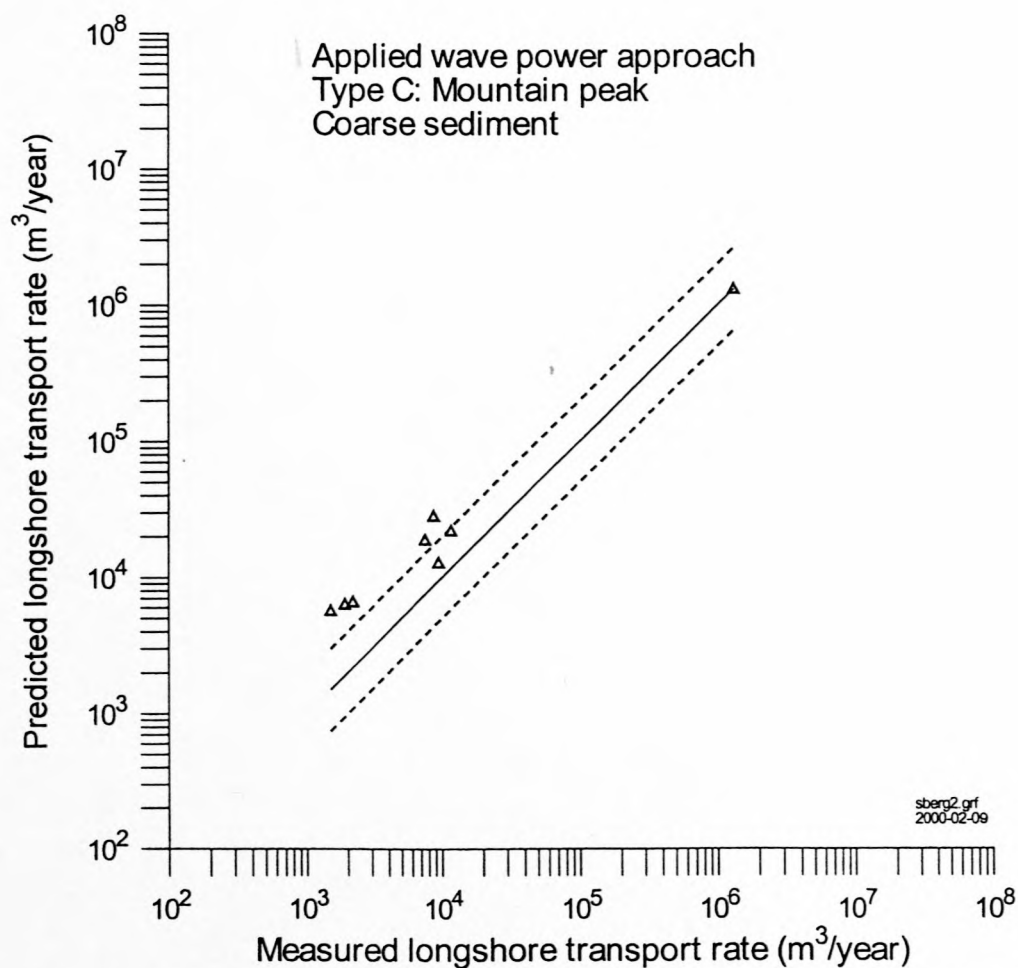


Figure: 5.29: Predicted versus measured longshore transport rates for coarse sediment for the applied wave power approach

APPENDIX A

REVIEW OF THE FIELD-DATA BASE FOR LONGSHORE SEDIMENT TRANSPORT

by

Schoonees, J S and Theron, A K (1993)
Coastal Engineering 19:1-25 (Reprinted with permission)

A1. The paper

The individual contributions by the two authors are as follows:

J S Schoonees

- concept of evaluating the field data
- compilation of references containing the data
- idea to plot the ranges of the data
- setting up the point rating system (parameters to consider and the sub-division)
- independent evaluation of data
- writing the first draft of the paper and editing it

A K Theron

- extraction of data from the references
- plotting the ranges of the data
- numerical value of weighting for each parameter
- independent evaluation of the data
- plotting the results of the evaluation
- editing the paper

Review of the field-data base for longshore sediment transport

J.S. Schoonees and A.K. Theron

*Division of Earth, Marine and Atmospheric Science and Technology, CSIR, P.O. Box 320,
7600 Stellenbosch, South Africa*

(Received 16 December 1991; accepted after revision 14 July 1991)

ABSTRACT

Schoonees, J.S. and Theron, A.K., 1993. Review of the field-data base for longshore sediment transport. *Coastal Eng.*, 19: 1-25.

A literature search was undertaken to collect field data on longshore sediment transport. This yielded a large number of data sets (273 points for bulk transport rates) from a variety of sites around the world. Data are especially lacking for transport rates exceeding $0.2 \times 10^6 \text{ m}^3/\text{year}$, significant wave heights higher than 1.8 m, sediment grain sizes coarser than 0.6 mm and beach slopes steeper than 0.06 ($= 1/14$). A point rating system was devised whereby the quality of the data could be assessed. The recording method and the accuracy thereof as well as the representativeness of the data were taken into account. It was found that the evaluation was done reasonably objectively and consistently. The data were divided into three categories. The highest score achieved in the evaluation was only 71% thus reflecting the difficulty of measuring longshore transport accurately. It is recommended that longshore transport formulae be calibrated against the data in the higher category (60% and better) and then be tested against all the other data. This will ensure that the formulae will be tested in as many different conditions and sites as possible without the lower quality data contributing to the calibration constants.

INTRODUCTION

General

Knowledge of longshore sediment transport is essential for the design of breakwaters at harbour entrances, navigation channels and dredging requirements, beach improvement schemes incorporating groynes, detached breakwaters and beach fill as well as for the determination of the stability of inlets and estuaries.

Formulae for the prediction of longshore transport rates can only be as good

Correspondence to: J.S. Schoonees, Division of Earth, Marine and Atmospheric Science and Technology, CSIR, P.O. Box 320, 7600 Stellenbosch, South Africa.

as the data on which they are based. Although this is especially true for empirical methods, even the most sophisticated formula requires verification. It is therefore of utmost importance to realise the limitations of the data.

Another important consideration is that, in order for a formula to be universally applicable, it should be verified under as many as possible different conditions and at different sites. The aim of this paper is therefore, firstly, to compile such a longshore sediment transport data base by listing all the relevant references and, secondly, to evaluate the quality of the data contained in these publications.

The data considered in this paper are only for particulate (non-cohesive) sediment (including sand, gravel and shingle) being transported alongshore from the swash zone across the surf zone to deep water. Both bulk (total rate across the shore) and local transport rates are considered. However, cases where only bedload or suspended load was measured are only included if the measurements were used to determine the total transport rate (for example Downing, 1984). Data sets are excluded where simultaneous wave and transport data are not available as in the case of Johnson (1957). Only field data are evaluated because of possible scale effects in laboratory investigations and/or because regular waves were used. Furthermore, the ultimate aim is to be able to predict longshore transport accurately in the field (Komar, 1988).

The data are not meant to provide average long-term data at (a) specific site(s). It is rather assumed that if a longshore transport formula is capable of accurately predicting transport rates for the data sets given herein, it can be used with reasonable confidence at similar sites to determine the long-term longshore sediment budget if representative wave and other input parameters are available. It would of course be even better to have site-specific calibration data before calculating average long-term transport rates.

It is well known that it is extremely difficult to measure sediment transport rates and the associated wave and current parameters accurately, especially in the surf zone. This will be illustrated in the evaluation of the data.

Previous studies

Das (1971) compiled laboratory and field data. He also summarized, among others, the site characteristics and the measuring techniques used by the earlier American investigators Watts (1953), Caldwell (1956), Moore and Cole (1960) and Komar (1969). Dean (1978) not only compiled but also evaluated the longshore transport data considering the measuring techniques used and investigating the variation of the dimensionless coefficient K in the SPM longshore transport formula (Komar, 1988):

$$I = KP_{ls}$$

where I is the immersed-weight transport rate and P_{ls} is the longshore energy flux factor.

One of Dean's conclusions was that the variability in the K values is quite large and that it is not known whether this is due to recording errors or to true variation in the factor K . In the present evaluation, only recording errors are addressed so as not to assume in effect a theoretical basis for any longshore transport formula.

Greer and Madsen (1978) provide a detailed critical review of the data sets collected by Watts (1953), Caldwell (1956) and Komar (1969). After giving a set of criteria to be adhered to, they concluded that the data "by Watts (1953) and Caldwell (1956) are of questionable quality" (the values of P_{ls} could be off by factors of 5 and 10 respectively). To darken the picture further, they found "that several of the basic assumptions underlying the use of tracers in sediment transport studies appear to have been violated" by Komar (1969).

Walton and Chiu (1979) and Bruno et al. (1981) list the methods of obtaining the data in the earlier studies. Bruno et al. also commented (mostly) on the accuracy of the sand tracer tests by Komar (1969), stating that the transport rate was probably overestimated due to the way the shore-parallel tracer displacement was determined from sediment samples taken close to the top of the seabed and because the thickness of the moving sediment layer was expected to increase in time.

More recently, Kamphuis et al. (1986) tabulated data from 9 field studies and Morfett (1990) briefly reviewed the longshore transport data base (including a number of newer studies such as Inman et al., 1980, and Kraus et al., 1982) concentrating on how accurately the variables were determined. Although deficiencies were noted, no firm conclusions were drawn in these studies regarding the overall accuracy of the data sets.

To conclude then, only Greer and Madsen (1978) provide an in-depth analysis of the accuracy of the data. Unfortunately, they could only review a few of the earlier studies.

FIELD-DATA BASE

Sources

Tables 1 (bulk transport rates) and 2 (local transport rates) summarize the field data available to the authors. As can be seen from these tables, the data were collected at a wide variety of sites around the world, yielding a large number of points of which 273 points give bulk transport rates. This is considerably more than the 41 data points used in the Shore Protection Manual by US Army, Corps of Engineers (1984).

A number of other field studies were also carried out where the longshore

TABLE I

Field data sources (bulk transport rates)

Data set No.	Reference(s)	Location	No. of points	Transport measured by	Wave height and period measured by	Wave angle measured by	Survey method
1	Caldwell (1956)	Anaheim Bay California	5	beach fill	hindcasting & step, float gauge	hindcasting & visual observed	hydro + topo echo sounder not described
2	Watts (1952)	South Lake Worth	3	deposition in trap & sand bypassing		visual observed	
3	Ishihara et al. (1958)	North Akashi Miyazu	10	accretion at temporary groyne	wind analysis (verified)	wind analysis (verified)	soundings
4	Adachi et al. (1959)	Miyazu Japan	7	accretion at off-shore breakwater	estimated wind analysis	not described	not described
5	Moore and Cole (1960)	Cape Thompson Alaska	8	growth of a spit	visual estimate	visual estimate	plane table survey
6	Delorme (1981)	North & Central Africa	1	not described (measured and estimated)	not described	not described	not described
7	Sato (1962)	Fukue, Atsumi Japan	5	accretion at breakwater	pressure gauge	wind analysis	not described
8	Sireyrol (1964)	Cotonou Benin	1	accretion at breakwater	not described	visual estimate	air photo analysis
9	Castanho (1966)	Lobito Angola	2	accretion at breakwater & spit	not described	calculated	not described
10	Fairchild (1977)	Ventnor (NJ) Nags Head (NC)	2	pump sampler	pressure gauge & staff gauge	not described	profiles + lead lines
11	Sato and Tanaka (1966)	Port Kashima Japan	2	accretion at breakwater	pressure gauge	visual observed	echo-sounder + rod & level
12	Bijker (1968)	Ivory Coast Abidjan	1	estimated	assumed estim.	not described	not described
13	Komar and Inman (1970)	El Moreno & Silver Strand	11	tracer	pressure gauges & dig. wave staffs	visual observed sensor array	not described
14	Duane and James (1980)	Point Mugu California	1	tracer	visual observed	visual observed	not described
15	Hou et al. (1980)	Taichung Harbour Taiwan	4	accretion at breakwater	ultrasonic gauge	wind analysis	profile & bathymetric
16	Lee (1975)	Lake Michigan	8	sampler	poles, posts	visual observed & photos	transit & stadia
17	Kana (1977)	Price Inlet South Carolina	25	sampler	visual observed staff	visual observed	not described

18	Bruno et al. (1981)	Channel Islands Harbor	18	accretion at off-shore breakwater	pressure gauge & LEO observations	pressure gauge & LEO observations	topo + bathy (fathometer)
19	Chang and Wang (1978), Wang and Chang (1978)	Santa Rosa I. (Bayside)	35	tracer	not described	not described	not described
20	Knoth and Nummedal (1977)	North Bull Island	5	tracer	not described	not described	not described
21	Inman et al. (1980)	Torrey Pines California	2	tracer & sampler	pressure gauges array & wave staffs	electromagnetic current meter	not described
22	Kana and Ward (1980)	Duck North Carolina	2	sampler	pressure gauge	radar & LEO observations	not described
23	Gable (1981)	Leadbetter, Santa Barbara	9	accretion at breakwater	pressure gauges array	pressure gauge	rod & level + (fathometer)
24	Dean et al. (1982)	Rudee inlet Virginia	3	deposition in trap (weir)	pressure gauges array	pressure gauge	rod & level + soundings
25	Nicholls and Wright (1991)	Southern England H.Bury Long Beach Hurst Castle Spit	6	tracer (aluminium)	visual observed	visual observed	beach profiles
26	Kraus et al. (1982)	Shi, Hir, Aji, Oar Japan	12	tracer	pressure gauge & photo poles	electromagnetic current meter	not described
27	Mangor et al. (1984)	Danish North Sea	6	deposition in trap & trench-backfill	Waverider & wind analysis	wind analysis	profiles & echosounder
28	Kooistra and Kamphuis (1984)	Pointe Sapin Canada	2	accretion at offsh. breakwater tracer	pressure gauge	electromagnetic current meter	beach + bathymetric
29	Bodge (1986)	Duck North Carolina	8	accretion at mobile groyne	pressure gauge & visual observed	radar imagery & visual observed	rod & level + transit
30	Laubscher et al. (1989)	Richards Bay South Africa	5	deposition in trap & dredging	Waverider	clinometer & VOS	survey beach + hydro
31	Kraus et al. (1982, 1988, 1989) Rosati et al. (1991)	Duck North Carolina	8	sampler (streamer)	photo poles & movie camera	not measured	infrared survey + transit
32	Voitsekovich (1986)	Ros., Pri., Kin. Black Sea	39	samples (siphon)	string gauge & poles	not described	not described
33	Chadwick (1989)	Shoreham Sussex, England	7	gravel trap	mes.SEM & visual, pole array measured	visual, pole array	tache survey & hydrographic profile &
34	Hou (1988)	Lin-Kou Northwest Taiwan	1	accretion at breakwater	pressure gauge	wind analysis	echo-sounder hydrographic
35	Caviglia et al. (1991)	Mar del Plata Argentina	4	accretion at break-water, dredge	pressure gauge	visual observed	
35	Total		273				

TABLE 2

Field data sources (local transport rates)

Data set No.	Reference(s)	Location	No. of points	Transport measured by	Wave height and period measured by	Wave angle measured by	Survey method
1	Sawaragi and Deguchi (1978)	Isonoura, Matsuho (Japan)	18	bedtrap	pressure gauge	not given	not described
2	Downing (1984)	Twin Harbor Beach (Wash.)	20	back-scatter-rometer	resistance gauge	not given	rod & level
3	Kraus et al. (1982)	Aji, Shi, Hir, Oar (Japan)	26	tracer	pressure gauge & photopoles waverider & wind analysis	electromagnetic current meter	not described
4	Mangor et al. (1984)	Danish North Sea	32	deposition in trench, backfill	wind analysis	not measured	echo-sounder
5	White (1987)	Torrey Pines & Scripps	25	tracer	pressure gauge	not measured	fathometer + rod & level
6	Bodge (1986)	Duck North Carolina	8	buildup against mobile groyne	pressure gauge & observed photopoles & movie camera	radar imagery & visual observ.	rod & level
7	Kraus et al. (1988, 1989)	Duck North Carolina	55	sampler (streamer trap)		not measured	+ transit infrared survey & transit
7	Total		184				

transport rate was determined together with wave and beach characteristics; unfortunately, most of the values of the variables are not given in the references. These studies include Iwagaki and Sawaragi (1962), Bonnefille and Pernecker (1967), Walton (1978), Swart and Fleming (1980), Maruyama et al. (1982) and Katoh et al. (1985). Although the data collected by Rosati et al. (1991) were discussed in their paper the report listing the complete data was not yet published and was therefore not evaluated.

Measuring techniques

Various methods were used to measure both the sediment transport rates and the wave characteristics (Tables 1 and 2). Sediment transport rates were obtained by measuring:

- accretion at a breakwater/groyne
- accretion plus bypassing
- erosion downdrift of a barrier
- growth of a spit;

and by the use of:

- tracers
- samplers
- gravel traps.

It is important to note whether the transport rate was determined over the long term (monthly and longer) or the short term (hourly or daily). The advantage of long-term data (typically accretion at a breakwater) is that the measured transport rates should be less variable (Dean, 1978), most probably because of natural smoothing of the data. The disadvantage is, however, that wave conditions change during a longer recording period. Furthermore, because this type of data usually is accretion or erosion adjacent to a breakwater, the structure influences the wave and current fields in its vicinity (Greer and Madsen, 1978 and Komar, 1988). On the other hand, wave conditions are usually more constant during shorter recording periods (Dean, 1978).

Another important consideration is the accuracy of the survey methods (Table 1) used to obtain the data for the calculation of volume differences. The seaward limit of the profiles, spacing of profiles, accuracy of the datum level, etc. are all factors to be taken into account.

Wave conditions were determined by a variety of methods ranging in sophistication from visual estimates, to wave hindcasting to the use of recorders such as pressure transducers (Table 1). Because of the sensitivity of longshore transport formulae to the wave incidence angle, the technique used to measure it is of particular interest; unfortunately, it is also one of the most difficult variables to measure accurately. Typical methods include visual es-

timates, the use of radar, aerial photography, hindcasting and an array of wave recorders (Table 1).

Additional factors influencing the accuracy of the data include, among others, the determination of the sediment grain sizes and the measurement of the nearshore currents.

Range of the data

When verifying the general validity of longshore transport formulae, it is important to know the range of the data used. For this reason, the distributions of the measured transport rates (S), significant breaker wave heights (H_{bs}), peak wave periods (T_p), wave incidence angles at the breaker line (θ_b), median grain sizes (D_{50}) and the beach slope in the surf zone ($\tan \alpha$) are plotted in Figs. 1a and b, and 2 to 6. In the case of the bulk transport rates, the units are m^3/year ($1 \text{ m}^3/\text{year} = 3.15576 \times 10^7 \text{ m}^3/\text{s}$). If the recording period was less than one year, it was assumed that the conditions persisted for a year thus making large rates possible. For data collected over the long term (monthly and longer), the maximum H_{bs} , T_p and θ_b were selected.

From Figs. 1a and b it is immediately apparent that almost all measured transport rates are less than $2 \times 10^6 \text{ m}^3/\text{year}$ ($0.0634 \text{ m}^3/\text{s}$) and of these, most are less than $0.1 \times 10^6 \text{ m}^3/\text{year}$ ($0.0317 \text{ m}^3/\text{s}$). The reason for this is obvious: predominantly lower waves occur and it is easier to measure during these conditions.

This trend can also be seen for the breaker height in Fig. 2 where few waves higher than 1.8 m were recorded. Here a larger variation in T_p values can be seen in Fig. 3. A bimodal distribution is evident with peaks at about 5 s and 12 s, which most probably is indicative of wind waves and swell. Despite this, wave periods lower than 8 s occur more frequently. Few data sets contain θ_b values exceeding 16° (Fig. 4). Typically the most common situation is small angles (5° or 10°). Angles were apparently often reported to the nearest 5° . If the intervals in Fig. 4 are reduced to 1° , pronounced local maxima are shown at 5° , 10° , 15° , 20° and 30° thus substantiating the above conclusion.

Most measurements were done on beaches with fine sand and especially in the range 0.20 mm to 0.25 mm (Fig. 5). Virtually no data were collected on beaches with sediment grain sizes between 0.6 mm and 15 mm. Realising the relation between grain size and beach slope, it is logical to expect that most of the data were collected on beaches with flat slopes; as is evident from Fig. 6, almost all the slopes fall between 0.01 ($= 1/100$) and 0.07 ($= 1/14$).

Bearing in mind that usually a few storms contribute to almost all the longshore transport at a site, it is critical that longshore transport formulae be verified against such conditions. In most cases this was not done except per-

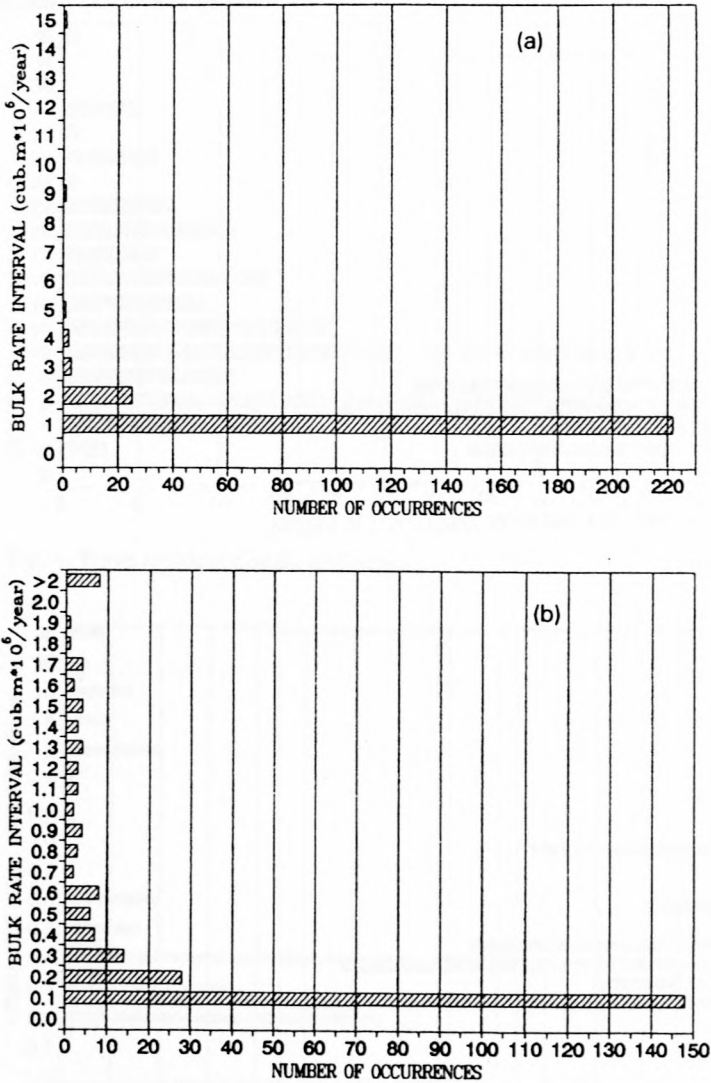


Fig. 1. Bulk rate histograms.

haps where the long-term accretion adjacent to a structure was monitored. Data are especially lacking for

$$S > 0.2 \times 10^6 \text{ m}^3/\text{year} \text{ (} 0.0634 \text{ m}^3/\text{s)}$$

$$H_{bs} > 1.8 \text{ m}$$

$$D_{50} > 0.6 \text{ mm}$$

$$\tan \alpha > 0.06 \text{ (= } 1/14)$$

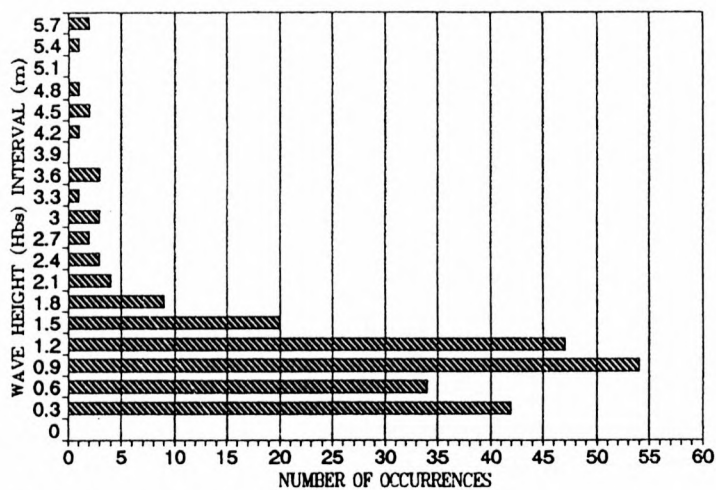


Fig. 2. Wave height histogram.

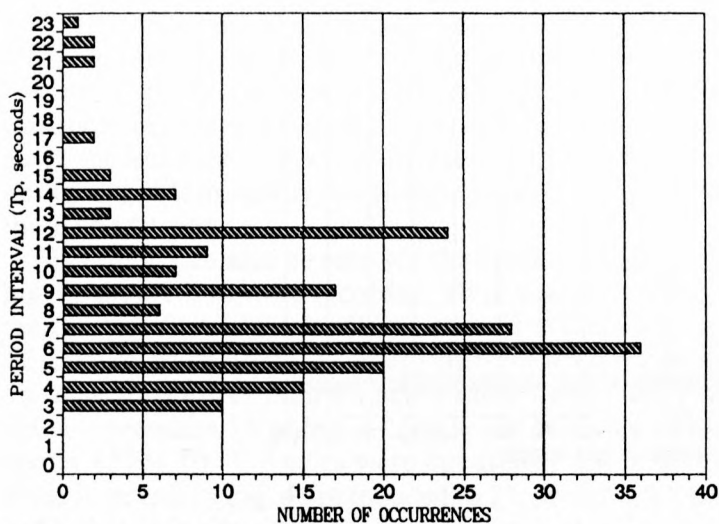


Fig. 3. Wave period histogram.

DATA EVALUATION

Method

A point-rating system was devised so that data sets could be compared with respect to overall quality of the data and suitability for testing longshore transport formulae. Keeping in mind the interdependence of the various physical factors that influence longshore transport rates, as well as the relative

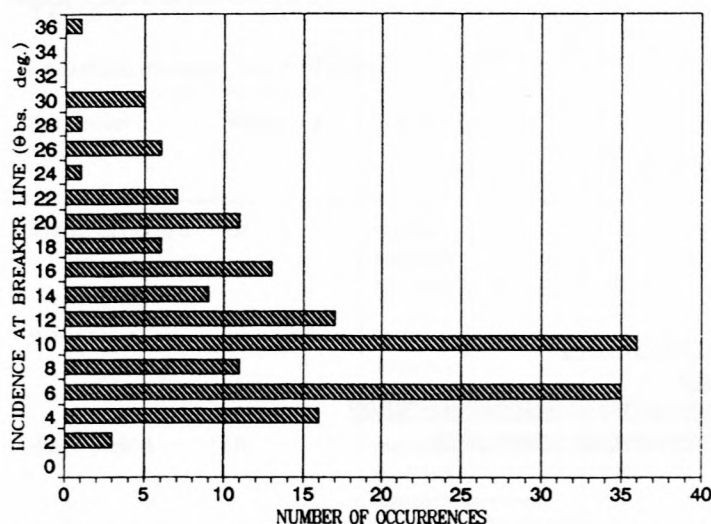


Fig. 4. Wave incidence angle histogram.

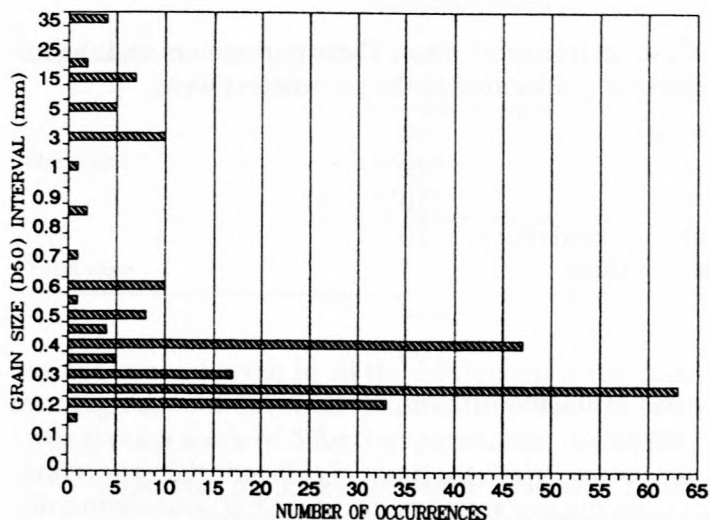


Fig. 5. Sediment grain size histogram.

importance of these factors, a point-rating system was compiled for the evaluation of the data sets relative to each other. This system is based on the point-rating systems developed previously for the comparative evaluation of the beach suitability of different beaches (CSIR, 1976, 1987; Schoonees and Bartels, 1991). Points were allocated to a data set according to the quality of the data of the six physical parameters deemed most appropriate (impor-

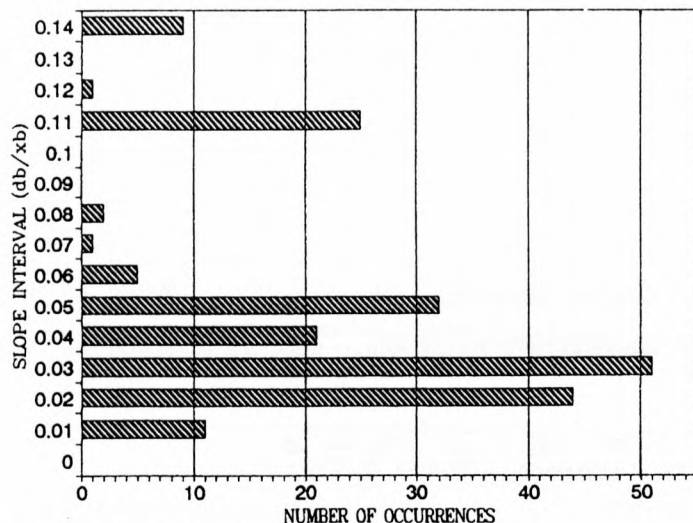


Fig. 6. Beach slope histogram.

tant) in determining longshore transport rates. These parameters and the relative importance ("weighting") allocated to the parameters were:

* longshore transport rate	40
* wave height	20
* wave period	10
* wave direction (angle of incidence)	20
* beach profile (bottom) slope	5
* sediment size	5
Total	100

The data sets were further evaluated with respect to each parameter in terms of three sub-divisions namely:

- method by which the data were determined for a specific parameter
- accuracy with which the data were determined or measured
- representativeness of the data

The data sets were each given a score out of a total of 10 points in terms of each of these sub-divisions with respect to each specific parameter.

The scores for the sub-divisions were added and after the relative weighting of the parameters had been applied, the total points were converted to give a total score out of 100.

Table 3 gives a hypothetical example of how this method was used to assess the quality of the data. Both authors did the evaluation independently in order to be able to judge the objectivity and consistency of the method.

It must be noted that full descriptions of how data were measured or deter-

TABLE 3

Longshore transport data evaluation

Parameter	Weighting	Sub-division	Max. points		Points of hyp. ref.	
				total		total
Transport rate	40	method	10	40	6	23
		accuracy	10		5	
		representativeness	10		6	
Wave height	20	method	10	20	6	12
		accuracy	10		6	
		representativeness	10		6	
Wave period	10	method	10	10	6	6
		accuracy	10		6	
		representativeness	10		6	
Wave angle	20	method	10	20	5	10
		accuracy	10		5	
		representativeness	10		5	
Beach slope	5	method	10	5	7	4
		accuracy	10		8	
		representativeness	10		7	
Grain size	5	method	10	5	6	4
		accuracy	10		8	
		representativeness	10		7	
Total score			100		58	

mined are not given in all the references. If the data for a specific parameter were given without description of how the data were obtained, the data set was given a score of 5 for that parameter. Although this may seem a bit arbitrary, it is felt that this is the most "fair" score that can be given under the circumstances. If a specific parameter was not measured or the data could not be determined from the information given in the reference, the data set was given a score of 0 for that parameter.

It must be stressed that this system primarily rates data sets relative to each other and with respect to longshore transport data, and that data sets receiving a lower score than the rest of the data sets, may nevertheless be quite usable, especially in respect of other parameters.

The parameters chosen and the relative weighting applied to these parameters will of course influence the evaluation and are debatable, but nevertheless the authors believe that based on current knowledge, the system gives a

fair method of evaluating longshore transport data as objectively as possible. A limited sensitivity analysis (described in the section "Discussion" below) has also been done to evaluate the effect of different weightings. It must, however, be kept in mind that the data are evaluated with regard to their suitability to predict total longshore transport rates. For example, if measured suspended sediment concentrations were extrapolated up to the sea bottom and then integrated through the water column to estimate the local longshore transport rate, the total score could be low. However, that does not necessarily mean that the accuracy of the measured sediment concentrations is poor.

Criteria

The most basic question concerning the measurements is: What exactly (transport rate or wave characteristic, etc.) was measured? (Nielsen, 1984), or alternatively, Was the total (real) transport rate (or wave characteristic, etc.) measured?

Based on the criteria set by Greer and Madsen (1978), Duane and James (1980), Bruno et al. (1981) and Madsen (1987) among others, points were allocated for each technique for measuring the transport rate to be given under the sub-division Method. To evaluate how representative the measured transport rate was, aspects such as the following were taken into account:

- Was it a total trap?
- Was only bedload or suspended load measured?
- Was the transport determined over the long term?
- Was the coverage considered to be adequate if samplers or traps were used?
- Did an offshore breakwater possibly contribute to overtrapping of sediment?

Similarly, the acquisition of the wave characteristics was evaluated giving, firstly, points for the method (lowest for assumed data, then hindcasted data and highest for accurately measured data). Secondly, aspects pertaining to the representativeness of the data included:

- Was it measured directly opposite the site?
- Was it recorded in deep water and then refracted in towards the shoreline?
- Were distributions or spectra of the wave characteristics given?
- Were the recordings done over the short or long term?

For beach slope, the following were taken into account: the spacing of survey lines, their seaward limit, their datum level and whether both beach and nearshore surveys were done and if so, whether they overlapped.

Adequate spatial and temporal coverage of the beach and nearshore zone

TABLE 4

Longshore transport data evaluation

No.	reference	location & data set	total
<i>Bulk transport rates</i>			
12	Bijker (1968)	Abidjan	19
4	Adachi et al. (1959)	Miyazu	24
10	Fairchild (1977)	Ventnor	36
3	Ishihara et al. (1958)	North Akashi, Miyazu	37
10	Fairchild (1977)	Nags Head	37
2	Watts (1953)	South Lake Worth	42
1	Caldwell (1956)	Anaheim Bay	46
17	Kana (1977)	Price Inlet	48
25	Nicholls and Wright (1991)	South England	48
6	Delorme (1981)	North Africa	49
5	Moore and Cole (1960)	Cape Thompson	50
8	Sireyjol (1964)	Cotonou	51
9	Castanho (1966)	Aveiro	52
9	Castanho (1966)	Lobito	52
20	Knoth and Nummedal (1977)	Bull Island	52
30	Laubscher et al. (1989, 1991)	Richards Bay	54
18	Bruno et al. (1981)	Channel Islands Harbor, 1	55
19	Chang and Wang (1978)	Santa Rosa Island	55
27	Mangor et al. (1984)	Danish North Sea	55
31	Kraus et al. (1989)	Duck	55
14	Duane and James (1980)	Point Mugu	56
29	Bodge (1986)	Duck, 2	56
15	Hou et al. (1980)	Taichung Harbour	57
16	Lee (1975)	Lake Michigan	57
22	Kana and Ward (1980)	Duck	57
29	Bodge (1986)	Duck, 3	57
33	Chadwick (1989)	Shoreham, M6, M7	57
11	Sato and Tanaka (1966)	Port Kashima	58
32	Viotsekhovich (1986)	Black Sea	58
34	Hou (1988)	North West Taiwan	58
35	Caviglia et al. (1991)	Mar del Plata	58
28	Kooistra and Kamphuis (1984)	Pointe Sapin NOV4	60
33	Chadwick (1989)	Shoreham, M1-M5	60
7	Sato (1962)	Fukue, Atsumi	61
29	Bodge (1986)	Duck, 4	61
13	Komar and Inman (1970)	El Moreno, Silver Strand	62
24	Dean et al. (1982, 1987)	Rudee Inlet	63
26	Kraus et al. (1982)	Japan	63
21	Inman et al. (1980)	Torrey Pines	64
18	Bruno et al. (1981)	Channel Islands Harbor, 2	67
23	Gable (1981)	Leadbetter Beach	68
28	Kooistra and Kamphuis (1984)	Pointe Sapin, OCT25	71
<i>Local transport rates</i>			
2	Downing	Twin Harbors Beach	44
1	Sawaragi and Deguchi	Isonoura	47
1	Sawaragi and Deguchi	Matsubo	49
6	White et al.	Torrey Pines, SIO	50
7	Kraus et al.	Duck	55
4	Mangor et al.	Danish North Sea	56
5	Bodge	Duck, 2	56
5	Bodge	Duck, 3	57
5	Bodge	Duck, 4	61
3	Kraus et al.	Japan	63

by sediment sampling were the primary factors for evaluating the sediment characteristics.

For all the Accuracy sub-divisions, a subjective rating out of 10 was given.

Results

The results of evaluating the overall quality of the longshore transport data are presented in Table 4 and Fig. 7. (Some references are listed more than once because the specific data sets contained in that reference differ in quality.) The data were sorted according to the final point rating (that is, the mean of the total score given by the two authors).

DISCUSSION

From Fig. 7, three categories of data can be distinguished for the bulk transport rates. Cut-off points were essentially arbitrarily chosen to be scores of 50% and 60%. It is clear from this graph that the majority of data sets fall in the middle category and that there is a very gradual increase in the point rating (accuracy) in this category. The largest gradients occur in the lower category and right at the top end of the higher category. The transition between the categories at both cut-off points is also gradual. From Table 4 and Fig. 7 it is clear that fewer studies yielding local transport rates were conducted. In addition, the range in the total scores are much less for the local rates (from a lowest score of 44% to a maximum score of 63%, being 19 percentage points) compared with 52 percentage points for the bulk rates (Table 4).

Inspection of Table 4 reveals that the poorer data sets are generally from the older references or from those where the purpose of the exercise was not necessarily to obtain good longshore transport data (for example, Nicholls

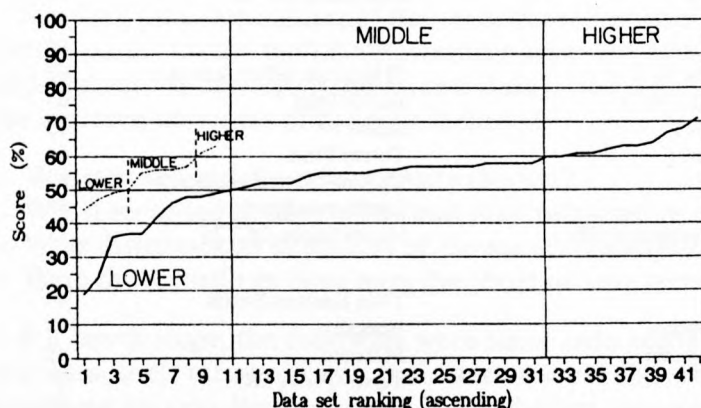


Fig. 7. Longshore transport data evaluation. (—) Bulk, (.....) local transport.

and Wright, 1991). However, this does not necessarily mean that older data sets are of poorer quality as can be seen from the Komar (1969) data falling in the higher category. With the development of better measurement techniques and equipment it is not surprising that most of the data sets in the higher category originated in recent years.

In interpreting the results, it must be borne in mind that a score of 0 points was given if a particular parameter was not measured or reported. For example, Kraus et al. (1989) did not measure the wave incidence angle because they conducted their exercise in the feeder current of a rip current. However, they measured the longshore current velocity. It can therefore be argued that their data are accurate because the incidence angle is usually only applied to predict the longshore current velocity. Table 5 lists the studies where one or more of the parameters were either not measured or not reported.

Greer and Madsen (1978) recommended that the data by Watts (1953) and Caldwell (1956) should be "excluded from establishing empirical sediment transport relationships" and that the data by Komar (1969) should not be "too heavily relied upon". The results of this review agree reasonably well with the former recommendation (because both the earlier studies fall in the lower category). Greer and Madsen based their recommendation concerning Komar's data mainly on the following arguments: (1) The lack of stationarity of the transporting system during the experiments at El Moreno beach; (2) The uncertainty about whether or not sufficient time was allowed between injection and sampling to ensure that equilibrium transport of tracer was reached during the exercise at Silver Strand Beach; and (3) the ambiguity in determining the thickness of the moving layer of sediment. Considering the extensive procedure followed by Kraus (1985) and Kraus et al. (1982) and the direct influence of this thickness on the transport rate, the third reason can be regarded as being the most important. Despite the fact that the proposed evaluation procedure is primarily comparative in nature, it is believed

TABLE 5

Studies with incomplete data listings

Reference	Parameter(s) either not measured or not reported
Watts (1953)	$\tan \alpha$
Adachi et al. (1959)	D_{50} and wave height
Delorme (1981)	$\tan \alpha$
Castanho (1966)	D_{50}
Fairchild (1977)	θ_b
Kraus et al. (1989)	θ_b *
Sawaragi and Deguchi (1978)	θ_b
Downing (1984)	θ_b *
White (1987)	θ_b *

*do contain detailed current measurements.

that some importance can be attached to the absolute value of the scores (the Komar, 1969 data got a score of 62%; Table 4). Normally, a score of 80% or higher is regarded as being good. It can therefore be argued that the cut-off point for the higher category should be 80% or rather another category say, an excellent category should be established. That would mean that no data points fall in this category (Table 4). It can thus be concluded that the data of Komar (1969) have deficiencies (which corresponds to the conclusion by Greer and Madsen, 1978) but still are amongst the best data sets available.

The individual scores allocated by the two authors were analyzed in order to assess the consistency and objectivity of the method. The mean difference in the total scores was +0.6 (out of 100) and the standard deviation 2.6 (out of 100). It can therefore be provisionally concluded that there was very little systematic difference between the scores given by the two authors. At the same time, the objectivity of the method is acceptable taking into account the subjectivity of estimating the accuracy of measurements.

As the weightings allocated to the different parameters are somewhat arbitrary, a limited sensitivity analysis was carried out. The weighting given to the longshore transport rate and to the wave direction were changed by plus or minus 10 points in both cases in order to assess what effect this would have on the data evaluation. These two parameters were chosen because the transport rate is the single most important parameter; and the wave direction was selected because it is also relatively important and because it is usually the most difficult parameter to measure accurately. Changing the weighting of the other parameters would have less effect on the data evaluation. The results of the sensitivity analysis are shown in Table 6. From the table it can be seen that the average changes in total scores are relatively small. Furthermore, the changes in category are all due to data sets moving from just below (or above) to just above (or below) the arbitrarily chosen category cut-off points. The

TABLE 6

Sensitivity analysis (on weighting of parameters)

Parameter	Change in weighting	Absolute change in total score of particular sets*			No. of data sets moving from one category** to the next
		max.	ave.	std. dev.	
Longshore transport rate (S)	+10	2	0.69	0.89	2
	-10	2	0.76	1.02	1
Wave direction (θ)	+10	5	1.19	1.34	3
	-10	6	1.60	1.61	4

*The absolute change is given out of 100; that is, for an absolute change of 2, the total score moved, for example, from 54% to 56% or from 54% to 52%.

**Category refers to either the lower, middle or higher category (Figs. 7 and 8).

conclusion is that the data evaluation is not overly sensitive to the weightings allocated to the different parameters. Keeping in mind that the data evaluation is of a comparative nature and that the aim is mainly to place the data sets in one of three main categories, the evaluation procedure is considered to be valid and meets the objective.

The data were evaluated only with regard to what was considered to be the most important parameters for longshore transport. Others factors like breaker type, the variation in the composition and grading of the bed material (and thus in settling velocity; see Nielsen, 1979, for example), porosity and specific gravity of the bed material, the effect of nearshore cell circulation (except for rip currents), tidal influence, the effect of cross-shore sediment transport, etc. were not included in the evaluation.

Separating the short- from the long-term bulk transport rates yielded Table 7 and Fig. 8. The trend in the accuracy of the data is very similar for both types of bulk rates, except that more short-term data sets have a ranking in the higher categories while more of the long-term data sets are in the lower category.

It is important that the random error in the measurement of the transport rates and therefore the consistency of the data, be determined. This can be done by using two or more samplers at essentially the same recording position (Kraus et al., 1989), by using different colours of sand tracer and/or different sampling strategies (spatial or temporal) (Chang and Wang, 1978; Inman et al., 1980; White, 1987), using more than one temporary groyne along a long straight beach or by combining more than one method; for example, a sand tracer test (using one or more colours of sand tracer) and/or using streamer traps combined with measuring the accretion next to a temporary groyne.

In the latter case, it could of course also be argued that the difference between two estimates will be due to the methods used as well as because of the random nature of the transport processes.

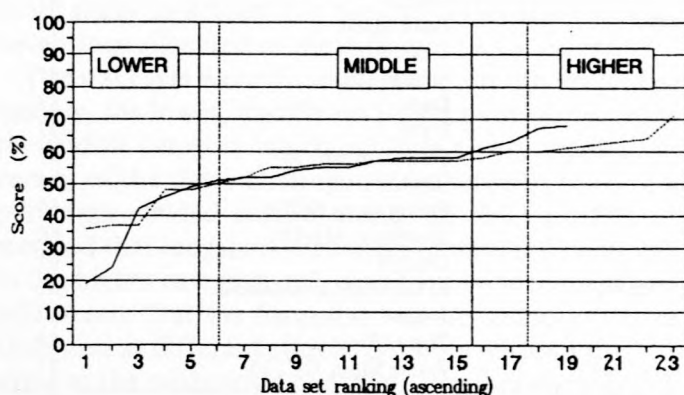


Fig. 8. (—) Long- and (.....) short-term bulk transport rates.

TABLE 7

Evaluation of short- and long-term bulk transport data

No.	reference	location & data set	total %
<i>Long-term rates</i>			
12	Bijker (1968)	Abidjan	19
4	Adachi et al. (1959)	Miyazu	24
2	Watts (1953)	South Lake Worth	42
1	Caldwell (1956)	Anaheim Bay	46
6	Delorme (1981)	North Africa	49
8	Sireyjol (1964)	Cotonou	51
9	Castanho (1966)	Aveiro	52
9	Castanho (1966)	Lobito	52
30	Laubscher et al. (1989, 1991)	Richards Bay	54
18	Bruno et al. (1981)	Channel Islands Harbor, 1	55
27	Mangor et al. (1984)	Danish North Sea	55
15	Hou et al. (1980)	Taichung Harbour	57
11	Sato and Tanaka (1966)	Port Kashima	58
34	Hou (1988)	North West Taiwan	58
35	Caviglia et al. (1991)	Mar del Plata	58
7	Sato (1962)	Fukue, Atsumi	61
24	Dean et al. (1982, 1987)	Rudee Inlet	63
18	Bruno et al. (1981)	Channel Islands Harbor, 2	67
23	Gable (1981)	Leadbetter Beach	68
<i>Short-term rates</i>			
10	Fairchild (1977)	Ventnor	36
3	Ishihara et al. (1958)	North Akashi, Miyazu	37
10	Fairchild (1977)	Nags Head	37
17	Kana (1977)	Price Inlet	48
25	Nicholls and Wright (1991)	South England	48
5	Moore and Cole (1960)	Cape Thompson	50
20	Knoth and Nummedal (1977)	Bull Island	52
19	Chang and Wang (1978)	Santa Rosa Island	55
31	Kraus et al. (1989)	Duck	55
14	Duane and James (1980)	Point Mugu	56
29	Bodge (1986)	Duck, 2	56
16	Lee (1975)	Lake Michigan	57
22	Kana and Ward (1980)	Duck	57
29	Bodge (1986)	Duck, 3	57
33	Chadwick (1989)	Shoreham, M6, M7	57
32	Viotsekhovich (1986)	Black Sea	58
28	Kooistra and Kamphuis (1984)	Pointe Sapin NOV4	60
33	Chadwick (1989)	Shoreham, M1-M5	60
29	Bodge (1986)	Duck, 4	61
13	Komar and Inman (1970)	El Moreno, Silver Strand	62
26	Kraus et al. (1982)	Japan	63
21	Inman et al. (1980)	Torrey Pines	64
28	Kooistra and Kamphuis (1984)	Pointe Sapin, OCT25	71

CONCLUSIONS AND RECOMMENDATIONS

A literature search was undertaken to collect field data on longshore transport. This yielded a large number of data sets for both bulk and local transport rates, far in excess of the 41 data points used by US Army, Corps of Engineers (1984). Altogether 273 data sets were collected for bulk transport rates. The data originated from a large variety of sites from around the world.

The transport rates were determined by measuring accretion and erosion rates adjacent to coastal structures and at sand spits, by using sand tracers and by different kinds of samplers and traps.

Most of the data were obtained during mild wave conditions for fine to medium sand. Data are especially lacking for:

$$S > 0.2 \times 10^6 \text{ m}^3/\text{year} \quad (0.0634 \text{ m}^3/\text{s})$$

$$H_{bs} > 1.8 \text{ m}$$

$$D_{50} > 0.6 \text{ mm}$$

$$\tan \alpha > 0.06 \quad (= 1/14)$$

A serious consequence of this lack of data is that longshore transport formulae are calibrated almost exclusively against data for mild conditions while, in the case of an average annual longshore transport budget, a few storms usually contribute by far the most to the total sediment transport. In other words, the most important predictions for which the formulae are used, are for conditions outside their calibration range. It is therefore strongly recommended that data be collected in these ranges.

A point rating system was devised to compare different data sets with regard to the most important parameters for longshore transport. It was found that the evaluation was done reasonably objectively and consistently within the limitations of evaluating the accuracy of measurements. A limited sensitivity study indicated that the data evaluation was not overly sensitive to the weightings allocated to the different parameters.

The data sets were divided, based on the evaluation, into three categories, namely, the lower, middle and higher categories. Most of the data sets fall in the middle category which exhibits a very gradual increase in the overall accuracy of the data. Distinguishing between short- and long-term bulk transport data yielded similar trends in the accuracy of the data. It is recommended that longshore transport formulae first be calibrated against the data in the higher category only and then be tested against all the other data. This will ensure that the formulae will be tested under as many different conditions and at different sites as possible without the lower quality data contributing to the calibration constants. Preferably only data having a score of 80% or more should be used for calibration. However, until such data are avail-

able, the data sets in the higher category will have to suffice. The goodness of fit to the data should then be interpreted with due cognisance of the accuracy rating of the data sets, taking Table 5 into account. This table shows what parameter(s) in some references are either not measured or not reported which could have influenced the rating.

It is already known that it is difficult to measure longshore transport rates, and the parameters that influence them, accurately. This is supported by the fact that the highest score achieved in the evaluation was only 71%. It is recommended that multiple measurements of the transport rate be made simultaneously in order to be able to estimate the random error involved in the data and to demonstrate the consistency of the measurements.

ACKNOWLEDGEMENT

The authors gratefully acknowledge the helpful comments by Prof. H. Hansson and Prof. A. Rooseboom from the Universities of Lund, Sweden and of Stellenbosch, South Africa respectively.

REFERENCES

- Adachi, S., Sawaragi, T. and Ogo, A., 1959. The effects of coastal structures on the littoral sand drifts. *Coastal Eng. Jpn.*, 2: 85-98.
- Bijker, E.W., 1968. Littoral drift as a function of waves and current. In: *Proc. 11th International Conf. on Coastal Eng.*, ASCE, London, Vol. 1, pp. 415-435.
- Bodge, K.R., 1986. Short-term impoundment of longshore sediment transport. Ph.D. thesis, University of Florida, Gainesville, 346 pp.
- Bonnefille, R. and Pernecker, L., 1967. Etude théorique et expérimentale du transport littoral. *Bulletin de la Direction des Etudes et Recherches, Série A (No. 3)*: 97-102 (in French).
- Bruno, R.O., Dean R.G., Gable, C.G. and Walton, T.L., 1981. Longshore sand transport study at Channel Islands Harbor, California. Technical paper no. 81-2, CERC, U.S. Army Corps of Engineers, Fort Belvoir. 48 pp.
- Caldwell, J.M., 1956. Wave action and sand movement near Anaheim Bay, California. U.S. Army, Beach Erosion Board, Tech. Memorandum 68, 21 pp.
- Castanho, J., 1966. Rebentação das ondas e transporte litoral. *Laboratorio Nacional de Engenharia Civil, Lisbon, Paper No. 275*, 278 pp. (in Portuguese).
- Caviglia, F.J., Pousa, J.L. and Lanfredi, N.W., 1991. A determination of the energy flux constant from dredge records. *J. Coastal Res.*, 7(2): 543-549.
- Chadwick, A.J., 1989. Field measurements and numerical model verification of coastal shingle transport. In: M.H. Palmer (Editor), *Advances in Water Modelling and Measurement*. BHRA, Cranfield, Bedford, pp. 381-402.
- Chang, T.T. and Wang, Y.H., 1978. Field verification of sediment transport model. In: *Proc. 26th Specialty Conf. of Hydraulics Div.*, University of Maryland, College Park, MD. ASCE, pp. 737-744.
- CSIR, 1976. Evaluation of beaches along the Natal South Coast. CSIR Report C/SEA 7604, National Research Institute for Oceanology, Stellenbosch.
- CSIR, 1987. Ondersoek na die omgewingsfaktore en daarmee gepaardgaande baaigeskiktheid

- van die strande aan die Noordoos-Valsbaai kus. CSIR Report C/SEA 8718/1, 2 and 3. National Research Institute for Oceanology, Stellenbosch (in Afrikaans).
- Das, M.M., 1971. Longshore sediment transport rates: A compilation of data. U.S. Army, Coastal Eng. Res. Center, Washington, DC, Miscellaneous Paper No. 1-71, 75 pp.
- Dean, R.G., 1978. Review of sediment transport relationships and the data base. In: Proc. of a Workshop on Coastal Sediment Transport with Emphasis on the National Sediment Transport Study, DEL-SG-15-78. Sea Grant College Program, Univ. of Delaware, Newark, DE, pp. 25-39.
- Dean, R.G., Berek, E.P., Gable, C.G. and Seymour, R.J., 1982. Longshore transport determined by an efficient trap. In: Proc. 18th International Conf. on Coastal Engineering, ASCE, Cape Town, Vol. 2, pp. 954-968.
- Dean, R.G., Berek, E.P., Bodge, K.R. and Gable, C.B., 1987. NSTS measurements of total longshore transport. In: Proc. of Coastal Sediments '87, New Orleans, LA, Vol. 1, pp. 652-667.
- Delorme, J.-L., 1981. Erosion des côtes due à des travaux portuaires et mesures visant à y remédier. In: 25 Congress of Permanent International Association of Navigation Congresses, Edinburgh. Pergamon Press, Oxford, Vol. 5, pp. 771-797 (in French).
- Downing, J.P., 1984. Suspended sand transport on a dissipative beach. In: Proc. 19th International Conf. on Coastal Eng., ASCE, Houston, TX, Vol. 2, pp. 1765-1781.
- Duane, D.B. and James, W.R., 1980. Littoral transport in the surf zone elucidated by a Eulerian sediment tracer experiment. *J. Sediment. Petrol.*, 50(3): 929-942.
- Fairchild, J.C., 1977. Suspended sediment in the littoral zone at Ventnor, New Jersey, and Nags Head, North Carolina. U.S. Army, Coastal Eng. Research Center, Fort Belvoir, Report TP 77-5, 97 pp.
- Gable, C.B., 1981. Report on data from the nearshore sediment transport study experiment at Leadbetter Beach, Santa Barbara, California, Jan-Feb, 1980. Institute of Marine Resources, University of California, IMR Report No. 80-5.
- Greer, M.N. and Madsen, O.S., 1978. Longshore sediment transport data: a review. In: Proc. 16th International Conf. on Coastal Eng., ASCE, Hamburg. Vol. 2, pp. 1563-1576.
- Hou, H., 1988. Study of shelf waves vs. sand drift in NW coast of Taiwan. In: Proc. 21st International Conf. on Coastal Eng., ASCE, Malaga, Vol. 2, pp. 1152-1165.
- Hou, H., Lee, C. and Lin, L., 1980. Relationship between alongshore wave energy and littoral drift in the midwest coast at Taiwan. Proc 17th International Conf. on Coastal Eng., ASCE, Sydney. Vol. 2, pp. 1255-1274.
- Inman, D.L., Zampol, J.A., White, T.E., Hanes, D.M., Waldorf, B.W. and Kastens, K.A., 1980. Field measurements of sand motion in the surf zone. In: Proc. 17th International Conf. on Coastal Eng., ASCE, Sydney. Vol. 2, pp. 1215-1234.
- Ishihara, T., Iwagaki, Y. and Murakami, M., 1958. On the investigation of beach erosion along the north coast of Akashi Strait. *Coastal Eng. in Japan*, Vol. 1, pp. 97-109.
- Iwagaki, Y. and Sawagari, T., 1962. A new method for estimation of the rate of littoral sand drift. *Coastal Eng. Jpn.*, 5: 67-79.
- Johnson, J.W., 1957. The littoral drift problem at shoreline harbors. *J. Waterways and Harbors Div., Proc. ASCE*, 83(WW1): Paper 1211, 37 pp.
- Kamphuis, J.W., Davies, M.H., Nairn, R.B. and Sayao, O.J., 1986. Calculation of littoral sand transport rate. *Coastal Eng.*, 10: 1-21.
- Kana, T.W., 1977. Suspended sediment transport at Price Inlet, S.C. In: Proc. of Coastal Sediments '77, Charleston, SC. ASCE, pp. 366-382.
- Kana, T.W. and Ward, L.G., 1980. Nearshore suspended sediment load during storm and post-storm conditions. In: Proc. 17th International Conf. on Coastal Eng., Sydney. ASCE, 1981, Vol. 2, pp. 1158-1173.
- Katoh, K., Tanaka, N., Kondoh, T., Akaishi, M. and Terasaki, K., 1985. Field observations of local sand movements in the surf zone using fluorescent sand tracer (second report). Report of the Port and Harbour Research Institute, Ministry of Transport, Japan, Vol. 24, No. 4.

- Knoth, J.S. and Nummedal, D., 1977. Longshore sediment transport using fluorescent tracer. In: *Proc. of Coastal Sediments '77*, Charleston, pp. 383–398.
- Komar, P.D., 1969. The longshore transport of sand on beaches. Ph.D thesis, Scripps Institute of Oceanography, University of California, San Diego.
- Komar, P.D., 1988. Environmental controls on littoral sand transport. In: *Proc. 21st International Conf. on Coastal Eng., ASCE, Malaga, Vol. 2*, pp. 1238–1252.
- Komar, P.D. and Inman, D.L., 1970. Longshore sand transport on beaches. *J. Geophys. Res.*, 76(30): 5914–5927.
- Kooistra, J. and Kamphuis, J.W., 1984. Scale effects in alongshore sediment transport rates. Canadian Coastal Sediment Study, Report No. C2S2-13, Kingston.
- Kraus, N.C., 1985. Field experiments on vertical mixing of sand in the surf zone. *J. Sediment. Petrol.*, 55(1): 3–14.
- Kraus, N.C., Isobe, M., Igarashi, H., Sasaki, T.O. and Horikawa, K., 1982. Field experiments on longshore sand transport in the surf zone. In: *Proc. 15th International Conf. on Coastal Eng., Cape Town, ASCE, Vol. 2*, pp. 969–988.
- Kraus, N.C., Gingerich, K.J. and Rosati, J.D., 1988. Towards an improved empirical formula for longshore sand transport. In: *Proc. 21st International Conf. on Coastal Eng., Malaga, ASCE, Vol. 2*, pp. 1182–1196.
- Kraus, N.C., Gingerich, K.J. and Rosati, J.D., 1989. Duck 85 surf zone sand transport experiment. U.S. Army Engineer Waterways Experiment Station, Tech. report CERC-89-5.
- Laubscher, W.I., Coppoolse, R.C., Schoonees, J.S. and Swart, D.H., 1991. A calibrated longshore transport model for Richards Bay. In: *Proc. of Coastal Sediments '91, ASCE, Seattle, Vol. 1*, pp. 197–211.
- Laubscher, W.I., Schoonees, J.S. and Swart, D.H., 1989. A calibrated longshore sediment transport model for Richards Bay. CSIR Report EMA-C 89121, Ematek, Stellenbosch.
- Lee, K.K., 1975. Longshore currents and sediment transport in west shore of Lake Michigan. *Water Resour. Res.*, 2(6): 1029–1032.
- Madsen, O.S., 1987. Use of tracers in sediment transport studies. In: *Proc. of Coastal Sediments '87, New Orleans, Vol. 1*, pp. 424–435.
- Mangor, K., Sørensen, T. and Navntoft, E., 1984. Shore approach at the Danish North Sea Coast, Monitoring of sedimentation in a dredged trench. In: *Proc. 19th International Conf. on Coastal Eng., ASCE, Houston, Vol. 2*, pp. 1816–1829.
- Maruyama, K., Kajima, R., Narihiro, A. and Kondo, K., 1982. Study on sediment transport in a power station harbour basin. In: *Proc. 18th International Conf. on Coastal Eng., ASCE, Cape Town, Vol. 2*, pp. 2357–2375.
- Moore, G.W. and Cole, J.Y., 1960. Coastal processes in the vicinity of Cape Thompson, Alaska. Geologic investigations in support of Project Chariot in the vicinity of Cape Thompson, Northwestern Alaska — Preliminary Report. Final Report U.S. Geol. Survey Trace Elements Investigations, Report No. 753.
- Morfett, J.C., 1990. A "virtual power" function for estimating the alongshore transport of sediment by waves. *Coastal Eng.*, 14: 439–456.
- Nielsen, P., 1979. Some basic concepts of wave sediment transport. Institute of Hydrodynamics and Hydraulic Engineering, Technical University of Denmark, Lyngby, Series paper No. 20.
- Nielsen, P., 1984. Field measurement of time-averaged suspended sediment concentrations under waves. *Coastal Eng.*, 8: 51–72.
- Nicholls, J.N. and Wright, P., 1991. Longshore transport of pebbles: Experimental estimates of K. In: *Proc. of Coastal Sediments '91, ASCE, Seattle, Vol. 1*, pp. 920–933.
- Rosati, J.D., Gingerich, K.J., Kraus, N.C., McKee Smith, J. and Beach, R.A., 1991. Longshore transport rate distributions measured in Lake Michigan. In: *Proc. of Coastal Sediments '91, ASCE, Seattle, Vol. 1*, pp. 156–169.

- Sato, S., 1962. Sand movement at Fukue Coast in Atsumi Bay, Japan, and its observation by radioactive glass sand. *Coastal Eng. Jpn.*, 5: 81-92.
- Sato, S. and Tanaka, N., 1966. Field investigation on sand drift at Port Kashima facing the Pacific Ocean. In: *Proc. 10th International Conf. on Coastal Eng., ASCE, Tokyo, Vol. 1*, pp. 595-614.
- Sawaragi, T. and Deguchi, I., 1978. Distribution of sand transport rate across a surf zone. In: *Proc. 16th International Conf. on Coastal Eng., ASCE, Tokyo, Vol. 2*, pp. 1596-1613.
- Schoonees, J.S. and Bartels, A., 1991. North-eastern False Bay: Physical environmental factors and bathing suitability. *Trans. of Royal Society of South Africa, False Bay Symposium, Cape Town, Vol. 47 (Parts 4 and 5)*, pp. 757-770..
- Sireyjol, P., 1964. Communication sur la construction du port de Cotonou (Dahomey). In: *Proc. 9th International Conf. on Coastal Eng., ASCE, Lisbon*, pp. 580-595 (in French).
- Swart, D.H. and Fleming, C.A., 1980. Longshore water and sediment movement. In: *Proc. 17th International Conf. on Coastal Eng., ASCE, Sydney, Vol. 2*, pp. 1275-1294.
- US Army, Corps of Engineers, 1984. *Shore Protection Manual, Volumes I and II. Coastal Engineering Research Center, Vicksburg.*
- Voitsekhovich, O.V., 1986. Longshore sediment transport — generalized relations and observation data. Ukrainian State Planning, Surveying, and Scientific Research Institute of Water-Management Construction. Translated from *Vodnye Resursy*, No. 5, September-October, 1986, pp. 108-115.
- Walton, T.L. (Jr.), 1978. Sediment trap at Panama City. In: *Proc. of Workshop on Coastal Sediment Transport, with Emphasis on the National Sediment Transport Study, DEL-SG-15-78. Sea Grant College Program, University of Delaware, Newark, DE*, pp. 93-94.
- Walton, T.L. (Jr.) and Chiu, T.Y., 1979. A review of analytical techniques to solve the sand transport equation and some simplified solutions. In: *Proc. Coastal Structures '79, Alexandria, Vol. 2*, pp. 809-837.
- Wang, Y.-H. and Chang, T.H., 1978. Littoral drift along bayshore of a barrier island. In: *Proc. 16th International Conf. on Coastal Eng., ASCE, Hamburg, Vol. 2*, pp. 1614-1625.
- Watts, G.M., 1953. A study of sand movement at South Lake Worth inlet, Florida. U.S. Army, Beach Erosion Board, Tech. Memo No. 42, 24 pp.
- White, T.E., 1987. Nearshore sand transport. Ph.D. thesis, University of California, San Diego, 210 pp.

A2. Details of the allocation of points in Schoonees and Theron (1993)

The following table summarizes the allocation of points as described on pages 10 to 16 in the paper:

ALLOCATION OF POINTS

Parameter	Sub-division				
	Method		Representativeness		
	Criterion	Points allocated	Points allocated before adjustment taking into account the adjacent criteria	Criterion	Point adjustment
Transport rate	Accretion or erosion	7	7	Not a total trap	-1
	Accretion at a groyne	6	6	Offshore breakwater possibly contributing to overtrapping	-1
	Accretion in a dredged trench	6	6	Only bedload measured	-1
	Accretion and bypassing	6	6	Only suspended load measured	-2
	Growth of a spit	6	6	Pumped samples used	-1
	Sand tracer study	4	4	Measurements done in a rip current	-1
	Using samplers or traps	5	5	Longshore current was calculated (not measured)	-1
	Estimated transport rate	2	2	Estimates of the transport used	-1
				Transport determined over the long term rather than during the measurement period	-1
				Streamer trap used.	+1
				Coverage of samplers/traps bad in the horizontal (surf zone) and/or vertical direction (water column)	-1
					-1

Wave height and period	Measured		8	7	Measured in deep water	-1
	Cameras (photopoles)		8	8	Refraction was carried out to obtain breakerline data	-1
	Hindcasted from wind data		4	4	Measurements were not done directly opposite the site	-1
	Observed using poles		6	7	Were the wave statistics used, measured over the recording period for the transport medium term long term	0 -1 -2
	Observed estimates		5	6	Distributions or wave spectra given	+1
	Assumed		2	2	The wave periods were determined by camera	-1 (for wave period only)
	Visual estimate		4	4	Measured in deep water	-1
	Observed by compass clinometer, or similar instrument		5	5	Refraction was carried out to obtain breakerline data	-1
	Cameras		6	7	Measurements were not done directly opposite the site	-1
	Radar		7	7	Were the wave statistics used measured over the recording period for the transport medium term long term	0 -1 -2
Wave angle	Array of meters		7	7	Distributions or wave spectra given	+1
	Hindcasted from wind data		2	2		
	Assumed		1	1		

Beach slope	Only a beach survey(s) was (were) done	6	6	Do the survey(s) extend far enough seawards: yes no	+1 -1
	Only a bathymetric survey(s) was (were) done	6	6	Are the profiles closely spaced? yes no	+1 -1
	Both beach and bathymetric surveys were done	7	7	Has the datum level been accurately determined? yes no	+1 -1
	Beach and bathymetric surveys were done which overlapped or an amphibious vehicle was used	8	8	Was the survey done during the measurement period/was the survey completed in a short time? yes no	+1 -1
	Photographs were used	5	5		
Grain size	Sieve analysis or by means of a settling tube	6*	6	Adequate spatial and temporal coverage of the beach by sampling	+1
	(* also adapt this value by applying the criteria for representativeness).			Part of a sand tracer study	+1
				Samples taken in nearshore zone	+1
				Samples taken away from the site	-1
				Grain sizes only estimated	-1

APPENDIX B

ANNUAL VARIATION IN THE NET LONGSHORE SEDIMENT TRANSPORT RATE

by

Schoonees, J S (2000)

Coastal Engineering Vol. 40: 141-160
(Reprinted with permission)

Annual variation in the net longshore sediment transport rate

J.S. Schoonees *

CSIR, PO Box 320, Stellenbosch 7599, South Africa

Received 1 June 1999; received in revised form 3 December 1999; accepted 13 January 2000

Abstract

The annual variation in the net longshore sediment transport rates at three South African and at one North African site is investigated. The net rates at these sites, given in the first table, show large variations. It was found that measurements of longshore transport rates should be conducted continuously for 5–8 years in order to obtain an accurate value (within 10%) of the true long-term mean net longshore transport rate. A second table was drawn up, which can be applied to determine the range in which the true mean rate will fall if measurements were done over a shorter period than the recommended 5–8 years. It is reasonable to expect that the conclusions are widely applicable, especially for exposed sites. It is recommended that an accurate assessment of the long-term mean net longshore transport rate at a site can best be made cost-effectively by doing limited site-specific measurements, calibrating the best longshore transport formula for the particular site, and predicting the transport rates using a representative wave climate. © 2000 Elsevier Science B.V. All rights reserved.

Keywords: Longshore sediment transport; Annual variations; Long-term mean transport rates; Richards Bay; Durban; Nouakchott

1. Introduction

Longshore sediment transport forms an integral part of the input required for the determination of dredging requirements at a port entrance. Detailed knowledge of the longshore transport is also necessary for the assessment of the beach evolution caused

* Tel.: +27-21-888-2563; fax: +27-21-888-2693.

E-mail address: kschoone@csir.co.za (J.S. Schoonees).

by the construction of breakwaters at harbour entrances or beach improvement schemes incorporating groynes, detached breakwaters and beach-fill. Longshore transport also plays an important role in the stability of inlets and estuaries. Normally, an average net longshore transport rate is used to determine the dredging requirements or the beach evolution at a particular site. This is usually followed by a sensitivity analysis to see what the effect would be if the true net longshore transport is considerably higher or lower than the assumed average rate, or even if a reversal in the transport direction would occur. This average rate is an estimate of the true long-term net longshore transport rate at the site.

In order to obtain the true long-term mean net longshore transport rate at a site, it is necessary to assess the annual variation in the net transport rates. This annual variation can be determined either by computing the longshore transport rates with a reliable formula from wave data spanning a number of years, or by measuring continuously the longshore transport over a number of years. In both cases, it must be known over how many consecutive years either the computations or the measurements should be done. This aspect (the required measurement period) will be determined based on the data from three sites on the South African coast. However, sometimes, it may not be possible to take measurements for this required period (e.g., due to time and cost limitations). An alternative question that needs to be resolved is: Within what range can the long-term mean net transport rate vary if measurements are done over a shorter-than-recommended period? This issue will also be addressed in this paper. While comparing the two ways of obtaining the true long-term mean net transport rate (predictions or measurements), another question arises: What is the most cost-effective way of obtaining the true long-term mean net longshore transport rate? An answer to this question will be given, again based on data from the three sites.

Previous work on the variation in longshore transport rates focused mainly on daily to monthly transport rates and their temporal fluctuations. Seymour and Castel (1985) analysed the daily transport rates at seven sites and determined statistics from them. Raw (1993) presented weekly to monthly transport rates at the Port of Durban determined from volumetric differences (calculated from surveys). In addition, he investigated the annual variation in the net longshore transport rates over a period of 7 years. In a study by Shi-Leng and Teh-Fu (1987), a longshore sediment transport formula (the Bijker, 1967 method) was calibrated against short-term measurements at Nouakchott, Mauritania (Fig. 1) on the Atlantic coast. This formula was then used, based on wave data, to calculate the net longshore sediment transport rates for 7 consecutive years (the data are listed in Shi-Leng and Teh-Fu, 1987). They found a definite variation in the annual transport, such that the ratio of the maximum of the mean value of the annual transport is 1.31, and the ratio of maximum to minimum is 1.89. They also showed that the annual net longshore transport rate follows the Gumbel distribution for their site. However, from all available literature, it appears that very little has been done on the length of time for which measurements should be taken continuously to ensure an accurate long-term mean net transport rate.

The sites, where time series data are available, are briefly described below. This description is followed by an explanation of the analysis method. Thereafter, the results of the analysis of the time series will be presented and discussed. The paper concludes

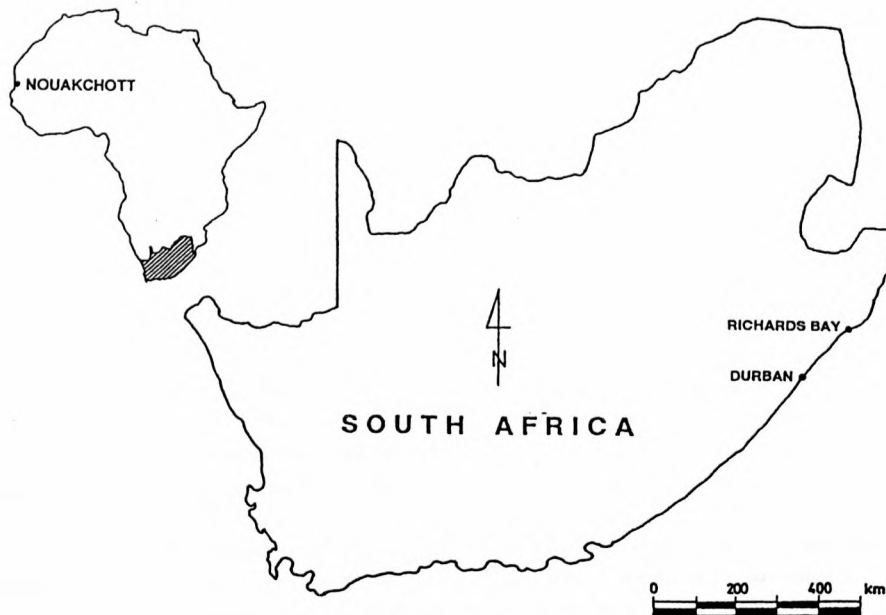


Fig. 1. Location map.

with a recommendation regarding the required period for determining the long-term net longshore transport rate. In addition, the range is given within which the true long-term mean net transport can vary if a shorter-than-recommended period has to suffice. The most cost-effective way of obtaining the true long-term mean net longshore transport rate is also determined.

2. Site characteristics and available data

2.1. General

The three sites, where time series data of the net longshore transport rates were available, are located on the east (Indian Ocean) coast of South Africa (Fig. 1). These are: Durban Bight, the sand trap of the Port of Durban, and the beaches around the Port of Richards Bay. For comparative purposes, the data for Nouakchott, Mauritania from Shi-Leng and Teh-Fu (1987) are also given.

2.2. Durban Bight

It is along the Durban Bight that the main bathing beaches of Durban are situated. The Durban Bight stretches from the entrance of the Port of Durban (between the south

and north breakwaters) in the south up to the mouth of the Mgeni River in the north (Fig. 2). (The river mouth is located just north of Survey Station A shown in Fig. 2.)

The dominantly northbound net longshore transport is interrupted by the breakwaters and entrance channel of the Port of Durban, and virtually all of this transport accumulates in and around the sand trap immediately south of the breakwaters (Fig. 3a and b).

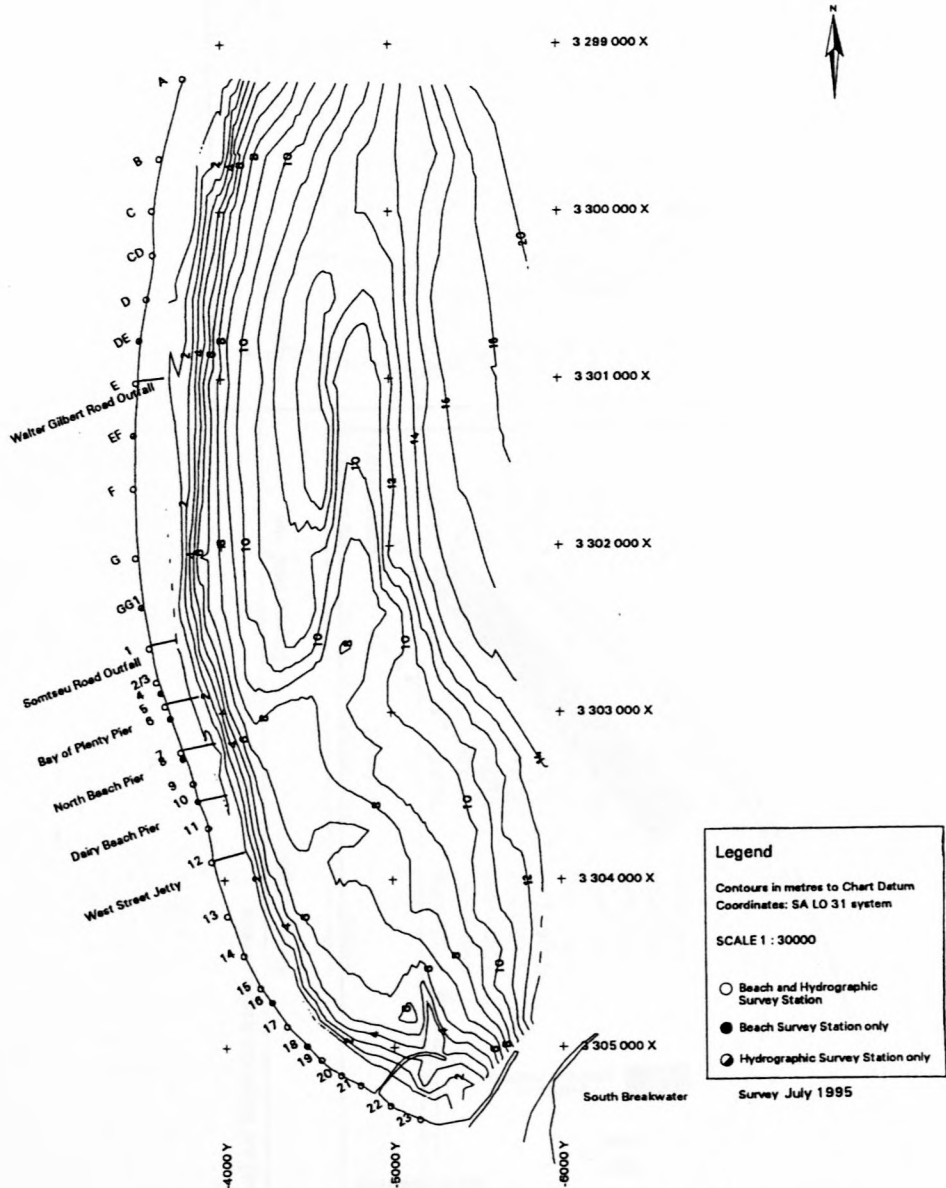


Fig. 2. Durban Bight reference map (from CSIR, 1996).

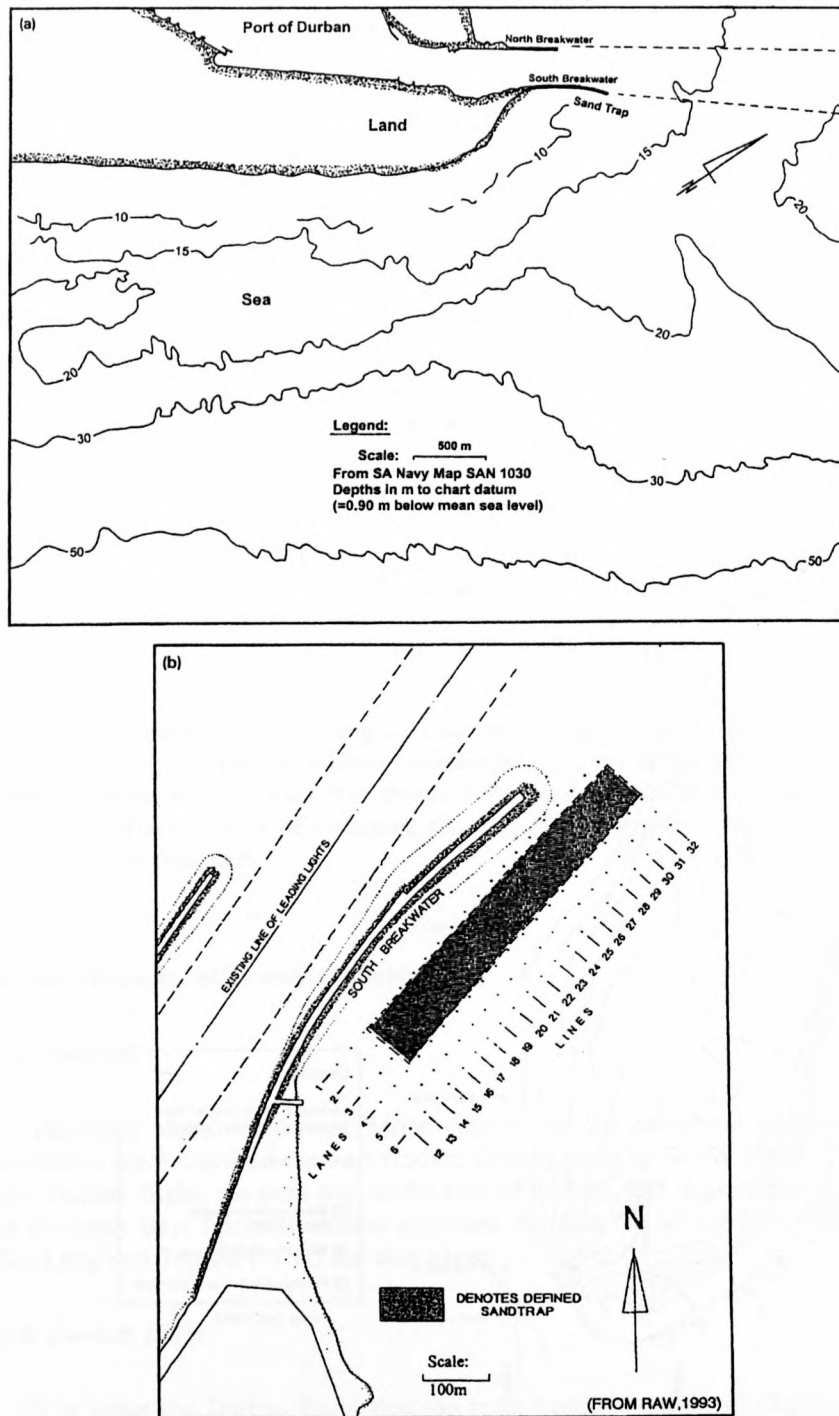


Fig. 3. (a) Bathymetry off the Port of Durban. (b) Sand trap at the Port of Durban.

Table 1
Annual net longshore transport rates

Durban Bight			Durban sand trap		Richards Bay		Nouakchott (from Shi-Leng and Teh-Fu, 1987)	
Period	Net loss rate (m ³ /year)	Period	Net longshore transport rate (m ³ /year)	Period	Net longshore transport rate (m ³ /year)	Period	Net longshore transport rate (m ³ /year)	
1985/1986	90,000	1986	420,000	1979/1980	1,020,000	1976	690,000	
1986/1987	120,000	1987	450,000	1980/1981	830,000	1977	970,000	
1987/1988	820,000	1988	360,000	1981/1982	850,000	1978	1,060,000	
1988/1989	210,000	1989	470,000	1982/1983	2,120,000	1979	780,000	
1989/1990	140,000	1990	590,000	1983/1984	1,880,000	1980	1,310,000	
1990/1991	430,000	1991	620,000	1984/1985	1,570,000	1981	1,140,000	
1991/1992	180,000	1992	560,000	1985/1986	-420,000	1982	1,040,000	
1992/1993	370,000			1986/1987	-260,000			
1993/1994	270,000			1987/1988	720,000			
1994/1995	380,000			1988/1989	1,010,000			
				1989/1990	-60,000			
				1990/1991	1,220,000			
				1991/1992	980,000			
				1992/1993	440,000			
Number of points	10		7		14		7	
Mean	300,000		500,000		850,000		1,000,000	
Standard deviation	220,000		100,000		750,000		210,000	
Coefficient of variation	0.73		0.19		0.88		0.21	

A trailing suction hopper dredger removes the sand from the sand trap and pumps the sand into a hopper just north of the north breakwater (the hopper is not shown in Fig. 2). Bypassing and beach nourishment are achieved by pumping the sand from the hopper along the beaches of the Durban Bight. The longshore transport potential along the Durban Bight is lower than the potential transport south of the harbour entrance, partially because of the protection against wave action offered by the breakwaters (the dominant deep-sea waves are from the south).

Monthly beach surveys have been done along the Durban Bight by using standard, accurate land surveying methods. Annual volumetric net loss rates were calculated from these surveys, representing the beach above chart datum. (Chart datum, which is approximately mean low-water spring tide level, is 0.90 m below mean sea level.) The volumes of sand bypassed are accurately determined in the hopper and are taken into account in assessing the net loss rates. These net loss rates are not equivalent to the net longshore transport rates. However, the loss rates are directly related to the longshore transport rates because longshore transport is the main mechanism for removing sand from the Durban Bight. It has been established that there is no major net long-term cross-shore transport of sand. Furthermore, it can be argued that the cross-shore losses are reasonably consistent from year to year because bypassing is conducted consistently. In any event, it is not the absolute values of the loss rates that are important in this analysis, but the variation in time of rates that were determined in a consistent manner.

The net loss rates that cover a 10-year period (Table 1) were taken from CSIR (1996). Fig. 4 illustrates the yearly variation in the net loss rates. Considerable variation

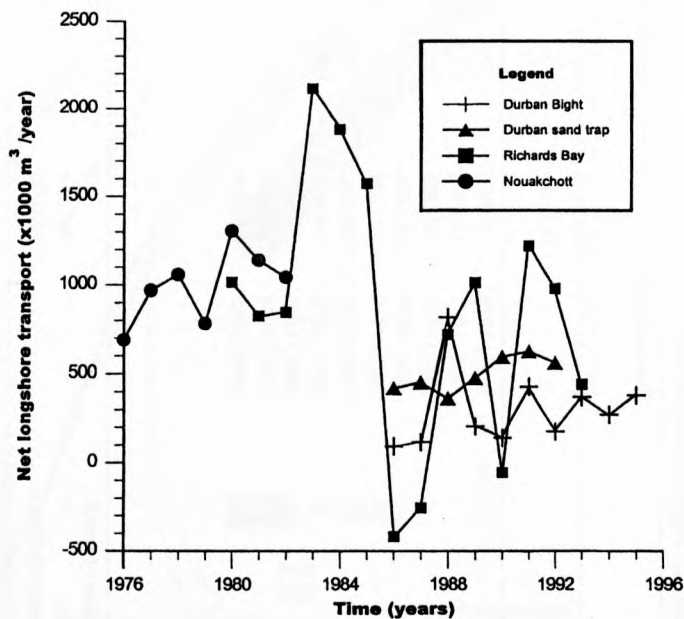


Fig. 4. Annual variation in the net longshore transport rate.

in these rates is apparent from this figure. The long-term mean rate is $300,000 \text{ m}^3/\text{year}$ with loss rates ranging between $90,000$ and $820,000 \text{ m}^3/\text{year}$ (Table 1).

More information about the bypassing operation, wave and sediment characteristics, tidal information, etc., can be obtained from Laubscher et al. (1990) and CSIR (1996).

2.3. Sand trap at the Port of Durban

As mentioned above, the net northbound longshore transport accumulates in the sand trap just south of the south breakwater of the Port of Durban (Fig. 3a and b). A hydrographic survey of the sand trap is carried out roughly every 2 weeks (Raw, 1993). Fig. 3b shows the spacing of the survey lines. The vertical accuracy of the surveys is of the order of 30 cm (Raw, 1993). Volumetric differences between surveys were computed and summed to obtain the net longshore transport rates for each year between 1986 and 1992. The annual variations in these rates (Table 1) can be seen in Fig. 4. Less variation is apparent in the sand trap data compared with the values for the Durban Bight (Fig. 4). The long-term average longshore transport rate for the sand trap is $500,000 \text{ m}^3/\text{year}$ (minimum value = $360,000 \text{ m}^3/\text{year}$; maximum value = $620,000 \text{ m}^3/\text{year}$; Table 1). Raw (1993) presented more detailed information on sand accumulation in the sand trap.

2.4. Richards Bay

The Port of Richards Bay (Fig. 5) was constructed on a sandy coast. Comprehensive monitoring has been undertaken, such as beach and hydrographic surveys, wave recordings by means of a Waverider and a clinometer (graded telescope), tide recordings and sediment grain size analyses. Fig. 5 shows the main beaches adjacent to the harbour, namely:

Southern beach	From Survey Stations TS2–TS17
Near-northern beach	Between TN2 and TN10
Far-northern beach	From TN10 to beyond TN18

Sand is dredged by a trailing suction hopper dredger from south of the harbour entrance and pumped onto the near-northern beach. As at Durban, the net longshore transport is usually towards the northeast.

Volumetric differences were computed from the annual beach and hydrographic surveys. By taking into account the volumes of material dredged, it was possible to calibrate a few longshore transport formulae (Coppoolse and Schoonees, 1991; Laubscher et al., 1991). The measured wave characteristics were used in this calibration together with a detailed refraction analysis. The Kamphuis (1990) formula fared the best. Fig. 6 shows the calibration which was carried out for the southern beach. Note that the coefficient of determination (R^2) is equal to 0.86, which means that the formula accounts for 86% of the variation. This high percentage is very good for sediment transport predictions.

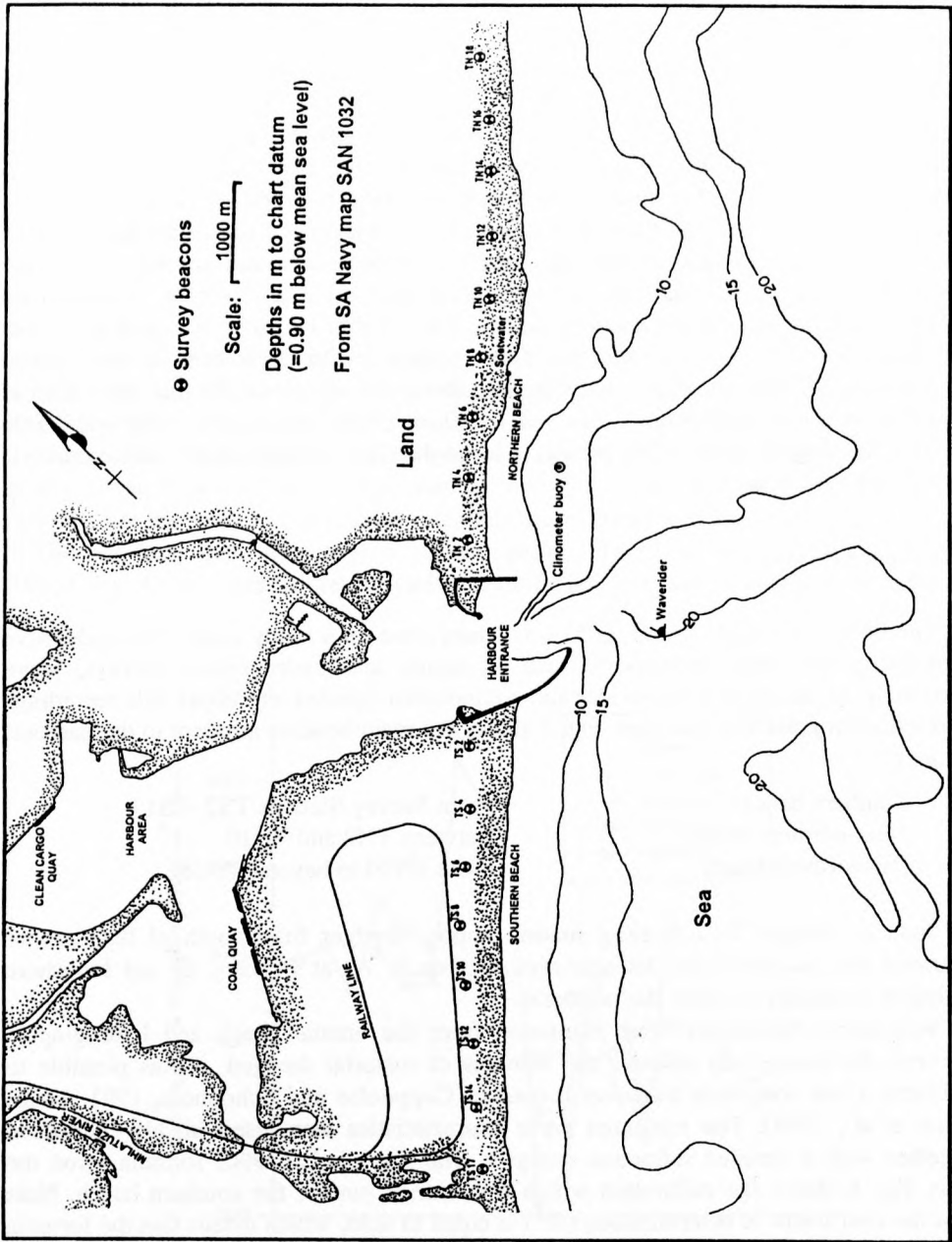


Fig. 5. Layout of the Port of Richards Bay (from CSIR, 1994).

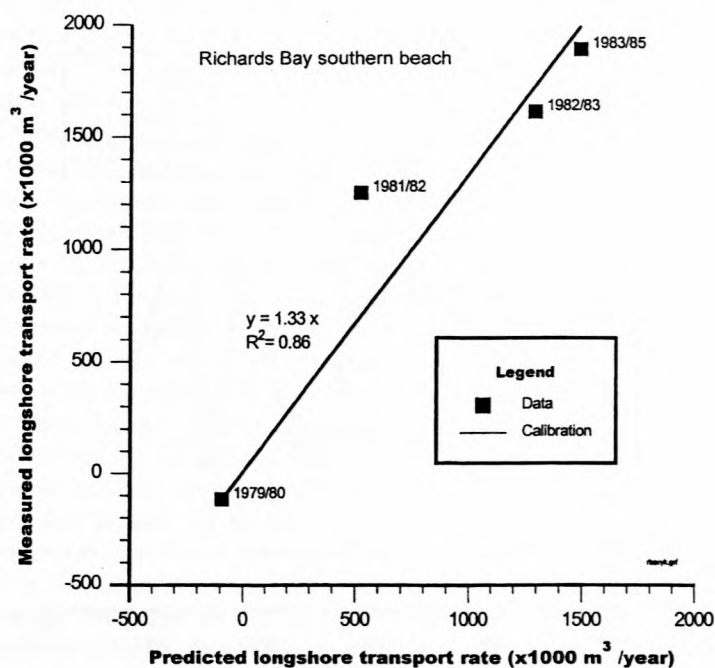


Fig. 6. Calibration of the Kamphuis formula using Richards Bay data.

Refraction results were also obtained for the near- and far-northern beaches and smoothened (averaged) for the specific beach, as was done for the southern beach. Each measured wave condition was then refracted out to deep sea, followed by refraction towards the particular beach. The calibrated Kamphuis formula was then employed to predict the longshore transport rate for each wave condition at each of the three beaches (CSIR, 1994). These rates were summed to obtain the net longshore transport rate for each year at each of the three beaches. Fig. 7 illustrates the variation in the net longshore transport rate over the 14 years from 1979/1980 to 1992/1993. Large differences in the net longshore transport rates are apparent from year to year in this figure. Reversals in the net longshore transport directions occurred a number of times on the southern beach and twice on the far-northern beach. The reasons for the frequent reversal in the net transport direction along the southern beach are the change in its orientation because of dredge spoil being pumped onto the beach (mostly in the 1970s) and shifts in the deep-sea wave direction. For the purpose of the analysis, the results for the three Richards Bay beaches were combined (Table 1), giving a long-term net north-eastbound longshore transport of 850,000 m³/year. The net rates vary from -420,000 to 2,120,000 m³/year (Table 1).

Detailed information about the site can be found in Swart (1981), CSIR (1989, 1994), Coppoolse and Schoonees (1991) and Laubscher et al. (1991). These references include descriptions of the wave recordings, tidal levels, refraction results, sediment grain sizes and the calibration of the longshore transport formula.

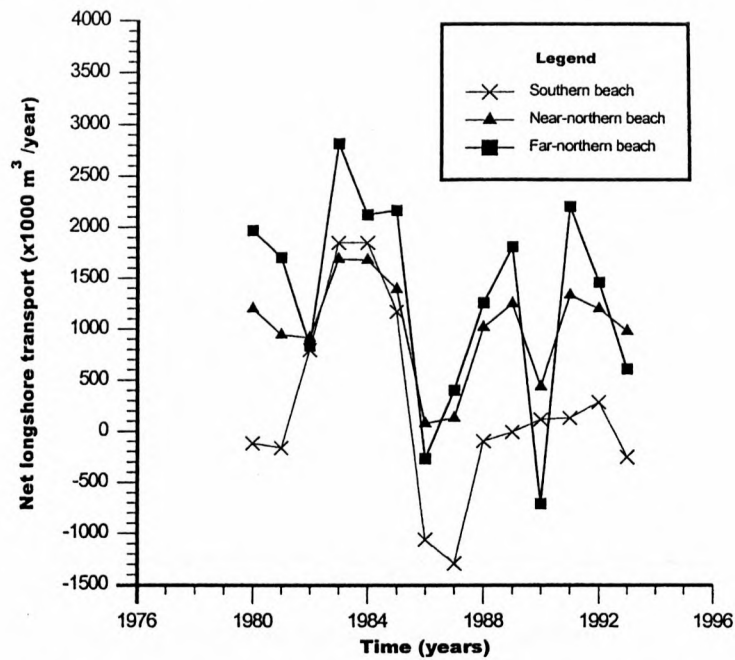


Fig. 7. Annual variation in the net longshore transport rate at Richards Bay.

2.5. Nouakchott

The data for Nouakchott from Shi-Leng and Teh-Fu (1987) are also contained in Table 1. The mean net longshore transport rate is 1,000,000 m³/year with the rates varying between 690,000 and 1,310,000 m³/year (Table 1).

3. Analysis method

The variation in the net longshore transport rate over time is characterised by two variables, namely, the standard deviation and the coefficient of variation. The coefficient of variation is defined as the standard deviation divided by the mean. These two variables are preferred above the ratio of the maximum rate to the minimum rate because they are the standard way in statistics of representing variation. In addition, if some of the net transport rates are negative (as for Richards Bay; Table 1), then the value of the abovementioned ratio is misleading. Both *running* and *floating* mean net longshore transport rates were used, as will be discussed below.

The running mean net transport rate is calculated as follows: the first point is the mean rate over 1 year; the second point is the mean rate of the first 2 years; the third

point is average of the first 3 years; and so on. A factor (f_t), being the running mean rate divided by the long-term mean net longshore transport rate, was plotted against time for each of the three sites. The advantage of plotting this factor, instead of just the running mean rate against time, is that it is known that the factor will tend towards unity. It is then easy to see over how many years the running average needs to be taken to ensure a variation of say, 20%, above and below the net long-term average rate. In this example, the required number of years over which the mean should be computed (say t_1) will be when the value of this factor (f_t) is consistently between 0.8 and 1.2. Measurements should therefore be done for t_1 years in this example to ensure an accuracy of 20% in the long-term value of the net longshore transport rate.

Another area of inquiry is the sequence of years during which consecutive measurements are taken. If, e.g., measurements are taken for 3 years at a site for a new port, and these happen to be 3 years with low net transport rates, the answer (mean net rate) will be too low. This could have severe cost implications if the dredging requirements for the port are underpredicted. To address this problem, the effect of the sequence of years on the final answer was also investigated.

However, due to cost limitations, it is usually not possible also to measure the longshore transport over the required number of years. Guidance is therefore needed on how much a shorter-term average can deviate from the long-term average rate. A *floating* average was used for this purpose. The floating average is computed over a specified number of years. For example, the floating average over 3 years is calculated as follows: the first mean value is the average of the first, second and third net rates; the second mean value is the average of the second, third and fourth net rates; the third mean value is the average of the third, fourth and fifth net rates, etc. A characteristic of this method is the fewer data points obtained if averaging is done over longer periods. For example, if averaging is done over 10 years, and 14 years of data are available, five data points (floating mean rates) are obtained. As for the running mean, the floating mean is divided by the long-term mean rate to obtain a factor (f_t) that will tend towards unity. Confidence bands based on the data can then be drawn in on a plot of this factor vs. the period over which the floating mean was computed. Therefore, for a certain confidence level, the factors can be obtained within which the estimate of the long-term rate will fall if measurements are taken during a period shorter than the recommended period.

4. Results and discussion

4.1. Variation in the net longshore transport rates

Fig. 4 shows the variation in the net longshore transport rates at the four sites (Durban Bight, Durban sand trap, Richards Bay and Nouakchott). The largest variations occur at Richards Bay and the Durban Bight; however, significant annual variation is evident for the Durban sand trap. Since all three South African sites are situated within

300 km of each other along an exposed coastline subject to roughly the same weather systems, reasonably similar variations in the annual rates at the three sites are to be expected. The smaller variation for the Durban sand trap data can be attributed to the following causes:

- The survey area at the sand trap does not cover the beach and nearshore area to its south, i.e., the area between the sand trap and the beach (Fig. 3b). This means that appreciable accretion can, e.g., occur there without it being reflected in the volumetric differences calculated for the sand trap. This area is important because it is well-known that most longshore transports occur within the surf zone. Despite this, very little sand eventually bypasses the sand trap and the adjacent beach and nearshore area as maintenance dredging of the entrance channel is not normally required.

- The side slopes of the sand trap are also not included in the survey area (Raw, 1993). As with the above condition, all sand is not accounted for in the volume calculation.

- It is unlikely that sand in the sand trap and in the lee of the breakwaters of the port will be transported southwards in the case of southbound longshore transport. This is because of the protection offered by the breakwaters and because sand is not easily transported up the slope and out of the sand trap. In contrast, the breakwaters at Richards Bay virtually do not affect the results there because long stretches of beach are included in the volumetric computations and not only a strip in the lee of the breakwaters as at the Durban sand trap.

- It is expected that the variation in the longshore transport arriving at the sand trap will be more than the variation in the accumulated volumes of sand in the sand trap, which are recorded by surveys roughly every 2 weeks. This is mostly because it is not possible to dredge the exact rate of sand as it arrives at the sand trap because of storms. The trapping of sand and the dredging of it thus, in effect, smoothen out some of the variation in the longshore transport.

Because the Durban sand trap data cover a shorter period than the other two South African sites, it can be argued that only a period with smaller variation in the net longshore transport rates is covered. However, this is not the case. Investigating the same period, 1986–1992, for the Durban Bight data as for the Durban sand trap data, it is found that the coefficient of variation was between 0.77 and 0.93 for the Durban Bight compared with 0.19 for the Durban sand trap. (The value 0.77 is obtained for the period 1985/1986 to 1991/1992 while 0.93 is calculated from 1986/1987 to 1992/1993; Table 1. The calculation of the coefficient of variation for these two periods is done because the respective periods for the Durban Bight and Durban sand trap do not coincide exactly.) Therefore, it is clear that the Durban sand trap data do not cover a period with smaller-than-normal variations in the net longshore transport rate. On the other hand, it could be that the Durban Bight variation is somewhat too large because the loss rates are dependent on when the surveys were done. That is, if a survey were done immediately after a storm, the loss rate from the beach would be higher than if the survey was conducted before the storm.

Comparing the annual variation in the net longshore sediment transport rate for the three South African (Indian Ocean) sites with the variation at Nouakchott on the Atlantic coast (Shi-Leng and Teh-Fu, 1987), it is clear that the variation at Nouakchott is larger

than the variation at the Durban sand trap, but lower than the variations found at the Durban Bight and at Richards Bay (Fig. 4 and Table 1). The values of the coefficient of variation are 0.19, 0.21, 0.73 and 0.88 for the Durban sand trap, Nouakchott, Durban Bight and Richards Bay, respectively. Although Shi-Leng and Teh-Fu (1987) give some information about the Nouakchott site, which is apparently along an exposed coastline on the west coast of north Africa, it is not possible to do a more detailed comparison.

4.2. Required measurement period

The factor (f_r) or ratio of the running mean net longshore transport divided by the long-term mean net longshore transport is plotted vs. time in Fig. 8 (S = longshore transport rate in this figure and in Figs. 9 and 10). Note that the long-term mean net longshore transport is the mean of the net longshore transport rates over the maximum number of years of data that are available, i.e., 10, 14 and 7 years, respectively, for the Durban Bight, Richards Bay and Durban sand trap data.

From Fig. 8, it can be seen that the factor f_r varies from about 0.3 to just over 1.6 for the data of the three sites. It is also clear that the Richards Bay and Durban Bight data exhibit the largest variations (as discussed above), while the Durban sand trap values show a slowly increasing trend towards unity.

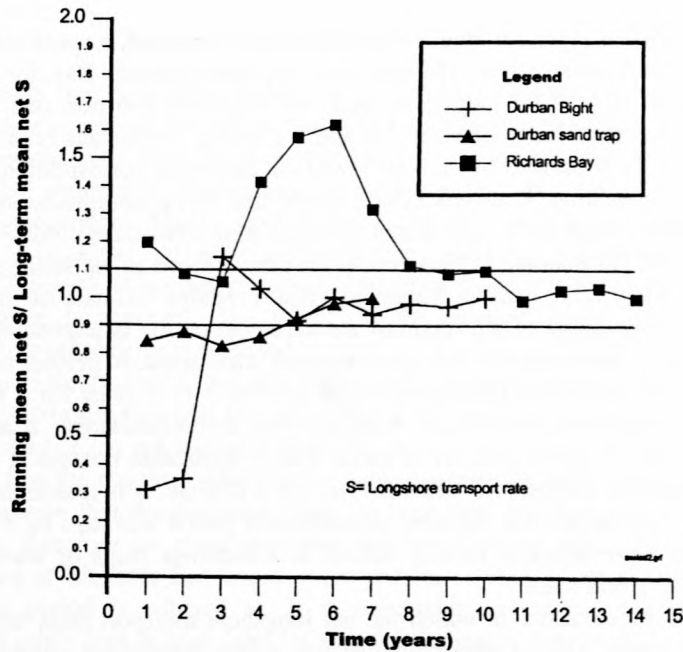


Fig. 8. Variation of the running mean net longshore transport rates over time.

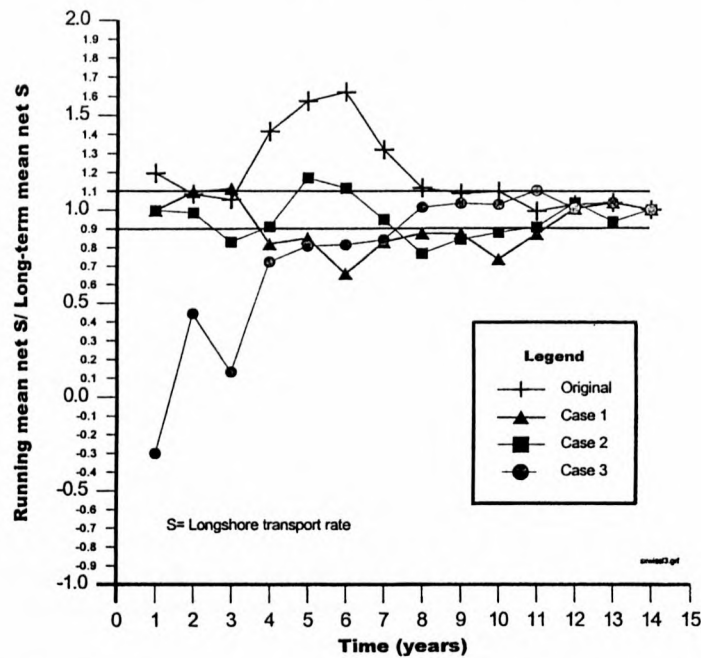


Fig. 9. Random variation of the net longshore transport rates at Richards Bay.

Fig. 8 also shows that the running mean needs to be computed, respectively, over 4, 5 and 8 years at the Durban Bight, Durban sand trap and Richards Bay for the running mean to be within 10% of the long-term mean net longshore transport rate. That is, the factor f_r will vary consistently between 0.9 and 1.1 in Fig. 8 after this number of years. A comparison of these periods (4–8 years) with the following corresponding periods in related fields is interesting. Rossouw (1989) found that wave measurements have to be done for 5 years or longer to be representative of the long-term wave climate. For fluvial sediment transport, Rooseboom (1992) concluded that a record of the sediment load of a river should be kept for 6 years or longer to yield a reliable estimate of the long-term mean load. This agreement of the required measurement period is interesting.

It is therefore recommended that the required measurement period to obtain an accurate long-term mean rate for exposed sites is from 5 to 8 years for a deviation of within 10% from the long-term mean. Although this recommendation is derived from three data sets only, it is believed to be more widely applicable because it agrees with the required recording period of 5 years for the wave climate. It is reasonable to expect that, for protected beaches, the required measurement period will also be 5–8 years or less because the wave attack is usually limited to a narrower range of wave directions compared with exposed sites.

The effect of the sequence in which the net longshore transport rates were obtained was also investigated. This is important because it is normally not known whether a cycle of high or low rates will be encountered during measurement.

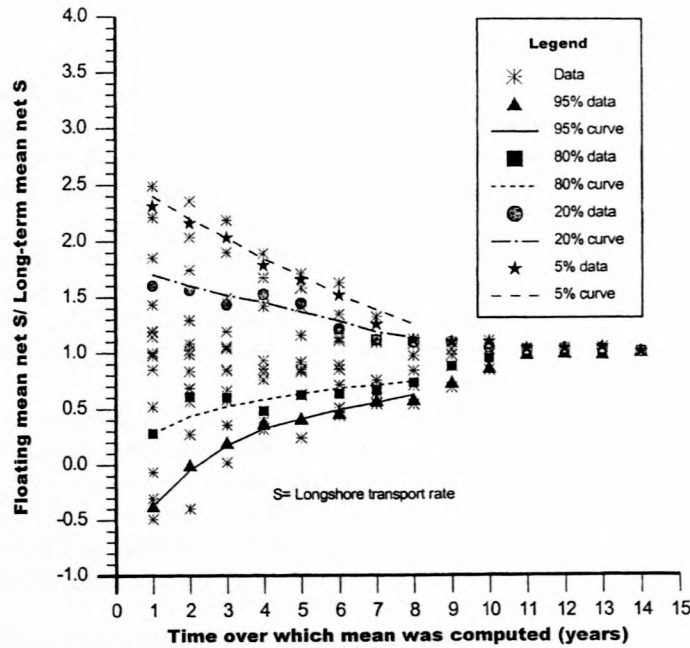


Fig. 10. Richards Bay: floating mean net longshore transport rate (S)/long-term mean net S .

The Richards Bay data were chosen for this investigation because the site yielded a data span over the longest period (14 years) and with large annual variations. A random number generator was used to alter the sequence in which the net transport rates occurred. The underlying assumption is therefore that the net transport rates are statistically independent. This is most probably not true, because weather patterns (and therefore wave patterns) can be distinguished over medium (5–10 years) and long terms (more than 10 years). However, maximum variations from year to year can be expected if independence is assumed. The effect on the required measurement period will therefore most probably be maximised.

Fig. 9 shows the factor (f_r , running mean rate/long-term mean rate) vs. time for the real (original) data for Richards Bay as in Fig. 8, together with three cases in which the order (sequence) of the net transport rates was varied in a random way. From Fig. 9, it can be seen that the required measurement period generally lies between 8 and 9 years in order to ensure that the deviation from the long-term mean is less than or equal to 10%. It can therefore be concluded that the sequence in which the net longshore transport rates at Richards Bay occur is not critical as long as the continuous required measurement period is adhered to. It is reasonable to assume that this finding is applicable to other sites as well (and/or that the finding is conservative) because of the large variations in net longshore transport rates found in Richards Bay.

4.3. Deviation of long-term mean transport rate from the short-term mean rate

Fig. 10 shows the variation in the factor (f_f) of the floating mean longshore transport divided by the long-term mean transport rate vs. the period over which the averaging was done. It should be recalled that the Richards Bay data set, which is the longest data set and shows the most variation, has been used. The data points fall within an approximately triangular area and are roughly symmetrical around 1.0. This is to be expected because the range of the values of the abovementioned factor should decrease as the period over which the averaging is done increases. Furthermore, because the net longshore transport rate can be negative, the data points will not be truncated where the factor is zero, as is the case for the sediment yield from river catchments (which cannot be less than zero; Rooseboom, 1992).

Four confidence bands (95%, 80%, 20% and 5%) were determined based on the occurrence of factor, f_f . The 95% limit indicates that 95% of the values of f_f will exceed the given value for the particular period over which the averaging was done. The data points showing the position of these four confidence limits (which were determined by means of linear interpolation) are also plotted in Fig. 10. Smooth lines were drawn through these points. Table 2, in which the values of f_f are tabulated, summarizes the confidence limits.

For example, if measurements, which were taken continuously over 2 years, yielded a mean net longshore transport rate of 300,000 m³/year, it would mean that the long-term mean net rate can vary as follows by using Table 2:

With a confidence of 90% (between 5% and 95%): from $-0.05 \times 300,000 = -15,000$ m³/year to $2.20 \times 300,000 = 660,000$ m³/year. This variation in the long-term net longshore transport rate will then have to be taken into account, as, e.g., in predicting accretion next to harbour breakwaters.

The values of the factor (f_f) tabulated in Table 2 are, strictly speaking, only applicable to the specific site. However, because Richards Bay lies on an exposed coast where large variations in the longshore transport regime occur (Fig. 7), it is believed that these values of f_f are more widely applicable. Engineering judgement is required to estimate how conservative these factors would be for protected coasts where the wave attack is usually limited to a narrower range of wave directions than that which occurs at Richards Bay. It is recommended that the above analysis be repeated for protected and partly protected coasts when data become available.

Table 2

Confidence bands of the factor, floating mean net longshore transport/true long-term mean net transport (Richards Bay data)

Confidence limit (%)	Period (years) over which the mean was computed							
	1	2	3	4	5	6	7	8
95	-0.37	-0.05	0.17	0.32	0.41	0.48	0.55	0.62
5	2.40	2.20	2.03	1.84	1.70	1.51	1.38	1.25
80	0.28	0.44	0.52	0.58	0.63	0.68	0.70	0.74
20	1.70	1.60	1.51	1.46	1.37	1.28	1.18	1.13

4.4. General discussion

An accurate assessment of the long-term mean net longshore transport rate at a site can be made in a number of ways (called options), as follows:

(1) The long-term mean net longshore transport rate may be known for nearby sites from long-term records. By inference, the long-term net rate at the new site can be determined. This can be done by comparing the wave climates, sand grain sizes, coastline orientations, beach and nearshore profiles, etc., of the particular site with the nearby sites.

(2) Measurements can be conducted over a 5–8 year period or over a shorter period and by using the values of f_t (floating mean rate/long-term mean rate) in Table 2 as explained above. Typical methods for doing these measurements are described in Schoonees and Theron (1993). Apart from the high costs involved in doing these measurements, such a long period is normally unacceptable for clients who commission this type of study.

(3) A representative wave climate can be used together with a well-calibrated longshore transport formula (Schoonees and Theron, 1996) to predict the long-term mean net transport rate.

(4) Limited site-specific measurements (e.g., by using short-term impoundment (Bodge, 1986) or other methods (Schoonees and Theron, 1993) can be made to calibrate a longshore transport formula (Schoonees and Theron, 1996) for the particular site. The calibrated formula can then be used with confidence in association with representative wave data to predict the long-term mean net rate.

In determining the average sediment yield of a river (or fluvial sediment transport), use has been made of almost continuous suspended sediment concentration measurements at a representative location (Rooseboom, 1992). In the sea, however, the cost of almost continuous concentration measurements is prohibitive. In addition, the zones of maximum concentration and transport shift all the time owing to changes in tidal levels, beach profiles, and wave heights. This means that the measuring point(s) (location) will have to shift continuously in order to measure within the zones where the maximum concentrations and transport occur. These zones are themselves difficult to determine before measurements are conducted.

It is recommended that the abovementioned option (4) (limited measurements, calibration and prediction) be carried out, possibly augmented by option (1) (inference of net rate from nearby sites). This is believed to be the most cost-effective method of determining the long-term mean net longshore transport rate.

The question may be asked: How many years of volume observations will it take to give a better estimate of the long-term mean transport rate than an estimate based on comprehensive wave data and the best longshore transport formula? Clearly, the answer will be the same number of years provided that the accuracies of the volume observations (the first method) and sediment transport predictions (the second method) are similar, assuming that the periods covered by both methods are equally representative of the long-term conditions. The factors that influence the accuracy of these methods include the accuracy of the following: the volume differences calculated from hydrographic surveys, the determination of dredged volumes, the measurement of wave

characteristics (especially the wave direction), and the longshore sediment transport formula used. Either of the two methods may be significantly more accurate in a specific instance, but this will have to be assessed in each case. In any event, a larger database than contained in this paper would be required to reach a firm conclusion.

5. Conclusions and recommendations

Based on data from three sites on the South African east coast, it was found that measurements of the longshore transport rates should be conducted continuously for 5–8 years in order to obtain an accurate value (within 10%) of the long-term mean net longshore transport rate. It was also found that the order (sequence) in which the net longshore transport rates occur is not critical as long as the required measurement period is adhered to. In other words, it does not matter whether the measurements start at a time when the net longshore transport rates are low or high.

Four confidence bands (95%, 80%, 20% and 5%) were determined for the factor f_t , the floating mean net longshore transport/long-term mean net transport, for different measurement periods (Table 2). This table can be used to estimate the long-term net transport rate if measurements were done over a shorter period than the 5–8 years recommended above. That is, if measurements cover only, e.g., a 2-year period, the values of f_t in Table 2 can be applied to determine the range in which the true long-term mean net transport rate will fall for a given confidence band.

Although the above conclusions are derived from data originating from specific sites, it is reasonable to expect that the conclusions are more widely applicable, especially for exposed sites (such as the three South African sites considered here). For protected sites, the above results are most probably conservative. It is recommended that the above analysis be repeated for protected and partly protected coasts when data become available.

It is also recommended that an accurate assessment of the long-term mean net longshore transport rate at a site can best be made cost-effectively by doing limited site-specific measurements, calibrating the best longshore transport formula (Schoonees and Theron, 1996) for the particular site, and predicting the transport rates using a representative wave climate. Measurements can be made using a variety of methods as described in Schoonees and Theron (1993). If possible, these predictions should be augmented by comparing the net rate with the net rates from nearby sites.

Acknowledgements

The comments by Prof. A. Rooseboom and André Theron are gratefully acknowledged. The work was carried out as part of a PhD study at the University of Stellenbosch. This study uses data obtained during contract work for Portnet and the City of Durban. Permission to apply the data is gratefully acknowledged.

References

- Bijker, E.W., 1967. Some considerations about scales for coastal models with movable bed. Publ. 50, Delft Hydraulics Laboratory, Delft.
- Bodge, K.R., 1986. Short-term impoundment of longshore sediment transport. PhD thesis, University of Florida, Gainesville.
- Coppoolse, R.C., Schoonees, J.S., 1991. Maintenance dredging at Richards Bay: sensitivity analysis of predictive models and the location of an offshore dump site. In: Paper D3, CEDA-PIANC Conference, Amsterdam.
- CSIR, 1989. A calibrated longshore sediment transport model for Richards Bay. CSIR Report EMA-C 89121, Stellenbosch, 1989.
- CSIR, 1994. Erosion and sedimentation problems at Richards Bay. CSIR Report EMAS-C 94035, Stellenbosch, 1994.
- CSIR, 1996. Durban beach monitoring. Progress Report: July 1994 to June 1995. Main Report. CSIR Report EMAS-C 96014/1, Vol. 1, Stellenbosch.
- Kamphuis, J.W., 1990. Alongshore sediment transport rate. In: 22nd Int. Conf. Coastal Eng., ASCE, Delft, Vol. 3, pp. 2402–2415.
- Laubscher, W.I., Coppoolse, R.C., Schoonees, J.S., Swart, D.H., 1991. A calibrated longshore transport model for Richards Bay. In: Coastal Sediments '91, ASCE, Seattle Vol. 1, pp. 197–211.
- Laubscher, W.I., Swart, D.H., Schoonees, J.S., Pfaff, W.M., Davis, A.B., 1990. The Durban beach restoration scheme after 30 years. In: 22 Int. Conf. Coastal Eng., ASCE, Delft Vol. 3, pp. 3227–3238.
- Raw, P.N., 1993. Determination of net longshore sediment transport rate in the sandtrap, Port of Durban, using volumetric calculations. Internal Portnet Report, Portnet, Durban.
- Rooseboom, A., 1992. Sediment transport in rivers and reservoirs: a Southern African perspective, Report 297/1. Water Research Commission, Pretoria.
- Rossouw, J., 1989. Design waves for the South African coastline. PhD thesis, Univ. of Stellenbosch, Stellenbosch.
- Schoonees, J.S., Theron, A.K., 1993. Review of the field data base for longshore sediment transport. Coastal Eng. 19, 1–25.
- Schoonees, J.S., Theron, A.K., 1996. Improvement of the most accurate longshore transport formula. In: 25 Int. Conf. Coastal Eng., ASCE, Orlando, FL Vol. 3, pp. 3652–3665.
- Seymour, R.J., Castel, D., 1985. Episodicity in longshore sediment transport. J. Waterways, Port, Coastal Ocean Eng. 111 (3), 542–551.
- Shi-Leng, X., Teh-Fu, L., 1987. Long-term variation of longshore sediment transport. Coastal Eng. 11, 131–140.
- Swart, D.H., 1981. Effect of Richards Bay harbour development on the adjacent coastline. In: 25 PIANC, Edinburgh Vol. 5, pp. 899–917.

APPENDIX C

LONGSHORE TRANSPORT FORMULAE

C.1 General

This appendix contains a summary of the available longshore transport formulae and how they were used. For brevity sake, not all the equations are given - the original references have to be consulted. However, sometimes the original references are not explicit and assumptions had to be made - these are presented. In other cases, curve fitting was required in order to program the methods. The two longshore transport formulae by Hallermeier (1982) were improved significantly while the range for the Larras, Bonnefille and Pernecker, 2 methods were extended by extrapolation.

The formulae are summarized per category as given in Chapter 2.

C.2 Energetics (Energy Flux) Approach

One of the earliest formulae and perhaps the best-known method, the **SPM formula** (SPM = Shore Protection Manual) is given in US Army, Corps of Engineers (1984):

$$S = K_1 P_{1s} f \quad (C1)$$

$(m^3/year)$

where K_1 = 1289 ($m^4 / (W \cdot year)$) for prototype conditions
= 578 for model data (Willis and Price, 1975 and Das, 1972)

P_{1s} = wave energy flux factor using the significant wave height in the calculation (W/m).
and f = frequency of occurrence

Development of the SPM formula was done, among others, by Scripps Institute of Oceanography (1947), Watts (1953), Caldwell (1956), Inman and Bagnold (1963), Komar (1969), Komar and Inman (1970) and Komar (1983).

Swart (1976a) adapted the coefficient $K_1 = 1289$ to be a function of the median grain size (D_{50}). His version of the **SPM formula** is

$$S = K_2 P_{1s} f \quad (C2)$$

where K_2 = $1876 \log_{10} (0,00146 / D_{50})$
 $(D_{50}$ in m)

Kamphuis and Readshaw (1978) and Vitale (1981) investigated whether K_1 is a function of the surf similarity parameter (or Iribarren number) ξ_{brms} :

$$\xi_{brms} = \frac{\tan \alpha}{(H_{brms} / L_0)^{0,5}}$$

where $\tan \alpha$ = bottom slope in the surf zone
 H_{brms} = root-mean-square breaker height
 $= H_{bs} / \sqrt{2}$ (H_{bs} = significant breaker height)
 L_0 = deep-water wavelength

It was decided to use the relationship proposed by Kamphuis and Readshaw (1978) and Readshaw (1979), namely:

$$K_p' = \begin{cases} 0,7 \xi_{brms} & \text{for } 0,4 < \xi_{brms} < 1,4 \\ \text{say for } \xi_{brms} < 1,4 \\ 1,24 & \text{for } \xi_{brms} \geq 1,4 \end{cases}$$

with Q_s (kg/s) = $K_p' P_{ls} / 2g$

$$\text{and } S = \frac{31\,557\,600\,Q_s\,f}{(1-p)\rho_s} \quad (C3)$$

where p = porosity of the sediment (assumed to be 0,4 for sand)
 ρ_s = density of the sediment (usually 2650 kg/m³ for sand)
 and 31 557 600 = number of seconds in one year

Bailard (1981) generalized the Bagnold (1963, 1966) energetics-based stream model. After integrating the local time-averaged longshore transport rate, Bailard (1984) obtained the following alternative equation for K_1 , (called K_3) valid for both model and prototype applications:

$$K_3 = 0,05 + 2,6 \sin^2 2\theta_b + 0,007 u_{mb} / w$$

where w = fall velocity of the sediment grains
 $u_{mb} = 0,5 \gamma (g d_b)^{0,5}$
 and γ = breaker index
 $= 0,8$

Bailard (1985) adds another term to the above equation namely, $0,0096 \tan \alpha$. However, choosing a very high value of $\tan \alpha$ of 0,2, it is clear that the estimated maximum value of this term is about 0,0019. For $\tan \alpha = 0,04$ a typical value, the term is only 0,00038. Because its contribution to K_3 is negligible, this term was omitted. Furthermore,

$$I_l = 0,5 K_3 P_{lx}$$

with I_l = immersed weight longshore transport rate

$$\text{and } S = \frac{31\,557\,600\, I_l \cdot f}{(\rho_s - \rho) g (1 - p)} \quad (C4)$$

Like the original SPM formula, the above variations to the SPM formula are bulk predictors. Svasek and Bakker (see Bakker, 1969, 1971 and Bakker *et al.*, 1971) and Komar (1977) devised methods to calculate the distribution of the longshore transport across the surf zone. The method by Komar has been used. He assumed that the local transport rate is proportional to the local product of the shear stress and the current velocity caused, firstly by only the wave orbital motion and secondly, by both the orbital motion and longshore velocity. Furthermore, he supposed that all the longshore transport occurs in the surf zone. He then calibrated the two formulations to obtain the same total transport rate (integrated across the surf zone) as for the SPM formula. The formulation applied here is the second formulation as given by Equation (19) in Komar (1977). The formula consists of a lengthy set of expressions utilizing the longshore current distribution by Komar (1975).

Watts (1953) empirically related the longshore transport rate to the wave energy flux factor. The **Watts formula** in SI units is:

$$S = 2223 f P_{lx}^{0,9} \quad (C5)$$

Similarly, **Caldwell** (1956) obtained his formula (given here in SI units):

$$S = 2505 f P_{lx}^{0,8} \quad (C6)$$

Manohar (1962) correlate the transport rate not only to the wave energy flux factor, but also to the grain size (assumed here to be the median grain size) and the relative density of the material to be transported. He obtained (in SI units):

$$S = 1,47 \cdot 10^5 f P_{lx}^{0,91} D_{50}^{0,59} (\rho / (\rho_s - \rho))^{0,41} \quad (C7)$$

Pyshkin *et al.* (1965) presented their equation, namely, the **Pyshkin-Maksimitchouk-Zaitz formula**:

$$S = 378,7 f H_{\alpha}^2 L_o (g / D_m)^{0,5} \sin 2\theta_o \quad (C8)$$

where D_m = mean sediment grain size

H_{α} = deep-water significant wave height

and subscript 0 denotes deep-water characteristics

It has been assumed that $D_m = D_{50}$. In the computations an equivalent H_{oe} and θ_{oe} have been used instead of H_{os} and θ_o . Parallel contours (and Snell's law) were assumed which made it possible to calculate H_{oe} (a significant wave height) and θ_{oe} from H_{bs} and θ_b . This formula can also be given in terms of P_{ls} .

Castanho (1966) considered bedload and suspended load separately and determined the energy dissipated by both spilling and plunging breakers (Sayao and Kamphuis, 1983 and Schoonees, 1997). The **Castanho formula**, using solitary wave theory, is:

$$S = \frac{31\,557\,600\, s_c\, P_{\#}\, f}{(\rho_s - \rho)\, g\, (1 - \rho)\, \tan \varnothing} \quad (C9)$$

$$\text{where } P_{\#} = 2,23\, \rho g\, (H_{bs}^3 / T) \sin \theta_b \cos \theta_b$$

$$\varnothing = \text{angle of repose of the sediment}$$

$$s_c = \text{fraction of the available energy flux}$$

The variable s_c is a function of the breaker type and $A_c \left(A_c = \frac{H_{bs} \tan \alpha}{L_b\, c_f \tan \theta_b} \right)$. In the latter equation

$$c_f = \text{roughness coefficient}$$

$$= f_{DW}/8 = g/C_h^2$$

$$\text{with } f_{DW} = \text{Darcy-Weisbach friction factor}$$

$$\text{and } C_h = \text{Chezy friction coefficient}$$

$$= 18 \log_{10} (12d/r) \text{ according to Swart (1976b). Swart's method to evaluate the bottom roughness } r \text{ in terms of the ripple characteristics (if any) was used in determining } C_h \text{ and thus } c_f.$$

To distinguish between spilling and plunging breakers, the method by Galvin (1968) was applied.

For spilling breakers and a rectangular longshore current velocity distribution through the surf zone

$$s_c = \varepsilon^3 \sin \theta_b / (1,78\, A_c)$$

$$\text{where } \varepsilon = \text{a velocity ratio}$$

$$= v / (C_b \sin \theta_b)$$

$$\text{with } v = \text{longshore current velocity}$$

and $C_b =$ wave celerity at the breakerline

ϵ is obtained from

$$3,44 A_c = \epsilon^2 / (1,07 - \epsilon)$$

(choose the positive root as the solution for ϵ).

For plunging breakers, Castanho gives

$$1,290 A_c = \epsilon^2 / (1,3 - \epsilon)$$

(In the process $b/m = 0,75$ and $C_p = 1,3$ - in Castanho's notation - have been used). The expressions for ϵ and s_c given by Sayao and Kamphuis (1983) for plunging breakers are incorrect.

The formula by Dean (1973) is given by

$$S = GfP_L \quad (C10)$$

where G in metric units (Schoonees, 1997) is:

$$G = \frac{2,9278 \cdot 10^7 K_4 (\gamma / 2)^{0,5} H_{bs}^{0,5} \tan \alpha \cos \theta_b}{C_{LH} g^{0,5} \rho (\rho_s / \rho - 1) (1 - p) w}$$

where $\gamma =$ breaker index (H_{bs}/d_b)

$C_{LH} =$ bottom friction coefficient by Longuet-Higgins (1970).

Dean (1973) obtained a preliminary value for $K_4 (= 0,00196)$ by equating his formula with the early version (1966) of the SPM formula at a specific point. The newer version of the SPM formula (U.S. Army, Corps of Engineers, 1984) predicts 82,5 % higher transport rates than before (Sayao and Kamphuis, 1983) because only prototype data were considered in its derivation. Consequently, the new rough estimate of K_4 for the case given by Dean (1973), is 0,00358. This value has been used for K_4 .

Walton and Chiu (1979a) presented the following formula for the bulk transport rate:

$$I_l = K_5 \chi P_L f$$

where $K_5 =$ 4,24 for prototype cases

$=$ 2,82 for model applications

and

$$\chi = \frac{\gamma(1 - K_{wc}) \tan \alpha}{f_w} \left(\frac{e_b \sin 2 \theta_b}{2 \tan \theta} + \frac{e_s L_b \cos \theta_b}{w T_p} \right)$$

$$\text{where } K_{wc} = \frac{\gamma^2 (3 - 2 \sin^2 \theta_b)}{8 + \gamma^2 (3 - 2 \sin^2 \theta_b)}$$

f_w = friction factor by Jonsson (1966)

e_b = bedload efficiency factor

e_s = suspended load efficiency factor

Walton and Chiu used the following values:

$$f_w = 0,02; \quad \tan \theta = 0,63; \quad \text{and} \quad \gamma = 0,8$$

Then

$$S = \frac{31\,557\,600\, I_t f}{(\rho_s - \rho) g (1 - p)} \quad (C11)$$

To determine e_b , Walton and Chiu used the graph of e_b versus the velocity by Bagnold (1966). The velocity is supposed to be half of the longshore current velocity at the breaker line (v_b) as is implied in the text. Curve fitting which was done to program the relationship, yielded:

$$e_b = \exp \left(m \ln \left(\frac{v_b / 2}{0,3048} \right) + c \right)$$

$$\text{where } m = 0,039 - 61,90 D_{50}$$

$$\text{and } c = -2,003 - 0,03 \ln (1\,000 D_{50})$$

with D_{50} in m and v_b in m/s.

In order to calculate e_s , the vertical sediment mixing coefficient (ϵ_s), the bottom reference concentration (C_o) and the mean concentration over depth (C_m) are needed. Walton and Chiu (1979a) gave an expression for ϵ_s in terms of the wave height and water depth. It has been assumed that the wave height equal to ($H_{bs}/2$) and a depth of half of d_b should be used. Their equation in metric units are

$$\epsilon_s = 8,547 \cdot 10^{-4} (H_{bs}/2)^{2,5} g^{0,5} / (0,5 d_b)$$

Walton and Chiu (1979a) gave only a graph (their Figure 4.10) to determine C_o in terms of, among others, the

wave height and water depth (variables H and d). They did not give an indication of where H and d should be evaluated. However, Walton and Chiu (1979b) stated that mean values of these variables across the surf zone should be used. Consequently, $H_{bs}/2$ and $d_b/2$ have been used for H and d . The equation for C_o was determined to be (from their graph)

$$C_o = 4,196 \cdot 10^{-4} (H^2 g / w^2 d) - 1,071$$

with $H = H_{bs}/2$ and $d = d_b/2$

Similarly, $d = d_b/2$ in the following equation for C_m :

$$C_m = C_o (1 - e^{-wd/e_s}) e_s / (wd)$$

Finally,

$$e_s = \frac{16 C_m w (\rho_s - \rho) T_p}{5 \rho_s \gamma^2 n L \cos \theta (1 - K_{wc}) \tan \alpha}$$

where according to Walton and Chiu (1979b), n , L and θ are the respective values at the breakerline.

Walton and Chiu (1979a) also derived a relationship for the local immersed weight longshore transport rate (i_l):

$$i_l = \frac{e_b \rho \gamma f_w L_b X^{0.5} v^2}{2 \tan \theta \cdot T_p \pi} + \frac{5 e_s \gamma^2 \rho g L_b d_b (1 - K_{wc}) \tan \alpha \cos \theta_b X^{1.5} v}{16 w T_p} \quad (C12)$$

where v = local longshore current velocity

X = x/x_b

with x = horizontal distance from the shoreline (still-water level).

x_b = surf-zone width.

(e_b , e_s , γ , $\tan \theta$, f_w , w and K_{wc} are the same as for the bulk transport rate). In the second term in Eq. (C12), it has been assumed that $\theta = \theta_b$ in $\cos \theta_b$. To derive equations for v , Walton and Chiu (1979a) followed the general approach by Longuet-Higgins (1970) but also took wave set-up into account. These are not repeated here; the relevant equations are (4.98), (4.100), (4.102) to (4.106) and (4.108) in Walton and Chiu (1979a). However, there is a typing error in their Eq. (4.108):

$$v = v_b \left(\frac{10}{49} X^{-2.5} \right) \text{ for } 1 < X \leq \infty$$

$$\text{and not } v = v_b \left(\frac{10}{49} X - 2.5 \right)$$

The first Hou, Lee and Lin (1980) formula is

$$I_{11} = 0.55 f P_{lrms}$$

and

$$S = \frac{31\,557\,600\,I_{11}}{(\rho_s - \rho)(1 - p)g} \quad (C13)$$

It has been assumed that the mean wave period used by Hou *et al.* (1980) is equal to T_z , the zero-crossing wave period. Their second formula is (in mks units):

$$I_{12} = 0.3428 f P_{lrms}^{1.0695}$$

and

$$S = \frac{31\,557\,600 \cdot I_{12}}{(\rho_s - \rho)(1 - p)g} \quad (C14)$$

Hallermeier (1982) derived two expressions for the total immersed weight longshore transport rate, namely, based on "bedload" (denoted by subscript AB) and "wave thrust" (denoted by subscript AW) considerations. Generally speaking, his relationships are:

$$I_l = m I_{AP}^n$$

where I_{AP} is either I_{AB} or I_{AW} .

and m and n are coefficients.

$$\text{Again } S = \frac{31\,577\,600\,I_l f}{(\rho_s - \rho)(1 - p)g} \quad (C15)$$

$$I_{AB} = \rho g (1 - p) H_e^{2.5} (1 + R_a)^3 \left(\frac{D_{50} \cdot \rho}{\rho_s - \rho} \right)^{0.5} \left(\frac{2\pi \sin \theta_e}{T_p \tan \alpha} \right) B$$

with d_e = an empirical maximum water depth for intense agitation of a sandy bed
 H_e = incident wave height according to linear wave shoaling at depth (d_e). (Significant wave height and T_p were used.)
 θ_e = wave direction at depth d_e
 R_a = reflection coefficient

$$= \frac{0,1 L_e \tan^2 \alpha}{H_e \cos \theta_e} = 0,1 \xi_e^2$$

where L_e = wavelength at depth d_e
 ξ_e = surf similarity parameter evaluated at depth d_e .

$$= \frac{\tan \alpha}{(H_e \cos \theta_e / L_e)^{0.5}}$$

$$B = 3 z^{-0.5} \left\{ \cos^{1.5} \theta_e \left[(4z^{0.6} - 4) + 15 \sin^2 \theta_e (1 - z^{-0.2}) \right] + z^{0.6} \right\}$$

and z is the following factor:

$$z = d_e / H_e$$

An iterative procedure based on Equations (A2) and (A3) of Hallermeier (1982) was used to calculate d_e , H_e and L_e .

For the second formula

$$I_{AW} = P_{ls}$$

Based on 57 laboratory tests which complied with certain criteria, Hallermeier then determined values for m and n for both I_{AB} and I_{AW} . The exponent n was found to be almost constant but m varied with ξ_e . Hallermeier, however, did not attempt to relate m to ξ_e . When this was done (in this study), significant improvements were found. The relationships obtained, were:

"Bedload" considerations (I_{AB}):

$$n = 0,79$$

$$m = 1,008 \xi_e$$

$$R^2 \text{ improved from } 0,49 \text{ to } 0,83$$

"Wave thrust" consideration (I_{AW}):

$$n = 0,93$$

$$m = 0,314 \xi_e + 0,044$$

$$R^2 \text{ increased from } 0,87 \text{ to } 0,95$$

(R^2 = coefficient of determination; values of n as given by Hallermeier).

Figures C1a and b show how the equations fit the data.

Bailard (1981, 1985) also developed a local longshore transport model; see under the SPM formula for his version for the bulk sediment transport rate. He simplified the formula for the local longshore current velocity given by Ostendorf and Madsen (1979) and used the values of 0,60 and 1,25 for the velocity moments u^*_3 and u^*_5 , respectively (Bailard, 1982). The relevant expressions for the longshore current velocity are Equations 13 to 21 in Bailard (1985). His Equation (22), a long and complicated formula, gives the local immersed weight transport rate.

Chadwick (1989) measured shingle transport in the field and presented three longshore transport predictors. His first formula is:

$$S = \frac{31\,557\,600\,K_6\,(P_{lrms} - P_o)}{(\rho_s - \rho)\,g\,(1 - p)} \quad (C16)$$

$$\text{with } K_6 = 0,0384$$

$$\text{and } P_o = \text{threshold value of } P_{lrms}$$

$$= 12,2$$

The second expression, an adaptation of the work by Van Hijum and Pilarczyk (1982) is:

$$Q_2 = 0,0013\,g\,D_{90}^2\,T_s\,W\,(W - 8,3)\,\sin\theta_b$$

$$(\text{m}^3/\text{s})$$

where Q_2 is the longshore transport rate; no transport if $W < 8,3$.

$$W = (H_{br} \cos^{0,5}\theta_b) / D_{90}$$

$$\text{Therefore } S = 31\,557\,600\,f\,Q_2 \quad (C17)$$

For the third expression, Chadwick (1989) modified the work by Brampton and Motyka (1984) to obtain:

$$Q_3 = \frac{K_7 P_{lrms} (1 - 8,1 D_{90} / H_{bs})}{(\rho_s - \rho) g (1 - p)}$$

(m³/s)with $K_7 = 0,0696$ If $8,1 D_{90}/H_{bs} \geq 1$, no transport occurs.Again $S = 31\,557\,600 f Q_3$ (C18)

C.3 Shear Stress (Modified Steady Flow) Approach

Iwagaki and Sawaragi (1962) adapted the Kalinske - Brown bedload formula (Rouse, 1950) and obtained the following equation for the total and bulk longshore transport rate:

$$S = \frac{8,583 \cdot 10^8 H_{bs}^{2/3} (\tan \alpha)^{4/3} T_z^{1/6} \cos \theta_b P_{ls}^{1,5}}{g^{5/3} (\rho_s - \rho)^{1,5} D_{50}^{0,5} (\sin 2 \theta_b)^{1/6} L_b^{1,5}} \quad (C19)$$

having assumed $H_{bs} = H'_{os}$ (as Iwagaki and Sawaragi did; H'_{os} = equivalent unrefracted deep-water significant wave height) and that the median grain size (D_{50}) = mean grain size.)

Bijker (1967) modified the bedload formula by Frijlink (1952) by introducing the average bed shear stress due to combined wave and current action instead of the bed shear stress because of current action alone. He gave the local bedload rate (S_{bl}) as:

$$S_{bl} = \frac{5 D_{50} \nu g^{0,5}}{C_h} \exp \left(\frac{-0,27 (\rho_s - \rho) D_{50} C_h^2}{\rho \mu \nu^2 (1 + 0,5 \{ \xi_{BK} u_o / \nu \}^2)} \right)$$

where μ = ripple coefficient

$$= (C_h / C_{D90})^{1,5}$$

and $C_{D90} = 18 \log_{10} (12d/D_{90})$; u_o = maximum orbital velocity at the bed according to linear theoryand ξ_{BK} = coefficient with two values, namely, ξ_1 and ξ_2

$$\xi_1 = 0,0575 C_h \text{ (Bijker 1967, 1971a and b)}$$

and $\xi_2 = C_h (f_w / (2g))^{0,5}$ (Swart, 1976b)

Similarly, two values of the bottom roughness r have been used to obtain C_{h1} and C_{h2} . For C_{h1} , $r = 2,5 D_{50}$ according to Nielsen (1979) and for C_{h2} , the method by Swart (1976b) has been applied for r in:

$$C_h = 18 \log_{10} (12 d/r)$$

Komar's (1975) longshore current velocity model with $C_{LH} = 0,0175$ (= friction factor by Longuet-Higgins, 1970) was utilized to compute the longshore current velocity v .

Bijker (1967) proceeded by utilizing the Einstein approach to get the local suspended load rate (s_{si}):

$$s_{si} = 1,83 s_{bi} \left[I_1 \ln (33d/r) + I_2 \right] \quad (C20)$$

where I_1 and I_2 are the Einstein integrals. These were numerically integrated to minimize calculation errors by following the approach by Nakato (1984).

Thus the total, local longshore transport rate (s_{ti}) is:

$$s_{ti} = (s_{bi} + s_{si}) f$$

(m³/s per m)

$$\text{or } s_{ti} = 31\,557\,600 f (s_{bi} + s_{si})$$

(m³/year per m)

Swart (1976b) adapted the England and Hansen (1967) formula in a manner similar to Bijker modifying Frijlink's equation. The **Engelund, Hansen and Swart formula** for the total, local longshore transport rate thus obtained, is (Swart and Fleming, 1980):

$$s_{ti} = \frac{0,05 v C_h (\tau_{wc} / \rho)^2 \rho f}{g^{2,5} D_{50} (\rho_s - \rho)} \quad (C21)$$

(m³/s per m)

with τ_{wc} = bed shear stress due to waves and current (Bijker, 1967)

ξ_2 and C_h were applied as for the Bijker formula using the bottom roughness r from the Swart (1976b) method. C_h is recalculated at each depth and not just at the breakerline. The longshore current velocity from the Komar (1975) approach was used in which $C_{LH} = 0,0175$.

Swart (1976b), Willis (1978, 1979), Van de Graaff and Van Overeem (1979) and Swart and Fleming (1980) presented different versions of how the Ackers and White (1973) formula for fluvial sediment transport can be adapted for oscillatory flow. Two of these, the Willis method and the Swart and Lenhoff version (Swart and Fleming, 1980) will be used.

The Ackers, White and Willis formula for total, local longshore transport is given in Willis (1979) neatly summarized as a lengthy series of equations which is not repeated here. The equation for the calibration coefficient (W_c) is (Willis, 1979):

$$W_c^2 = 0,04141 D_{gr} + 0,20354$$

where D_{gr} = dimensionless grain size

The longshore current velocity computed with the Komar (1975) method ($C_{LH} = 0,0175$) was used.

The Ackers, White, Swart and Lenhoff formula which gives the total, local longshore transport rate, is described in Swart and Fleming (1980). The main aspects are the following (Swart and Fleming, 1980):

- An instantaneous mobility number and efficiency term are calculated and averaged over one wave period.
- Vector addition of the instantaneous velocity and shear stress at the bed is carried out.
- A new critical mobility number was determined (see also Lenhoff, 1982).

The extensive set of equations given in Swart and Fleming (1980) is not repeated here. The longshore current velocity by the same authors was applied.

Sawaragi and Deguchi (1978) related the total local longshore sediment transport rate to a factor F , called the "non-dimensional force of the sediment transport". F is related to the excess shear stress as follows:

$$F = \frac{u_*^2 - u_{*c}^2}{(\rho_s / \rho - 1) g D_{50}}$$

(Note: In the definition of F in Sawaragi and Deguchi (1978) the density factor ρ_s / ρ is incorrect. The version in their Figure 14 is correct as confirmed by Horikawa, 1988).

where u_* = shear velocity

$$= (\tau_m / \rho)^{0.5}$$

with τ_m = bottom shear stress

$$= \left\{ \left(\frac{v}{2 u_{bm} \cos \theta_b} + \tan \theta_b \right)^2 + 1 \right\}^{0,5} \tau_{ym}$$

$$\text{and } \tau_{ym} = 0,5 f_w \rho u_{bm}^2$$

$$u_{bm} = \text{"the maximum water particle velocity by waves" (Sawaragi and Deguchi, 1978)}$$

$$= \{ g (d + H) \}^{0,5} H / (2d)$$

$$u_{*c} = \text{critical bottom shear stress as given by Iwagaki in 1956 for sediment movement in open channels. His empirical set of equations is contained in Sawaragi and Deguchi (1978); it is important to note that } D_{50} \text{ in these equations must be in cm, thus necessitating transforming } u_{*c} \text{ to mks units as well.}$$

It has been assumed that no refraction takes place in the surf zone so that the wave incidence angle is θ_b everywhere in the surf zone.

Sawaragi and Deguchi (1978) used the Riedel *et al.* (1972) method to determine $f_w (=2f_y; f_y$ used by Sawaragi and Deguchi):

$$f_w = 0,25 (a_o/r)^{-0,77} \text{ for } 0,1 < a_o/r \leq 25 \quad (4.44)$$

$$\text{with } a_o = \text{amplitude of the orbital excursion at the bed obtained from linear theory.}$$

To eliminate an iterative solution to the Riedel *et al.* (1972) equation for $a_o/r > 25$, a curve was fitted through points obtained from it. A very good fit resulted (Figure C2) in the expression:

$$f_w = 0,1 \exp \left\{ -1,443 + 4,616 (a_o / r)^{-0,2175} \right\}$$

$$\text{for } a_o/r > 25$$

Sawaragi and Deguchi do not specify how to determine the bottom roughness r . This variable was assumed to be equal to $2,5 D_{50}$ (Nielsen, 1979).

The longshore transport rate (q) is then given by:

$$q = v D_{50} 86 F^{3,7} \quad \text{for } F \geq 0,3$$

$$(\text{m}^3/\text{s per m})$$

$$\begin{aligned}
 &= v D_{50} 23 F^{4.5} \quad \text{for } F < 0,3 \\
 \text{and } s &= 31\,557\,600 f q \\
 &(\text{m}^3/\text{year per m})
 \end{aligned} \tag{C22}$$

This local rate is integrated across the surf zone and beyond.

Sawaragi and Deguchi (1978) applied the longshore current velocity as predicted by the Longuet-Higgins (1970) method with a lateral mixing factor $P = 0,4$, $C_{LH} = 0,01$ and $\alpha = 0,41$ and using the significant breaker wave height as the wave height parameter.

Madsen (1978) gave a total, local longshore transport rate based on the Shields number as:

$$q = 1,7 w D_{50} \left(\frac{f_{wc}}{g (\rho_s / \rho - 1) D_{50}} \right)^3 u_b^5 v$$

$$\begin{aligned}
 \text{where } u_b &= \text{"maximum orbital velocity associated with the wave motion as a function of distance} \\
 &\quad \text{from the shore" (Madsen, 1978)} \\
 &= 0,4 (gd)^{0,5} \\
 f_{wc} &= \text{friction factor} \\
 &= 0,02
 \end{aligned}$$

$$\begin{aligned}
 \text{Then } s_i &= 31\,557\,600 f q \text{ (m}^3/\text{year per m)}, \text{ which is integrated across the surf zone and beyond.} \\
 &\tag{C23}
 \end{aligned}$$

It was assumed that the representative grain size is D_{50} . Furthermore, as in the example calculations by Madsen, the breakerline corresponding to the root-mean-square wave height was used. He assumed that no longshore transport occurs outside the surf zone because he integrates only from the shoreline up to the breakerline and then compared the calculated value to the total, bulk transport rate measured. The Longuet-Higgins (1970) longshore current velocity method is employed with a lateral mixing factor P of 0,25.

Ostendorf and Madsen (1979) proposed a "linear longshore sediment transport model" based on their "linear longshore current model." They assumed that the transport rate is a function of the Shields number. If Q (kg/s) is their total bulk longshore transport rate then

$$S = \frac{31\,557\,600 Q f}{(1 - p) \rho_s} \tag{C24}$$

Q can be calculated from a long series of equations such as their Equations (4-60), (4-61), (4-72), (4-74), (4-75). Ostendorf and Madsen (1979) found that their calibration constant $\zeta = 660$ which fitted laboratory data reasonably. Because field data are overpredicted by a factor 5 (Ostendorf and Madsen, 1979), $\zeta = 660/5 = 132$ was used. In addition, their λ_1 was taken to be 1, thus assuming no shore-normal groyne. The wave characteristics at the breakerline read into the computer program were refracted out to 20 m water depth using Snell's law whereafter a new breakerline was determined using the empirical breaking criterion combined with non-linear wave theory by Ostendorf and Madsen (1979). The bottom roughness was taken as D_{50} in accordance with Ostendorf and Madsen. Their linear longshore current velocity model represented by their Equations (3-76), (4-37) and (4-49), was used.

C.4 Approach Using the Product of the Shear Stress and the Longshore Current Velocity

Watanabe (1985), Watanabe *et al.* in Horikawa (1988) and Watanabe *et al.* (1991) treated sediment transport due to wave and current action by considering transport by waves (in the direction of the waves) and by a mean current. The latter, can be regarded as being the longshore transport (Horikawa, 1988) if the mean current is assumed to be the longshore current velocity. The **Watanabe formula** for total, local transport is:

$$q_c = A_c v (\tau - \tau_c) / (\rho g)$$

$$\text{and } s_i = 31\,557\,600 f q_c \quad (C25)$$

(m³/year per m)

$$\text{with } A_c = 0,5 \text{ for model applications (Watanabe, 1985).}$$

$$= 2,0 \text{ for prototype cases (Watanabe et al., 1991)}$$

$$\tau = \text{maximum shear stress at the bottom}$$

and f_w evaluated by means of the Tanaka and Shuto (1981) method and taking the bottom roughness $r = D_{50}$.

$$\tau_c = \text{critical shear stress}$$

$$\text{with } \tau_c = 0 \text{ in the surf zone}$$

$$= (\rho_s - \rho) g D_{50} \psi_c \tanh^2 (K_c (x - x_b) / x_b)$$

outside the surf zone

$$\text{and } K_c = 1,0$$

$$\psi_c = \text{factor different for fine to coarse sand}$$

$$\text{where } \delta_L = \text{represents the thickness of the oscillatory boundary layer}$$

and assuming D_{50} is the relevant grain size. The bulk transport rate is obtained by integrating the local rate across the surf zone and beyond.

Bodge (1986) was particularly interested in the cross-shore distribution of the longshore sediment transport. He evaluated a number of total, local transport models by comparing these against his field and laboratory data.

The **Bodge formula** require considerable computations as is described in detail in Chapter 9 in Bodge (1986). It is necessary to calculate the profile characteristics (such as x_m), the wave set-up and set-down, the slope of the mean water level and of $H^2 d^{0.5}$, the cross-shore variation of wave height and the longshore current velocity (Bodge, 1986). The most important relationships are his Equations (9.13), (9.14) and (9.27) to (9.30). (Note: the d contained in his Equation (9.13) should be omitted; it is a typing error). The following values were used in the computations:

$$\begin{aligned}\gamma &= 0,8 \\ c_f &= 0,10 \text{ (Bodge gave a range of 0,05 to 0,15)} \\ k_3 &= \text{coefficient in his Equation (9.28)} \\ &= 0,057 \text{ s for model applications} \\ &= 0,48 \text{ s for prototype cases (Bodge, 1986)}\end{aligned}$$

In addition, the equation for A given by Dean (1987) has been modified to be in mks units:

$$A = 0,5082 w^{0.44}$$

The equations for the longshore current velocity (v) given by Bodge are only valid if $x_m < x_b$. Outside this range, that is, $x_m > x_b$, one has a planar beach slope. In these cases, the Komar (1975) method has been used for v with $C_{LH} = 0,0175$.

Finally, it should be noted that Bodge assumed that all longshore transport occurs only in the surf zone.

Kraus *et al.* (1988) analysed sediment transport measurements taken in a cross-flow tank by Katori *et al.* (1984) and data from the SUPERDUCK experiment. Following Katori *et al.*, the **Kraus, Gingerich and Rosati total, local formula 3** is:

$$s_i = 31\,557\,600 \Phi w D_{50} f \quad (C26)$$

($\text{m}^3/\text{year per m}$)

$$\begin{aligned}\text{with } \Phi &= \text{"dimensionless flow power"} \\ &= 0,85 S_h^{1.1}\end{aligned}$$

$$\text{and } S_h = \frac{(\tau_m - \tau_c) v}{\rho [(\rho_s - \rho) g D_{50} / \rho]^{1.5}}$$

$$\tau_m = 0,5 f_w \rho (u_o^2 + v^2)$$

where u_o is calculated with the local root-mean-square wave height according to linear theory.

In order to compute f_w with the explicit formula by Swart (1974), it was assumed that the bottom roughness is equal to $2,5 D_{50}$ (Engelund and Hansen, 1967 and Nielsen, 1979). The Komar (1975) method with $C_{LH} = 0,0175$ was used for the longshore current velocity. Integration was done across the surf zone and beyond to obtain the bulk transport rate.

Morfett (1990) derived a bulk longshore transport formula for both sand and gravel by considering the "virtual" wave power. The expression is:

$$\begin{aligned} I_l &= 10\,500 P_* D_* & (C27) \\ \text{and } P_* &= P (\sin \theta_b)^{0,75} \\ P &= \text{"virtual" wave power} \\ &= P_+^{1,5} g^{-0,833} (\rho_s - \rho)^{-0,5} u^{0,75} \end{aligned}$$

$$\text{with } P_+ = \rho (u_+^3 - u_{+cr}^3)$$

$$\begin{aligned} \text{and } u_+ &= \text{dissipation velocity} \\ &= (D_T/\rho)^{0,333} \\ D_T &= \text{total rate of energy dissipation per unit area} \\ &= D_B + D_F \end{aligned}$$

where subscript B denotes "due to wave breaking" and subscript F is "due to bed shear stress"

$$u_{+cr} = \text{critical dissipation velocity}$$

Morfett (1990) used:

$$D_F = \rho C_w u_0^3$$

where his $C_w = \delta C$ from O'Connor and Yoo (1988) (Morfett, pers. comm., 1990) as determined in the latter reference. He adapted the equation by O'Connor and Yoo (1987) to obtain

$$D_B = \rho g C_{bD} H_{bs}^3 / 8$$

with C_{bD} determined from Equation (5) in Morfett (1990) with the factors $K_D = 1,3$ and $m = 0,33$ and his $T_D = T_z$ where there are no currents (Morfett, pers. comm., 1990).

Morfett distinguished between sand and gravel to determine incipient motion criteria and u_{+cr} . For the gravel he gives a simple expression (it was assumed that $D_{50} > 2$ mm for gravel according to US Army, Corps of Engineers, 1984). To determine the equivalent value for sand, he (Morfett, pers. comm, 1990) proposed the bottom roughness stipulated by Van Rijn (1989), using the relationships for the Shield curve by Van Rijn

(1984) and the drag coefficient (C_D) by Morsi and Alexander (1972). (It was assumed that $C_D = 0,488$ for Reynolds numbers greater than 50 000.)

C.5 Approach Using Dimensional Analysis

The Kamphuis, Davies, Nairn and Sayao (1986) bulk formula is given by:

$$Q = 1,28 \tan \alpha_K H_{bs}^{3,5} \sin 2 \theta_b / D_{50}$$

with Q = longshore transport rate in kg/s

$\tan \alpha_K$ = beach slope, defined by d_b/x_b

$$\text{Thus } S = \frac{31\,557\,600\,Q}{\rho_s (1 - p)} \quad (C28)$$

Sánchez-Arcilla *et al.* (1988) also used dimensional analysis and derived the following expressions (the Sánchez-Arcilla, Vidoar and Pous bulk formula):

$$I_t = 0,5 (\rho_s - \rho) A_s \xi^{0,5222} 10^{-0,1908\xi} H_{bs}^{2,5} \sin 2 \theta_b g^{1,5} \cdot (S_h^c - S_{hcr}^c)$$

$$\text{and } S = \frac{31\,557\,600\,I_t f}{(\rho_s - \rho) g (1 - p)} \quad (C29)$$

where according to Sánchez-Arcilla, pers. comm., (1990) :

A_s = coefficient = $4,88 \cdot 10^{-3}$

S_h = a version of the Shields parameter

$$= \rho H_{bs} / (\rho_s D_{50})$$

The exponent of ξ is 0,5222, not 0,5 and

c = 0,4419, not 0,44 as in Sanchez-Arcilla *et al.* (1988)

Furthermore, 0,5 is included as a factor on the right hand side of Equation (C29)

and the exponent of 10 is -0,1908 ξ , not -8 ξ as appeared in Sánchez-Arcilla *et al.* (1988).

The critical Shields parameter, S_{hcr} , = 12,77 (ξ is the surf similarity parameter or Iribarren number). It has been supposed that the significant wave height should be used.

Kamphuis (1990, 1991) presented the results of extensive model tests and calibrated a formula against these data and then tested it also against published field data. This resulted in:

$$Q = 1,3 \cdot 10^{-3} (\rho / T_p) L_o^{1,25} H_{bs}^2 (\tan \alpha_K)^{0,75} (1/D_{50})^{0,25} (\sin 2\theta_b)^{0,6}$$

(Q is the underwater mass transport rate in kg/s)

$$\text{and } S = \frac{31\,557\,600 f Q}{(1-p)(\rho_s - \rho)} \quad (C30)$$

L_o is calculated with T_p .

D.6 Approach Using the Suspended Sediment Concentration and the Longshore Current Velocity

Fleming (Fleming and Hunt (1976), Fleming (1977) and Swart and Fleming (1980)) developed a total, local longshore transport formula by integrating the product of the suspended sediment concentration (C) and longshore current velocity (v) over depth. He gave the following equations:

$$C(z) = 0,52 (C_o / 0,52)^{z/z_e} \text{ for } 0 \leq z \leq z_e$$

$$C = C_o \exp \left\{ J_m (1 - (z/z_e)^{0,75}) \right\} \text{ for } z_e < z \leq d$$

where C_o = bottom reference concentration
 z_e = small specified height above the bed.

The variation with distance from the bed of the longshore current velocity was assumed to be:

$$v(z) = (8/7) v (z/d)^{1/7}$$

Fleming presented equations for C_o , J_m and z_e . The longshore current velocity by Swart and Fleming (1980) has been used.

In a similar development, Swart and Fleming (1980) applied the formulation of Nielsen *et al.* (1978) for the concentration together with their own longshore current velocity model (as explained for the Fleming formula) to get the **Nielsen formula**. The concentration is given by:

$$C(z) = C_o (1 / (1 + \sigma V))^{1/V}$$

with $V = (\text{variance of } w) / w_{50}^2$

and w_{50} = fall velocity of the median grain size

σ = parameter including the eddy diffusivity

Nielsen *et al.* (1978) and Nielsen (1979, 1985) gave expressions for C_o . Integration over the depth and across the surf zone and beyond was conducted.

Tsuchiya (1982) presented a bulk longshore transport formula:

$$S_T = C_1 (\rho / \rho_s) I_T d_b^{2,5} g^{0,5} \sin 2 \theta_b \quad (m^3/s)$$

where $C_1 = 5 \pi c_2 \alpha_T / (16 f_w)$

and $c_2 = 0,2$

$f_w = 0,3$

$\alpha_T = L_b H_{bs} / (2 T_p g d_b^{1,5})$

For prototype conditions:

$I_T = 0,3$

Therefore

$$S = 31\,557\,600 f S_T \quad (C31)$$

It has been assumed that the significant wave height and the peak wave period are the relevant wave characteristics.

Voitsekhovich (1986) presented his bulk formula in terms of the mean concentration and mean longshore current velocity in the surf zone:

$$Q = k_b v_{mean} C_{mean} w_e \quad (kg/s)$$

with $k_b =$ factor to incorporate bedload = 1,2

$v_{mean} =$ mean longshore current velocity in the surf zone

$C_{mean} =$ mean concentration in the surf zone

$w_e =$ cross-sectional area of the transport zone which extends up to a depth d_v (d_v is typically 1 to 1,5 d_b).

$$S = \frac{31\,557\,600 Q f}{(1 - p) \rho_s} \quad (C32)$$

Voitsekhovich gave the following equations for v_{mean} , C_{mean} and w_e :

$$V_{\text{mean}} = \frac{33,3 H_c^2 \sin 2 \theta_b}{T_z^2 (g d_{\text{mean}})^{0,5}}$$

where H_c = the characteristic wave height corresponding to a 10 % occurrence in the wave height distribution

$$= 1,072 H_{bs} \text{ (assuming a Rayleigh distribution)}$$

d_{mean} = mean depth from the shoreline to depth d_v

$$= 0,5 d_v \text{ if a planar beach is considered}$$

where d_v = $0,09 \gamma L_b$

$$\text{Further } C_{\text{mean}} = \frac{0,5 \cdot 10^{-4} \varepsilon H_c^2 (1 + \sin 2 \theta_b)}{d_{\text{mean}} T_z (g D_{50})^{0,5}}$$

where ε = $1,65 \cdot 10^3 \text{ kg/m}^3$ (Voitsekhovich, 1986)

$$w_e = \frac{0,4 \cdot 10^{-2} g d_b T_z^2}{k_w \tan \alpha \gamma^2} \quad (\text{assuming a planar beach})$$

with k_w = a profile factor

$$= d_v / (2 d_{\text{mean}})$$

$$= 1 \text{ if a planar beach is considered}$$

It has been assumed that the mean wave period is equal to T_z .

Deigaard *et al.* (1986) derived a detailed model for predicting the longshore transport rate. The Deigaard, Fredsøe and Hedegaard formula applied here is their schematized version as given by:

For $H_o/D_{50} < 3 \cdot 10^4$:

$$Q_s = Q_{s, \text{max}} \left((f(\theta_o)) \right)^{2,5} \quad (\text{grain volume/s})$$

$$\text{where } f(\theta_o) = \sin \left\{ 2 \theta_o \left[1 - 0,4 \frac{\theta_o}{90^\circ} \left(1 - \frac{\theta_o}{90^\circ} \right) \right] \right\}$$

with θ_o in degrees

$$\text{and } Q_{s,\max} = \Phi_o H_o \tan^{0,5} \alpha \left((\rho_s / \rho - 1) g D_{50}^3 \right)^{0,5}$$

$$\text{with } \Phi_o = \left(H_o / (10^4 D_{50}) \right)^{P_D} \cdot 1,8 \cdot 10^7 (H_o / L_o)^{0,42}$$

$$\begin{aligned} \text{and } P_D &= 2,79 + 0,069 \ln (H_o / L_o) \\ &\quad - 1,67 (1,46 + 0,187 \ln (H_o / L_o) - w_*)^2 \end{aligned}$$

$$w_* = w / (g D_{50})^{0,5}$$

For H_o and θ_o the equivalent deep-water wave characteristics H_{oe} (a significant wave height) and θ_{oe} were used (determined from H_{bs} and θ_b and assuming Snell's law).

Finally,

$$S = \frac{31\,557\,600 \cdot f \cdot Q_s}{(1 - p)} \quad (C33)$$

C.7 Empirical Formulae

The formula by Sauvage de Saint Marc, Vincent and Larras is based on early work by Sauvage de Saint Marc and Vincent (1954) and Larras (1957, 1961) - see also Delorme (1981). This formula is (Schoonees, 1997):

$$S = \frac{31\,557\,600 K_{10} g H_{os}^2 T_x f(\theta)}{(H_{os} / L_o)} \quad (C34)$$

where K_{10} = a dimensionless factor dependent on the grain size and the nature of the waves.

H_{os} = deep-water significant wave height

$f(\theta)$ = $\sin(7\theta_{15}/4)$ for $\theta_{15} < 25^\circ$

where θ_{15} = wave incidence angle at 15 m water depth

Two values for K_{10} have been used, namely, by Delorme (1981):

$$K_{10} = 1,8 \cdot 10^{-6} D_{50}^{-0,5} \text{ for } 0,2 \text{ mm} < D_{50} < 1,0 \text{ mm}$$

(assuming that D_{50} (in m) is the representative grain size).

and $K_{10} = 4 \cdot 10^{-6}$ for $0,15 \text{ mm} < D_{50} < 0,5 \text{ mm}$

H_{oe} has been used instead of H_{os} (H_{oe} was determined by assuming Snell's law together with H_{bs} and θ_b).

Larras and Bonnefille (1965), Larras (1966) and Bonnefille and Pernecker (1967) also investigated longshore transport. The Larras, Bonnefille and Pernecker formula is:

$$S = \frac{K_{11} f H_{os}^3}{T_z} f(\theta_o) \quad (C35)$$

having supposed H_{os} is the relevant deep-water wave height and T_z is the wave period to be used.

Two versions of the formula have been programmed, namely, firstly that due to Larras (1966) and, secondly, the version by Bonnefille and Pernecker (1967). Larras (1966) gave:

$$K_{11} = 0,00175 \left(\frac{3,5 \cdot 10^6 D_{50}}{10^{12} D_{50}^4 + 2} \right)^n$$

where $n = (11 - 100 H_{os}/L_o)/10$

(D_{50} is in m and H_{os}/L_o is dimensionless).

and $f(\theta_o) = \sin(7\theta_o/4)$

According to Bonnefille and Pernecker (1967), K_{11} can be found from a series of graphs provided that the grain size and the deep-water wave steepness are known. These graphs can be closely approximated (Figure C3a to h) by an equation of the form

$$K_{11} = (c/D_{50}) \exp \left[-0,5 \left(\frac{\log_{10} (1000 D_{50}) - b}{a} \right)^2 \right]$$

where a, b and c have the following values:

H_{os}/L_o	a	b	c
0,01	0,356	0,140	$1,956 \cdot 10^{-3}$
0,02	0,373	0,160	$0,459 \cdot 10^{-3}$
0,03	0,373	0,177	$0,207 \cdot 10^{-3}$
0,04	0,342	0,143	$0,128 \cdot 10^{-3}$
0,05	0,359	0,185	$0,078 \cdot 10^{-3}$
0,06	0,361	0,189	$0,056 \cdot 10^{-3}$
0,07	0,353	0,178	$0,039 \cdot 10^{-3}$
0,08*	0,360	0,201	$0,290 \cdot 10^{-4}$
0,09*	0,360	0,196	$0,200 \cdot 10^{-4}$
0,10*	0,360	0,200	$0,143 \cdot 10^{-4}$
0,11*	0,360	0,191	$0,913 \cdot 10^{-5}$
0,12*	0,360	0,196	$0,667 \cdot 10^{-5}$

* extrapolated values - see Figure C3a

In addition, (H_{os}/L_o) in prototype applications must be multiplied by 2,75 to obtain the corresponding $(H_{os}/L_o)_{model}$ (Bonnefille and Pernecker, 1967) to be used in the above equation for K_{11} . Also

$$f(\theta_o) = \frac{\sin(7\theta_o/4)}{\sin 35^\circ}$$

H_{oe} was used instead of H_{os} (H_{oe} was calculated by assuming Snell's law and using H_{bs} and θ_b).

The **Kraus, Isobe, Igarashi, Sasaki and Horikawa** bulk formula (Kraus *et al.*, 1982) is:

$$S = \frac{14990 H_{bs}^2 v_{mean} f}{\tan \alpha} \quad (C36)$$

where v_{mean} = mean longshore current velocity in the surf zone

and the constant $14990 = (31\,557\,600 \cdot 3,8 \cdot 10^{-4}) / 0,8$ where the breaker index was supposed to be equal to 0,8 as Kraus *et al.* (1982) did.

It was assumed the v_{mean} is equal to the longshore current velocity at the mid-surf position (v_m) according to Komar (1975):

$$v_m = 2,7 u_m \sin \theta_b \cos \theta_b$$

$$\text{with } u_m = \left(\frac{g H_{bs}^2}{4 d_b} \right)^{0,5}$$

Kraus *et al.* (1988) derived three empirical formulae based on longshore transport measurements taken during the DUCK85 and SUPERDUCK experiments. The first of the **Kraus, Gingerich and Rosati** formulae, is a bulk predictor:

$$1: I_l = 2,7 (R - R_c)$$

where R = the discharge parameter

$$= v_{mean} H_{brms} x_{brms}$$

where x_{brms} = width of the surf zone with the breakerline determined where H_{brms} breaks.

$$R_c = 3,9 \text{ m}^3/\text{s}$$

and

$$S = \frac{31\,557\,600 I_l}{(\rho_s - \rho) g (1 - p)} \quad (C37)$$

Again $v_{\text{mean}} = v_m$ according to Komar (1975) as was also done by Kraus *et al.* (1988).

The **second and third formulae** give total, local immersed weight longshore transport rates which have to be integrated to obtain bulk transport rates, namely,

$$2a : i = 2 \cdot 10^{-4} \left[\rho g H_{\text{rms}} v \left(1 + 20 \frac{dH}{dx} \right) - 770 \right] \quad (\text{kg/s per m})$$

where H_{rms} = the local root-mean-square wave height

and $\frac{dH}{dx}$ = local cross-shore gradient in wave height

$$\text{and } 2b : i = 1,5 \cdot 10^{-4} \left[\rho g H_{\text{rms}} v \left(1 + 20 \frac{dH}{dx} + 1,8 \frac{s_v}{v} \right) - 2400 \right] \quad (\text{kg/s per m})$$

with s_v = standard deviation of the longshore current velocity over an averaging interval.

s_v/v = 0,20 (assumed based on the mean of the two measured values of 0,02 and 0,37 given by Kraus *et al.*, 1988).

dH/dx was found by differentiating the empirical expression by Anderson and Fredsøe (1983) for the cross-shore variation of H through the surf zone:

$$H/d = 0,5 + 0,3 \exp \left(\frac{-0,11(x_b - x)}{x_b \tan \alpha} \right)$$

where x = distance from the (still-water) shoreline

x_b = width of the surf zone.

Van der Meer (1990) reanalysed the model results obtained by Van Hijum and Pilarczyk (1982) on shingle beaches and used the wave characteristics at the breakerline as the relevant parameters. He also adapted the SPM formula to extend the range of the formula to sandy beaches. His expressions are:

$$\text{For } P_v = H_{bs} / \left((\rho_s / \rho - 1) D_{n50} \right) > 50$$

$$S = 119\,919 H_{bs}^2 f C_o \sin 2 \theta_b \quad (\text{C38a})$$

For $10 \leq P_v \leq 50$:

$$S = 37\,869 \, g \, D_{n50} \, T_p \, H_{bs} \, v_v \, f \cos^{0.5} \theta_b \sin \theta_b \quad (\text{C38b})$$

For $P_v < 10$:

No equation available (later Van der Meer and Veldsman, 1992 produce an equation in this range; it was, however, not used)

where $119\,919 = 0,0038 \cdot 31\,557\,600$

C_o = wave celerity in deep water

$$= (gT_p) / (2\pi)$$

$37\,869 = 0,0012 \cdot 31\,557\,600$

and $D_{n50} = (M_{50} / \rho_s)^{1/3}$

with M_{50} = median mass of the grains

$$v_v = H_{bs} \cos^{0.5} \theta_b / D_{n50} - 11$$

(no transport occurs if $H_{bs} \cos^{0.5} \theta_b / D_{n50}$ is less than 11)

It has been assumed that Equation (C38b) is valid for $P_v = 10$ and $P_v = 50$.

C.8 Formulae Excluded from the Analysis

Apart from some early versions of the SPM formula that have been superseded and excluded (for example, Savage, 1962 and Das, 1972), the following models were not included:

- (1) Bajorunas (1960, 1970) - 2 formulae
- (2) Edelman (1963) - 2 formulae
- (3) Ijima, Sato, Aono and Ishi (in Horikawa, 1978)
- (4) Ijima, Sato and Tanaka (in Horikawa, 1978) - 2 formulae
- (5) Ichikawa, Ochiai, Tomita and Murobuse (in Horikawa, 1978)
- (6) Tsuchiya (1982), the local longshore sediment transport rate
- (7) McDougal and Hudspeth (1983) - 2 formulae
- (8) Deigaard *et al* (1986) - the detailed, local formula
- (9) Morfett (1991)
- (10) Oelerich (1990)

Schoonees (1997) critically evaluated the formulae numbered (1) to (5) above. He found that in the formulae by Bajorunas (1960, 1970), the objectivity of the choice of certain parameters in the derivation can be seriously

questioned. These formulae should therefore not be used. In the case of the Edelman expressions, it was found that one constant lacks a numerical value; furthermore, the expressions are almost similar to the SPM formula. Castanho (1966) used some of the Edelman concepts in the derivation of his equation (which is included).

Schoonees (1997) also showed that the Japanese formulations (numbers (3) - (5) above) generally apply to specific sites only because they were derived for sites with steep beach slopes, very coarse sediment and low waves. He therefore cautioned against using these equations in a general manner.

The formulation for local longshore transport by Tsuchiya (1982) is incomplete and can thus not be implemented.

The formulae numbered (7) to (10) above, require extensive computations in order to apply them. In addition, most of the elements of the approach contained in McDougal and Hudspeth (1983) are present in a number of the models that were included.



Figure 2.10: Predicted versus Measured (mmol). The plot shows the relationship between predicted and measured values for various parameters. The data points are scattered around the 1:1 line, indicating a good correlation between the predicted and measured values.

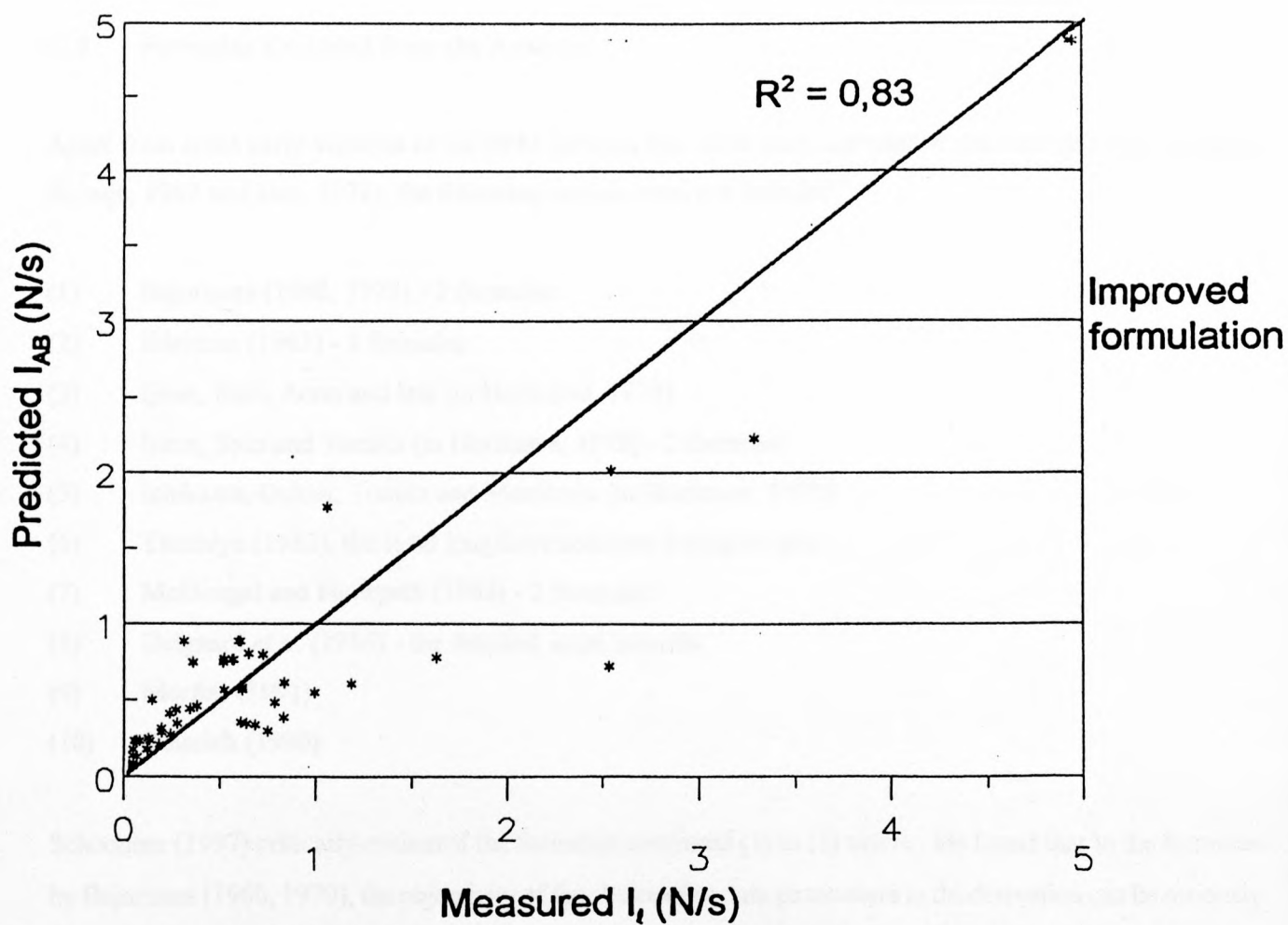
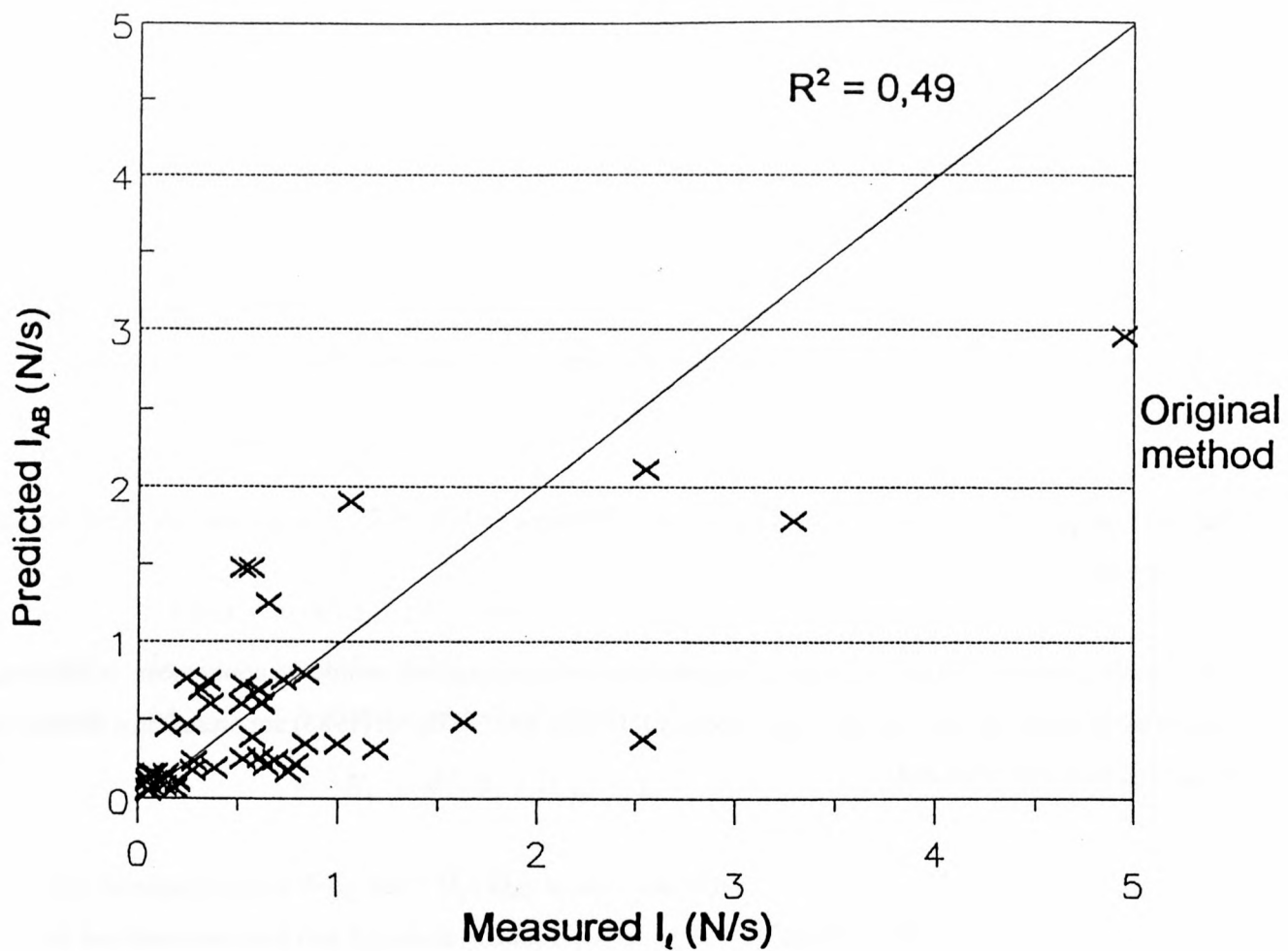


Figure C1a: Predicted immersed weight longshore transport rates (based on bedload) against measured rates (Hallermeier formula)

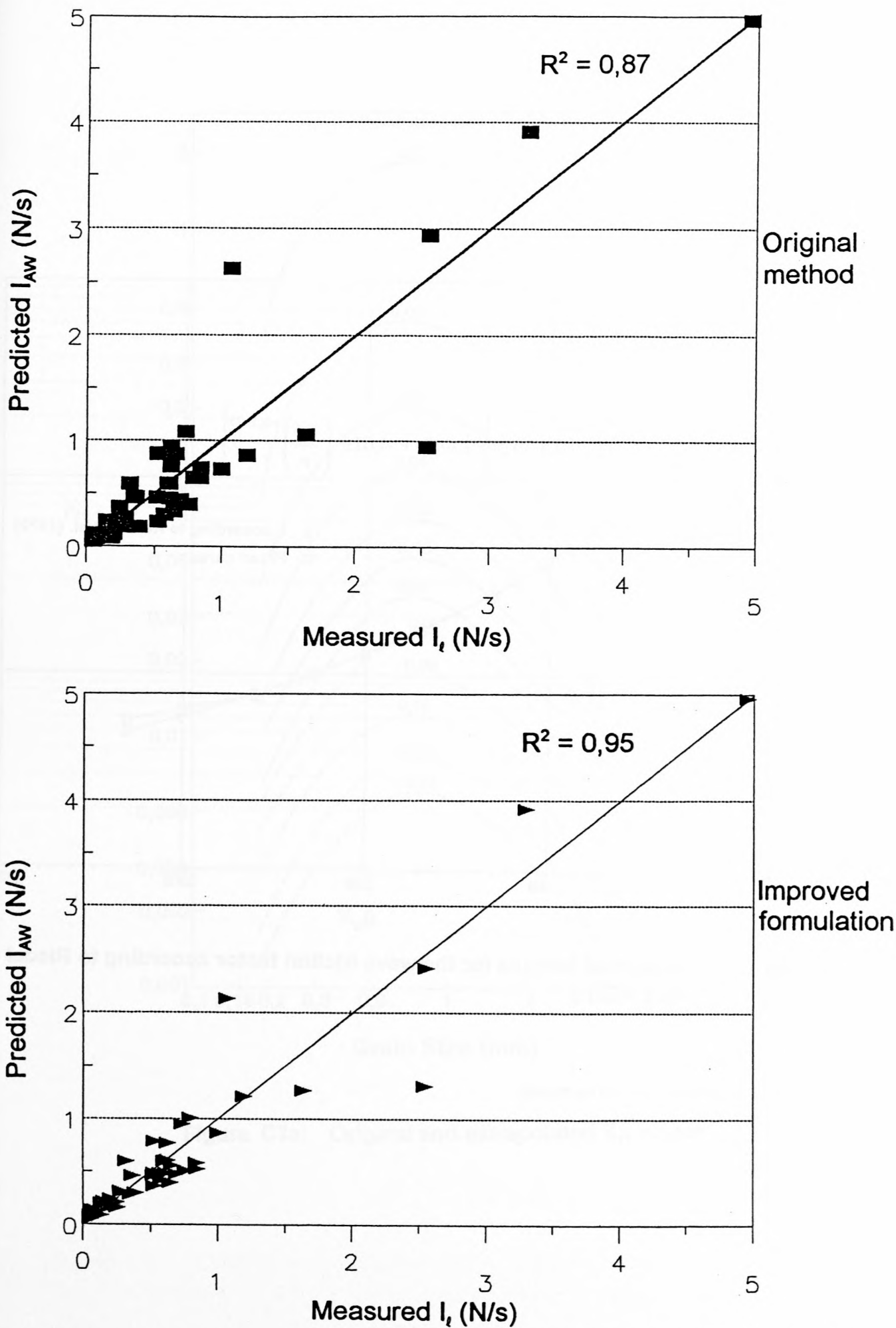


Figure C1b: Predicted immersed weight longshore transport rates (based on wave thrust) against measured rates (Hallermeier formula)

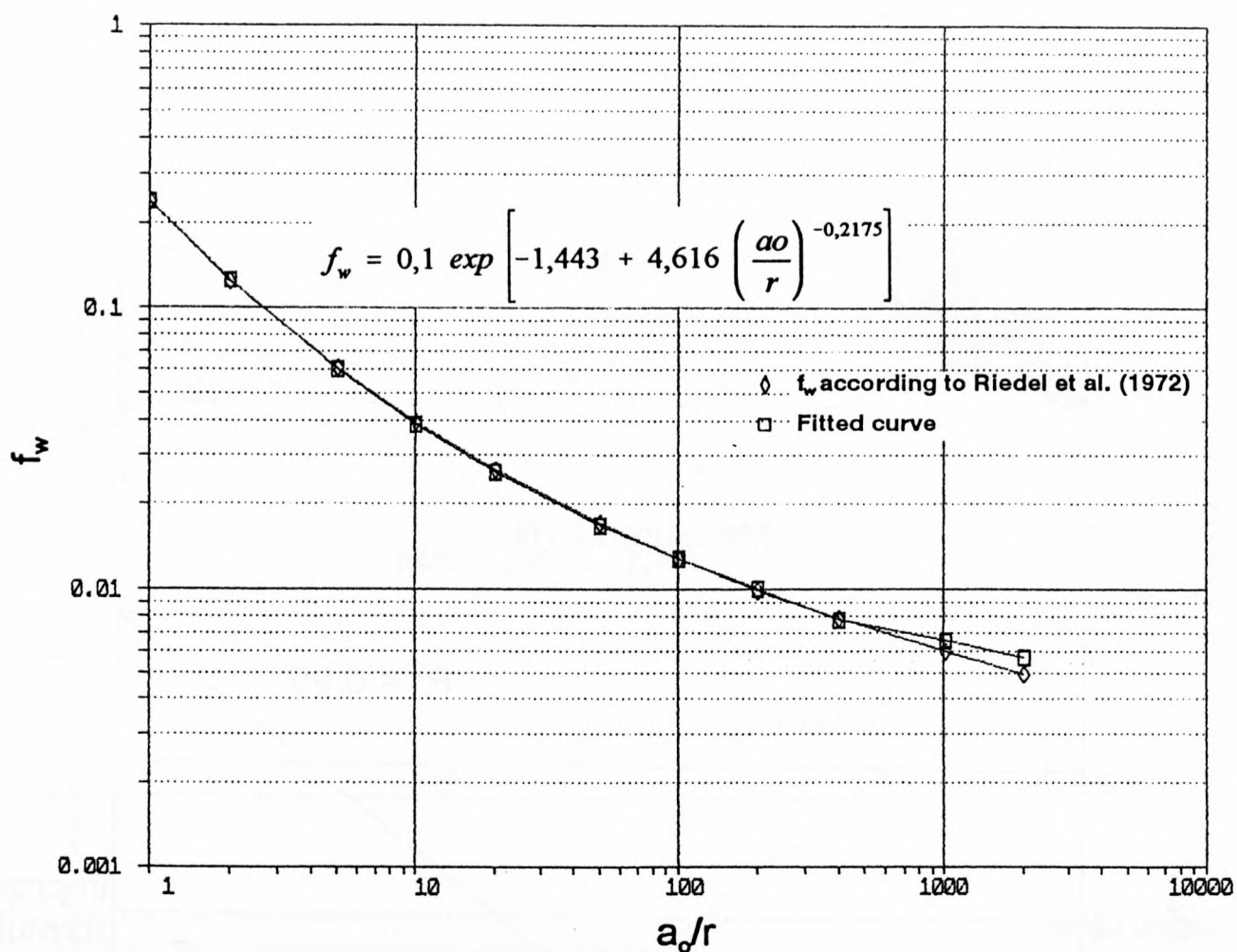
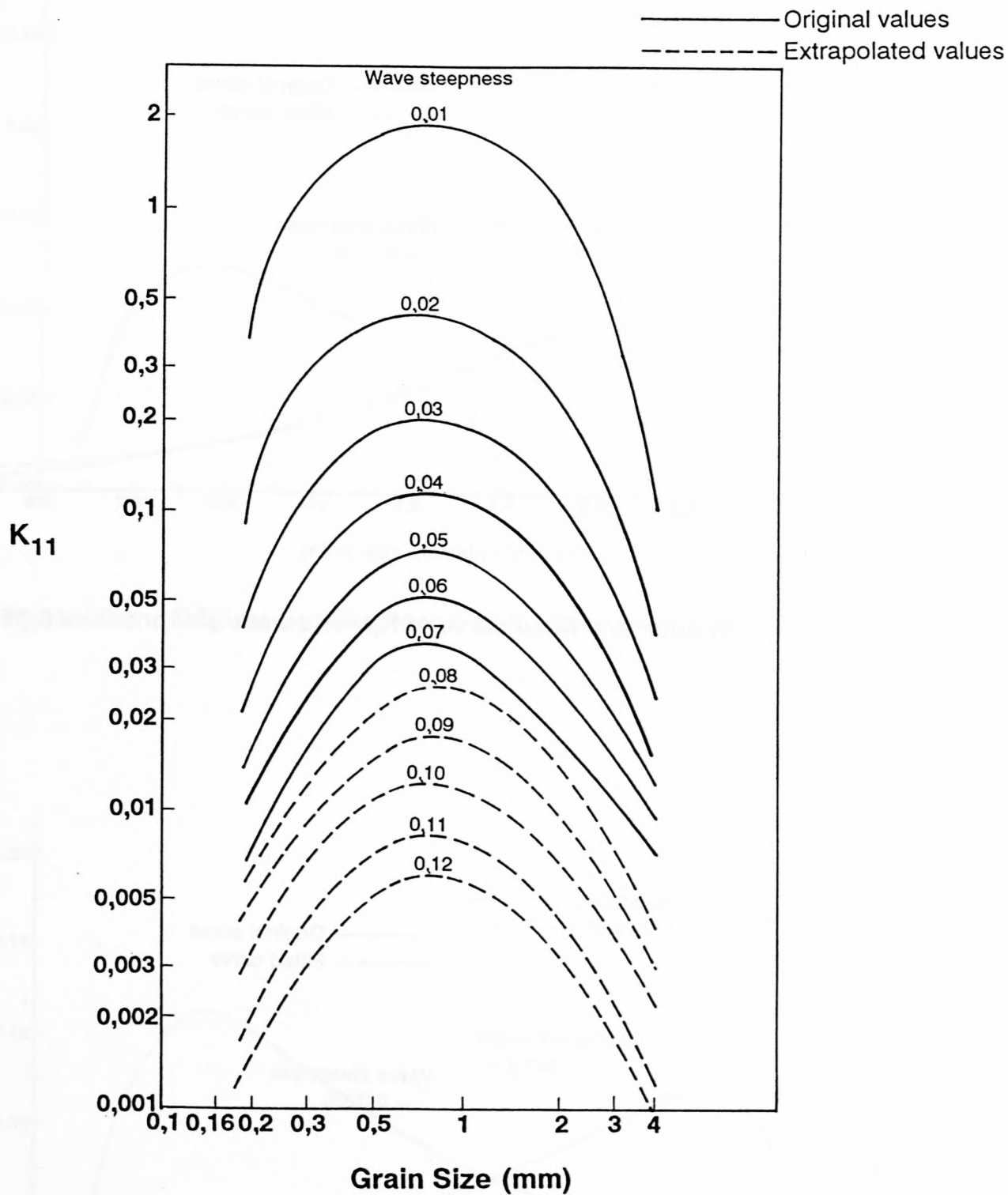


Figure C2: Analytical formula for the wave friction factor according to Riedel et al. (1972)



(Modified from Bonnefille and Pernecker, 1967)

Figure C3a: Original and extrapolated K_{11} values

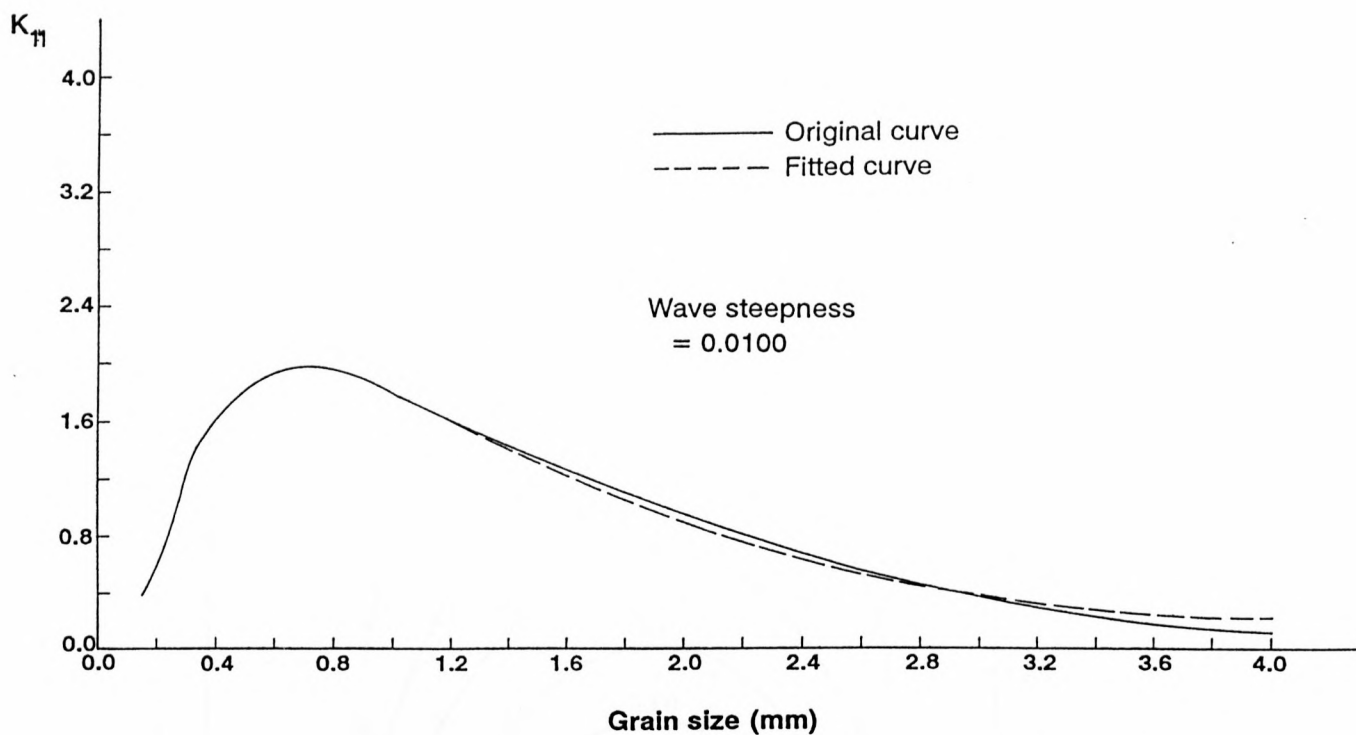


Figure C3b: Original and fitted curve of K_{11} for a wave steepness of 0,01

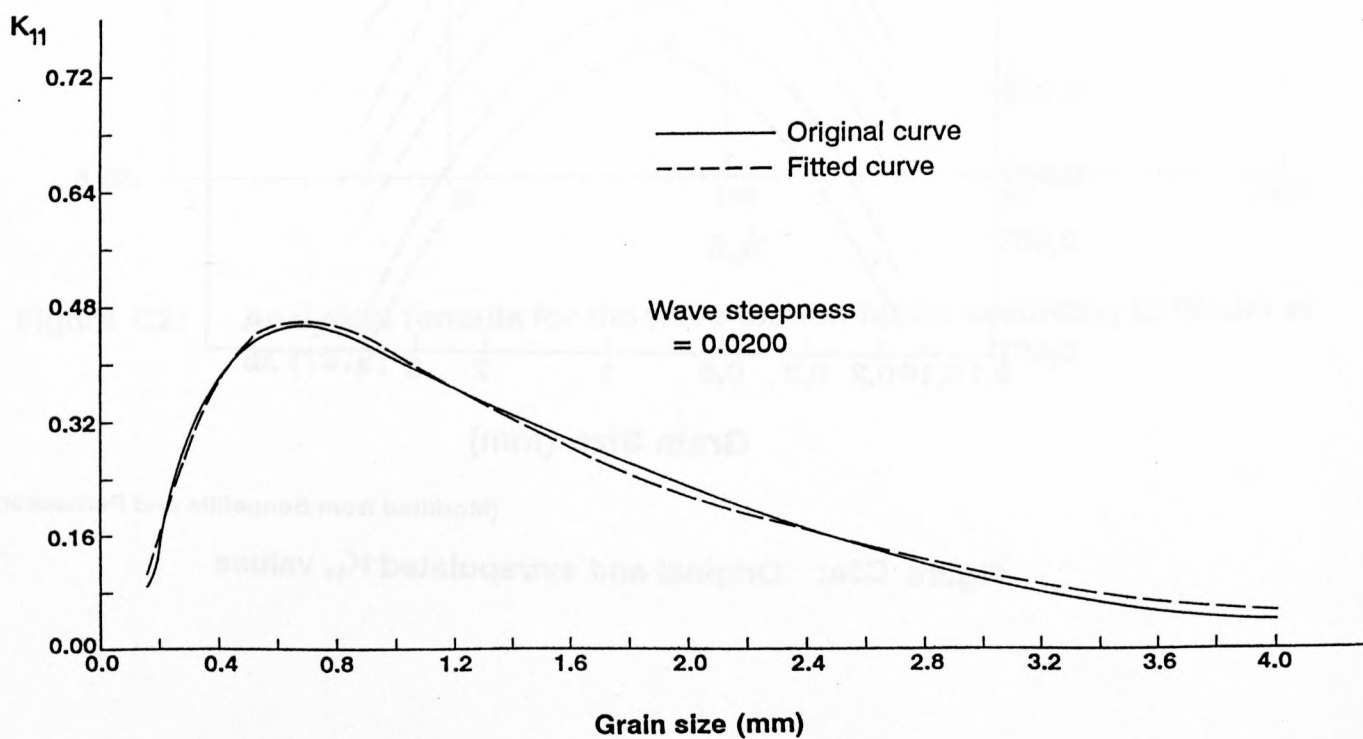


Figure C3c: Original and fitted curve of K_{11} for a wave steepness of 0,02

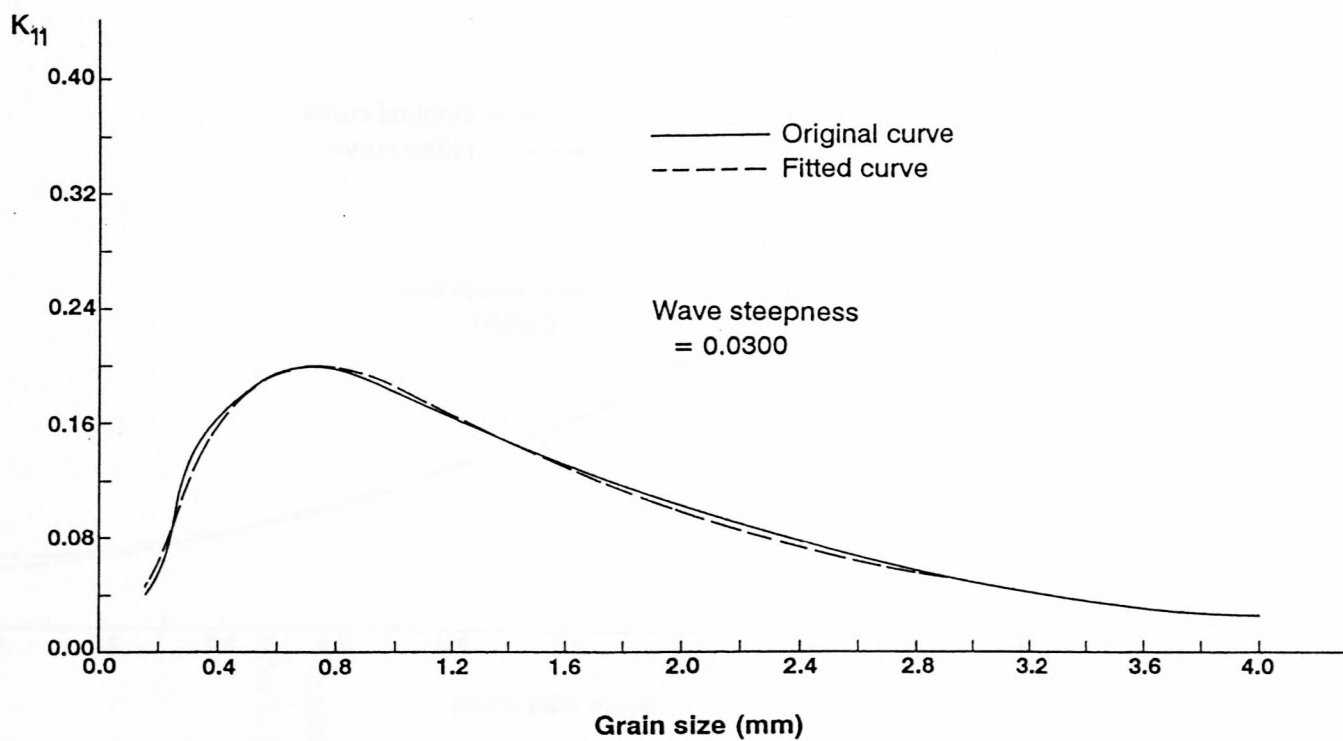


Figure C3d: Original and fitted curve of K_{11} for a wave steepness of 0,03

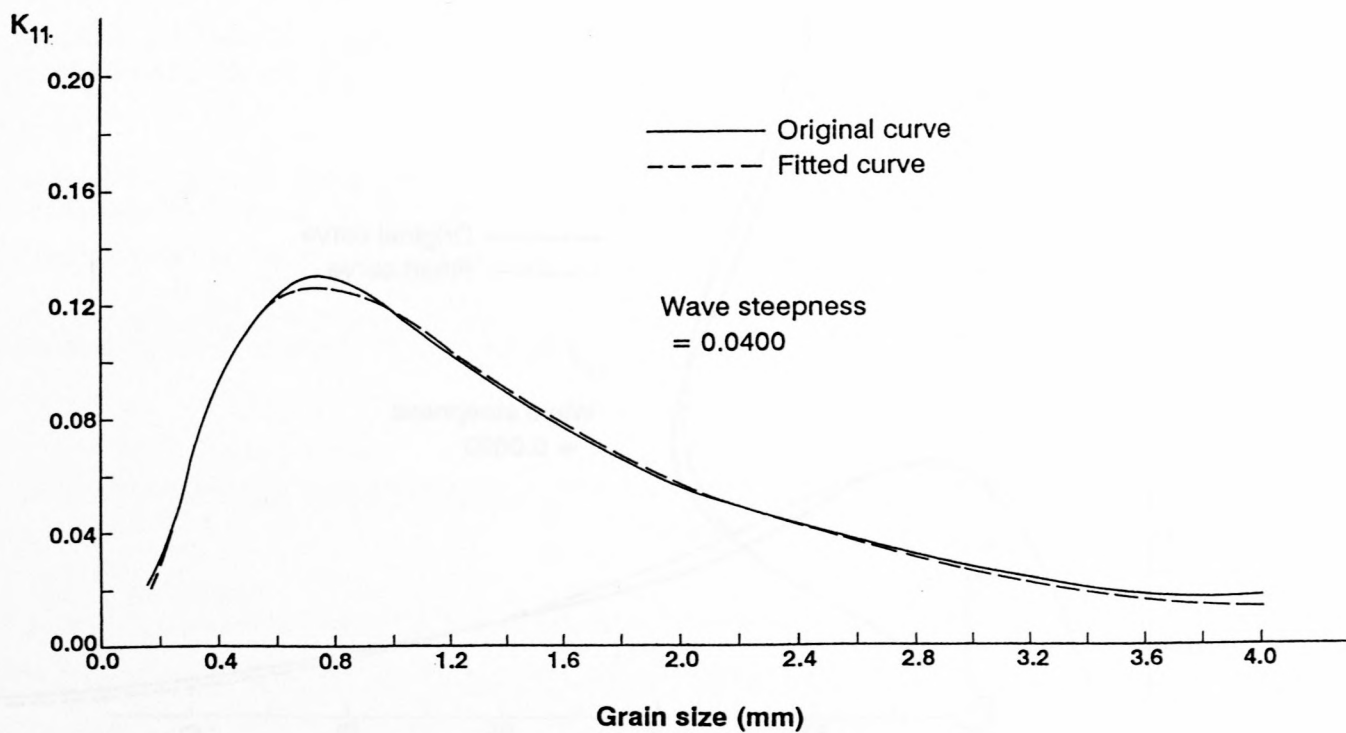


Figure C3e: Original and fitted curve of K_{11} for a wave steepness of 0,04

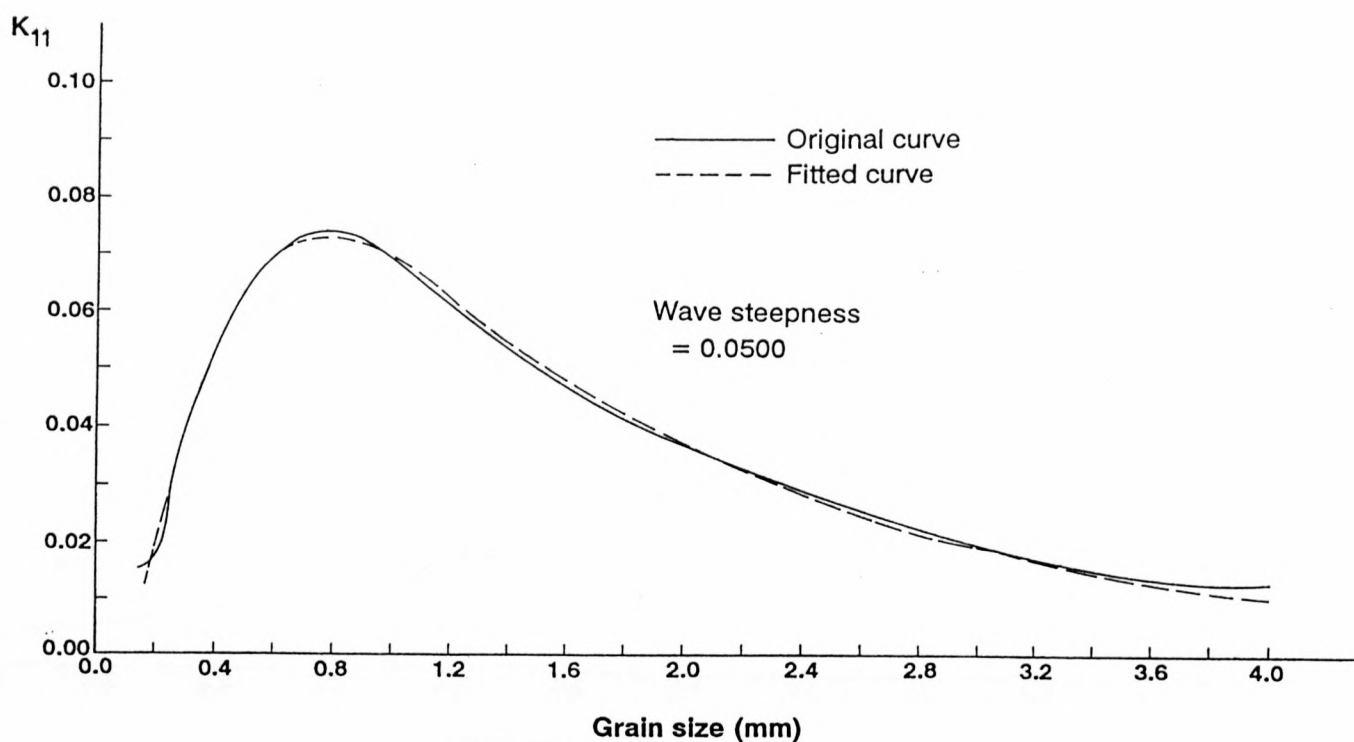


Figure C3f: Original and fitted curve of K_{11} for a wave steepness of 0,05

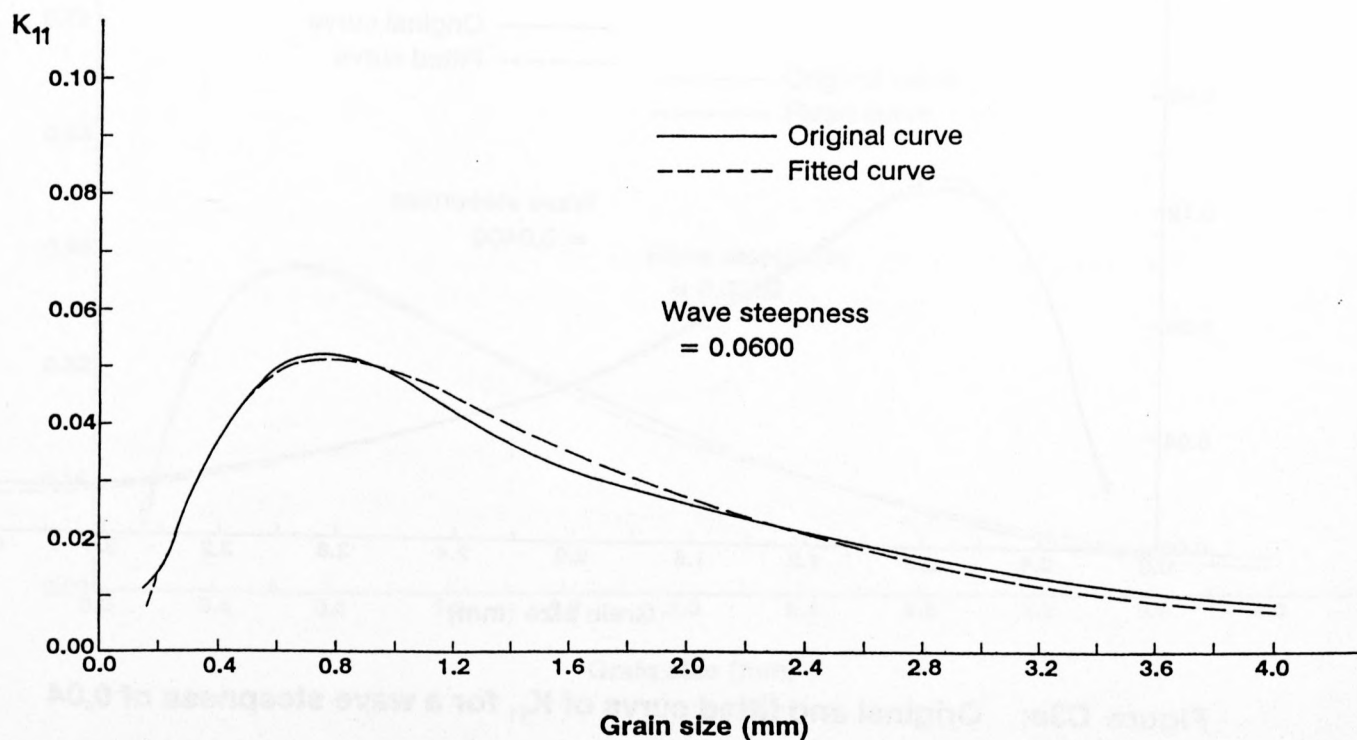


Figure C3g: Original and fitted curve of K_{11} for a wave steepness of 0,06

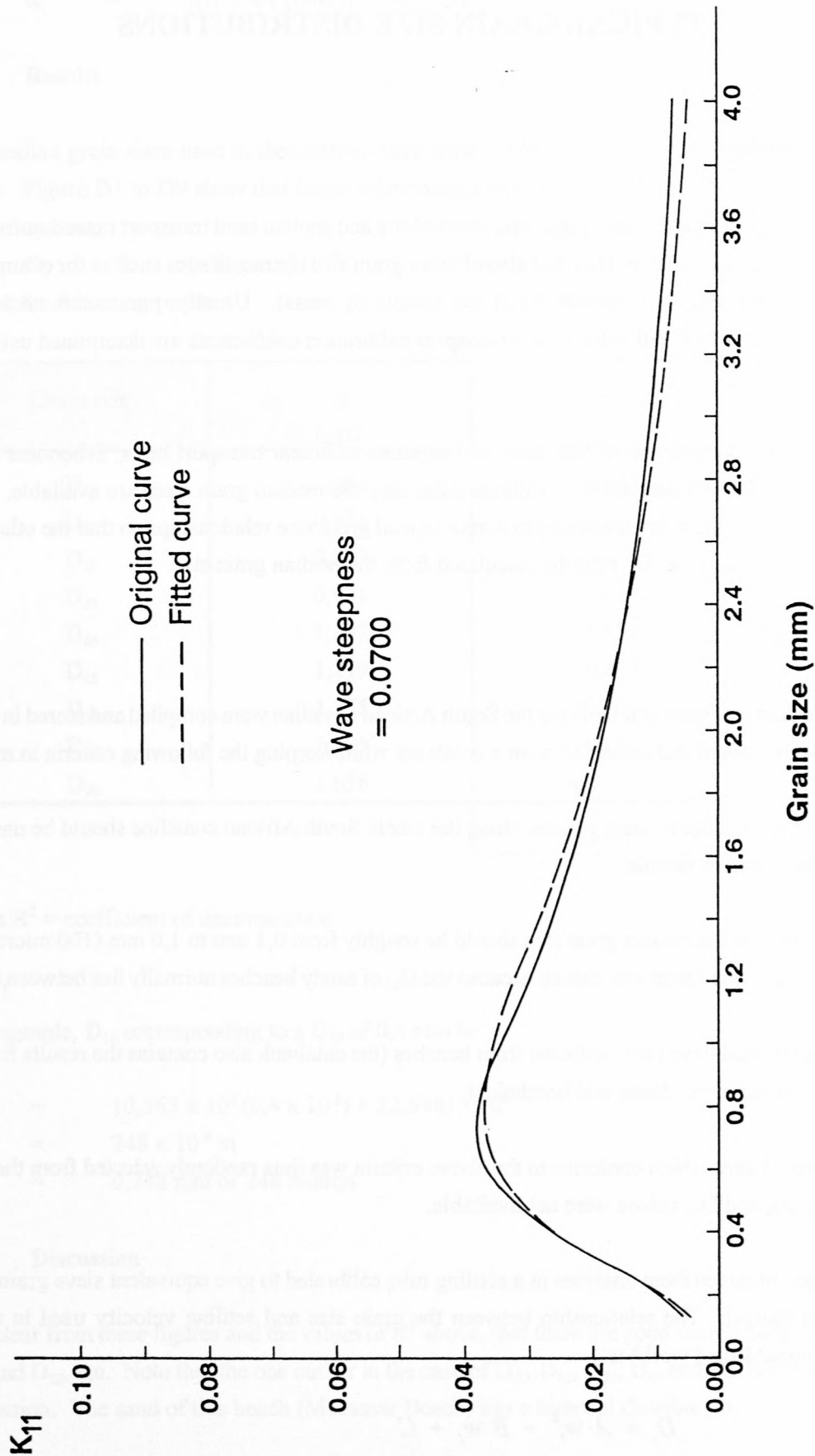


Figure C3h: Original and fitted curve of K_{11} for a wave steepness of 0,07

APPENDIX D

TYPICAL GRAIN SIZE DISTRIBUTIONS

D.1 Introduction

Predictions of sand concentrations, longshore, cross-shore and aeolian sand transport rates require knowledge of not only the median grain size (D_{50}), but also of other grain size characteristics such as for example, D_{35} and D_{90} (D_i is the grain size that exceeds $i\%$ of the sample by mass). Usually, parameters such as the bed roughness, friction factors, fall velocity and transport calibration coefficients are determined using the grain size as input.

In a comprehensive compilation of field data on longshore sediment transport rates, Schoonees and Theron (1993) found that for virtually all the available data, only the median grain sizes are available. In order to utilize these data, it is therefore necessary to derive typical grain size relationships so that the other grain size characteristics (for example, D_{35}) can be calculated from the median grain size.

D.2 Method

The grain size data that were available for the South African coastline were compiled and stored in a databank. Data points were chosen and extracted from a databank while keeping the following criteria in mind:

- Sand from a large number of sites along the whole South African coastline should be used to ensure a representative sample.
- The range of the median grain size should be roughly from 0,1 mm to 1,0 mm (100 microns to 1 000 microns). This range was chosen because the D_{50} of sandy beaches normally lies between these limits.
- Samples must have been collected from beaches (the databank also contains the results from samples taken in estuaries, dunes and boreholes).

A sample from 33 sites which conforms to the above criteria was thus randomly selected from the data. At 4 sites, the D_{25} , D_{60} and D_{75} values were not available.

The grain sizes, obtained from analyses in a settling tube calibrated to give equivalent sieve grain sizes, were tabulated and plotted. The relationship between the grain size and settling velocity used in the analysis (Schoonees, unpublished work) is:

$$D_i = A w_i^2 + B w_i + C \quad (D1)$$

where w_i = settling velocity corresponding to D_i
and A = $2,973 \cdot 10^{-2}$
 B = $4,173 \cdot 10^{-3}$

$$\begin{aligned} C &= 6,738 \cdot 10^{-5} \\ \therefore w_i &= [(B^2 - 4A(C-D_i))^{0,5} - B] / 2A \end{aligned} \quad (D2)$$

D.3 Results

The median grain sizes used in the analysis vary from 0,144 mm to 1,206 mm, thus covering the required range. Figure D1 to D9 show that linear relationships exist between D_{10} and D_{50} , D_{16} and D_{50} , etc. Linear regression being

$$D_i = (a D_{50} + b) / 10^6 \quad (D3)$$

yielded the following results:

Grain size	a $\times 10^6$	b	R^2
D_{10}	0,563	22,598	0,920
D_{16}	0,675	7,560	0,946
D_{25}	0,823	-10,126	0,981
D_{35}	0,921	-18,062	0,982
D_{60}	1,092	-3,553	0,998
D_{65}	1,219	-29,821	0,992
D_{75}	1,335	-40,222	0,987
D_{84}	1,495	-50,096	0,970
D_{90}	1,656	-65,143	0,948
Mean R^2			0,969

where R^2 = coefficient of determination

For example, D_{10} corresponding to a D_{50} of 0,4 mm is:

$$\begin{aligned} D_{10} &= \{0,563 \times 10^6 (0,4 \times 10^{-3}) + 22,598\} / 10^6 \\ &= 248 \times 10^{-6} \text{ m} \\ &= 0,248 \text{ mm or } 248 \text{ micron} \end{aligned}$$

D.4 Discussion

It is clear from these figures and the values of R^2 above, that there are good correlations between D_{10} and D_{50} , D_{16} and D_{50} , etc. Note that the one outlier in the case of D_{60} , D_{65} , D_{75} , D_{84} and D_{90} has been neglected for the regression. The sand of this beach (Macassar Beach) has a bimodal distribution.

Although these relationships are not necessarily universally applicable, it is felt that they provide good first estimates of D_{10} , D_{16} , D_{25} , D_{35} , D_{60} , D_{65} , D_{75} , D_{84} , D_{90} if D_{50} is known, especially in the light of the high values of the coefficient of determination and the wide variety of beaches from which the sand was selected. It is

D.3

therefore reasonable to use these relationships. Of course, where the grain size distributions have been reported (Sato, 1962; Fairchild, 1973, 1977; Duane and James, 1980; Nicholls, 1985; Nicholls and Wright, 1991) they were used. These grain size distributions are contained in the following table:

Reference	Site	D ₁₀ (mm)	D ₂₅ (mm)	D ₃₅ (mm)	D ₅₀ (mm)	D ₆₀ (mm)	D ₆₅ (mm)	D ₇₅ (mm)	D ₈₄ (mm)	D ₉₀ (mm)
Sato (1962)	Fukue Coast, Atsumi Bay	1,40	2,35	2,80	3,50	4,10	4,50	5,50	7,30	10,10
Fairchild (1972, 1977)	Ventnor	0,164	0,176	0,190	0,200	0,206	0,214	0,241	0,261	0,314
	Nags Head	0,235	0,250	0,268	0,290	0,305	0,332	0,388	0,451	0,610
Duane and James (1980)	Point Mugu	0,115	0,130	0,140	0,154	0,170	0,180	0,197	0,205	0,242
Nicholls (1985);	Solent Beach	23,3	32,8	36,3	42,3	45,5	53,5	60,0	65,0	84,5
Nicholls and Wright (1991)	Hurst Castle Spit	28,0	30,0	32,0	34,0	36,0	37,0	42,0	43,0	46,0

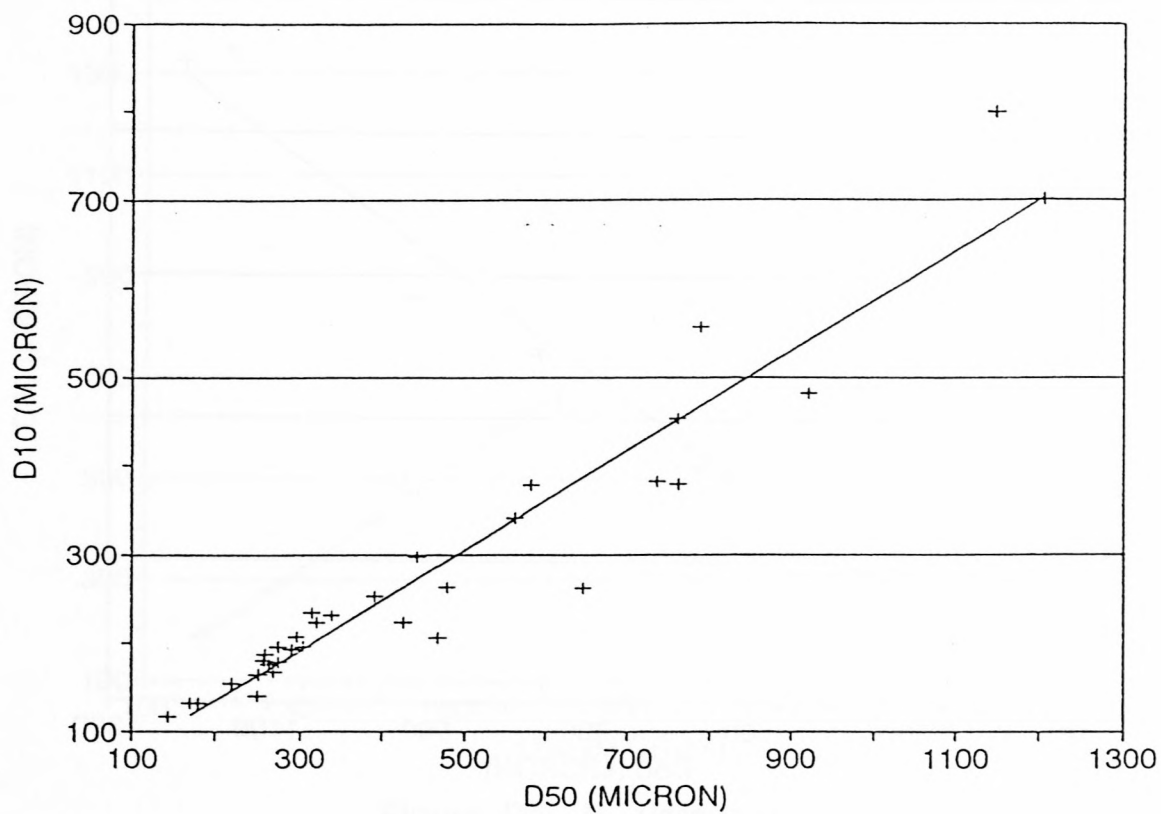


Figure D1: D₁₀ versus D₆₀

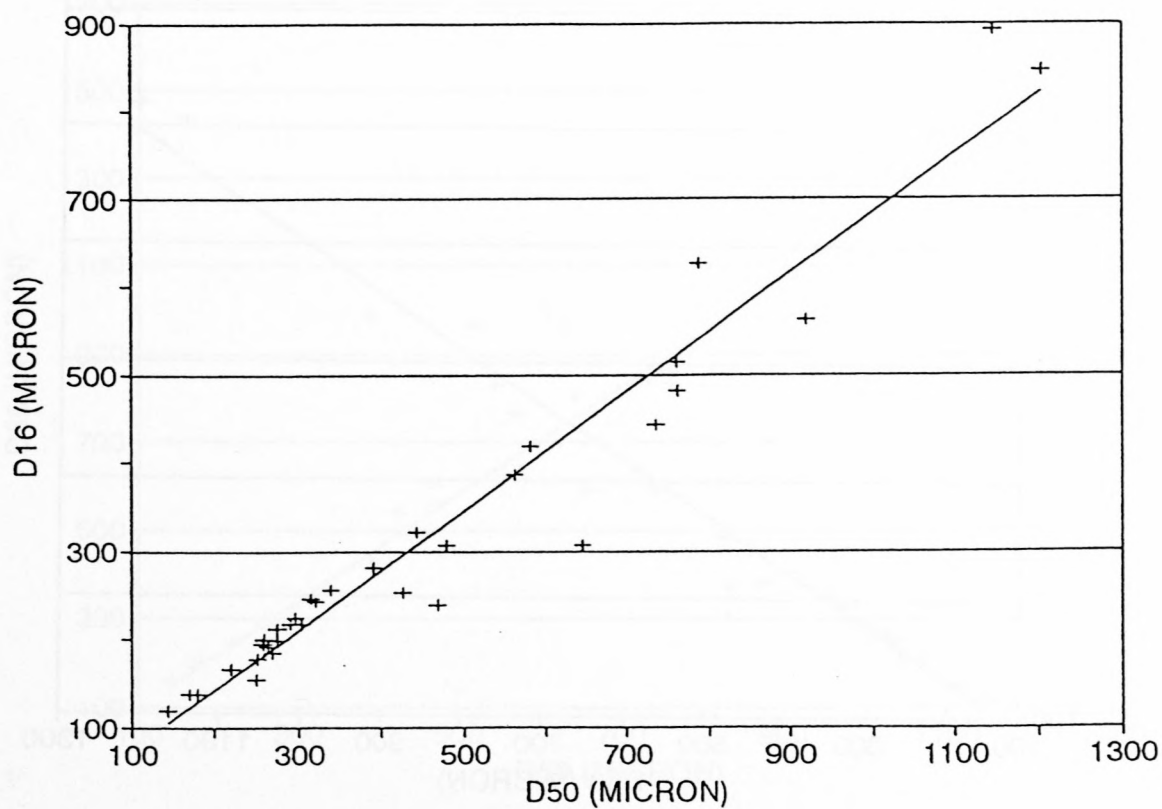


Figure D2: D₁₆ versus D₆₀

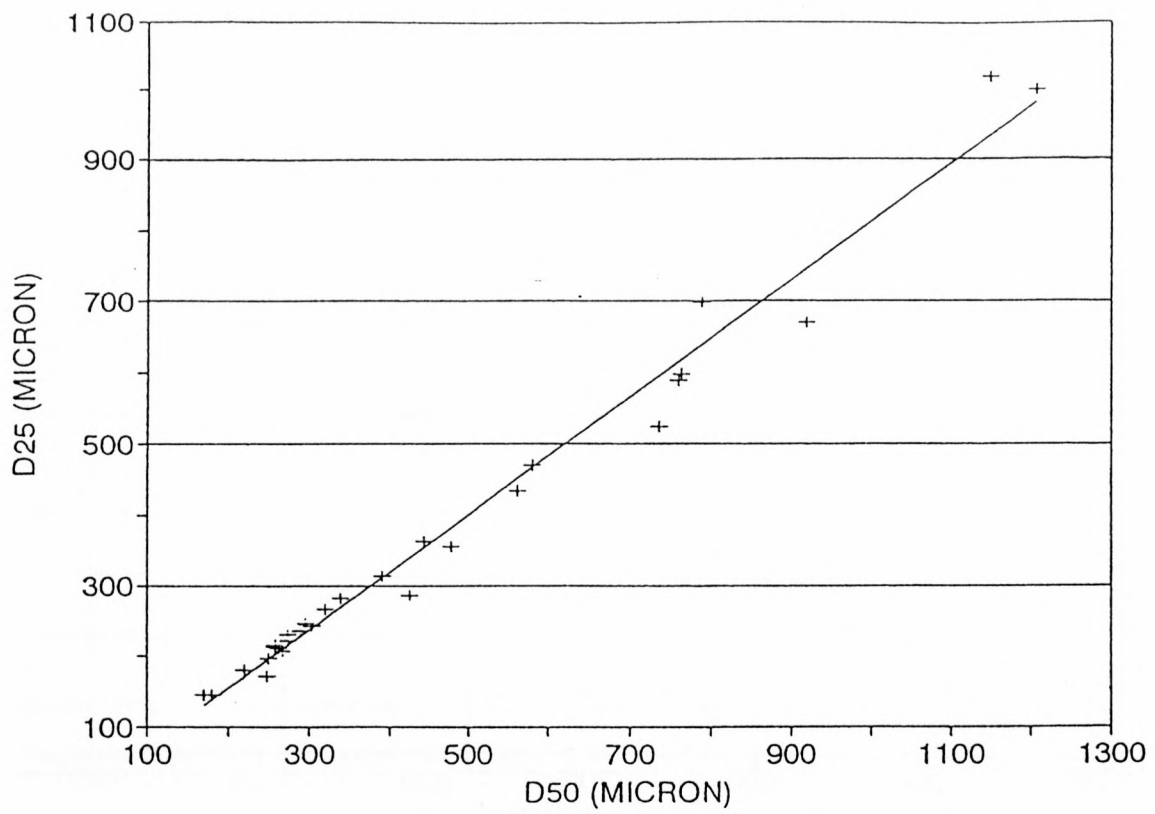


Figure D3: D₂₅ versus D₅₀

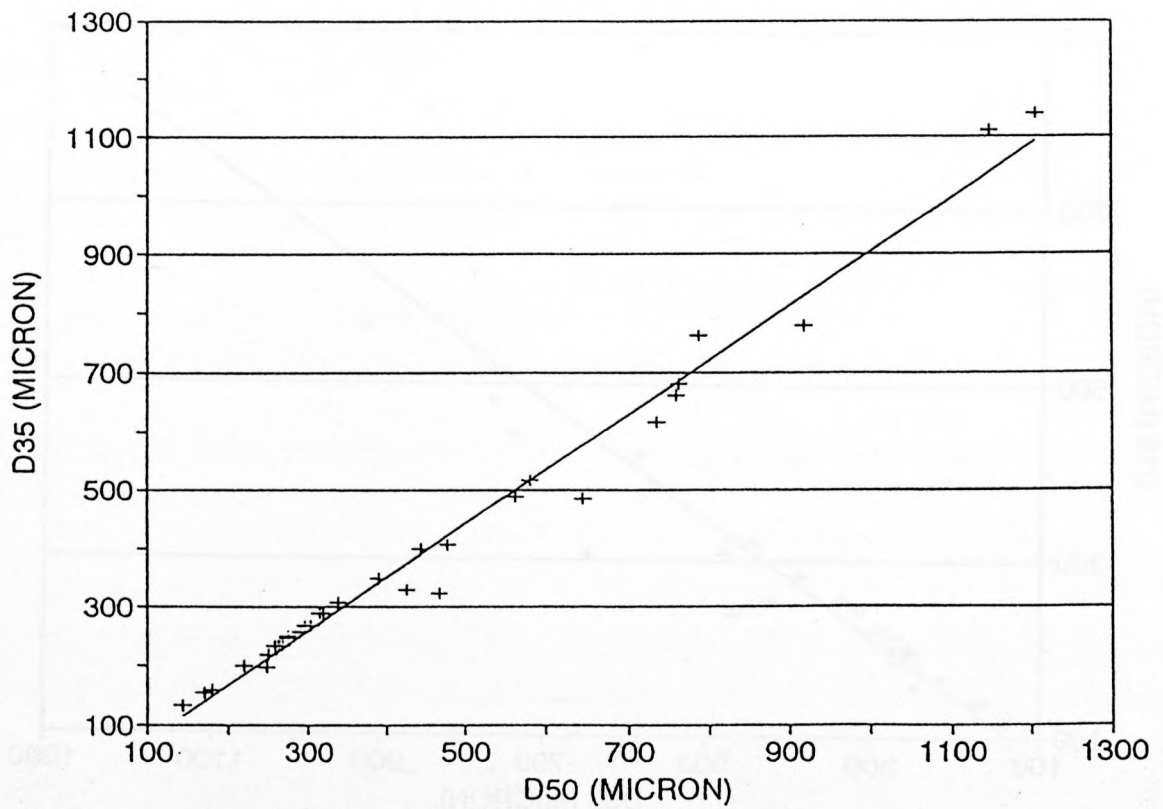


Figure D4: D₃₅ versus D₅₀

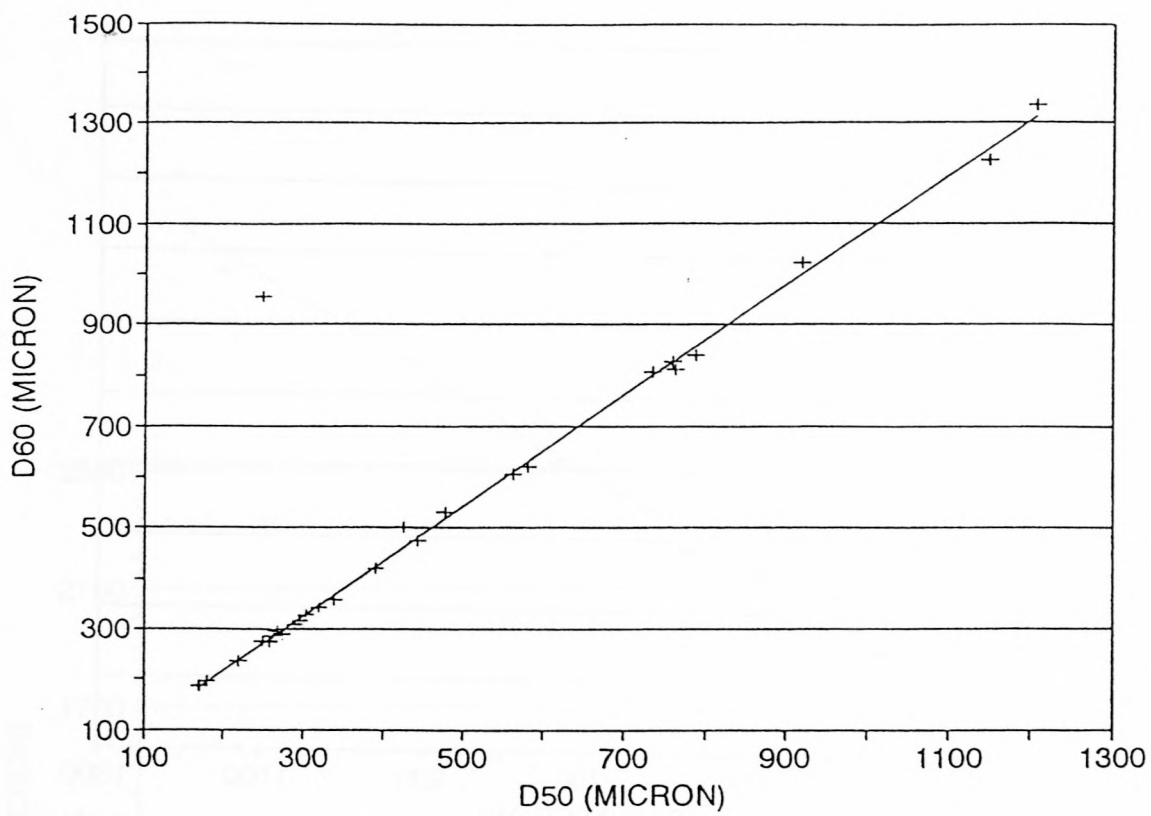


Figure D5: D_{60} versus D_{50}

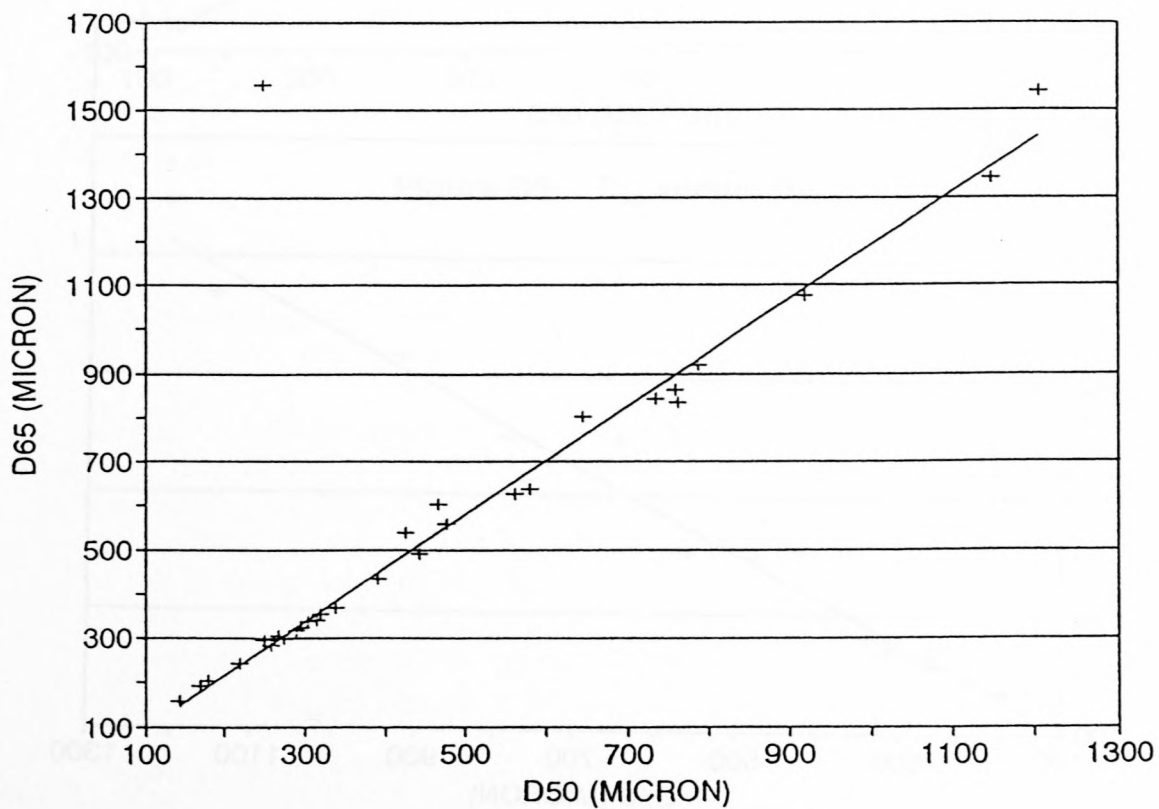


Figure D6: D_{65} versus D_{50}

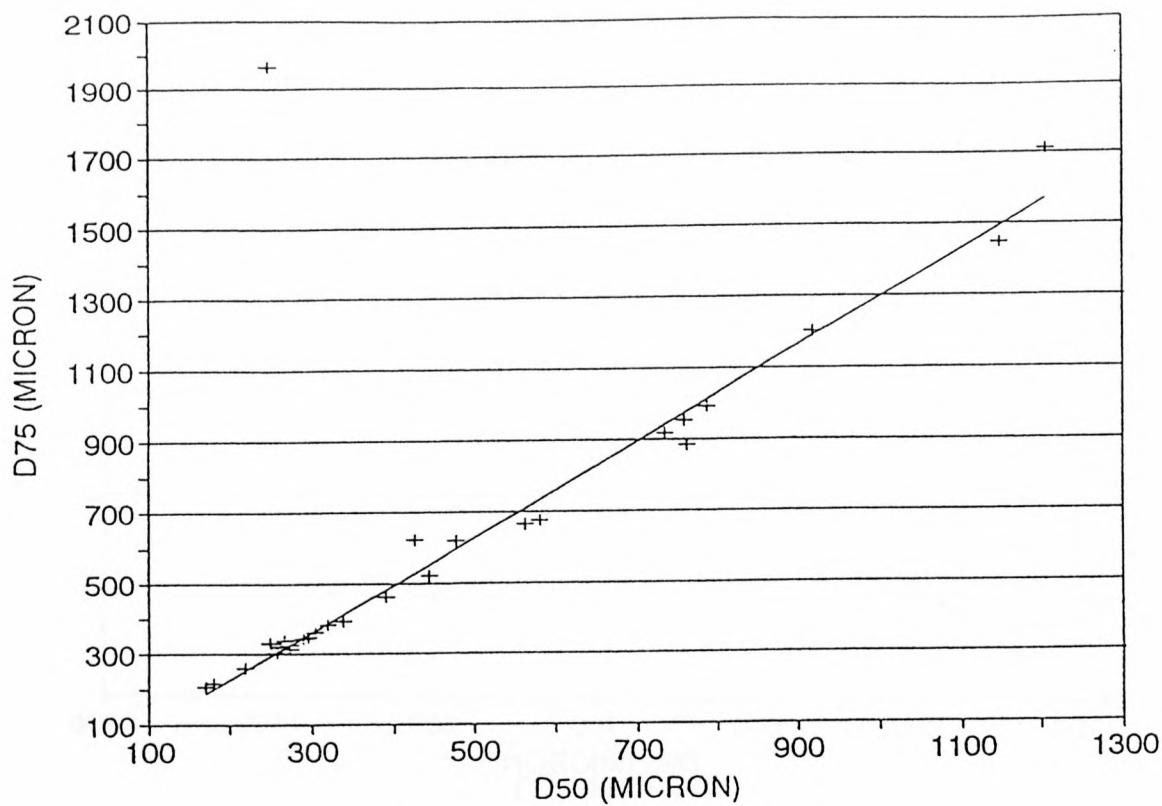


Figure D7: D_{75} versus D_{50}

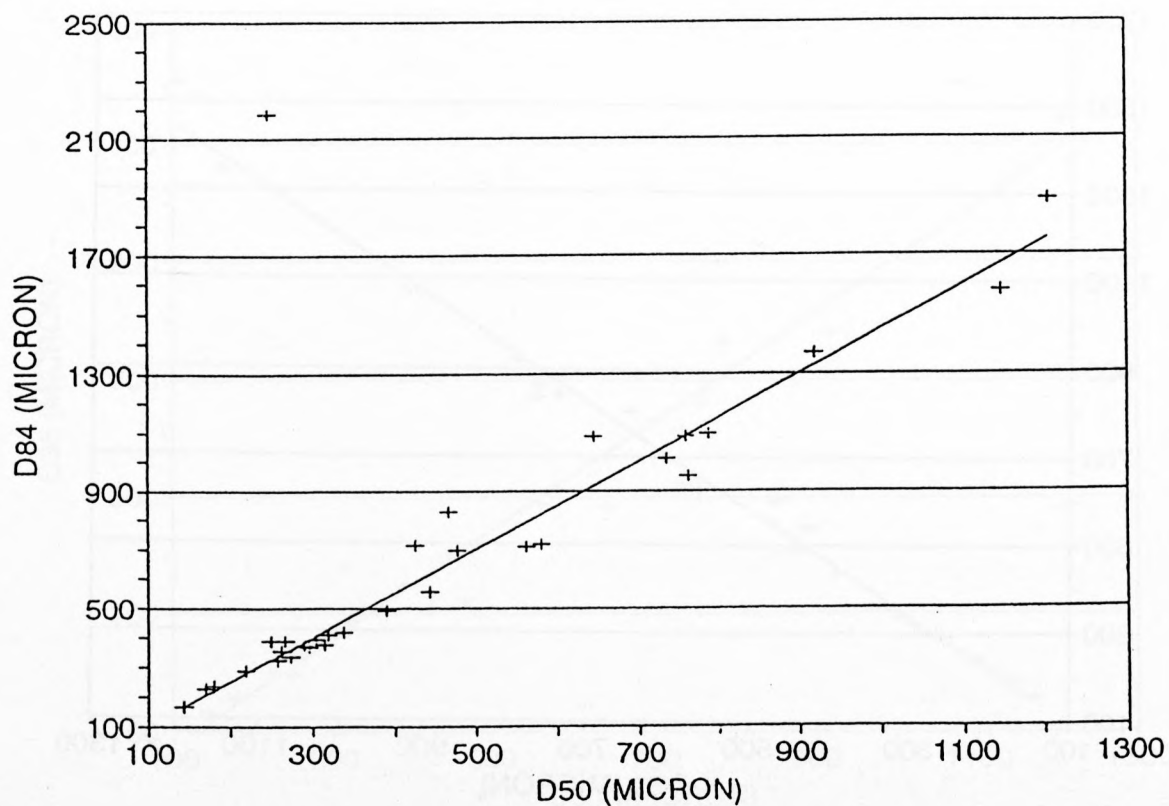


Figure D8: D_{84} versus D_{50}

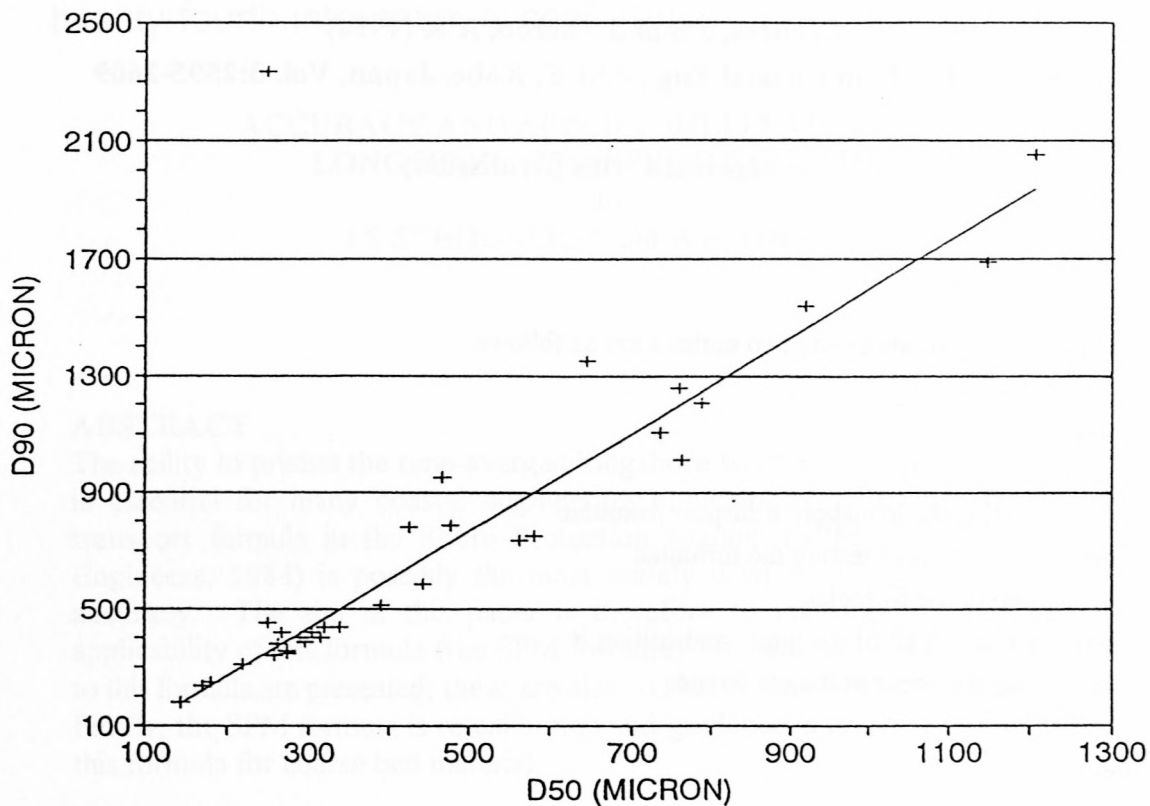


Figure D9: D_{90} versus D_{50}

APPENDIX E

ACCURACY AND APPLICABILITY OF THE SPM LONGSHORE TRANSPORT FORMULA

by

Schoonees, J S and Theron, A K (1994)

24 Intern. Conf. on Coastal Eng., ASCE, Kobe, Japan, Vol. 3:2595-2609

(Reprinted with permission)

The individual contributions by the two authors are as follows:

J S Schoonees

- programming the longshore transport formulae
- devising methods of testing the formulae
- evaluation of the formulae
- writing a first draft of the paper and editing it
- presenting the paper at the conference

A K Theron

- extraction of the data from the references
- plotting of the figures
- idea to also plot the results only for the data in the higher category (Figure 5)
- editing the paper

Coastal Engineering 1994

Proceedings of the
twenty-fourth international conference

ACCURACY AND APPLICABILITY OF THE SPM LONGSHORE TRANSPORT FORMULA

by

J S SCHOONEES* and A K THERON*

ABSTRACT

The ability to predict the time-averaged longshore sediment transport rate accurately is essential for many coastal engineering applications. Because the longshore transport formula in the Shore Protection Manual (SPM; US Army, Corps of Engineers, 1984) is possibly the most widely used, it is important to know its accuracy. The aim of this paper is therefore to investigate the accuracy and applicability of this formula (the SPM formula). In addition, a number of variations to this formula are presented; these are also tested against a comprehensive data set. Finally, the SPM formula is re-calibrated and guidance is given regarding the use of this formula for coarse bed material.

INTRODUCTION

The ability to predict the time-averaged longshore sediment transport rate accurately is essential for the design of breakwaters at harbour entrances, navigation channels and dredging requirements, beach improvement schemes incorporating groynes, detached breakwaters and beach fill as well as for the determination of the stability of inlets and estuaries.

Because the longshore transport formula in the Shore Protection Manual (SPM; US Army, Corps of Engineers, 1984) is possibly the most widely used, it is important to know its accuracy. The aim of this paper is therefore to investigate the accuracy and applicability of this formula (the SPM formula). In addition, a number of variations to this formula have been presented; these will also be tested against a comprehensive data set. Finally, the SPM formula is re-calibrated and guidance is given regarding the use of this formula for coarse bed material.

* Research Engineers, CSIR, P O Box 320, Stellenbosch, 7599, South Africa

The data considered in this paper are only for particulate (non-cohesive) sediment (including sand, gravel and shingle) being transported alongshore from the swash zone across the surf zone to deep water. Only bulk (total rate across the shore) and not local transport rates are considered. These bulk rates include both the bedload and suspended load. Only field data are used because of possible scale effects in laboratory investigations and/or because regular waves were used. Furthermore, the ultimate aim is to be able to predict longshore transport accurately in the field (Komar, 1988).

The data are not meant to provide average long-term data at (a) specific site(s). It is rather assumed that if a longshore transport formula is capable of accurately predicting transport rates for the data sets given herein, it can be used with reasonable confidence at similar sites to determine the long-term longshore sediment budget if representative wave and other input parameters are available. It would of course be even better to have site-specific calibration data before calculating average long-term transport rates.

Previous studies where a few longshore transport formulae have been tested against data are Swart (1976), Fleming *et al.* (1986) and Kamphuis *et al.* (1986). Schoonees (1994) evaluated 51 formulae against an extensive data base. This paper reports the findings of the above-mentioned study with regard to the SPM formula and variations thereof. Two of the most important papers on the development of the SPM formula are Komar and Inman (1970) and Komar (1988). The latter study in which the dependency of the SPM formula on sediment grain size, beach slope and wave steepness was investigated, is partially revised here with a bigger data base.

DATA

Schoonees and Theron (1993) compiled and reviewed almost all the available field data on longshore transport. They used a point rating system to assess the quality of the data in detail. Two data sets, namely Data Sets 1 and 2, were extracted from the data contained in Schoonees and Theron (1993) together with their point ratings.

Data Set 1 containing 123 data points, consists of data where all the required parameters are available. Table 1 summarizes this data set and gives the point ratings in percentages according to Schoonees and Theron (1993). Data Set 2 includes Data Set 1 and contains other measurements totalling 240 data points. These other measurements are usually where only values of the energy flux factor, the longshore transport rate and the median grain size are available. Table 2 lists the sources of Data Set 2.

It is important to note that the data ranges of the particular Data Set 1 are:

0,058	<	H_{bs} (m)	<	3,400
2,32	<	T_p (s)	<	16,60
0,30	<	θ_b (°)	<	35,00
0,0070 (=1/142,9)	<	beach slope	<	0,1380 (=1/7,2)

0,154	<	D_{50} (mm)	<	15,000
600	<	S ($m^3/year$)	<	14 793 000

From the above values it is clear that the data ranges of this data set (and therefore also Data Set 2) are quite wide. Most conditions encountered on natural beaches are covered and the data were collected on beaches from a variety of sites from around the world. These give credibility to the conclusions drawn in this comparison with data.

FORMULAE

One of the earliest longshore transport formulae and perhaps the best-known method, the **SPM formula** (SPM = Shore Protection Manual) is given in US Army, Corps of Engineers (1984):

$$S = K_1 P_{ls} \quad (m^3/yr)$$

where

$$K_1 = 1289 \text{ (m}^4\text{/(W.yr) for prototype beaches}$$

$$P_{ls} = \text{wave energy flux factor using the significant wave height in the calculation. (W/m)}$$

$$= E_b n_b C_b \sin \theta_b \cos \theta_b$$

with

$$E = \text{wave energy density}$$

$$= \rho g H_{bs}^2 / 8$$

$$\rho = \text{density of sea water (kg/m}^3\text{)}$$

$$g = \text{gravitational acceleration (m/s}^2\text{)}$$

$$H_{bs} = \text{significant breaker wave height (m)}$$

$$n_b = 0,5 \left(1 + (4\pi d_b / L_b) / (\sinh 4\pi d_b / L_b) \right)$$

and

$$d_b = \text{breaker depth (m)}$$

$$L_b = \text{wavelength at the breaker line (m)}$$

$$C_b = \text{wave celerity at the breaker line (m/s)}$$

$$= (L_b / T_p)$$

$$T_p = \text{peak wave period}$$

and

$$\theta_b = \text{wave incidence angle at the breaker line}$$

An alternative formulation of the SPM is:

$$I = \frac{K_r P_{ls}}{K_r P_{lr}}$$

with I = immersed weight longshore transport rate
 P_{lr} = energy flux factor using the root-mean square breaker height
 where K_s = 0,5 (0,78) = 0,39 if the significant breaker height is used in P_{ls}
 K_r = 0,78 if the root-mean-square breaker height (H_{brms}) is used in P_{lr}

Development of the SPM formula was done, among others, by the Scripps Institute of Oceanography (1947), Watts (1953), Caldwell (1956), Inman and Bagnold (1963), Komar (1969), Komar and Inman (1970) and Komar (1988).

Swart (1976) adapted the coefficient $K_1 = 1289$ to be a function of the median grain size (D_{50}). His version of the **SPM formula** which appears to differ from the SPM formula given above because of several implications, is

$$S = K_2 P_{ls} \quad (m^3/yr)$$

where $K_2 = 1876 \log_{10} (0,00146 / D_{50})$
 (D_{50} in m)

This equation together with a relationship proposed by Bruno *et al* (1981) will be shown later. Komar (1988) maintained that there is no significant relationship between K_1 and D_{50} . This issue will be discussed further based on all the data.

Kamphuis and Readshaw (1978) and Vitale (1981) investigated whether K_1 is a function of the surf similarity parameter (or Iribarren number) ξ_b :

$$\xi_b = \frac{\tan \alpha}{(H_{brms} / L_o)^{0,5}}$$

where $\tan \alpha$ = bottom slope in the surf zone

$$H_{brms} = H_{bs} / \sqrt{2}$$

$$L_o = \text{deep-sea wavelength}$$

Vitale (1981) used a mean wave height (measured in relatively deep water) instead of H_{brms} . To prevent the need for calculation of the wave height at the breaker line, it was decided to use the relationship proposed by Kamphuis and Readshaw (1978) and Readshaw (1979), namely:

$$K_p' = 0,7 \xi_b \quad \text{for } 0,4 < \xi_b < 1,4$$

(say for $\xi_b < 1,4$)

$$1,24 \quad \text{for} \quad \xi_b \geq 1,4$$

$$\text{with } Q_s \text{ (kg/s)} = K_p' P_{ls} / 2g$$

$$\text{and } S = \frac{31\,557\,600\, Q_s}{(1-p) \rho_s} \quad (m^3/yr)$$

$$\text{where } p = \text{porosity of the sediment (assumed to be 0,4 for sand)}$$

$$\rho_s = \text{density of the sediment (usually } 2650 \text{ kg/m}^3 \text{ for sand)}$$

$$\text{and } 31\,557\,600 = \text{number of seconds in one year}$$

Bailard (1981) generalized the Bagnold (1963, 1966) energetics-based stream model. After integrating the local time-averaged longshore transport rate, Bailard (1984) obtained the following alternative equation for K_1 , (called K_3) valid for both model and prototype applications:

$$K_3 = 0,05 + 2,6 \sin^2 2\theta_b + 0,007 \, u_{mb} / w$$

$$\text{where } w = \text{fall velocity of the sediment grains}$$

$$u_{mb} = 0,5 \, \gamma (g d_b)^{0,5}$$

$$\text{and } \gamma = \text{breaker index} = 0,8$$

Bailard (1985) adds another term the equation for K_3 namely, $0,0096 \tan \alpha$. However, choosing a very high value of the beach slope ($\tan \alpha$) of 0,2, it is clear that the estimated maximum value of this term is about 0,0019. For $\tan \alpha = 0,04$, a typical value, the term is only 0,00038. Because its contribution to K_s is negligible, this term was omitted. Furthermore:

$$I = 0,5 \, K_3 \, P_{ls}$$

$$\text{and } S = \frac{31\,557\,600 \, I}{(\rho_s - \rho) \, g \, (1 - p)} \quad (m^3/yr)$$

Watts (1953) empirically related the longshore transport rate to the wave energy flux factor. The **Watts formula** in SI units is:

$$S = 2223 \, P_{ls}^{0,9}$$

Similarly, **Caldwell (1956)** obtained his formula (given here in SI units):

$$S = 2505 \, P_{ls}^{0,8} \quad (m^3/yr)$$

EVALUATION OF FORMULAE

Method of Testing

The results of the testing of the formulae will be presented in a number of ways in order to facilitate interpretation. These are:

- * A plot of the predicted longshore transport rates (S_p) versus the measured rates (S_m).
- * The relative standard error of estimate (σ) was calculated (Kamphuis, *et al*, 1986):

$$\sigma = \sum_{i=1}^n \left[\frac{(\log S_{p,i} - \log S_{m,i})^2}{n-1} \right]^{0.5}$$

where n = number of data points

i = number of the particular data point

- * The discrepancy ratio (r_d) (Van Rijn, 1984) and its distribution were determined.

$$r_{d,i} = S_{p,i} / S_{m,i}$$

A histogram of the percentage occurrence versus r_d gives this distribution.

(The residuals ($e_i = S_{m,i} - S_{p,i}$) were computed and plotted against S_p to check whether there is a systematic trend in the residuals, or not - these are not shown. Refer to Schoonees (1994)).

Results

Table 3 lists the relative standard error of estimate (σ) and the percentage occurrence of the discrepancy ratio (r_d) within certain limits for the formulae. For example, the percentage of the predicted transport rates for which the discrepancy ratio falls between 0,5 and 2 or between 0,25 and 4 can be read from this table.

Figures 1 and 2 show the predicted longshore transport rates (S_p) versus the measured rates (S_m) for the SPM and the SPM, Kamphuis and Readshaw formulae respectively. The histogram of the discrepancy ratios for the SPM, Kamphuis and Readshaw formula is contained in Figure 3. Refer to Schoonees (1994) for similar figures of the other formulae. Note that in these figures m^3/yr means m^3/yr .

Discussion

A first impression when examining Figures 1 and 2 and Table 3 is that considerable scatter exists in the predicted longshore transport rates. Based on this particular data set, the SPM, Kamphuis and Readshaw formula gives the best answer of the six formulae over the full range of measured longshore transport rates ($\sigma=0,515$; r_d between 0,5 and 2: 65,0%). Even so this formula tends to underpredict high transport rates (Figure 2). This is an area of concern because at a particular site, most

of the longshore transport occurs during a few storms so that it is important to predict high transport rates accurately.

It is interesting to note that the SPM formula, perhaps the best known and most used predictor, does not fare very well. Although one can argue that its poor performance at low transport rates (Figure 1) can be attributed to a lack of an incipient motion criterion, it is still clear that it over-predicts in the range $1,5 \times 10^4 \text{ m}^3/\text{year}$ to $1,5 \times 10^6 \text{ m}^3/\text{year}$. What is, however, comforting is that for high transport rates ($> 1,5 \times 10^6 \text{ m}^3/\text{year}$) the SPM predicts transport rates accurately. That is, for the few data points in this range. However, two of the oldest formulae, namely, the Caldwell and Watts methods, also do not have an incipient motion criterion but both appear to be more accurate than the SPM and the SPM and Swart formulae (compare $\sigma=0,579$ (Caldwell) and $0,685$ (Watts) to $0,708$ (SPM) and $0,720$ (SPM and Swart)). In fact, adapting the SPM formula for grain size (SPM and Swart method) caused a slight decrease in the accuracy of the predictions. The similar answers of these two predictors can, however, merely indicate that most of the data points were collected for grain sizes between $0,2 \text{ mm}$ to $0,4 \text{ mm}$ as indeed found by Schoonees and Theron (1993). In this grain size range the SPM and Swart formula gives very similar answers to the SPM formula.

It is interesting to note that the original SPM, Kamphuis and Readshaw formula was only calibrated against laboratory data and therefore no field data of Data Set 1 were used in its derivation. The second-best formula (Caldwell's) only used a few of the data points, especially when compared to the 41 points of Data Set 1 included in the calibration of the SPM formula.

FURTHER CALIBRATION OF THE SPM FORMULA

One can argue that the SPM formula is not applicable for coarse-grained sediment which are included in Data Set 1. In addition, the data points for which only S and P_b are available, should also be used.

Figure 4 shows the data in Data Set 2 with a distinction being made between fine - ($D_{50} < 1 \text{ mm}$) and coarse-grained ($D_{50} > 1 \text{ mm}$) sediment. It is clear from this figure that except for some minor overlap, two different populations of points are apparent. For the fine-grained sediment (206 data points) the best fit relationship is:

$$I = 0,20 P_b \quad (R^2 = \text{coefficient of determination} = 0,72) \quad (1)$$

Considerable scatter is evident. If the recommendation by Schoonees and Theron (1993) is followed whereby only data in their higher category (point rating 60% and better) is used (Tables 1 and 2), 46 data points are retained. Figure 5 illustrates the result while the equation is:

$$I = 0,41 P_b \quad (R^2 = 0,77) \quad (2)$$

or $I = 0,82 P_{lr}$ (i.e. $K_r = 0,82$)

Unfortunately, the scatter is not significantly reduced and the range of P_{ls} values is much smaller. In comparing Equations 1 and 2, it is clear that the elimination of the lower quality data, more than doubled the value of K_s . $K_r = 0,82$ is an increase of the value of 0,57 proposed by Komar (1988) based on 70 of the data points in Data Set 1. The value in the original formula is 0,78 which is derived from 41 data points (US Army, Corps of Engineers, 1984). Kraus *et al.* (1982) found $K = 0,58$ based on their data and those of Komar (1969), which are 25 data points. It would of course be even better to have site-specific calibration data before calculating longshore transport rates. The foregoing illustrates the great uncertainties involved in using the SPM formula and in view of this we recommend that the SPM, Kamphuis and Readshaw formula preferably be used.

Both Swart (1976) and Bruno *et al.* (1981) presented relationships between K_s and D_{50} . Figure 6 shows these relationships together with the data having median grain sizes below or equal to 1 mm. From this figure it is clear that a single relationship between K_s and D_{50} will not explain all the scatter shown in Figures 4 and 6. The same applies if the settling velocity instead of the median grain size is used. Although this correlates with the finding of Komar (1988), the authors believe that a longshore transport formula must contain either D_{50} or the settling velocity. It is also evident from Figure 6 that neither of the relationships by Swart and Bruno *et al.* are generally valid. The relationship by Bruno *et al.* (1981) almost forms an upper envelope to the values.

Returning to Figure 4, a very approximate line through the coarse-grained sediment is:

$$I = 0,01 P_{ls} \quad (R^2 = 0,11) \quad (3)$$

Because of the considerable scatter in the data and the very low R^2 , this equation should only be used to obtain a rough order of magnitude of the longshore transport rate. For these coarse-grained data as well, no single relationship between K_s and D_{50} (figure not shown) will explain all the scatter shown in Figure 4. Clearly, further work is required. For example, an incipient motion criterion (see e.g. Chadwick, 1989, Brampton and Motyka, 1984 and Van Hijum and Pilarczyk, 1982) is necessary.

CONCLUSIONS

The data ranges of Data Sets 1 and 2 are quite wide and as such, cover most conditions encountered on natural beaches.

Of the six formulae (SPM formula and variations thereof), tested against Data Set 1, the SPM, Kamphuis and Readshaw method fared the best. The standard error of estimate for this method was 0,515 while 65,0% of the time, the discrepancy ratio (r_d) fell between 0,5 and 2.

By using only the data from Data Set 2 that fall in the higher (better) category of Schoonees and Theron (1993) - 46 data points -, the best fit relationship for sand ($D_{50} < 1 \text{ mm}$) is:

$$I = 0,41 P_b \quad (R^2 = 0,77)$$

Unfortunately, significant scatter is still evident (Figure 5). It was also found that no single relationship between K_s and the median grain size (or the settling velocity) will explain all the scatter in the data. In view of the uncertainties involved in using the SPM formula it is recommended that the SPM, Kamphuis and Readshaw formula preferably be used.

For coarse grained sediment ($D_{50} > 1 \text{ mm}$) 34 data points were available which yielded an approximate relationship:

$$I = 0,01 P_b \quad (R^2 = 0,11)$$

Because of the considerable scatter evident in Figure 4 and very low R^2 , this equation should only be used to obtain an order of magnitude of the transport. Again, no single relationship between K_s and the median grain size (or settling velocity) will explain all the scatter in the data.

REFERENCES

- Adachi, S., Sawaragi, T. and Ogo, A., 1959. The effects of coastal structures on the littoral sand drifts. *Coastal Engineering in Japan*, Vol. 2 : 85 - 98.
- Bagnold, R.A. (1963). *Mechanics of marine sedimentation*. The sea, Vol. 3, The earth beneath the sea. Hill, M.N. (Ed.). Inter-science Publ., New York, pp. 507-528.
- Bagnold, R.A. (1966). An approach to the sediment transport problem from general physics. U.S. Dept. of the interior, Geological Survey Prof. Paper 422-I. 37 pp.
- Bailard, J.A., 1981. "An energetics total load sediment transport model for a plane sloping beach," *J. Geophysical Res.*, Vol. 86, no. c11, pp 10938-10954.
- Bailard, J.A. (1984). A simplified model for longshore sediment transport. 19 International Conf. on Coastal Eng., Houston, Texas, Vol 2: 1454-1470.
- Bailard, J.A. (1985). Simple models for surfzone sediment transport. NCEL technical note N-1740. Naval Civil Eng. Lab., Port Hueneme California.
- Bijker, E.W., 1968. Littoral drift as a function of waves and current. Proc. 11th International Conf. on Coastal Eng., ASCE, London. Vol 1 : 415-435.
- Bodge, K.R., 1986. Short-term impoundment of longshore sediment transport. Ph.D. thesis, University of Florida, Gainesville. 346 pp.
- Brampton A and Motyka J M (1984). Modelling the plan shape of shingle beaches. *Estuarine Studies*, Vol. 12, Springer Verlag.
- Bruno, R.O., Dean R.G., Gable, C.G. and Walton, T.L., 1981. Longshore sand transport study at Channel Islands Harbor, California. Technical paper no. 81-2, CERC, U.S. Army Corps of Engineers, Fort Belvoir. 48pp.
- Caldwell, J.M., 1956. Wave action and sand movement near Anaheim Bay, California. U.S. Army, Beach Erosion Board, Tech. Memorandum 68. 21pp.
- Castanho, J., 1966. Rebentação das ondas e transporte litoral. Laboratório Nacional de Engenharia Civil, Lisbon, Paper No. 275. (in Portuguese) 278pp.
- Chadwick, A.J., 1989. Field measurements and numerical model verification of coastal shingle transport. *Advances in Water Modelling and Measurement*, Palmer, M H (ed.), BHRA,

- Cranfield, Bedford.
- Chang, T.T. and Wang, Y.H., 1978. Field verification of sediment transport model. Proc. 26th Specialty Conf. of Hydraulics Div., ASCE, University of Maryland, Maryland. pp. 737-744.
- Dean, R.G., 1978. Review of sediment transport relationships and the data base. Proc. of a workshop on coastal sediment transport with emphasis on the National Sediment Transport Study, DEL-SG-15-78. Sea Grant College Program, Univ. of Delaware, Newark, Delaware, pp. 25-39.
- Dean, R.G., Berek, E.P., Bodge, K.R. and Gable, C.B., 1987. NSTS measurements of total longshore transport. Proc. of Coastal Sediments '87, New Orleans, Louisiana, Vol. 1 : 652-667.
- Dean, R.G., Berek, E.P., Gable, C.G. and Seymour, R.J., 1982. Longshore transport determined by an efficient trap. Proc. 18th International Conf. on Coastal Engineering, ASCE, Cape Town. Vol. 2 : 954-968.
- Delorme, J.-L., 1981. Erosion des côtes due à des travaux portuaires et mesures visant à y remédier. Permanent International Association of Navigation Congresses, Edinburgh (in French). Vol. 5 : 771-797.
- Duane, D.B. and James, W.R., 1980. Littoral transport in the surf zone elucidated by a Eulerian sediment tracer experiment. J. Sedimentary Petrology, Vol. 50 (No. 3) : 929-942.
- Fairchild, J.C., 1977. Suspended sediment in the littoral zone at Ventnor, New Jersey, and Nags Head, North Carolina. U.S. Army, Coastal Eng. Research Center, Fort Belvoir, Report TP 77-5. 97pp.
- Fleming, C A, Pinchin, B M and Nairn R B (1986). Evaluation of models of nearshore processes. 20 Intern. Conf. on Coastal Eng., ASCE, Taipei, Taiwan, Volume 2: 1116-1131.
- Gable, C.B., 1981. Report on data from the nearshore sediment transport study experiment at Leadbetter Beach, Santa Barbara, California, Jan-Feb, 1980. Institute of Marine Resources, University of California, IMR Report No. 80-5.
- Hou, H., 1988. Study of shelf waves vs. sand drift in NW coast of Taiwan. Proc. 21st International Conf. on Coastal Eng., ASCE, Malaga. Vol.2 : 1152-1165.
- Hou, H., Lee, C. and Lin, L., 1980. Relationship between alongshore wave energy and littoral drift in the midwest coast at Taiwan. Proc 17th International Conf. on Coastal Eng., ASCE, Sydney. Vol. 2 : 1255-1274.
- Inman, D.L. and Bagnold, R.A. (1963). Littoral processes. The Sea, Vol. 3, The earth beneath the sea. Hill, M.N. (Ed.) Interscience Publ., New York, pp. 529-551.
- Inman, D.L., Zampol, J.A., White, T.E., Hanes, D.M., Waldorf, B.W. and Kastens, K.A., 1980. Field measurements of sand motion in the surf zone. Proc. 17th International Conf. on Coastal Eng., ASCE, Sydney. Vol. 2 : 1215-1234.
- Ishihara, T., Iwagaki, Y. and Murakami, M., 1958. On the investigation of beach erosion along the north coast of Akashi Strait. Coastal Eng. in Japan, Vol. 1 : 97-109.
- Kamphuis, J W and Readshaw, J S (1978). A model study of alongshore sediment transport rate. 16th International Conf. on Coastal Eng, Hamburg. Vol. 2: 1656-1674.
- Kamphuis, J.W., Davies, M.H., Nairn, R.B. and Sayao, O.J., 1986. Calculation of littoral sand transport rate. Coastal Engineering, Vol. 10 : 1-21.
- Kana, T.W., 1977. Suspended sediment transport at Price Inlet, S.C. Proc. of Coastal Sediments '77. Charleston. pp. 366-382.
- Kana, T.W. and Ward, L.G., 1980. Nearshore suspended sediment load during storm and post-storm conditions. Proc. 17th International Conf. on Coastal Eng., ASCE, Sydney. Vol. 2 : 1158-1173.
- Knoth, J.S. and Nummedal, D., 1977. Longshore sediment transport using fluorescent tracer. Proc. of Coastal Sediments '77, Charleston. pp. 383-398.
- Komar, P.D., 1969. The longshore transport of sand on beaches. Ph.D thesis, Scripps Institute of Oceanography, University of California, San Diego.
- Komar, P.D., 1988. Environmental controls on littoral sand transport. 21st International Conf. on Coastal Eng., ASCE, Malaga. Vol. 2 : 1238-1252.
- Komar, P.D. and Inman, D.L., 1970. Longshore sand transport on beaches. J. Geophys. Res., Vol. 76 (No. 30) : 5914-5927.

- Kooistra, J. and Kamphuis, J.W., 1984. Scale effects in alongshore sediment transport rates. Canadian Coastal Sediment Study, Report No. C2S2-13. Kingston.
- Kraus, N.C., Isobe, M., Igarashi, H., Sasaki, T.O. and Horikawa, K., 1982. Field experiments on longshore sand transport in the surf zone. Proc. 15th International Conf. on Coastal Eng., Cape Town, ASCE, Vol. 2 : 969-988.
- Lee K.K., 1975. Longshore currents and sediment transport in west shore of Lake Michigan. Water Resources Research. Vol. II, No. 6 : 1029-1032.
- Laubscher, W.I., Schoonees, J.S. and Swart, D.H., 1989. A calibrated longshore sediment transport model for Richards Bay. CSIR Report EMA-C 89121, Ematek, Stellenbosch.
- Moore, G.W. and Cole, J.Y., 1960. Coastal processes in the vicinity of Cape Thompson, Alaska. Geologic investigations in support of Project Chariot in the vicinity of Cape Thompson, Northwestern Alaska - Preliminary Report. Final Report U.S. Geol. Survey Trace Elements Investigations, Report No. 753.
- Nicholls, J.N. and Wright, P., 1991. Longshore transport of pebbles: Experimental estimates of K. Proc. of Coastal Sediments '91, ASCE, Seattle. Vol. 1 : 920-933.
- Readshaw, W.J.S. (1979). A model study of alongshore sediment transport M.Sc. thesis, Dept. of Civil Engineering, Queen's University, Kingston.
- Sato, S., 1962. Sand movement at Fukue Coast in Atsumi Bay, Japan, and its observation by radioactive glass sand. Coastal Eng. in Japan, Vol. 5 : 81-92.
- Sato, S. and Tanaka, N., 1966. Field investigation on sand drift at Port Kashima facing the Pacific Ocean. Proc. 10th International Conf. on Coastal Eng., ASCE, Tokyo. Vol. 1 : 595-614.
- Schoonees, J S (1994). Longshore sediment transport in terms of the applied wave power concept. PhD thesis, University of Stellenbosch, Stellenbosch (in preparation).
- Schoonees, J S and Theron, A K (1993). Review of the field data base for longshore sediment transport. Coastal Engineering 19:1-25.
- Scripps Institute of Oceanography (1947). A statistical study of wave conditions at five locations along the California Coast. University of California, San Diego, Wave Report no. 68.
- Sireyjol, P., 1964. Communication sur la construction du port de Cotonou (Dahomey). Proc. 9th International Conf. on Coastal Eng., ASCE, Lisbon, (in French) pp. 580-595.
- Swart, D H (1976). Predictive equations regarding coastal transports. 15th International Conf On Coastal Eng, Honolulu, Hawaii. Vol 2: 1113-1132.
- U.S. Army, Corps of Engineers, 1984. Shore Protection Manual, Volumes I and II, Coastal Engineering Research Center, Vicksburg.
- Van Hijum, E and Pilarczyk, K W (1982). Equilibrium profile and longshore transport of coarse material under regular and irregular wave attack. Publikasie Nr 274. Delft Hidroulika-laboratorium, Delft, Holland.
- Van Rijn, L.C. (1984). Sediment transport, Part I: Bed load transport. J. Hydr. Eng., ASCE, Vol. 110 (10): 1431-1456.
- Vitale, P. (1981). Movable-bed laboratory experiments comparing radiation stress and energy flux factor as predictors of longshore transport rate. U.S. Army Coastal Eng. Res. Center, Fort Belvoir, Miscellaneous Report No. 81-4. 94 pp.
- Voitsekhovich, O.V., 1986. Longshore sediment transport - generalized relations and observation data. Ukrainian State Planning, Surveying, and Scientific-Research Institute of Water-Management Construction. Translated from Vodnye Resursy, No. 5, September - October, 1986, pp. 108-115, .
- Wang, Y-H and Chang, T.H., 1978. Littoral drift along bayshore of a barrier island. Proc. 16th International Conf. on Coastal Eng., ASCE, Hamburg. Vol. 2 : 1614-1625.
- Watts, G.M., 1953. A study of sand movement at South Lake Worth inlet, Florida. U.S. Army, Beach Erosion Board, Tech. memo No. 42. 24 pp.

TABLE 1: DATA SET 1

Data set no.	Reference(s)	Location	No of points	Point rating (%)
1	Caldwell (1956)	Anaheim Bay California	5	46
2	Watts (1952)	South Lake Worth	3	42
4	Adachi <i>et al</i> (1959)	Miyazu Japan	8	24
5	Moore and Cole (1960)	Cape Thompson Alaska	1	50
6	Delorme (1981)	North & Central Africa	5	49
8	Sireyjol (1964)	Cotonou Benin	1	51
9	Castanho (1966)	Lobito Angola	2	52
10	Fairchild (1977)	Ventnor (NJ) Nags Head (NC)	2	36 37
12	Bijker (1968)	Ivory Coast Abidjan	1	19
13	Komar and Inman (1970)	El Moreno & Silver Strand	11	62
14	Duane and James (1980)	Point Mugu California	1	56
16	Lee (1975)	Lake Michigan	8	57
17	Kana (1977)	Price Inlet South Carolina	25	48
18	Bruno <i>et al</i> (1981)	Channel Islands Harbour	18	55, 67
21	Inman <i>et al</i> (1980)	Torrey Pines California	2	64
22	Kana and Ward (1980)	Duck North Carolina	2	57
23	Gable (1981) Dean <i>et al</i> (1982)	Leadbetter Santa Barbara	9	68
28	Kooistra and Kamphuis (1984)	Pointe Sapin Canada	2	60, 71
29	Bodge (1986)	Duck North Carolina	8	56,57,61
32	Voitsekhovich (1986)	Ros. Pri. Kin. Black Sea	39	58
33	Chadwick (1989)	Shoreham Sussex England	7	57,60

TABLE 2: DATA SET 2

Data Set 1 plus the following data:

Data set no.	Reference(s)	Location	No of points	Point rating (%)
3	Ishihara <i>et al</i> (1958)	North Akashi Miyazu	10 7	37
7	Sato (1962)	Fukue, Atsumi Japan	5	61
11	Sato and Tanaka (1966)	Port Kashima Japan	2	58
15	Hou <i>et al</i> (1980)	Taichung Harbour Taiwan	4	57
19	Chang and Wang (1978) Wang and Chang (1978)	Santo Rosa Island (Bayside)	35	55
20	Knoth and Nummedal (1977)	North Bull Island	5	52
24	Dean <i>et al</i> (1987)	Rudee inlet Virginia	3	63
25	Nicholls and Wright (1991)	Southern England H. Bury Long Beach Hurst Castle Spit	6	48
26	Kraus <i>et al</i> (1982)	Shi. Hir. Aji. Oar. Japan	12	63
30	Laubscher <i>et al</i> (1989)	Richards Bay South Africa	5	54
34	Hou (1988)	Lin-Kou Northwest Taiwan	1	58

TABLE 3: RELATIVE STANDARD ERROR OF ESTIMATE (σ) AND PERCENTAGE OCCURRENCE OF THE DISCREPANCY RATIOS (r_d) FOR EACH FORMULA

NAME OF FORMULA	NUMBER OF DATA POINTS	σ	PERCENTAGE OCCURRENCE OF r_d BETWEEN:	
			0,5 and 2	0,25 and 4
SPM	119	0,708	42,0	58,0
SPM and Swart	119	0,720	42,0	58,0
SPM, Kamphuis and Readshaw	123	0,515	65,0	95,1
SPM and Bailard (bulk transport rate)	119	0,741	46,2	66,7
Watts	123	0,685	42,2	65,0
Caldwell	123	0,579	56,1	75,6

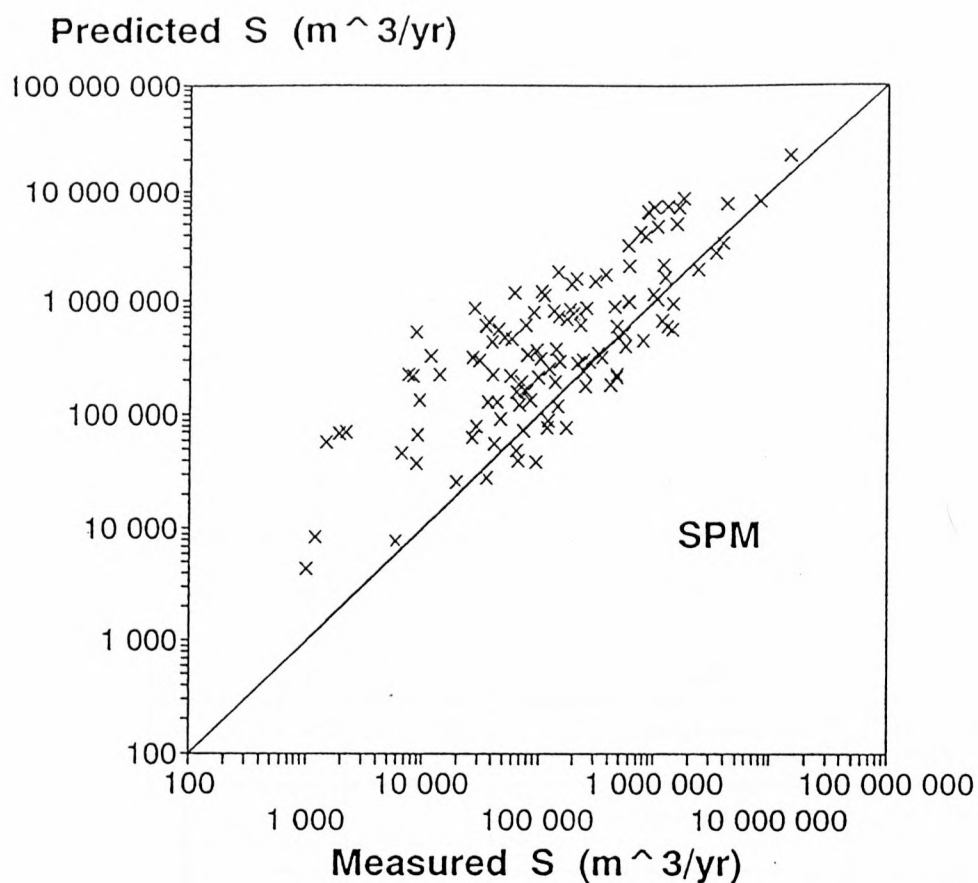


Figure 1: Predicted longshore transport rates versus measured rates for the SPM formula.

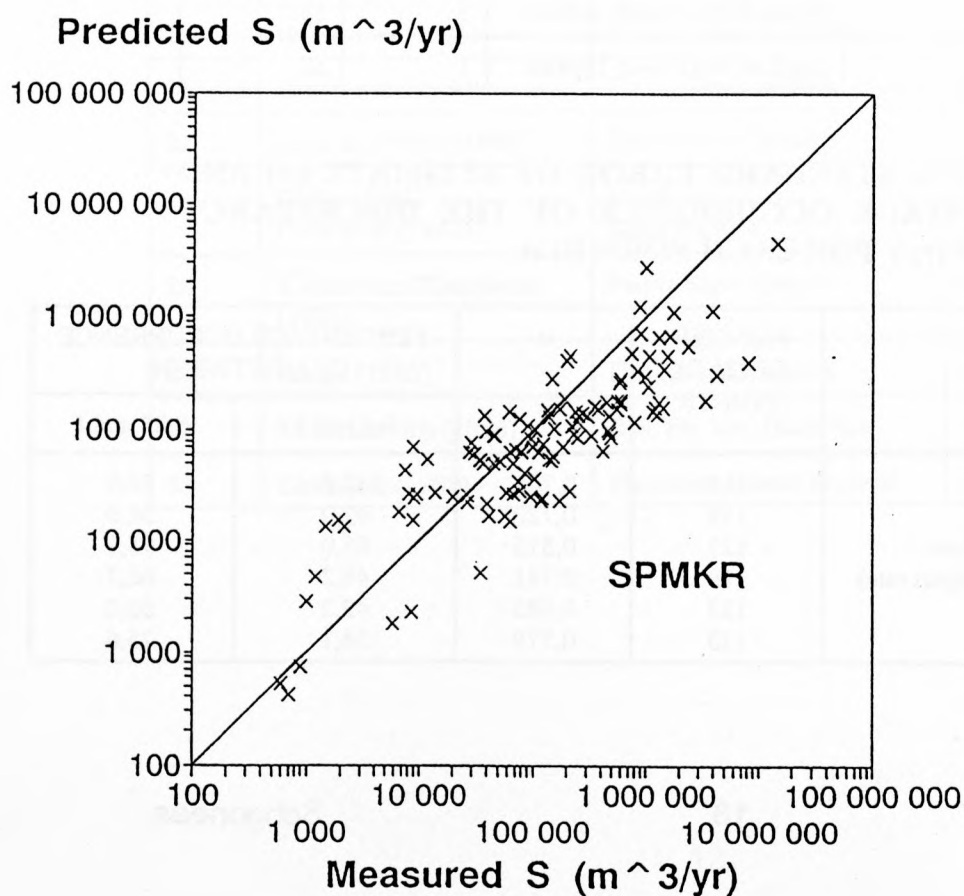


Figure 2: Predicted longshore transport rates versus measured rates for the SPM, Kamphuis and Readshaw formula.

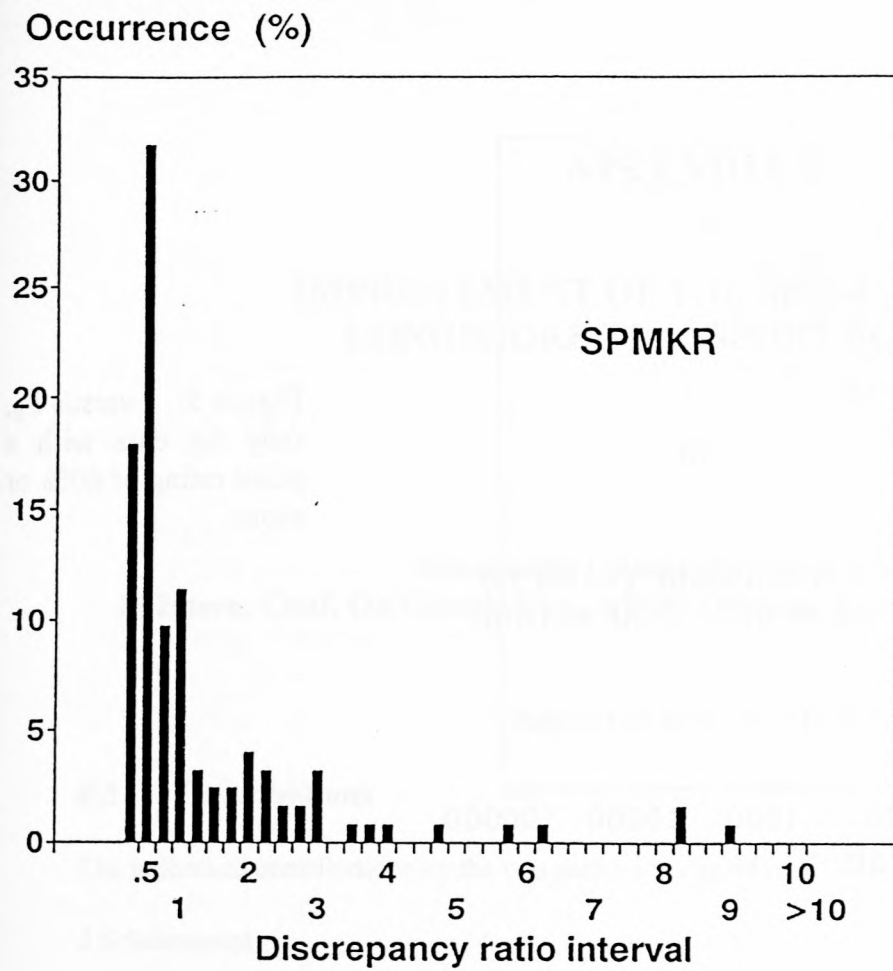


Figure 3: Histogram of the discrepancy ratios for the SPM, Kamphuis and Readshaw formula.

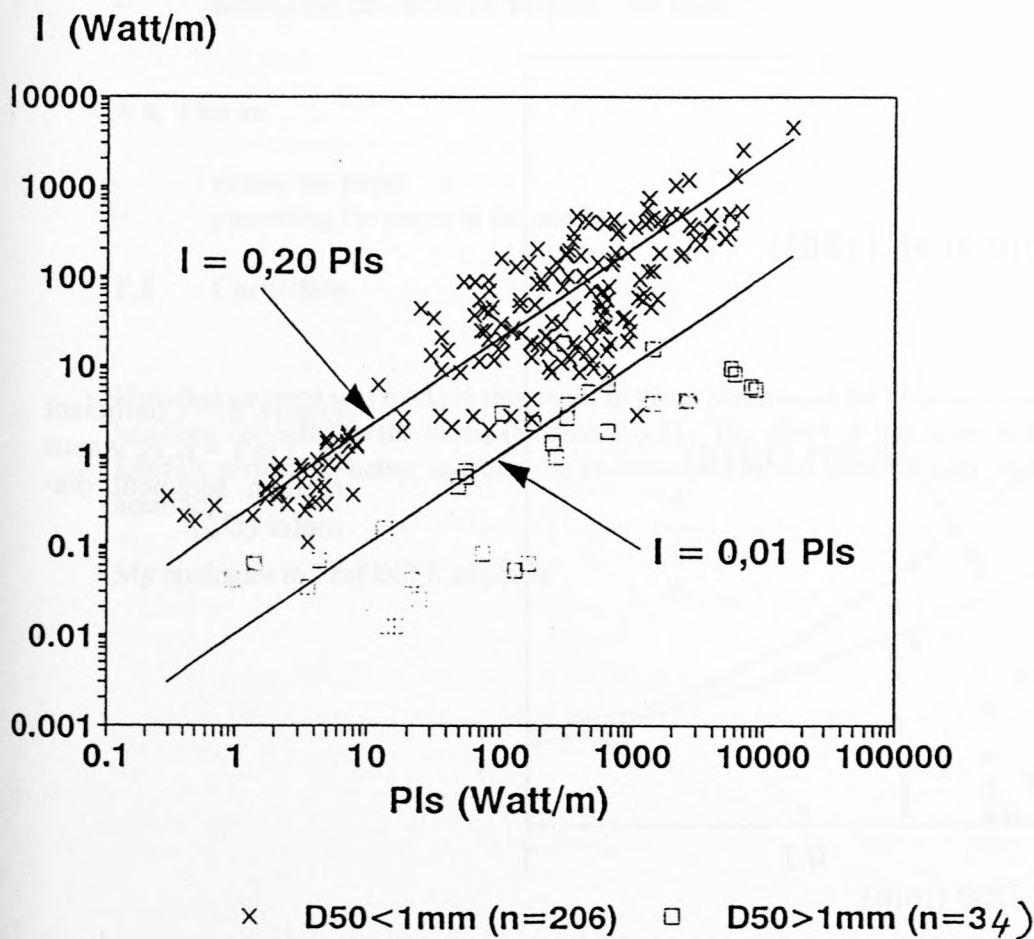


Figure 4: Immersed weight longshore transport rate (I) versus wave energy flux factor (P_b) for Data Set 2.

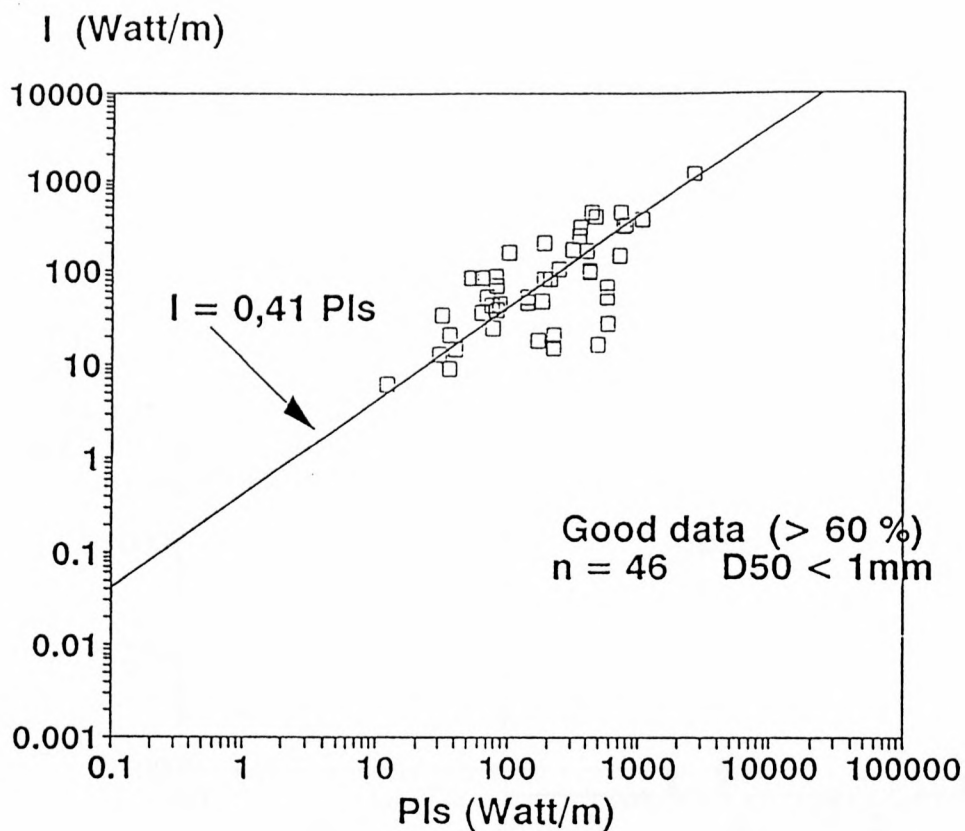


Figure 5: I versus P_{Is} , only for data with a point rating of 60% or more.

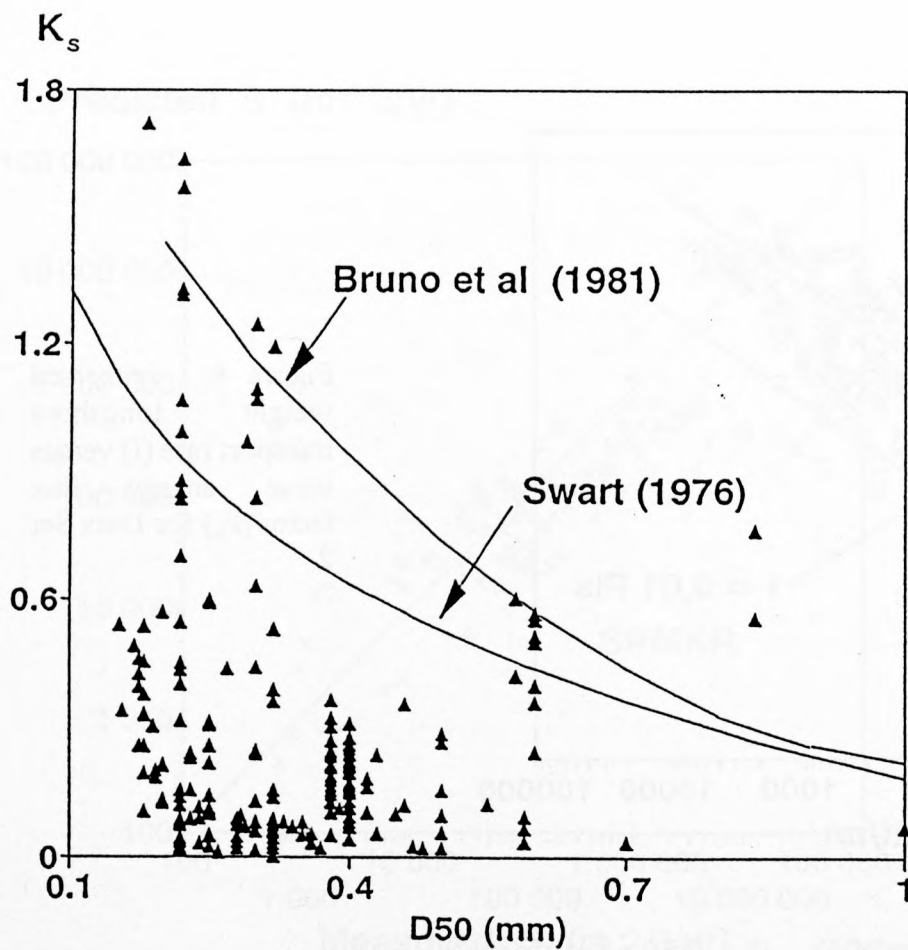


Figure 6: Coefficient (K_s) in $I = K_s P_{Is}$ versus median sediment diameter (D_{50}).

APPENDIX F

IMPROVEMENT OF THE MOST ACCURATE LONGSHORE TRANSPORT FORMULA

by

Schoonees, J S and Theron, A K (1996)

25 Intern. Conf. On Coastal Eng., ASCE, Orlando, Florida, USA, Vol. 3:3652-3665

(Reprinted with permission)

F.1 Contributions

The individual contributions by the two authors are as follows:

J S Schoonees

- evaluation of longshore transport formulae
- testing of the package deal approach
- recalibration of the Kamphuis formula
- confidence intervals for the Kamphuis formula
- writing the first draft of the paper and editing it

A K Theron

- editing the paper
- presenting the paper at the conference

F.2 Correction

Note that an error was made in this paper in the application of the original Kamphuis formula. This error has been corrected in the thesis (Section 4.6.5). The effect of this error is that the original Kamphuis formula performed better and that the recalibration of this formula only slightly improved (by 2%) its accuracy.

My apologies to Prof Bill Kamphuis.

IMPROVEMENT OF THE MOST ACCURATE LONGSHORE TRANSPORT FORMULA

by
J S Schoonees¹ and A K Theron¹

ABSTRACT

The ability to predict the longshore sediment transport rate accurately is essential for many coastal engineering applications. Because of the existence of a large number of existing longshore transport formulae, it is important to know which formula to use/apply. Thus, the most universally applicable formula was identified and tested against a comprehensive data set. This formula (Kamphuis formula) was also re-calibrated and guidance is given regarding its use.

INTRODUCTION

The ability to predict the time-averaged longshore sediment transport rate accurately is essential for the design of breakwaters at harbour entrances, navigation channels and their dredging requirements, beach improvement schemes incorporating groynes, detached breakwaters and beach fill as well as for the determination of the stability of inlets and estuary mouths.

Because of the large number of existing longshore transport formula it is important to know which formula to apply in practice. The aim of this paper is therefore to identify the most universally applicable formula and to test this formula against a comprehensive field data database. Finally, this formula is re-calibrated and guidance is given regarding its use.

The data considered in this paper are only for particulate (non-cohesive) sediment (including sand, gravel and shingle) being transported alongshore from the swash zone across the surf zone to deep water. Bulk (total rate calculated perpendicular to the shoreline) as well as local (at a specific point)

¹Research Engineers, CSIR, P O Box 320, Stellenbosch, 7599, South Africa

point) transport rates are considered. These bulk rates include both the bedload and the suspended load. Only field data are used because laboratory investigations often contain possible scale effects and/or use regular waves. Furthermore, the ultimate aim is to be able to predict longshore transport accurately in the *field* (Komar, 1988).

It is assumed that if a longshore transport formula is capable of predicting transport rates accurately for the wide ranging data sets described herein, it can be used with reasonable confidence at similar sites to determine the long-term longshore sediment transport budget if representative wave and other input parameter data are available. It would of course be preferable to have site-specific calibration data before calculating average long-term transport rates at a specific site.

Previous studies where longshore transport formulae have been tested against data include Swart (1976), Fleming *et al.* (1986) and Kamphuis *et al.* (1986). These studies entailed a relatively small number of formulae and limited data. Schoonees (1996) evaluated 52 formulae against an extensive data base. This paper reports some of the findings of the above-mentioned study, with specific regard to the Kamphuis formula (Kamphuis, 1991).

FIELD DATA ANALYSIS

Schoonees and Theron (1993) compiled and reviewed almost all the available field data on longshore transport (as recorded up to 1993).

The data were collected at a wide variety of sites around the world, yielding a large number of data-points, of which 273 points give bulk transport rates. (This is considerably more than the 41 data points used in the Shore Protection Manual by US Army, Corps of Engineers, 1984). Included in the database are also 184 points which give local transport rates.

A point rating system was devised whereby the quality of the data could be assessed. The recording method and the accuracy thereof as well as the representativeness of the data were taken into account. It was found that this evaluation was done reasonably objectively and consistently (Schoonees and Theron, 1993).

According to this evaluation, the data sets were assigned to three categories, namely, the lower, middle and higher quality categories. Most of the data sets fell in the middle category which exhibited a very gradual increase in the overall accuracy of the data within this category. Distinguishing between short- and long-term bulk transport data yielded similar trends in the accuracy of the data. The highest score achieved in the data evaluation was only 71%, thus reflecting the difficulty of measuring longshore transport accurately.

EVALUATION OF LONGSHORE TRANSPORT FORMULAE

The method used in this study to evaluate the longshore transport formulae, was to compare the predicted longshore transport rates to the measured rates and to calculate the relative standard error of estimate (σ). (For a definition of σ , see Schoonees and Theron (1994)). The lower σ is, the better the predictions by the particular formula. In addition the residuals (e_i = measured transport rate - predicted rate) and the distribution of the discrepancy ratio (r_d = predicted/measured rate) were also determined. (The residuals were plotted against the predicted rates to check whether there are systematic trends in the residuals - these are not shown here (Schoonees, 1996)). The longshore transport formulae were also tested under as many different conditions and at as many sites as possible.

From the above-mentioned field data database, Data Set 1 containing 123 points was extracted (see Schoonees and Theron, 1994 for a full description of Data Set 1). In Data Set 1 all the parameters required for testing the transport formulae are available. This same data set was used to evaluate existing longshore transport formulae as well as a newly derived formula (Schoonees, 1996) based on the applied wave power concept.

It is important to note that the data ranges of Data Set 1 are:

0,058	< H_{bs} (significant breaker height, m)	< 3,400
2,32	< T_p (peak wave period, s)	< 16,60
0,30	< θ_b (breaking wave angle, °)	< 35,00
0,007 (=1/143)	< beach slope	< 0,138 (=1/7,2)
0,154	< D_{50} (median grain size, mm)	< 15,000
600	< S (longshore transport rate, m ³ /year)	< 14 793 000

From the above values it is clear that the data ranges of this data set are quite wide. Most conditions encountered on natural beaches are covered and the data were collected on beaches from a variety of sites from around the world. These factors give credibility to the conclusions drawn in this comparison of predicted versus measured transport rates.

In total, 52 different longshore transport formulae were evaluated (Schoonees, 1996). These formulae were classified into different categories with regard to the theories on which they are based. The following three formulae were found to be the most accurate as tested against Data Set 1:

Order of accuracy	Name of the formula	Relative standard error of estimate (σ)	Category
1	Kamphuis (1991)	0,393	Dimensional analysis
2	Van Hijum, Pilarczyk and Chadwick (1989)	0,417	Energetics (energy flux)
3	Van der Meer (1990)	0,447	Empirical

These formulae are all bulk (total rate) as opposed to detailed predictors. Figures 1, 2 and 3 illustrate the fit of the predicted transport rates against the measured rates (log-log scales).

The formulae were also ranked according to the highest percentage of discrepancy ratios (r_d) between 0,5 and 2 (i.e. under or over prediction by a factor of 2; $r_d = 1$ indicates perfect agreement). A similar ranking of the "best" five formulae was found. However, it was found that σ provides a better way to judge the accuracy of a formula than using the percentage of r_d between 0,5 and 2. This is because, when applying a transport formula to determine a longshore transport budget at a site, a single badly predicted transport rate can distort the calculated budget greatly. At the same time, however, the above-mentioned percentage of r_d can still be very high compared to σ which would be affected greatly by a single badly predicted rate. Therefore σ is a better yardstick.

Dimensional analysis incorporating all relevant variables ensured that the Kamphuis formula contains the most important parameters. The three top formulae (Kamphuis; Van Hijum, Pilarczyk and Chadwick and Van der Meer) are relatively simple. These "simpler" methods performed well probably because a lower degree of inaccuracy is or can be introduced by having fewer (but all the most important) parameters. It is very difficult to acquire accurate input data; and the more parameters incorporated in a formula, the more input data is required (thereby potentially increasing the noise).

It is common practice to compare the predictions from different longshore transport formulae when computing the annual longshore transport regime at a site. Swart and Fleming (1980) advocated the use of a so-called package deal approach. In this approach, the highest and lowest transport rates predicted by six formulae were ignored and the median of the remaining values was determined. The question then remains whether better results can be achieved by means of this or a related method. Three approaches were tried

(Schoonees, 1996). Firstly, by considering the median of the predictions by the five best formulae; secondly, by determining the mean of the three middle values after discarding the highest and lowest predictions; and thirdly, by computing a weighted mean transport of the five predictions. The variation in the transport rates predicted by the five best formulae was investigated. It was found (Schoonees, 1996) that these predictions are reasonably consistent; that is, the individual formulae do not yield excessive outliers. It can therefore be concluded that none of the package deal approaches yield better answers than the best formula (the Kamphuis method) and as such, are not worth pursuing if the above-mentioned five best formulae are used. The reason for this probably lies in the consistency (reliability) of the five best formulae.

RECALIBRATION OF THE KAMPHUIS FORMULA

The Kamphuis formula can be written as follows:

$$\begin{aligned} S &= (31\,557\,600 \cdot 1.3 \cdot 10^{-3}) x_{Kamphuis} \\ &= 41\,024,88 x_{Kamphuis} \text{ (m}^3\text{/yr)} \end{aligned} \quad (1)$$

$$\begin{aligned} x_{Kamphuis} = & \frac{1}{(1 - \rho) \rho_s} \cdot (\rho / T_p) L_o^{1,25} H_{bs}^2 (\tan \alpha_K)^{0,75} \\ & \cdot (1/D_{50})^{0,25} (\sin 2\theta_b)^{0,6} \end{aligned} \quad (2)$$

where ρ = porosity
 ρ_s = density of the sediment grains
 ρ = density of sea water
 L_o = deep-water wavelength
 $\tan \alpha_K$ = beach slope to the breaker line

See Kamphuis (1991) for a more comprehensive definition of all the parameters.

Equation (1), the original Kamphuis formula, is plotted on *linear scales* in Figure 4a and b. Note that Figure 4b shows the detail of Figure 4a for $x_{Kamphuis}$ values up to 80 (instead of 200). The 80%, 90% and 95% confidence intervals for the predicted responses of the original Kamphuis formula are also shown in Figures 4a and b. Despite the fact that the Kamphuis formula fares the best of the 52 formulae tested, it is immediately apparent that the confidence intervals are very wide. For example, at the 80% confidence level, the predicted transport rate for $x_{Kamphuis} = 8,7$ varies between -1 290 000 m³/year and + 2 004 000 m³/year (predicted rate = +357 000 m³/year) - Figure 4b. The coefficient of determination (R^2) is 0,284.

Illustrated in Figure 5 is the best-fit straight line through all the data (called S_{Kamphuis} recalibrated, 1):

$$S = 88\,248 + 61\,892 x_{\text{Kamphuis}} (m^3/\text{year}) \quad (3)$$

If Equation (3) is used, it is evident that the lowest transport rate that can be predicted, is 88 248 m^3/year , which is when $x_{\text{Kamphuis}} = 0$. This is clearly unacceptable, because the transport rate must be zero if $x_{\text{Kamphuis}} = 0$. Furthermore, it can be seen from Figure 4a that there are three main outliers (which fall beyond the 95% confidence limit) and that Equation (3) fits the higher transport rates better than the original Kamphuis formula. Therefore, disregarding the three main outliers and fitting the line through the origin, the following equation is found:

$$S = 75\,549 x_{\text{Kamphuis}} (m^3/\text{year}) \quad (4)$$

This relationship, S_{Kamphuis} recalibrated 2, is shown in Figure 5a and b (the latter Figure 5b again presents the detail of Figure 5a). Although this formula fits the high transport rates well, it over predicts significantly for x_{Kamphuis} values below 10 (Figure 5b). This is caused by two influential points where transport rates higher than $3 \times 10^6 m^3/\text{year}$ were measured (Figures 5a and b). (Remember that the three main outliers, although shown, have not been used in this regression).

To eliminate this problem all the data points (123) were again considered to yield the third regression line, the S_{Kamphuis} recalibrated, 3:

$$S = 63\,433 x_{\text{Kamphuis}} (m^3/\text{year}) \quad (5)$$

This formula fits the data reasonably well over the whole range (Figures 5a and b). It gives virtually the same answers at high x_{Kamphuis} values than the first recalibrated formula Equation (3). It also fits the data at lower transport rates quite well. R^2 is 0,620 and thus Equation (5) explains 62% of the variance in the data (which is a 118% improvement compared with Equation (1)). However, the standard error of estimate (σ) for this formulation is 0,405, which is slightly poorer than the 0,393 of the original Kamphuis equation. The reasons for this apparent contradiction are:

- The least squares approach (Equations (3), (4) and (5)) minimizes $\sum (S_{m,i} - S_{p,i})^2$ while the standard error of estimate (σ) uses $(\log S_{p,i} - \log S_{m,i})^2$. (Subscripts m and p denote "measured" and "predicted" respectively while i is the number of the data point).
- The effect of a few data points with high transport rates act as influential points in the least squares approach. On the other hand, the number of data points at low transport rates play an important role in the value of the standard error of estimate (σ).

To investigate the effect of such low rates on the standard error of estimate, certain data points below a cut-off transport rate were temporarily disregarded and σ re-calculated. The result was the following:

Cut-off measured transport rate (m ³ /year)	Number of data points	σ for $S = 63433 \times x_{\text{Kamphuis}}$ (Equation 5)	σ for the original Kamphuis formula (Equation 1)
0	123	0,405	0,393
5 000	115	0,392	0,393
10 000	106	0,368	0,380
25 000	103	0,365	0,383
50 000	87	0,324	0,377
100 000	68	0,299	0,374

These values have been plotted in Figure 6. It is clear from the above table that except when very low transport rates of less than 5 000 m³/year are included, Equation (5) is superior to the original Kamphuis formulation. Figure 6 shows that the original Kamphuis formula is relatively insensitive to the cut-off transport rate. On the other hand, the standard error of estimate decreases significantly (to only 0,299 compared to 0,374 of the original formula, which is a 20% improvement) for Equation (5), if the cut-off transport rate increases. If a cut-off rate of 50 000 m³/year is applied, σ reduces from 0,377 to 0,324, a 14% improvement. This finding is important because relatively few storm conditions at any site usually contribute the major part of the longshore sediment transport budget. It is therefore important that the higher transport rates are predicted accurately.

In order to obtain an indication of which wave conditions would cause such cut-off transport rates, the following typical values were chosen:

$T_p = 10\text{s}$, $\theta_b = 2^\circ$, $D_{50} = 0,3\text{ mm}$ and $\tan\alpha = 1/25 (= 0,04)$. It was also assumed that these wave conditions will occur throughout the year.

Using the *original* Kamphuis formula, the longshore transport was then computed for a range of wave heights:

H_{bs} (m)	Longshore transport rate ($S_{Kamphuis}$) ($m^3/year$)
0,1	2 007
0,3	18 067
0,5	50 187
0,7	98 366

For this particular (typical) case, it is clear that relatively low wave heights of about 0,5 m and 0,7 m will already cause transport rates of about 50 000 $m^3/year$ and 100 000 $m^3/year$ respectively. For these cut-off rates, the standard errors of estimate are 0,299 and 0,324 respectively (Figure 6). Equation (5) is therefore judged to be "good".

Instead of using the least squares approach, the question may also be asked: What value of K will cause the minimum standard error of estimate (σ) when using *all* the data points? That is, K in:

$$S = Kx_{Kamphuis} \quad (m^3/year) \tag{6}$$

Computations with different K values yielded the following:

K	σ
30 000	0,438
41 025 (Equation (1))	0,393
45 000	0,388
48 000	0,387
49 000	0,387
50 000	0,387
55 000	0,391
64 433 (Equation (5))	0,405
70 000	0,420

These data have been plotted in Figure 7. From this figure it is evident that the minimum standard error of estimate(s) is 0,387. It can also be seen that σ is not very sensitive with regard to the value of K near the turning point: $\sigma = 0,387$ even if K varies from 48 000 to 50 000. Taking the accuracy of predicted transport rates during storms into account, the preferred (rounded off) equation is:

$$\begin{array}{lll} S & = & 50\,000 \times x_{\text{Kamphuis}} \text{ (m}^3\text{/year)} \\ \text{with } R^2 & = & 0,397 \end{array} \quad (7)$$

FINAL RECOMMENDATIONS

The least squares as well as the minimum standard error of estimate approaches were used to recalibrate the Kamphuis formula, yielding Equations (5) and (7) respectively. Finally the recommended procedure for calculating longshore sediment transport is as follows:

For obtaining bulk longshore transport rates, it is recommended that **Equation (5)** be applied at sites where the significant wave heights normally exceed say, 0,3 m and where the sediment grain size is usually less than 1 mm; that is, at partially protected and exposed sites (i.e. relatively high transport rates). Only at sites where very calm conditions prevail and/or where the sediment is coarse, is **Equation (7)** expected to yield better answers. The considerably higher R^2 for Equation (5) compared with the corresponding value for Equation (7) supports the preference for Equation (5). A significant improvement of 118% according to R^2 and up to 20% in σ in the predicted transport rates was obtained.

REFERENCES

- Chadwick, A J (1989). Field measurements and numerical model verification of coastal shingle transport. *Advances in Water Modelling and Measurement*, Palmer, M H (ed), BHRA, Cranfield, Bedford.
- Fleming, C A, Pinchin, B M and Nairn R B (1986). Evaluation of models of nearshore processes. *20 Intern. Conf. on Coastal Eng.*, ASCE, Taipei, Taiwan, Vol 2: 1116-1131.
- Kamphuis, J W (1991). Alongshore sediment transport rate. *J. Waterways, Port, Coastal and Ocean Eng.*, ASCE, Vol. 117(6): 624-640.
- Kamphuis, J W, Davies, M H, Nairn, R B and Sayao, O J (1986). Calculation of littoral sand transport rate. *Coastal Engineering*, Vol 10: 1-21.
- Komar, P D (1988). Environmental controls on littoral sand transport. *21st Intern. Conf. on Coastal Eng.*, ASCE, Malaga. Vol 2: 1238-1252.
- Schoonees, J S (1996). Longshore sediment transport in terms of the applied wave power concept. *PhD thesis*, University of Stellenbosch, Stellenbosch (in preparation).
- Schoonees, J S and Theron, A K (1993). Review of the field data base for longshore sediment transport. *Coastal Engineering* Vol. 19: 1-25.
- Schoonees J S and Theron, A K (1994). Accuracy and applicability of the SPM longshore transport formula. *24 Intern. Conf. on Coastal - Eng.* ASCE, Kobe, Japan. Vol 3: 2595-2609.
- Swart, D H (1976). Predictive equations regarding coastal transports. *15th Intern. Conf on Coastal Eng.* ASCE, Honolulu, Hawaii. Vol 2: 1113-1132.
- Swart, D H and Fleming, C A (1980). Longshore water and sediment movement. *17th Intern. Conf. on Coastal Eng.*, ASCE, Sydney. Vol 2: 1275-1294.
- U S Army, Corps of Engineers (1984). *Shore Protection Manual*, Volumes I and II, Coastal Engineering Research Center, Vicksburg.
- Van der Meer, J A W (1990). Static and dynamic stability of loose materials. In: *Coastal protection*, Pilarczyk K W (ed), Balkema, Rotterdam.

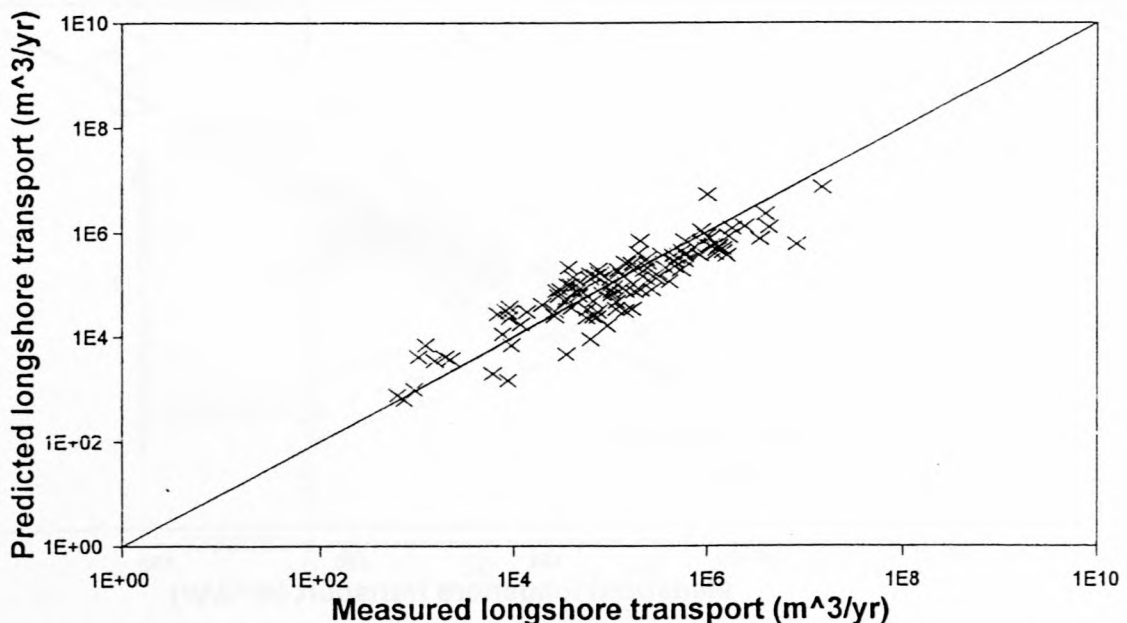


Figure 1: Predicted versus measured longshore transport rates for the Kamphuis formula

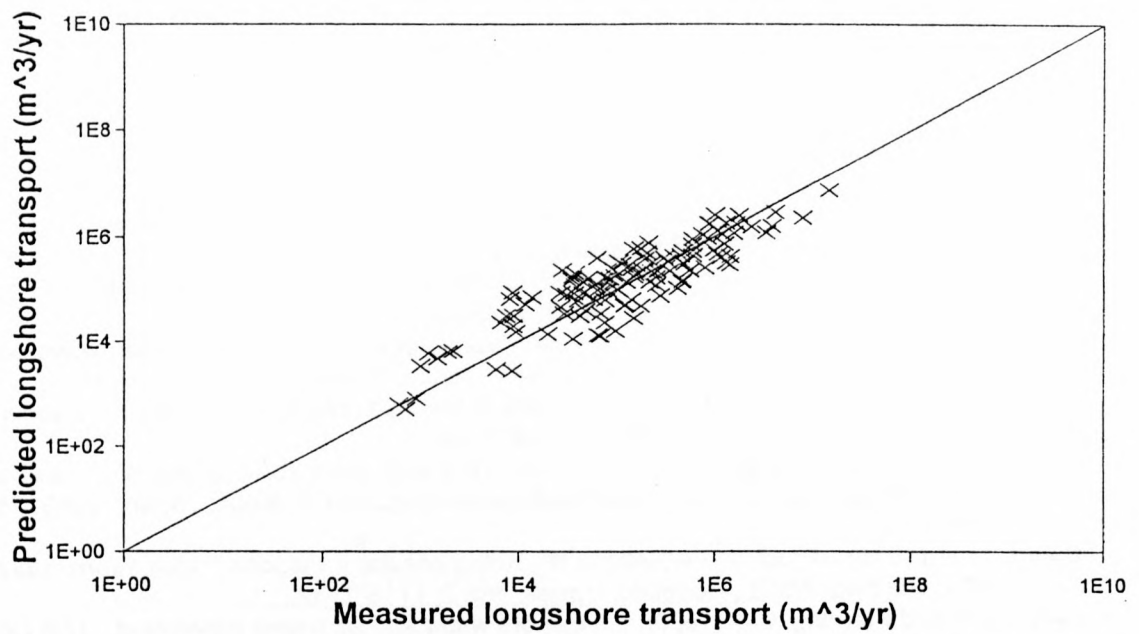


Figure 2: Predicted versus measured longshore transport rates for the Van Hijum, Pilarczyk and Chadwick formula

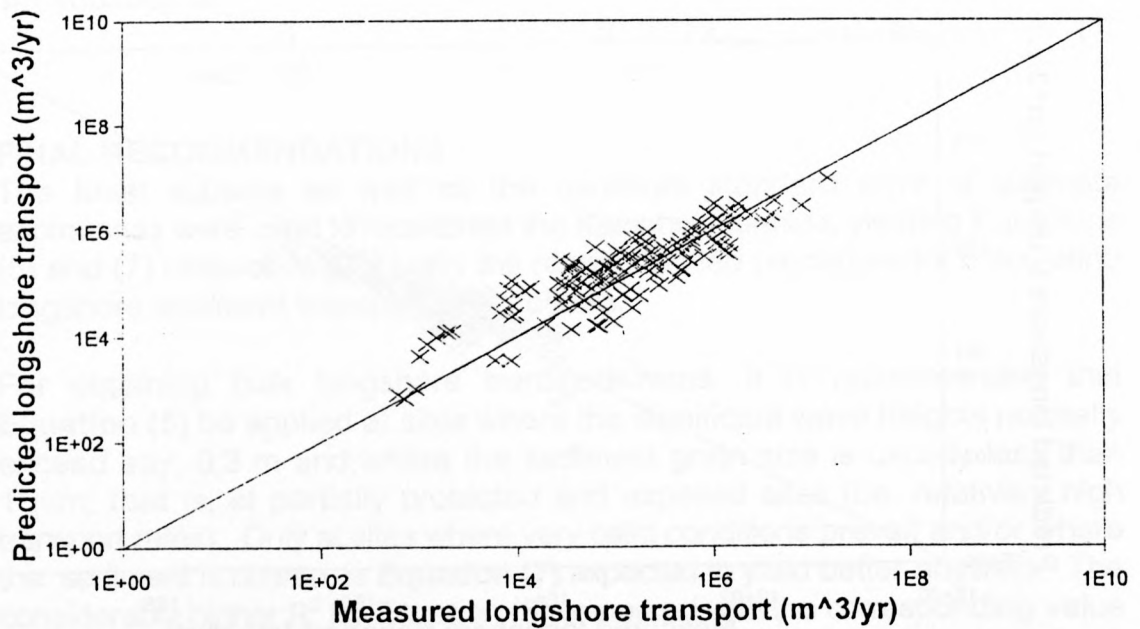


Figure 3: Predicted versus measured longshore transport rates for the Van der Meer formula

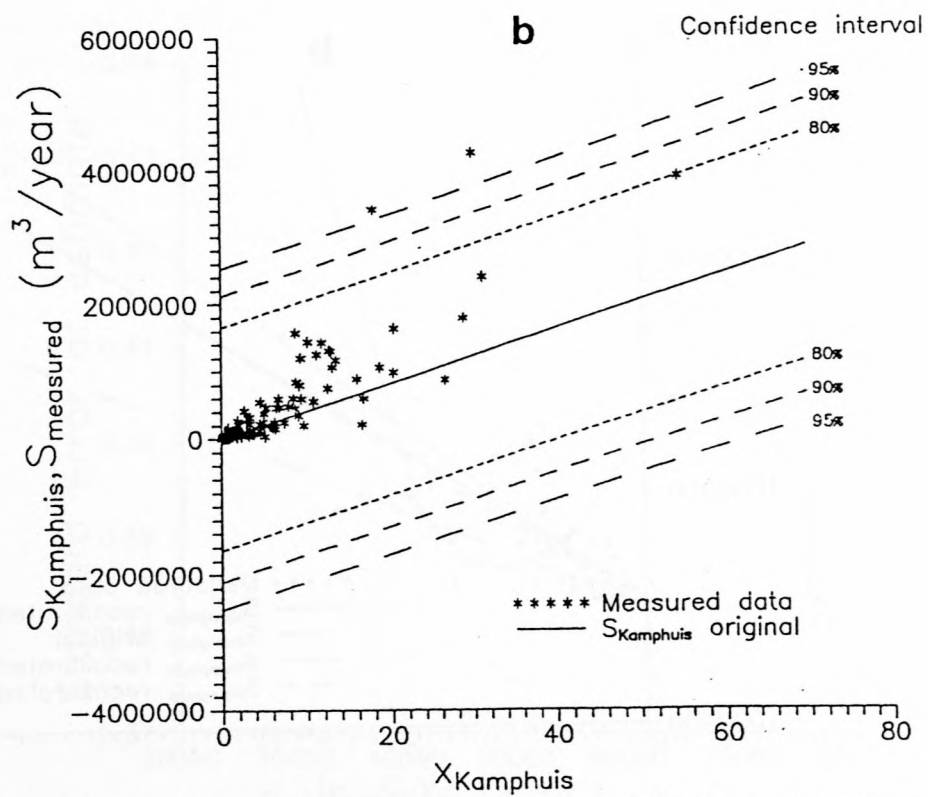
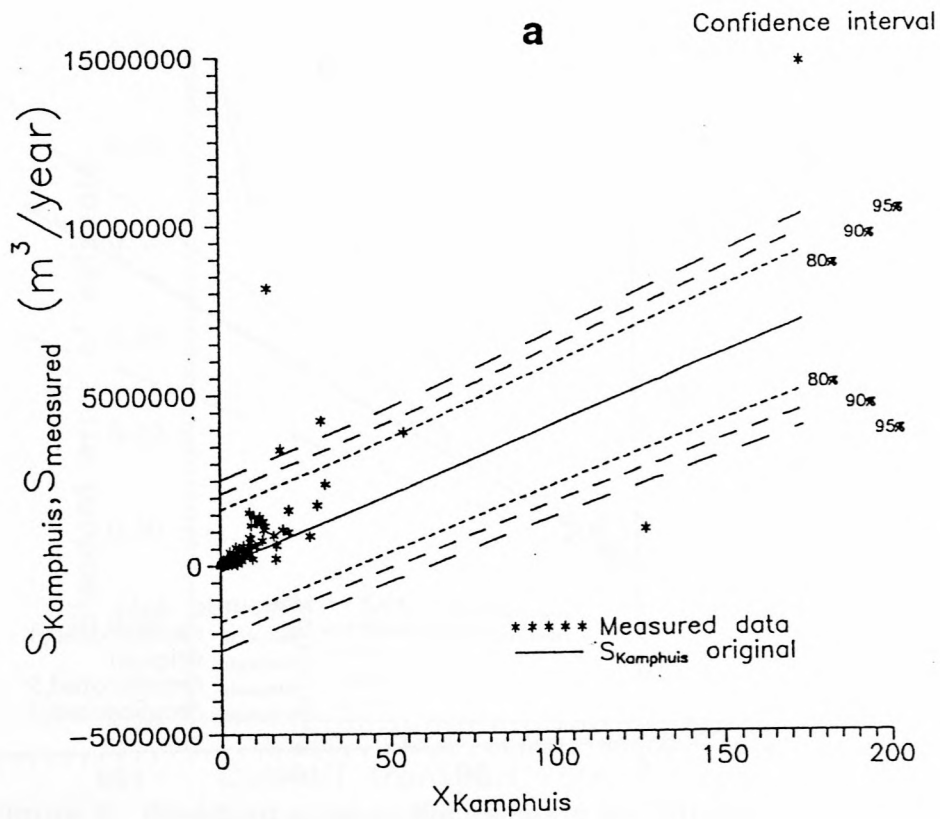


Figure 4: Confidence intervals for the original Kamphuis Formula

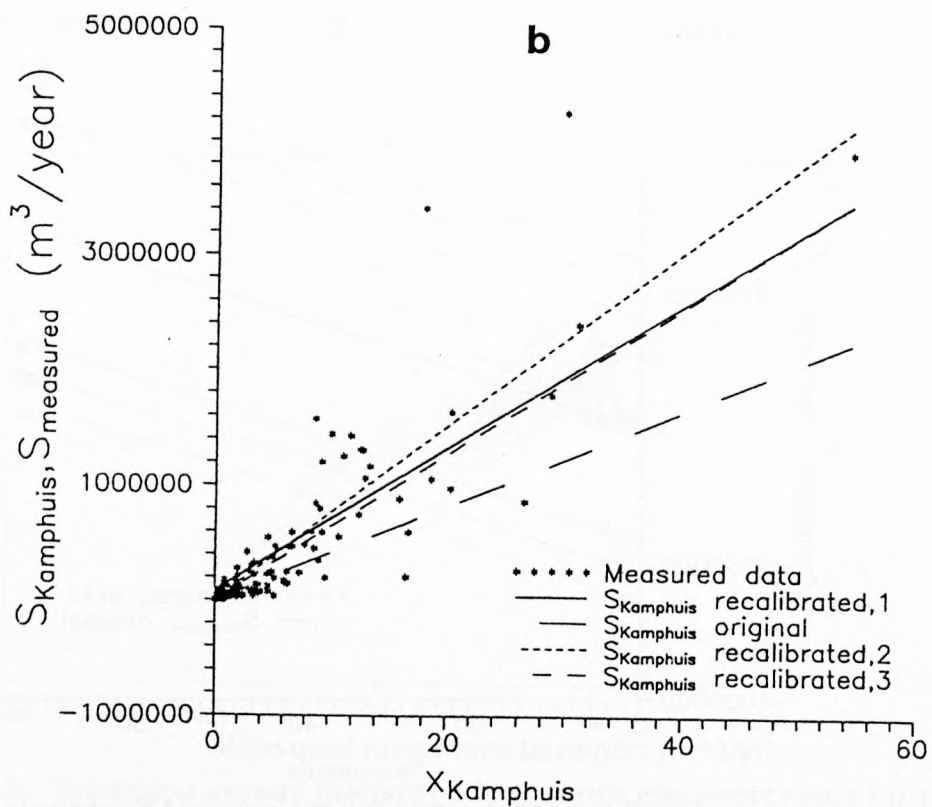
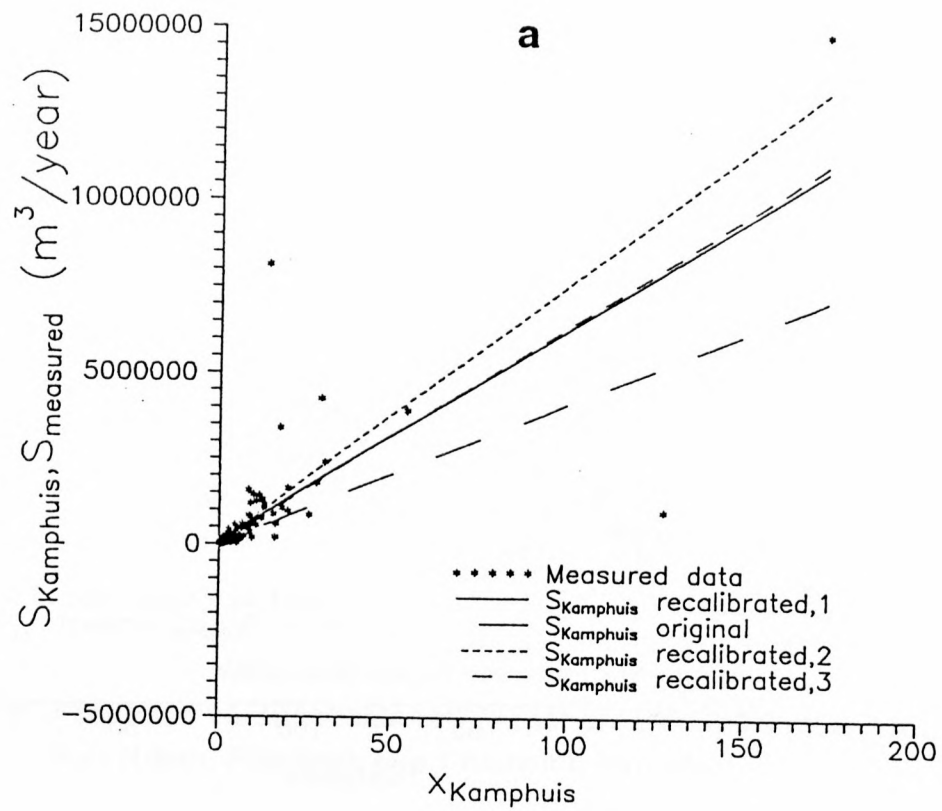


Figure 5: Recalibration of the kamphuis formula

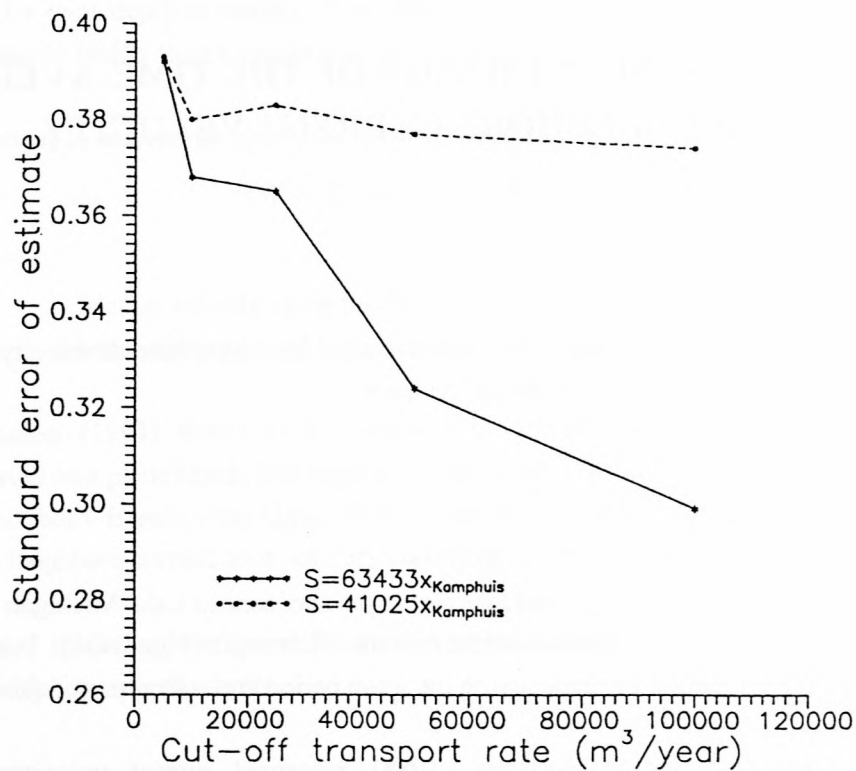


Figure 6: Standard error of the estimate for different cut-off rates

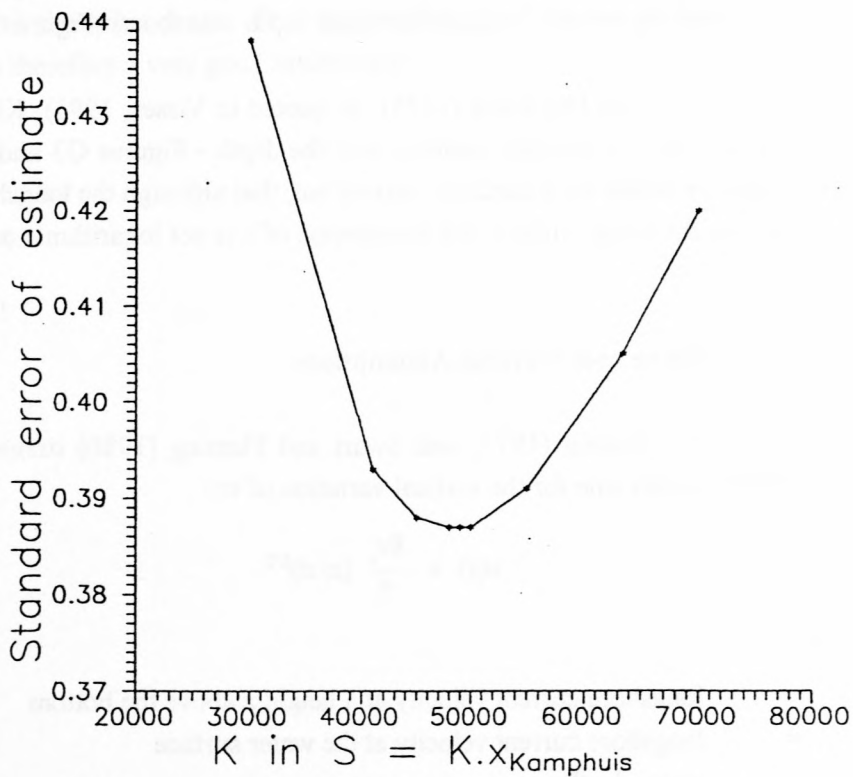


Figure 7: Minimizing the standard error of estimate for the Kamphuis formula

APPENDIX G

VERTICAL DISTRIBUTION OF THE TIME-AVERAGED LONGSHORE CURRENT VELOCITY

G1 General

To examine the vertical distribution of the time-averaged longshore current velocity(v), it is necessary to consider both measurements and theoretical evidence.

G2 Measurements

Meadows (1976) measured the longshore current in the surf zone in Lake Michigan with ducted impeller flowmeters. He found that v is almost constant over the water depth (Figure G1). In addition, fluctuations in v occurred within a period coincident with the wave period and a long period (about 80 s).

Isobe (1983) (as discussed in Horikawa, 1988), measured current velocities in the field with electromagnetic current meters in and beyond the surf zone. Averaging was done over 20 minutes and between 2 and 5 instruments were used at a specific measuring position. Irrespective of the current magnitude, an almost constant velocity through the water depth was found (Figure G2).

In the laboratory, Mizuguchi and Horikawa (1978) (as quoted in Visser, 1991), Kim *et al.* (1986) and Visser (1991) all found that v is virtually uniform over the depth - Figures G3 and G4. Visser (1991) showed in his experiments which were carefully carried out, that although the longshore current velocity is somewhat higher near the water surface, the distribution of v is not logarithmic as is the case in open channel flow .

G.3 Theoretical Evidence and Previous Assumptions

Fleming and Hunt (1976), Fleming (1977) and Swart and Fleming (1980) *assumed* for the sake of simplicity a one-seventh power rule for the vertical variation of v :

$$v(z) = \frac{8v_s}{7} (z/d)^{1/7}$$

where $v(z)$ = longshore current velocity at a height z above the bottom
 v_s = longshore current velocity at the water surface
and d = water depth

Svendsen and Lorentz (1989) determined theoretically the three-dimensional velocity variation over depth in combined undertow and longshore currents. They concluded that v is not logarithmically distributed but

G.2

that the variation of v over depth is modest. Furthermore they state that a uniform velocity over depth would be much closer to reality than a logarithmic profile.

Nairn (1990), however, in analogy to open channel flow assumed a logarithmic vertical distribution:

$$v(z) = 2,5 u_* \ln (30 z/r)$$

where u_* = friction velocity using the O'Connor and Yoo (1988) method
 r = bed roughness

Dong and Anastasiou (1991) found in a numerical model of longshore currents generated by monochromatic waves on a plane beach, that outside the surf zone, v is uniform over depth. Inside the surf zone, they predicted that v is somewhat higher at the water surface. Generally speaking, however, they concluded that the longshore current does not vary considerably over the water depth.

Therefore theoretical investigations (apart from arbitrary assumptions) also indicate a near constant longshore current velocity over the depth.

G.4 Conclusion

Based on measurements and theoretical evidence, it is clear that the longshore current velocity is almost constant throughout the water depth. That is, from the top of the boundary layer to the water surface. Taking $v = v_{gem}$ is therefore a very good assumption.

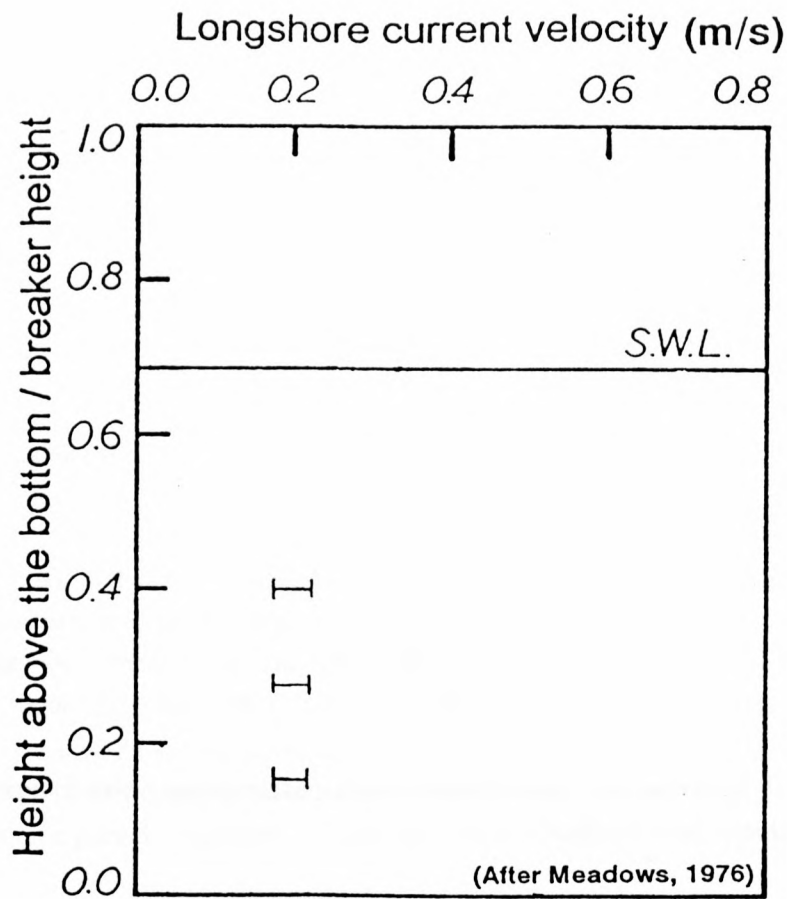


Figure G1: Measured longshore current velocity fluctuations over the water depth

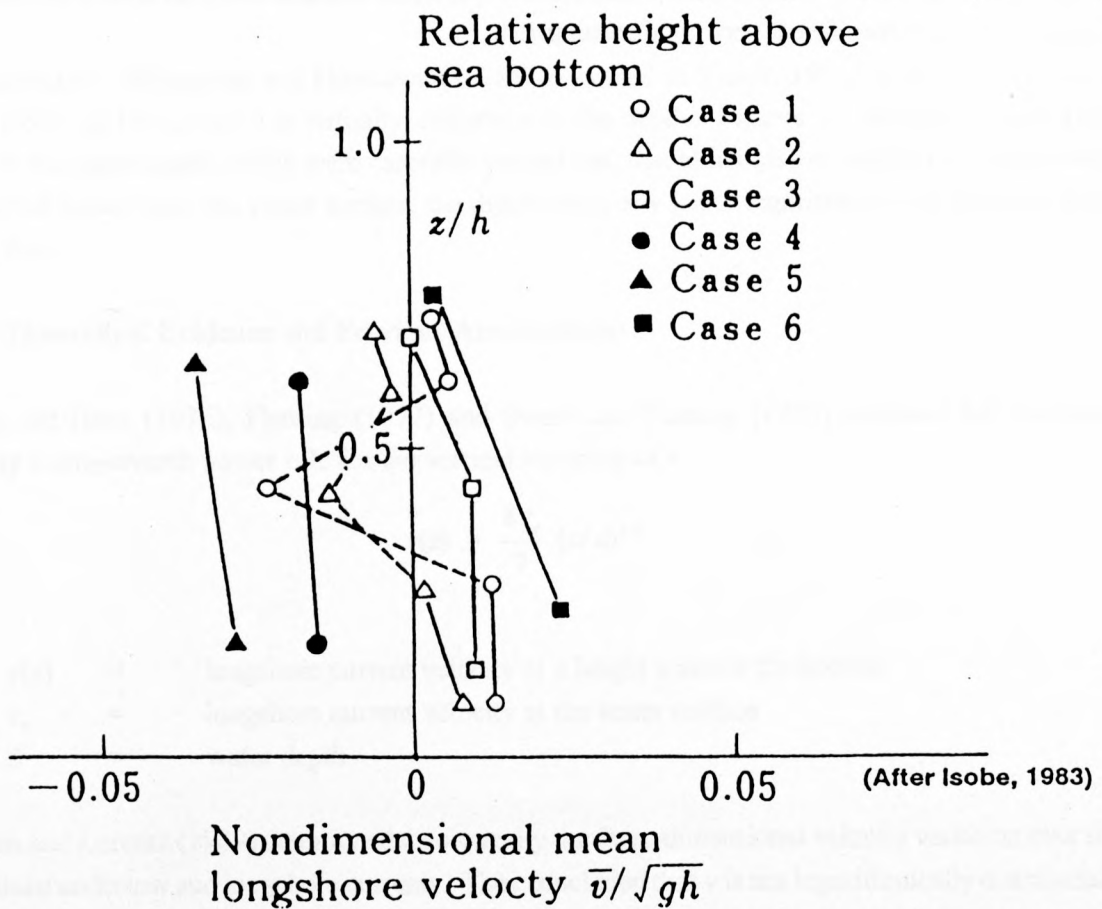


Figure G2: Vertical distribution of the mean longshore current velocity

APPENDIX H

SEDIMENT CONCENTRATIONS : EXTRAPOLATION METHOD, CONSISTENCY OF THE DATA AND DETAILED CALIBRATIONS

H.1 Extrapolation Method

Van Rijn (1991) described three possible methods to extrapolate the concentration measurements (profile) to the bed in order to determine a mean sediment concentration. (The bed is taken to be situated half the bedform height below the crest of the bed form - Figure H1). Methods 1 and 2 give respectively a lower and an upper limit (Van Rijn, 1991). On the other hand, Method 3 (which was used in this thesis) gives a realistic estimate because it uses an exponential extrapolation and it is known that the concentration is distributed exponentially through the depth. Van Rijn (1991) explains Method 3 as follows:

“The sediment concentrations between the bed and the first measuring point are represented by (Figure H1):

$$C = e^{Az+B} \text{ for } 0 < z < z_1 \quad (H1)$$

in which:

z = height above bed
 A, B = coefficients.

The A and B coefficients are determined by a linear regression method applying the measured concentrations of the first three measuring points above the bed, as follows:

$$A = \frac{3\sum_1^3(z_k \ln C_k) - \sum_1^3(z_k)\sum_1^3(\ln C_k)}{3\sum_1^3(z_k z_k) - (\sum_1^3 z_k)^2}$$
$$B = \frac{\sum_1^3(z_k z_k)\sum_1^3(\ln C_k) - \sum_1^3(z_k)\sum_1^3(z_k \ln C_k)}{3\sum_1^3(z_k z_k) - (\sum_1^3 z_k)^2}$$

$$(k = 1, 2 \text{ or } 3)$$

Applying Equation (H1), the sediment concentrations are computed in 50 (equidistant) points between the bed (defined at $z = 0$ m) and the first measuring point ($z = z_1$). The maximum concentration is assumed to be 1 590 kg/m³.

The depth-integrated suspended sediment load (Ls3) is computed as:

$$Ls3 = \sum_{i=1}^N 0,5 (C_i + C_{i-1})(z_i - z_{i-1})$$

in which:

C_i = sediment concentration at height z_i above bed
 N = total number of points (including extrapolated values)".

The mean time-averaged concentration over the depth (C_{gem}) is then:

$$C_{gem} = Ls3/d \quad (H2)$$

(d = water depth)

H.2 Consistency of the Sediment Concentration Data

Nielsen (1984) measured sediment concentrations repeatedly in the field and Dette and Uliczka (1986) measured the same in the big wave flume in Hannover. The data from these consistency runs are given and analysed in Table H1. Figures H2 to H4 illustrate these repeated concentration measurements as well as two other examples (Figure H5). (In these latter two examples the concentrations were not measured at exactly the same heights above the bed and could therefore not be included in Table H1).

From Table H1 it is evident that the percentage variation (= 100 times the standard deviation/mean concentration) ranges from 12,9% to 148,7% with a mean value of 38,5%. For the field data of Nielsen (1984) there is apparently no significant change in the percentage variation over the depth. The opposite is true for the laboratory data of Dette and Uliczka (1986): the accuracy increases with the elevation above the bed. However, the data are too limited to draw firm conclusions about the trends with height above the bed. The factor (f_c) = maximum concentration/minimum concentration at a particular elevation varies between about 1,4 and 19,9 with an average value of approximately 3,2 (Table H1). It can therefore be concluded that an error band of about 38,5% exists around the mean measured concentrations; or, the ratio between the maximum and minimum concentration can be expected to be on average approximately 3,2. This means that even if a particular theoretical model is perfect, it can only be calibrated against these data to be accurate within an average factor of 3,2.

Naturally the question now arises as to what are the reasons for these large variations in measured concentrations. These reasons can be summarized as:

- A certain length of record (sampling interval) is required to obtain a proper time-averaged concentration. In a study undertaken in a wave (water) tunnel, Nakato (1974) found that he had to sample over about 100 cycles to obtain a reasonably steady average concentration. For commonly occurring waves in the field, this means the following:

Wave period (s)	Sampling interval (minutes)
5	8,3
10	16,7
12	20,0
15	25,0
20	33,3

Because wave breaking in the surf zone causes larger variations in concentrations than in Nakato's wave tunnel data, the above-mentioned sampling intervals should be regarded as minimum values. However, Nielsen (1984) typically sampled over 3,5 minutes. Schoonees (1990) compared concentrations taken over an hour with concentrations from samples which were pumped over 10

minutes to 15 minutes. The former data exhibited much less scatter. It is therefore recommended that the sampling interval should not be less than 30 minutes (preferably an hour or longer). This recommendation resulted in a significant improvement in the consistency of concentration measurements during a subsequent field exercise (CSIR, 1995).

- Nielsen (1984) attributed the large difference in concentration profiles (Figure H5) to temporal variations in the bottom configuration. He showed that there is almost no change in water motion (Figure H6). Whilst the concentrations varied considerably (Figure H5), Bosman and Steetzel (1986) and Nielsen (1979) also showed that the concentration profile differs above the crests or troughs of bedforms and that averaging is required for consistent results.
- Another important factor is that beach profile changes take place as environmental conditions vary. In this process the bed armours itself (for example, by forming sand bars) until an equilibrium profile is attained. Dette and Uliczka (1986) found even after the profile had reached equilibrium, that the profile shape fluctuated around this equilibrium profile and that the location of each breaker influences the concentration in a random way.
- If different methods are used to measure the concentrations (as was done to obtain the data in Van Rijn, 1991), then the efficiency (Bosman, 1982) and the disturbance of the flow among others, may differ from instrument to instrument.
- Another source of inaccuracy is the extrapolation of the concentration profile to the bed because the mean concentration is dependent on this procedure.

H.3 Initial Calibration of the Mean Concentration (Inside the Surf Zone) for the Applied Wave Power Method

General

$$C_{gem} = a_2 (D_b/d)^{e_1} \quad (H3)$$

As explained in Chapter 5, the model which will be calibrated is:

where	C_{gem}	=	time- and depth-averaged sediment concentration
	D_b	=	energy dissipation per unit time and area due to wave breaking
	d	=	water depth
and	e_1	=	$a_1 w/u_*$
with a_1 and a_2 being calibration coefficients.			
	w	=	sediment fall velocity
	u_*	=	shear velocity

Initially it was assumed that $a_1 = 2,089$. This means that the value of a_1 is identical in the surf zone as in river flow. Figures H7 to H10 shows the results of the Dean, Battjes and Janssen, Dally *et al.* and Morfett methods, respectively. When comparing these figures, the following can be seen:

- Considerable scatter is evident on all these figures. However, the method by Battjes and Janssen appears to be the most promising and it was felt that the value of a_1 should be optimized for this method.
- Figures H7, H9 and H10 contain considerably fewer data points than in Figure H8. This is because the methods by Dean, Dally *et al.* and Morfett requires the beach slope. Unfortunately the database by Van Rijn (1991) only gives the local bottom slope around the location where the measurement was done. Some of the original references give the general beach slope (or a beach profile) in the surf zone and the required slope can thus be obtained. Not all the original references could be found, thus limiting the number of data points. In addition, for the derivation based on the Dally *et al.* (1985) approach, Equations (5.33) or (5.37) - see Chapter 5 - in a few cases either not produced a solution for the breaker height or gave an unrealistic answer (e.g. the local wave height in the surf zone is higher than the breaker height).
- The outliers in Figures H7 and H9 are points 754, 755 and 758 where Dette and Uliczka (1986) measured concentrations under regular waves. For regular waves it was assumed in these figures that the significant wave height for irregular waves was equivalent to the mean wave height for regular waves. Because the root-mean-square wave height (H_{rms}) represents the energy of the wave spectrum and the mean wave height likewise for regular waves, it can be argued they are equivalent. Since $H_s = \sqrt{2} H_{rms}$, it was tested whether better correlations could be obtained with $H_s = \sqrt{2}$ (mean wave height). This approach resulted in a reduction in the scatter as shown in Figures H7 and H9; however, it was not a significant improvement. This idea was therefore not pursued further.

Testing whether the concentration is related to the difference between D_b and the energy dissipation under equilibrium conditions

Because Kriebel and Dean (1984) and Kriebel (1990) related the cross-shore transport rate to a factor ($D_b - D_{eq}$) and obtained reasonably good predictions, it was decided to test the following similar hypothesis:

$$C_{gem} = a_2(D_{b,Dean}/d - D_{eq}/d)^{0.1} \quad (H4)$$

with $D_{eq} =$ wave energy dissipation per unit area under equilibrium conditions. That is, if the beach profile is concave (Dean, 1977) : $y = Ax^{0.67}$

$$= 5\rho g^{1.5}\gamma^2 A^{1.5}/24 \quad (H5)$$

and D_b is computed from Equation (5.28) in Chapter 5.

where

y	=	vertical co-ordinate of the profile
x	=	horizontal co-ordinate of the profile (runs from the still-water line seawards)
A	=	constant depending on the sediment grain size or fall velocity
γ	=	breaker index
	=	significant breaker height/depth at the breaker line

Figure H11 illustrates the results: considerable scatter is apparent. This approach was therefore not pursued further.

Optimizing a_1 and a_2 for the Battjes and Janssen method

Marquart's maximum neighbourhood method (Daniel and Wood, 1980) was used to optimize the values of a_1 and a_2 . Figure H12 shows the results if all the data points are retained. Because it appears that three outliers are present (numbers 147, 588 and 592) which contribute significantly to the scatter, the calibration was repeated without these three points. The following equation with 33 degrees of freedom was found:

$$C_{gem} = 0,047 \cdot 10^{-3} (D_{b,BJ}/d)^{1,94w/u} \quad (H6)$$

Figure H13 illustrates that a reasonably good fit is obtained with $a_1 = 1,94$. Compared with Figure H12, the higher concentrations are also predicted better (Figure H13).

The ranges of the data are reasonably wide as can be seen from the following:

0,45	<	H_s (m)	<	2,20
4,1	<	T_p (s)	<	18,5
0,78	<	d (m)	<	3,4
0,170	<	D_{50} (mm)	<	0,330
0,0085	<	C_{gem} ($\times 10^{-3} m^3/m^3$)	<	1,4074

The data were also collected from seven different investigations at a variety of sites and as such, are reasonably representative of a wide range of conditions.

Kamphuis (1995) found differences in a comparison between two- and three-dimensional (3D) beach profiles. He attributed the differences to local turbulence induced by the head-on collision of the incoming breaking wave with the down-rush from the previous wave for the 2D case. In the 3D tests, this phenomenon is much less pronounced. It can therefore be argued that only field data should be considered. Another possible reason for using only field data, is to eliminate the effect of using only regular waves (instead of wave spectra).

If only field data on suspended sediment concentrations are used, the equation for C_{gem} (Figure H14) is:

$$C_{gem} = 0,060 \cdot 10^{-3} (D_{b,BJ} / d)^{1,94 w/u} \quad (H7)$$

H.4 Detailed Calibration of the Mean Concentration (Outside the Surf Zone) for the Applied Wave Power Method

General

As explained in Chapter 5, the model which will be calibrated is:

$$C_{gem} = a_2 (D_f/d)^{e_1} \quad (H8)$$

where $e_1 = a_1 w/u$.

with a_1 and a_2 two calibration coefficients.

Initial calibration and assessment of the accuracy of two outliers

Again the data compiled by Van Rijn (1991) were used - see Section 5.4. Initially the ripple dimensions were

computed with the Van Rijn (1991) method and $a_1 = 2,089$ (as for river flow) was assumed. By using the measured ripple dimensions only minor changes in $(D_f/d)^{e1}$ were found. This indicates in a qualitative way that the Van Rijn (1991) method is accurate. Henceforth measured ripple dimensions were used if available. If not, the Van Rijn (1991) method was applied.

Figure H15 shows the results (above each point its number (or id) is given). From this figure it is apparent that there is considerable scatter. The two main outliers are Points 8 and 51, both from Nielsen (1984). Fortunately, Nielsen measured at virtually the same positions and during almost the same conditions a number of times (Nielsen, 1984). Points 6 to 8 and 48 to 54 were done in this way. Points 7 and 8 and 49 and 51 especially can be directly compared:

Parameter	Point Number			
	7	8	49	51
H_s (m)	0,47	0,44	0,62	0,49
T_p (s)	9,7	9,8	12,4	11,8
d (m)	1,42	1,29	1,22	1,21
ripple height (m)	0,150	0,150	0,080	0,075
ripple length (m)	0,500	0,500	0,600	0,500
C_{gem} (m^3/m^3)	0,2406	0,6660	0,0597	0,8036

Note the similarity in the wave and seabed conditions as given in the table above. This is also the case for Points 6 to 8 and 48 to 54 as presented by Nielsen (1984). Despite the similarity, the values of C_{gem} vary considerably, namely from 0,2406 to 0,6660 for Points 7 and 8 (a factor of 2,8) and between 0,0597 and 0,8036 (a factor of 13,5) for Points 49 and 51. From Figure H15 it can be seen that the mean concentrations of Points 6 and 7 and Points 48 to 54 (excluding 51) are similar despite some scatter. It can therefore be concluded that the accuracy of Points 51 and 8 is highly questionable. What then are the causes for their inaccuracy? As discussed above and in Section 5.4, it is hypothesised that the sampling period is too short considering the temporal variation in sediment concentrations due to small changes in the bed configuration. Measurement error can also not be ruled out totally. Consequently, Points 51 and 8 were left out in the calibration that follows.

Data ranges

The ranges of the data consisting of 47 remaining data points outside the surf zone were as follows:

0,20	≤	H_s (m)	≤	1,55
4,6	≤	T_p (s)	≤	16,6
1,10	≤	d (m)	≤	3,00
0,110	≤	D_{50} (mm)	≤	0,500
0,0111	≤	C_{gem} ($\times 10^{-3} m^3/m^3$)	≤	0,3400
0,095	≤	H_s/d	≤	0,589

The data therefore covers a reasonably wide range.

Final calibration

If the value of a_1 is also optimized, the following equation is found (Figure H16):

$$C_{\text{gem}} = 0,051 \cdot 10^{-3} (D_f/d)^{1,16w/u*} \quad (3.49)$$

However, in order to improve the fit, it was investigated whether a_2 was a function of the local surf similarity parameter, or the factor H_s/L , or the factor H_s/d . The best result was obtained by the H_s/d factor. Although the scatter is still large (Figure 5.8), a line was fitted through the data giving:

$$a_2 = 0,15 \cdot 10^{-3} (H_s/d) \quad (H10)$$

Figure 5.9 illustrates the measured versus the predicted mean concentrations in which

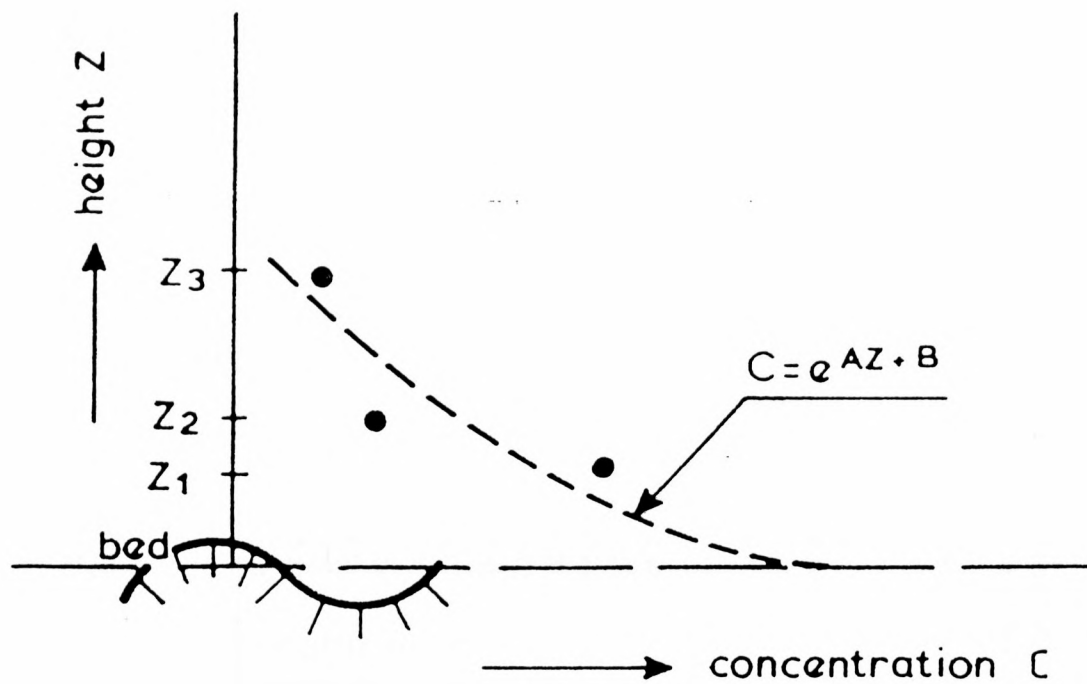
$$C_{\text{gem}} = 0,15 \cdot 10^{-3} (H_s/d) (D_f/d)^{1,16w/u*} \quad (3.51)$$

This figure (note the linear scales) shows that despite some scatter, this equation can predict the mean concentrations reasonably well over quite a wide range of conditions.

Table H1: Consistency of Repetitive Time-Averaged Concentration Measurements

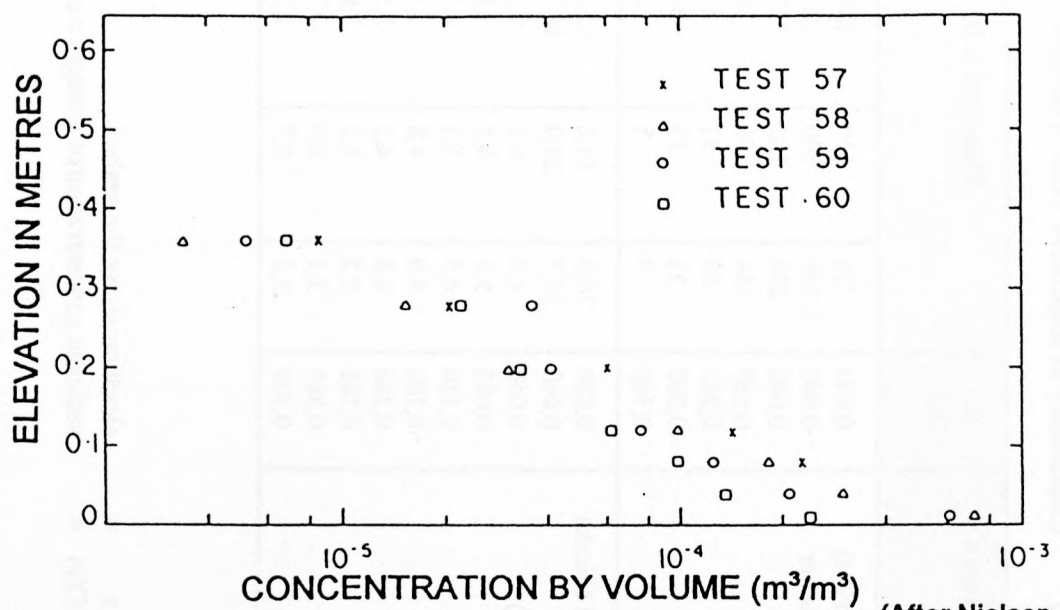
Reference	Z (m)	Measured C (z)			Mean C(z)	Standard deviation s _d	% variation = 100 s _d /mean C(z)	$f_c = \frac{\text{Maximum } C(z)}{\text{Minimum } C(z)}$
Nielsen (1984) (C in parts per million)	0,010	720	610	240	523,3	251,5	48,1	3,00
	0,040	2 700	300	210	836,5	1 244,1	148,7	19,85
	0,080	230	182	127	159,3	58,6	36,8	2,35
	0,120	134	99	76	92,8	31,4	33,9	2,16
	0,200	60	31	41	41,3	13,2	21,1	1,94
	0,280	21	15	36	21,0	10,7	50,8	3,00
	0,360	9	3	5	6,0	2,6	43,0	3,00
	0,020	20,6	43,6	42,4	31,6	13,2	41,8	2,21
	0,040	10,7	23,0	16,7	17,8	5,4	30,4	2,15
	0,060	4,3	8,0	6,1	7,6	3,3	43,0	2,77
Dette and Uliczka (1986) (C in g/l)	0,085	5,4	6,5	4,9	6,5	1,9	28,9	1,86
	0,110	4,5	5,2	4,3	5,3	1,3	24,2	1,65
	0,160	4,0	4,8	3,9	5,0	1,5	30,1	1,82
	0,260	3,8	4,3	3,5	4,3	0,9	20,6	1,57
	0,385	3,2	3,1	2,9	3,3	0,5	16,0	1,41
	0,585	3,1	2,9	2,7	3,1	0,4	13,9	1,37
	0,910	2,5	2,7	2,2	2,6	0,3	12,9	1,36
Mean							38,5	3,15
Standard deviation							30,6	4,34

(Note: z = elevation above the seabed
C(z) = sediment concentration at a height z above the bed.)



(After Van Rijn, 1991)

Figure H1: Extrapolation of the concentration profile (Method 3)



(After Nielsen, 1984)

Figure H2: Four successive profiles measured over well-developed vortex ripples in a bar trough

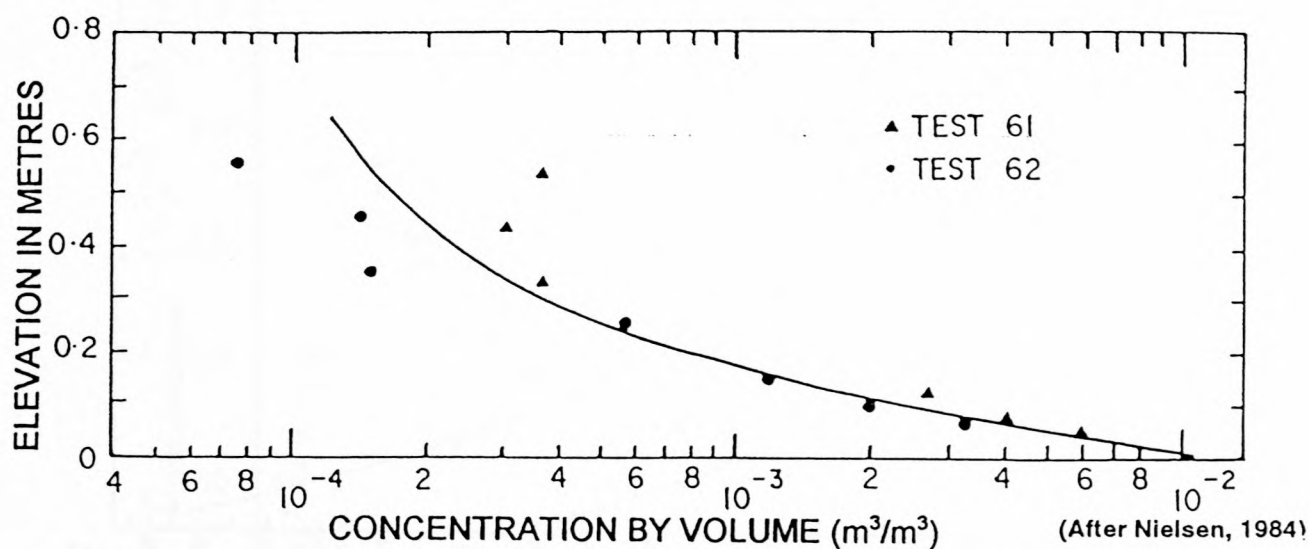


Figure H3: Concentrations measured over a flat bed under plunging breakers

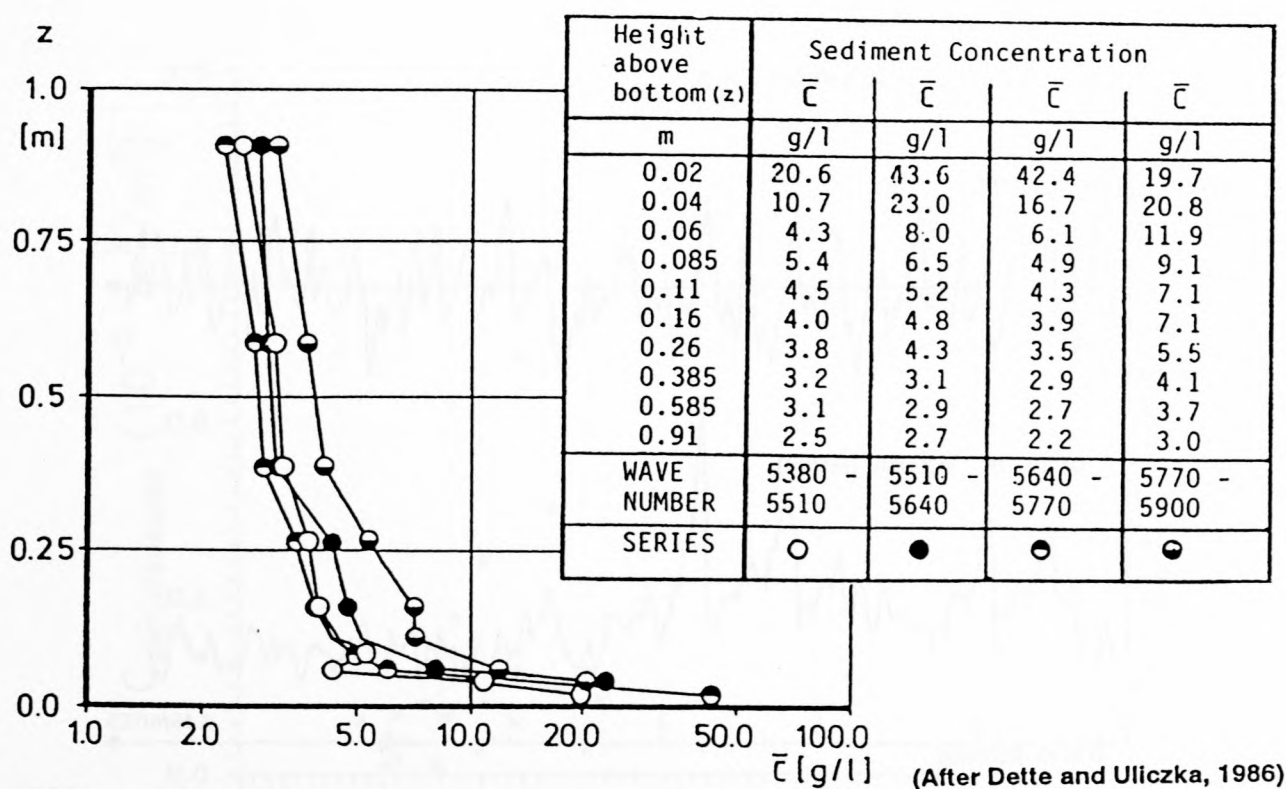
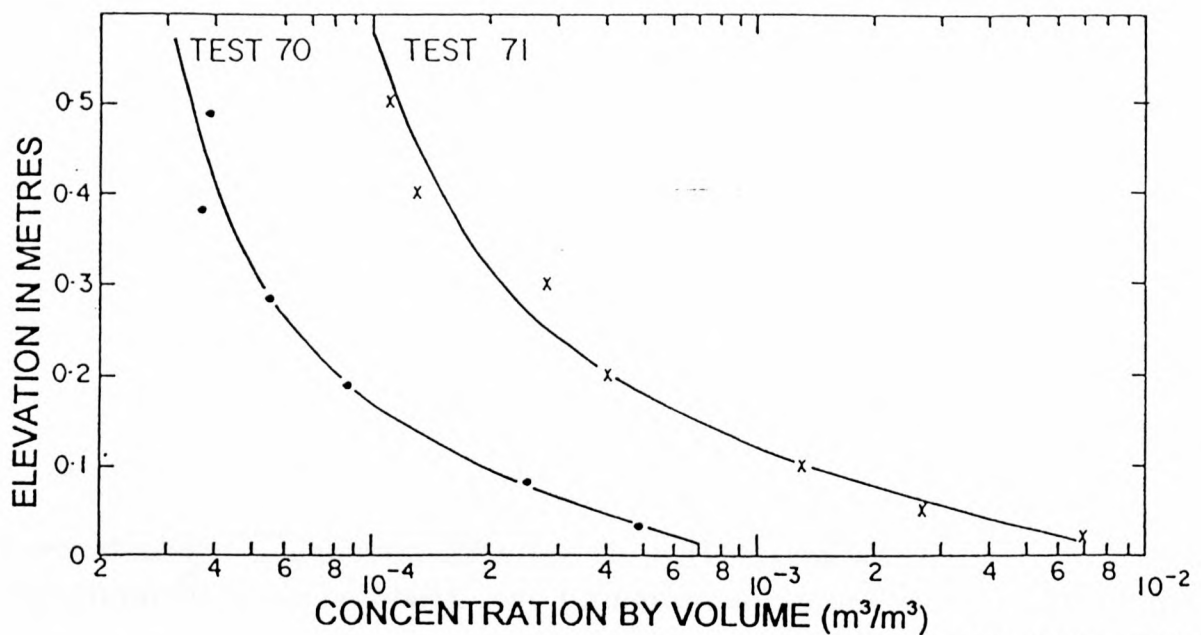
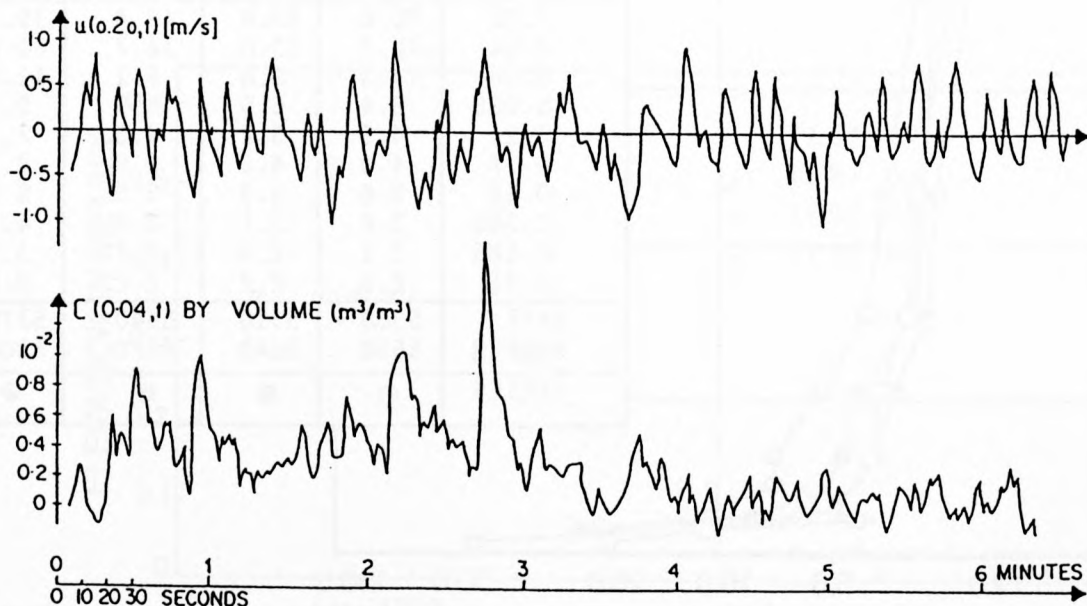


Figure H4: Repeated concentration measurements at the same position over the quasi-equilibrium profile developed from the dune without foreshore and Jonswap wave spectrum



(After Nielsen, 1984)

Figure H5: Two concentration profiles measured under identical wave conditions at the same location, over megaripples. The level of activity has changed considerably due to the temporal variation of the megaripple pattern



(After Nielsen, 1984)

Figure H6: Simultaneous time series of shore-normal velocities (u) and instantaneous sediment concentrations (C). For the first 3 minutes, the area around the sediment detector was much more active than during the last half of the record. There is no corresponding change in the water motion, so the change must be due to subtle changes in the megaripple topography.

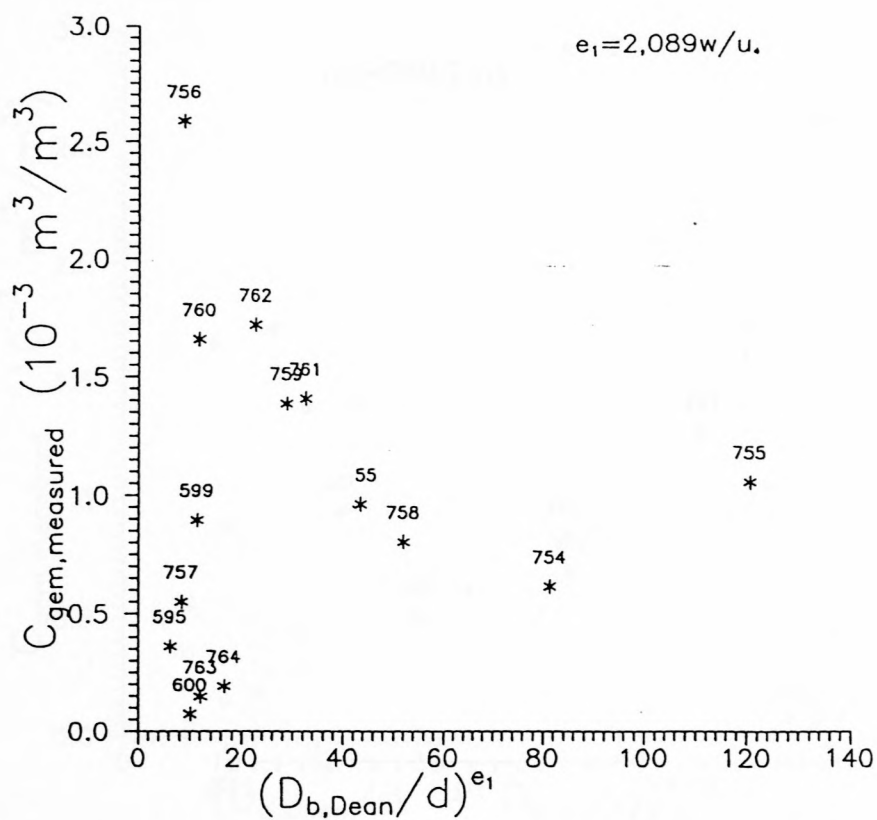


Figure H7: Measured mean concentration as a function of the energy dissipation per unit time and volume to the power e_1 (Dean method)

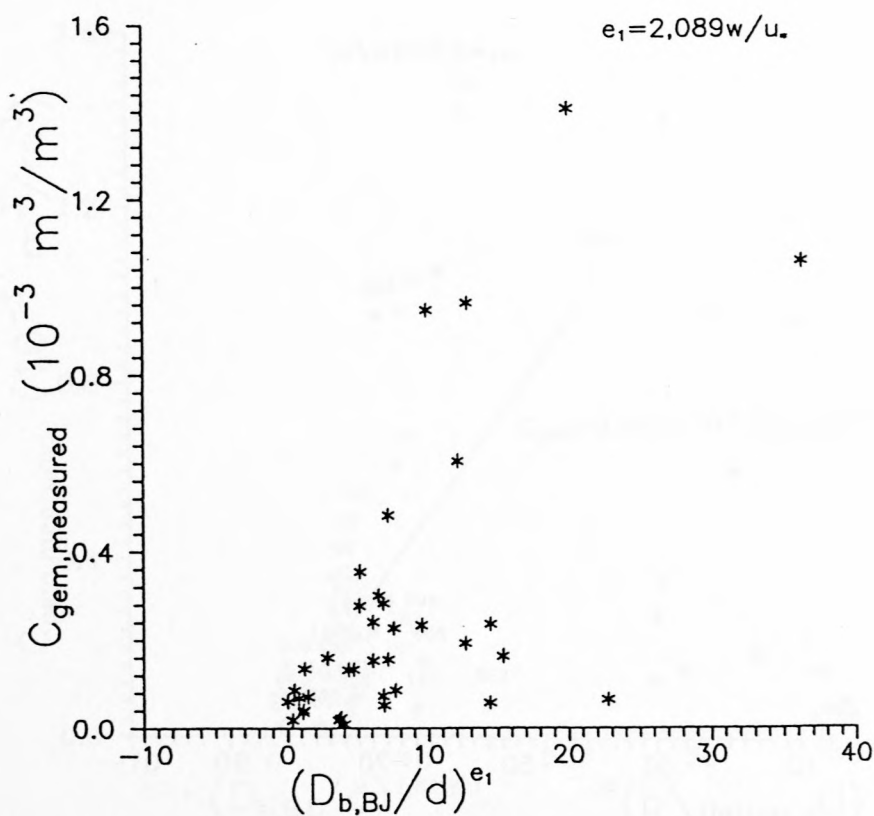


Figure H8: Measured mean concentration as a function of the energy dissipation per unit time and volume to the power e_1 (Battjes and Janssen method)

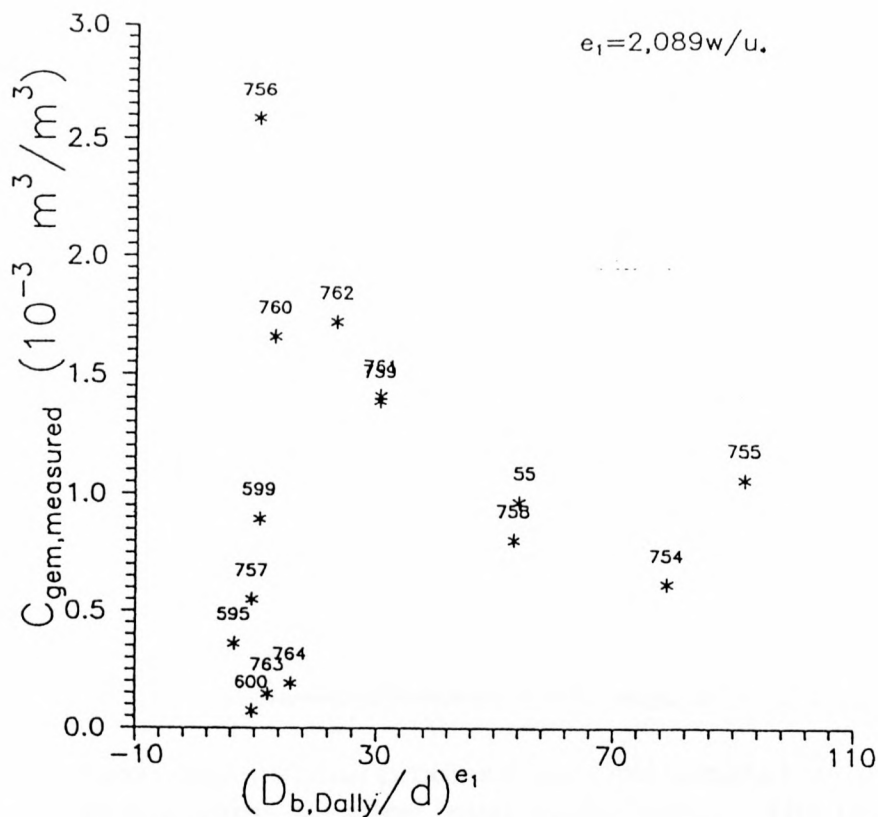


Figure H9: Measured mean concentration as a function of the energy dissipation per unit time and volume to the power e_1 (derived from the Dally method)

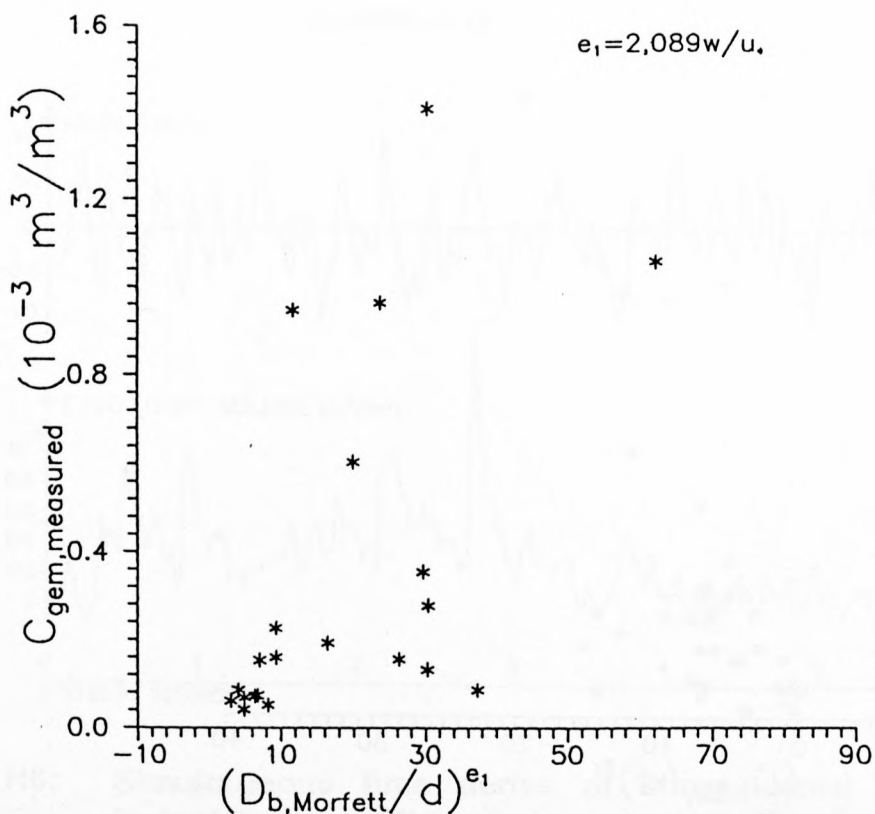


Figure H10: Measured mean concentration as a function of the energy dissipation per unit time and volume to the power e_1 (Morfett method)

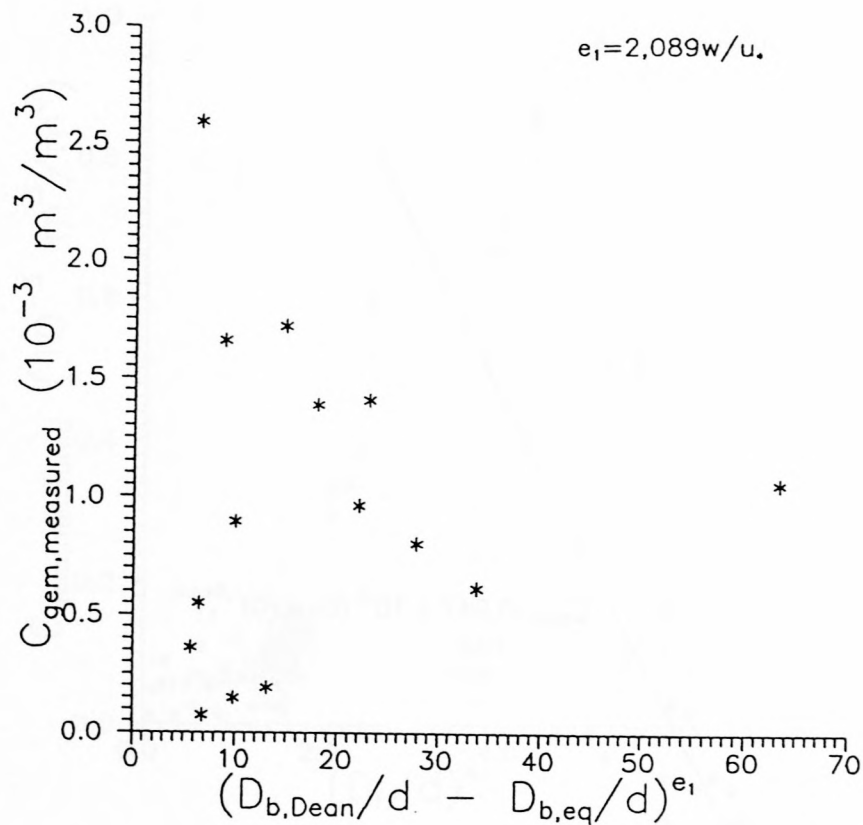


Figure H11: Measured mean concentration as a function of $(D_{b,Dean}/d - D_{b,eq}/d)^{e_1}$

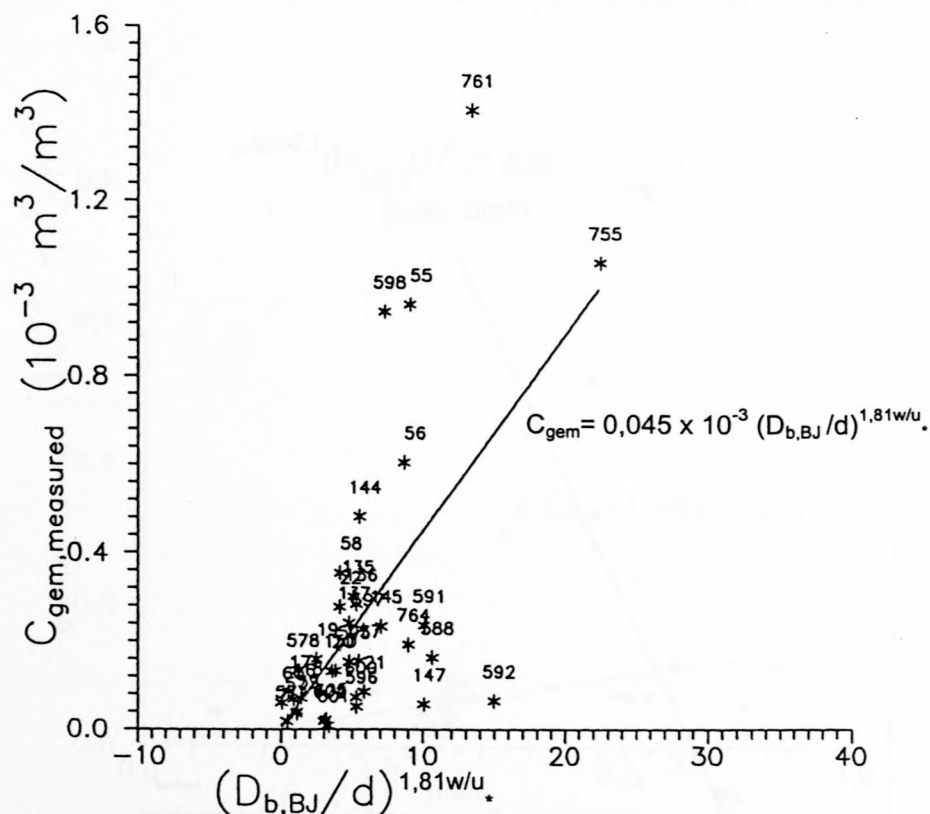


Figure H12: Measured mean concentration as a function of the energy dissipation per unit time and volume to the power e_1 ($e_1 = 1,81 w/u.$; Battjes and Janssen method)

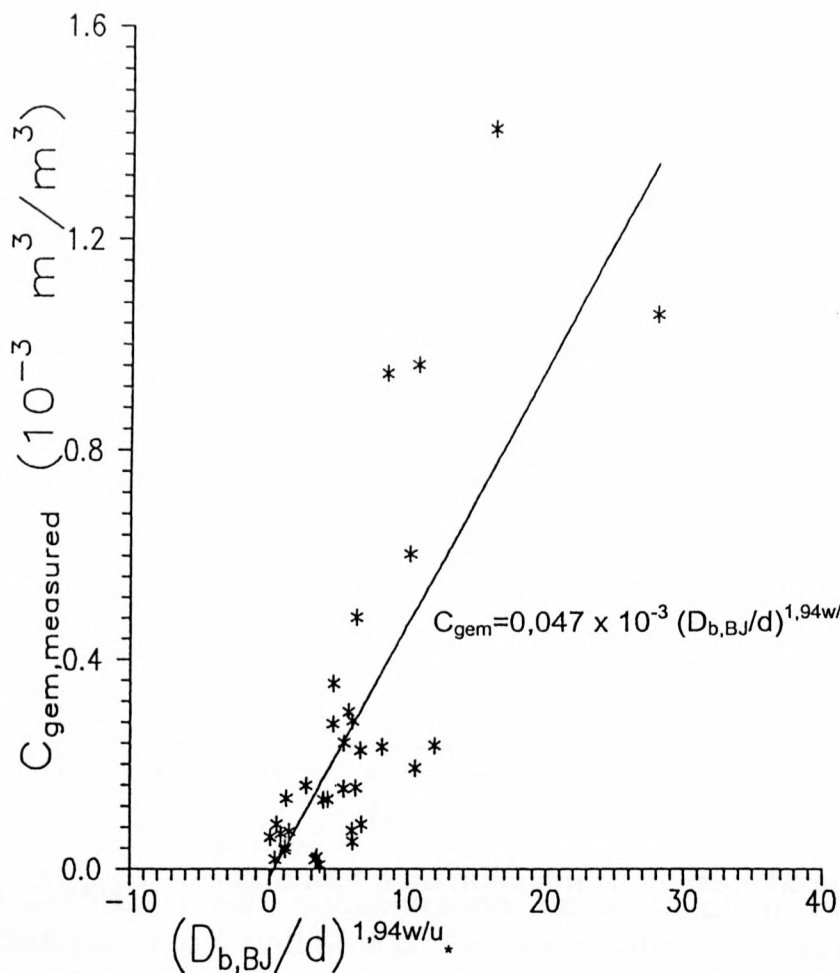


Figure H13: Measured mean concentration as a function of the energy dissipation per unit time and per unit volume to the power e_1 ($e_1 = 1,94 \text{ w/u.}$; Battjes and Janssen method)

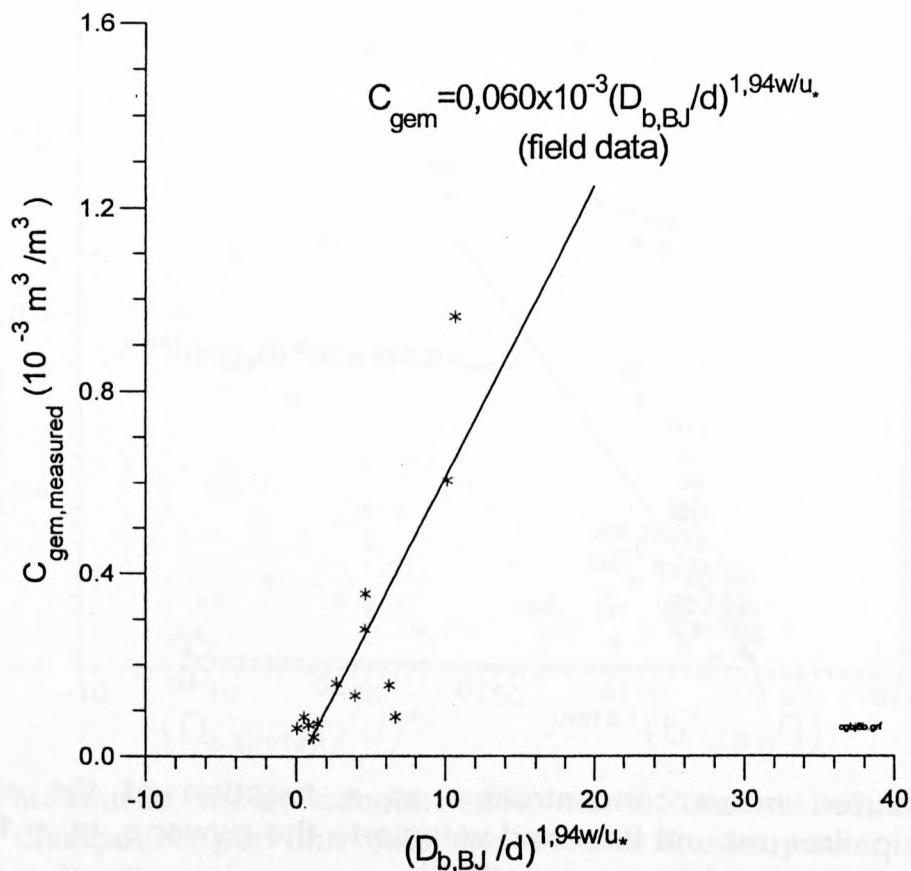


Figure H14: Mean concentration as a function of the energy dissipation per unit time and volume to the power e_1 (Battjes and Janssen method; field data)

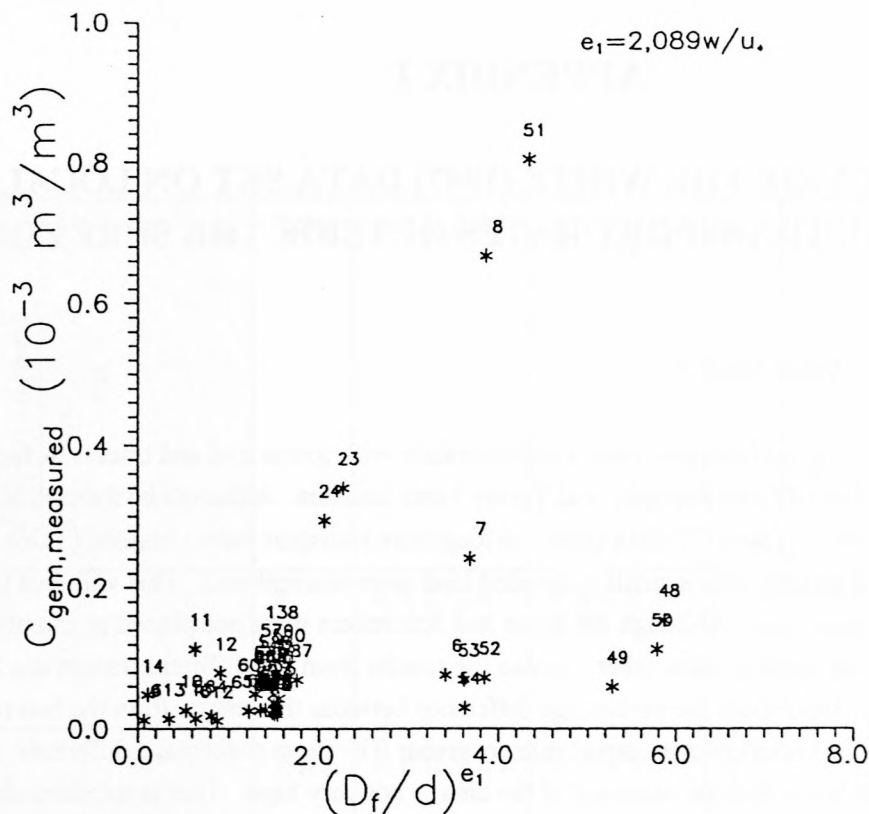


Figure H15: Measured mean concentration versus the energy dissipation per unit time and volume to the power e_1

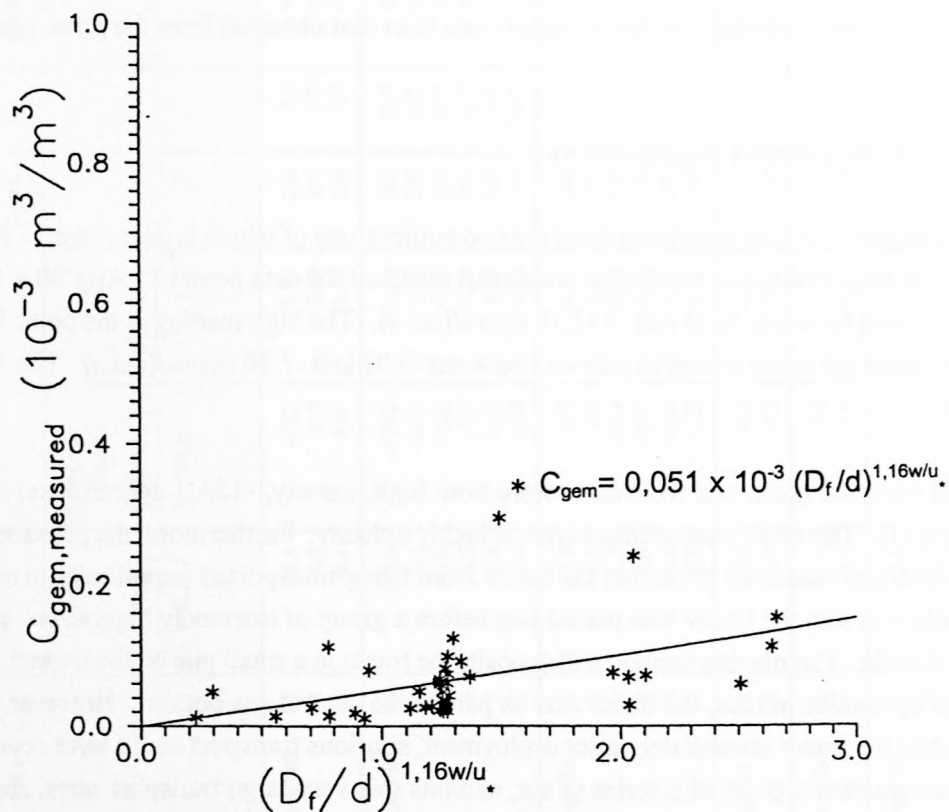


Figure H16: Measured mean concentration versus $(D_f/d)^{1,16w/u}$

APPENDIX I

ACCURACY OF THE WHITE (1987) DATA SET ON LOCAL LONGSHORE TRANSPORT RATES OUTSIDE THE SURF ZONE

I.1 Accuracy of the Whole Data Set

White (1987) measured the local transport rates simultaneously with green and red tracers at two beaches, namely, the Scripps Institute of Oceanography and Torrey Pines beaches. Although he focused his attention mainly on cross-shore transport, some 25 data points on longshore transport were obtained (Table I1). Most of the time, sheet flow conditions with a small suspended load were encountered. This will thus be a severe test for the theoretical model used. Although the green and red tracers were not placed at exactly the same locations (3 m apart) it was close to each other. Hence the results from the different tracers can be used to judge the accuracy of the data. Both the percentage difference between the results from the two tracers and the factor $f = \text{higher transport rate} / \text{lower transport rate}$ are given. The mean percentage difference is 67% and the mean $f = 8,3$ which indicate that the accuracy of the data is not very high. This is substantiated by:

- For 4 data points the sand and water is moving in different directions. These points were subsequently disregarded, thus leaving 21 data points.
- On a few occasions the transport is in different directions according the two tracers (Table I1). This happened especially at low rates.
- The red tracer usually yielded a higher transport rate than that obtained from the green tracer (Table I1).

I.2 Accuracy of Data Point 11 August '80 #1

In the calibration (Chapter 5) it was found that there are two outliers, one of which is data point 11 August '80 #1. From Table I1 it can be seen that conditions are almost identical for data points 11 Aug '80 # 1 to 6. Yet the mean transport varied between -0,02 and -152,10 dynes/(cm.s). The high reading is the point 11 Aug '80 # 1; for the other 5 points the mean transport rate was between -0,02 and -7,10 dynes/(cm.s). The reasons for this are the following:

The transport rates from the green and red tracers were both high, namely, -125,0 dynes/(cm.s) and -179,1 dynes/(cm.s) - Table I1). Therefore measurement error is highly unlikely. Furthermore, the placement method of using a dual cylindrical container prevented the tracer from being transported unnaturally in suspension. A possible explanation is that the tracer was placed just before a group of extremely high waves in the wave spectrum reached the site. The placing method still deposits the tracer in a small pile on the bottom. If the pile is initially flattened by smaller waves, the tracer acts as part of the natural sea bottom. However, if a group of high waves reached the tracer immediately after deployment, spurious transport could have occurred. The fact that the first measurement point of a series of six, exhibits this very large transport rates, supports this explanation. Therefore the data point 11 Aug '80 # 1 was ignored.

No valid reasons could be found for leaving the other outlier out and thus it was retained.

Table 11: Local Longshore Transport Rates outside the Surf Zone Measured by White (1987)

Date and point number	Local longshore transport			d Depth (cm)	T _r (s)	H _r (cm)	v (cm/s)	Bottom slope α (°)	D ₅₀ (μm)	f	Transport difference $\left(= \frac{i(\text{red}) - i(\text{green})}{i(\text{red})} \cdot 100 \right)$ (%)
	i(green tracer) $\left(\frac{\text{dynes}}{\text{cm.s}} \right)$	i(red tracer) $\left(\frac{\text{dynes}}{\text{cm.s}} \right)$	\bar{i} $\left(\frac{\text{dynes}}{\text{cm.s}} \right)$								
23 June '80 #1 3 4	-34,4	-33,2	-33,80	230	7,7	91	-1,6	1,66	250	1,04	-3
	-8,0	-9,7	-8,90	230	7,7	91	0,9	1,66	250	-	18
	-6,1	-4,80	-5,50	230	7,7	91	0,9	1,66	250	-	100
11 Aug '80 #1 2 3 4 5 6	-125,0	-179,0	-152,10	260	22,7	42	-3,1	1,26	218	1,43	30
	-0,2	-2,10	-1,10	260	22,7	42	-3,8	1,26	218	10,50	90
	-0,06	0,03	-0,05	260	22,7	42	-3,6	1,26	218	2,00	300
	-6,6	-7,7	-7,10	260	22,7	42	-3,4	1,26	218	1,17	13
	-0,4	-0,02	0,20	260	22,7	42	-3,4	1,26	218	20,00	25
	-0,04	0,00	0,02	260	22,7	42	-3,6	1,26	218	-	-38
12 Sep '80 #1 2 3 4 5 6	-47,3	-2,3	-24,80	280	13,7	75	-3,1	1,43	182	20,57	-1966
	-1,1	-1,6	-1,30	280	13,7	75	-3,6	1,43	182	1,45	28
	-0,3	-0,04	-0,18	280	13,7	75	-3,9	1,43	182	7,50	900
	-0,6	-0,05	-0,33	280	13,7	75	-4,4	1,43	182	12,00	1320
	-0,2	-0,12	-0,17	280	13,7	75	-4,6	1,43	182	1,67	-75
	-0,2	0,22	-0,21	280	13,7	75	-3,7	1,43	182	1,10	14
3 Aug '84 #1 2	0,03	-0,9	-0,50	500	9,1	113	-2,1	1,15	177	30,0	103
	-0,09	-0,5	-0,30	500	9,1	113	-2,6	1,15	177	5,56	81
10 Aug '84 #1 2	0,31	7,6	4,00	310	10,0	83	9,2	0,69	201	24,52	105
	11,3	14,6	12,90	310	10,0	83	7,9	0,69	201	1,29	53
29 Aug '84 #1 2 3	1,1	7,7	-3,30	430	10,0	69	-5,8	1,49	206	-	114
	0,4	0,4	-0,02	430	10,0	69	-4,9	1,49	206	-	193
	5,4	6,1	5,70	430	10,0	69	-4,6	1,49	206	-	16
26 Sept '84 #1 2 3	0,15	0,8	0,50	320	11,4	72	7,2	1,32	183	5,33	82
	-0,01	-0,05	-0,03	320	11,4	72	7,8	1,32	183	-	80
	0,59	0,31	0,45	320	11,4	72	7,9	1,32	183	1,90	90
										$\bar{f} = 8,28$	Mean = 67

i = local longshore transport in terms of immersed weight \bar{i} = mean transport rate from the green and red tracers

\bar{f} = mean factor f where f = maximum i / minimum i

APPENDIX J

ACCURACY OF ONE DATA POINT OF THE KRAUS *ET AL.* (1982) DATA SET ON LOCAL LONGSHORE TRANSPORT INSIDE THE SURF ZONE

The data point under consideration is the outlier (in Figure 5.16) located at $\xi_i = 0,37$, which was obtained at Ajigaura Beach in 1979 with sampling done after 120 minutes (Table 3 in Kraus *et al.* (1982)).

Kraus *et al.* (1981) provide additional information about the same data set contained in Kraus *et al.* (1982). Of specific interest is a bathymetric map of the Ajigaura beach site (depicted in Figure 3 in Kraus *et al.* (1981)). Figure J1 shows the beach profile through the points where sand samples were taken. It can be seen from this figure that the beach is generally flat and even (beach slope is about 1/47) in the surf zone except for a steeper slope near the shoreline. No distinct sand bar is present in the surf zone.

Figure J1 also illustrates the cross-shore distribution of the local longshore transport rate. When moving shorewards from the breakerline, the measured local longshore transport rate initially decreases rapidly. This is to be expected because the most intense breaking and turbulence are usually found at the breakerline. Normally this decreasing trend in the local transport rate continues towards the shoreline unless a sand bar is present. A secondary peak in the local longshore transport is generally found at the shoreline on a steep beach. However, the outlier which is roughly in the middle of the surf zone (denoted by “reported value” on Figure J1), is considerably higher than the other two measured transport rates despite the absence of a pronounced sand bar. It is unlikely that this high measured value is correct.

It was estimated that the measured transport rate should have been between $40 \times 10^{-6} \text{ m}^2/\text{s}$ and $80 \times 10^{-6} \text{ m}^2/\text{s}$. The value midway between these two values namely, $60 \times 10^{-6} \text{ m}^2/\text{s}$, is also shown (as “expected value”) on Figure J1. If $60 \times 10^{-6} \text{ m}^2/\text{s}$ is assumed to be correct value, then the corresponding a_4 value for this outlier will be about 390×10^{-6} . The data point will therefore plot in a realistic position just above the curve (solid line) in Figure 5.16.

Based on the morphology of the surf zone at Ajigaura Beach (as represented by the beach profile) and typical wave breaking, it is concluded that the measured transport rate denoted by “reported value” in Figure J1, is incorrect.

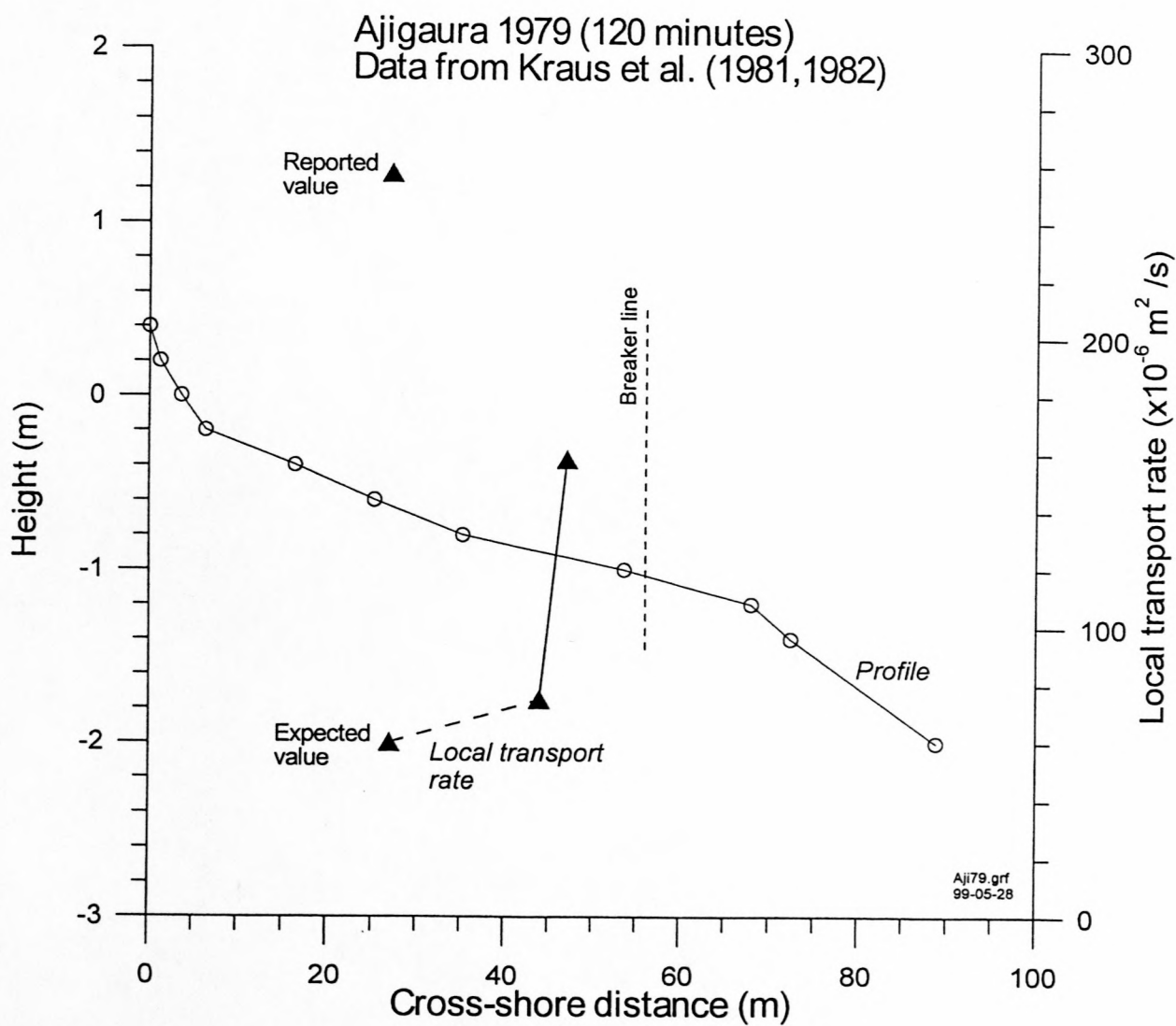


Figure J1: Beach profile and local longshore transport rates at Ajigaura Beach